HETEROBIMETALLIC LANTHANIDE HELICATES: DECIPHERING SUBSTITUENT EFFECTS BY CRYSTALLOGRAPHY AND NMR ANALYSES

THÈSE N^{O} 3519 (2006)

PRÉSENTÉE LE 19 MAI 2006

À LA FACULTÉ SCIENCES DE BASE

Laboratoire de chimie supramoléculaire des lanthanides

SECTION DE CHIMIE ET GÉNIE CHIMIQUE

ÉCOLE POLYTECHNIQUE FÉDÉRALE DE LAUSANNE

POUR L'OBTENTION DU GRADE DE DOCTEUR ÈS SCIENCES

PAR

Thomas Binderup JENSEN

M.Sc. in Chemistry, University of Copenhagen, Danemark
et de nationalité danoise

acceptée sur proposition du jury:

Prof. K. Johnsson, président du jury
Prof. J.-C. Bünzli, directeur de thèse
Prof. M. Albrecht, rapporteur
Prof. C. Piguet, rapporteur
Prof. K. Severin, rapporteur

ÉCOLE POLYTECHNIQUE
FÉDÉRALE DE LAUSANNE

Lausanne, EPFL
2006

Acknowledgements

I would like to express my gratitude to Professor Jean-Claude Bünzli for giving me the opportunity to work on the present project in his research group.

I would also like the thank the president of the jury Professor Kai Johnsson as well as the other members of the jury Professor Markus Albrecht, Professor Claude Piguet and Professor Kay Severin for having accepted the task of judging my work.

Dr. Rosario Scopelliti deserves thanks for having determined the solid state structures in the present work by means of X-ray diffraction.

Thanks to former and present collaborators at the Laboratory of Lanthanide Supramolecular Chemistry for having made it a pleasant place to work.

And finally, thanks to my family and my wife, Micaela, for all the rest.

Table of contents

Résumé

Basés sur le ligand L^{AB}, les nouveaux ligands hétéroditopiques L^{AB2}, L^{AB3}, L^{AB4} et L^{AB5} ont été synthétisés. Les cinq ligands ont été conçus pour leur capacité à former sélectivement des complexes hétérométalliques de type $[LnLn'(L)_3](ClO_4)_6$ en présence d'un couple de lanthanides $Ln(ClO_4)_3$ et $Ln'(ClO_4)_3$ en solution.

X = Y = H L^{AB}

X = H Y = NEt_2 L^{AB2}

X = H Y = Cl L^{AB3}

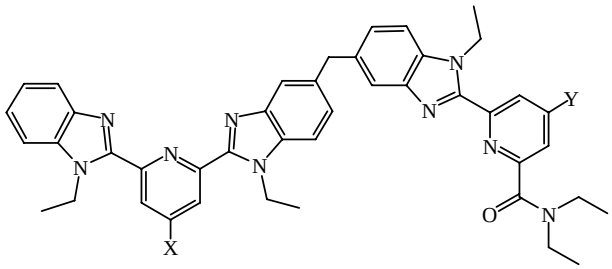

X = NEt_2 Y = H L^{AB4}

X = Cl Y = H L^{AB5}

Dans le ligand L^{AB} le site *benzimidazole-pyridine-benzimidazole* (bpb) a une préférence de complexation marquée pour les cations Ln^{3+} du début et du milieu de la série. Le site *benzimidazole-pyridine-amide* (bpa) a, quant à lui, une plus grande affinité pour les ions lanthanides de la fin de la série. Dans une solution La^{3+}:Lu^{3+}:L^{AB} = 1:1:3 la proportion du complexe hétérodimétallique $[LaLu(L^{AB})_3]^{6+}$ dépasse 90 %, le pourcentage étant inférieur pour des couples d'ions lanthanides plus proches.

Les substituants sur les nouveaux ligands modifient la densité de charge de l'atome d'azote de la pyridine. Le groupe électrodonneur NEt_2 dans L^{AB2} augmente la dureté du groupe bpa, ce qui devrait améliorer la sélectivité du ligand. Une amélioration comparable était attendue pour L^{AB5}, dans lequel le substituant électroattracteur Cl diminue la dureté du groupe bpb du ligand. Les deux autres nouveaux ligands L^{AB3} et L^{AB4}, par contre, n'étaient pas anticipés comme des améliorations du ligand L^{AB} et ont été synthétisés pour comparaison.

Dû à la tendance de L^{AB2} et L^{AB5} de former des proportions élevées des isomères *HHT (Head-Head-Tail ; Tête-Tête-Queue)*, leurs sélectivités se sont révélées inférieures aux valeurs anticipées. Les proportions des complexes hétérodimétalliques n'ont atteint, respectivement, que 65 et 92 %, pour le couple de lanthanides LaLu. Les ligands L^{AB3} et L^{AB5} ont donné comme prévu des pourcentages (87 et 79 %) des complexes hétérodimétalliques inférieurs à L^{AB}.

Pour expliquer l'équilibre entre les isomères *Tête-Tête-Tête* et *Tête-Tête-Queue,* des études par RMN à température variable ont été réalisées. Les valeurs de H et S ont été déterminées pour 26 complexes différents. Les résultats ont permis de voir que les équilibres sont contrôlés par des effets enthalpiques et entropiques faibles, les différences entre les deux isomères n'étant que de quelques $kJ \cdot mol^{-1}$.

Les structures de cinq complexes du ligand L^{AB3} ont été analysées par diffraction des rayons X. Les structures contiennent des hélicates à trois brins *HHH*-$[LnLn'(L^{AB3})_3]^{6+}$.

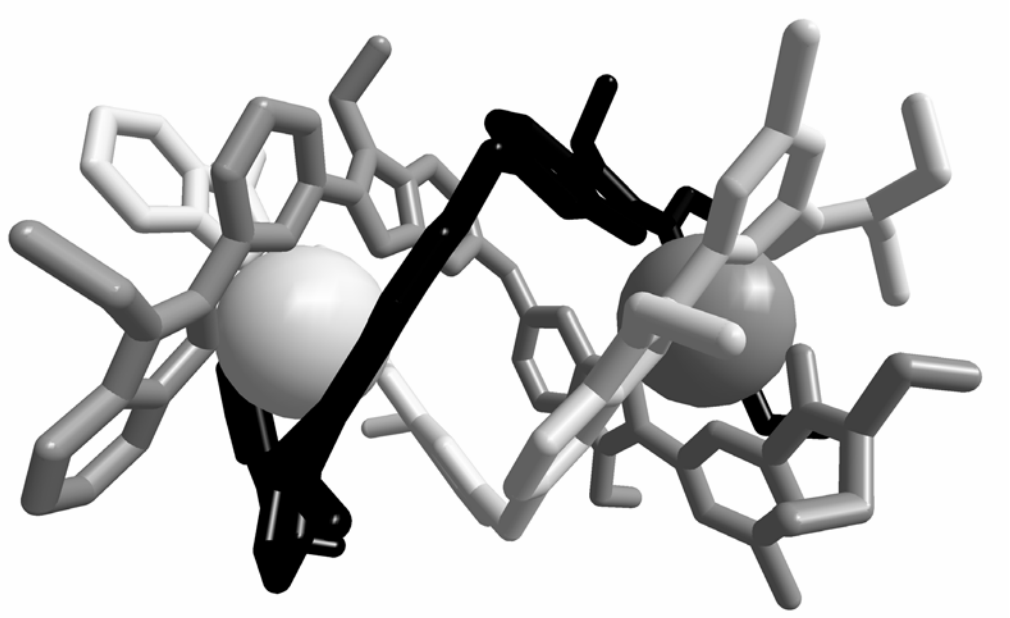

Afin d'obtenir des informations sur la structure des complexes en solution, les déplacements paramagnétiques induits par les ions lanthanides (Lanthanide Induced Shift) ont été étudiés. L'extraction des facteurs structurels a démontré que tous les complexes sont isostructuraux dans l'acétonitrile. La comparaison avec la structure à l'état solide déterminée par diffraction des rayons X a prouvé que cette dernière constitue un modèle correct pour représenter les complexes en solution. Enfin, une nouvelle méthode pour séparer les termes de contact et pseudo contact est proposée, qui tient compte de la variation du paramètre de champ cristallin B_0^2 le long de la série.

Mots-clés

Hélicates; auto-assemblage; chimie supramoléculaire; déplacement chimique paramagnétique; complexes hétérodimétallique.

Summary

Based on the ligand L^{AB} the new heterobitopic ligands L^{AB2}, L^{AB3}, L^{AB4} and L^{AB5} have been designed and synthesised. The five ligands were designed to selectively form heterobimetallic complexes of composition $[LnLn'(L)_3](ClO_4)_6$ when reacted with a pair of lanthanide ions $Ln(ClO_4)_3$ and $Ln'(ClO_4)_3$ in solution.

X = Y = H L^{AB}

X = H Y = NEt_2 L^{AB2}

X = H Y = Cl L^{AB3}

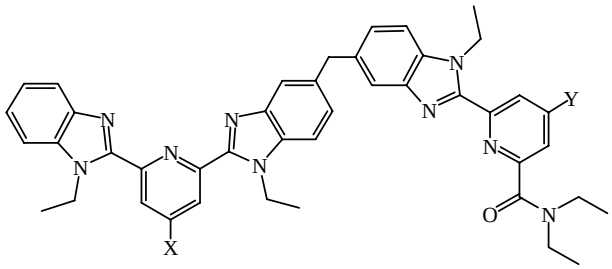

X = NEt_2 Y = H L^{AB4}

X = Cl Y = H L^{AB5}

The *benzimidazole-pyridine-benzimidazole* (bpb) moiety codes for the larger and softer lanthanide ions, while the *benzimidazole-pyridine-amide* (bpa) moiety codes for the smaller and harder ions of the lanthanide series. When reacted with 1/3 equivalent La^{3+} and 1/3 equivalent Lu^{3+} L^{AB} forms in excess of 90 % $[LnLn'(L)_3]^{6+}$, the percentage being lower for pairs of lanthanide ions closer in size.

The substituents on the new ligands modify the hardness of the nitrogen atom of the pyridyl group. The electron donating NEt_2 group in L^{AB2} increases the hardness of the bpa group, which should improve the selectivity of the ligand. A similar improvement was expected for L^{AB5} in which the electron withdrawing Cl substituent makes the bpb moiety of the ligand softer. The two other new ligands L^{AB3} and L^{AB4} were, based on similar arguments, not expected to exhibit improved selectivity and were synthesised for comparison.

Due to the tendency of L^{AB2} and L^{AB5} to form high proportions of *HHT* (*Head-Head-Tail*) isomers their selectivity turned out to be lower than anticipated. The proportion of heterobimetallic complexes reaches only 65 and 92 %, respectively, for the LaLu couple of lanthanides. The ligands L^{AB3} and L^{AB4}, as expected, also give lower yields (up to 87 and 79 %) of heterobimetallic complexes.

To investigate the details of the *Head-Head-Head/Head-Head-Tail* equilibrium variable temperature NMR measurements were carried out and the H and S values were determined for 26 different complexes. It was found that the equilibria were characterised by a subtle

interplay of enthalpic and entropic effects, with the two isomers differing only by a few kJ/mol.

Structures of five complexes of L^{AB3} were determined by X-ray diffraction. The structures contain molecular ions of composition $[LnLn'(L)_3]^{6+}$ in which the three ligand strands are wrapped around the two lanthanide ions in a helical fashion.

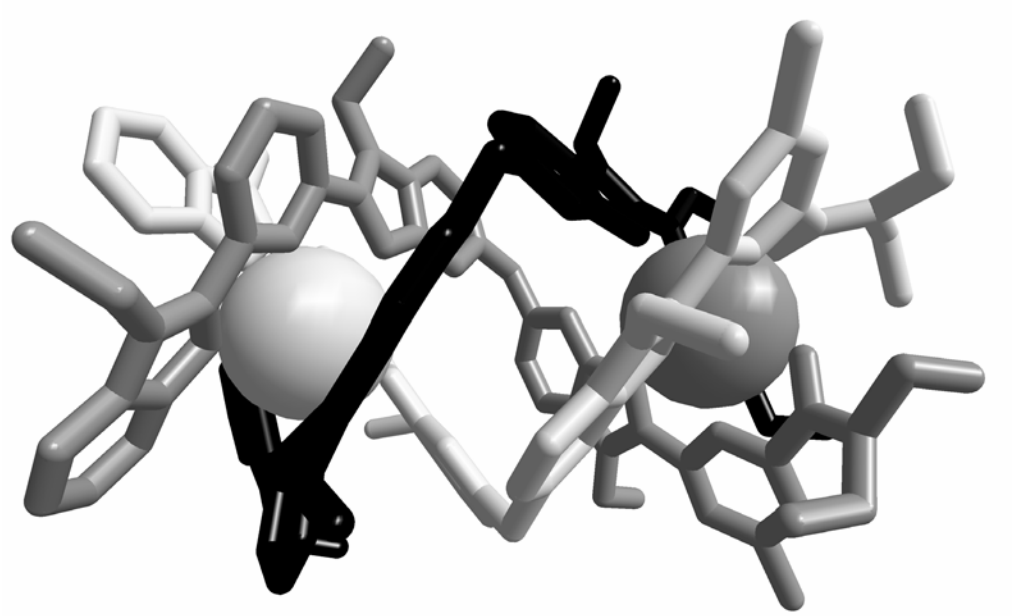

To obtain information about the structure of the complexes in solution analysis of the lanthanide induced paramagnetic shift has been carried out. The so-called one proton analysis showed that contributions from two paramagnetic lanthanide ions in the same complex are additive. Extraction of structural factors demonstrated that the complexes of all the ligands are isostructural in solution. Comparison with the X-ray data proved that the solid state structures are maintained in solution. Finally, a modified one proton analysis has been devised to separate contact and pseudo contact shifts while taking into account the variation of the crystal field parameter B_0^2 along the lanthanide series.

Keywords

Helicates; self-assembly; supramolecular chemistry; lanthanide induced shift; lanthanide induced relaxation; bimetallic complexes.

1 Introduction

Interest in the chemistry of lanthanide complexes has been increasing in recent years due to their fascinating photophysical and magnetic properties.[1,2,3,4] One reason for this has been the potential application of lanthanide complexes for biomedical purposes, especially as relaxation reagents for magnetic resonance imaging (MRI) and luminescent probes.

1.1 Chemical properties of the lanthanides

The most stable oxidation state for all the lanthanides is 3+ with the only notable exceptions being the Ce(IV) and Eu(II) ions. The Ln(III) ions are typical hard ions with a preference for ligands with hard donor atoms, oxygen in particular.

The chemical properties of the lanthanides are similar due to their comparable sizes and shielded valence electron shells, which is also manifested in a lack of preferred coordination geometry. Between Ln(III) ions adjacent in the lanthanide series the size difference is only a few pm and even between La(III) and Lu(III) the difference in ionic radius is less than 20 pm, significantly smaller than for example the difference between the Na^+ and K^+ ions.

It is possible to fine-tune the coordination properties of a ligand by modifying the hardness of the ligator atoms. The simplest method is to exchange the ligator atom when designing the ligand, for example a nitrogen atom for an oxygen atom. Further improvement can be obtained by changing atoms or groups bonded to the ligator atoms since this can modify the electron density. It should however be emphasised that since the hardness of a lanthanide atom only depends of its size, only relatively small differences in hardness are observed within the lanthanide series. A ligand designed to form complexes with the larger lanthanide ions will thus also form complexes with the smaller lanthanide ions, the complexation constants being expected to vary smoothly, but not much, along the lanthanide series.

Regarding coordination geometry of lanthanide complexes, common arrangements include eight-coordinate square anti-prisms and nine-coordinate tricapped trigonal prisms. The high coordination number reflects the large size of the lanthanide ions whereas the geometries mentioned minimize the interligand repulsion for small, monodentate ligands, for example water molecules. Other coordination numbers (6-12) and coordination geometries (often with

a high degree of deviation from regular coordination polyhedra) are however also found, reflecting the non-directional character of the metal-ligand interaction. Should a specific coordination geometry of a lanthanide ion be wished, it has to be built into the design of the ligand.

1.2 Luminescence

Regarding photophysical aspects, several lanthanide ions display interesting luminescence properties, e.g. Eu(III) (red emission) and Tb(III) (green emission). However, due to the f-f transitions being parity forbidden, lanthanides have weak electronic absorption bands. Furthermore, the weak interaction between 4f and ligand electrons does not provide a mechanism for enhancing the absorbance, as is the case for d-d transitions in transition metal complexes. For the purpose of developing luminescent applications, it is therefore desirable to have a ligand capable of absorbing photons and subsequently transfer the energy to the lanthanide ion; this is commonly known as the antenna effect.

To minimise unwanted de-excitation of the exited states, groups with high energy vibrations (OH, NH) should be avoided since they provide a non-radiative pathway for relaxation of the molecule following the initial absorption of light. This demand should be met not only within the ligand, but also in the coordination sphere of the lanthanide ion, meaning that a further property of the ligand should be that it coordinatively saturates the metal ion leaving no room for solvent molecules or counter ions. The kinetic lability of lanthanide complexes implies that complexes with polydentate ligands, especially with attractive intra- or inter-ligand-ligand interactions, are preferable over complexes with monodentate ligands, the latter being more susceptible to (partial) solvatisation.

Some examples of ligands meeting the latter criteria are given in Chart 1.[5,6,7,8,9]

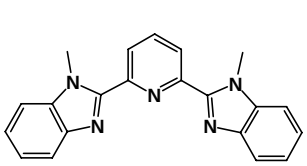

L^1

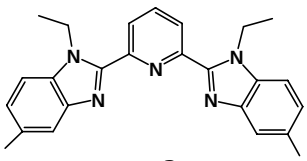

L^2

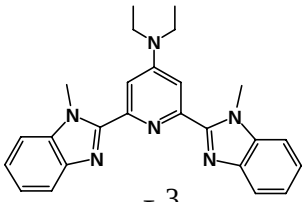

L^3

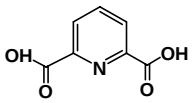

L^4

Chart 1 Ligands L^1, L^2, L^3 and L^4

While the design of an organic ligand with a large molar absorption coefficient is rather easy, the energy transfer requires that the relative energy levels of ligand and lanthanide ion are well-matched. The energy levels of the ligands can be modified by changing substituents as exemplified by the addition of a NEt_2 substituent in L^3.

1.3 Polymetallic complexes

Designing compounds containing two or more lanthanide ions is of interest for several reasons. For example, fixing two lanthanide ions in close proximity allows for magnetic interaction and energy transfer to take place between them.

An example of a ligand used to synthesise bimetallic complexes is shown in Chart 2.[10] L^5 forms dimeric $[Eu_2(L^5)_4]^{6+}$ complexes in which one of the ligands bridges the two Eu(III) ions.

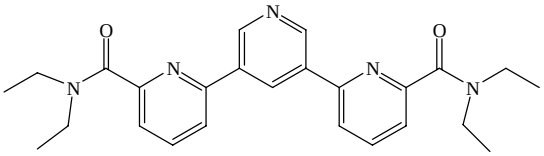

L^5

Chart 2 Ligand L^5

Further examples of ligands used for synthesising bimetallic complexes are L^7 ad L^8 shown in Chart 3.[11,12] These are derived from the ligand L^6 (DOTA), whose Gd complexes are used as contrast agents in MRI. The examples given here illustrate well how strategies used for designing monometallic complexes can be extended to yield bimetallic complexes.

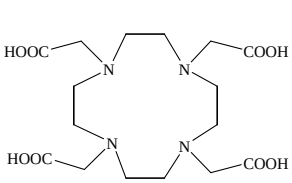

L^6 (DOTA)

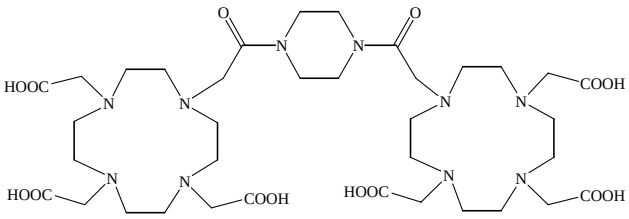

L^7

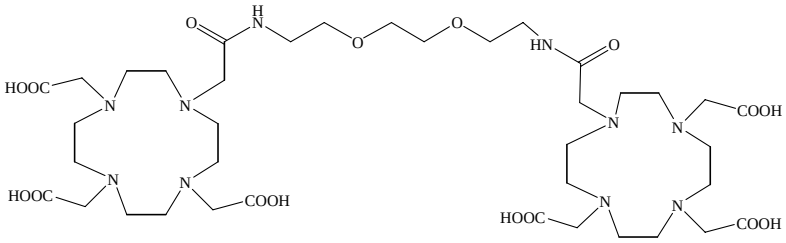

L^8

Chart 3 Ligands L^6, L^7 and L^8

1.4 Helicates

Helical structures are found not only in manmade molecules,[13,14,15] but also in nature. The most famous example is without a doubt DNA (Figure 1), which exists in solution as a double helix held together by hydrogen bonding.[16] Despite being obviously unrelated to the present work it still deserves mentioning, not only for its importance in biological systems, but also because it is aesthetically pleasing.

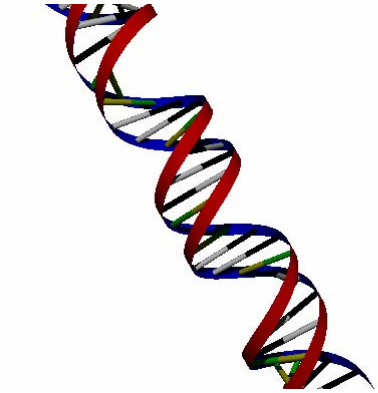

Figure 1 The DNA double helix

The term "helicate" was introduced by Lehn in 1987 to describe complexes containing two or more metal ions connected by two ligand strands wrapped in a helical fashion around the metal centers.[17] A large number of single, double and triple stranded helicates are now known.[18,19,20,21,22,23]

Here we are interested in a subgroup of helicates, triple stranded helicates containing two lanthanide ions. Few such complexes have been described in the literature.

An early example was the $Ln_2(L^9)_3(NO_3)_6$ (Ln = Pr, Nd, Sm, Er) complexes in which three bridging L^9 ligands are arranged in a helical fashion.[24] L^{10} and L^{11} form uncharged complexes of composition $[Ln_2(L)_3]$ (Ln = Sm, Eu, Nd).[25]

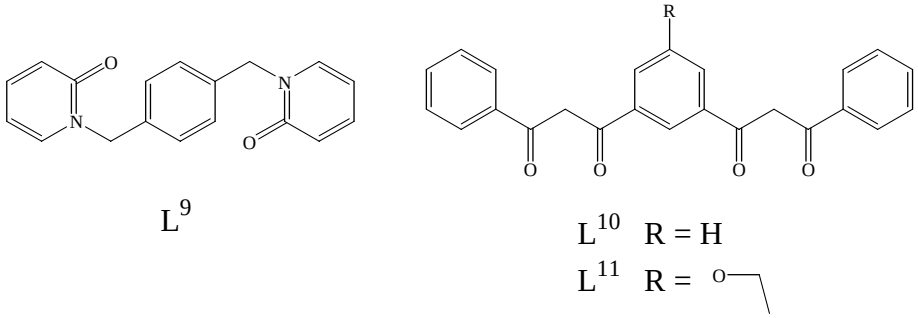

L^9 L^{10} R = H L^{11} R = O

Chart 4 Ligands L^9, L^{10} and L^{11}

The ligands L^{12} and L^{13} in Chart 5 form helicates in aqueous solution, which is less common due to the high solvatisation energy of the lanthanide ions in water.[26]

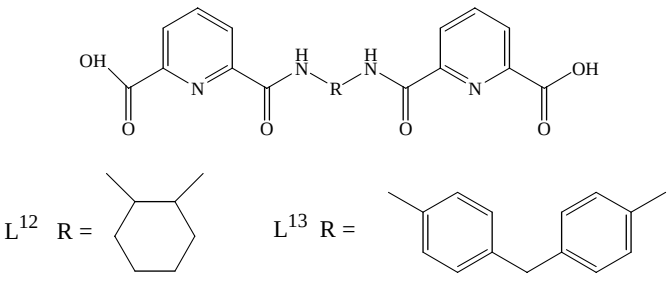

L^{12} R = L^{13} R =

Chart 5 Ligands L^{12} and L^{13}

The family of homoditopic ligands shown in Chart 6 form the background of the present project. L^A [27,28,29] was the first example of a ligand self-assembling with lanthanide ions in CD_3CN solution to form triple stranded bimetallic helicates of composition $[Ln_2(L)_3]^{6+}$. The

ligands L^{B},[30] L^{E} and L^{F} [31] yield analogous complexes, while deprotonated L^{C} [32,33,34,35,36] forms uncharged $[Ln_2(L^{C})_3]$ in aqueous solution

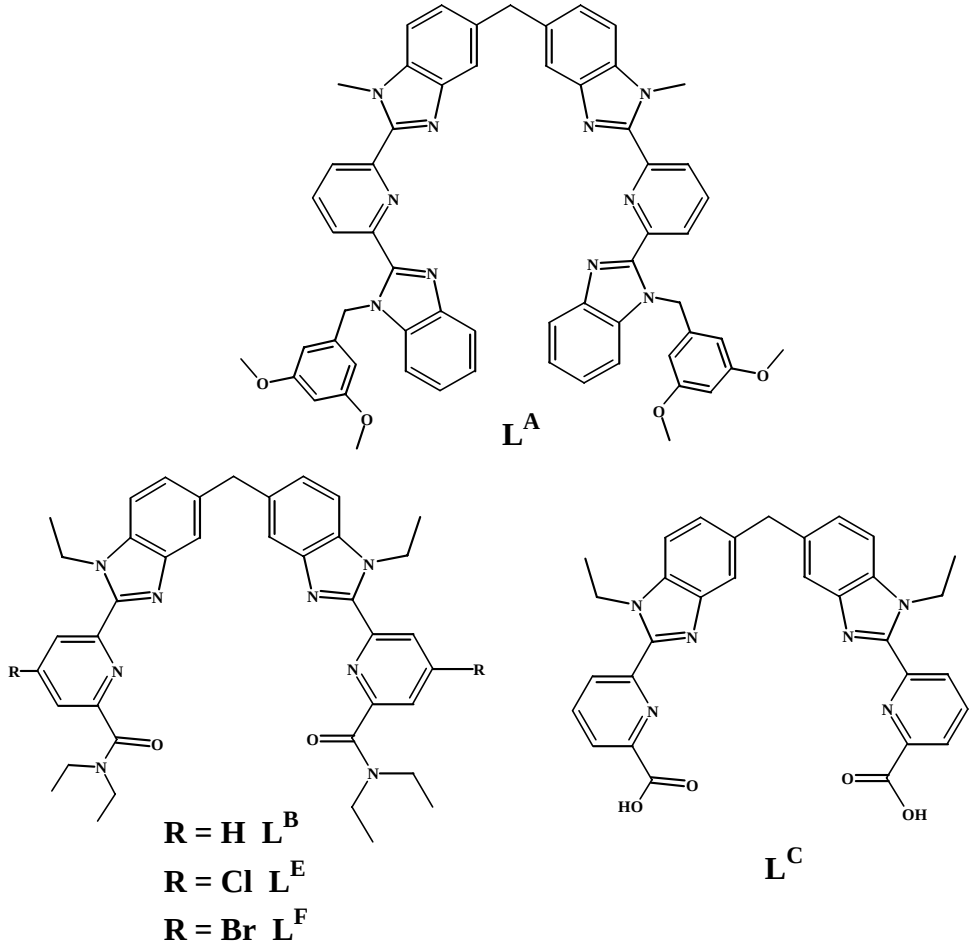

Chart 6 Ligands L^{A}, L^{B}, L^{C}, L^{E} and L^{F}

1.5 Heteropolymetallic complexes

Finally, the design of heteropolymetallic compounds would yield complexes with the combined magnetic and/or photophysical properties of several lanthanide ions. This would provide the opportunity of having molecules emitting at two different wavelengths or edifices containing one luminescent and one magnetic probe.

Several strategies for synthesising and isolating heteropoly metallic complexes can be applied.

Reaction of a ligand with one equivalent of Ln and subsequently one equivalent of Ln' is potentially problematic since this strategy would depend on the initially formed complex to be

kinetically stable. It is, however, not impossible, as demonstrated by Costes and co-workers[37,38,39] who have synthesised and characterised a large number of heterobimetallic complexes with the tripodal ligand L^{14} (Chart 7).

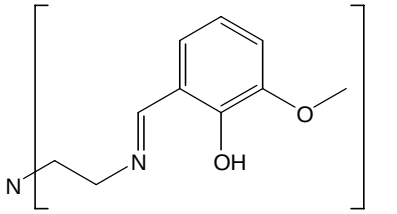

L^{14}

Chart 7 Ligand L^{14}

A second strategy is the formation in solution of several homo- and heteropolymetallic edifices followed by separation. An example is ligand L^{15} which forms trimetallic sandwich complexes of composition $[Ln_3(L^{15}\text{-}3H)_2]$ in D_2O.[40,41,42,43] In the presence of a mixture of lanthanide ions heterotrimetallic complexes $[Ln_2Ln'(L^{15}\text{-}3H)_2]$ and $[LnLn'Ln''(L^{15}\text{-}3H)_2]$ are formed in statistical proportions slightly modified by the preference of the ligand for the smaller lanthanide ions.[44,45]

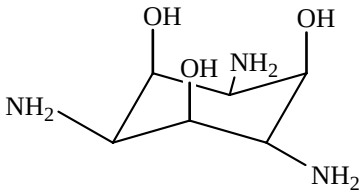

L^{15}

Chart 8 Ligand L^{15}

The problem in this strategy lies in the difficulty in separating the heterometallic complexes from the other components of the reaction mixture due to the kinetic lability of lanthanide complexes.

The third strategy is based on the simultaneous recognition of two different lanthanide ions. This will be the strategy of our choice as outlined in the following.

1.6 L^{AB} and related ligands

The philosophy behind the design of heterobimetallic lanthanide complexes consists of constructing ligands that are combinations of monomeric building blocks, each with a preference for either large or small lanthanide ions

1.6.1 Monomeric building blocks

The challenge in designing ligands with a pronounced preference for a specific lanthanide ion lies in the similar chemical properties of the trivalent lanthanide ions. The only difference between them is a slight decrease in ionic radius along the lanthanide series,[46] too small to base the selectivity of a ligand on the size (or rather its bite, when as here multidentate ligands are being considered). The variation in ionic radius is the cause of the electrostatic trend usually observed: complexation constants are larger for the smaller lanthanide ions. Such a behaviour is of course of no use to us, since a heterobitopic ligand constructed from two such monomeric building blocks would not have one coordination unit showing preference for the larger lanthanide ions.

A remarkable exception to the rule of increased complexation constant with increasing atom number is ligand L^1. It forms complexes of composition $[Ln(L^1)_3]^{3+}$ with all the lanthanides and the complexes of the smaller lanthanide ions are significantly less stable than the complexes of the lanthanides of the first half of the lanthanide series.[5,6] This unusual behaviour has its origin in the helical wrapping of the three ligand strands around the lanthanide ion; weak interstrand interactions between neighbouring strands stabilise the ligands in a conformation which creates a coordination cavity that is too large to accommodate the smaller lanthanide ions. In the design of a heterobitopic ligand envisaged to exhibit selectivity towards a pair of different lanthanide ions L^1 is therefore an ideal candidate for the coordination unit coded for the larger of the two ions. The behaviour of L^1 is also displayed by the closely related homoditopic ligand L^A (Chart 6) for which a similar decrease in stability is observed along the lanthanide series: 20 $\log\beta_{23}^{La} \approx \log\beta_{23}^{Eu}$ 22; $\log\beta_{23}^{Lu}$ = 17.5(4).[27]

For the other coordination unit the choice is less limited and ligand L^{16} and L^{18} (Chart 9) were chosen. The replacement of one of the benzimidazole groups of L^1 with an amide or carboxylic acid group eliminates the possibility of the interstrand interactions that were the

basis for the preference of L^1 for the larger lanthanide ions. No stability constant have been measured for L^{16} complexes of the larger lanthanides, but the closely related ligand L^{17} [47] displays the expected electrostatic trend with $\beta_{13}^{Lu} \approx 2\ \beta_{13}^{La}$ and the same behaviour has been observed[8] for complexes with L^{18}.*

Other reasons for this choice of building block is the improved luminescence properties with respect to L^1 as well as the future potential for preparing helicates in aqueous solution with the incorporation of L^{18} (cf. the complexes of L^C mentioned above).

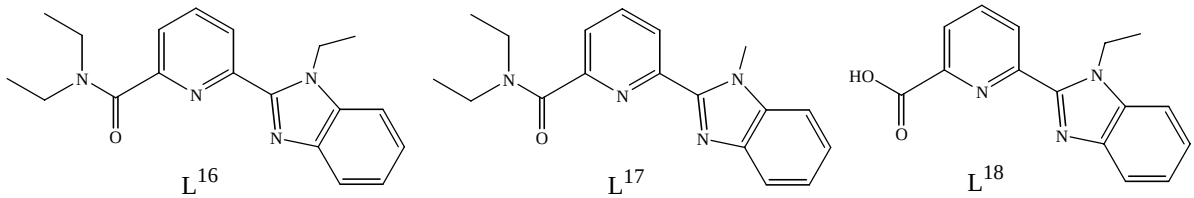

L^{16} L^{17} L^{18}

Chart 9 Ligands L^{16}, L^{17} and L^{18}

1.6.2 Design and properties of L^{AB}, L^{AC} and L^{BC}

Based on these three building blocks ligands L^{AB} and L^{AC} (Chart 10) were designed and synthesised.[8,48,80] For reasons of comparison L^{BC} was also synthesised.

Ligand L^{AB} showed the best selectivity of the three ligands towards a pair of lanthanide ions sufficiently different in size; for the LaLu couple the proportion of heterobimetallic complexes of composition $[LaLu(L^{AB})_3]^{6+}$ exceeds 90 % in acetonitrile as determined by ES-MS and NMR. As expected, the selectivity depends on the size difference and the percentage approaches 50 %, the statistical value (see Chapter 4.2; page 64), for ions adjacent in the lanthanide series. In the heterobimetallic complexes, NMR measurements indicate that the smaller lanthanide ion is coordinated by the bpa (*benzimidazole-pyridine-amide*) moiety of the ligand while the larger ion is coordinated by the bpb (*benzimidazole-pyridine-benzimidazole*) moiety, as predicted during the design of the ligand.

* The stability constants given for complexes of L^{16} in Ref. 47 are in fact those measured for L^{18}. See Ref. 8.

With L^{BC} only 31 % heterobimetallic complexes are formed for the LaLu couple. The low selectivity is in accordance with what was anticipated for this ligand in which both coordination units have a preference for the smaller lanthanide ions.

L^{AC} gave smaller percentages of heterobimetallic complexes than L^{AB} for all LnLn' couples examined. This was traced back to a pronounced tendency of L^{AC} to form *HHT* (*Head-Head-Tail*) isomers in which one of the ligand strands in the complex are oriented in the opposite direction of the two others. The formation of mixed benzimidazole/carboxylate coordination cavities in the *HHT* isomer reduces the selectivity of the ligand.

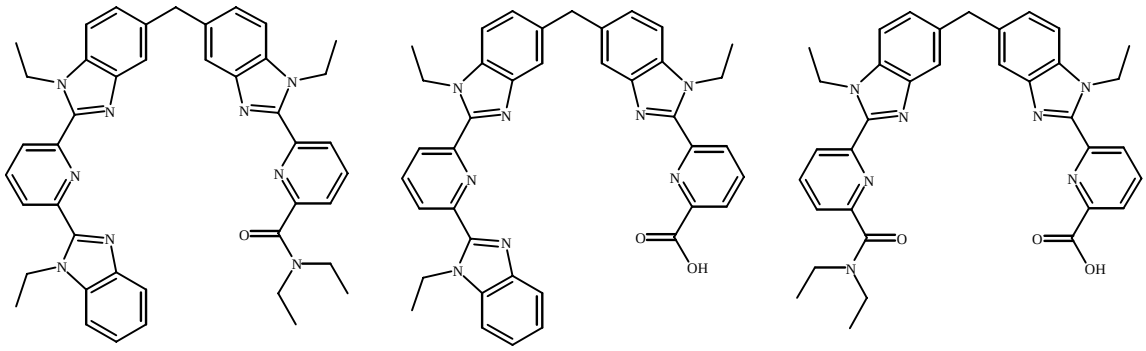

L^{AB} L^{AC} L^{BC}

Chart 10 Ligands L^{AB}, L^{AC} and L^{BC}

1.6.3 Ligands L^{BAB}, L^{BAAB}, L^{Aa} and L^{Ba}

The concept behind the design of L^{AB} has been extended to the heterotritopic ligand L^{BAB} and the heterotetratopic ligand L^{BAAB} (Chart 11). L^{BAB} forms homo- and heterotrimetallic lanthanide containing helicates in CD_3CN solution and in the solid state.[49,50,51,52,53,54,55] Ligand L^{BAAB} reacts with Eu(III) ions to yield $[Eu_4(L^{BAAB})_3]^{12+}$.[56] A model for the site selective binding has been developed using these complexes as examples.[57,58,59]

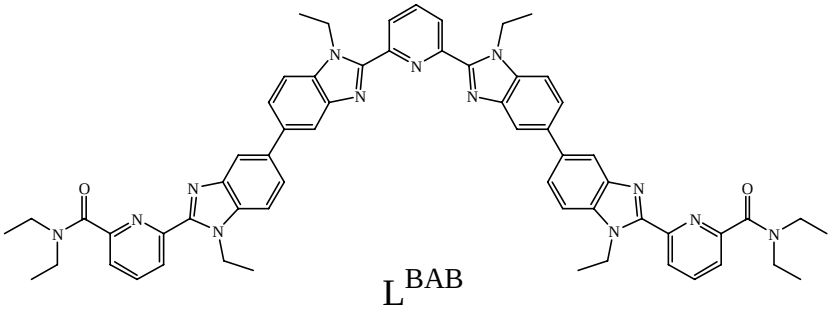

L^{BAB}

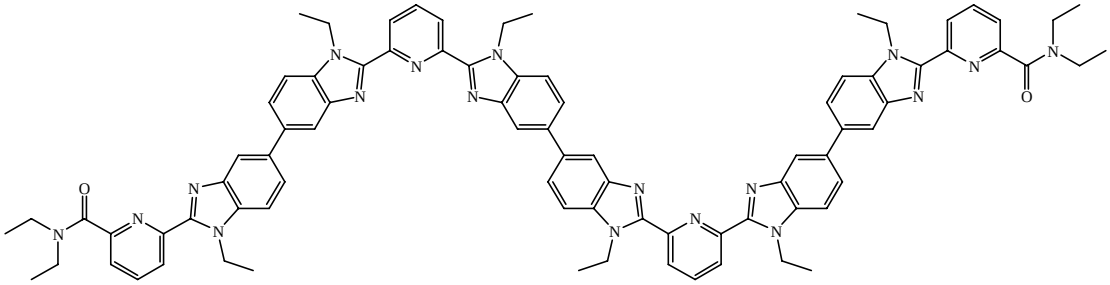

L^{BAAB}

Chart 11 Ligands L^{BAB} and L^{BAAB}

Closely related in concept are the ligands L^{Aa} [60,61] and L^{Ba} [62,63,64,65,66,67,68,69,70,71,72,73] (Chart 12) which are designed to complex one lanthanide ion and one transition metal ion. With divalent transition metal ions complexes of the type $[M(II)Ln(L)_3]^{5+}$ (M = Cr, Fe, Co, Zn, Ru) are formed, while trivalent transition metal ions give $[M(III)Ln(L)_3]^{6+}$ (M = Cr, Co).

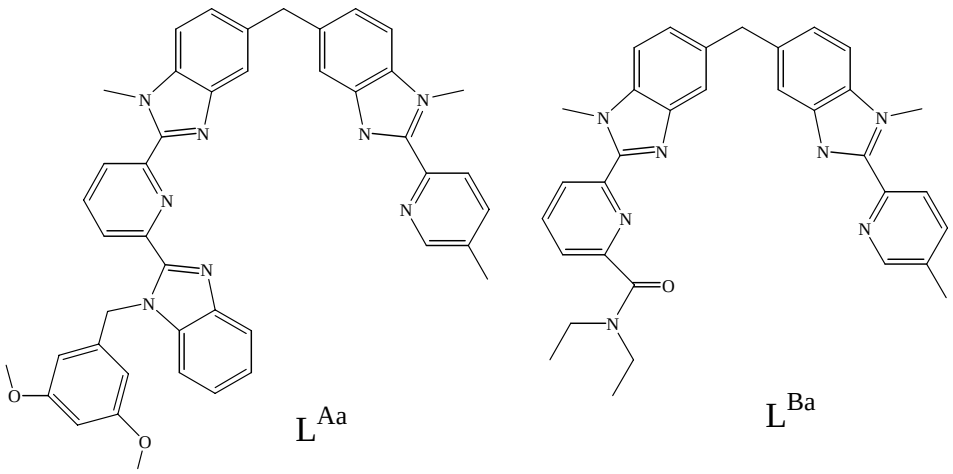

L^{Aa} L^{Ba}

Chart 12 Ligands L^{Aa} and L^{Ba}

1.7 Purpose of the present project

The goal of the present Ph.D. project is to understand the origin of and, if possible, improve the selectivity of ligand L^{AB} since for practical applications a better selectivity for pairs of ions displaying a small difference in ionic radius would be desirable.

The strategy for the design of the new ligands is based on the modification of the hardness of a pyridyl N donor atom by the introduction of a substituent on the *para* position of the pyridyl group of one moiety of L^{AB}.

X = Y = H L^{AB}

X = H Y = NEt_2 L^{AB2}

X = H Y = Cl L^{AB3}

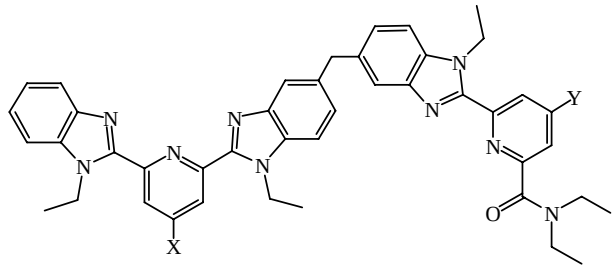

X = NEt_2 Y = H L^{AB4}

X = Cl Y = H L^{AB5}

Chart 13 Ligands L^{AB}, L^{AB2}, L^{AB3}, L^{AB4} and L^{AB5}

In L^{AB2} a NEt_2 group is introduced in the *para* position of the pyridyl group of the bpa (*benzimidazole-pyridine-amide*) moiety of L^{AB} which codes for the smaller, harder lanthanide ions from the latter half of the lanthanide series. It is assumed that the introduction of an electron donating NEt_2 group will increase the hardness of the N donor atom and the preference of this unit towards smaller lanthanide ions and thus improve the overall selectivity of the ligand towards pairs of different lanthanide ions.

In the case of L^{AB5}, a Cl substituent is placed in the *para* position of the pyridyl group of the bpb (*benzimidazole-pyridine-benzimidazole*) moiety of L^{AB}. As this is the softer of the two coordination compartments it is expected that the electron withdrawing Cl substituent will decrease the hardness of the N atom and, again, improve the selectivity of the ligand.

To complement the studies the ligands L^{AB3} and L^{AB4} are designed for comparison with ligands L^{AB2} and L^{AB5}. In these two ligands the substituents (Cl for L^{AB3} and NEt_2 for L^{AB4}) are placed on the "wrong" moieties of the ligand and the selectivity is therefore expected to be less good than for L^{AB}.

The purpose of the project is to determine if, how and why the substituents change the structure of the complexes in solution and in the solid state as well as their speciation in solution.

The project consists of the following parts:

- Synthesis of the ligands following strategies developed for related mono- and dimeric ligands.
- Preparation of solid samples and determination of their structures by means of X-ray diffraction. Of particular interest here is whether the introduction of substituents on the new ligands induces changes in the interstrand interactions or in the geometry of the coordination polyhedra of the lanthanide ions.
- Determination of the selectivity of the ligands towards a pair of different lanthanide ions by measurements of the speciation of complexes in CD_3CN solution by means of NMR spectroscopy.
- Determination of the thermodynamic parameters H and S for the *HHH*/*HHT* equilibrium from variable temperature NMR spectroscopy in order to better our understanding of the factors influencing the relative stabilities of the two isomers.
- Analysis of the lanthanide induced shift of paramagnetic complexes in solution. This includes extraction of structural information and comparison thereof with data obtained for other complexes in solution as well as with solid state structures. As part hereof an improved method is proposed which eliminate the effect of the variation of the crystal field parameter B_0^2 along the lanthanide series.

2 Ligand synthesis and characterisation

2.1 Ligand synthesis

The asymmetric ligands L^{AB}, L^{AB2}, L^{AB3}, L^{AB4} and L^{AB5} were synthesised using strategies developed for related symmetric ligands.[27,30,31] The syntheses are outlined in Scheme 1 - Scheme 7.

The two key reactions are the conversion of a carboxylic acid to an amide via an acid chloride intermediate (**6**, **8**, **16**, **18**, **22**, **24**, **29**, **31**, **32**, **33**, **34**, **35**, **36**, **37** and **38**) and a modified Phillips coupling to close the ring of a benzimidazole group (**9**, **19**, **25**, **30** and the final step of the syntheses of all five ligands).

The compounds **2**[74], **3**[75], **5**[76], **6**[32], **7**[32], **8**[32], **9**[32], **10**, **12**[31,77], **13**[31,77], **14**[78,79], **21**[31], **22**[31], **23**[31], **31**[80], **32** and L^{AB} were prepared according to published procedures, while **28** was synthesised by two different paths. The more direct route via **29** and **30** gave low yields since the ester function of **29** was partially hydrolysed during the reduction to **30**. Protecting with an amide function led to **25**, which proved impossible to hydrolyse directly to **28**. Instead **26** was obtained, which gave the desired product through the intermediate **27**.

The details are given in the experimental section (pages 307 ff.).

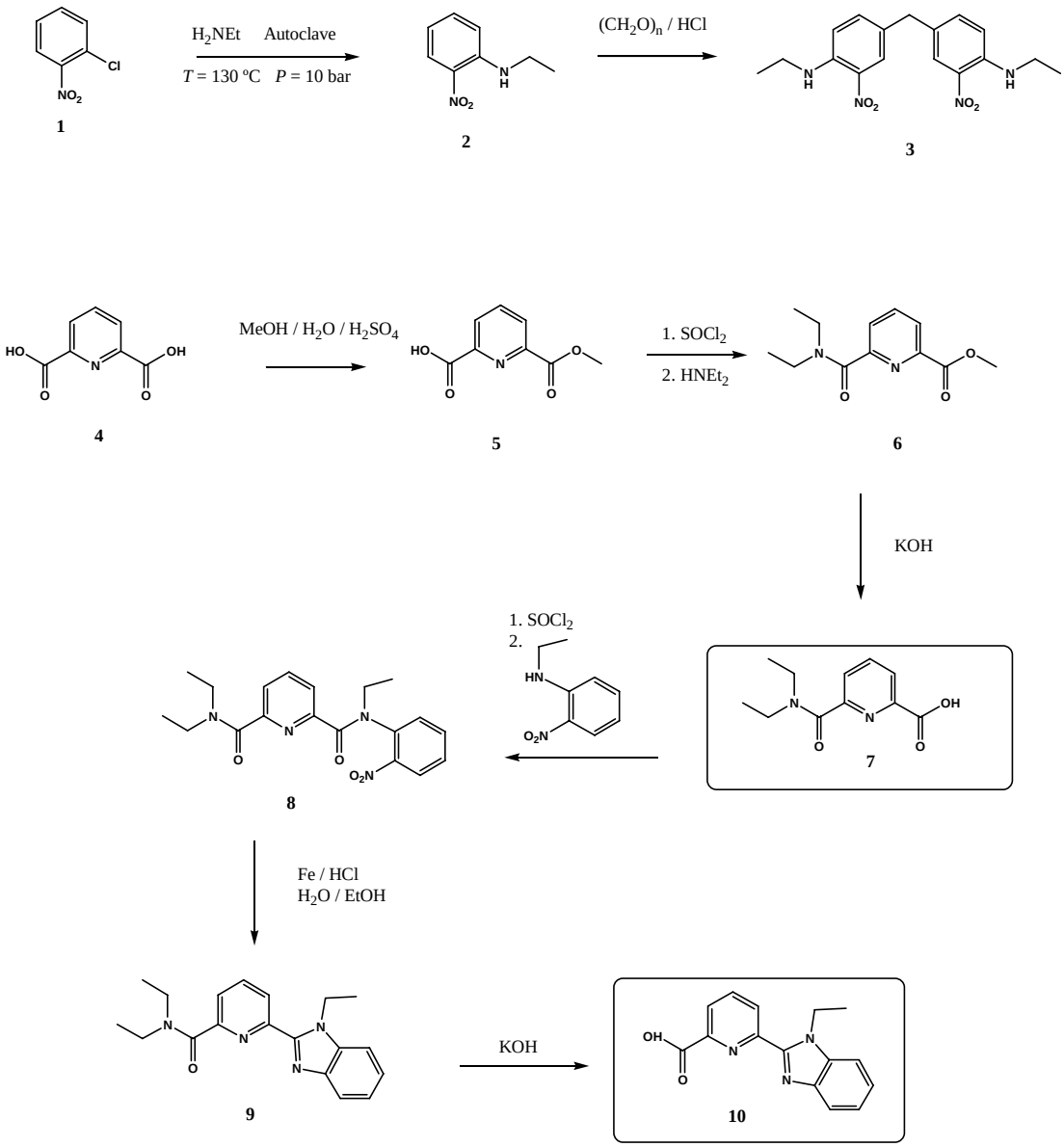

Scheme 1 Ligand synthesis: building blocks

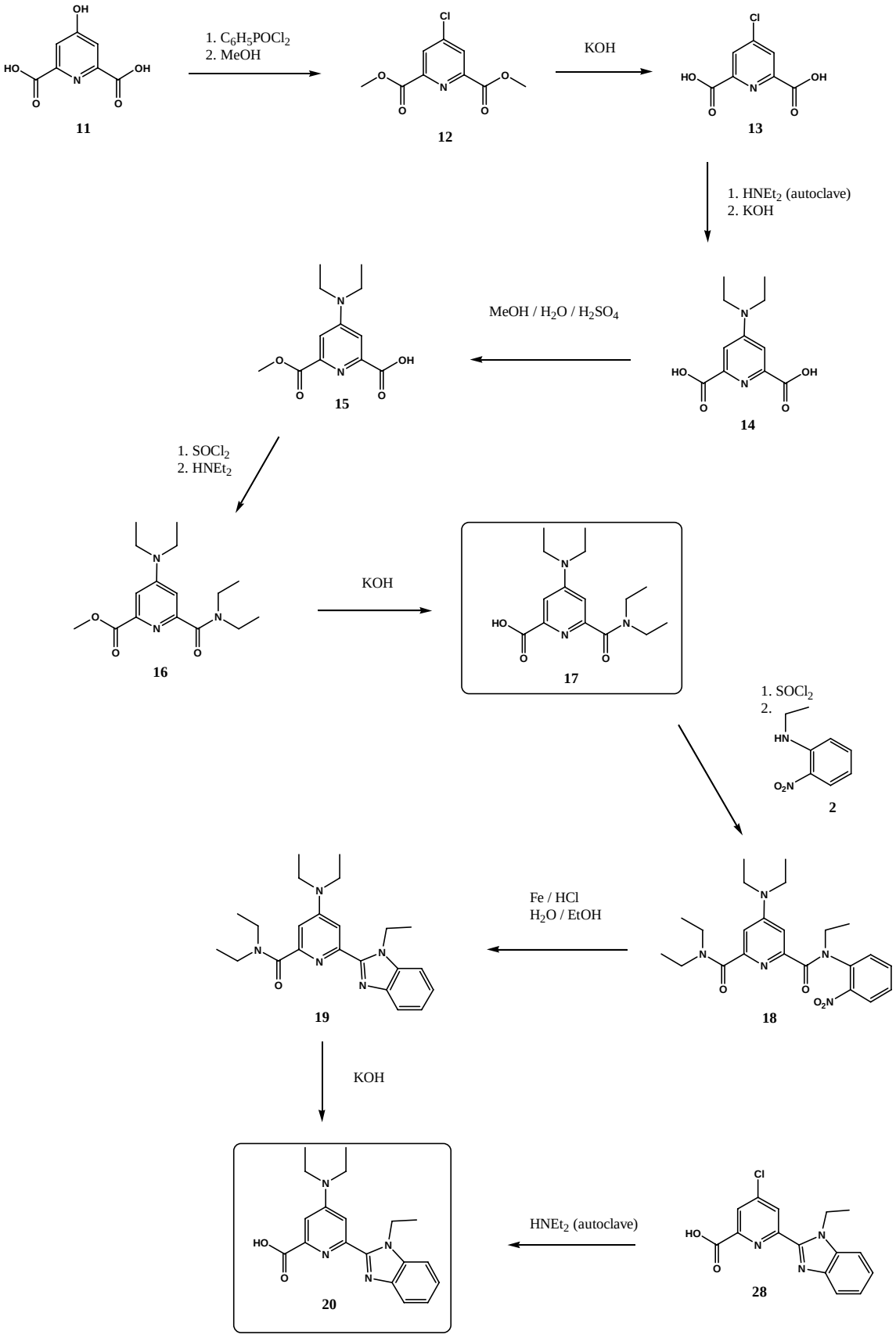

Scheme 2 Ligand synthesis: building blocks

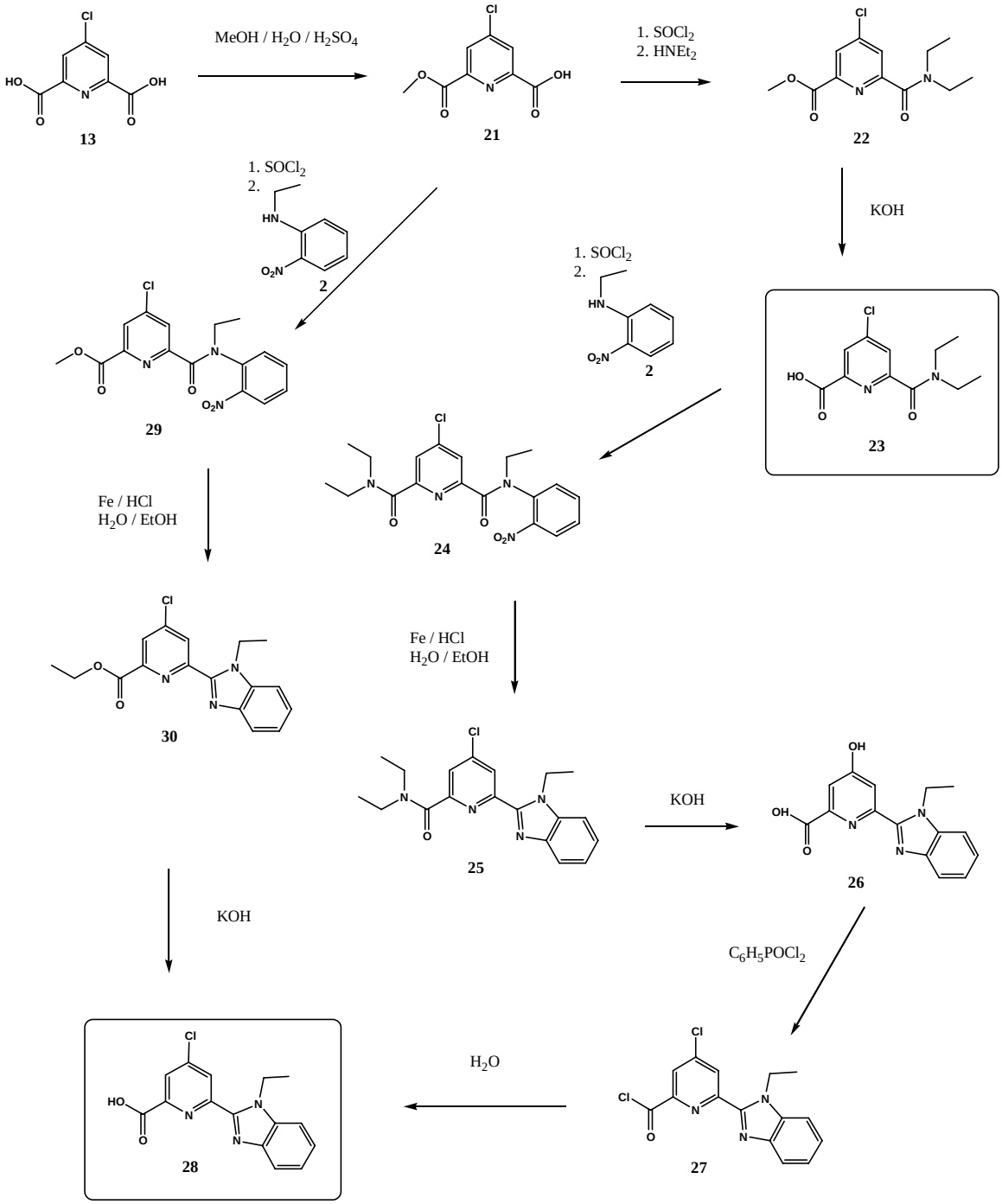

Scheme 3 Ligand synthesis: building blocks

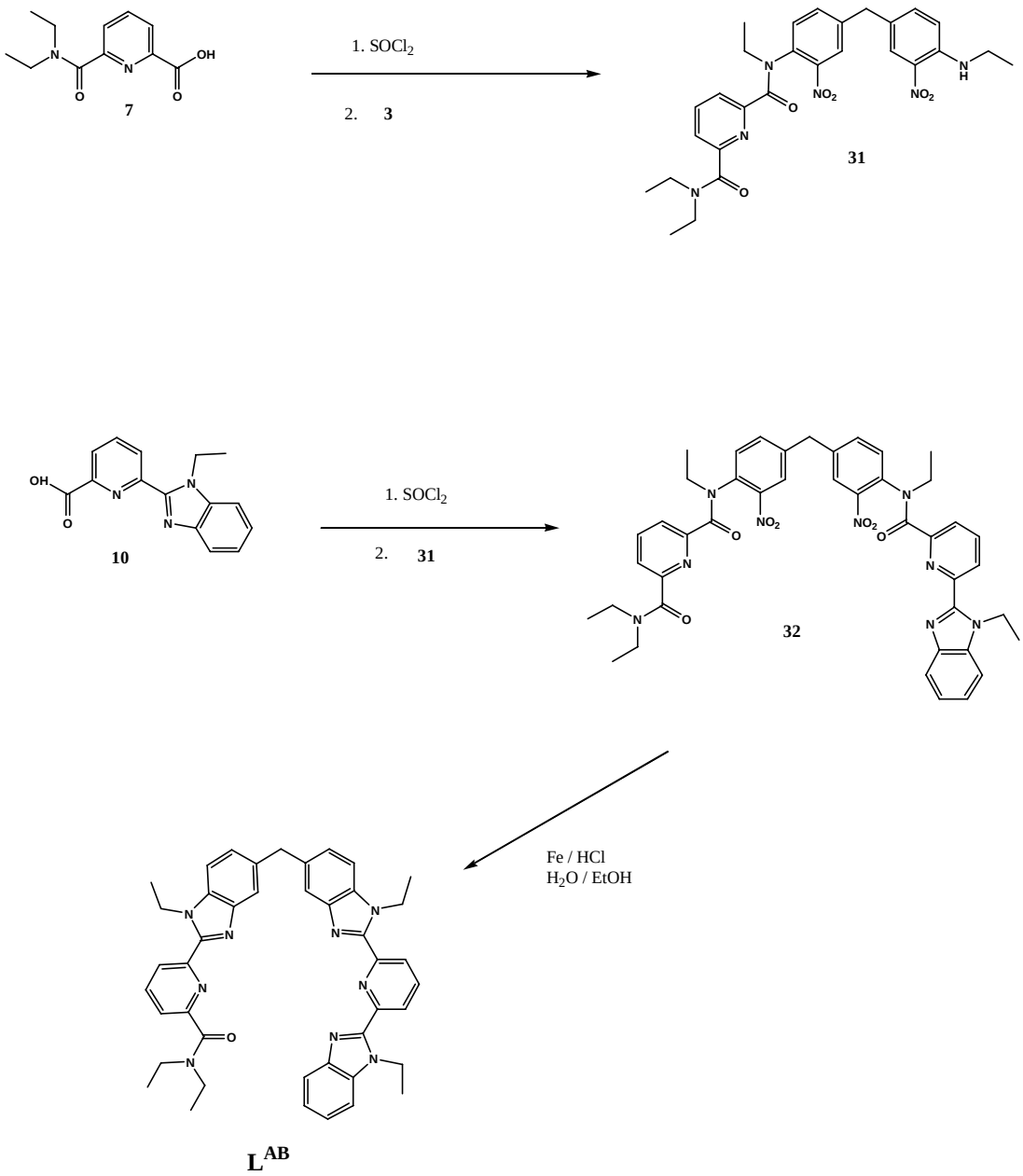

Scheme 4 Synthesis of L^{AB}

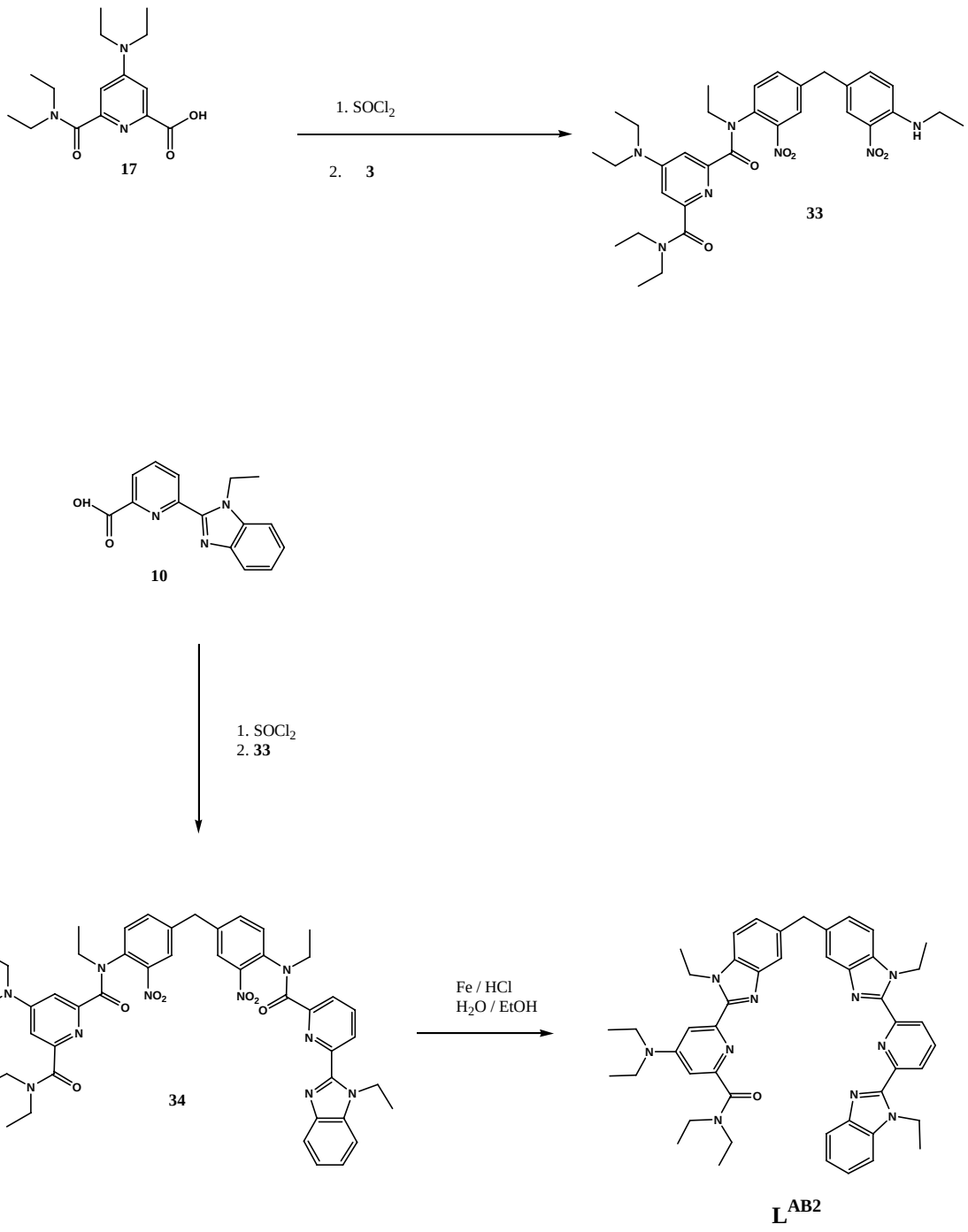

Scheme 5 Synthesis of L^{AB2}

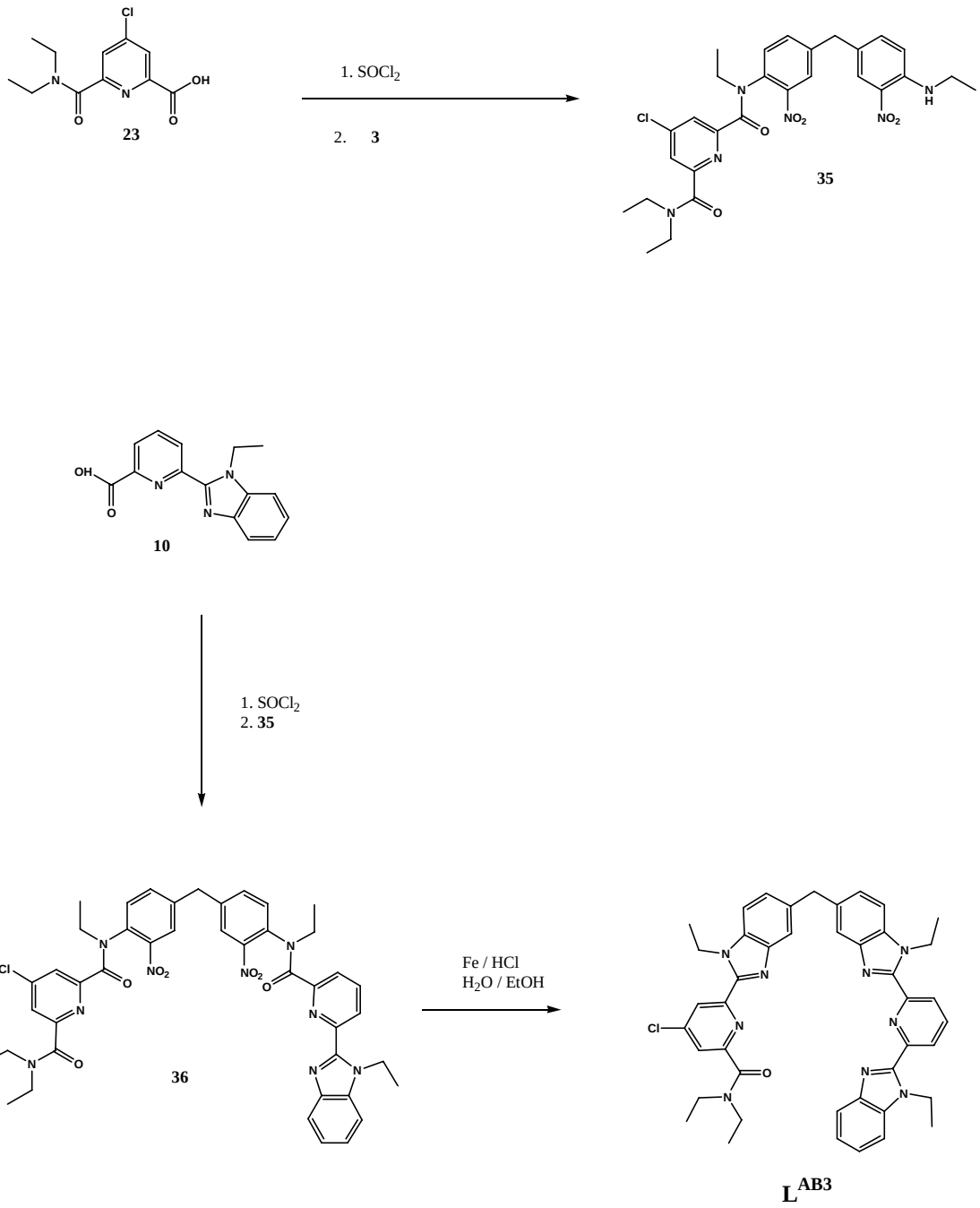

Scheme 6 Synthesis of L^{AB3}

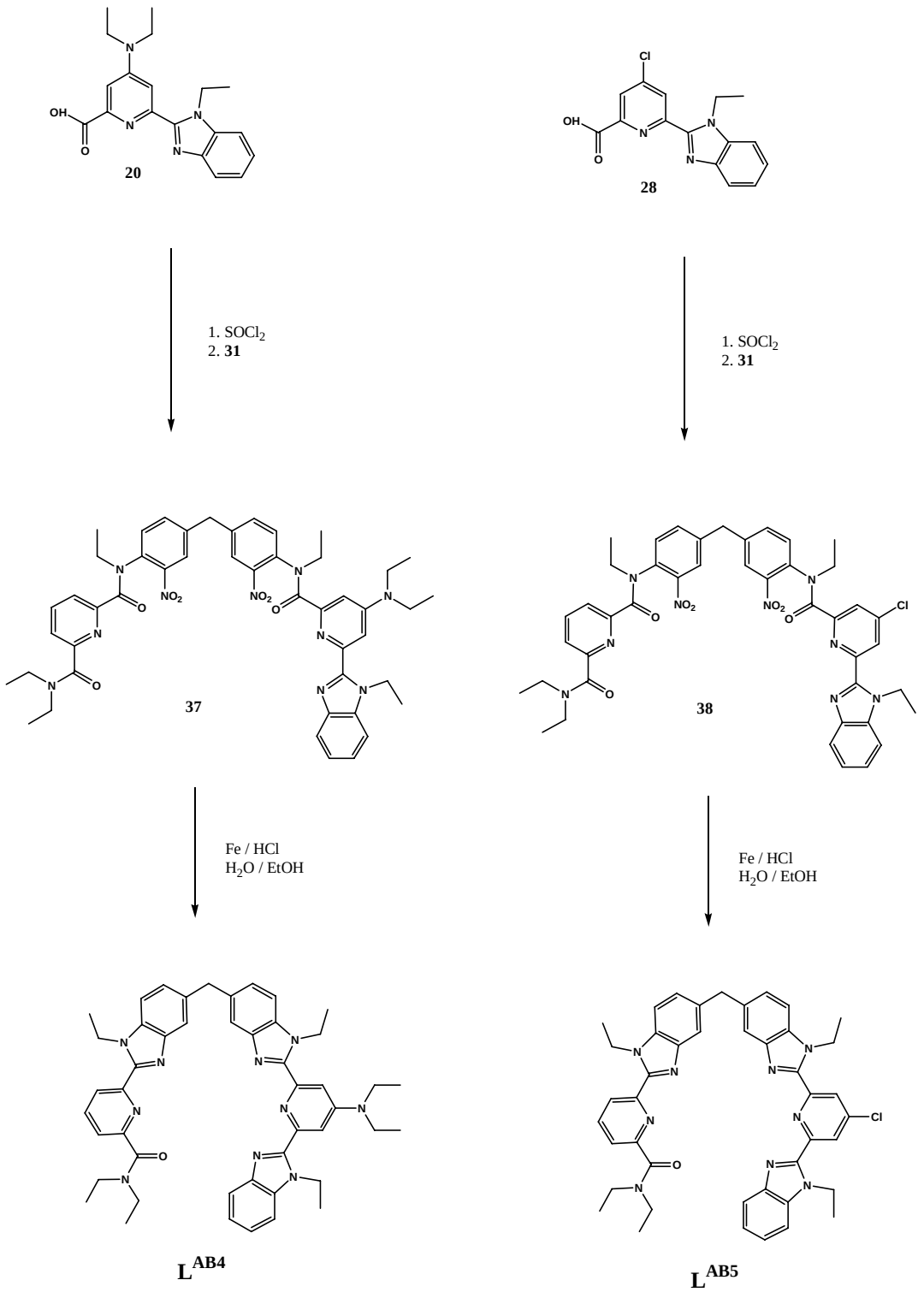

Scheme 7 Synthesis of L^{AB4} and L^{AB5}

2.2 Ligand characterisation in solution

^{1}H NMR spectra (1D, 2D COSY and 2D ROESY) of the free ligands L^{AB2}, L^{AB3}, L^{AB4} and L^{AB5} have been measured in $CDCl_3$ solution at 400 MHz. The 1D spectra are shown in Figure 2 - Figure 5.

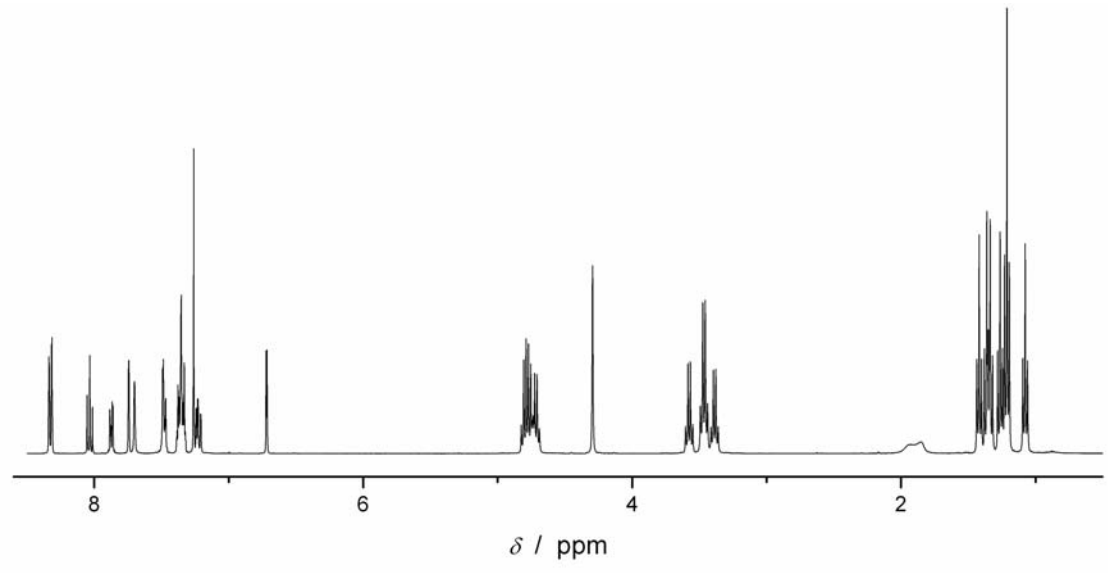

Figure 2 ^{1}H NMR spectrum of L^{AB2} in $CDCl_3$

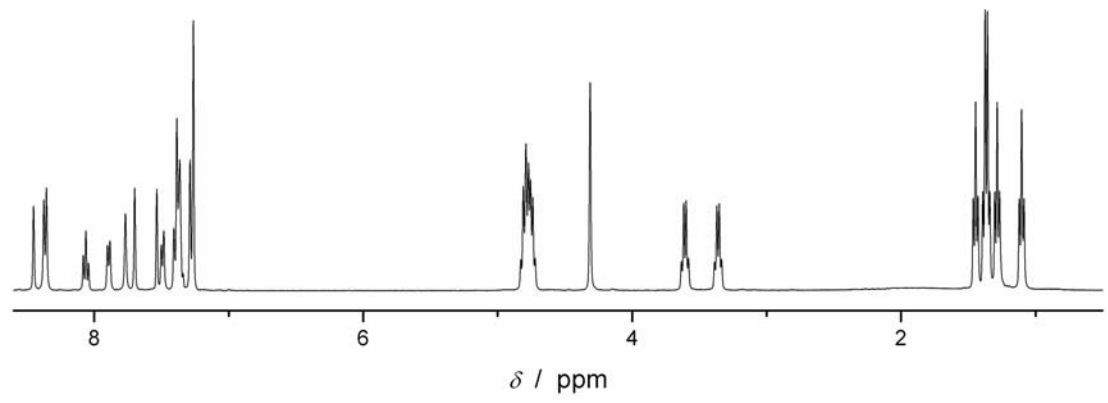

Figure 3 ^{1}H NMR spectrum of L^{AB3} in $CDCl_3$

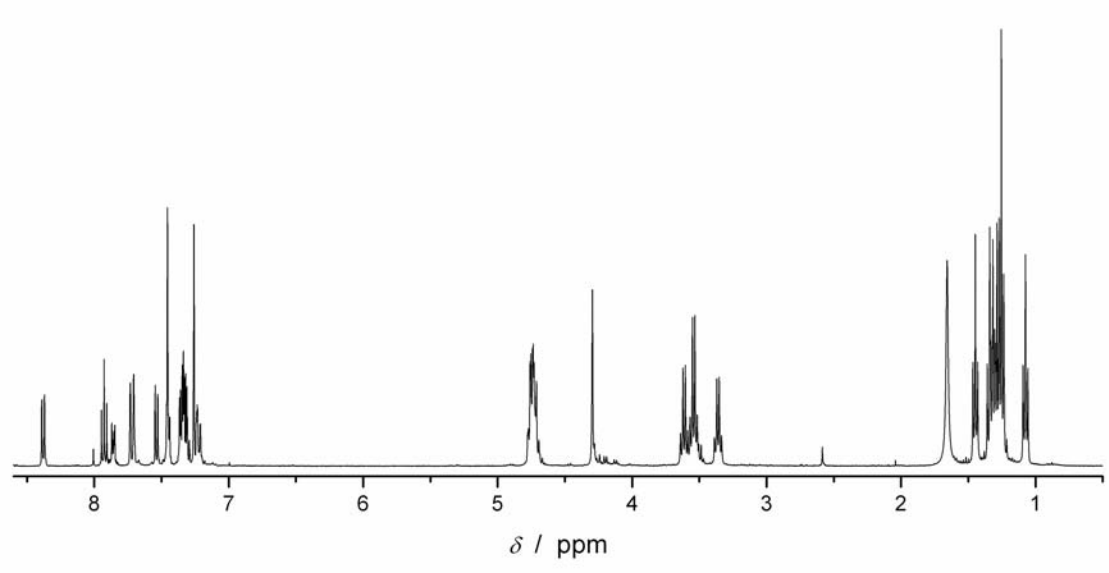

Figure 4 ^{1}H NMR spectrum of L^{AB4} in $CDCl_3$

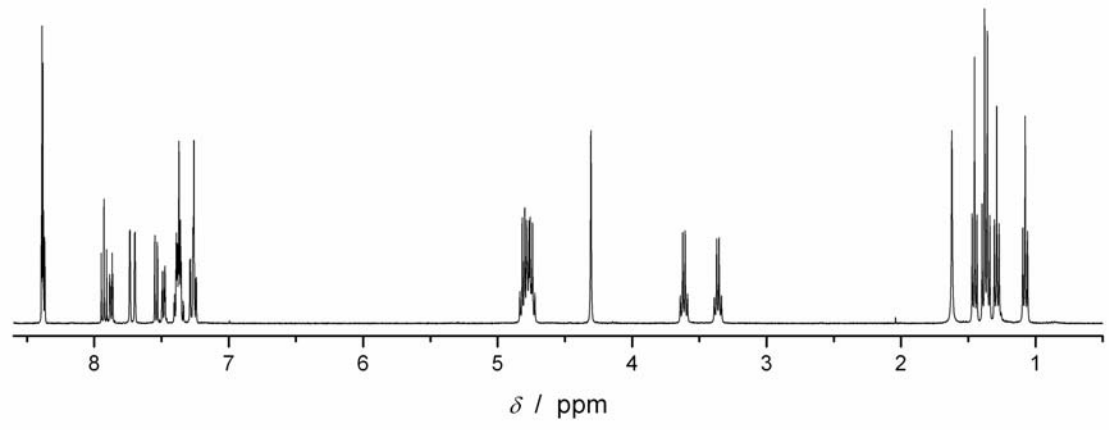

Figure 5 ^{1}H NMR spectrum of L^{AB5} in $CDCl_3$

The proton numbering of all five ligands is shown in Scheme 8 and the assignment of the spectra of the four new ligands is given in Table 1 - Table 4.

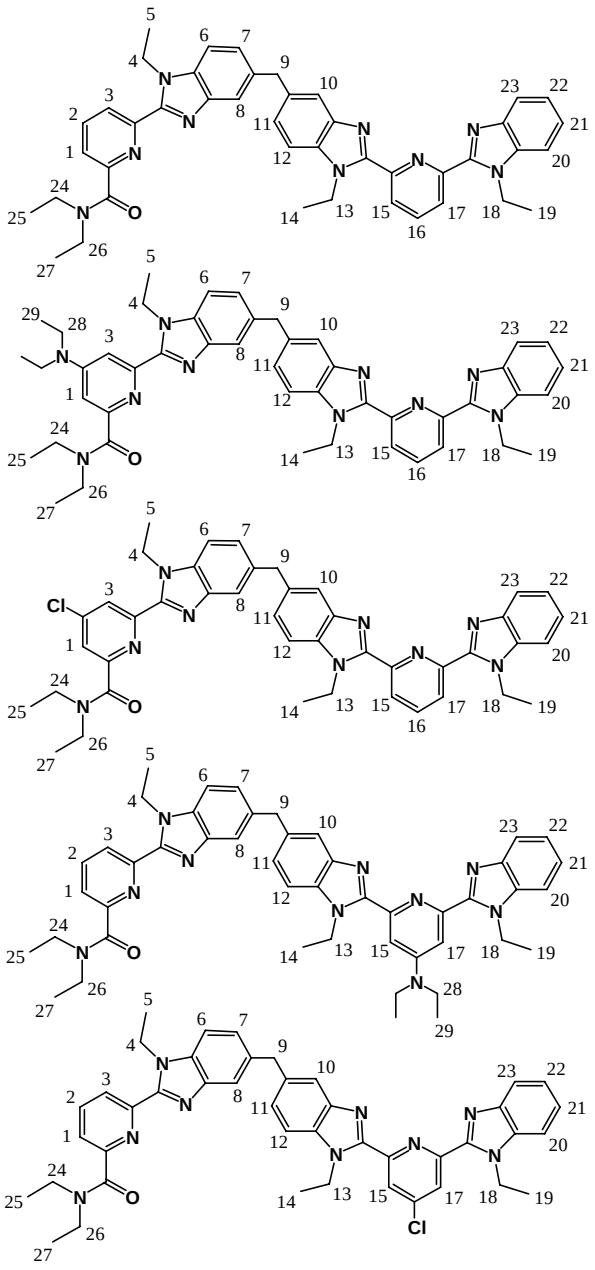

Chart 14 Proton numbering of the ligands

Table 1 ^{1}H NMR of L^{AB2} in $CDCl_3$

	15 and 17		16	23	8 and 10		1 or 3	20	6, 12, 21, 22		7 and 11		3 or 1
δ / ppm	8.33		8.03	7.87	7.74	7.70	7.49	7.48	7.32 – 7.38		7.24	7.22	6.72
	2 x dd 2H		t 1H	dd 1H	s 1H	s 1H	d 1H	dd 1H	m 4H		dd 1H	dd 1H	d 1H
J / Hz	7.8; 2.2		7.9	6.6; 2.0			2.2	6.1; 2.7			8.3; 1.6	8.3; 1.6	2.6
	9	18	4 or 13	13 or 4	24 or 26	28	26 or 24	19	5 and 14		25 or 27	29	27 or 25
δ / ppm	4.29	4.80	4.76	4.72	3.58	3.47	3.39	1.36	1.42	1.34	1.26	1.21	1.08
	s 2H	q 2H	q 2H	q 2H	q 2H	q 4H	q 2H	t 3H	t 3H	t 3H	t 3H	t 6H	t 3H
J / Hz		7.1	7.1	7.1	7.1	7.1	7.1	7.1	7.2	7.2	7.1	7.1	7.1

Table 2 ^{1}H NMR of L^{AB3} in $CDCl_3$

	3	15 and 17	16	23	8 and 10		1	20	6, 12, 21, 22	7 and 11
δ / ppm	8.45	8.37	8.06	7.89	7.77	7.70	7.53	7.49	7.33-7.42	7.28
	d 1H	d 2H	t 1H	dd 1H	s 1H	s 1H	d 1H	dd 1H	m 4H	d 2H
J / Hz	1.5	7.8	7.9	6.7; 1.7			2.0	6.1; 2.1		8.4
	18	13	4	9	24 and 26		5	19	14	25 and 27
δ / ppm	4.80	4.78	4.75	4.31	3.61	3.36	1.45	1.38	1.36	1.28	1.10
	q 1H	q 1H	q 1H	s 2H	q 2H	q 2H	t 3H	t 3H	t 3H	t 3H	t 3H
J / Hz	7.2	7.3	7.1		7.1	7.1	7.1	7.2	7.0	7.2	7.1

Table 3 ^{1}H NMR of L^{AB4} in $CDCl_3$

	1 or 3	2	23	8 and 10		3 or 1	15 and 17		20	6, 12, 21, 22		7 and 11	
δ / ppm	8.38	7.93	7.86	7.73	7.71	7.54	7.46	7.45	7.45	7.28 – 7.38		7.25	7.22
	dd 1H	t 1H	dd 1H	s 1H	s 1H	dd 1H	d 1H	d 1H	dd 1H	m 4H		dd 1H	dd 1H
J / Hz	8.1; 1.2	7.9	6.8; 2.2			7.8; 1.1	2.4	2.4	6.5; 1.3			8.3; 1.8	8.3; 1.8
	4, 13, 18		9	24 or 26	28	26 or 24	5	14 and 19		25 or 27	29	27 or 25	
δ / ppm	4.68 – 4.79		4.30	3.61	3.54	3.36	1.45	1.34	1.32	1.29	1.26	1.08	
	m 6H		s 2H	q 2H	q 4H	q 2H	t 3H	t 3H	t 3H	t 3H	t 6H	t 3H	
J / Hz				7.1	7.1	7.1	7.2	7.1	7.1	7.0	7.2	7.1	

Table 4 ^{1}H NMR of L^{AB5} in $CDCl_3$

	15 and 17		1 or 3	2	23	8 and 10		3 or 1	20	6, 12, 21, 22	7 or 11
δ / ppm	8.39	8.38	8.38	7.93	7.87	7.74	7.70	7.54	7.49	7.33 – 7.41	7.27
	d 1H	d 1H	dd 1H	t 1H	dd 1H	d 1H	d 1H	dd 1H	dd 1H	m 4H	dd 1H
J / Hz	1.9	1.9	8.2; 1.1	7.9	7.3; 2.0	1.3	1.3	7.7; 1.1	7.4; 1.8		8.6; 1.5
	11 or 7	18	13	4	9	24 and 26		5	19	14	25 and 27
δ / ppm	7.25	4.81	4.77	4.75	4.31	3.61	3.36	1.45	1.38	1.29	1.29	1.08
	dd 1H	q 2H	q 2H	q 2H	s 2H	q 2H	q 2H	t 3H	t 3H	t 3H	t 3H	t 3H
J / Hz	8.0; 1.5	7.2	7.2	7.1		7.1	7.1	7.1	7.2	7.2	7.1	7.1

The chemical shift values found are similar to those determined for L^{AB} (less than 0.05 ppm of difference) with the obvious exception of the protons of the substituted pyridine moiety.

NOE signals are observed between H24 and H26, H25 and H26, H24 and H27, H25 and H27, H4 and H6, H12 and H13, H18 and H20. The NOE signals observed between the hydrogens of the bridging methylene group (H9) and all neighbouring benzimidazole hydrogens (H7, H8, H10 and H11) are indicative of free rotation about the methylene group. The absence of signals between pyridine hydrogens (H1, H3, H15 and H17) and ethyl groups (e.g. H4, H5, H24 and H25) indicate that the nitrogen atoms of the pyridine groups are oriented in a *transoid* fashion with respect to the other potentially ligating atoms as indicated in Chart 15. The same kind of structure (free rotation around the central CH_2 group and *transoid* conformation of the pyridine N atoms with respect to the neighbouring pair of potential ligator atoms) has also been observed for other ligands of this type (L^{AB}, L^{AC}, L^{BC} [80] and L^{G} [81]).

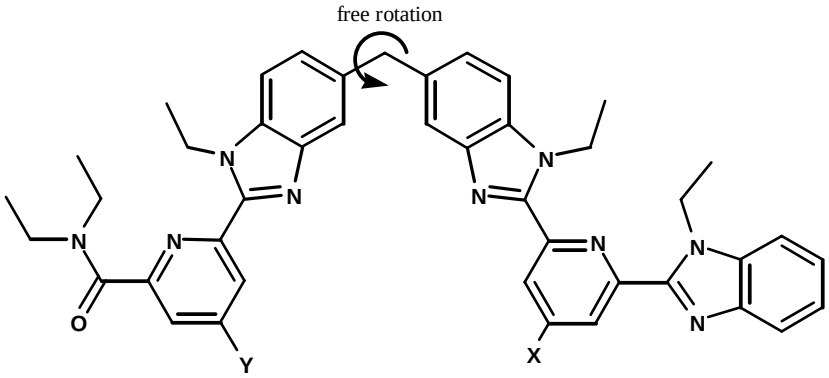

Chart 15 Solution structure of the ligands

3 Isolation and structure of the helicates

3.1 Isolation of the complexes

Solid samples of homobimetallic complexes have been synthesised by reacting a weighed amount of ligand (5-15 mg) with 2/3 equivalents of $Ln(ClO_4)_3$ in acetonitrile solution. After evaporation of the solvent the complexes were redisolved in CH_3CN:CH_3CH_2CN (1:1) and precipitated by slow diffusion of ^{t}BuOMe (see Experimental section; page 325).

Despite numerous crystallisation experiments having been carried out with complexes of all the four new ligands the only samples to yield crystals of sufficient quality for X-ray diffraction were the Ce_2, Pr_2, Sm_2, PrLu and NdLu *HHH* helicates* with L^{AB3} in addition to the complexes with L^{AB} already reported.[80] In particular, we were unable to crystallise a *HHT* complex.

3.2 X-ray structural investigation

The complexes, of general formula $[LnLn'(L^{AB3})_3](ClO_4)_6 \cdot xCH_3CN \cdot yCH_3CH_2CN$, crystallised with different content of solvent molecules: Ce_2 (x = 5; y = 2), Pr_2 (x = 6; y = 4), PrLu (x = 7; y = 3), NdLu (x = 5; y = 2) and Sm_2 (x = 5; y = 2).

The crystallographic data are given in Table 5 and Table 6.

* In the following LnLn' or $LnLn'(L)_3$ signifies (depending on the context) $[LnLn'(L)_3]^{6+}$ or $[LnLn'(L)_3](ClO_4)_6$. In this notation Ln is coordinated by the bpb unit of the ligand and Ln' by bpa one.

Table 5 Crystallographic data for $[LnLn'(L^{AB3})_3](ClO_4)_6 \cdot x\ CH_3CN \cdot y\ CH_3CH_2CN$

	Ce_2	Pr_2	PrLu
x; y	5; 2	6; 4	7; 3
formula	$C_{145}\ H_{151}\ Ce_2\ Cl_9\ N_{34}\ O_{27}$	$C_{153}\ H_{164}\ Cl_9\ N_{37}\ O_{27}\ Pr_2$	$C_{152}\ H_{162}\ Cl_9\ Lu\ N_{37}\ O_{27}\ Pr$
mol weight	3401.29	3554.08	3574.12
temp (K)	140(2)	140(2)	140(2)
crystal system	monoclinic	triclinic	triclinic
space group	$P\ 2_1/n$	P	P
a (Å)	30.819(10)	15.0272(13)	15.0634(11)
b (Å)	15.113(2)	19.214(2)	19.3270(18)
c (Å)	34.771(11)	30.105(2)	30.237(2)
α (°)	90	103.87(1)	104.10(1)
β (°)	109.79(3)	101.42(1)	100.84(1)
γ (°)	90	95.75(1)	96.22(1)
V ($Å^3$)	15238.71(700)	8171.42(130)	8274.88(110)
F(000)	6976	3656	3664
Z	4	2	2
D_c ($Mg \cdot m^{-3}$)	1.482	1.444	1.434
μ(Mo Kα) (mm^{-1})	0.830	0.817	1.108
crystal size (mm)	0.35×0.31×0.15	0.30×0.19×0.15	0.30×0.19×0.15
reflections measured	81966	48975	49646
unique reflections	25902	25306	25563
no. of parameters	1901	1839	1880
constraints	679	687	680
GoF on F^2 [b]	0.927	0.796	0.854
R1 [$I > 2\sigma(I)$] [a]	0.1175	0.0816	0.0787
wR2 [a]	0.3923	0.2346	0.2317

[a] $R = \Sigma| |F_o| - |F_c| |/\Sigma|F_o|$, $wR2 = \{\Sigma [w(F_o^2-F_c^2)^2]/ \Sigma [w(F_o^2)^2]\}^{1/2}$; [b] GoF = $\{\Sigma [w(F_o^2-F_c^2)^2]/(n-p)\}^{1/2}$

Table 6 Crystallographic data for $[LnLn'(L^{AB3})_3](ClO_4)_6 \cdot x\ CH_3CN \cdot y\ CH_3CH_2CN$

	NdLu	Sm_2
x; y	5; 2	5; 2
formula	$C_{145}H_{151}Cl_9LuN_{34}\ NdO_{27}$	$C_{145}\ H_{151}\ Cl_9\ N_{34}\ O_{27}\ Sm_2$
mol weight	3440.26	3421.75
temp (K)	140(2)	140(2)
crystal system	monoclinic	monoclinic
space group	P 2_1/n	P 2_1/n
a (Å)	30.992(3)	31.0945(17)
b (Å)	15.0821(9)	15.0822(7)
c (Å)	34.666(3)	34.758(2)
α (°)	90	90
β (°)	109.251(7)	109.264(5)
γ (°)	90	90
V (Å^3)	15297(2)	15388.0(14)
F(000)	7036	7008
Z	4	4
D_c (Mg·m^{-3})	1.494	1.477
μ(Mo Kα) (mm^{-1})	1.216	0.993
crystal size (mm)	0.35×0.31×0.15	0.35×0.31×0.15
reflections measured	87058	86796
unique reflections	25615	26082
no. of parameters	1883	1901
constraints	679	679
GoF on F^2 [b]	0.878	0.996
R1 [$I > 2\sigma(I)$] [a]	0.0933	0.1013
wR2 [a]	0.3022	0.3376

The structures (Figure 6) consist of isolated helical *HHH*-$[LnLn'(L^{AB3})_3]^{6+}$ molecular ions formed by two lanthanide ions and three ligand strands, perchlorate counter ions and solvent molecules (acetonitrile and propionitrile). No particular features were observed in the solvent molecules or counter ions apart from some disorder. The triclinic and monoclinic structures differ only slightly in the packing of the molecules. The molecular ions (Figure 7 and Figure 8) are similar in overall structure to the structures already reported for the L^{AB} complexes.[80] They are present in the unit cell as a racemic mixture of the two *P* and *M* enantiomers (right- and left-handed screw).

In the Pr_2 complex two methyl groups (C127 and C129 – corresponding to H25 and H27 in the NMR data) of one of the carboxamide groups are disordered.

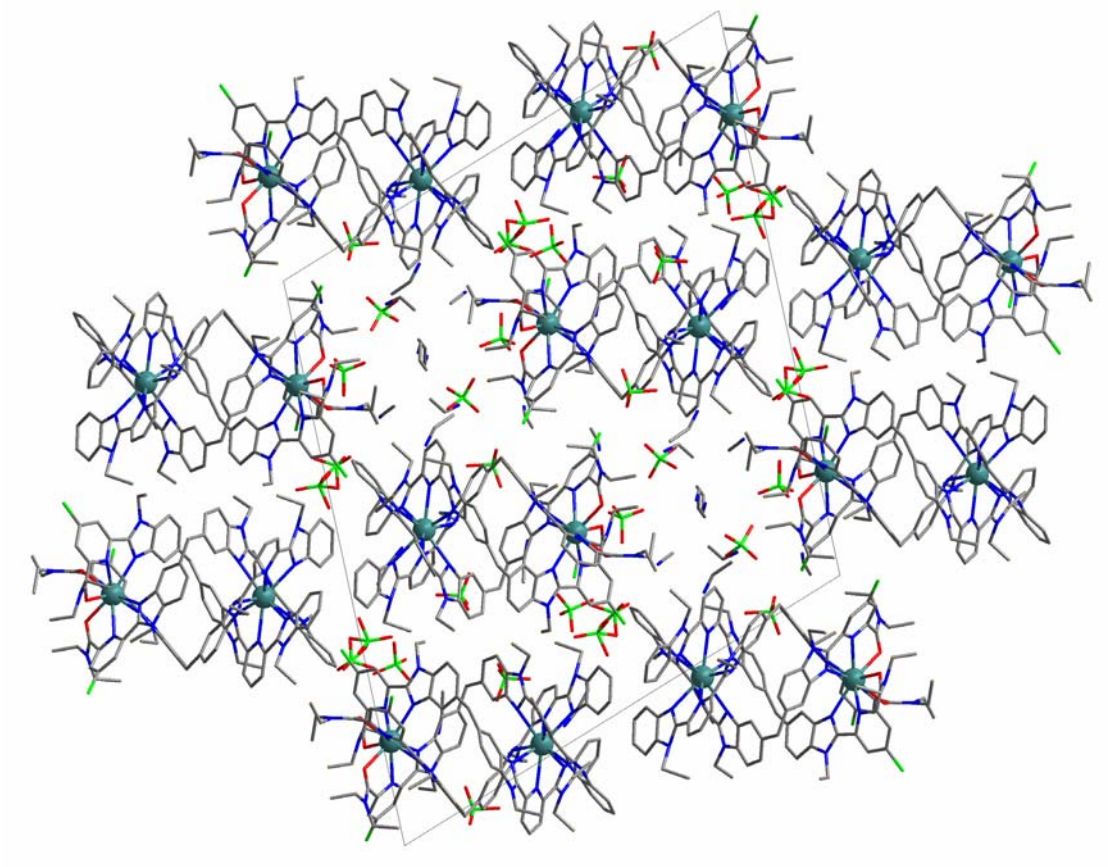

Figure 6 Structure of $[Ce_2(L^{AB3})_3](ClO_4)_6 \cdot 5CH_3CN \cdot 2CH_3CH_2CN$ viewed along the *b* axis

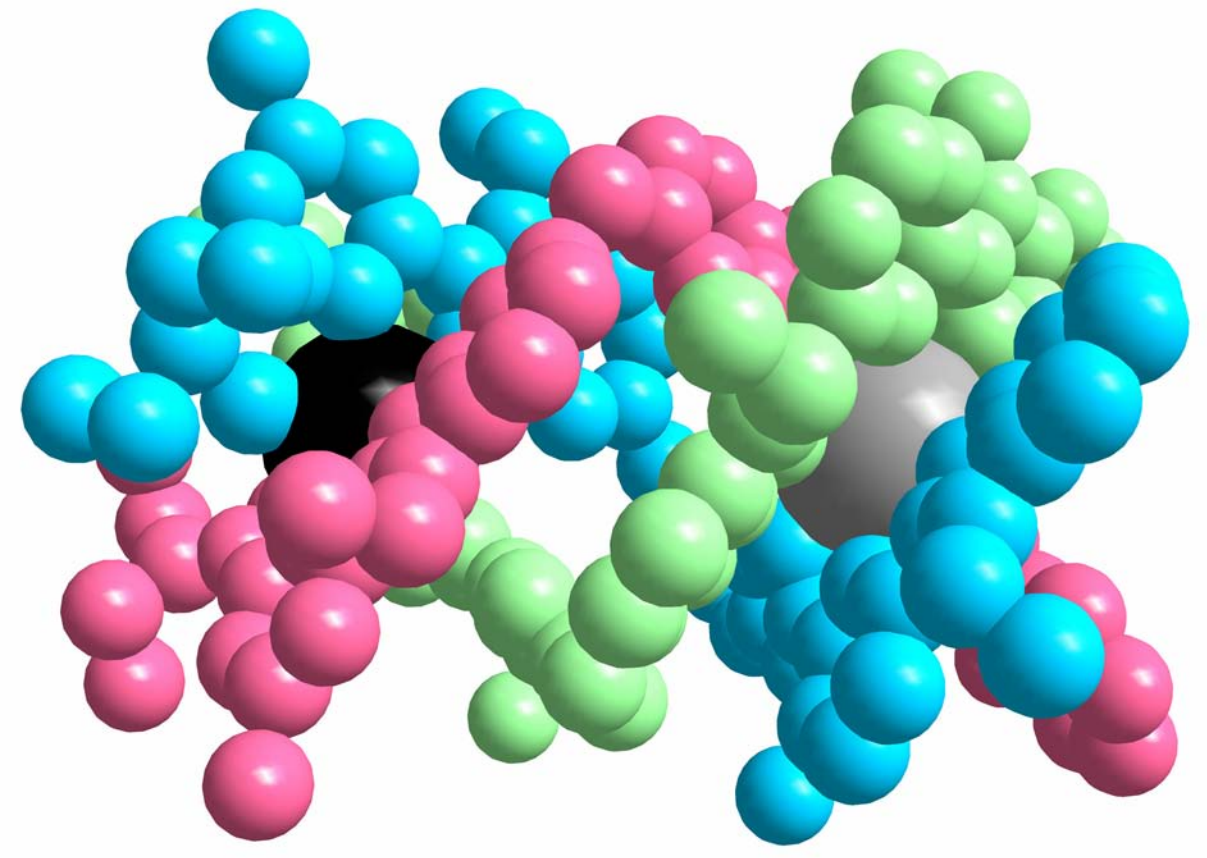

Figure 7 Structure of the $[NdLu(L^{AB3})_3]^{6+}$ molecular ion.

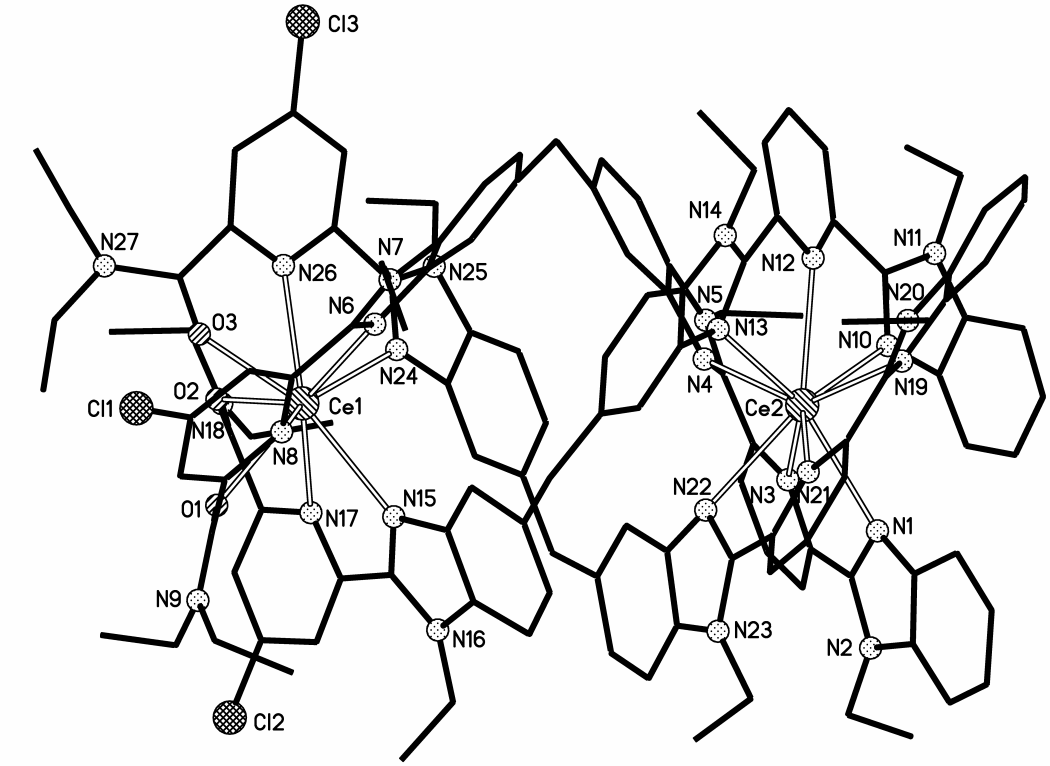

Figure 8 Structure of the $[Ce_2(L^{AB3})_3]^{6+}$ molecular ion with partial atom numbering scheme.

3.3 Assignment of Ln and Ln' in the bpb and bpa cavities

The structures of the heterobimetallic PrLu and NdLu complexes have been solved under the assumption that the smallest of the two lanthanide ions (Lu in both cases) is coordinated by the bpa (*benzimidazole-pyridine-carboxamide*) moiety of the ligand and the largest lanthanide ion (Pr or Nd) is coordinated by the bpb (*benzimidazole-pyridine-benzimidazole*) moiety.

For the PrLu compound 4 different models have been tried in order to check if this assumption is valid. The models Pr(bpb)Pr(bpa), Lu(bpb)Lu(bpa), Lu(bpb)Pr(bpa) and Pr(bpb)Lu(bpa) give the R1 values 0.0816, 0.0853, 0.0943 and 0.0787, respectively. This proves, as it was also done for the L^{AB} complexes, that the assignment of the Pr and Lu in the two coordination cavities is correct.

This approach is, however, too simple to take into account partial occupancies of the two coordination sites. NMR studies in CD_3CN showed that the PrLu solution contains 88 % PrLu, 8 % Pr_2 and 4 % Lu_2 (Chapter 4.2; page 64). It would be reasonable to assume that a similar composition would be found in the solid state. Attempts to refine the crystal structure with the occupancies treated as variables did unfortunately not lead to better R1 factors due to the relative low quality of the crystal in combination with the very large number of variables. To better ascertain the heterometallic model, we have turned to a careful analysis of the Ln-X bond lengths.

3.4 Ln(III)-ligand distances

Distances from the lanthanide ions to the coordinating nitrogen and oxygen atoms are given in Table 7 and Table 8 with values calculated for the L^{AB} complexes given for comparison.

Table 7 Ln-N distances (Å) in the benzimidazole-pyridine-benzimidazole moiety of L^{AB3} and L^{AB} complexes.

	Terminal benzimidazole		average	Pyridine		average	Bridging benzimidazole		average
L^{AB3} complexes									
Ce	N1	2.68(3)		N3	2.69(3)		N4	2.62(1)	
Ce_2	N10	2.63(3)	2.66(3)	N12	2.68(1)	2.679(8)	N13	2.62(3)	2.63(1)
	N19	2.68(2)		N21	2.67(1)		N22	2.64(2)	
Pr	N1	2.65(1)		N3	2.66(2)		N4	2.64(2)	
Pr_2	N10	2.62(2)	2.62(4)	N12	2.61(2)	2.64(3)	N13	2.68(2)	2.62(8)
	N19	2.58(1)		N21	2.65(2)		N22	2.53(1)	
Pr	N1	2.63(1)		N3	2.64(1)		N4	2.63(1)	
PrLu	N10	2.63(1)	2.627(5)	N12	2.63(1)	2.637(5)	N13	2.66(1)	2.62(6)
	N19	2.62(1)		N21	2.64(2)		N22	2.55(1)	
Nd	N1	2.63(1)		N3	2.67(1)		N4	2.60(1)	
NdLu	N10	2.59(1)	2.63(3)	N12	2.61(1)	2.64(3)	N13	2.59(1)	2.60(1)
	N19	2.65(1)		N21	2.64(1)		N22	2.61(1)	
Sm	N1	2.598(9)		N3	2.60(1)		N4	2.621(9)	
Sm_2	N10	2.612(9)	2.62(2)	N12	2.632(9)	2.60(3)	N13	2.585(9)	2.60(2)
	N19	2.65(1)		N21	2.579(9)		N22	2.592(8)	
L^{AB} complexes[80]									
La LaEu			2.65(2)			2.65(2)			2.64(3)
La LaTb			2.67(4)			2.64(1)			2.64(3)
Pr PrEr			2.62(2)			2.65(3)			2.63(4)
Pr PrLu			2.60(2)			2.62(5)			2.64(5)
Eu Eu_2			2.60(4)			2.58(5)			2.60(7)

Table 8 Ln-N and Ln-O distances (Å) in the benzimidazole-pyridine-carboxamide moiety of L^{AB3} and L^{AB} complexes.

	Bridging benzimidazole			Pyridine			Carboxamide		
			average			average			average
L^{AB3} complexes									
Ce	N6	2.64(3)		N8	2.61(1)		O1	2.47(2)	
Ce_2	N15	2.68(3)	2.66(2)	N17	2.70(2)	2.66(4)	O2	2.48(2)	2.46(2)
	N24	2.65(3)		N26	2.66(1)		O3	2.44 (4)	
Pr	N6	2.70(2)		N8	2.69(2)		O1	2.48(1)	
Pr_2	N15	2.60(1)	2.63(6)	N17	2.68(2)	2.67(2)	O2	2.47(1)	2.45(4)
	N24	2.59(2)		N26	2.65(2)		O3	2.41(1)	
Lu	N6	2.60(1)		N8	2.63(2)		O1	2.40(1)	
PrLu	N15	2.54(1)	2.56(3)	N17	2.58(1)	2.59(4)	O2	2.35(1)	2.35(5)
	N24	2.55(1)		N26	2.55(1)		O3	2.31(1)	
Lu	N6	2.59(1)		N8	2.58(1)		O1	2.40(1)	
NdLu	N15	2.62(1)	2.59(2)	N17	2.61(1)	2.57(5)	O2	2.37(1)	2.37(3)
	N24	2.57(1)		N26	2.52(1)		O3	2.34(1)	
Sm	N6	2.63(1)		N8	2.566(9)		O1	2.418(8)	
Sm_2	N15	2.620(9)	2.62(2)	N17	2.64(1)	2.60(4)	O2	2.410(8)	2.40(2)
	N24	2.597(9)		N26	2.59(1)		O3	2.382(8)	
L^{AB} complexes[80]									
Eu LaEu			2.59(1)			2.62(1)			2.40(2)
Eu Eu_2			2.59(4)			2.615(7)			2.401(6)
Tb LaTb			2.53(2)			2.57(2)			2.35(2)
Er PrEr			2.49(3)			2.52(6)			2.29(2)
Lu PrLu			2.46(1)			2.55(4)			2.31(3)

Standard deviation of the average defined as $[\Sigma_i(d_{average}-d_i)^2]/(n-1)]^{1/2}$ with $n = 3$.

In the bpb (benzimidazole-pyridine-benzimidazole) unit the bond lengths vary as expected (Ce bonds longest, Sm bonds shortest). In the two Pr containing complexes the bond lengths are the same within 0.02 Å. All bpb bond lengths in the Pr complexes are very similar (± 0.03 Å) to those found for the L^{AB} complexes. This is in line with the bpb unit being identical in the two ligands. The measured bond lengths also support the assignment of the PrLu and NdLu complexes with the Pr or Nd ion in the bpb site and the Lu ion in the bpa site.

In the bpa (benzimidazole-pyridine-carboxamide) unit the relative Ln-X distances of the Ce, Pr and Sm containing complexes again follow the usual trend of lanthanide ion sizes. There are no L^{AB} complexes with lanthanide ions larger than Eu(III) available for direct comparison,

but the Ln-X distances are as expected longer in these three complexes than in the L^{AB} complexes.

The bpa bond lengths in the two Lu containing complexes (PrLu and NdLu) are longer than expected based on the bond lengths in the other complexes, both of L^{AB} and L^{AB3}. Since the only difference between the two ligands is a Cl substituent in the *para* position of the pyridyl group of the bpa moiety this is not surprising. The expected softening of the nitrogen donor atom would indeed lead to an increase of the bond length in the complexes with the hard lanthanide ions. Note also that increased bond lengths are observed for all nine donor atoms in the bpa unit, not only for the three pyridyl nitrogen atoms. This indicates that the Cl substituent leads to a larger structural distortion of the complex than a mere expansion of the Ln(III)-N(pyridyl) bond. An alternative explanation could be that the two LnLu complexes (Ln = Pr or Nd) are contaminated with LnLn complexes in which the bpa site is occupied by the larger Ln ion. As mentioned earlier such a partial occupancy would not be unreasonable, but could not be determined directly from the refinement of the crystal structures due to the low quality of the crystals.

3.5 Coordination polyhedra – angles

The coordination polyhedra around the two lanthanide ions can best be described as slightly distorted tricapped trigonal prisms. The two prisms are defined by the six coordinating benzimidazole nitrogen atoms (bpb site) or by three benzimidazole nitrogen atoms and the three oxygen atoms of the carboxamide groups (bpa site). In both cases three pyridyl nitrogen atoms cap the prisms.

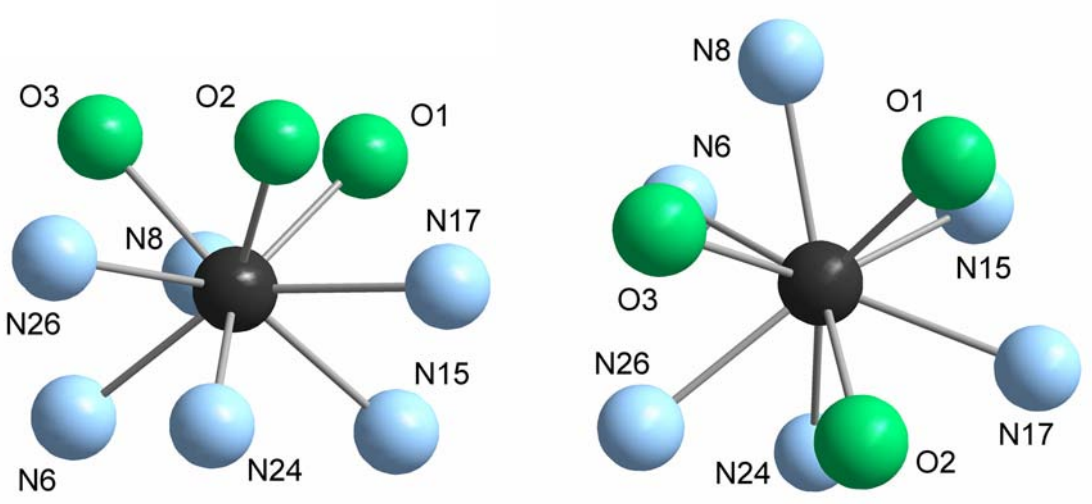

Figure 9 Two views of the bpa unit in the $Ce_2(L^{AB3})_3$ complex

Table 9 Definition of planes in the coordination polyhedra

Name	Atom numbers	Description	Coordination unit
P1	O1, O2, O3	Carboxamide oxygen	bpa
P2	N8, N17, N26	Pyridyl nitrogen	
P3	N6, N15, N24	Bridging benzimidazole nitrogen	
P4	N4, N13, N22	Bridging benzimidazole nitrogen	bpb
P5	N3, N12, N21	Pyridyl nitrogen	
P6	N1, N10, N19	Terminal benzimidazole nitrogen	

Angles describing the coordination polyhedra were calculated following a procedure previously employed for the analysis of complexes of L^{AB} and L^{C}.[80,32]

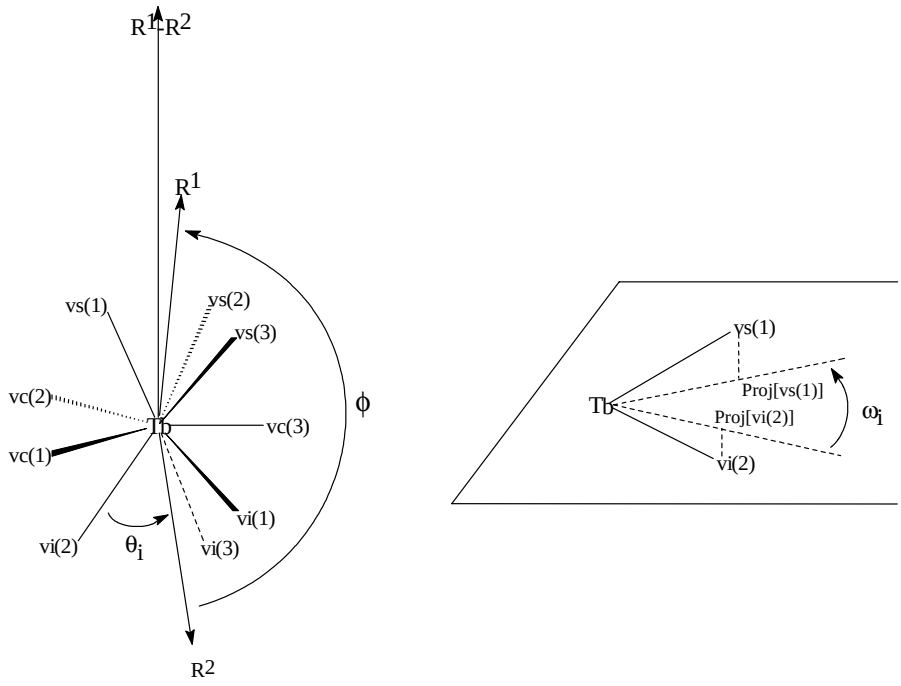

Figure 10 Definition of angles in the coordination polyhedra

Figure 10 illustrates the angles calculated. The vectors vs(n), vc(n) and vi(n) are vectors from the lanthanide ion to the coordinating atoms where s, c and i mean *supérieur* (upper), *cappant* (capping) and *inférieur* (lower), respectively and n (= 1, 2 or 3) numbers the ligand strands. The vector R1 is the sum of vs(1), vs(2) and vs(3) and passes through the midpoint of the triangle defined by the three upper coordinating atoms. A similar relationship holds for R2 and vi(1), vi(2) and vi(3). R1-R2 is the difference between the two vectors and is equal to a vector between the two midpoints of the upper and lower coordination triangles – it is also equal to the pseudo C_3 axis of the prism. The projection vector Proj[vs(1)] is the projection of

vs(1) onto a plane perpendicular to (R1-R2) and similarly for the other eight projection vectors.

The angle Φ is the angle between R1 and R2. The θ angles are between the vs(n) vectors and R1 and between the vi(n) vectors and R2 and describe the elongation of the prism. The angles ω are the angles between pairs of projection vectors and describe the twist of the prism. The angles α and β are the angles between planes and the angles between a plane and a plane normal to the molecular (Ln-Ln') axis, respectively. Distances between planes are calculated as distances between midpoints of the coordinating triangles.

All angles have been compared to the values calculated for a perfect tricapped prism as well as to values calculated for lanthanide complexes of L^{AB}. All calculations of the L^{AB} complexes have been redone using the published .cif files yielding results that are very similar (but not identical) to the values published, which were not calculated from the .cif files of the final refinement.[80]

Note that the angle α between the upper and lower coordination triangle cannot be determined from the angle Φ (the latter depends on the position of the lanthanide ion whereas the former does not). Unfortunately, it appears that this error has been made in the analysis of the L^{AB} complexes.[80]

Table 10 Angles (º) and distances (Å) in the benzimidazole-pyridine-carboxamide coordination polyhedron of L^{AB3} and L^{AB} complexes

	Φ	θ(P1) θ(P3)	ω (P1-P3) interstrand ω(P1-P2) intrastrand	α P1-P2 P1-P3 P2-P3	β P1 P2 P3	Distances P1 - P2 P2 - P3	Distances Ln – P1 Ln – P2 Ln – P3
L^{AB3} complexes							
Ce Ce_2	178.4	47(1) 54(1)	15(1) 56(2)	1.0 2.6 2.0	6.8 7.3 6.7	1.491 1.768	1.679 0.189 1.578
Pr Pr_2	177.3	49.1(3) 54(3)	14(2) 57(2)	1.2 2.7 3.7	2.4 3.4 0.4	1.419 1.740	1.605 0.186 1.549
Lu PrLu	178.2	47.3(7) 53(2)	10.1(7) 59(1)	0.8 3.6 3.3	2.9 2.9 1.1	1.380 1.741	1.594 0.215 1.523
Lu NdLu	178.4	46.6(6) 53(1)	11.0(6) 58(2)	1.3 2.1 0.9	7.1 6.9 6.2	1.445 1.737	1.630 0.185 1.552
Sm Sm_2	179.1	46.9(4) 53(1)	12.3(7) 57.3(7)	0.9 2.2 1.4	6.9 7.0 6.2	1.459 1.748	1.642 0.184 1.563
L^{AB} complexes							
Eu LaEu	179.6	46.6(1) 54(1)	11.0(8) 56.7(4)	1.1 1.2 2.1	4.2 3.6 4.3	1.471 1.683	1.646 0.175 1.507
Eu Eu_2	178.2	46.5(4) 53.8(4)	11.3(8) 57.4(6)	1.1 1.5 2.4	4.3 3.5 4.5	1.508 1.671	1.653 0.145 1.526
Tb LaTb	179.2	46.9(4) 54(2)	11(1) 57(2)	0.6 4.0 3.8	3.4 3.9 5.3	1.432 1.673	1.607 0.175 1.494
Er PrEr	177.1	45.8(9) 52.6(5)	8.2(6) 59(2)	1.2 2.2 1.0	2.5 2.2 2.8	1.379 1.735	1.596 0.219 1.513
Lu PrLu	179.8	46(2) 53(2)	10(1) 57(2)	2.8 3.3 3.2	2.9 1.1 4.2	1.417 1.652	1.594 0.179 1.471
Regular trigonal tricapped prism	180	θ(P1) = θ(P3)	0 60	0 0 0	0 0 0	d(P1-P2)= d(P2-P3)	0

Table 11 Angles (°) and distances (Å) in the benzimidazole-pyridine-benzimidazole coordination polyhedron of L^{AB3} and L^{AB} complexes

	Φ	θ(P4) θ(P6)	ω (P4-P6) interstrand ω(P4-P5) intrastrand	α P4-P5 P4-P6 P5-P6	β P4 P5 P6	Distances P4 – P5 P5 – P6	Distances Ln – P4 Ln – P5 Ln – P6
L^{AB3} complexes							
Ce Ce_2	178.9	50(1) 53.4(6)	15(1) 51.9(5)	1.6 2.6 1.0	4.9 6.1 6.8	1.712 1.577	1.698 0.013 1.578
Pr Pr_2	179.4	50(3) 52(2)	15(3) 52(1)	1.7 6.1 4.4	1.8 0.3 4.2	1.709 1.563	1.672 0.034 1.592
Pr PrLu	178.7	50(2) 52(2)	14(3) 53(2)	1.2 4.9 4.0	1.8 0.7 3.3	1.704 1.592	1.681 0.022 1.611
Nd NdLu	178.9	50(1) 53(1)	14(1) 52.0(3)	1.6 3.2 1.7	5.8 6.3 7.9	1.693 1.581	1.681 0.011 1.582
Sm Sm_2	179.2	50(1) 53(1)	13(1) 52.9(6)	1.9 3.2 1.3	5.9 6.6 7.7	1.701 1.580	1.685 0.014 1.584
L^{AB} complexes							
La LaEu	177.4	49(1) 52(3)	16(3) 52(2)	1.4 6.2 5.6	3.5 4.8 9.4	1.729 1.611	1.716 0.011 1.606
La LaTb	177.4	50(1) 53(4)	16(2) 52(2)	1.6 6.2 5.4	2.8 4.3 8.9	1.719 1.597	1.706 0.012 1.598
Pr PrEr	178.4	50(1) 53(2)	15(2) 53.1(7)	2.1 3.9 3.2	2.2 4.3 5.3	1.689 1.583	1.678 0.010 1.588
Pr PrLu	178.0	50.7(9) 53(1)	15.8(3) 52.1(8)	1.2 2.1 1.8	3.5 2.8 4.6	1.701 1.537	1.668 0.031 1.563
Eu Eu_2	177.3	49(2) 51(4)	13(3) 53(3)	2.7 8.9 6.8	2.4 5.2 11.2	1.722 1.609	1.692 0.025 1.612
Regular trigonal tricapped prism	180	θ(P4) = θ(P6)	0 60	0 0 0	0 0 0	d(P4-P5) = d(P5-P6)	0

All coordination polyhedra are very close to being regular trigonal tricapped prisms.

The principal deviations are observable in the angles ω, which describe the twist between the upper and lower faces of the prism. In the bpa unit this angle is 15(1), 14(2), 10.1(7), 11.0(6) and 12.3(7) for the Ce_2, Pr_2, PrLu, NdLu and Sm_2 complexes, respectively. These values are slightly larger than found for the L^{AB} complexes, but the difference is probably not significant. In the bpb unit the angle is 15(1), 15(3), 14(3), 14(1) and 13(1) for the five

complexes, which is comparable to the values calculated for the L^{AB} complexes. This is as expected since the bpb coordination units are identical in the two ligands.

In the bpa unit the lanthanide ion is displaced from the plane defined by the capping atoms (P2). The distance from lanthanide ion to P2 is 0.189, 0.186, 0.215, 0.185 and 0.184 Å in the Ce_2, Pr_2, PrLu, NdLu and Sm_2 complexes, which is similar to the values calculated for the L^{AB} complexes. In the bpb unit, which is more symmetric, the corresponding distance (Ln(III)-P5) is smaller: 0.013, 0.034, 0.022, 0.011 and 0.014 Å as was also found for the L^{AB} complexes.

All other angles calculated for the coordination polyhedra are very close to the values expected for a regular trigonal tricapped prism.

There appears to be no significant difference between the coordination polyhedra in the complexes of the two ligands. The introduction of the Cl substituent does not strongly influence the coordination geometry, as least not in an obvious way.

3.6 Helical pitch

The helical pitch of a helicate is defined as the distance necessary for a ligand to make a complete (360 º) turn around the pseudo C_3 axis of the complex.

Table 12 Pitch and LnLn' distances in L^{AB3} and L^{AB} complexes

	L^{AB3}				
LnLn'	Ce_2	Pr_2	PrLu	NdLu	Sm_2
Pitch (Å)	13.3(1)	13.4(1)	13.2(2)	13.2(1)	13.3(1)
d(Ln-Ln') (Å)	9.10(15)	9.23(3)	9.18(2)	9.14(4)	9.18(2)

	L^{AB}				
LnLn'	LaEu	LaTb	PrEr	PrLu	Eu_2
Pitch (Å)	13.4(2)	13.4(2)	13.2(1)	13.21(2)	13.5(2)
d(Ln-Ln') (Å)	9.207(4)	9.199(5)	9.219(4)	9.215(5)	9.352(8)

The values of helical pitch (average value for the three ligand strands) and Ln-Ln' distances given in Table 12 exhibit no particular features. Changing the LnLn' pair or introducing a Cl substituent in going from L^{AB} to L^{AB3} does not induce any significant changes.

3.7 Interstrand π-π interactions

Angles and distances between the aromatic rings of the ligands in the complexes have been analysed to establish whether intramolecular interstrand stacking interactions play a significant role in the stability of the complexes. The monoclinic $Ce_2(L^{AB3})_3$ and the triclinic $Pr_2(L^{AB3})_3$ structures were chosen to represent the two types of structures; the $LaEu(L^{AB})_3$ structure was included in the analysis for comparison.

Least square planes and centroids were calculated for 5 planes for each ligand strand as defined in Table 13. For the two benzimidazole groups in the bpb moiety of the ligands planes defined only by the imidazole rings (denoted with *i*) were also calculated.

Table 13 Definition of planes

	$LaEu(L^{AB})_3$			$Ce_2(L^{AB3})_3$ and $Pr_2(L^{AB3})_3$		
	L^1	L^2	L^3	L^1	L^2	L^3
bpb moiety						
terminal benzimidazole	*1*: C27-33; N8-9	*2*: C70-76; N17-18	*3*: C113-119; N26-27	*1*: C1-7; N1-2	*2*: C44-50; N10-11	*3*: C87-93; N19-20
imidazole only	*1i*: C27-29; N8-9	*2i*: C70-72; N17-18	*3i*: C113-115; N26-27	*1i*: C1,6-7; N1-2	*2i*: C44,49-50; N10-11	*3i*: C87,92-93; N19-20
pyridine	*4*: C22-26; N7	*5*: C65-69; N16	*6*: C108-112; N25	*4*: C8-12; N3	*5*: C51-55; N12	*6*: C94-98; N21
bridging benzimidazole	*7*: C15-21; N5-6	*8*: C58-64; N14-15	*9*: C101-107; N23-24	*7*: C13-19; N4-5	*8*: C56-62; N13-14	*9*: C99-105; N22-23
imidazole only	*7i*: C17-18,21; N5-6	*8i*: C60-61,64; N14-15	*9i*: C103-104, 107; N23-24	*7i*: C13-14,19; N4-5	*8i:* C56-57.62; N13-14	*9i*: C99-100, 105; N22-23
bpa moiety						
bridging benzimidazole	*10*: C7-13; N3-4	*11*: C50-56; N12-13	*12*: C93-99; N21-22	*10*: C21-27; N6-7	*11*: C64-70; N15-16	*12*: C107-113; N24-25
pyridine	*13*: C2-6; N2	*14*: C45-49; N11	*15*: C88-92; N20	*13*: C28-32; N8	*14*: C71-75; N17	*15*: C114-118; N26

For each pair of adjacent planes the angle and the distance between the centroids were calculated; the results are listed in Table 14.

Table 14 Angles and distances between planes

	$LaEu(L^{AB})_3$		$Ce_2(L^{AB3})_3$		$Pr_2(L^{AB3})_3$	
Planes	Angle	*d*	Angle	*d*	Angle	*d*
1 - 6	47.3 º	4.185 Å	42.5 º	4.220 Å	48.4 º	4.250 Å
2 - 4	39.6 º	4.011 Å	62.7 º	4.472 Å	51.6 º	4.391 Å
3 - 5	42.8 º	4.028 Å	48.0 º	4.279 Å	57.7 º	4.436 Å
1i - 9i	11.5 º	3.997 Å	9.1 º	3.496 Å	28.4 º	3.831 Å
2i - 7i	23.1 º	3.746 Å	36.0 º	4.158 Å	15.8 º	3.695 Å
3i - 8i	33.9 º	4.029 Å	16.6 º	3.837 Å	10.4 º	3.924 Å
4 - 9	26.6 º	3.688 Å	22.8 º	3.842 Å	46.6 º	4.367 Å
5 - 7	28.3 º	3.931 Å	20.9 º	3.653 Å	29.8 º	3.904 Å
6 - 8	28.8 º	3.980 Å	39.0 º	4.119 Å	22.4 º	3.597 Å
7 - 12	25.3 º	4.151 Å	26.1 º	4.025 Å	27.1 º	4.288 Å
8 - 10	27.7 º	4.278 Å	19.9 º	4.556 Å	24.0 º	4.250 Å
9 - 11	26.3 º	4.437 Å	22.9 º	4.121 Å	33.1 º	4.148 Å
10 - 15	76.2 º	4.808 Å	53.2 º	4.364 Å	81.5 º	4.896 Å
11 - 13	86.4 º	5.063 Å	84.8 º	5.381 Å	84.7 º	5.190 Å
12 - 14	88.3 º	5.309 Å	81.4 º	5.035 Å	88.0 º	5.060 Å

As can be seen in Table 14 most of the planes are not parallel or close enough to conclude that there are strong π-π interactions. The most parallel pairs of planes (*1i - 9i* for $LaEu(L^{AB})_3$ and $Ce_2(L^{AB3})_3$; *3i - 8i* for $Pr_2(L^{AB3})_3$; see Figure 11) have angles of 9.1 - 11.5 ° and distances of 3.5 - 4.0 Å. The limit for stacking interactions is usually considered to be 3.5 Å, twice the van der Waals "half-thickness" of an aromatic molecule.[82] Therefore, strictly speaking, only one π-π interaction, in $Ce_2(L^{AB3})_3$, meet these criteria. For comparison, the distance between layers in graphite is 3.35 Å.

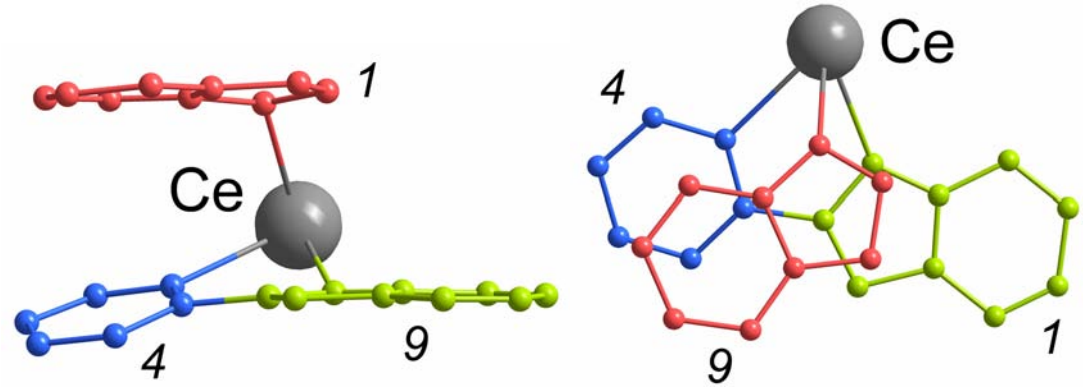

Figure 11 Planes *1*, *4* and *9* of the $Ce_2(L^{AB3})_3$ complex. *1i* and *9i* are the two imidazole rings.

This should be compared to the values found for monomeric complexes of the ligands (Chart 1) L^1 (9.1°; 3.1 - 3.3 Å),[5,6] L^2 (1 °; 3.08 - 3.22 Å)[7] and L^3 (5.5 °; 3.5 Å).[8]
In the other bimetallic lanthanide-containing helicates investigated to date these distances also tend to be longer than what has been found in the monometallic complexes mentioned above, indicating weaker interactions. For the homobimetallic complexes $[Eu_2(L^A)_3](ClO_4)_6$,[27] $[Tb_2(L^B)_3](ClO_4)_6$,[30] $[Eu_2(L^C\text{-}2H)_3]$ and $[Tb_2(L^C\text{-}2H)_3]$[32] (Chart 6) for instance, interstrand benzimidazole-benzimidazole distances of 3.7 - 4.6 Å have been found, which means that the π-π interactions are weak.

Interestingly, the differences between the L^{AB} complex and the L^{AB3} complexes are not significantly larger than the differences between the two L^{AB3} complexes. This indicates that the differences in angles and distances may be caused by packing effects in the crystal and not by the effect of the Cl substituent on the L^{AB3} ligand.

3.8 A second Ce_2 crystal

A second, triclinic, crystal of the $Ce_2(L^{AB3})_3$ complex was also obtained under similar crystallisation conditions as the first one. The crystal was unfortunately not of sufficient quality to do the final refinement of the structure and the result can therefore not be presented here.

Table 15 Crystal data for $[Ce_2(L^{AB3})_3](ClO_4)_6 \cdot 10\ CH_3CN$

formula	$C_{149}H_{156}Ce_2Cl_9N_{37}O_{27}$
mol weight	3496.43
crystal system	triclinic
space group	*P*
a (Å)	15.1477(28)
b (Å)	19.2690(47)
c (Å)	30.1647(60)
α (°)	103.405(19)
β (°)	101.239(16)
γ (°)	96.333(17)
Z	2

However, as seen in Table 15 the unit cell (space group and dimensions) is very similar to what was found for the Pr_2 and PrLu complexes (Table 5). This serves to demonstrate that the same complex can crystallise with different unit cells and numbers of solvent molecules. The observation may be trivial, but is nevertheless included here to avoid that the opposite is assumed: that the different unit cell of the Ce_2, Sm_2 and NdLu complexes compared to the Pr_2 and PrLu ones is the manifestation of a fundamental difference in the structure of the three complexes.

4 Speciation in solution

The study of the speciation of solutions containing ligands and lanthanide ions will fall in two parts. Firstly we will examine the homobimetallic complexes in solutions containing two identical lanthanide ions and secondly we will turn our attention to heterobimetallic complexes in solutions containing two different lanthanide ions in order to evaluate the selectivity of the ligands. Proportions of the various species will be determined by integration of the NMR signals. For a complete assignment of the spectra of the *HHH* isomers of the complexes, see Chapter 5.2.2, Table 23 - Table 30 (page 83).

4.1 Homobimetallic complexes

In a CD_3CN solution containing La^{3+} ions ($c_{La} \approx 10^{-2}$ M) and L^{AB} in the ratio 2:3 the only species that can be observed by ^1H NMR is the $[La_2(L^{AB})_3]^{6+}$ complex.[80] The analogous Lu^{3+} solution also contains a few percent of complexes with different composition, probably $[Lu_2(L^{AB})_2]^{6+}$, $[Lu(L^{AB})]^{3+}$, $[Lu(L^{AB})_2]^{3+}$ and/or $[Lu(L^{AB})_3]^{3+}$, but the main species here is still the 2:3 complex.

For complexes of the symmetrical ditopic ligand L^B spectrophotometric titrations have been carried out in acetonitrile and the stability constants β of the 2:2 and 2:3 species have been determined for all lanthanides except Pm.[53] The values for log β_{23} range from 25.0(2) to 26.0(2); the β_{22} are between 18.9(1) and 20.1(5). Using these values it is possible to calculate the percentage of the 2:2 species to 1.0 - 4.9 % in a solution with 2:3 stoichiometry and $c_{Ln\ total} = 10^{-2}$ M.

In the present study the ^1H NMR spectra of CD_3CN solutions containing $Ln(ClO_4)_3$ (Ln = La, Ce, Pr, Nd, Sm, Eu, Y or Lu) and L (= L^{AB}, L^{AB2}, L^{AB3}, L^{AB4} or L^{AB5}) in a 2:3 ratio and $c_{Ln\ total} \approx 10^{-2}$ M were measured. Based on the observations on the L^{AB} solutions and L^B stability constants mentioned above it is reasonably assumed that all complexes formed are of the composition $[Ln_2(L)_3]^{6+}$.

For a $Ln_2(L)_3$ complex two isomers are possible (Figure 12):

- *HHH* (*Head-Head-Head)* in which all three ligands are oriented in the same direction and the benzimidazole-pyridine-benzimidazole (bpb) moieties are coordinated to the same lanthanide ion.
- *HHT* (*Head-Head-Tail)* where one of the three ligand strands binds the benzimidazole-pyridine-benzimidazole moiety to the lanthanide ion which is coordinated by the benzimidazole-pyridine-amide (bpa) moieties of the other two ligands.

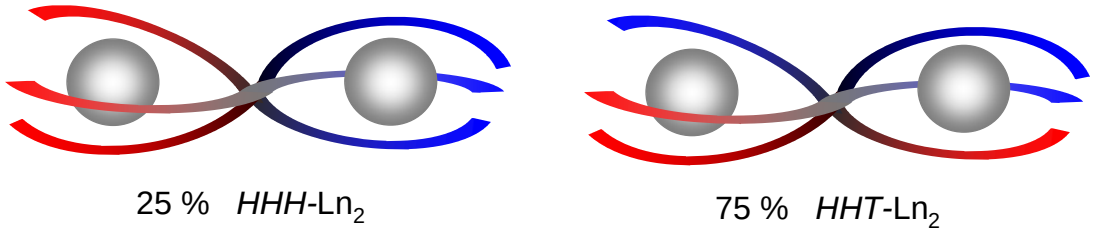

Figure 12 *HHH* and *HHT* isomers

For the *HHH* isomer the macroscopic formation constant β_{LnLn}^{HHH} is equal to $\left(k_{Ln}^{\alpha}\right)\cdot\left(k_{Ln}^{\beta}\right)\cdot\left(u^{HHH}\right)\cdot\left(u_{LnLn}^{HHH}\right)$ where $\left(k_{Ln}^{\alpha}\right)$ and $\left(k_{Ln}^{\beta}\right)$ are the absolute affinity constants of site α (the bpa-bpa-bpa site) and β (bpb-bpb-bpb), respectively, for Ln; u^{HHH} is the pre-organisation energy (including attractive and repulsive interactions between strands) of the formation of an "empty" triple helix from three ligands and u_{LnLn}^{HHH} describes the Ln-Ln (Coulomb) repulsion.[53,54,55,57,58,59] The similar constant for the *HHT* isomer, β_{LnLn}^{HHT}, can be written as $3\cdot\left(k_{Ln}^{\gamma}\right)\cdot\left(k_{Ln}^{\delta}\right)\cdot\left(u^{HHT}\right)\cdot\left(u_{LnLn}^{HHT}\right)$ where γ stands for the bpa-bpa-bpb site and δ is the bpa-bpb-bpb one; the factor 3 is the degeneracy. Thus, a total of 8 parameters are necessary to describe the system if no simplifications are made.

If the four affinity constants were all the same, the pre-organisation energies the same for the two isomers and the two Ln-Ln repulsion parameters were equal, the equilibrium constant for the *HHH* ⇆ *HHT* isomerisation would be 3, corresponding to a distribution of 25 % *HHH* and 75 % *HHT*. We will refer to this as the statistical distribution; corresponding to the

complexation of two identical lanthanide ions by a homobitopic ligand. Although this description is obviously oversimplified, it serves as a reference point in the later discussion.

In the NMR spectra the *HHH* isomer gives only one set of signals since the three ligand strands are equivalent; the *HHT* isomer, in which the ligand strands are not equivalent, gives three sets of signals, one for each ligand.

An example of partial spectra is given in Figure 13. The L^{AB2} ligand contains 6 methyl groups and the *HHH* isomer should thus give 6 signals in the region shown. The *HHT* isomer should give $3 \cdot 6 = 18$ signals. In the spectra of both the La and the Lu solutions this is also what is observed; in each spectrum there are two sets of signals with different intensities. Even in the 600 MHz spectra there is substantial overlap of lines; nevertheless, counting the most intense set gives 15 – 18 signals, whereas the less intense set contains at least 2 resonances, the rest being obscured by the more intense set of signals.

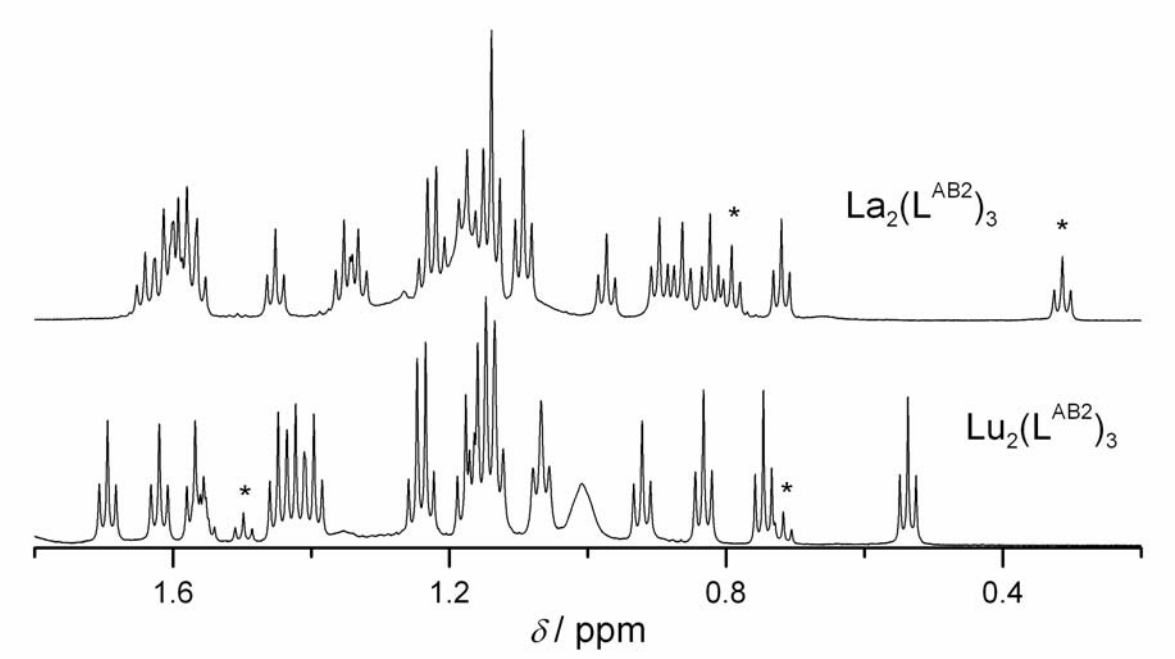

Figure 13 CH_3 region of the 600 MHz ^{1}H NMR spectra of homobimetallic $Ln_2(L^{AB2})_3$ solutions. $c_{Ln} \approx 10^{-2}$ M * *HHH* complexes

Similarly, in Figure 14 are given partial spectra of La complexes of all the 5 ligands. The helical wrapping of the ligands causes the benzimidazole protons H8 and H10 (Chart 14 (page 37) for proton numbering) to be shifted out of the usual aromatic region spectrum and appear relatively isolated around 5.8 – 6.2 ppm. There are 6 *HHT* signals in the 5.2 – 6.3 ppm region, two for each of the two protons (H8 and H10) of each of the three ligand strands. The

different speciation of the complexes of the 5 ligands is immediately obvious with the *HHT* signals dominating the $La_2(L^{AB2})_3$ spectrum and being virtually absent in the spectrum of the $La_2(L^{AB4})_3$ complexes.

In all spectra the two sets of resonance with different intensities were assigned to the *HHH* and *HHT* isomers based on the number of lines.

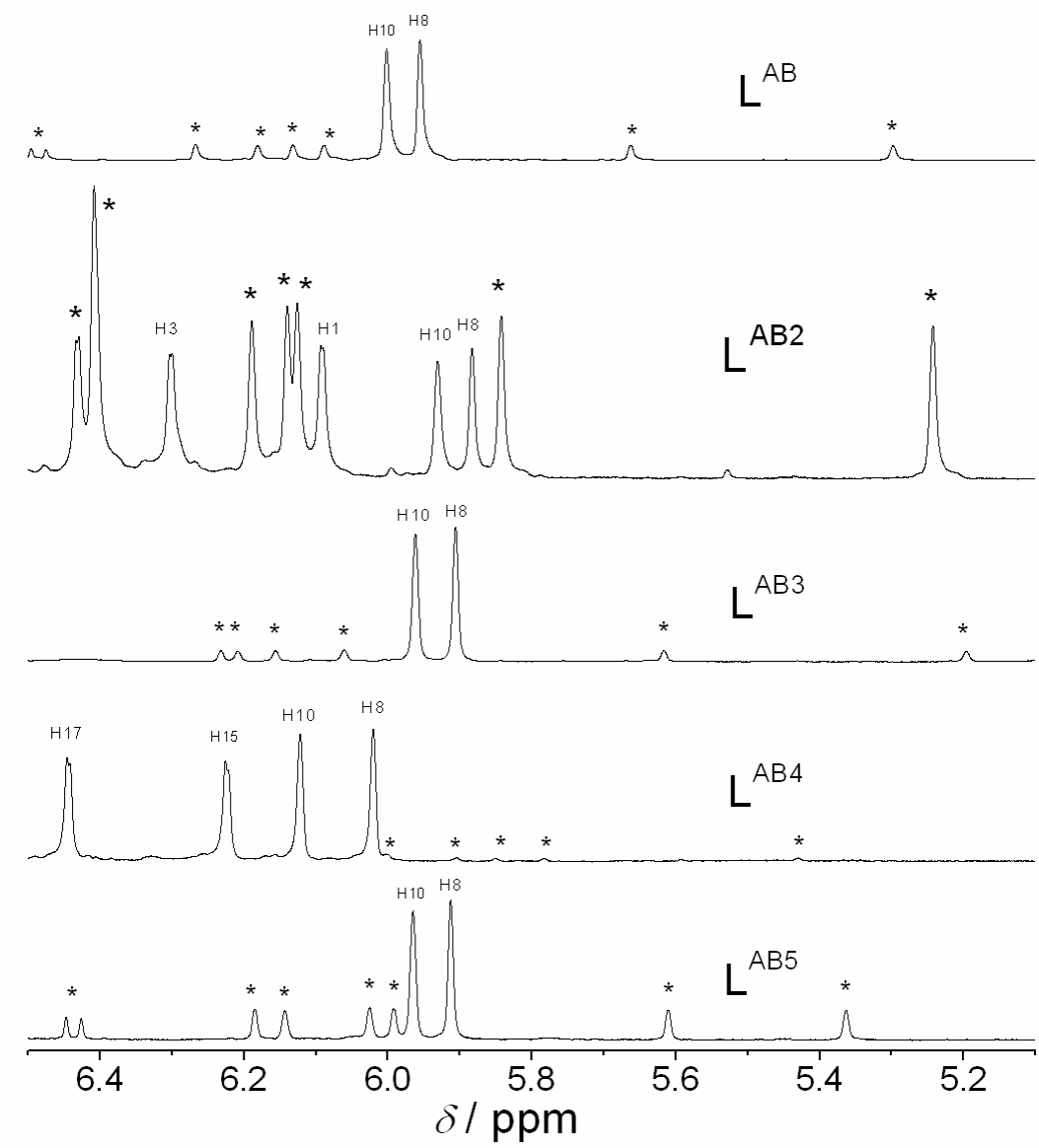

Figure 14 Partial NMR spectra of $La_2(L)_3$ CD_3CN solutions. * indicates *HHT* signals. $c_{Ln\ total} \approx 10^{-2}$ M

Percentages of the two isomers were calculated from the integrated line intensities. In most cases, several lines (up to 10) were used for each isomer.

The majority of the percentages were re-calculated from the thermodynamic parameters determined by variable temperature NMR (see Chapter 7 (page 281) where a more detailed

description of the spectra can be found). The exceptions were $Ce_2(L^{AB})_3$, $Ce_2(L^{AB3})_3$, all of the $Nd_2(L)_3$ and all of the L^{AB4} complexes. $Y_2(L^{AB4})_3$ has not been measured.

The results are given in Table 16 and Figure 15. Based on the variation of intensities within sets of signals the absolute errors are estimated to be less than 5 % for the L^{AB2} solutions and less than 10 % for the solutions of the other four ligands.

Table 16 Percentage of *HHH* isomer

	L^{AB}	L^{AB2}	L^{AB3}	L^{AB4}	L^{AB5}
La_2	73	20	79	96	60
Ce_2	69	13	79	95	53
Pr_2	67	12	87	93	53
Nd_2	69	15	87	95	55
Sm_2	65	11	85	95	56
Eu_2	69	8	85	96	54
Y_2	63	8	82		61
Lu_2	68	6	86	94	60

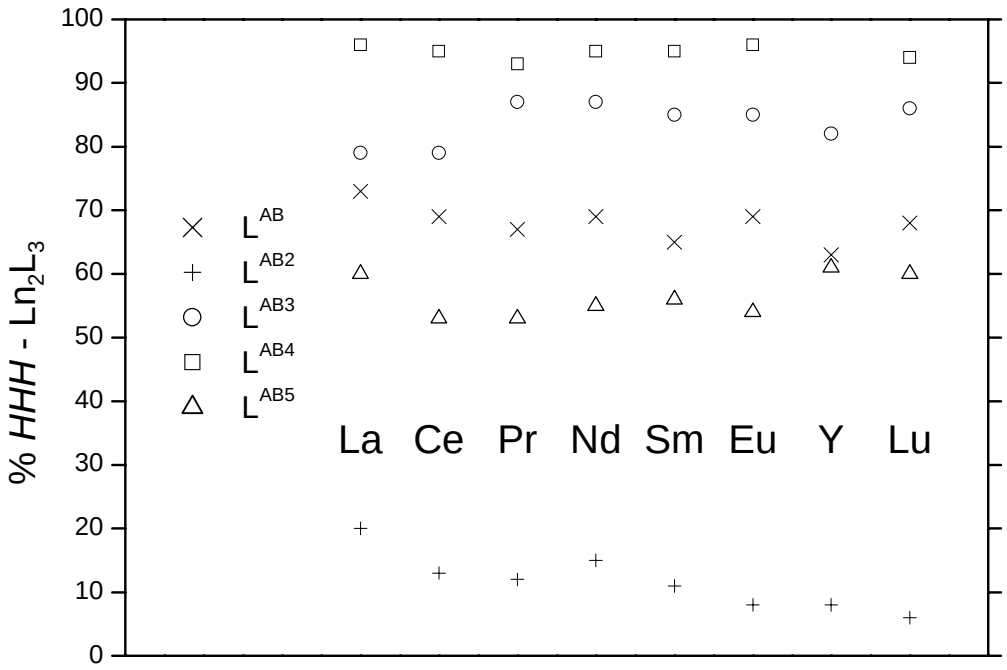

Figure 15 *HHH* percentages in $Ln_2(L)_3$ CD_3CN solutions. $c_{Ln} \approx 10^{-2}$ M

Interestingly, percentages of *HHH* isomer in the complexes of L^{AB} are between 63 and 73 %, far from the statistical value of 25 %, meaning that this heterobitopic ligand favours the *HHH* isomer over the *HHT* one.

The introduction of a Cl substituent in L^{AB3} and L^{AB5} only changes the *HHH* percentages by a few percent when compared to the complexes of the L^{AB} ligand. The *HHH* percentages of the L^{AB3} complexes are 6 -20 % (average 16 %) higher than the L^{AB} ones, the L^{AB5} values are 2 – 16 % (average 11 %) lower.

The NEt_2 substituent on the L^{AB2} and L^{AB4} ligands, on the other hand, has a dramatic effect on the percentage of *HHH* isomer; compared to the values of the L^{AB} complexes they are 53 - 62 % (average 56 %) lower for the L^{AB2} complexes and 23 - 30 % (average 26 %) higher for the L^{AB4} complexes

The effect caused by the substituents exhibits methodical behaviour not only in magnitude, but also in sign. For a pair of ligands with different substituents (L^{AB2}/L^{AB3} or L^{AB4}/L^{AB5}) substituted on the same moiety (bpa or bpb) the change when compared to L^{AB} is opposite in sign. Similarly, pairs of ligands with the same substituent on different moieties (L^{AB2}/L^{AB4} or L^{AB3}/L^{AB5}) also show deviations from L^{AB} of opposite signs.

The *HHH/HHT* equilibrium will be treated in more detail in Chapter 7 (page 281).

4.2 Heterobimetallic complexes

For solutions containing a pair of different lanthanide ions the number of possible species increases to eight. Apart from the *HHH* and *HHT* isomers of each of the two homobimetallic complexes, four heterobimetallic complexes are possible: the *HHH* and *HHT* isomers of the $LnLn'(L)_3$ and $Ln'Ln(L)_3$ complexes. Note that in this notation *HHH*-$LnLn'(L)_3$ signifies that the Ln and Ln' ions are coordinated by the bpb and bpa moieties of the ligand, respectively. In the *HHT*-$LnLn'(L)_3$ complex Ln is coordinated by two bpb and one bpa units and Ln' by one bpb and two bpa units. Changing the coordination mode of a second ligand leads to *HHT*-$Ln'Ln(L)_3$ (note the reversed order of Ln and Ln') and the last possible isomer is *HHH*-$Ln'Ln(L)_3$.

The isomers are illustrated in Figure 16 together with their "statistical" distribution, their percentages in solution if only the degeneracies of the different possibilities were taken into account. For any possible combinations of metal ions (Ln_2, Ln'_2, LnLn' and Ln'Ln) the statistical concentration of the *HHT* isomer is three times the concentration of the *HHH* one.

A more detailed description in terms of macroscopic formation constants like it was outlined for the homobimetallic complexes would require a total of 16 parameters: $\left(k_{Ln}^{\alpha}\right),\left(k_{Ln}^{\beta}\right),\left(k_{Ln}^{\gamma}\right),\left(k_{Ln'}^{\delta}\right),\left(k_{Ln'}^{\alpha}\right),\left(k_{Ln'}^{\beta}\right),\left(k_{Ln'}^{\gamma}\right),\left(k_{Ln'}^{\delta}\right),\left(u^{HHH}\right),\left(u^{HHT}\right),\left(u_{LnLn}^{HHH}\right),\left(u_{LnLn'}^{HHH}\right),\left(u_{Ln'Ln'}^{HHH}\right),\left(u_{LnLn}^{HHT}\right)$, $\left(u_{LnLn'}^{HHT}\right)$ and $\left(u_{Ln'Ln'}^{HHT}\right)$.[53,54,55,57,58,59]

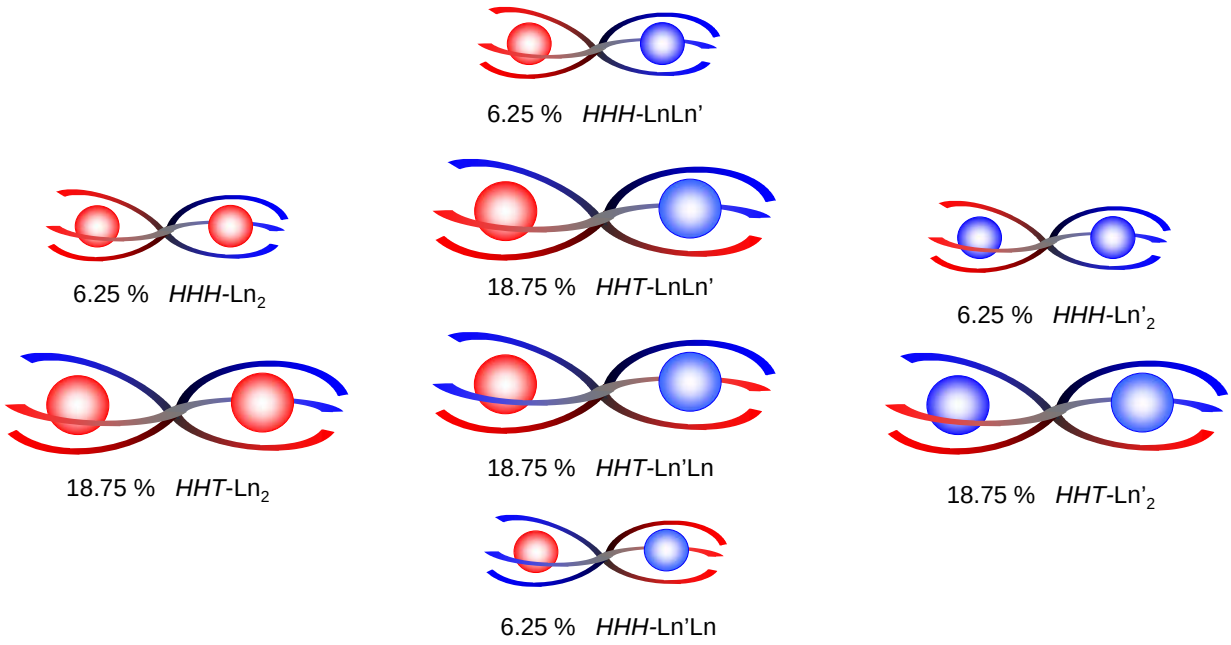

Figure 16 Ln_2, Ln'_2, LnLn' and Ln'Ln isomers

The complexes were studied in CD_3CN solution by means of ^1H NMR spectroscopy. In all cases the Ln:Ln':L ratio was fixed at 1:1:3 ($c_{Ln} \approx 10^{-2}$ M). It has been demonstrated[80] for complexes with L^{AB} that ES-MS measurements yield essentially the same results as NMR regarding the relative concentrations of homo- and heterobimetallic complexes despite the more diluted solutions ($c_{Ln} \approx 10^{-3}$ M) used for ES-MS. However, since ES-MS yields no information on the relative concentrations of *HHH* and *HHT* isomers no such measurements will be presented here.

Fortunately, it was found that for large differences of sizes between the two lanthanide ions the only heterobimetallic isomer formed out of the four possibilities is the *HHH*-LnLn'$(L)_3$ one (e.g. *HHH*-CeLu$(L^{AB3})_3$ and not *HHT*-CeLu$(L^{AB3})_3$, *HHT*-LuCe$(L^{AB3})_3$ or *HHH*-LuCe$(L^{AB3})_3$; Figure 17).

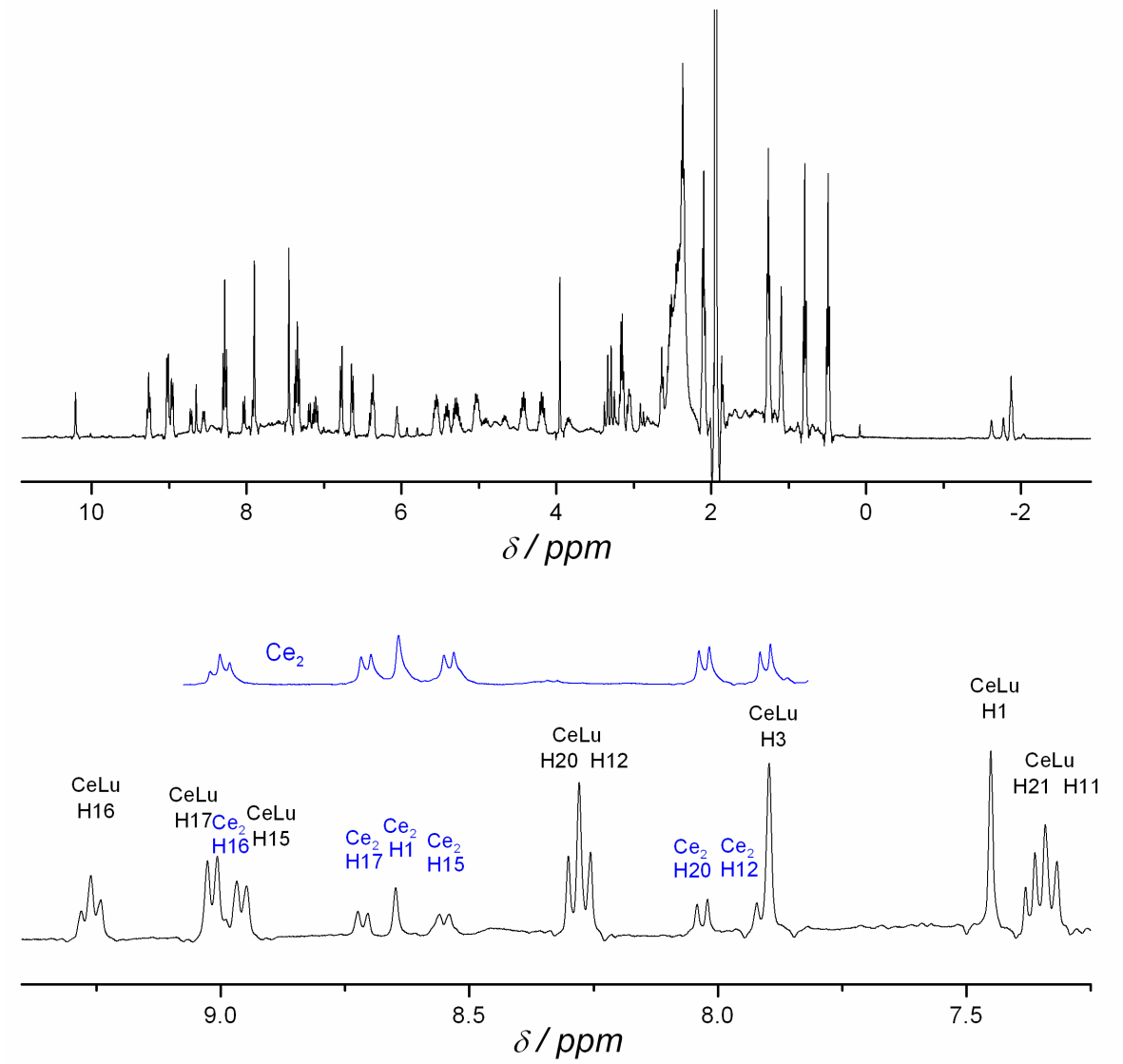

Figure 17 NMR spectrum of the CeLu$(L^{AB3})_3$ complex (top). An excerpt of the spectrum is shown below with part of the $Ce_2(L^{AB3})_3$ spectrum inserted. $c_{Ln\ total} \approx 10^{-2}$ M.

For smaller size difference other heterobimetallic isomers were observed, but the isomer with the larger ion in the bpb site was still the major one.

The solutions of the heterobimetallic complexes also contain homobimetallic species. Again, the composition depends on the size difference of the two lanthanides. The spectrum of the LaCe$(L^{AB3})_3$ complex is given as an example in Figure 18. The solution contains not only the complex of interest, but also CeLa$(L^{AB3})_3$, $La_2(L^{AB3})_3$ and $Ce_2(L^{AB3})_3$ in considerable

amounts. This should be compared with the relatively small amounts of homobimetallic complexes seen in Figure 17.

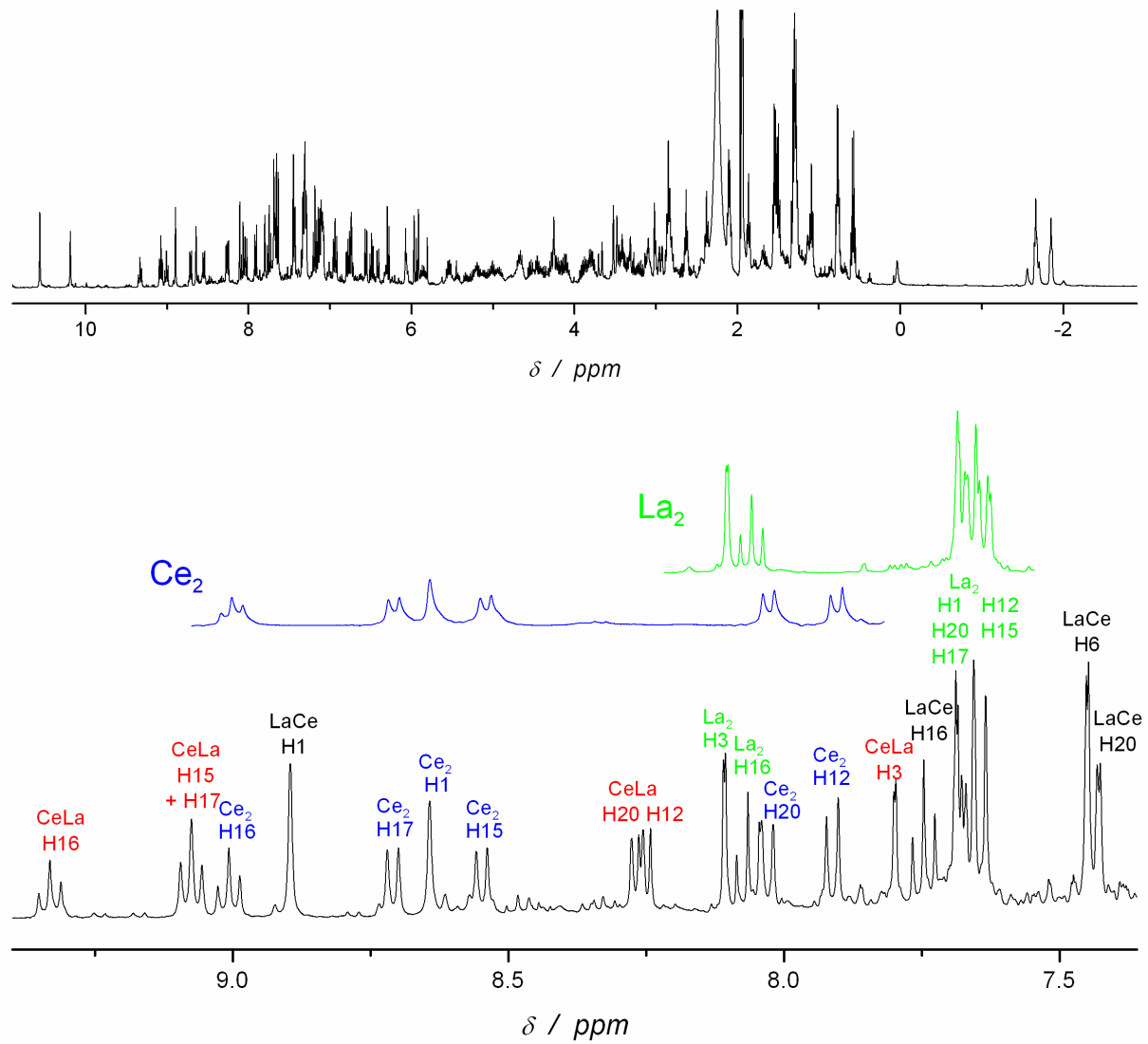

Figure 18 NMR spectrum of the LaCe(L^{AB3})$_3$ complex (top). An excerpt of the spectrum is shown below with parts of the Ce_2(L^{AB3})$_3$ and La_2(L^{AB3})$_3$ spectra inserted. $c_{Ln\ total} \approx 10^{-2}$ M.

As a final example partial spectra of La_2, Lu_2 and LaLu complexes of L^{AB2} are shown in Figure 19. Here it is obvious how high percentages of *HHT* isomer can further complicate the spectra.

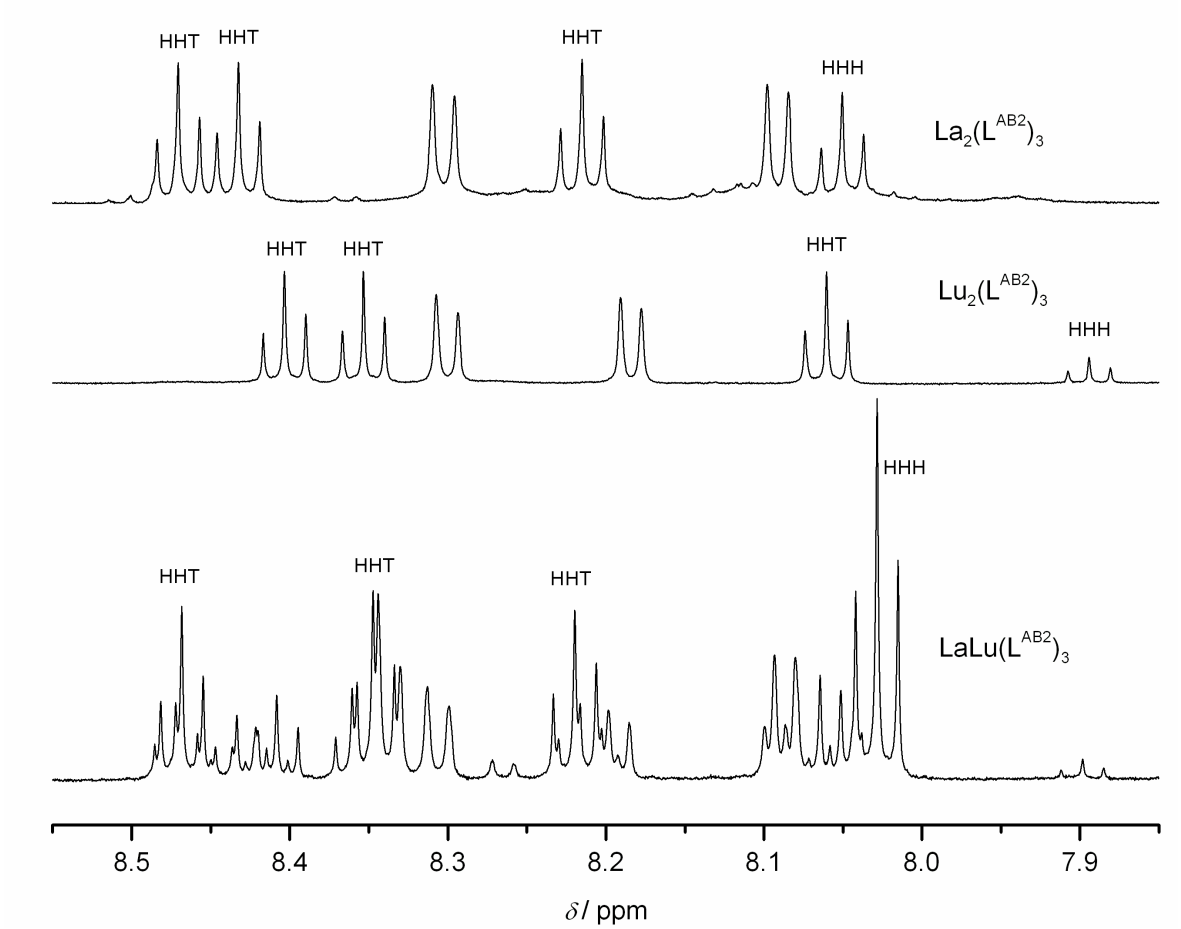

Figure 19 Partial 600 MHz ^{1}H NMR spectra of $La_2(L^{AB2})_3$, $Lu_2(L^{AB2})_3$ and $LaLu(L^{AB2})_3$ solutions. Signals of H16 for the *HHH* and *HHT* isomers are indicated. $c_{Ln\ total} \approx 10^{-2}$ M.

The relative concentrations of the different complexes in solution were determined by integration of their respective signals in the NMR spectra. Homobimetallic signals were assigned by comparison with spectra of homobimetallic solutions. The *HHH* and *HHT* isomers of heterobimetallic complex were identified by counting the signals. In the *HHH* isomer all three ligand strands are equivalent and only one set of signals is observed; the *HHT* isomer gives three sets of signals since the ligand strands are no longer equivalent. Typically 3-5 well isolated signals of each isomer were used for the calculation of the concentrations. The relative errors are estimated to be ≈ 5 – 10 %. A complete assignment of all *HHH* complexes of L^{AB}, L^{AB3}, L^{AB4} and L^{AB5} can be found in Chapter 5 (page 83).

The speciation of complexes is listed in Table 17 - Table 21.

Table 17 Composition in % of L^{AB} complexes in solution

			LnLn'		Ln'Ln			Ln_2		Ln'_2	
Ln	Ln'	$r_{Ln\text{-}Ln'}$	*HHH*	*HHT*	*HHT*	*HHH*	Total hetero	*HHH*	*HHT*	*HHH*	*HHT*
La	Ce	2	25	5		12	42	23	6	21	7
La	Pr	3.7	30			11	41	21	6	23	9
La	Nd	5.3	41			10	51	14	4	22	9
Eu	Lu	8.8	73				73	12	4	9	2
La	Eu	9.6	64				64	13	5	13	5
Sm	Lu	10	84				84	9		7	
Nd	Lu	13.1	90				90	6		4	
Pr	Lu	14.7	95				95	4		1	
Ce	Lu	16.4	92				92	5		3	
La	Lu	18.4	96				96	2		2	

Table 18 Composition in % of L^{AB2} complexes in solution

			LnLn'		Ln'Ln			Ln_2		Ln'_2	
Ln	Ln'	$r_{Ln\text{-}Ln'}$	*HHH*	*HHT*	*HHT*	*HHH*	Total hetero	*HHH*	*HHT*	*HHH*	*HHT*
Eu	Lu	8.8	4	17			21	10	47	3	19
Nd	Lu	13.1	7	18	2		27	5	32	3	31
Pr	Lu	14.7	18	33			51	2	21	3	24
Ce	Lu	16.4	21	39			60	3	18	2	17
La	Lu	18.4	27	34	4		65	3	13	1	17

Table 19 Composition in % of L^{AB3} complexes in solution

			LnLn'		Ln'Ln			Ln_2		Ln'_2	
Ln	Ln'	$r_{Ln\text{-}Ln'}$	*HHH*	*HHT*	*HHT*	*HHH*	Total hetero	*HHH*	*HHT*	*HHH*	*HHT*
La	Ce	2	30			19	49	28		23	
La	Pr	3.7	33			15	48	26		25	
La	Nd	5.3	45			12	57	16		28	
Eu	Lu	8.8	75				75	18		8	
La	Eu	9.6	63				63	18		19	
Sm	Lu	10	65				65	24		11	
Nd	Lu	13.1	70				70	14		15	
Pr	Lu	14.7	88				88	8		4	
Ce	Lu	16.4	80				80	10		10	
La	Lu	18.4	87				87	9		4	

Table 20 Composition in % of L^{AB4} complexes in solution

			LnLn'		Ln'Ln			Ln_2		Ln'_2	
Ln	Ln'	$r_{Ln\text{-}Ln'}$	*HHH*	*HHT*	*HHT*	*HHH*	Total hetero	*HHH*	*HHT*	*HHH*	*HHT*
La	Ce	2	34			14	48	10		41	
La	Pr	3.7	41			13	54	24		23	
La	Nd	5.3	54			7	61	16		23	
Eu	Lu	8.8	62				62	14		24	
La	Eu	9.6	75				75	14		12	
Nd	Lu	13.1	68				68	16		16	
Pr	Lu	14.7	82				82	13		5	
Ce	Lu	16.4	76				76	14		11	
La	Lu	18.4	79				79	11		9	

Table 21 Composition in % of L^{AB5} complexes in solution

			LnLn'		Ln'Ln			Ln_2		Ln'_2	
Ln	Ln'	$r_{Ln\text{-}Ln'}$	*HHH*	*HHT*	*HHT*	*HHH*	Total hetero	*HHH*	*HHT*	*HHH*	*HHT*
La	Ce	2	24	12		9	45	15	12	16	12
La	Pr	3.7	29	9		7	45	17	13	13	12
La	Nd	5.3	39	9		4	52	14	10	13	12
La	Sm	8.4	47	9			56	14	11	9	10
Eu	Lu	8.8	39	13			52	15	11	11	11
La	Eu	9.6	48	9			57	10	9	10	15
Sm	Lu	10	57	9			66	10	8	7	9
Nd	Lu	13.1	71	9			80	6	6	5	4
Pr	Lu	14.7	63	7			70	9	9	8	5
Ce	Lu	16.4	79	13			92	4	1	2	1
La	Lu	18.4	77	15			92	3	1	1	1

The total percentage of the four heterobimetallic isomers is illustrated in Figure 20 as a function of the difference in ionic radius between the two lanthanide ions.

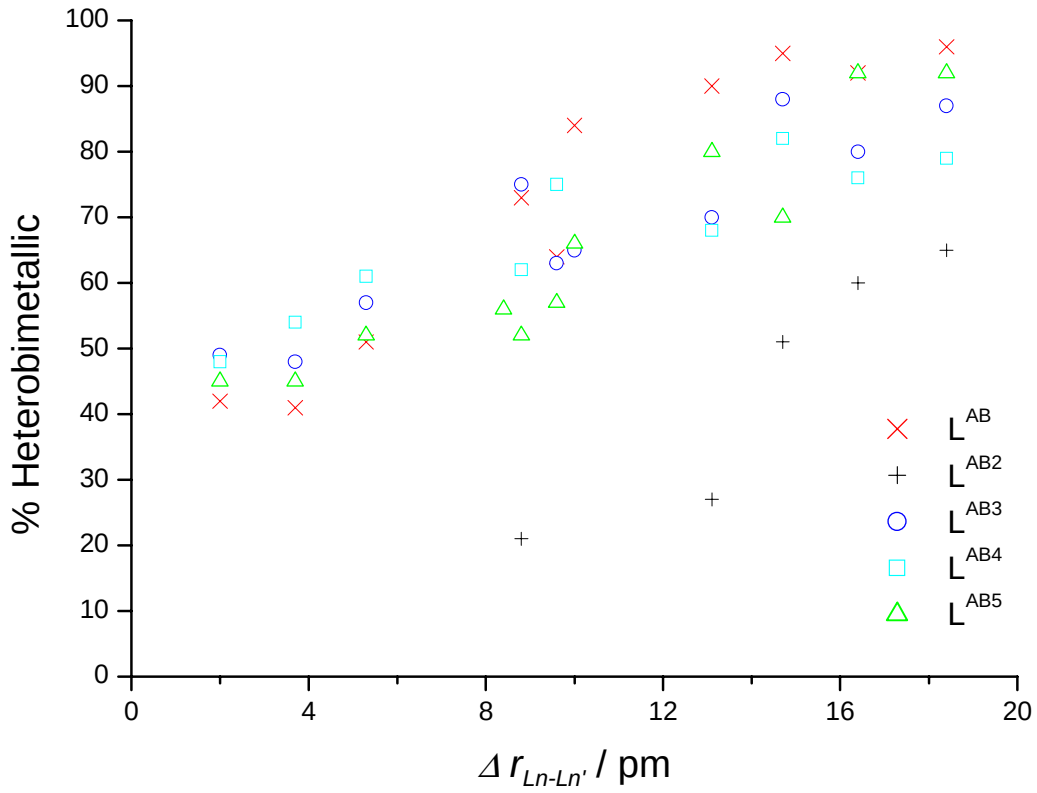

Figure 20 Percentage of hetero species in solution

As can be seen in Table 17 - Table 21 and Figure 20 the general trend is as expected that the selectivity towards a pair of lanthanide ions increases with the size difference. For pairs of similar lanthanide ions the distribution is close to statistical (50 %).

Unfortunately, none of the new ligands represents an improvement over L^{AB} when it comes to forming high percentages of heterobimetallic complexes. The problem can be traced back to the *HHH*/*HHT* equilibrium. The two ligands that were hoped to be more selective when reacted with a pair of different lanthanide ions (L^{AB2} and L^{AB5}) are unfortunately also the ligands that form higher percentages of *HHT* complexes than L^{AB}. This leads, in particular in the case of L^{AB2}, to lower selectivity.

The two other ligands, L^{AB3} and L^{AB4}, behave as predicted. According to the reasoning on which their design is based they should not constitute an improvement over L^{AB} in selectivity and this is indeed what is observed.

It is expected that the energetics of the complex formation is dominated by ion-dipole lanthanide-ligand interactions. Interstrand interactions between two ligands in the same complex are, however, not expected to be negligible. These latter interactions can be both attractive (van der Waals) and repulsive (sterical effects) in character.

For example, that the *HHH*-$Lu_2(L^{AB2})_3$ complex is formed in such a low proportion could point to a repulsive interaction being responsible for the behaviour of the L^{AB2} ligand, this repulsion being strengthened by the ligands being closer to each other in the complexes of the smaller Lu ion compared to the La complexes. It could also be taken as evidence of a positive interaction in the *HHT* complex and the argument involving the relative sizes of the lanthanide ions could be repeated.

These interactions are not necessarily sterical in nature, even though it would be tempting to ascribe the different behaviour of the L^{AB2} to problems with the relatively bulky NEt_2 substituent. Indeed adding a group at the 4-postion of the pyridine has been done apparently without hindering complex formation.[81] It is known that a potentially important contribution to the formation of triple helicates is the interstrand π-π interaction between aromatic groups and it could be that the effect of the substituents is a modification of the conjugated π electron system. While these π-π interactions are weak in the *HHH* isomer (page 55) they could be more important in the *HHT* isomer, for which no structural information is available.

In the following chapters the structures of the complexes in solution will be examined and the *HHH*/*HHT* equilibrium will be studied in more detail.

5 Lanthanide induced shift

5.1 Introduction

The concept of lanthanide induced paramagnetic shift (LIS) is easily understood by referring to Figure 21 in which partial spectra of the LnLu(L^{AB})$_3$ series of complexes are shown. As can be seen, the methyl signals (H5, H14, H19, H25 and H27) of the diamagnetic LaLu complex are in the same region as in the spectrum of the free ligand although slightly shifted due to the conformation change of the ligand upon complexation. The signals in the spectra of complexes containing paramagnetic lanthanide ions are shifted with respect to their positions in the LaLu spectrum; this is the so-called lanthanide induced shift.

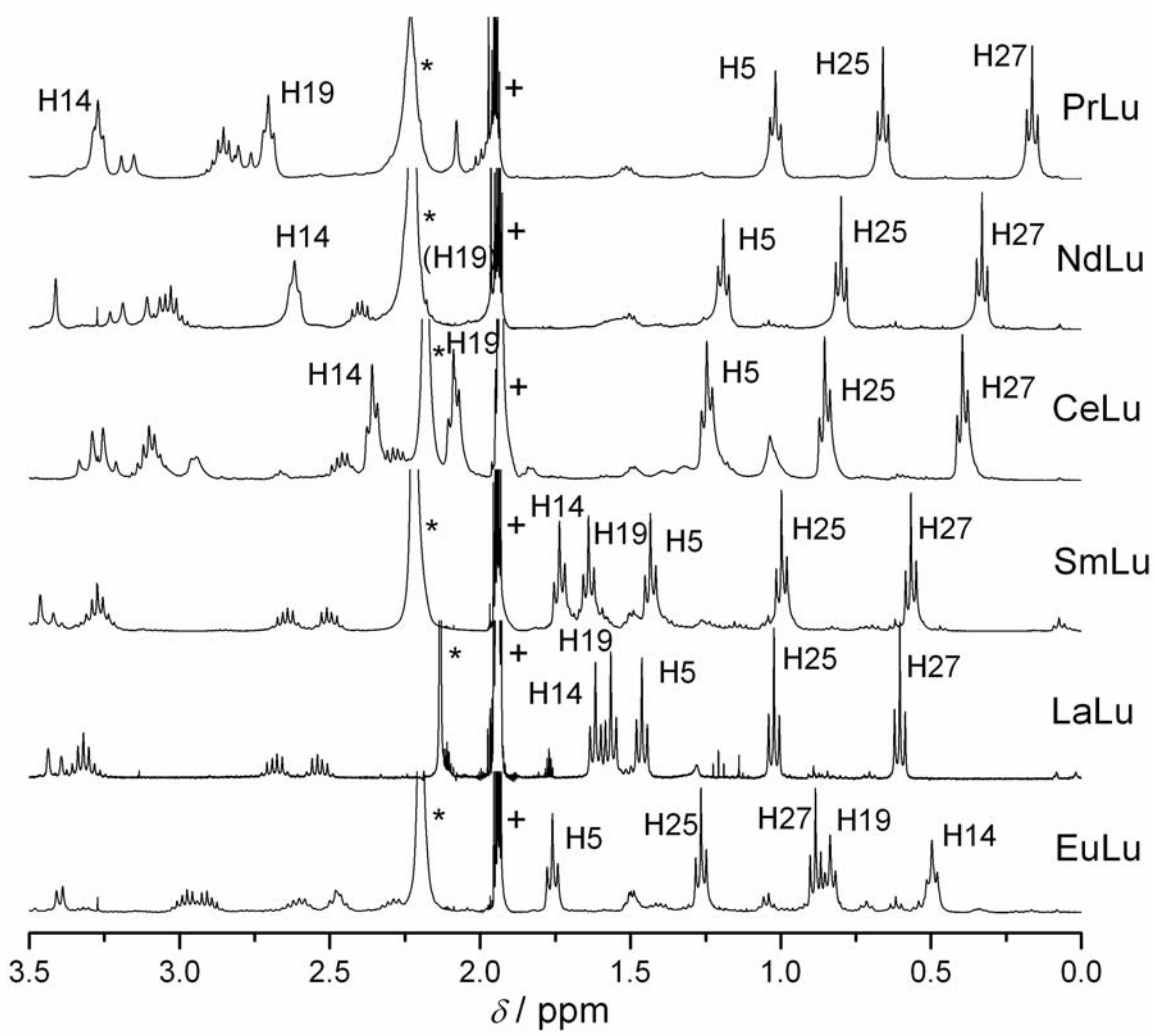

Figure 21 Methyl NMR signals of some L^{AB} complexes (* = H_2O; + = solvent)

A closer inspection reveals that the shifts are far from being random in sign and magnitude. This observation suggests that the phenomenon can be described with a simple model and in fact it can.[83]

The lanthanide induced paramagnetic shift of a proton, Hi, in a compound with one paramagnetic lanthanide ion Ln_j can be obtained by subtracting the chemical shift of a suitable isostructural diamagnetic reference compound from the measured chemical shift and is the sum of the contact (through chemical bonds) and pseudo contact (dipolar; through space) contributions:

$$\Delta_{i,j} = \delta_{i,j} - \delta_{i,dia} = \Delta_c + \Delta_{pc} \qquad (1)$$

For a compound with at least a threefold axis this can be expressed rather simply as

$$_{i,j} = F_i \langle S_z \rangle_j + C_j B_0^2 G_i \qquad (2)$$

where the first term is the contact and the second term the pseudo-contact term, respectively. Both terms depend on parameters characteristic of the paramagnetic Ln ion (the spin expectation value $<S_Z>_j$, the second-order magnetic axial anisotropy value for the free ion C_j, and the ligand field parameter B_0^2) and of the Hi nucleus (the hyperfine coupling constant F_i and the geometric factor G_i ($= (3\cos^2\theta_i - 1)/r_i^3$). In the latter, r_i is the Ln···H_i distance between the proton and the paramagnetic lanthanide ion and θ_i the angle between the Ln···H_i vector and the molecular axis, which in the complexes investigated here is taken as the Ln-Ln vector. Values of $<S_Z>_j$ and C_j (scaled to -100 for Dy) have been calculated theoretically at room temperature and can be found in the literature.[84,85,86,87] The values are given in Table 22.

Table 22 Values of $\langle S_z \rangle_j$ and C_j

	$\langle S_z \rangle_j$	C_j
Ce	-0.974	-6.3
Pr	-2.956	-11
Nd	-4.452	-4.2
Sm	0.224	-0.7
Eu	7.5	4
Tb	31.853	-86
Dy	28.565	-100
Ho	22.642	-39
Er	15.382	33
Tm	8.21	53
Yb	2.589	22

The experimental data can be treated in different ways. In the following chapters three distinct approaches will be examined and compared:

- The one proton (Reilley) method (Chapter 5.3; page 93) is a simple way to separate contact and pseudo contact contributions to the lanthanide induced shift. It is easily extended to complexes including two paramagnetic lanthanide ions. It is, however, based on the not necessarily valid assumption that the crystal field parameter B_0^2 is the same for all lanthanides.
- The two proton (Geraldes) method (Chapter 5.6; page 175) eliminates the crystal field parameter problem associated with the one proton analysis and yields structural parameters that can be used to compare solution structure to the structure of a complex in the solid state. The disadvantage of this approach is that it gives no information regarding the contact term.
- The modified one proton method that we propose (Chapter 5.7; page 223) introduces a novel approach to circumventing the crystal field parameter problem while still not loosing contact term information. Also, the variation of the crystal field parameter (discarded in the two proton method) can be examined.

5.2 Results

5.2.1 NMR spectra

Three series of complexes were measured for each ligand:

$[Ln_2(L)_3]^{6+}$ (Ln = La, Ce, Pr, Nd, Sm, Eu, Y, Lu)

$[LaLn(L)_3]^{6+}$ (Ln = Ce, Pr, Nd, Sm, Eu) in which the La ion is in the bpb site

$[LnLu(L)_3]^{6+}$ (Ln = La, Ce, Pr, Nd, Sm, Eu) in which the Lu ion is in the bpa site

All complexes were investigated in deuterated acetonitrile (CD_3CN) solution ($c \approx 10^{-2}$ M) by means of ^{1}H NMR spectroscopy at 400 MHz. In addition to 1D spectra, 2D spectra (COSY and ROESY) have also been measured.

Spectra of some diamagnetic complexes are given in Figure 22 - Figure 24. Paramagnetic homobimetallic $Ln_2(L)_3$ spectra are shown in Figure 25 - Figure 29. Finally, Figure 30 - Figure 37 contain spectra of mixed diamagnetic/paramagnetic complexes ($LaLn(L)_3$ and $LnLu(L)_3$).

The number of signals of the *HHH* isomers in the spectra corresponds to the expected number for one ligand, meaning that the three ligand strands are equivalent and that the solution structure has (possibly time-averaged) C_3 symmetry. The only slightly unusual feature is the diastereotopic signals of all the CH_2 groups, which appear as two doublets ($^2J \approx 15$ Hz, H9/H9') and two pseudo sextets (H4/H4', H13/H13', H18/H18', H24/H24', H26/H26'). The pseudo sextets are in fact doublets of quartets with $^2J \approx 2 \cdot {}^3J$. Also worth mentioning is the NOE observed between pyridine protons and nearby CH_2 protons indicating that the conformation of the pyridine has changed compared to that found in the free ligand where this coupling is absent. This is in accordance with the structure of the ligand being so that the ligator atoms (5xN + O) are turned towards the lanthanide ions, which differs from the structure of the free ligand in solution, where the pyridine N atom is in a transoid conformation relative to the neighbouring pair of ligator atoms.

All expected intrastrand NOE were observed: H3-H4/H4', H3-H5, H4/H4'-H6, H5-H6, H7-H9/H9', H8-H9', H9/H9'-H11, H12-H13/H13', H12-H14, H13/H13'-H15, H14-H15, H17-H18/H18', H17-H19, H18/H18'-H20, H19-H20, H24/H24'-H1, H24/H24'-H26/H26',

H24/H24'-H27 and H25-H26/H26'. When compared to the solid state structures, these interactions correspond to H-H distances of less than 3 Å.

It is perhaps worth noting that that the observed NOE involving diastereotopic methylene protons of the ethyl groups are similar for both protons. For example, H4 and H4' both interact with H3 with the same magnitude (as far as can be observed in the spectra). This is an indication of a certain freedom of movement, not necessarily free rotation of the ethyl group, but at least some degree of wriggling. The absence of totally free rotation is deducted from the observed interstrand NOE: H4'-H11, H6-H14 and H7-H14 (all corresponding to distances less than 3 Å in the solid state structures) are seen in several spectra whereas H5-H11, H6-H13/H13' and H7-H13/H13' (distances of about 5 Å) are absent. The general "pointing direction" of these two ethyl groups in the solid state seems to be replicated in the solution structure of the complexes.

A different behaviour is observed for H9 and H9', which in some spectra exhibit asymmetric coupling (H7-H9, H8-H9', H9'-H11), in agreement with the expected greater rigidity of the bridging group in comparison to the ethyl groups. The absence of interaction between H9/H9' and H10 is further evidence of loss of free rotation around the bridging methylene group as is observed for the free ligand in solution.

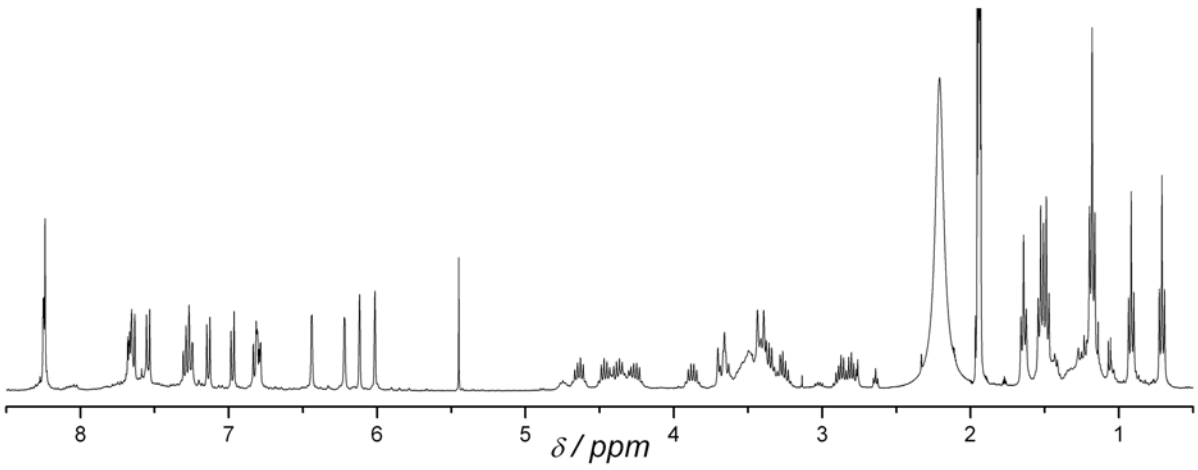

Figure 22 ^{1}H NMR spectrum of $La_2(L^{AB4})_3$

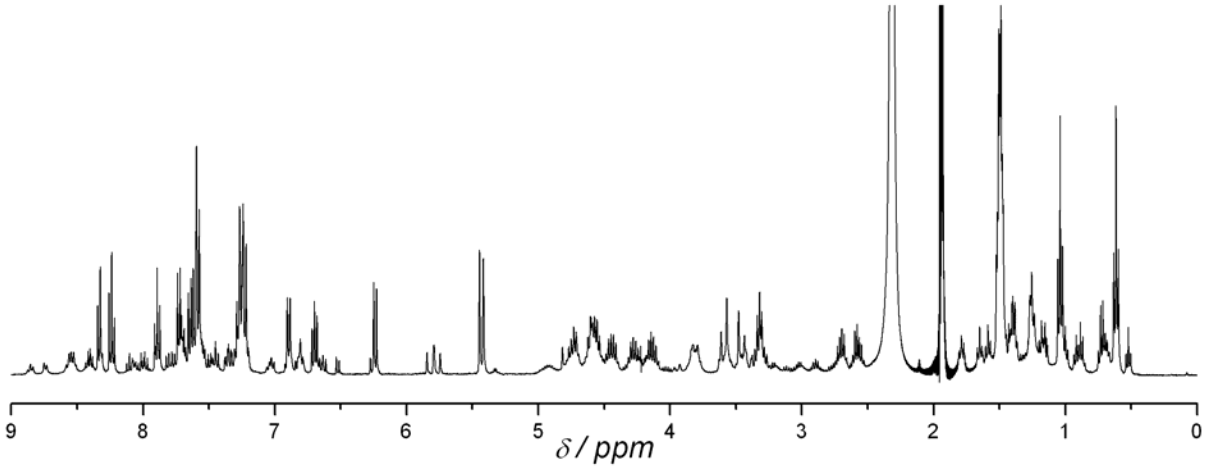

Figure 23 ^{1}H NMR spectrum of $Lu_2(L^{AB})_3$

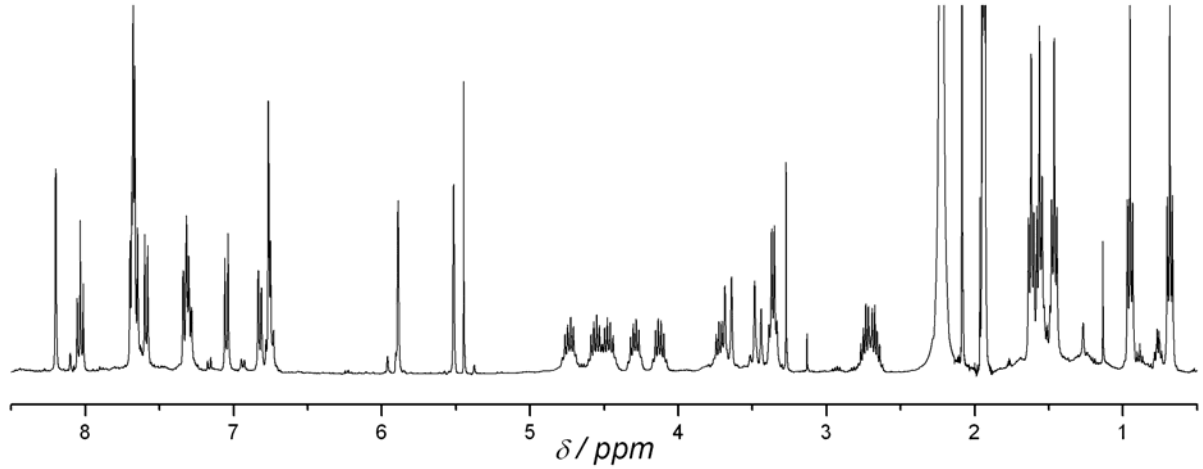

Figure 24 ^{1}H NMR spectrum of $LaLu(L^{AB3})_3$

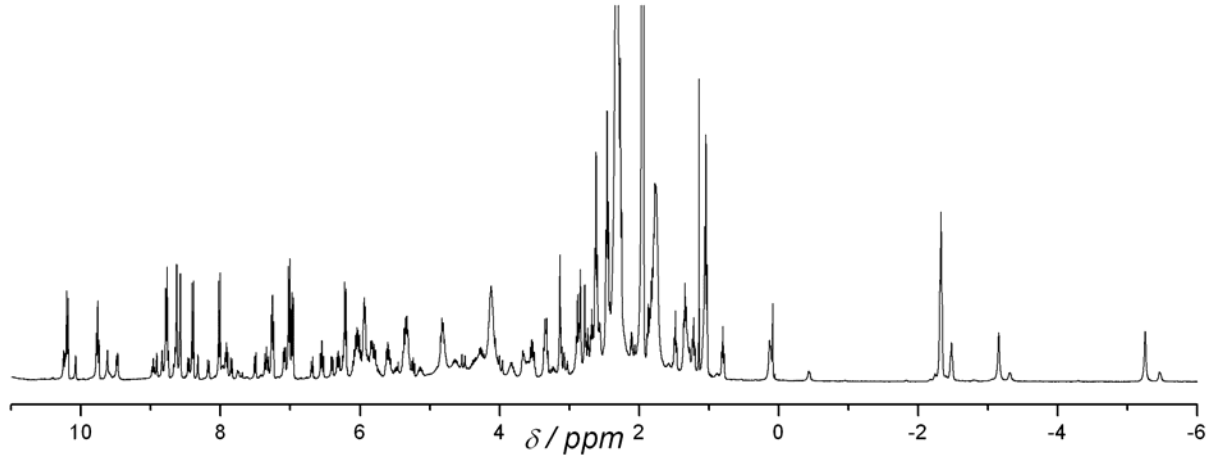

Figure 25 ^{1}H NMR spectrum of $Ce_2(L^{AB4})_3$

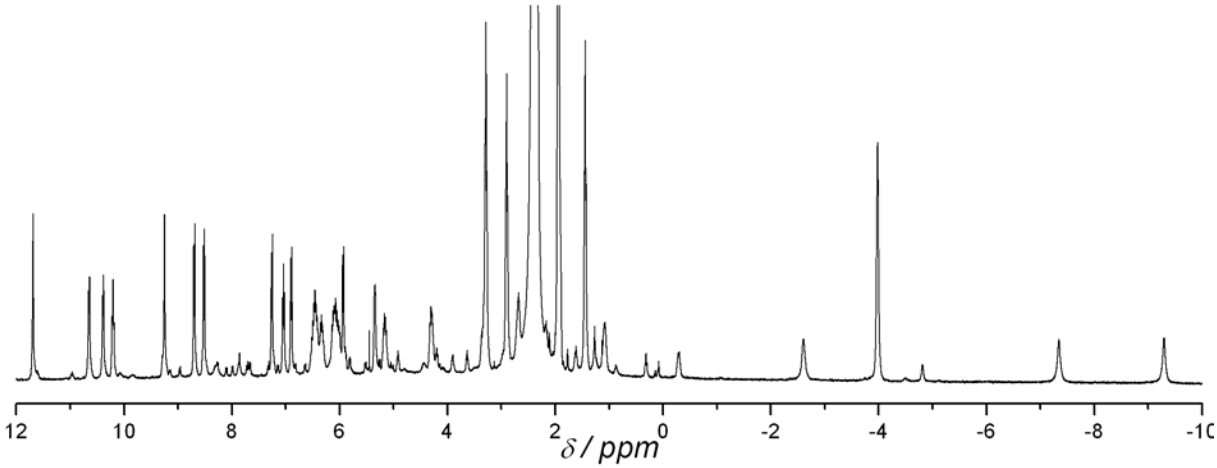

Figure 26 ^{1}H NMR spectrum of $Pr_2(L^{AB3})_3$

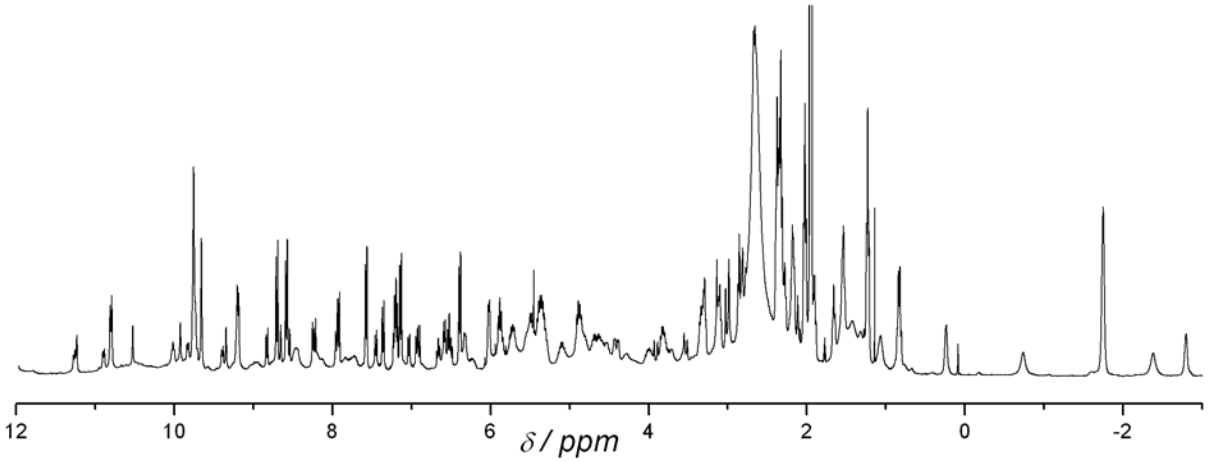

Figure 27 ^{1}H NMR spectrum of $Nd_2(L^{AB5})_3$

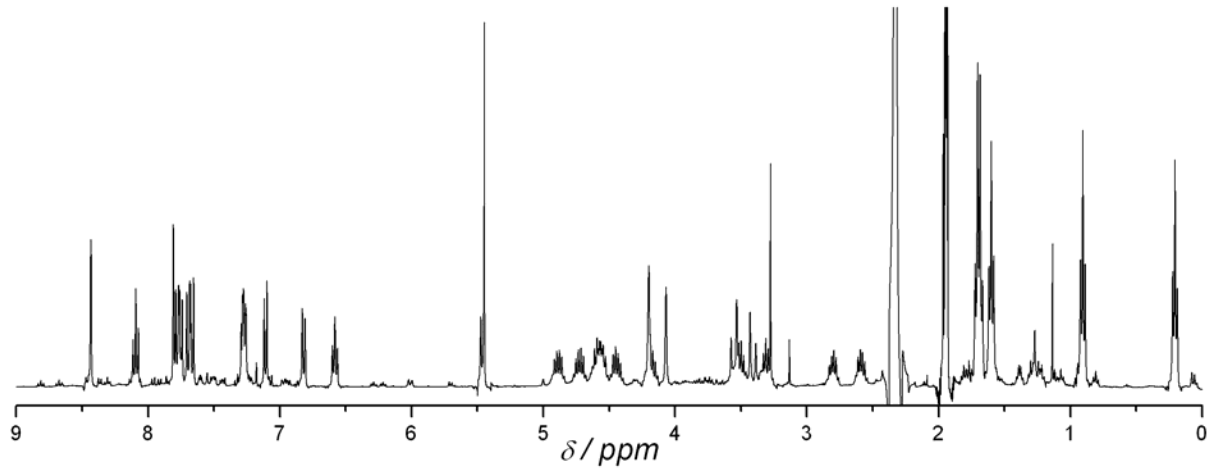

Figure 28 ^{1}H NMR spectrum of $Sm_2(L^{AB3})_3$

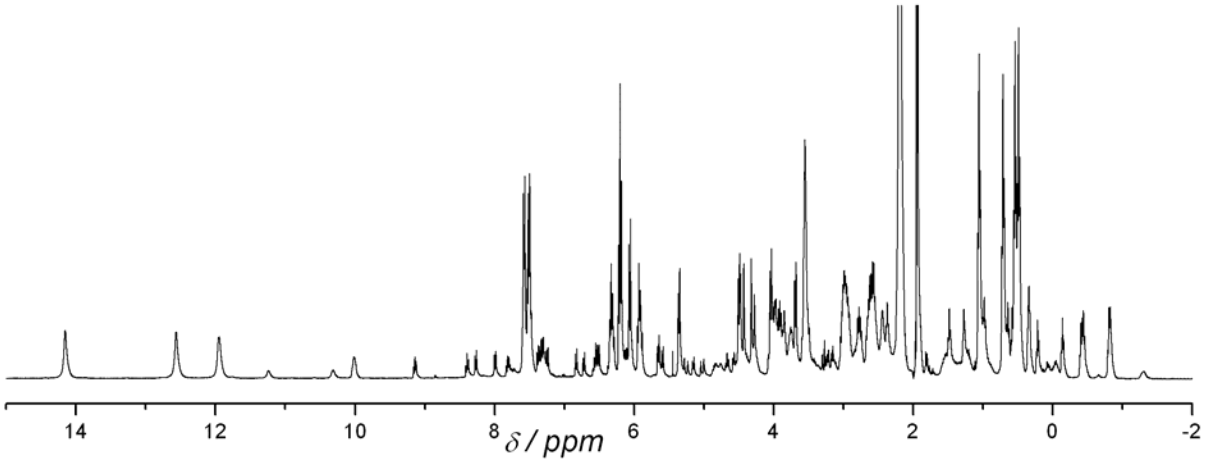

Figure 29 ^{1}H NMR spectrum of $Eu_2(L^{AB})_3$

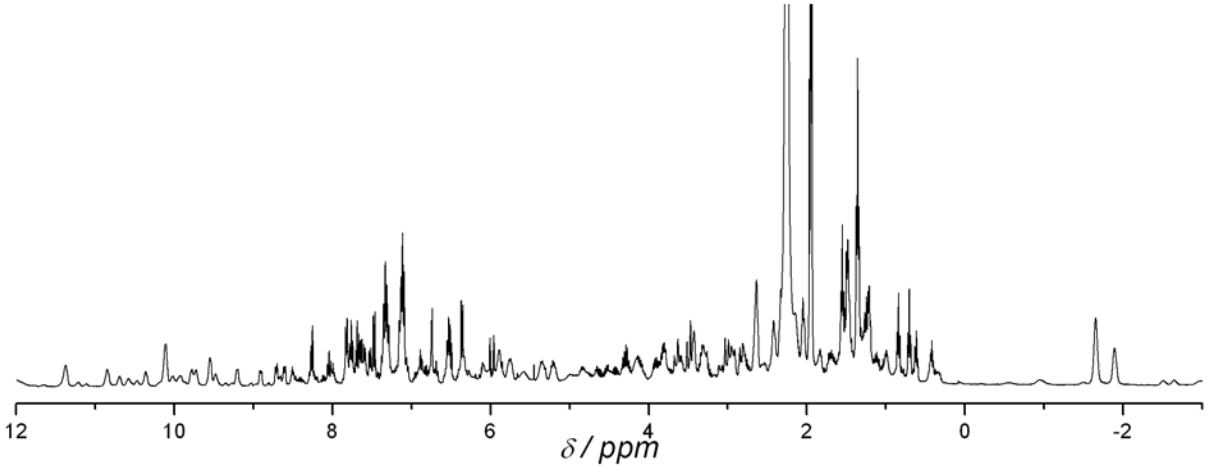

Figure 30 ^{1}H NMR spectrum of $LaNd(L^{AB})_3$

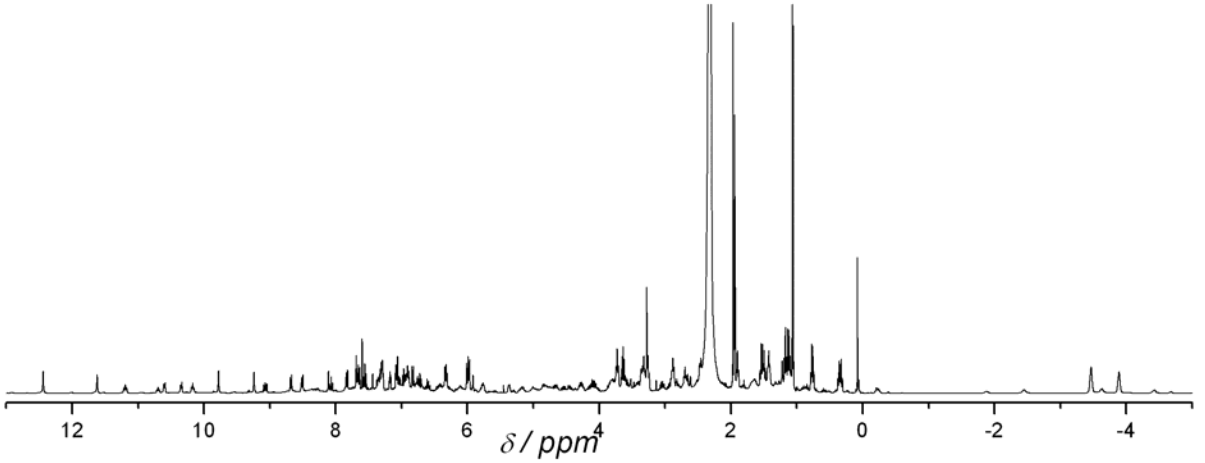

Figure 31 ^{1}H NMR spectrum of $LaPr(L^{AB3})_3$

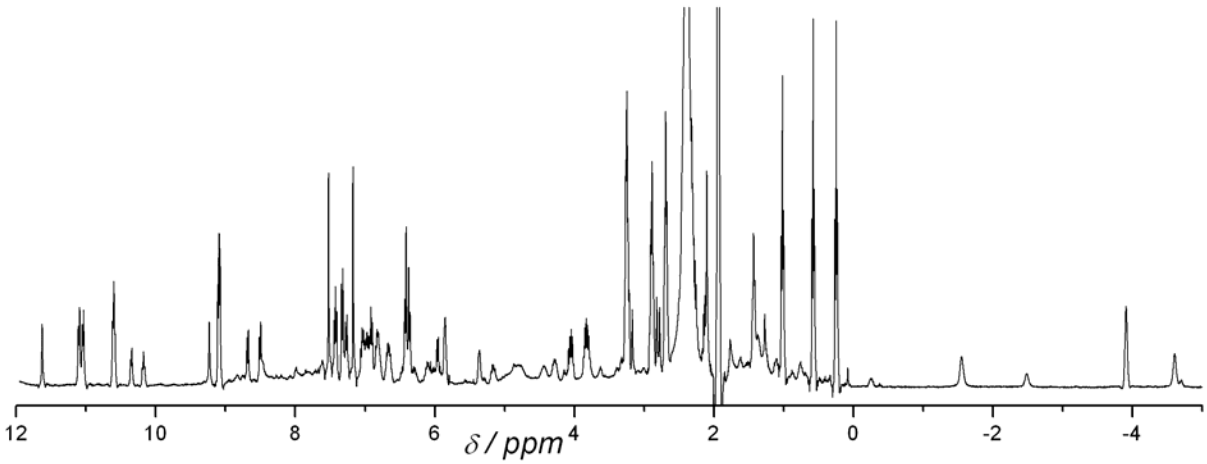

Figure 32 ^{1}H NMR spectrum of PrLu(L^{AB3})$_3$

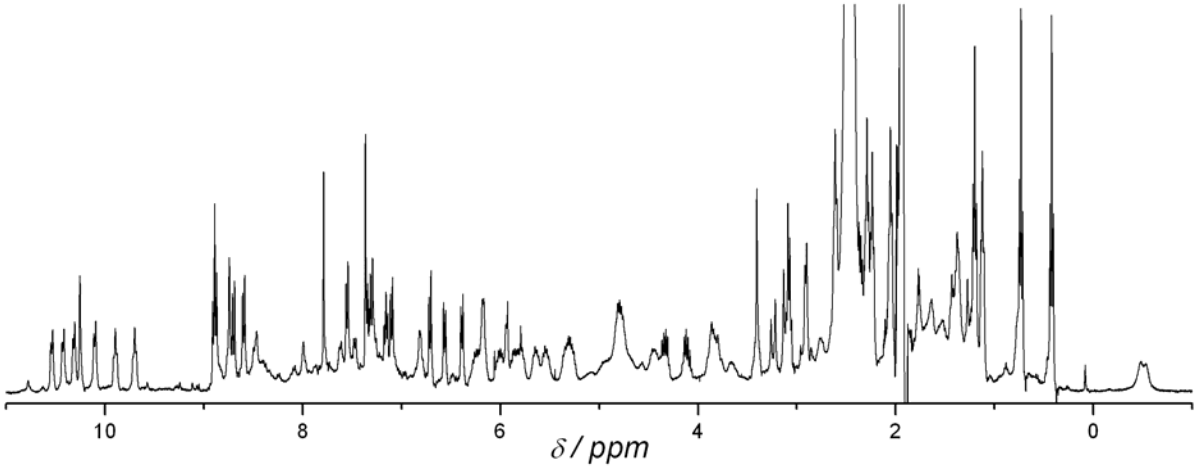

Figure 33 ^{1}H NMR spectrum of NdLu(L^{AB3})$_3$

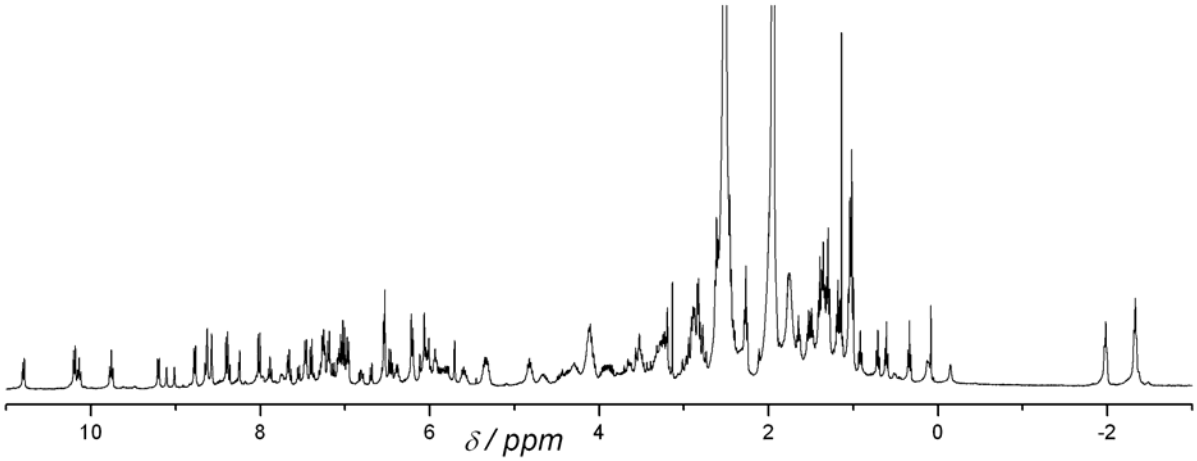

Figure 34 ^{1}H NMR spectrum of LaCe(L^{AB4})$_3$

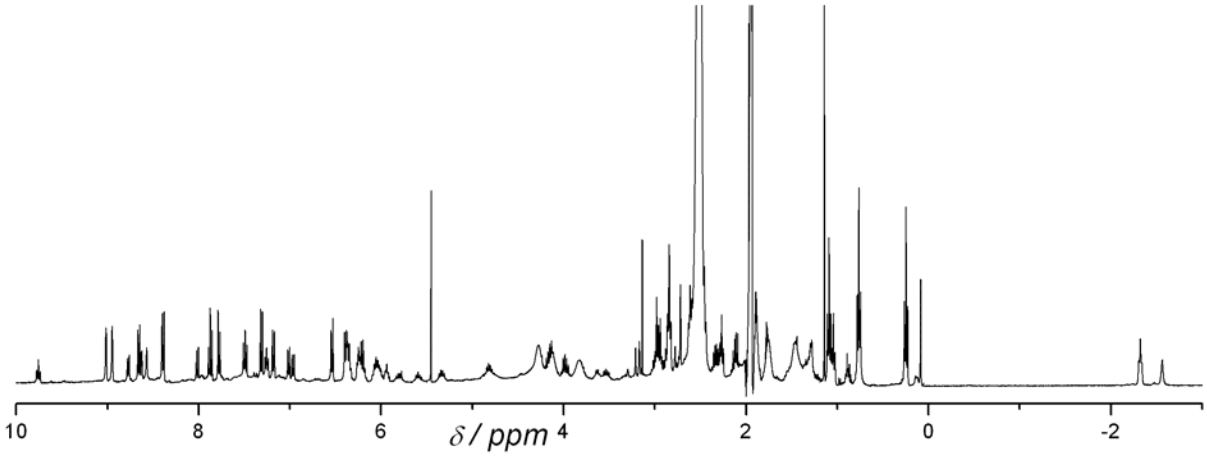

Figure 35 ^{1}H NMR spectrum of CeLu(L^{AB4})$_3$

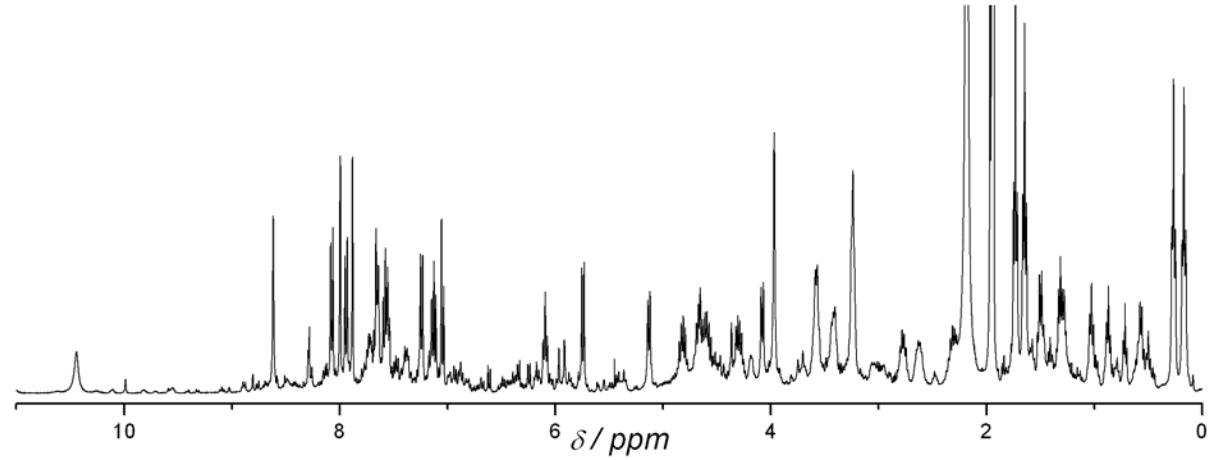

Figure 36 ^{1}H NMR spectrum of LaEu(L^{AB5})$_3$

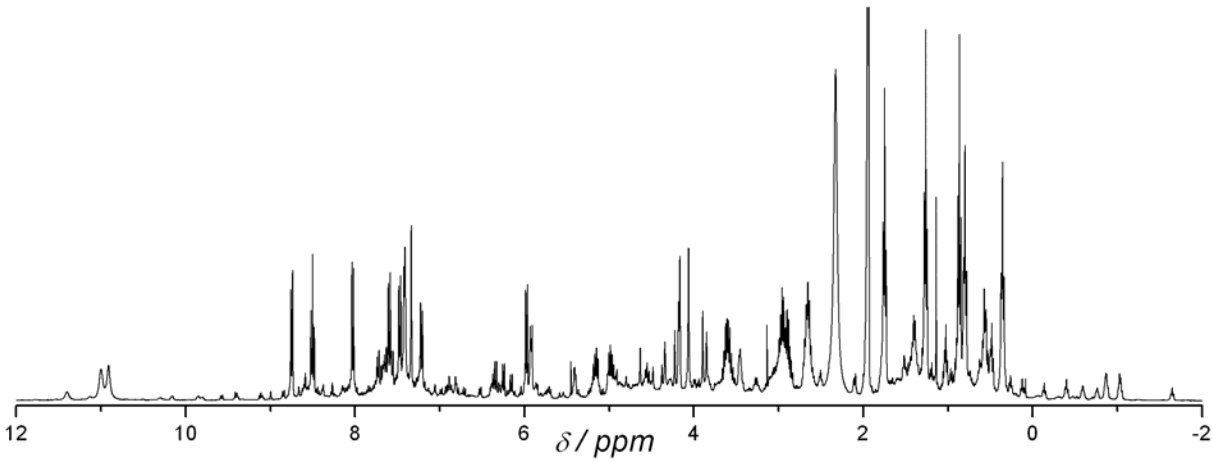

Figure 37 ^{1}H NMR spectrum of EuLu(L^{AB5})$_3$

5.2.2 Chemical shifts

The assignment of the spectra has not been straightforward, but has been aided by the large number of complexes measured.

The homobimetallic complexes are relatively simple since the only two species present in the solution are the *HHH* and *HHT* isomers with the former being dominant for complexes of L^{AB}, L^{AB3}, L^{AB4} and L^{AB5}. With the aid of COSY and ROESY spectra as well as application of LIS theory to the final values they were easily assigned. It helped that the spectra of L^{AB}, L^{AB3} and L^{AB5} complexes are so similar (with the exception of the protons close to the Cl substituents in the two latter). The large proportion of *HHT* isomer in the solutions of the complexes of L^{AB2} unfortunately made it impossible to assign the spectra due to the large number of lines of comparable intensity. The complexes therefore had to be left out of the analysis of lanthanide induced shifts.

Due to the large size difference of the two lanthanide ions the LnLu spectra contain only relatively small amounts of homobimetallic complexes and were therefore also not too difficult to assign. Finally, the spectra of the LaLn complexes were the most complicated. Apart from homobimetallic complexes the solutions also contained varying amounts of LnLa, depending on the relative sizes of Ln and La, with Ln = Ce being the most critical. In some cases the complex of interest was only present in a 25 % amount. However, in combination with the other spectra, the LaLn spectra could be assigned assuming that (Ln_2) = (Ln in bpa) + (Ln in bpb). In other words the lanthanide induced paramagnetic shifts of two lanthanides in the same complex are additive. As a last control all data were checked using the following criteria: the chemical shift value of a given proton should be approximately the same for complexes of the same pair of lanthanide ions with two different ligands (e.g. $LaCe(L^{AB})_3$ and $LaCe(L^{AB3})_3$) since it was found to be so for the "easily" assigned spectra. Only the complexes of L^{AB4} seemed to deviate significantly. Plots according to one proton (Reilley) model (*vide infra*) should be (at least approximately) linear. Finally, the slopes of the two proton (Geraldes) plots (*vide infra*) should be comparable to the values calculated from the solid state structures – or rather, if they are not it could be indicative of a wrong assignment. Comparing with the solid state structures using the Geraldes plots have also been the method used to assign the diastereotopic methylene group protons H4/H4', H9/H9', H13/H13', H18/H18', H24/H24' and H26/H26' (which one is HX and which one is HX').

The final assignment of the spectra is given in Table 23 - Table 30. For the proton numbering of the ligands see Chart 14 (page 37).

Table 23 Chemical shift values of diamagnetic complexes of L^{AB} and L^{AB3}

	L^{AB}				L^{AB3}			
	LaLu	La_2	Y_2	Lu_2	LaLu	La_2	Y_2	Lu_2
H1	7.73	7.69	7.73	7.73	7.67	7.68	7.69	7.67
H2	8.25	8.25	8.25	8.23				
H3	8.35	8.26	8.32	8.32	8.20	8.10	8.19	8.21
H4	4.46	4.42	4.56	4.60	4.47	4.44	4.58	4.59
H4'	4.70	4.62	4.73	4.73	4.73	4.67	4.77	4.78
H5	1.46	1.50	1.51	1.50	1.46	1.49	1.51	1.50
H6	7.03	7.12	7.20	7.22	7.05	7.17	7.22	7.27
H7	6.79	6.88	6.89	6.89	6.82	6.94	6.93	6.94
H8	5.60	5.96	5.54	5.42	5.52	5.91	5.49	5.38
H9	3.42	3.45	3.47	3.46	3.46	3.49	3.50	3.50
H9'	3.64	3.65	3.61	3.59	3.66	3.68	3.64	3.63
H10	5.93	6.01	5.56	5.45	5.89	5.96	5.49	5.38
H11	7.31	7.30	7.27	7.25	7.33	7.31	7.29	7.27
H12	7.66	7.63	7.65	7.60	7.67	7.64	7.65	7.63
H13	4.28	4.26	4.42	4.43	4.29	4.28	4.44	4.46
H13'	3.69	3.72	4.06	4.13	3.71	3.76	4.09	4.16
H14	1.61	1.54	1.53	1.51	1.62	1.53	1.54	1.53
H15	7.57	7.60	7.60	7.57	7.59	7.64	7.61	7.60
H16	8.02	8.05	7.92	7.89	8.03	8.06	7.93	7.90
H17	7.64	7.65	7.60	7.57	7.65	7.66	7.63	7.61
H18	4.10	4.11	4.27	4.27	4.13	4.12	4.27	4.29
H18'	4.55	4.54	4.56	4.56	4.56	4.54	4.58	4.59
H19	1.55	1.54	1.51	1.50	1.56	1.54	1.51	1.50
H20	7.68	7.67	7.66	7.65	7.69	7.67	7.66	7.65
H21	7.29	7.29	7.28	7.28	7.29	7.30	7.28	7.28
H22	6.75	6.74	6.71	6.70	6.76	6.74	6.72	6.71
H23	6.75	6.74	6.36	6.24	6.75	6.73	6.34	6.24
H24	3.30	3.35	3.32	3.33	3.36	3.41	3.35	3.36
H24'	3.30	3.23	3.32	3.33	3.36	3.31	3.35	3.36
H25	1.02	0.84	1.01	1.04	0.95	0.76	0.92	0.97
H26	2.53	2.75	2.65	2.59	2.68	2.81	2.76	2.71
H26'	2.68	2.84	2.72	2.71	2.73	2.94	2.76	2.77
H27	0.60	0.70	0.64	0.62	0.68	0.77	0.71	0.69

Table 24 Chemical shift values of diamagnetic complexes of L^{AB4} and L^{AB5}

	L^{AB4}			L^{AB5}			
	LaLu	La_2	Lu_2	LaLu	La_2	Y_2	Lu_2
H1	7.73	7.67	7.73	7.76	7.71	7.75	7.75
H2	8.24	8.24	8.23	8.27	8.28	8.27	8.26
H3	8.36	8.24	8.33	8.38	8.28	8.36	8.37
H4	4.52	4.46	4.60	4.51	4.47	4.61	4.67
H4'	4.72	4.64	4.73	4.76	4.68	4.76	4.78
H5	1.46	1.49	1.51	1.47	1.51	1.52	1.51
H6	7.05	7.14	7.21	7.06	7.16	7.22	7.25
H7	6.72	6.80	6.81	6.84	6.93	6.91	6.92
H8	5.64	6.02	5.52	5.55	5.97	5.51	5.41
H9	3.38	3.41	3.39	3.45	3.47	3.49	3.49
H9'	3.67	3.69	3.63	3.70	3.72	3.67	3.66
H10	6.03	6.12	5.60	5.91	5.91	5.52	5.41
H11	7.27	7.26	7.21	7.40	7.38	7.38	7.35
H12	7.60	7.54	7.55	7.70	7.67	7.71	7.70
H13	4.31	4.26	4.36	4.29	4.26	4.49	4.51
H13'	3.67	3.66	3.96	3.88	3.94	4.24	4.29
H14	1.69	1.64	1.58	1.43	1.31	1.44	1.44
H15	6.21	6.22	6.21	7.50	7.56	7.52	7.51
H17	6.44	6.44	6.33	7.53	7.54	7.48	7.47
H18	3.89	3.88	4.08	4.25	4.28	4.35	4.37
H18'	4.30	4.38	4.47	4.53	4.52	4.57	4.58
H19	1.54	1.53	1.52	1.51	1.49	1.48	1.47
H20	7.66	7.65	7.61	7.72	7.69	7.72	7.70
H21	7.29	7.29	7.26	7.39	7.38	7.34	7.35
H22	6.82	6.82	6.76	6.88	6.88	6.82	6.80
H23	6.99	6.98	6.48	6.68	6.61	6.31	6.19
H24	3.33	3.35	3.33	3.33	3.37	3.33	3.35
H24'	3.33	3.25	3.33	3.38	3.27	3.33	3.35
H25	1.06	0.92	1.05	1.05	0.87	1.02	1.06
H26	2.57	2.81	2.59	2.55	2.77	2.63	2.60
H26'	2.71	2.88	2.72	2.70	2.84	2.70	2.72
H27	0.61	0.71	0.62	0.62	0.72	0.64	0.63
H28	3.49	3.51	3.40				
H28'	3.42	3.42	3.40				
H29	1.18	1.18	1.10				

Table 25 Chemical shift values of paramagnetic Ln_2 complexes of L^{AB} and L^{AB3}

	L^{AB}					L^{AB3}				
	Ce_2	Pr_2	Nd_2	Sm_2	Eu_2	Ce_2	Pr_2	Nd_2	Sm_2	Eu_2
H1	8.98	9.82	9.19	7.87	5.35	8.64	9.25	8.75	7.81	6.04
H2	10.01	10.92	9.76	8.49	6.33					
H3	10.65	12.31	10.81	8.63	4.49	10.20	11.69	10.29	8.73	5.04
H4	4.99	5.34	4.84	4.60	4.00	4.90	5.16	4.78	4.60	4.10
H4'	5.59	6.24	5.34	4.86	3.90	5.54	6.11	5.29	4.89	4.13
H5	2.67	3.34	2.32	1.72	0.49	2.63	3.28	2.30	1.70	0.53
H6	7.17	7.30	7.54	7.09	6.21	7.18	7.26	7.54	7.11	6.25
H7	6.35	5.96	6.37	6.78	7.50	6.39	5.93	6.37	6.82	7.57
H8	-1.94	-7.81	-0.88	4.05	12.56	-1.62	-7.35	-0.63	4.07	12.02
H9	2.84	2.38	2.84	3.37	4.29	2.88	2.43	2.86	3.40	4.32
H9'	3.13	2.54	2.95	3.53	4.45	3.09	2.43	2.92	3.55	4.53
H10	-2.06	-9.59	-2.85	4.17	14.15	-1.77	-9.30	-2.72	4.20	13.86
H11	7.09	6.93	7.12	7.27	7.57	7.08	6.90	7.10	7.27	7.60
H12	7.91	8.51	8.59	7.69	6.19	7.90	8.52	8.61	7.70	6.19
H13	4.99	6.40	5.88	4.72	2.62	5.03	6.44	5.88	4.73	2.61
H13'	4.67	6.03	5.34	4.43	2.55	4.66	6.02	5.36	4.44	2.57
H14	2.09	2.85	2.40	1.67	0.71	2.11	2.90	2.44	1.69	0.69
H15	8.51	10.33	10.08	7.76	4.04	8.54	10.39	10.13	7.78	4.01
H16	9.00	10.19	9.70	8.09	5.92	9.00	10.20	9.72	8.09	5.91
H17	8.71	10.63	10.32	7.73	3.68	8.71	10.65	10.35	7.75	3.66
H18	4.99	6.30	5.55	4.16	2.78	5.01	6.33	5.56	4.16	2.76
H18'	5.26	6.46	6.02	4.55	2.98	5.25	6.49	6.03	4.56	2.93
H19	1.84	2.29	2.04	1.59	1.05	1.86	2.33	2.06	1.60	1.03
H20	8.02	8.67	8.69	7.65	6.06	8.03	8.70	8.71	7.66	6.04
H21	7.10	7.01	7.12	7.27	7.51	7.12	7.04	7.16	7.28	7.50
H22	6.01	5.31	5.89	6.57	7.57	6.05	5.35	5.93	6.58	7.56
H23	2.59	-2.74	1.33	5.45	11.94	2.40	-2.61	1.13	5.46	11.87
H24	3.76	4.28	3.79	3.40	2.57	3.84	4.30	3.86	3.49	2.74
H24'	3.07	3.14	3.30	3.25	3.02	3.22	3.34	3.39	3.30	3.04
H25	1.18	1.52	1.20	0.99	0.54	1.09	1.44	1.13	0.91	0.40
H26	1.53	0.85	1.85	2.51	3.75	1.69	1.09	2.10	2.59	3.66
H26'	2.59	2.43	2.58	2.66	2.92	2.81	2.68	2.75	2.81	3.02
H27	-2.24	-4.42	-1.85	0.07	3.55	-1.88	-3.98	-1.58	0.21	3.38

Table 26 Chemical shift values of paramagnetic Ln_2 complexes of L^{AB4} and L^{AB5}

	L^{AB4}					L^{AB5}				
	Ce_2	Pr_2	Nd_2	Sm_2	Eu_2	Ce_2	Pr_2	Nd_2	Sm_2	Eu_2
H1	8.77	9.53	9.05	7.81	5.57	8.97	9.79	9.19	7.88	5.39
H2	9.76	10.56	9.58	8.42	6.57	9.99	10.88	9.75	8.50	6.36
H3	10.20	11.65	10.48	8.52	4.93	10.61	12.25	10.82	8.65	4.53
H4	4.82	5.07	4.71	4.56	4.17	4.99	5.32	4.88	4.70	4.08
H4'	5.34	5.91	5.17	4.81	4.25	5.63	6.28	5.38	4.93	3.96
H5	2.46	3.05	2.18	1.67	0.71	2.66	3.34	2.33	1.72	0.47
H6	7.01	7.04	7.39	7.03	6.42	7.20	7.30	7.57	7.12	6.24
H7	6.21	5.75	6.21	6.66	7.52	6.38	5.93	6.39	6.81	7.57
H8	-3.16	-9.95	-1.91	3.94	14.17	-1.54	-7.75	-0.74	4.13	12.34
H9	2.75	2.10	2.74	3.29	4.26	2.85	2.33	2.83	3.39	4.36
H9'	2.86	2.27	2.78	3.49	4.85	3.17	2.57	3.01	3.60	4.51
H10	-5.26	-14.68	-5.39	3.38	18.65	-1.85	-8.81	-2.38	4.17	13.57
H11	6.97	6.68	6.95	7.19	7.65	7.13	6.88	7.14	7.35	7.73
H12	8.01	8.64	8.61	7.63	5.93	7.88	8.39	8.58	7.72	6.33
H13	5.93	7.56	6.48	4.26	1.43	4.94	6.18	5.73	4.70	3.05
H13'	5.59	7.56	6.04	4.68	1.02	4.68	5.81	5.33	4.48	2.95
H14	2.61	3.51	2.75	1.86	0.34	2.02	2.86	2.38	1.55	0.54
H15	8.57	11.25	9.97	6.65	0.84	8.21	9.81	9.66	7.62	4.61
H17	8.63	11.12	9.97	6.80	1.14	8.32	9.95	9.76	7.61	4.32
H18	6.02	7.79	6.39	4.52	1.12	4.94	6.12	5.35	4.31	2.95
H18'	6.05	8.08	6.68	4.81	1.51	5.12	6.24	5.87	4.58	3.24
H19	2.27	2.93	2.37	1.70	0.64	1.83	2.30	2.02	1.57	1.02
H20	8.40	9.23	8.95	7.74	5.70	8.02	8.61	8.70	7.72	6.15
H21	7.25	7.23	7.25	7.28	7.42	7.17	7.03	7.20	7.35	7.63
H22	5.93	5.07	5.87	6.58	7.97	6.15	5.41	6.02	6.68	7.66
H23	0.12	-6.03	-0.52	5.11	15.44	2.60	-2.24	1.32	5.47	11.46
H24	3.53	3.95	3.66	3.46	2.83	3.77	4.28	3.82	3.45	2.60
H24'	2.86	2.81	3.17	3.22	3.24	3.08	3.11	3.33	3.28	3.04
H25	1.04	1.26	1.11	0.99	0.77	1.20	1.51	1.23	1.01	0.57
H26	1.33	0.47	1.72	2.49	4.03	1.58	0.87	1.93	2.53	3.72
H26'	2.33	2.05	2.44	2.64	3.26	2.60	2.45	2.65	2.69	2.95
H27	-2.33	-4.57	-1.91	0.06	3.64	-2.15	-4.31	-1.75	0.10	3.49
H28	4.12	4.79	4.15	3.56	2.75					
H28'	4.12	4.79	4.15	3.63	2.53					
H29	1.73	2.34	1.87	1.28	0.27					

Table 27 Chemical shift values of paramagnetic LnLn' complexes of L^{AB}

	LaCe	LaPr	LaNd	LaEu	CeLu	PrLu	NdLu	SmLu	EuLu
H1	9.21	10.33	9.55	5.04	7.50	7.22	7.42	7.68	8.03
H2	10.22	11.39	10.11	6.01	8.03	7.81	7.98	8.20	8.51
H3	10.98	13.08	11.37	3.96	8.03	7.67	7.93	8.27	8.75
H4	5.27	5.92	5.21	3.47	4.17	3.83	4.12	4.47	4.95
H4'	5.89	6.90	5.76	3.47	4.39	4.03	4.30	4.64	5.14
H5	2.88	3.78	2.64	0.15	1.25	1.01	1.19	1.43	1.76
H6	7.41	7.82	7.82	5.70	6.75	6.43	6.71	7.07	7.57
H7	6.50	6.29	6.54	7.19	6.60	6.36	6.55	6.80	7.16
H8	-0.20	-4.10	1.48	10.54	3.98	2.07	3.41	5.17	7.57
H9	2.93	2.58	3.02	3.91	3.31	3.16	3.21	3.44	3.81
H9'	3.52	3.45	3.50	3.93	3.24	2.77	3.09	3.54	4.16
H10	2.85	0.95	3.42	8.78	1.04	-4.70	-0.53	4.58	11.48
H11	7.08	6.89	7.12	7.55	7.31	7.33	7.30	7.31	7.33
H12	7.28	7.00	7.34	8.03	8.26	9.12	8.89	7.72	5.83
H13	3.83	3.58	3.91	4.66	5.43	7.01	6.20	4.63	2.29
H13'	3.27	2.94	3.31	4.12	5.06	6.75	5.69	4.24	2.20
H14	1.27	1.10	1.36	1.85	2.36	3.26	2.62	1.73	0.49
H15	7.08	6.71	7.15	8.07	8.97	11.11	10.46	7.80	3.58
H16	7.71	7.49	7.76	8.34	9.28	10.66	9.93	8.13	5.66
H17	7.25	7.02	7.32	8.00	9.03	11.16	10.58	7.82	3.40
H18	3.74	3.52	3.81	4.47	5.30	6.87	5.82	4.47	2.47
H18'	4.23	4.03	4.30	4.85	5.57	7.01	6.29	4.77	2.60
H19	1.30	1.15	1.36	1.79	2.09	2.70	2.25	1.64	0.83
H20	7.42	7.26	7.47	7.92	8.29	9.12	8.92	7.74	5.83
H21	7.07	6.93	7.11	7.50	7.35	7.42	7.34	7.30	7.33
H22	6.46	6.27	6.51	7.01	6.35	5.84	6.17	6.63	7.33
H23	6.26	5.97	6.35	7.19	2.96	-1.72	1.55	5.58	11.48
H24	4.00	4.82	4.13	2.26	3.09	2.85	3.03	3.27	3.59
H24'	3.28	3.63	3.59	2.72					
H25	1.37	1.95	1.48	0.21	0.86	0.65	0.80	0.99	1.26
H26	1.77	1.34	2.14	3.47	2.29	1.95	2.20	2.51	2.91
H26'	2.82	3.03	2.95	2.62	2.47	2.25	2.40	2.64	2.97
H27	-2.01	-3.96	-1.65	3.34	0.40	0.16	0.33	0.56	0.88

Table 28 Chemical shift values of paramagnetic LnLn' complexes of L^{AB3}

	LaCe	LaPr	LaNd	LaEu	CeLu	PrLu	NdLu	SmLu	EuLu
H1	8.90	9.78	9.08	5.70	7.45	7.17	7.36	7.62	7.97
H3	10.56	12.44	10.76	4.43	7.90	7.52	7.79	8.14	8.61
H4	5.18	5.76	5.31	3.62	4.18	3.82	4.11	4.49	4.98
H4'	5.86	6.75	5.70	3.62	4.43	4.05	4.34	4.68	5.18
H5	2.85	3.73	2.58	0.18	1.26	1.01	1.20	1.43	1.76
H6	7.44	7.83	7.85	5.72	6.78	6.42	6.71	7.09	7.58
H7	6.56	6.33	6.60	7.25	6.63	6.36	6.56	6.84	7.22
H8	0.04	-3.60	1.58	10.10	3.95	2.10	3.40	5.10	7.57
H9	2.99	2.64	3.08	3.97	3.36	3.19	3.24	3.48	3.86
H9'	3.50	3.34	3.49	3.97	3.27	2.80	3.11	3.57	4.20
H10	3.02	1.21	3.64	8.54	1.09	-4.61	-0.48	4.54	11.46
H11	7.09	6.91	7.13	7.58	7.33	7.33	7.30	7.33	7.36
H12	7.28	7.07	7.38	8.03	8.27	9.08	8.88	7.73	5.86
H13	3.89	3.64	3.97	4.66	5.41	7.03	6.18	4.63	2.32
H13'	3.32	3.04	3.41	4.12	5.03	6.66	5.64	4.25	2.22
H14	1.28	1.12	1.36	1.84	2.37	3.25	2.61	1.75	0.52
H15	7.13	6.83	7.24	8.06	8.96	11.04	10.43	7.81	3.61
H16	7.75	7.56	7.81	8.33	9.26	10.60	9.89	8.14	5.67
H17	7.30	7.07	7.38	8.00	9.02	11.10	10.54	7.83	3.41
H18	3.78	3.64	3.87	4.47	5.29	6.81	5.86	4.46	2.48
H18'	4.24	4.07	4.33	4.84	5.55	6.96	6.25	4.77	2.62
H19	1.31	1.17	1.39	1.78	2.09	2.69	2.24	1.64	0.83
H20	7.42	7.31	7.50	7.91	8.29	9.10	8.90	7.74	5.83
H21	7.10	6.96	7.15	7.49	7.36	7.42	7.34	7.31	7.31
H22	6.49	6.32	6.55	6.99	6.36	5.85	6.18	6.63	7.32
H23	6.28	5.98	6.38	7.14	3.06	-1.55	1.53	5.59	11.46
H24	4.11	4.85	4.19	2.37	3.16	2.88	3.08	3.31	3.65
H24'	3.41	3.84	3.66	2.77					
H25	1.30	1.90	1.38	0.03	0.79	0.57	0.73	0.93	1.21
H26	1.95	1.65	2.31	3.32	2.44	2.12	2.36	2.65	3.02
H26'	3.08	3.33	3.12	2.65	2.52	2.28	2.43	2.71	3.02
H27	-1.56	-3.47	-1.30	3.21	0.49	0.25	0.42	0.64	0.96

Table 29 Chemical shift values of paramagnetic LnLn' complexes of L^{AB4}

	LaCe	LaPr	LaNd	LaEu	CeLu	PrLu	NdLu	EuLu
H1	9.20	10.33	9.51	5.01	7.31	6.94	7.28	8.26
H2	10.13	11.25	9.99	6.07	7.87	7.55	7.84	8.71
H3	10.80	12.74	11.12	4.16	7.78	7.27	7.73	9.08
H4	5.59	6.06	5.28	3.49	3.98	3.50	3.96	5.27
H4'	5.80	6.90	5.77	3.49	4.16	3.66	4.12	5.45
H5	2.60	3.75	2.58	0.15	1.09	0.76	1.07	1.96
H6	7.46	7.94	7.88	5.68	6.54	6.08	6.53	7.83
H7	6.47	6.31	6.52	7.05	6.39	6.08	6.36	7.23
H8	-0.15	-3.95	1.45	10.61	2.72	0.16	2.47	9.22
H9	2.87	2.54	2.99	3.91	3.19	3.01	3.11	3.79
H9'	3.53	3.44	3.53	3.91	2.96	2.34	2.88	4.58
H10	3.19	1.25	3.80	8.69	-2.56	-10.41	-3.17	16.17
H11	7.04	6.81	7.06	7.53	7.18	7.12	7.15	7.41
H12	7.19	6.92	7.26	7.97	8.39	9.27	8.90	5.58
H13	3.85	3.60	3.95	4.68	6.21	8.18	6.76	1.07
H13'	3.19	2.88	3.28	4.08	6.04	8.18	6.36	0.62
H14	1.39	1.23	1.46	1.92	2.84	3.86	2.94	0.12
H15	5.71	5.39	5.82	6.67	9.01	11.96	10.29	0.39
H17	6.06	5.83	6.15	6.78	8.95	11.62	10.17	0.84
H18	3.50	3.30	3.59	4.25	6.36	8.26	6.63	0.74
H18'	4.08	3.87	4.15	4.73	6.36	8.61	6.90	1.18
H19	1.30	1.14	1.35	1.77	2.52	3.31	2.55	0.41
H20	7.40	7.24	7.46	7.89	8.65	9.65	9.14	5.45
H21	7.07	6.93	7.12	7.49	7.49	7.62	7.44	7.21
H22	6.54	6.37	6.61	7.06	6.25	5.67	6.12	7.72
H23	6.53	6.24	6.61	7.37	0.76	-4.91	0.02	15.03
H24	3.93	4.70	4.08	2.34	2.96	2.62	2.94	3.82
H24'	3.24	3.53	3.52	2.77	2.96	2.64	2.94	3.82
H25	1.35	1.87	1.45	0.34	0.76	0.49	0.73	1.44
H26	1.70	1.20	2.16	3.57	2.11	1.71	2.08	3.18
H26'	2.77	2.90	2.94	2.77	2.33	2.00	2.30	3.18
H27	-1.98	-3.87	-1.53	3.25	0.24	-0.08	0.22	1.10
H28	3.25	3.30	3.32	3.67	4.27	5.05	4.27	2.58
H28'	3.25	3.15	3.23	3.58	4.27	5.05	4.27	2.37
H29	1.02	0.92	1.05	1.32	1.89	2.57	1.98	0.12

Table 30 Chemical shift values of paramagnetic LnLn' complexes of L^{AB5}

	LaCe	LaPr	LaNd	LaEu	CeLu	PrLu	NdLu	SmLu	EuLu
H1	9.19	10.26	9.49	5.13	7.54	7.27	7.46	7.70	8.03
H2	10.21	11.35	10.05	6.09	8.10	7.85	8.00	8.22	8.50
H3	11.00	13.04	11.29	4.08	8.10	7.74	8.01	8.31	8.75
H4	5.25	5.87	5.21	3.58	4.23	3.89	4.17	4.51	4.98
H4'	5.94	6.89	5.76	3.58	4.47	4.12	4.38	4.70	5.16
H5	2.90	3.80	2.61	0.17	1.27	1.04	1.22	1.44	1.75
H6	7.42	7.83	7.85	5.74	6.79	6.45	6.74	7.09	7.60
H7	6.53	6.31	6.60	7.24	6.62	6.35	6.57	6.83	7.21
H8	-0.33	-4.31	1.30	10.44	4.02	2.25	3.58	5.15	7.34
H9	2.92	2.57	3.03	3.97	3.31	3.14	3.21	3.46	3.87
H9'	3.56	3.42	3.54	3.97	3.31	2.84	3.14	3.59	4.20
H10	2.70	1.01	3.57	8.62	1.36	-4.05	-0.12	4.64	10.91
H11	7.15	6.93	7.18	7.65	7.36	7.33	7.34	7.39	7.47
H12	7.31	7.03	7.38	8.07	8.25	9.02	8.87	7.77	5.97
H13	3.85	3.55	3.94	4.67	5.32	6.78	6.02	4.64	2.63
H13'	3.49	3.17	3.54	4.30	5.06	6.50	5.61	4.37	2.68
H14	1.03	0.86	1.13	1.65	2.31	3.25	2.57	1.64	0.36
H15	7.00	6.66	7.11	7.99	8.66	10.55	9.97	7.68	4.16
H17	7.14	6.90	7.23	7.88	8.65	10.46	9.97	7.67	4.06
H18	3.96	3.72	3.99	4.60	5.26	6.66	5.71	4.52	2.65
H18'	4.23	4.03	4.30	4.82	5.44	6.71	6.08	4.64	2.90
H19	1.24	1.09	1.30	1.73	2.09	2.71	2.21	1.60	0.80
H20	7.47	7.31	7.53	7.94	8.30	9.06	8.90	7.77	5.92
H21	7.17	7.02	7.21	7.58	7.42	7.45	7.39	7.39	7.42
H22	6.61	6.42	6.66	7.13	6.48	5.95	6.28	6.74	7.42
H23	6.16	5.87	6.27	7.04	3.22	-1.21	1.87	5.60	11.00
H24	4.02	4.82	4.15	2.31	3.11	2.89	3.06	3.29	3.58
H24’	3.28	3.59	3.60	2.77	3.16	2.92	3.09	3.32	3.62
H25	1.38	1.96	1.47	0.26	0.90	0.70	0.84	1.02	1.26
H26	1.83	1.40	2.20	3.42	2.30	2.04	2.26	2.52	2.85
H26'	2.87	3.06	2.95	2.63	2.51	2.28	2.44	2.67	2.95
H27	-1.95	-3.86	-1.52	3.24	0.43	0.20	0.36	0.58	0.86

5.3 One proton (Reilley) analysis

5.3.1 Diamagnetic references

The analysis of lanthanide induced shift requires the choice of a complex to be used as diamagnetic reference. Available for this purpose are complexes with the diamagnetic La(III) and Lu(III) ions and the choice is based on considerations of size since the reference must have the same structure as the paramagnetic complexes investigated. A complex of La should be used for complexes of the lighter lanthanides while a Lu complex would be more suitable for the heavier lanthanides. In this work the paramagnetic ions (Ce, Pr, Nd and Eu) belong to the first half of the lanthanide series and the best choice of diamagnetic reference should be the complex where the paramagnetic ion is replaced by La.

Comparing the ^{1}H NMR spectra of the two diamagnetic complexes $La_2(L^{AB})_3$ and $Lu_2(L^{AB})_3$ (Table 23) gives an idea of how significant the choice of reference complex is. The differences of the chemical shift values are typically around 0.1 - 0.2 ppm. For H8 and H10, which are the hydrogen atoms most sensitive to size induced changes of the tightness of the helical wrapping, the differences of chemical shift values between the La and Lu complexes are more than 0.5 ppm. These differences are one order of magnitude smaller than the lanthanide induced shifts and the choice of reference complex is thus not expected to change significantly the outcome of the analysis. The differences are, however, large enough to influence the quality of the analysis.

As an alternative to using one single diamagnetic complex as reference the average of the La and Lu chemical shifts could be used as reference. Concerning the sizes of the ions, taking the average of the ionic radii of the La and Lu ions gives a value close to the radius of Eu, slightly larger than the average size of the four paramagnetic lanthanide ions studied here.

Eventually it was decided to utilise a weighted average of the La and Lu chemical shifts with the initial presumption (based on the argument of size) that there should be a slight overweight of La in this virtual reference complex.

The chemical shift of each proton Hi in the virtual reference complex was then calculated from the chemical shift of a La complex and a Lu complex as $(\delta_i)^{Ref} = (x\cdot(\delta_i)^{La} + (100 - x)\cdot(\delta_i)^{Lu})/100$, where x is the La percentages ranging from 0 to 100.

For the paramagnetic LaLn complexes the La_2 complex was used as La reference and LaLu as Lu reference. All these complexes have La in the bpb coordination site and only the La percentage in the bpa site is varied.

Similarly, LaLu and Lu_2 served as La and Lu references, respectively, for the LnLu paramagnetic complexes. In all these complexes there is a Lu ion in the bpa site.

For the paramagnetic Ln_2 complexes the La_2 complex was used as La reference. As for the Lu reference either LaLu or Lu_2 was used.

The problematic protons close to the so-called magic angles (54.7° and 125.3°) were excluded since they have structural factors $G_i \approx 0$, which causes problems in the separation of contact and pseudo contact shift. For the Ln_2 and LaLn complexes H24' and H26' were disregarded and for the LnLu complexes H11 and H21 were left out of the calculations.

To determine the appropriate weights a preliminary one proton analysis was carried out and the average proton agreement factor (AF_i; page 125) of all the protons calculated.

The results of these calculations are shown in Figure 38 - Figure 41. Note the overall similar appearance of all graphs. In all cases a combination of the two diamagnetic references is better than using only one reference. La is a better reference than Lu, and the optimal La percentage is larger than 50, which as mentioned above is as expected based on the relative sizes of all the ions involved. The only exception from this rule is the $LaLn(L^{AB})_3$ series of complexes for which Lu is a better reference than La and for which the optimal La percentage is 40.

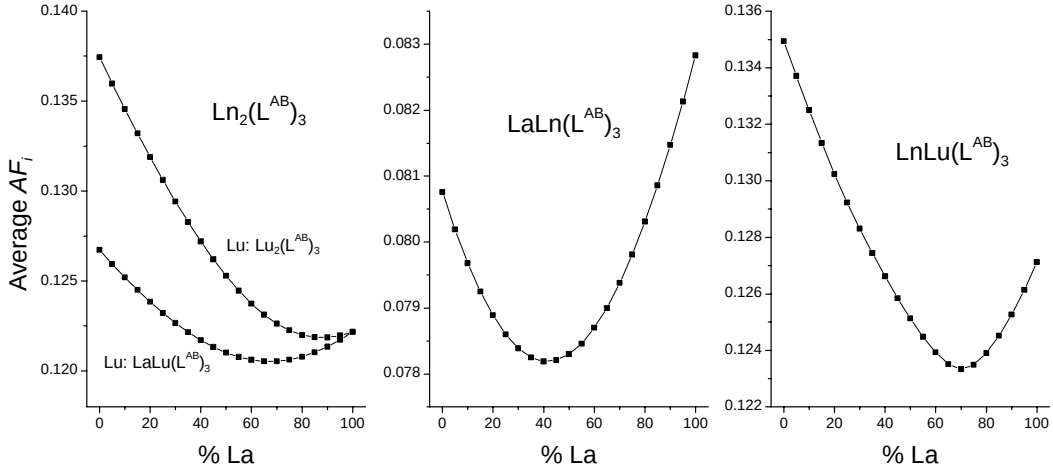

Figure 38 Average AF_i of L^{AB} complexes as function of La percentage of the reference complex

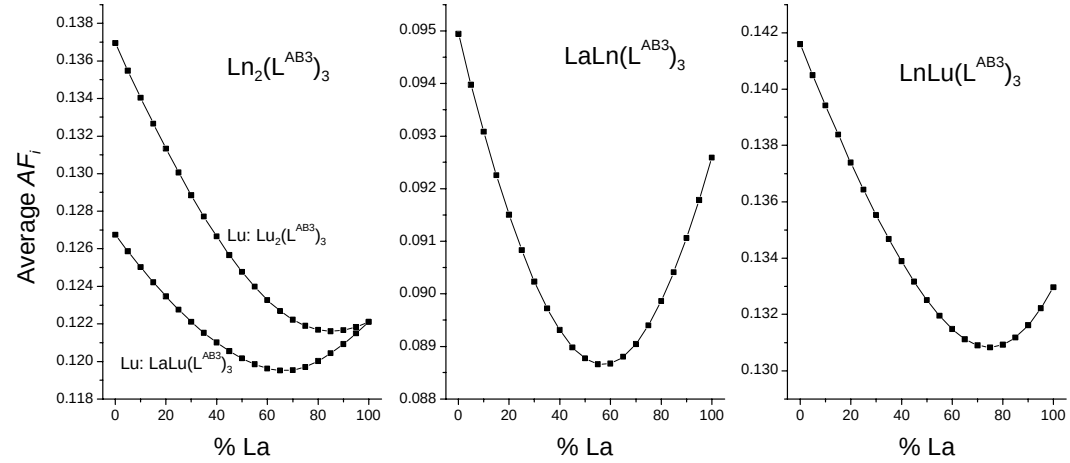

Figure 39 Average AF_i of L^{AB3} complexes as function of La percentage of the reference complex

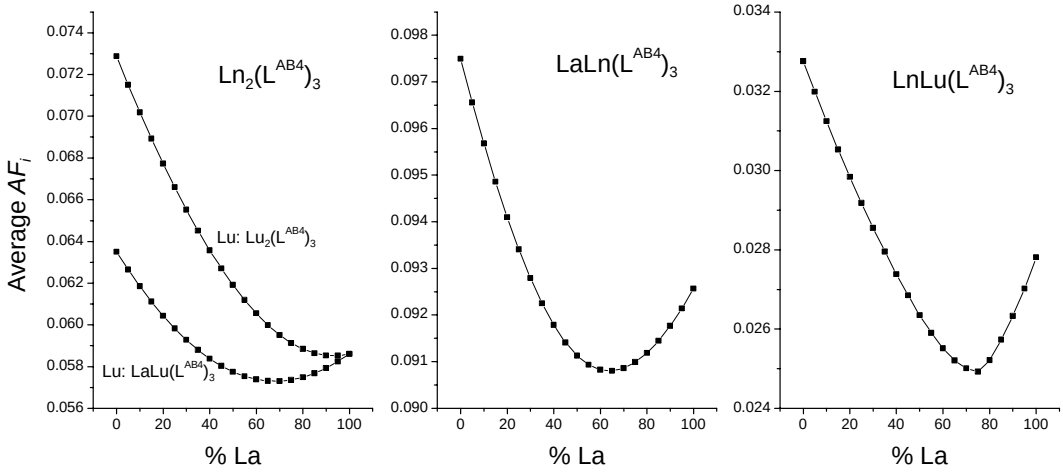

Figure 40 Average AF_i of L^{AB4} complexes as function of La percentage of the reference complex

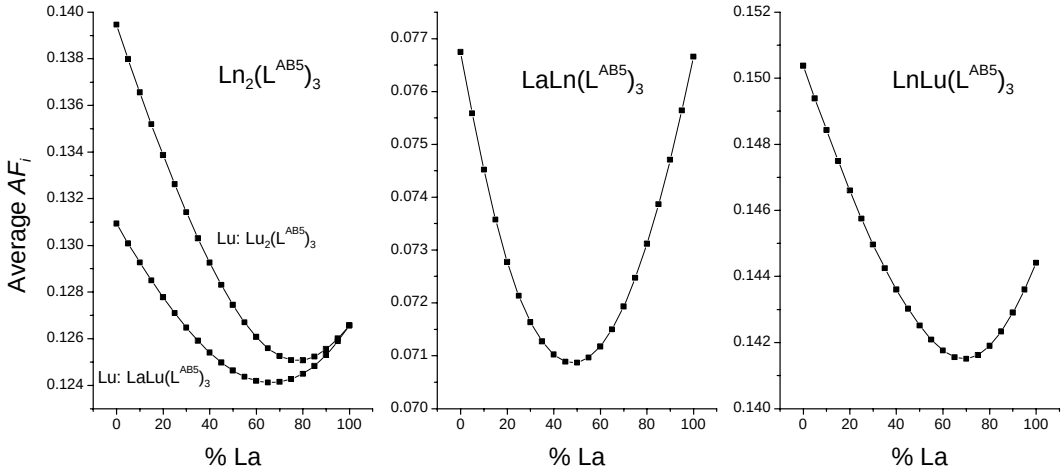

Figure 41 Average AF_i of L^{AB5} complexes as function of La percentage of the reference complex

The average AF_i could typically be reduced by about 5 % compared to using only one reference complex.

The optimal virtual reference complexes obtained in this way were:

$Ln_2(L^{AB})_3$: 65 % $La_2(L^{AB})_3$ and 35 % $LaLu(L^{AB})_3$
$LaLn(L^{AB})_3$: 40 % $La_2(L^{AB})_3$ and 60 % $LaLu(L^{AB})_3$
$LnLu(L^{AB})_3$: 70 % $LaLu(L^{AB})_3$ and 30 % $Lu_2(L^{AB})_3$
$Ln2(L^{AB3})_3$: 65 % $La_2(L^{AB3})_3$ and 35 % $LaLu(L^{AB3})_3$
$LaLn(L^{AB3})_3$: 55 % $La_2(L^{AB3})_3$ and 45 % $LaLu(L^{AB3})_3$
$LnLu(L^{AB3})_3$: 75 % $LaLu(L^{AB3})_3$ and 25 % $Lu_2(L^{AB3})_3$
$Ln2(L^{AB4})_3$: 70 % $La_2(L^{AB4})_3$ and 30 % $LaLu(L^{AB4})_3$
$LaLn(L^{AB4})_3$: 65 % $La_2(L^{AB4})_3$ and 35 % $LaLu(L^{AB4})_3$
$LnLu(L^{AB4})_3$: 75 % $LaLu(L^{AB4})_3$ and 25 % $Lu_2(L^{AB4})_3$
$Ln2(L^{AB5})_3$: 65 % $La_2(L^{AB5})_3$ and 35 % $LaLu(L^{AB5})_3$
$LaLn(L^{AB5})_3$: 50 % $La_2(L^{AB5})_3$ and 50 % $LaLu(L^{AB5})_3$
$LnLu(L^{AB5})_3$: 70 % $LaLu(L^{AB5})_3$ and 30 % $Lu_2(L^{AB5})_3$

The chemical shift values calculated for these "virtual reference complexes" as weighted averages are given in Table 31.

Table 31 Chemical shifts of virtual reference complexes

	L^{AB}			L^{AB3}			L^{AB4}			L^{AB5}		
	Ln_2	LaLn	LnLu	La_2	LnLn	LnLu	La_2	LnLn	LnLu	La_2	LnLn	LnLu
	65 % La_2 35% LaLu	40 % La_2 60 % LaLu	70 % LaLu 30 % Lu_2	65 % La_2 35% LaLu	55 % La_2 45 % LaLu	75 % LaLu 25 % Lu_2	70 % La_2 30% LaLu	65 % La_2 35 % LaLu	75 % LaLu 25 % Lu_2	65 % La_2 35% LaLu	50 % La_2 50 % LaLu	70 % LaLu 30 % Lu_2
H1	7.70	7.71	7.73	7.68	7.68	7.67	7.69	7.69	7.73	7.73	7.74	7.76
H2	8.25	8.25	8.24				8.24	8.24	8.24	8.28	8.28	8.27
H3	8.29	8.31	8.34	8.14	8.15	8.20	8.28	8.28	8.35	8.32	8.33	8.38
H4	4.43	4.44	4.50	4.45	4.45	4.50	4.48	4.48	4.54	4.48	4.49	4.56
H4'	4.65	4.67	4.71	4.69	4.70	4.74	4.66	4.67	4.72	4.71	4.72	4.77
H5	1.49	1.48	1.47	1.48	1.48	1.47	1.48	1.48	1.47	1.50	1.49	1.48
H6	7.09	7.07	7.09	7.13	7.12	7.11	7.11	7.11	7.09	7.13	7.11	7.12
H7	6.85	6.83	6.82	6.90	6.89	6.85	6.78	6.77	6.74	6.90	6.89	6.86
H8	5.83	5.74	5.55	5.77	5.73	5.49	5.91	5.89	5.61	5.82	5.76	5.51
H9	3.44	3.43	3.43	3.48	3.48	3.47	3.40	3.40	3.38	3.46	3.46	3.46
H9'	3.65	3.64	3.63	3.67	3.67	3.65	3.68	3.68	3.66	3.71	3.71	3.69
H10	5.98	5.96	5.79	5.94	5.93	5.76	6.09	6.09	5.92	5.91	5.91	5.76
H11	7.30	7.31	7.29	7.32	7.32	7.32	7.26	7.26	7.26	7.39	7.39	7.39
H12	7.64	7.65	7.64	7.65	7.65	7.66	7.56	7.56	7.59	7.68	7.69	7.70
H13	4.27	4.27	4.33	4.28	4.28	4.33	4.28	4.28	4.32	4.27	4.28	4.36
H13'	3.71	3.70	3.82	3.74	3.74	3.82	3.66	3.66	3.74	3.92	3.91	4.00
H14	1.56	1.58	1.58	1.56	1.57	1.60	1.66	1.66	1.66	1.35	1.37	1.43
H15	7.59	7.58	7.57	7.62	7.62	7.59	6.22	6.22	6.21	7.54	7.53	7.50
H16	8.04	8.03	7.98	8.05	8.05	8.00						
H17	7.65	7.64	7.62	7.66	7.66	7.64	6.44	6.44	6.41	7.54	7.54	7.51
H18	4.11	4.10	4.15	4.12	4.12	4.17	3.88	3.88	3.94	4.27	4.27	4.29
H18'	4.54	4.55	4.55	4.55	4.55	4.57	4.36	4.35	4.34	4.52	4.53	4.55
H19	1.54	1.55	1.54	1.55	1.55	1.55	1.53	1.53	1.54	1.50	1.50	1.50
H20	7.67	7.68	7.67	7.68	7.68	7.68	7.65	7.65	7.65	7.70	7.71	7.71
H21	7.29	7.29	7.29	7.30	7.30	7.29	7.29	7.29	7.28	7.38	7.39	7.38
H22	6.74	6.75	6.74	6.75	6.75	6.75	6.82	6.82	6.81	6.88	6.88	6.86
H23	6.74	6.75	6.60	6.74	6.74	6.62	6.98	6.98	6.86	6.63	6.65	6.53
H24	3.33	3.32	3.31	3.39	3.39	3.36	3.34	3.34	3.33	3.36	3.35	3.34
H24'	3.25	3.27	3.31	3.33	3.33	3.36	3.27	3.28	3.33	3.31	3.33	3.37
H25	0.90	0.95	1.03	0.83	0.85	0.96	0.96	0.97	1.06	0.93	0.96	1.05
H26	2.67	2.62	2.55	2.76	2.75	2.69	2.74	2.73	2.58	2.69	2.66	2.57
H26'	2.78	2.74	2.69	2.87	2.85	2.74	2.83	2.82	2.71	2.79	2.77	2.71
H27	0.67	0.64	0.61	0.74	0.73	0.68	0.68	0.68	0.61	0.69	0.67	0.62
H28							3.50	3.50	3.47			
H28'							3.42	3.42	3.42			
H29							1.18	1.18	1.16			

5.3.2 LIS values

Using these "virtual lanthanide complexes" as references values the lanthanide induced shifts have been calculated. The values are given in Table 32 - Table 37.

Table 32 LIS of Ln_2 complexes of L^{AB} and L^{AB3}

	L^{AB}					L^{AB3}				
	Ce_2	Pr_2	Nd_2	Sm_2	Eu_2	Ce_2	Pr_2	Nd_2	Sm_2	Eu_2
H1	1.28	2.12	1.49	0.17	-2.35	0.96	1.57	1.07	0.13	-1.64
H2	1.76	2.67	1.51	0.24	-1.92					
H3	2.36	4.02	2.52	0.34	-3.80	2.07	3.56	2.16	0.60	-3.10
H4	0.56	0.91	0.41	0.17	-0.43	0.45	0.71	0.33	0.15	-0.35
H4'	0.94	1.59	0.69	0.21	-0.75	0.85	1.42	0.60	0.20	-0.56
H5	1.18	1.85	0.83	0.23	-1.00	1.15	1.80	0.82	0.22	-0.95
H6	0.08	0.21	0.45	0.00	-0.88	0.05	0.13	0.41	-0.02	-0.88
H7	-0.50	-0.89	-0.48	-0.07	0.65	-0.51	-0.97	-0.53	-0.08	0.67
H8	-7.77	-13.64	-6.71	-1.78	6.73	-7.39	-13.12	-6.40	-1.70	6.25
H9	-0.60	-1.06	-0.60	-0.07	0.85	-0.60	-1.05	-0.62	-0.08	0.84
H9'	-0.52	-1.11	-0.70	-0.12	0.80	-0.58	-1.24	-0.75	-0.12	0.86
H10	-8.04	-15.57	-8.83	-1.81	8.17	-7.71	-15.24	-8.66	-1.74	7.92
H11	-0.21	-0.37	-0.18	-0.03	0.27	-0.24	-0.42	-0.22	-0.05	0.28
H12	0.27	0.87	0.95	0.05	-1.45	0.25	0.87	0.96	0.05	-1.46
H13	0.72	2.13	1.61	0.45	-1.65	0.75	2.16	1.60	0.45	-1.67
H13'	0.96	2.32	1.63	0.72	-1.16	0.92	2.28	1.62	0.70	-1.17
H14	0.53	1.29	0.84	0.11	-0.85	0.55	1.34	0.88	0.13	-0.87
H15	0.92	2.74	2.49	0.17	-3.55	0.92	2.77	2.51	0.16	-3.61
H16	0.96	2.15	1.66	0.05	-2.12	0.95	2.15	1.67	0.04	-2.14
H17	1.06	2.98	2.67	0.08	-3.97	1.05	2.99	2.69	0.09	-4.00
H18	0.88	2.19	1.44	0.05	-1.33	0.89	2.21	1.44	0.04	-1.36
H18'	0.72	1.92	1.48	0.01	-1.56	0.70	1.94	1.48	0.01	-1.62
H19	0.30	0.75	0.50	0.05	-0.49	0.31	0.78	0.51	0.05	-0.52
H20	0.35	1.00	1.02	-0.02	-1.61	0.35	1.02	1.03	-0.02	-1.64
H21	-0.19	-0.28	-0.17	-0.02	0.22	-0.18	-0.26	-0.14	-0.02	0.20
H22	-0.73	-1.43	-0.85	-0.17	0.83	-0.70	-1.40	-0.82	-0.17	0.81
H23	-4.15	-9.48	-5.41	-1.29	5.20	-4.34	-9.35	-5.61	-1.28	5.13
H24	0.43	0.95	0.46	0.07	-0.76	0.45	0.91	0.47	0.10	-0.65
H24'	-0.18	-0.11	0.05	0.00	-0.23	-0.11	0.01	0.06	-0.03	-0.29
H25	0.28	0.62	0.30	0.09	-0.36	0.26	0.61	0.30	0.08	-0.43
H26	-1.14	-1.82	-0.82	-0.16	1.08	-1.07	-1.67	-0.66	-0.17	0.90
H26'	-0.19	-0.35	-0.20	-0.12	0.14	-0.06	-0.19	-0.12	-0.06	0.15
H27	-2.91	-5.09	-2.52	-0.60	2.89	-2.62	-4.72	-2.32	-0.53	2.64

Table 33 LIS of Ln_2 complexes of L^{AB4} and L^{AB5}

	L^{AB4}					L^{AB5}				
	Ce_2	Pr_2	Nd_2	Sm_2	Eu_2	Ce_2	Pr_2	Nd_2	Sm_2	Eu_2
H1	1.08	1.84	1.36	0.12	-2.12	1.24	2.06	1.46	0.15	-2.34
H2	1.52	2.32	1.34	0.18	-1.67	1.71	2.60	1.47	0.22	-1.92
H3	1.92	3.37	2.20	0.24	-3.35	2.30	3.94	2.51	0.34	-3.79
H4	0.34	0.59	0.23	0.08	-0.31	0.51	0.84	0.40	0.22	-0.40
H4'	0.68	1.25	0.51	0.15	-0.41	0.92	1.57	0.67	0.22	-0.75
H5	0.98	1.57	0.70	0.19	-0.77	1.16	1.84	0.83	0.22	-1.03
H6	-0.10	-0.07	0.28	-0.08	-0.69	0.08	0.18	0.45	0.00	-0.89
H7	-0.57	-1.03	-0.57	-0.12	0.74	-0.52	-0.97	-0.51	-0.09	0.67
H8	-9.07	-15.86	-7.82	-1.97	8.26	-7.36	-13.57	-6.56	-1.69	6.52
H9	-0.65	-1.30	-0.66	-0.11	0.86	-0.61	-1.13	-0.63	-0.07	0.90
H9'	-0.82	-1.41	-0.90	-0.19	1.17	-0.54	-1.14	-0.70	-0.11	0.80
H10	-11.35	-20.77	-11.48	-2.71	12.56	-7.76	-14.72	-8.29	-1.74	7.66
H11	-0.29	-0.58	-0.31	-0.07	0.39	-0.26	-0.51	-0.25	-0.04	0.34
H12	0.45	1.08	1.05	0.07	-1.63	0.20	0.71	0.90	0.04	-1.35
H13	1.66	3.29	2.21	-0.02	-2.85	0.67	1.91	1.46	0.43	-1.22
H13'	1.93	3.90	2.38	1.02	-2.64	0.76	1.89	1.41	0.56	-0.97
H14	0.96	1.86	1.10	0.21	-1.32	0.67	1.51	1.03	0.20	-0.81
H15	2.35	5.03	3.75	0.43	-5.38	0.67	2.27	2.12	0.08	-2.93
H17	2.19	4.68	3.53	0.36	-5.30	0.78	2.41	2.22	0.07	-3.22
H18	2.14	3.91	2.51	0.64	-2.76	0.67	1.85	1.08	0.04	-1.32
H18'	1.69	3.72	2.32	0.45	-2.85	0.60	1.72	1.35	0.06	-1.28
H19	0.74	1.40	0.84	0.17	-0.89	0.33	0.80	0.52	0.07	-0.48
H20	0.75	1.58	1.30	0.09	-1.95	0.32	0.91	1.00	0.02	-1.55
H21	-0.04	-0.06	-0.04	-0.01	0.13	-0.21	-0.35	-0.18	-0.03	0.25
H22	-0.89	-1.75	-0.95	-0.24	1.15	-0.73	-1.47	-0.86	-0.20	0.78
H23	-6.86	-13.01	-7.50	-1.87	8.46	-4.03	-8.87	-5.31	-1.16	4.83
H24	0.19	0.61	0.32	0.12	-0.51	0.41	0.92	0.46	0.09	-0.76
H24'	-0.41	-0.46	-0.10	-0.05	-0.03	-0.23	-0.20	0.02	-0.03	-0.27
H25	0.08	0.30	0.15	0.03	-0.19	0.27	0.58	0.30	0.08	-0.36
H26	-1.41	-2.27	-1.02	-0.25	1.29	-1.11	-1.82	-0.76	-0.16	1.03
H26'	-0.50	-0.78	-0.39	-0.19	0.43	-0.19	-0.34	-0.14	-0.10	0.16
H27	-3.01	-5.25	-2.59	-0.62	2.96	-2.84	-5.00	-2.44	-0.59	2.81
H28	0.62	1.29	0.65	0.06	-0.75					
H28'	0.70	1.37	0.73	0.21	-0.89					
H29	0.55	1.16	0.69	0.10	-0.91					

Table 34 LIS of LaLn complexes of L^{AB} and L^{AB3}

	L^{AB}				L^{AB3}			
	LaCe	LaPr	LaNd	LaEu	LaCe	LaPr	LaNd	LaEu
H1	1.50	2.62	1.84	-2.67	1.22	2.10	1.40	-1.98
H2	1.97	3.14	1.86	-2.24				
H3	2.67	4.77	3.06	-4.35	2.42	4.30	2.62	-3.72
H4	0.83	1.48	0.77	-0.97	0.73	1.31	0.86	-0.83
H4'	1.22	2.23	1.09	-1.20	1.16	2.05	1.00	-1.08
H5	1.40	2.30	1.16	-1.33	1.37	2.25	1.10	-1.30
H6	0.34	0.75	0.75	-1.37	0.32	0.71	0.73	-1.40
H7	-0.33	-0.54	-0.29	0.36	-0.33	-0.56	-0.29	0.36
H8	-5.94	-9.88	-4.26	4.80	-5.69	-9.37	-4.15	4.40
H9	-0.50	-0.85	-0.41	0.48	-0.49	-0.84	-0.40	0.49
H9'	-0.12	-0.19	-0.14	0.29	-0.17	-0.33	-0.18	0.30
H10	-3.11	-5.01	-2.54	2.82	-2.91	-4.72	-2.29	2.61
H11	-0.23	-0.42	-0.19	0.24	-0.23	-0.41	-0.19	0.26
H12	-0.37	-0.65	-0.31	0.38	-0.37	-0.58	-0.27	0.38
H13	-0.44	-0.69	-0.36	0.39	-0.39	-0.64	-0.31	0.38
H13'	-0.43	-0.76	-0.39	0.42	-0.42	-0.70	-0.33	0.38
H14	-0.31	-0.48	-0.22	0.27	-0.29	-0.45	-0.21	0.27
H15	-0.50	-0.87	-0.43	0.49	-0.49	-0.79	-0.38	0.44
H16	-0.32	-0.54	-0.27	0.31	-0.30	-0.49	-0.24	0.28
H17	-0.39	-0.62	-0.32	0.36	-0.36	-0.59	-0.28	0.34
H18	-0.36	-0.58	-0.29	0.37	-0.34	-0.48	-0.25	0.35
H18'	-0.32	-0.52	-0.25	0.30	-0.31	-0.48	-0.22	0.29
H19	-0.25	-0.40	-0.19	0.24	-0.24	-0.38	-0.16	0.23
H20	-0.26	-0.42	-0.21	0.24	-0.26	-0.37	-0.18	0.23
H21	-0.22	-0.36	-0.18	0.21	-0.20	-0.34	-0.15	0.19
H22	-0.29	-0.48	-0.24	0.26	-0.26	-0.43	-0.20	0.24
H23	-0.49	-0.78	-0.40	0.44	-0.46	-0.76	-0.36	0.40
H24	0.68	1.50	0.81	-1.06	0.72	1.46	0.80	-1.02
H24'	0.01	0.36	0.32	-0.55	0.08	0.51	0.33	-0.56
H25	0.42	1.00	0.53	-0.74	0.45	1.05	0.53	-0.82
H26	-0.85	-1.28	-0.48	0.85	-0.80	-1.10	-0.44	0.57
H26'	0.08	0.29	0.21	-0.12	0.23	0.48	0.27	-0.20
H27	-2.65	-4.60	-2.29	2.70	-2.29	-4.20	-2.03	2.48

Table 35 LIS of LaLn complexes of L^{AB4} and L^{AB5}

	L^{AB4}				L^{AB5}			
	LaCe	LaPr	LaNd	LaEu	LaCe	LaPr	LaNd	LaEu
H1	1.51	2.64	1.82	-2.68	1.46	2.53	1.76	-2.61
H2	1.89	3.01	1.75	-2.17	1.94	3.08	1.78	-2.19
H3	2.52	4.46	2.84	-4.12	2.67	4.71	2.96	-4.25
H4	1.11	1.58	0.80	-0.99	0.76	1.38	0.72	-0.91
H4'	1.13	2.23	1.10	-1.18	1.22	2.17	1.04	-1.14
H5	1.12	2.27	1.10	-1.33	1.41	2.31	1.12	-1.32
H6	0.35	0.83	0.77	-1.43	0.31	0.72	0.74	-1.37
H7	-0.30	-0.46	-0.25	0.28	-0.36	-0.58	-0.29	0.36
H8	-6.04	-9.84	-4.44	4.72	-6.09	-10.07	-4.46	4.68
H9	-0.53	-0.86	-0.41	0.51	-0.54	-0.89	-0.43	0.51
H9'	-0.15	-0.24	-0.15	0.23	-0.15	-0.29	-0.17	0.26
H10	-2.90	-4.84	-2.29	2.60	-3.21	-4.90	-2.34	2.71
H11	-0.22	-0.45	-0.20	0.27	-0.24	-0.46	-0.21	0.26
H12	-0.37	-0.64	-0.30	0.41	-0.38	-0.65	-0.31	0.39
H13	-0.43	-0.68	-0.33	0.40	-0.43	-0.73	-0.34	0.40
H13'	-0.47	-0.78	-0.38	0.42	-0.42	-0.74	-0.37	0.39
H14	-0.27	-0.43	-0.20	0.26	-0.34	-0.51	-0.24	0.28
H15	-0.51	-0.83	-0.40	0.45	-0.53	-0.87	-0.42	0.46
H17	-0.38	-0.61	-0.29	0.34	-0.40	-0.64	-0.31	0.35
H18	-0.38	-0.58	-0.29	0.37	-0.31	-0.54	-0.27	0.34
H18'	-0.27	-0.48	-0.20	0.38	-0.30	-0.50	-0.23	0.30
H19	-0.23	-0.39	-0.18	0.24	-0.26	-0.41	-0.20	0.23
H20	-0.25	-0.41	-0.19	0.24	-0.24	-0.40	-0.18	0.24
H21	-0.22	-0.36	-0.17	0.20	-0.22	-0.37	-0.18	0.20
H22	-0.28	-0.45	-0.21	0.24	-0.27	-0.46	-0.22	0.25
H23	-0.45	-0.74	-0.37	0.39	-0.48	-0.77	-0.38	0.40
H24	0.59	1.36	0.74	-1.00	0.67	1.47	0.80	-1.04
H24'	-0.04	0.25	0.24	-0.51	-0.05	0.27	0.28	-0.56
H25	0.38	0.90	0.48	-0.63	0.42	1.00	0.51	-0.70
H26	-1.03	-1.53	-0.57	0.84	-0.83	-1.26	-0.46	0.76
H26'	-0.05	0.08	0.12	-0.05	0.10	0.29	0.18	-0.14
H27	-2.66	-4.55	-2.21	2.58	-2.62	-4.53	-2.19	2.57
H28	-0.25	-0.20	-0.18	0.17	1.46	2.53	1.76	-2.61
H28'	-0.17	-0.27	-0.19	0.16	1.94	3.08	1.78	-2.19
H29	-0.16	-0.26	-0.13	0.14	2.67	4.71	2.96	-4.25

Table 36 LIS of LnLu complexes of L^{AB} and L^{AB3}

	L^{AB}					L^{AB3}				
	CeLu	PrLu	NdLu	SmLu	EuLu	CeLu	PrLu	NdLu	SmLu	EuLu
H1	-0.23	-0.51	-0.31	-0.05	0.30	-0.22	-0.50	-0.31	-0.05	0.30
H2	-0.21	-0.43	-0.26	-0.04	0.27					
H3	-0.31	-0.67	-0.41	-0.07	0.41	-0.30	-0.68	-0.41	-0.06	0.41
H4	-0.33	-0.67	-0.38	-0.03	0.45	-0.32	-0.68	-0.39	-0.01	0.48
H4'	-0.32	-0.68	-0.41	-0.07	0.43	-0.31	-0.69	-0.40	-0.06	0.44
H5	-0.22	-0.46	-0.28	-0.04	0.29	-0.21	-0.46	-0.27	-0.04	0.29
H6	-0.34	-0.66	-0.38	-0.02	0.48	-0.33	-0.69	-0.40	-0.02	0.48
H7	-0.22	-0.46	-0.27	-0.02	0.34	-0.22	-0.49	-0.29	-0.01	0.37
H8	-1.57	-3.48	-2.14	-0.38	2.02	-1.54	-3.39	-2.09	-0.39	2.09
H9	-0.12	-0.27	-0.22	0.01	0.38	-0.11	-0.28	-0.23	0.01	0.39
H9'	-0.39	-0.86	-0.54	-0.09	0.54	-0.38	-0.85	-0.54	-0.08	0.55
H10	-4.75	-10.49	-6.32	-1.21	5.69	-4.67	-10.37	-6.24	-1.22	5.70
H11	0.02	0.04	0.01	0.02	0.04	0.01	0.01	-0.02	0.01	0.04
H12	0.62	1.48	1.25	0.08	-1.81	0.61	1.42	1.22	0.07	-1.80
H13	1.11	2.69	1.88	0.31	-2.04	1.08	2.70	1.85	0.30	-2.01
H13'	1.24	2.93	1.87	0.42	-1.62	1.21	2.84	1.82	0.43	-1.60
H14	0.78	1.68	1.04	0.15	-1.09	0.77	1.65	1.01	0.15	-1.08
H15	1.40	3.54	2.89	0.23	-3.99	1.37	3.45	2.84	0.22	-3.98
H16	1.30	2.68	1.95	0.15	-2.32	1.26	2.60	1.89	0.14	-2.33
H17	1.41	3.54	2.96	0.20	-4.22	1.38	3.46	2.90	0.19	-4.23
H18	1.15	2.72	1.67	0.32	-1.68	1.12	2.64	1.69	0.29	-1.69
H18'	1.02	2.46	1.74	0.22	-1.95	0.98	2.39	1.68	0.20	-1.95
H19	0.56	1.17	0.72	0.11	-0.71	0.55	1.15	0.70	0.10	-0.72
H20	0.62	1.45	1.25	0.07	-1.84	0.61	1.42	1.22	0.06	-1.85
H21	0.06	0.13	0.05	0.01	0.04	0.07	0.13	0.05	0.02	0.02
H22	-0.39	-0.90	-0.57	-0.11	0.60	-0.39	-0.90	-0.57	-0.12	0.57
H23	-3.64	-8.32	-5.05	-1.02	4.88	-3.56	-8.17	-5.09	-1.03	4.84
H24	-0.22	-0.46	-0.28	-0.04	0.28	-0.20	-0.48	-0.28	-0.05	0.29
H25	-0.17	-0.38	-0.23	-0.04	0.23	-0.17	-0.39	-0.23	-0.02	0.26
H26	-0.26	-0.60	-0.35	-0.04	0.36	-0.25	-0.57	-0.33	-0.04	0.33
H26'	-0.22	-0.44	-0.29	-0.05	0.28	-0.22	-0.46	-0.31	-0.03	0.28
H27	-0.21	-0.45	-0.28	-0.05	0.27	-0.19	-0.43	-0.26	-0.04	0.28

Table 37 LIS of LnLu complexes of L^{AB4} and L^{AB5}

	L^{AB4}				L^{AB5}				
	CeLu	PrLu	NdLu	EuLu	CeLu	PrLu	NdLu	SmLu	EuLu
H1	-0.42	-0.79	-0.45	0.53	-0.22	-0.49	-0.30	-0.06	0.27
H2	-0.37	-0.69	-0.40	0.47	-0.17	-0.42	-0.27	-0.05	0.23
H3	-0.57	-1.08	-0.62	0.73	-0.28	-0.64	-0.37	-0.07	0.37
H4	-0.56	-1.04	-0.58	0.73	-0.33	-0.67	-0.39	-0.05	0.42
H4'	-0.56	-1.06	-0.60	0.73	-0.30	-0.65	-0.39	-0.07	0.39
H5	-0.38	-0.71	-0.40	0.49	-0.21	-0.44	-0.26	-0.04	0.27
H6	-0.55	-1.01	-0.56	0.74	-0.33	-0.67	-0.38	-0.03	0.48
H7	-0.35	-0.66	-0.38	0.49	-0.24	-0.51	-0.29	-0.03	0.35
H8	-2.89	-5.45	-3.14	3.61	-1.49	-3.26	-1.93	-0.36	1.83
H9	-0.19	-0.37	-0.27	0.41	-0.15	-0.32	-0.25	0.00	0.41
H9'	-0.70	-1.32	-0.78	0.92	-0.38	-0.85	-0.55	-0.10	0.51
H10	-8.48	-16.33	-9.09	10.25	-4.40	-9.81	-5.88	-1.12	5.15
H11	-0.08	-0.14	-0.11	0.16	-0.02	-0.05	-0.04	0.00	0.09
H12	0.80	1.68	1.31	-2.01	0.55	1.32	1.17	0.07	-1.73
H13	1.89	3.86	2.44	-3.25	0.96	2.42	1.66	0.28	-1.73
H13'	2.30	4.44	2.62	-3.12	1.06	2.50	1.61	0.37	-1.32
H14	1.18	2.20	1.28	-1.54	0.88	1.82	1.14	0.21	-1.07
H15	2.80	5.75	4.08	-5.82	1.16	3.05	2.47	0.18	-3.34
H17	2.54	5.21	3.76	-5.57	1.14	2.95	2.46	0.16	-3.45
H18	2.42	4.32	2.69	-3.20	0.97	2.37	1.42	0.23	-1.64
H18'	2.02	4.27	2.56	-3.16	0.90	2.17	1.54	0.09	-1.65
H19	0.99	1.78	1.02	-1.13	0.59	1.21	0.71	0.10	-0.70
H20	1.00	2.00	1.49	-2.20	0.59	1.35	1.19	0.06	-1.79
H21	0.21	0.34	0.16	-0.07	0.04	0.07	0.01	0.01	0.04
H22	-0.56	-1.14	-0.69	0.92	-0.38	-0.91	-0.58	-0.12	0.56
H23	-6.10	-11.77	-6.84	8.17	-3.31	-7.74	-4.66	-0.93	4.47
H24	-0.37	-0.71	-0.39	0.49	-0.23	-0.45	-0.28	-0.05	0.24
H24'	-0.37	-0.69	-0.39	0.49	-0.21	-0.45	-0.28	-0.05	0.25
H25	-0.30	-0.57	-0.33	0.38	-0.15	-0.35	-0.21	-0.03	0.21
H26	-0.47	-0.87	-0.50	0.61	-0.27	-0.53	-0.31	-0.04	0.29
H26'	-0.38	-0.71	-0.41	0.47	-0.20	-0.43	-0.27	-0.04	0.24
H27	-0.37	-0.69	-0.39	0.49	-0.19	-0.42	-0.26	-0.04	0.24
H28	0.80	1.58	0.80	-0.89					
H28'	0.86	1.64	0.86	-1.05					
H29	0.73	1.41	0.82	-1.04					

The lanthanide induced shift values calculated for the complexes of the four ligands are compared in Figure 42 with the values of the L^{AB} complexes as reference values. The straight lines in the figures correspond to a perfect match between the LIS values of L^{AB} and any other given ligand.

It is immediately clear that the values calculated for the complexes of the ligands L^{AB3} and L^{AB5} are very similar to the L^{AB} values. The complexes of L^{AB4}, on the other hand, seem to deviate significantly. This is the first indication of differences induced by the substituents (Cl or NEt_2) on the ligands. Note that both L^{AB3} and L^{AB5} contain a Cl substituent on the bpa and bpb moiety, respectively, whereas L^{AB4} is NEt_2 substituted on the bpb moiety. The conclusion to draw here is that that a Cl substituent does not induce a significant change on the level of LIS.

Another feature of the plots is that the LaLn complexes of L^{AB4} deviate very little from the complexes of L^{AB} when compared to the differences seen for the Ln_2 and LnLu series of complexes. This is in concordance with the position of the paramagnetic lanthanide ion in the complexes. In the LaLn complexes the paramagnetic probe is situated in the bpa coordination cavity of the complex, a fair distance from the NEt_2 substituent and any structural or electronic changes it may cause. It is therefore reasonable that very little difference is observed on the LIS level. In the two other series of complexes (Ln_2 and LnLu) there is a paramagnetic ion in the bpb cavity, which is in the immediate vicinity of the NEt_2 substituent. Any change induced by the substituent would be immediately reflected in the lanthanide induced shifts.

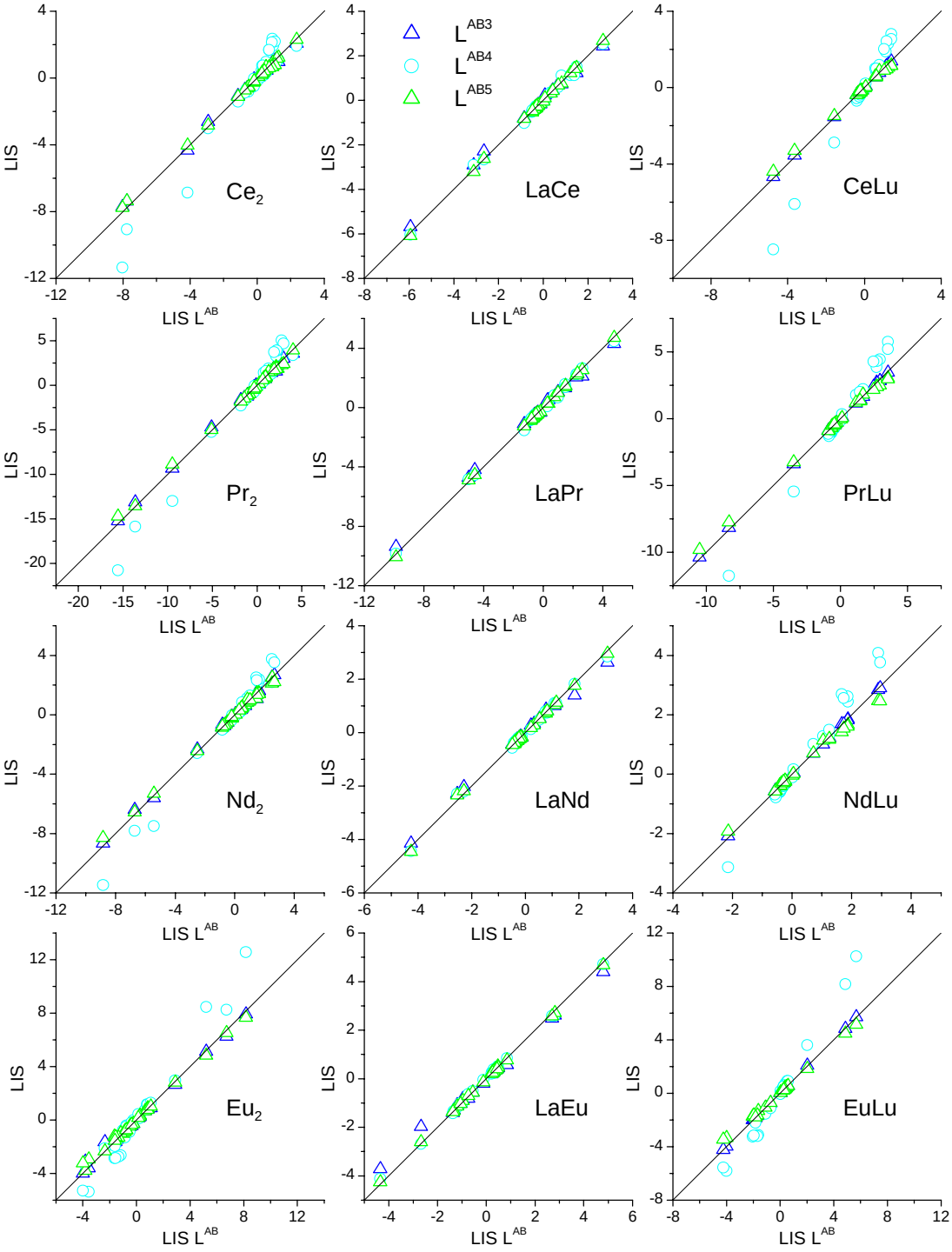

Figure 42 Comparison of the lanthanide induced shift

5.3.3 Theory: Monometallic complexes

In order to investigate the different contributions to the LIS a simple method has been developed to separate contact and pseudo contact terms of axial complexes.[88,89] Dividing Eq. (2) with C_j or $<S_z>_j$, respectively, yields the equations

$$\frac{\Delta_{i,j}}{C_j} = B_0^2 G_i + \left(\frac{< S_z >_j}{C_j} \right) \cdot F_i \qquad (3)$$

$$\frac{\Delta_{i,j}}{\langle S_z \rangle_j} = F_i + \left(\frac{C_j}{\langle S_z \rangle_j} \right) \cdot B_0^2 G_i \qquad (4)$$

As can be seen from eq. (3) a plot of $\Delta_{i,j}/C_j$ versus $<S_Z>_j/C_j$ for one proton and all the complexes of an isostructural series yields F_i as slope. Similarly, plots of $\Delta_{i,j}/<S_Z>_j$ versus $C_j/<S_Z>_j$ according to eq. (4) yield $B_0^2 G_i$ as slopes. In both cases it is assumed that the complexes are isostructural (having the same values of G_i) and that the crystal field parameter B_0^2 is the same for all complexes regardless of the lanthanide ion.

5.3.4 Theory: Bimetallic complexes

For a complex with two non-equivalent lanthanide ions the lanthanide induced shift can be expressed as a simple sum of the contributions of the two individual ions

$$\left(\Delta i, j\right)^{total} = \delta_{ij} - \delta_{i,dia} = \left(\Delta i, j\right)^{bpa} + \left(\Delta i, j\right)^{bpb} \qquad (5)$$

The two coordination sites of the complex are here labelled bpa and bpb.

It is assumed here that the two lanthanide ions are magnetically independent, that is that the Ln···Ln' distance is so large than there is no magnetic coupling between them. For the complexes studied here this assumption is justified by Ln(bpa)···Ln(bpb) distances larger than 9 Å and lack of electronic relay through the ligand strands in view of the methylene bridge linking the two coordinating units.

Using the expressions for the contact and pseudo contact terms from Eq. (2) the lanthanide induced shift can be written as

$$\left(\mathrm{i,j} \right)^{total} = \left(\mathrm{F_i^{bpa}} + \mathrm{F_i^{bpb}} \right) \left\langle \mathrm{S_Z} \right\rangle_{\mathrm{j}} + \left(B_0^{2\,bpa} G_i^{bpa} + B_0^{2\,bpb} G_i^{bpb} \right) \mathrm{C_j} \qquad (6)$$

Dividing eq. (7) with C_j or $<S_z>_j$, respectively, yields the equations

$$\frac{\left(\Delta i,j\right)^{total}}{C_j} = B_0^{2\,bpa} G_i^{bpa} + B_0^{2\,bpb} G_i^{bpb} + \left(\frac{\left\langle S_z \right\rangle_j}{C_j}\right) \cdot \left(F_i^{bpa} + F_i^{bpb}\right) \qquad (7)$$

$$\frac{\left(\Delta i,j\right)^{total}}{\left\langle S_z \right\rangle_j} = F_i^{bpa} + F_i^{bpb} + \left(\frac{C_j}{\left\langle S_z \right\rangle_j}\right) \cdot \left(B_0^{2\,bpa} G_i^{bpa} + B_0^{2\,bpb} G_i^{bpb}\right) \qquad (8)$$

These two equations are both expressions of straight lines. In a manner similar to what was described for the monometallic one proton analysis (Eqs. (3) and (4)) plotting of the data in this way can be used to isolate contact and pseudo contact contributions to the total lanthanide induced shift. For example, a plot according to Eq. (7) yields a straight line with the slope equal to $\left(F_i^{bpa} + F_i^{bpb}\right)$ and $\left(B_0^{2\,bpa} G_i^{bpa} + B_0^{2\,bpb} G_i^{bpb}\right)$ can be obtained as the slope of a plot according to Eq. (8).

Although the contact and pseudo contact contributions can easily be separated in this way the results are always sums of contributions of the two lanthanide ions. There is no straightforward method of separating these.

5.3.5 Separation of contact and pseudo contact parameters

Separation of contact and pseudo contact contributions to the lanthanide induced shift was carried out by linear fitting of the calculated LIS values (Table 32 - Table 37) to Equations (3), (4), (7) and (8).

Examples of plots are shown in Figure 43 - Figure 48. A complete set is given in Appendix 1 (pages 327 ff.). The plots are seen to be linear although not all of them are perfect.

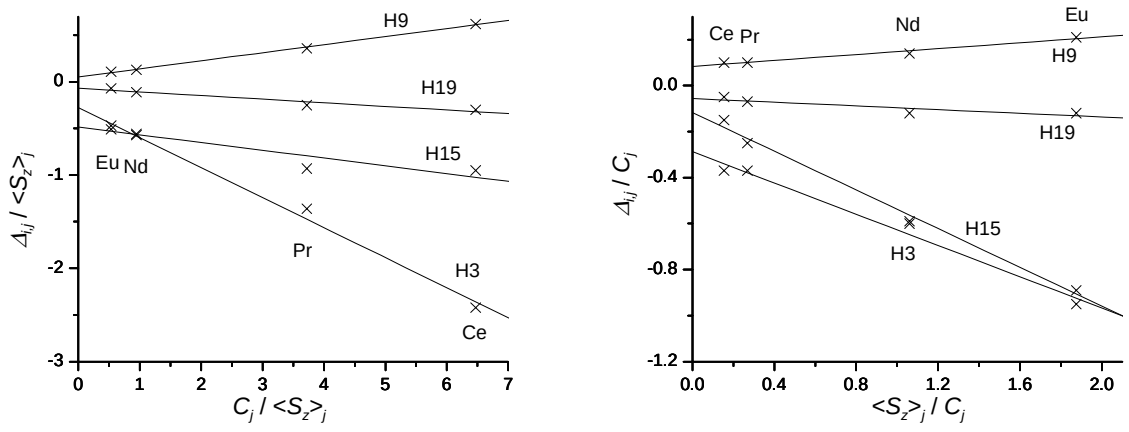

Figure 43 Selected Reilley plots of $Ln_2(L^{AB})_3$ complexes

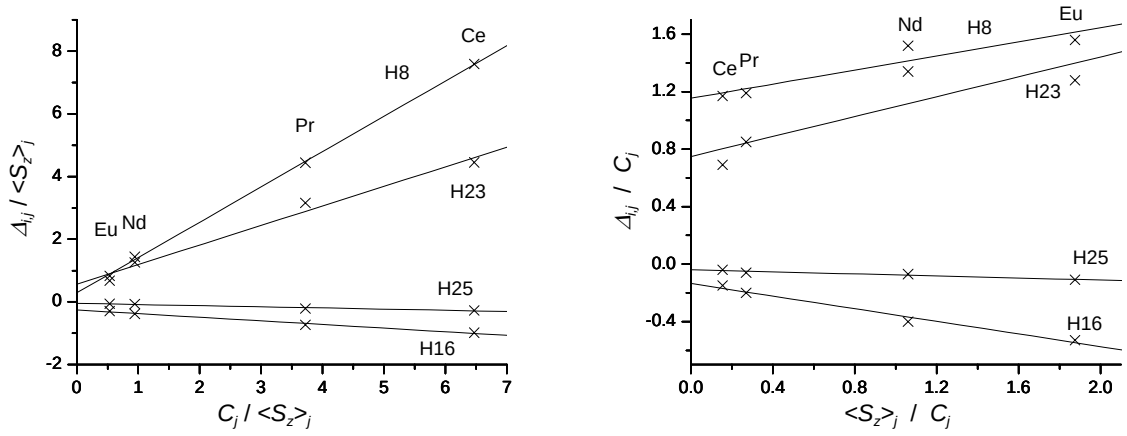

Figure 44 Selected Reilley plots of $Ln_2(L^{AB3})_3$ complexes

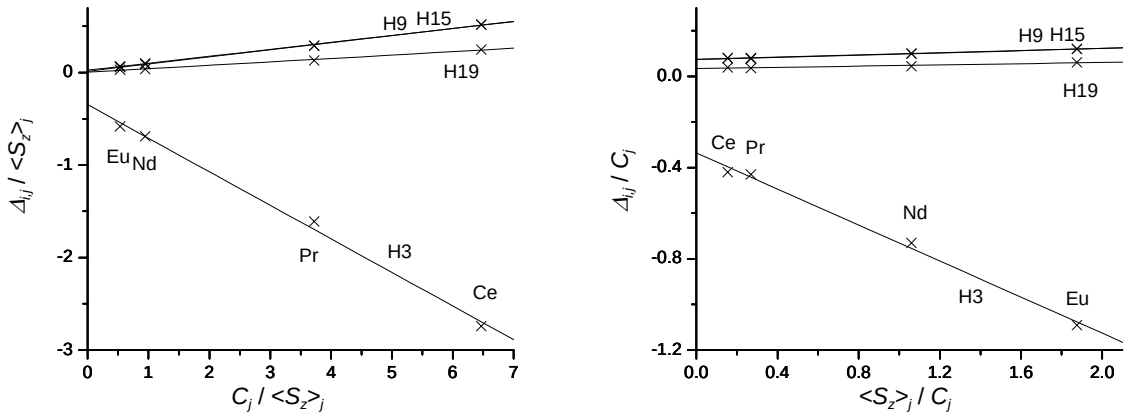

Figure 45 Selected Reilley plots of $LaLn(L^{AB})_3$ complexes

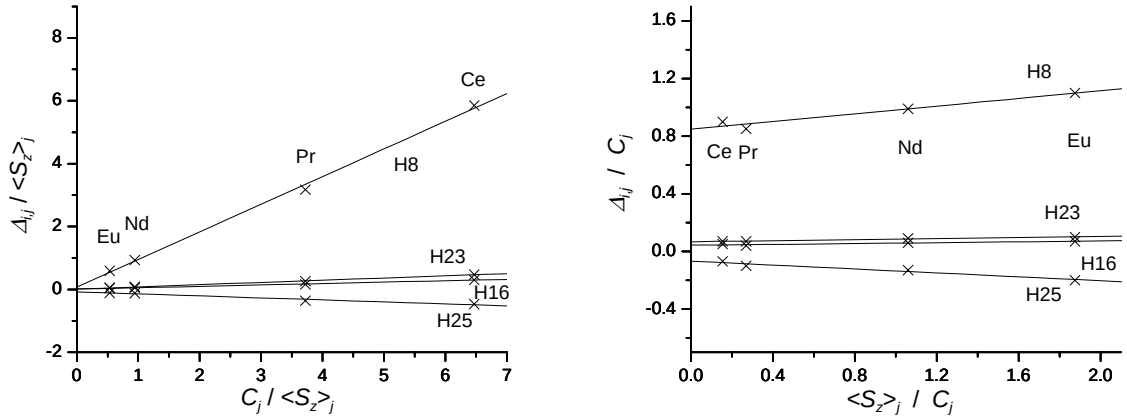

Figure 46 Selected Reilley plots of $LaLn(L^{AB3})_3$ complexes

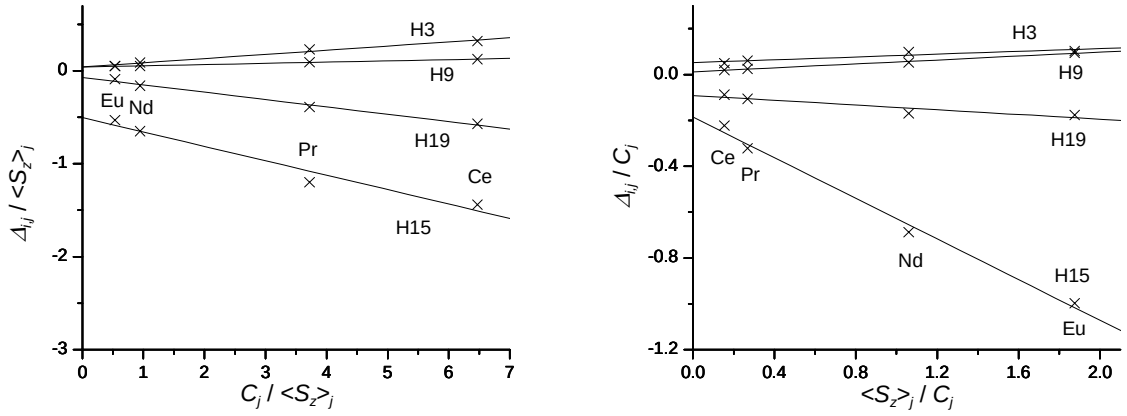

Figure 47 Selected Reilley plots of LnLu(L^{AB})$_3$ complexes

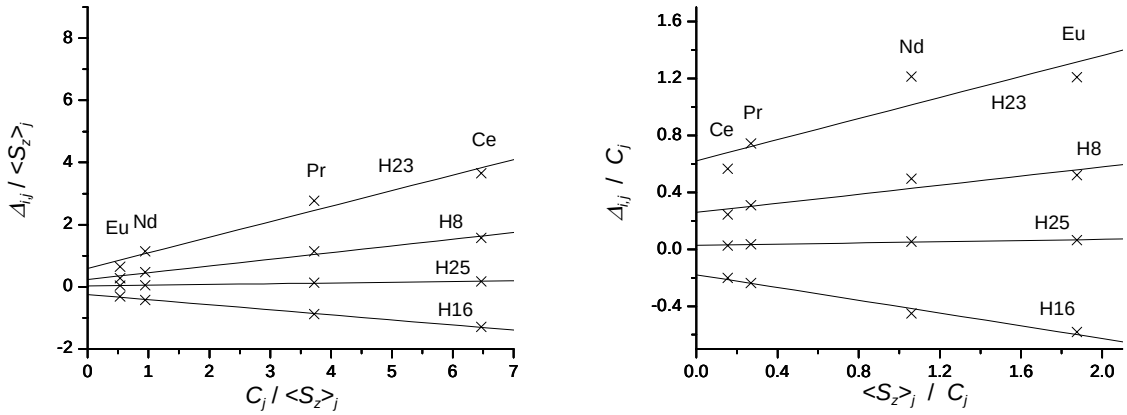

Figure 48 Selected Reilley plots of LnLu(L^{AB3})$_3$ complexes

Results of the one proton analysis (slopes, intercepts and correlation coefficients according to Equations (3), (4), (7) and (8)) are given in Table 38 - Table 49.

Table 38 One proton analysis of Ln_2 complexes of L^{AB}

	Plots of $\Delta_{i,j}/\langle S_z\rangle_j$ vs. $C_j/\langle S_z\rangle_j$			Plots of $\Delta_{i,j}/C_j$ vs. $\langle S_z\rangle_j/C_j$		
	$B_0^2G_i$ (slope)	F_i (intercept)	Correlation coefficient	$B_0^2G_i$ (intercept)	F_i (slope)	Correlation coefficient
H1	-0.17(2)	-0.18(6)	0.991	-0.14(2)	-0.23(2)	0.990
H2	-0.26(2)	-0.08(9)	0.992	-0.23(2)	-0.13(2)	0.978
H3	-0.32(2)	-0.27(8)	0.996	-0.29(4)	-0.34(3)	0.990
H4	-0.086(3)	-0.01(1)	0.998	-0.082(3)	-0.014(3)	0.963
H4'	-0.146(3)	-0.02(1)	0.999	-0.142(3)	-0.023(3)	0.985
H5	-0.18(1)	-0.01(4)	0.997	-0.17(1)	-0.04(1)	0.931
H6	0.005(3)	-0.11(1)	0.752	0.012(7)	-0.121(6)	0.998
H7	0.072(2)	0.042(7)	0.999	0.068(4)	0.049(4)	0.994
H8	1.18(2)	0.31(7)	1.000	1.20(6)	0.28(6)	0.958
H9	0.085(3)	0.06(1)	0.999	0.079(7)	0.069(6)	0.992
H9'	0.071(5)	0.09(2)	0.995	0.08(1)	0.068(9)	0.983
H10	1.18(5)	0.7(2)	0.998	1.3(2)	0.5(2)	0.881
H11	0.031(1)	0.014(4)	0.999	0.029(3)	0.019(3)	0.974
H12	-0.015(7)	-0.20(3)	0.839	-0.024(8)	-0.183(7)	0.998
H13	-0.09(3)	-0.3(1)	0.915	-0.14(5)	-0.17(5)	0.927
H13'	-0.13(2)	-0.18(9)	0.967	-0.19(7)	-0.08(7)	0.657
H14	-0.07(1)	-0.11(4)	0.976	-0.09(2)	-0.07(2)	0.934
H15	-0.08(2)	-0.49(9)	0.923	-0.12(3)	-0.42(3)	0.996
H16	-0.117(8)	-0.25(3)	0.995	-0.13(2)	-0.22(2)	0.993
H17	-0.10(2)	-0.52(8)	0.955	-0.12(2)	-0.47(2)	0.998
H18	-0.12(2)	-0.19(8)	0.970	-0.16(5)	-0.11(4)	0.873
H18'	-0.09(2)	-0.23(7)	0.954	-0.12(1)	-0.16(4)	0.946
H19	-0.040(7)	-0.07(3)	0.969	-0.05(1)	-0.04(1)	0.919
H20	-0.025(6)	-0.21(2)	0.951	-0.031(5)	-0.199(5)	0.999
H21	0.027(3)	0.01(1)	0.989	0.024(3)	0.016(2)	0.978
H22	0.106(5)	0.08(2)	0.998	0.12(2)	0.05(2)	0.920
H23	0.60(7)	0.6(3)	0.986	0.7(1)	0.4(1)	0.897
H24	-0.060(6)	-0.07(2)	0.990	-0.06(1)	-0.07(1)	0.968
H24'	0.035(6)	-0.06(2)	0.969	0.032(7)	-0.047(6)	0.982
H25	-0.041(4)	-0.03(2)	0.990	-0.045(4)	-0.025(3)	0.982
H26	0.17(1)	0.02(4)	0.997	0.16(2)	0.05(1)	0.939
H26'	0.029(2)	0.010(6)	0.997	0.034(7)	0.003(7)	0.327
H27	0.436(8)	0.14(3)	1.000	0.430(7)	0.156(6)	0.998

Table 39 One proton analysis of Ln_2 complexes of L^{AB3}

	Plots of $\Delta_{i,j}/\langle S_z\rangle_j$ vs. $C_j/\langle S_z\rangle_j$			Plots of $\Delta_{i,j}/C_j$ vs. $\langle S_z\rangle_j/C_j$		
	$B_0^2G_i$ (slope)	F_i (intercept)	Correlation coefficient	$B_0^2G_i$ (intercept)	F_i (slope)	Correlation coefficient
H1	-0.13(1)	-0.12(5)	0.991	-0.11(2)	-0.15(1)	0.991
H3	-0.29(2)	-0.22(6)	0.997	-0.26(2)	-0.26(2)	0.993
H4	-0.069(4)	0.00(1)	0.997	-0.066(3)	-0.012(3)	0.941
H4'	-0.133(3)	0.00(1)	0.999	-0.132(4)	-0.006(4)	0.735
H5	-0.18(1)	-0.01(4)	0.997	-0.16(1)	-0.04(1)	0.939
H6	0.010(5)	-0.11(2)	0.841	0.02(1)	-0.123(9)	0.995
H7	0.0731(8)	0.051(3)	1.000	0.0734(9)	0.0502(8)	1.000
H8	1.13(2)	0.29(6)	1.000	1.16(7)	0.24(6)	0.937
H9	0.085(3)	0.06(1)	0.998	0.080(4)	0.068(4)	0.997
H9'	0.081(6)	0.09(2)	0.995	0.09(1)	0.07(1)	0.981
H10	1.13(6)	0.7(2)	0.997	1.3(2)	0.5(2)	0.870
H11	0.0347(9)	0.017(3)	0.999	0.033(2)	0.019(1)	0.994
H12	-0.011(8)	-0.21(3)	0.704	-0.02(1)	-0.186(9)	0.998
H13	-0.09(3)	-0.3(1)	0.926	-0.14(5)	-0.17(4)	0.938
H13'	-0.13(3)	-0.2(1)	0.962	-0.18(7)	-0.09(7)	0.682
H14	-0.07(1)	-0.12(4)	0.975	-0.10(2)	-0.07(2)	0.920
H15	-0.08(3)	-0.50(9)	0.915	-0.11(3)	-0.43(3)	0.996
H16	-0.115(9)	-0.25(3)	0.994	-0.13(2)	-0.22(2)	0.993
H17	-0.10(2)	-0.53(8)	0.949	-0.12(2)	-0.47(2)	0.998
H18	-0.12(2)	-0.19(8)	0.970	-0.16(4)	-0.11(4)	0.893
H18'	-0.08(2)	-0.24(8)	0.944	-0.12(4)	-0.17(4)	0.954
H19	-0.042(7)	-0.07(3)	0.971	-0.06(1)	-0.04(1)	0.926
H20	-0.026(6)	-0.21(2)	0.946	-0.032(6)	-0.202(5)	0.999
H21	0.026(3)	0.01(1)	0.988	0.022(4)	0.014(3)	0.945
H22	0.101(5)	0.08(2)	0.997	0.11(2)	0.05(1)	0.935
H23	0.62(6)	0.6(2)	0.991	0.7(2)	0.3 (1)	0.870
H24	-0.064(3)	-0.05(1)	0.998	-0.064(5)	-0.051(5)	0.992
H24'	0.022(6)	-0.05(2)	0.927	0.02(1)	-0.046(9)	0.964
H25	-0.038(5)	-0.04(2)	0.985	-0.040(5)	-0.034(4)	0.983
H26	0.17(1)	0.00(4)	0.996	0.15(2)	0.03(2)	0.804
H26'	0.007(3)	0.02(1)	0.870	0.010(3)	0.016(2)	0.978
H27	0.393(2)	0.144(7)	1.000	0.393(4)	0.144(4)	0.999

Table 40 One proton analysis of Ln_2 complexes of L^{AB4}

	Plots of $\Delta_{i,j}/\langle S_z\rangle_j$ vs. $C_j/\langle S_z\rangle_j$			Plots of $\Delta_{i,j}/C_j$ vs. $\langle S_z\rangle_j/C_j$		
	$B_0^2G_i$ (slope)	F_i (intercept)	Correlation coefficient	$B_0^2G_i$ (intercept)	F_i (slope)	Correlation coefficient
H1	-0.14(1)	-0.18(5)	0.992	-0.12(2)	-0.21(2)	0.994
H2	-0.22(2)	-0.07(7)	0.992	-0.20(2)	-0.11(2)	0.981
H3	-0.26(2)	-0.26(6)	0.996	-0.23(3)	-0.31(3)	0.993
H4	-0.053(1)	-0.007(5)	0.999	-0.050(5)	-0.013(5)	0.886
H4'	-0.107(3)	-0.01(1)	0.999	-0.113(7)	0.002(6)	0.250
H5	-0.151(7)	-0.01(3)	0.998	-0.143(7)	-0.025(6)	0.947
H6	0.032(2)	-0.100(7)	0.996	0.038(8)	-0.109(7)	0.995
H7	0.081(1)	0.052(5)	1.000	0.079(3)	0.056(2)	0.998
H8	1.37(2)	0.39(9)	1.000	1.38(5)	0.39(5)	0.986
H9	0.095(4)	0.07(1)	0.998	0.096(4)	0.062(4)	0.996
H9'	0.115(6)	0.09(2)	0.997	0.110(5)	0.097(5)	0.997
H10	1.66(2)	0.88(9)	1.000	1.7(1)	0.8(1)	0.985
H11	0.042(1)	0.032(5)	0.999	0.044(1)	0.028(1)	0.998
H12	-0.042(2)	-0.198(8)	0.998	-0.044(2)	-0.194(2)	1.000
H13	-0.221(3)	-0.28(1)	1.000	-0.23(1)	-0.26(1)	0.998
H13'	-0.27(1)	-0.25(5)	0.998	-0.30(3)	-0.21(3)	0.979
H14	-0.135(3)	-0.11(1)	1.000	-0.141(7)	-0.103(7)	0.996
H15	-0.288(9)	-0.58(3)	0.999	-0.297(8)	-0.559(8)	1.000
H17	-0.263(7)	-0.57(3)	0.999	-0.26(1)	-0.56(1)	1.000
H18	-0.301(9)	-0.23(4)	0.999	-0.32(4)	-0.21(3)	0.978
H18'	-0.23(2)	-0.30(7)	0.994	-0.26(3)	-0.25(2)	0.991
H19	-0.106(3)	-0.08(1)	0.999	-0.11(1)	-0.06(1)	0.971
H20	-0.0857(5)	-0.213(2)	1.000	-0.085(2)	-0.214(2)	1.000
H21	0.005(1)	0.009(5)	0.914	0.001(5)	0.015(4)	0.921
H22	0.129(4)	0.09(1)	0.999	0.133(4)	0.083(4)	0.998
H23	0.99(2)	0.68(7)	1.000	1.03(7)	0.61(7)	0.988
H24	-0.024(9)	-0.06(3)	0.878	-0.029(9)	-0.051(9)	0.973
H24'	0.070(9)	-0.05(3)	0.985	0.063(8)	-0.038(7)	0.967
H25	-0.010(6)	-0.03(2)	0.794	-0.016(5)	-0.017(5)	0.937
H26	0.21(1)	0.03(4)	0.997	0.20(2)	0.06(1)	0.945
H26'	0.075(5)	0.01(2)	0.996	0.071(4)	0.019(4)	0.963
H27	0.452(8)	0.14(3)	1.000	0.445(8)	0.158(7)	0.998
H28	-0.091(6)	-0.06(2)	0.996	-0.097(6)	-0.050(5)	0.989
H28'	-0.102(3)	-0.07(1)	0.999	-0.105(3)	-0.063(3)	0.998
H29	-0.076(4)	-0.09(2)	0.997	-0.080(4)	-0.079(3)	0.998

Table 41 One proton analysis of Ln_2 complexes of L^{AB5}

	Plots of $\Delta_{i,j}/\langle S_z\rangle_j$ vs. $C_j/\langle S_z\rangle_j$			Plots of $\Delta_{i,j}/C_j$ vs. $\langle S_z\rangle_j/C_j$		
	$B_0^2G_i$ (slope)	F_i (intercept)	Correlation coefficient	$B_0^2G_i$ (intercept)	F_i (slope)	Correlation coefficient
H1	-0.16(2)	-0.18(6)	0.990	-0.14(3)	-0.23(2)	0.990
H2	-0.25(2)	-0.08(8)	0.992	-0.22(2)	-0.13(2)	0.978
H3	-0.31(2)	-0.28(8)	0.996	-0.28(3)	-0.34(3)	0.991
H4	-0.077(3)	-0.01(1)	0.999	-0.076(3)	-0.014(3)	0.960
H4'	-0.143(3)	-0.02(1)	1.000	-0.138(4)	-0.025(4)	0.980
H5	-0.18(1)	-0.02(4)	0.997	-0.16(1)	-0.05(1)	0.942
H6	0.007(4)	-0.11(2)	0.738	0.014(8)	-0.123(7)	0.997
H7	0.0751(7)	0.047(3)	1.000	0.074(3)	0.049(3)	0.997
H8	1.12(2)	0.36(7)	1.000	1.17(7)	0.27(6)	0.951
H9	0.087(2)	0.066(6)	1.000	0.082(6)	0.073(6)	0.994
H9'	0.076(5)	0.08(2)	0.996	0.08(1)	0.065(9)	0.981
H10	1.15(4)	0.6(2)	0.999	1.3(2)	0.4(2)	0.880
H11	0.038(1)	0.025(5)	0.999	0.037(3)	0.025(3)	0.987
H12	-0.004(6)	-0.19(2)	0.452	-0.01(1)	-0.177(9)	0.997
H13	-0.08(3)	-0.2(1)	0.920	-0.14(6)	-0.12(6)	0.819
H13'	-0.10(2)	-0.17(8)	0.957	-0.15(7)	-0.08(6)	0.644
H14	-0.09(1)	-0.11(5)	0.982	-0.12(4)	-0.06(4)	0.752
H15	-0.05(3)	-0.4(1)	0.815	-0.09(3)	-0.35(3)	0.992
H17	-0.07(2)	-0.44(8)	0.901	-0.10(3)	-0.39(2)	0.996
H18	-0.09(2)	-0.17(8)	0.948	-0.11(2)	-0.12(2)	0.974
H18'	-0.07(2)	-0.21(8)	0.921	-0.11(5)	-0.13(4)	0.899
H19	-0.046(7)	-0.06(3)	0.976	-0.06(2)	-0.04(2)	0.868
H20	-0.021(4)	-0.21(2)	0.960	-0.027(5)	-0.194(5)	0.999
H21	0.031(2)	0.012(6)	0.997	0.029(2)	0.017(2)	0.984
H22	0.107(7)	0.08(2)	0.996	0.12(2)	0.05(2)	0.863
H23	0.58(6)	0.6(2)	0.989	0.7(1)	0.3(1)	0.862
H24	-0.058(6)	-0.07(2)	0.990	-0.06(1)	-0.07(1)	0.976
H24'	0.043(6)	-0.06(2)	0.982	0.042(9)	-0.055(8)	0.979
H25	-0.039(3)	-0.03(1)	0.993	-0.042(3)	-0.026(3)	0.990
H26	0.170(8)	0.02(3)	0.998	0.16(2)	0.05(2)	0.906
H26'	0.0296(2)	0.0047(7)	1.000	0.0292(8)	0.0053(8)	0.980
H27	0.426(6)	0.14(2)	1.000	0.421(5)	0.150(5)	0.999

Table 42 One proton analysis of LaLn complexes of L^{AB}

	Plots of $\Delta_{i,j}/\langle S_z\rangle_j$ vs. $C_j/\langle S_z\rangle_j$			Plots of $\Delta_{i,j}/C_j$ vs. $\langle S_z\rangle_j/C_j$		
	$B_0^2G_i$ (slope)	F_i (intercept)	Correlation coefficient	$B_0^2G_i$ (intercept)	F_i (slope)	Correlation coefficient
H1	-0.20(1)	-0.22(5)	0.996	-0.18(1)	-0.26(1)	0.997
H2	-0.28(2)	-0.12(8)	0.995	-0.27(2)	-0.16(2)	0.988
H3	-0.36(2)	-0.35(6)	0.998	-0.34(2)	-0.39(2)	0.997
H4	-0.121(2)	-0.059(7)	1.000	-0.118(4)	-0.066(3)	0.997
H4'	-0.184(1)	-0.067(5)	1.000	-0.187(5)	-0.062(4)	0.995
H5	-0.21(1)	-0.05(4)	0.998	-0.202(8)	-0.069(8)	0.988
H6	-0.030(3)	-0.15(1)	0.990	-0.02(1)	-0.17(1)	0.996
H7	0.048(3)	0.02(1)	0.997	0.045(3)	0.024(2)	0.990
H8	0.92(3)	0.1(1)	0.999	0.88(3)	0.16(3)	0.965
H9	0.076(2)	0.019(8)	0.999	0.073(2)	0.024(2)	0.994
H9'	0.015(3)	0.02(1)	0.974	0.010(6)	0.030(5)	0.971
H10	0.47(2)	0.09(9)	0.997	0.45(2)	0.14(2)	0.979
H11	0.0340(6)	0.012(2)	1.000	0.033(2)	0.014(2)	0.978
H12	0.0552(9)	0.018(3)	1.000	0.053(2)	0.022(2)	0.992
H13	0.066(4)	0.01(2)	0.996	0.064(4)	0.019(4)	0.960
H13'	0.065(1)	0.023(4)	1.000	0.065(3)	0.022(3)	0.984
H14	0.048(3)	0.00(1)	0.996	0.044(3)	0.012(3)	0.934
H15	0.075(2)	0.023(6)	1.000	0.074(2)	0.026(1)	0.997
H16	0.048(2)	0.013(6)	0.999	0.047(2)	0.016(1)	0.993
H17	0.059(4)	0.01(1)	0.996	0.056(3)	0.018(3)	0.972
H18	0.054(3)	0.01(1)	0.997	0.050(3)	0.021(3)	0.980
H18'	0.048(2)	0.010(8)	0.998	0.045(3)	0.016(3)	0.976
H19	0.037(2)	0.007(8)	0.997	0.034(3)	0.013(3)	0.959
H20	0.038(2)	0.008(7)	0.998	0.036(2)	0.013(2)	0.984
H21	0.033(2)	0.008(6)	0.998	0.031(1)	0.011(1)	0.987
H22	0.043(2)	0.010(6)	0.999	0.042(1)	0.013(1)	0.989
H23	0.073(4)	0.01(2)	0.997	0.070(4)	0.022(3)	0.978
H24	-0.096(8)	-0.10(3)	0.993	-0.103(7)	-0.086(7)	0.994
H24'	0.01(1)	-0.09(4)	0.495	0.000(9)	-0.073(8)	0.987
H25	-0.059(8)	-0.08(3)	0.983	-0.064(7)	-0.063(7)	0.989
H26	0.13(1)	0.00(4)	0.993	0.11(3)	0.05(3)	0.779
H26'	-0.010(6)	-0.03(2)	0.766	-0.02(2)	-0.01(2)	0.541
H27	0.396(9)	0.13(3)	1.000	0.387(8)	0.153(7)	0.998

Table 43 One proton analysis of LaLn complexes of L^{AB3}

	Plots of $\Delta_{i,j}/\langle S_z\rangle_j$ vs. $C_j/\langle S_z\rangle_j$			Plots of $\Delta_{i,j}/C_j$ vs. $\langle S_z\rangle_j/C_j$		
	$B_0^2G_i$ (slope)	F_i (intercept)	Correlation coefficient	$B_0^2G_i$ (intercept)	F_i (slope)	Correlation coefficient
H1	-0.17(1)	-0.15(4)	0.996	-0.15(1)	-0.18(1)	0.997
H3	-0.33(1)	-0.28(5)	0.998	-0.31(2)	-0.32(2)	0.996
H4	-0.103(5)	-0.07(2)	0.998	-0.11(2)	-0.06(2)	0.923
H4'	-0.176(2)	-0.052(8)	1.000	-0.177(5)	-0.051(5)	0.991
H5	-0.207(9)	-0.05(3)	0.998	-0.197(9)	-0.066(8)	0.986
H6	-0.027(4)	-0.15(1)	0.979	-0.02(2)	-0.17(1)	0.993
H7	0.048(2)	0.019(6)	0.999	0.046(2)	0.023(2)	0.993
H8	0.88(3)	0.1(1)	0.999	0.85(3)	0.13(2)	0.968
H9	0.073(2)	0.021(7)	0.999	0.070(3)	0.027(3)	0.988
H9'	0.0236(9)	0.023(4)	0.998	0.021(4)	0.027(4)	0.979
H10	0.44(2)	0.08(8)	0.998	0.42(2)	0.12(2)	0.981
H11	0.0341(7)	0.013(3)	1.000	0.032(3)	0.016(3)	0.973
H12	0.056(4)	0.01(1)	0.995	0.050(6)	0.021(6)	0.939
H13	0.059(3)	0.01(1)	0.998	0.056(3)	0.020(3)	0.983
H13'	0.063(2)	0.013(8)	0.999	0.061(2)	0.018(2)	0.987
H14	0.044(3)	0.01(1)	0.996	0.040(4)	0.013(3)	0.941
H15	0.074(4)	0.01(1)	0.998	0.070(4)	0.021(3)	0.977
H16	0.045(2)	0.010(8)	0.998	0.042(2)	0.015(2)	0.984
H17	0.054(2)	0.011(9)	0.998	0.050(3)	0.018(3)	0.974
H18	0.051(6)	0.01(2)	0.988	0.044(6)	0.021(6)	0.932
H18'	0.047(3)	0.01(1)	0.995	0.042(5)	0.015(4)	0.927
H19	0.036(2)	0.004(8)	0.996	0.032(5)	0.012(4)	0.883
H20	0.039(4)	0.00(1)	0.990	0.034(4)	0.011(4)	0.900
H21	0.0297(9)	0.007(3)	0.999	0.028(3)	0.010(2)	0.950
H22	0.039(2)	0.007(6)	0.999	0.037(2)	0.012(2)	0.977
H23	0.070(3)	0.01(1)	0.999	0.067(2)	0.017(2)	0.985
H24	-0.103(4)	-0.09(2)	0.998	-0.107(4)	-0.079(3)	0.998
H24'	0.00(1)	-0.09(4)	0.244	-0.01(1)	-0.07(1)	0.978
H25	-0.063(8)	-0.08(3)	0.986	-0.07(1)	-0.07(1)	0.982
H26	0.12(1)	-0.02(5)	0.990	0.11(2)	0.01(1)	0.554
H26'	-0.035(3)	-0.02(1)	0.992	-0.04(1)	-0.008(9)	0.500
H27	0.342(2)	0.143(7)	1.000	0.339(7)	0.147(7)	0.998

Table 44 One proton analysis of LaLn complexes of L^{AB4}

	Plots of $\Delta_{i,j}/\langle S_z\rangle_j$ vs. $C_j/\langle S_z\rangle_j$			Plots of $\Delta_{i,j}/C_j$ vs. $\langle S_z\rangle_j/C_j$		
	$B_0^2G_i$ (slope)	F_i (intercept)	Correlation coefficient	$B_0^2G_i$ (intercept)	F_i (slope)	Correlation coefficient
H1	-0.20(1)	-0.22(5)	0.996	-0.18(2)	-0.25(2)	0.996
H2	-0.27(2)	-0.11(7)	0.995	-0.26(2)	-0.15(2)	0.989
H3	-0.34(2)	-0.32(6)	0.998	-0.32(3)	-0.37(2)	0.996
H4	-0.17(2)	-0.01(6)	0.990	-0.15(2)	-0.05(2)	0.919
H4'	-0.170(7)	-0.09(3)	0.998	-0.18(1)	-0.06(1)	0.978
H5	-0.166(8)	-0.10(3)	0.997	-0.174(7)	-0.085(7)	0.993
H6	-0.031(3)	-0.16(1)	0.989	-0.02(1)	-0.17(1)	0.994
H7	0.045(3)	0.01(1)	0.994	0.042(3)	0.015(3)	0.962
H8	0.93(4)	0.1(1)	0.998	0.90(3)	0.15(3)	0.964
H9	0.080(4)	0.02(1)	0.998	0.074(5)	0.027(5)	0.972
H9'	0.021(2)	0.014(7)	0.992	0.018(3)	0.020(2)	0.986
H10	0.44(1)	0.09(6)	0.999	0.42(1)	0.12(1)	0.989
H11	0.033(2)	0.019(7)	0.997	0.034(3)	0.017(2)	0.981
H12	0.055(2)	0.019(6)	0.999	0.052(5)	0.025(4)	0.973
H13	0.064(4)	0.01(1)	0.997	0.060(4)	0.021(4)	0.968
H13'	0.072(3)	0.01(1)	0.999	0.070(3)	0.019(2)	0.984
H14	0.040(2)	0.007(9)	0.997	0.037(4)	0.014(3)	0.948
H15	0.077(3)	0.01(1)	0.998	0.073(3)	0.021(3)	0.982
H17	0.058(3)	0.01(1)	0.997	0.054(3)	0.016(3)	0.972
H18	0.057(4)	0.01(2)	0.994	0.052(5)	0.020(4)	0.959
H18'	0.040(2)	0.018(9)	0.997	0.03(1)	0.028(9)	0.905
H19	0.035(1)	0.009(5)	0.999	0.033(2)	0.013(2)	0.975
H20	0.038(2)	0.007(7)	0.998	0.036(2)	0.012(2)	0.972
H21	0.033(1)	0.006(5)	0.998	0.032(1)	0.009(1)	0.980
H22	0.043(2)	0.005(8)	0.998	0.040(2)	0.010(2)	0.969
H23	0.069(3)	0.01(1)	0.998	0.067(4)	0.017(3)	0.963
H24	-0.082(9)	-0.10(3)	0.987	-0.089(8)	-0.086(8)	0.992
H24'	0.01(1)	-0.09(4)	0.737	0.01(1)	-0.071(9)	0.984
H25	-0.053(7)	-0.07(3)	0.984	-0.060(6)	-0.052(6)	0.989
H26	0.16(1)	-0.01(5)	0.994	0.14(2)	0.03(2)	0.684
H26'	0.010(6)	-0.03(2)	0.751	0.00(1)	-0.01(1)	0.574
H27	0.40(1)	0.11(4)	0.999	0.39(1)	0.135(9)	0.995
H28	0.04(1)	-0.01(4)	0.931	0.03(1)	0.008(9)	0.524
H28'	0.024(2)	0.011(8)	0.992	0.026(6)	0.010(5)	0.787
H29	0.024(1)	0.005(4)	0.998	0.023(1)	0.006(1)	0.975

Table 45 One proton analysis of LaLn complexes of L^{AB5}

	Plots of $\Delta_{i,j}/\langle S_z\rangle_j$ vs. $C_j/\langle S_z\rangle_j$			Plots of $\Delta_{i,j}/C_j$ vs. $\langle S_z\rangle_j/C_j$		
	$B_0^2G_i$ (slope)	F_i (intercept)	Correlation coefficient	$B_0^2G_i$ (intercept)	F_i (slope)	Correlation coefficient
H1	-0.19(1)	-0.21(5)	0.995	-0.17(2)	-0.25(2)	0.996
H2	-0.28(2)	-0.11(8)	0.995	-0.26(2)	-0.15(2)	0.989
H3	-0.37(2)	-0.32(6)	0.998	-0.34(3)	-0.38(2)	0.996
H4	-0.111(1)	-0.058(4)	1.000	-0.109(2)	-0.062(2)	0.999
H4'	-0.185(1)	-0.055(5)	1.000	-0.185(3)	-0.055(3)	0.997
H5	-0.213(9)	-0.04(4)	0.998	-0.202(9)	-0.066(8)	0.984
H6	-0.025(3)	-0.16(1)	0.987	-0.02(1)	-0.17(1)	0.995
H7	0.053(3)	0.01(1)	0.997	0.049(3)	0.020(3)	0.980
H8	0.94(3)	0.1(1)	0.999	0.91(3)	0.14(2)	0.970
H9	0.081(3)	0.02(1)	0.998	0.077(3)	0.026(3)	0.985
H9'	0.0205(5)	0.021(2)	0.999	0.019(2)	0.023(2)	0.992
H10	0.49(3)	0.0(1)	0.995	0.45(3)	0.12(3)	0.940
H11	0.036(1)	0.016(4)	0.999	0.036(2)	0.015(1)	0.991
H12	0.056(1)	0.017(4)	1.000	0.054(3)	0.021(3)	0.985
H13	0.065(2)	0.014(6)	0.999	0.062(2)	0.019(2)	0.989
H13'	0.063(1)	0.020(4)	1.000	0.064(3)	0.019(2)	0.983
H14	0.052(4)	0.00(1)	0.994	0.047(4)	0.011(3)	0.916
H16	0.080(3)	0.01(1)	0.998	0.078(3)	0.020(3)	0.982
H17	0.060(3)	0.01(1)	0.998	0.057(3)	0.015(2)	0.975
H18	0.0452(5)	0.019(2)	1.000	0.0444(8)	0.0207(7)	0.999
H18'	0.045(2)	0.010(6)	0.999	0.041(3)	0.016(3)	0.963
H19	0.039(2)	0.006(9)	0.997	0.037(2)	0.011(2)	0.969
H20	0.036(1)	0.008(5)	0.999	0.033(3)	0.013(3)	0.950
H21	0.0326(9)	0.007(3)	0.999	0.0318(8)	0.0091(7)	0.994
H22	0.041(1)	0.010(4)	0.999	0.040(1)	0.0120(9)	0.995
H23	0.074(4)	0.01(1)	0.997	0.071(4)	0.015(3)	0.957
H24	-0.095(8)	-0.10(3)	0.993	-0.102(7)	-0.085(6)	0.994
H24'	0.02(1)	-0.09(4)	0.764	0.01(1)	-0.078(9)	0.987
H25	-0.059(8)	-0.07(3)	0.982	-0.065(8)	-0.058(7)	0.986
H26	0.13(1)	0.00(4)	0.994	0.11(2)	0.03(2)	0.737
H26'	-0.014(4)	-0.02(2)	0.921	-0.021(8)	-0.010(7)	0.711
H27	0.394(9)	0.11(3)	1.000	0.384(9)	0.136(8)	0.996

Table 46 One proton analysis of LnLu complexes of L^{AB}

	Plots of $\Delta_{i,j}/\langle S_z\rangle_j$ vs. $C_j/\langle S_z\rangle_j$			Plots of $\Delta_{i,j}/C_j$ vs. $\langle S_z\rangle_j/C_j$		
	$B_0^2G_i$ (slope)	F_i (intercept)	Correlation coefficient	$B_0^2G_i$ (intercept)	F_i (slope)	Correlation coefficient
H1	0.033(3)	0.03(1)	0.989	0.039(8)	0.022(7)	0.910
H2	0.031(2)	0.026(6)	0.997	0.035(5)	0.019(5)	0.941
H3	0.044(4)	0.04(1)	0.993	0.052(9)	0.031(9)	0.929
H4	0.047(2)	0.040(8)	0.998	0.051(3)	0.034(3)	0.992
H4'	0.045(3)	0.05(1)	0.994	0.052(8)	0.033(7)	0.958
H5	0.031(2)	0.030(8)	0.996	0.036(6)	0.022(5)	0.946
H6	0.0476(8)	0.040(3)	1.000	0.0485(7)	0.0387(7)	1.000
H7	0.031(2)	0.032(6)	0.997	0.033(2)	0.028(2)	0.997
H8	0.22(2)	0.24(9)	0.989	0.27(6)	0.15(5)	0.896
H9	0.0132(7)	0.041(3)	0.997	0.012(3)	0.043(3)	0.996
H9'	0.054(5)	0.06(2)	0.990	0.06(1)	0.04(1)	0.930
H10	0.68(7)	0.7(3)	0.989	0.8(2)	0.4(2)	0.856
H11	-0.0037(8)	0.004(3)	0.961	-0.006(3)	0.007(2)	0.905
H12	-0.067(6)	-0.22(2)	0.993	-0.074(7)	-0.204(6)	0.999
H13	-0.14(2)	-0.26(8)	0.979	-0.18(4)	-0.19(4)	0.958
H13'	-0.17(3)	-0.2(1)	0.978	-0.23(6)	-0.12(6)	0.828
H14	-0.109(9)	-0.12(3)	0.993	-0.13(2)	-0.09(2)	0.954
H15	-0.15(2)	-0.50(8)	0.981	-0.19(3)	-0.44(3)	0.996
H16	-0.169(7)	-0.25(3)	0.998	-0.19(3)	-0.22(3)	0.987
H17	-0.15(2)	-0.53(7)	0.984	-0.18(2)	-0.48(2)	0.998
H18	-0.16(2)	-0.21(8)	0.981	-0.20(4)	-0.13(4)	0.927
H18'	-0.13(2)	-0.25(7)	0.981	-0.16(4)	-0.19(3)	0.969
H19	-0.079(6)	-0.07(2)	0.995	-0.09(2)	-0.05(1)	0.926
H20	-0.066(4)	-0.22(2)	0.996	-0.072(5)	-0.209(4)	1.000
H21	-0.011(2)	0.004(7)	0.974	-0.016(6)	0.012(6)	0.822
H22	0.053(7)	0.07(2)	0.985	0.06(1)	0.05(1)	0.950
H23	0.51(6)	0.6(2)	0.986	0.6(1)	0.4(1)	0.907
H24	0.031(2)	0.029(8)	0.995	0.036(6)	0.021(5)	0.938
H25	0.023(3)	0.03(1)	0.988	0.028(5)	0.018(4)	0.944
H26	0.037(5)	0.04(7)	0.985	0.044(7)	0.028(7)	0.943
H26'	0.031(2)	0.029(7)	0.997	0.035(7)	0.022(6)	0.921
H27	0.029(3)	0.03(1)	0.992	0.034(6)	0.021(6)	0.928

Table 47 One proton analysis of LnLu complexes of L^{AB3}

	Plots of $\Delta_{i,j}/\langle S_z\rangle_j$ vs. $C_j/\langle S_z\rangle_j$			Plots of $\Delta_{i,j}/C_j$ vs. $\langle S_z\rangle_j/C_j$		
	$B_0^2G_i$ (slope)	F_i (intercept)	Correlation coefficient	$B_0^2G_i$ (intercept)	F_i (slope)	Correlation coefficient
H1	0.031(4)	0.04(1)	0.986	0.038(8)	0.023(7)	0.909
H3	0.043(5)	0.05(2)	0.988	0.05(1)	0.031(9)	0.921
H4	0.045(3)	0.05(1)	0.996	0.049(3)	0.039(3)	0.994
H4'	0.044(4)	0.05(2)	0.991	0.051(7)	0.034(6)	0.965
H5	0.030(3)	0.03(1)	0.992	0.034(5)	0.022(4)	0.962
H6	0.046(3)	0.05(1)	0.996	0.050(4)	0.038(3)	0.992
H7	0.030(3)	0.04(1)	0.992	0.033(3)	0.032(2)	0.995
H8	0.22(2)	0.24(8)	0.991	0.26(5)	0.16(4)	0.930
H9	0.011(1)	0.046(6)	0.982	0.011(3)	0.045(3)	0.997
H9'	0.053(5)	0.06(2)	0.990	0.06(1)	0.04(1)	0.934
H10	0.67(7)	0.7(3)	0.988	0.8(2)	0.4(2)	0.866
H11	-0.0035(2)	0.0074(6)	0.998	-0.0037(6)	0.0077(5)	0.995
H12	-0.066(4)	-0.21(2)	0.996	-0.071(4)	-0.204(4)	1.000
H13	-0.14(2)	-0.27(9)	0.973	-0.18(4)	-0.19(4)	0.957
H13'	-0.17(2)	-0.21(9)	0.979	-0.22(6)	-0.12(5)	0.842
H14	-0.108(8)	-0.11(3)	0.994	-0.12(2)	-0.08(2)	0.961
H15	-0.15(2)	-0.50(8)	0.982	-0.18(3)	-0.44(2)	0.997
H16	-0.164(6)	-0.25(2)	0.999	-0.18(2)	-0.22(2)	0.992
H17	-0.15(2)	-0.52(7)	0.985	-0.17(2)	-0.48(2)	0.999
H18	-0.15(2)	-0.21(8)	0.982	-0.19(4)	-0.14(4)	0.925
H18'	-0.13(2)	-0.25(7)	0.980	-0.16(3)	-0.19(3)	0.975
H19	-0.077(5)	-0.07(2)	0.995	-0.09(1)	-0.05(1)	0.948
H20	-0.065(4)	-0.22(1)	0.997	-0.068(3)	-0.210(3)	1.000
H21	-0.012(1)	0.004(4)	0.992	-0.015(5)	0.009(4)	0.842
H22	0.054(7)	0.07(3)	0.985	0.07(1)	0.05(1)	0.931
H23	0.50(6)	0.6(2)	0.985	0.6(1)	0.4(1)	0.896
H24	0.028(4)	0.04(2)	0.979	0.035(6)	0.023(6)	0.937
H25	0.023(3)	0.03(1)	0.985	0.027(4)	0.021(4)	0.973
H26	0.035(4)	0.04(2)	0.986	0.042(7)	0.024(7)	0.932
H26'	0.031(3)	0.03(1)	0.993	0.037(9)	0.021(9)	0.870
H27	0.027(3)	0.03(1)	0.989	0.032(5)	0.022(5)	0.954

Table 48 One proton analysis of LnLu complexes of L^{AB4}

	Plots of $\Delta_{i,j}/\langle S_z\rangle_j$ vs. $C_j/\langle S_z\rangle_j$			Plots of $\Delta_{i,j}/C_j$ vs. $\langle S_z\rangle_j/C_j$		
	$B_0^2G_i$ (slope)	F_i (intercept)	Correlation coefficient	$B_0^2G_i$ (intercept)	F_i (slope)	Correlation coefficient
H1	0.0604(6)	0.041(2)	1.000	0.062(3)	0.039(2)	0.996
H2	0.0526(5)	0.037(2)	1.000	0.054(2)	0.035(2)	0.997
H3	0.082(1)	0.058(4)	1.000	0.085(4)	0.054(4)	0.995
H4	0.0804(3)	0.054(1)	1.000	0.0802(2)	0.0546(2)	1.000
H4'	0.0807(7)	0.057(3)	1.000	0.082(2)	0.054(2)	0.998
H5	0.0550(3)	0.037(1)	1.000	0.056(1)	0.036(1)	0.999
H6	0.0787(9)	0.053(4)	1.000	0.077(2)	0.057(2)	0.998
H7	0.04998(7)	0.0385(3)	1.000	0.0500(2)	0.0384(2)	1.000
H8	0.415(6)	0.29(2)	1.000	0.43(3)	0.26(2)	0.992
H9	0.0242(7)	0.039(2)	0.999	0.023(1)	0.042(1)	0.999
H9'	0.100(1)	0.075(5)	1.000	0.103(6)	0.070(5)	0.995
H10	1.23(3)	0.8(1)	0.999	1.29(8)	0.71(7)	0.989
H11	0.0094(6)	0.014(2)	0.995	0.0086(7)	0.0159(6)	0.999
H12	-0.095(1)	-0.212(5)	1.000	-0.092(6)	-0.216(5)	0.999
H13	-0.255(8)	-0.31(3)	0.999	-0.264(7)	-0.295(7)	0.999
H13'	-0.326(6)	-0.27(2)	1.000	-0.34(2)	-0.24(2)	0.995
H14	-0.168(1)	-0.121(5)	1.000	-0.171(6)	-0.117(6)	0.998
H15	-0.356(5)	-0.59(2)	1.000	-0.359(6)	-0.583(5)	1.000
H17	-0.317(4)	-0.56(2)	1.000	-0.31(1)	-0.57(1)	0.999
H18	-0.34(1)	-0.25(4)	0.999	-0.34(2)	-0.25(2)	0.994
H18'	-0.28(2)	-0.31(6)	0.997	-0.30(2)	-0.27(2)	0.995
H19	-0.143(3)	-0.08(1)	1.000	-0.15(1)	-0.076(9)	0.986
H20	-0.124(1)	-0.221(5)	1.000	-0.121(4)	-0.227(4)	1.000
H21	-0.033(2)	0.003(6)	0.998	-0.036(6)	0.007(6)	0.656
H22	0.076(3)	0.09(1)	0.999	0.078(2)	0.080(2)	0.999
H23	0.87(1)	0.69(6)	1.000	0.90(4)	0.63(4)	0.996
H24	0.0532(7)	0.038(3)	1.000	0.0539(6)	0.0367(6)	1.000
H24'	0.0529(1)	0.0372(5)	1.000	0.0530(3)	0.0372(3)	1.000
H25	0.0426(7)	0.031(2)	1.000	0.044(2)	0.028(2)	0.994
H26	0.0665(4)	0.046(2)	1.000	0.067(2)	0.045(1)	0.999
H26'	0.0551(8)	0.037(3)	1.000	0.057(4)	0.033(3)	0.990
H27	0.0533(2)	0.0369(9)	1.000	0.0535(7)	0.0367(6)	1.000
H28	-0.119(5)	-0.07(2)	0.999	-0.126(7)	-0.053(6)	0.987
H28'	-0.125(2)	-0.076(8)	1.000	-0.127(2)	-0.072(2)	0.999
H29	-0.103(1)	-0.087(5)	1.000	-0.105(2)	-0.083(2)	1.000

Table 49 One proton analysis of LnLu complexes of L^{AB5}

	Plots of $\Delta_{i,j}/\langle S_z\rangle_j$ vs. $C_j/\langle S_z\rangle_j$			Plots of $\Delta_{i,j}/C_j$ vs. $\langle S_z\rangle_j/C_j$		
	$B_0^2G_i$ (slope)	F_i (intercept)	Correlation coefficient	$B_0^2G_i$ (intercept)	F_i (slope)	Correlation coefficient
H1	0.031(4)	0.03(1)	0.987	0.038(8)	0.020(8)	0.872
H2	0.023(4)	0.03(2)	0.968	0.031(9)	0.018(9)	0.830
H3	0.040(5)	0.04(2)	0.985	0.048(8)	0.027(8)	0.932
H4	0.047(2)	0.040(9)	0.997	0.052(6)	0.031(5)	0.974
H4'	0.042(4)	0.04(1)	0.992	0.049(8)	0.030(7)	0.941
H5	0.030(2)	0.027(8)	0.996	0.035(5)	0.019(5)	0.947
H6	0.046(2)	0.043(7)	0.998	0.048(2)	0.039(2)	0.998
H7	0.035(2)	0.033(8)	0.996	0.038(3)	0.027(3)	0.990
H8	0.21(2)	0.20(8)	0.990	0.26(5)	0.13(4)	0.897
H9	0.0175(5)	0.043(2)	0.999	0.016(2)	0.045(2)	0.998
H9'	0.053(6)	0.06(2)	0.987	0.07(2)	0.04(1)	0.889
H10	0.63(7)	0.6(3)	0.987	0.8(2)	0.3(2)	0.828
H11	0.0026(2)	0.0089(9)	0.992	0.002(1)	0.010(1)	0.990
H12	-0.057(4)	-0.21(2)	0.994	-0.063(5)	-0.199(5)	0.999
H13	-0.13(2)	-0.23(8)	0.970	-0.17(4)	-0.16(4)	0.939
H13'	-0.15(2)	-0.18(9)	0.977	-0.20(6)	-0.10(5)	0.781
H14	-0.125(9)	-0.11(3)	0.995	-0.15(3)	-0.08(3)	0.899
H15	-0.13(2)	-0.44(8)	0.970	-0.16(3)	-0.37(3)	0.994
H17	-0.12(2)	-0.44(7)	0.976	-0.15(2)	-0.39(2)	0.997
H18	-0.13(2)	-0.20(8)	0.978	-0.16(3)	-0.14(2)	0.973
H18'	-0.12(2)	-0.22(6)	0.979	-0.15(4)	-0.15(3)	0.954
H19	-0.085(5)	-0.07(2)	0.996	-0.10(2)	-0.05(1)	0.924
H20	-0.062(3)	-0.21(1)	0.998	-0.064(2)	-0.205(2)	1.000
H21	-0.0079(6)	0.007(2)	0.994	-0.010(2)	0.010(2)	0.952
H22	0.052(8)	0.07(3)	0.978	0.07(2)	0.05(1)	0.912
H23	0.47(6)	0.5(2)	0.982	0.6(1)	0.3(1)	0.898
H24	0.033(2)	0.024(7)	0.997	0.038(8)	0.016(7)	0.845
H24'	0.030(3)	0.03(1)	0.992	0.037(8)	0.017(8)	0.847
H25	0.022(3)	0.02(1)	0.984	0.027(6)	0.016(5)	0.908
H26	0.039(2)	0.026(8)	0.997	0.044(7)	0.018(6)	0.891
H26'	0.028(3)	0.03(1)	0.991	0.034(7)	0.018(7)	0.875
H27	0.027(3)	0.03(1)	0.989	0.034(8)	0.017(7)	0.860

The value of F_i can be determined either as the slope of a plot according to Eq. (3) or as the intercept of plot according to Eq. (4) (and *vice versa* for $B_0^2 G_i$). In practice all parameters used for further treatment have been determined as slopes, since this gives lower standard errors. The reason for this is probably that all values of $C_j/\langle S_Z \rangle_j$ and $\langle S_Z \rangle_j / C_j$ are positive for the paramagnetic lanthanide ions in this study, meaning that all intercepts have to be determined as extrapolations. This choice may thus not be generally applicable for any set of lanthanide ions. Note that the numerical values of F_i and $B_0^2 G_i$ are similar, regardless of whether they have been determined as slopes or intercepts.

The fits according to eq. (4) are excellent with almost all correlation coefficients being larger than 0.98 (Table 42 - Table 49). In all complex series correlation coefficients (when viewed as a whole for the entire ligand) were lower for the fits to (3) than for the fits to (4). No certain explanation is given for this. It could be related to the calculated values of $\langle S_z \rangle_j$ and C_j, the problem could also arise from the crystal field parameter B_0^2. It is usually assumed when treating lanthanide induced shift that this parameter is the same for the whole lanthanide series, but when actually measured it turns out that this is not the case.[90,94]

Some of the low correlation coefficients can be explained by the protons in question being close to one of the so-called magic angles (54.74º and 125.26º) which causes the structural factors G_i ($= (3\cos^2\theta_i - 1)/r_i^3$) to be close to 0. Using the crystal structures available as general structural models (i.e. for a moment disregarding *which* lanthanide ions are in the structure) it is seen from Table 87 - Table 94 (*vide infra*) that placing the paramagnetic lanthanide ion in either the bpa or bpb cavity leaves some protons close to a so-called magic angle. Examining the calculated G_i factors and the averages thereof (Table 95 - Table 102) it is evident that the average G_i factors for these protons are small and (when the standard deviations are also considered) could be zero.

With the paramagnetic lanthanide ion placed in the bpb site the potential problematic protons are H11 (5 solid state structures out of 8 exhibit a standard deviation on the average of G_i of more than 100 %), H20 (5 out of 8), H21 (8 out of 8) and H22 (3 out of 8). This is reflected in the correlation coefficients of the plots involving the four series of LnLu complexes, in which the paramagnetic lanthanide ion is in the bpb cavity. For the L^{AB} complexes (Table 46) the lowest correlation coefficients are for H21 (0.822) and H11 (0.961) for the plots according to

equations (3) and (4), respectively. H21 also has the lowest correlation coefficients for the Eq. (3) plots of the LnLu series of the ligands L^{AB3} (0.842; Table 47) and L^{AB4} (0.656; Table 48). For the L^{AB5} series of complexes (Table 49) H11 (correlation coefficient 0.990) and H21 (0.952) are not the most problematic protons; there are 14 protons with correlation coefficients lower than 0.9. This underlines that the so-called magic angles are not the only factor influencing the quality of the plots.

Placing the Ln ion in the bpa cavity causes problems for H6 (4 out of 8 solid state structures) and H26 (8 out of 8), in the sense that these two protons are close to a so-called magic angle when the average of the three ligand strands is used. A closer look at the angles calculated for the individual ligand strands of the L^{AB3} complexes reveals that all four methylene protons of the carboxamide group (H24, H24', H26 and H26') could be problematic since the values for two strands are below (101.05° – 119.27°) and for the third strand above (129.99° – 158.61°) one of the so-called magic angles (125.26º). This is in accordance with the analysis of the LIS data since H24', H26 and H26' have low correlation coefficients of the plots for the LaLn series for all four ligands (Table 42 - Table 45).

For complexes with paramagnetic lanthanide ions in both the bpa and bpb cavities (Ln_2) the problem with the so-called magic angles should be less pronounced since no protons are close to the magic angles of both lanthanides. It is, however, noteworthy that most of the protons with low correlation coefficients in the LIS analysis (Table 38 - Table 41) are among those pointed out as problematic protons above.

The hyperfine coupling constants (F_i) of the contact terms determined by the Reilley method are generally speaking as expected with appreciable values ($|F_i|$ 0.07) mostly for protons topologically close to the paramagnetic lanthanide ion.

The separation of contact and pseudo contact terms can certainly be said to be successful considering the overall good correlations of the plots according to Eqs. (3), (4), (7) and (8), but the analysis is not flawless. For some protons with large pseudo contact shifts the contact shifts seem to be too large. Examples: In LnLu F_8 is about one third of F_{10} even though separated from Ln by four additional bonds. In LaLn F_8 and F_{10} are about equal despite a bond difference of four. In the LaLn series F_{27} is very large compared to F_{26} and $F_{26'}$. Bond counting would have it smaller and the large value is no doubt related to

insufficient separation from the very large pseudo contact shift (H26 and H26' being closer to the so-called magic angle than H27). This is not to say that the one proton separation is not useful, but only to point out that a critical sense should be applied whenever comparing contact terms of different protons. We will return to this problem in the modified one proton analysis (Chapter 5.7; page 223).

5.3.6 Comparing contact and pseudo contact parameters

F_i and $B_0^2 G_i$ parameters of complexes of the four different ligands are compared in Figure 49. It is obvious (as it was by the comparison of LIS of the complexes, Figure 42) that the complexes of the two Cl substituted ligands L^{AB3} and L^{AB5} are very similar to those of L^{AB} whereas the L^{AB4} complexes deviate significantly.

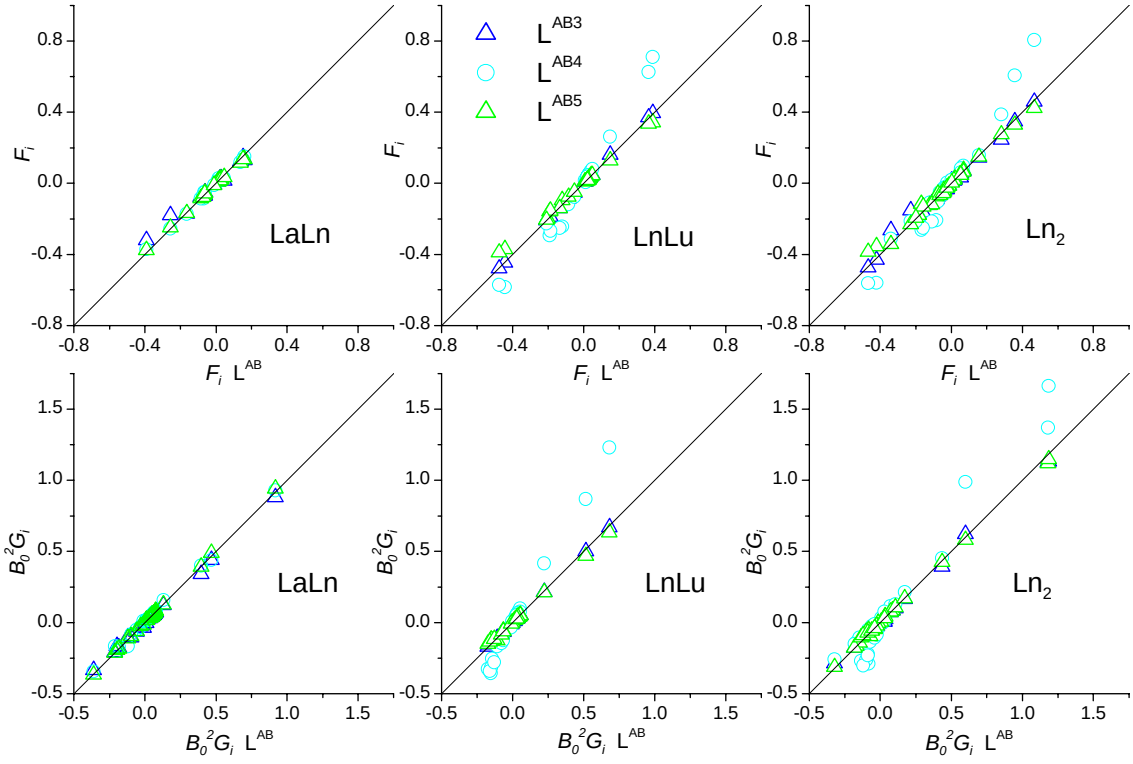

Figure 49 Comparing contact and pseudo contact parameters

Interestingly, the largest difference between L^{AB3} and L^{AB5} complexes and those of L^{AB} are seen for the two protons in *cis* position to the Cl substituent on a pyridine group coordinated to the paramagnetic lanthanide ion (H1 and H3 in LaLn$(L^{AB3})_3$; H15 and H17 in LnLu$(L^{AB5})_3$). In both cases, the difference is apparent as a decrease in the numerical value of the F_i parameter, indicating reduced overlap between lanthanide and ligand orbitals. This is in

line with what would be expected since the electron-withdrawing Cl substituent leads to reduced electron density of the N ligator of the ligand. The difference is only significant for the contact (and not the pseudo contact) parameter, indicating that the effect induced by the Cl substituent is electronic in nature and not accompanied by a structural change.

Note that the F_i parameters for H15 and H17 in $LnLu(L^{AB4})_3$ are displaced in the opposite direction with respect to what was found for $LnLu(L^{AB5})_3$ in accordance with the electron-*donating* character of the NEt_2 substituent.

As mentioned above some of the contact parameters seem to be too large, most likely a result of less-than-perfect separation from their pseudo contact counterparts, especially when the latter are dominating the LIS. Thus it would be premature to conclude too much based on the F_i parameters of H8, H10 and H23 in the $LnLu(L^{AB4})_3$ and $Ln_2(L^{AB4})_3$ complexes and their apparent deviation from the values of the same protons in the L^{AB} complexes. It is at this point of the analysis very possible that this is due to a structural change (as opposed to an electronic effect), which strongly influences the pseudo contact shift of these three protons (the closest to the paramagnetic lanthanide ion in the bpb coordination cavity in these two series of complexes). A change in the B_0^2 parameter is also possible and we will have to wait for two proton and the modified one proton analyses before we can give a conclusive answer to this question.

5.3.7 Recalculation of contact and pseudo contact shifts

The contact and pseudo contact contributions to the total lanthanide induced shift have been calculated using values of F_i and $B_0^2 G_i$ determined as the slopes of plots according to Equations. (3), (4), (7) or (8) and subsequently multiplied by $\langle S_z \rangle_j$ or C_j. The results are given in Table 50 - Table 61.

Table 50 Contact and pseudo contact terms of Ln_2 complexes of L^{AB}

	Ce_2		Pr_2		Nd_2		Eu_2	
	Δ_c	Δ_{pc}	Δ_c	Δ_{pc}	Δ_c	Δ_{pc}	Δ_c	Δ_{pc}
H1	0.22(2)	1.1(1)	0.68(7)	1.8(2)	1.0(1)	0.70(7)	-1.7(2)	-0.67(6)
H2	0.13(2)	1.6(1)	0.38(6)	2.8(3)	0.57(9)	1.1(1)	-1.0(1)	-1.03(9)
H3	0.33(3)	2.0(1)	1.0(1)	3.6(2)	1.5(1)	1.36(9)	-2.5(3)	-1.29(9)
H4	0.013(3)	0.54(2)	0.040(8)	0.94(4)	0.06(1)	0.36(1)	-0.10(2)	-0.34(1)
H4'	0.023(3)	0.92(2)	0.069(9)	1.60(4)	0.10(1)	0.61(1)	-0.18(2)	-0.58(1)
H5	0.04(1)	1.14(7)	0.12(3)	2.0(1)	0.18(5)	0.76(4)	-0.30(8)	-0.72(4)
H6	0.118(6)	-0.03(2)	0.36(2)	-0.06(4)	0.54(3)	-0.02(1)	-0.91(5)	0.02(1)
H7	-0.048(4)	-0.45(1)	-0.14(1)	-0.79(2)	-0.22(2)	-0.302(8)	0.37(3)	0.287(7)
H8	-0.27(6)	-7.4(1)	-0.8(2)	-13.0(2)	-1.3(3)	-4.96(8)	2.1(4)	4.72(8)
H9	-0.067(6)	-0.53(2)	-0.20(2)	-0.93(3)	-0.31(3)	-0.36(1)	0.51(4)	0.34(1)
H9'	-0.067(9)	-0.45(3)	-0.20(3)	-0.78(5)	-0.30(4)	-0.30(2)	0.51(7)	0.28(2)
H10	-0.5(2)	-7.5(3)	-1.4(5)	-13.0(6)	-2.1(8)	-5.0(2)	4(1)	4.7(2)
H11	-0.018(3)	-0.197(7)	-0.056(9)	-0.34(1)	-0.08(1)	-0.131(5)	0.14(2)	0.125(4)
H12	0.178(7)	0.09(4)	0.54(2)	0.16(7)	0.82(3)	0.06(3)	-1.37(6)	-0.06(3)
H13	0.16(5)	0.5(2)	0.5(1)	1.0(3)	0.7(2)	0.4(1)	-1.3(4)	-0.3(1)
H13'	0.08(7)	0.8(2)	0.2(2)	1.5(3)	0.4(3)	0.6(1)	-0.6(5)	-0.5(1)
H14	0.07(2)	0.45(7)	0.22(6)	0.8(1)	0.33(9)	0.30(5)	-0.6(1)	-0.28(5)
H15	0.41(3)	0.5(2)	1.25(8)	0.9(3)	1.9(1)	0.3(1)	-3.2(2)	-0.3(1)
H16	0.21(2)	0.74(5)	0.65(5)	1.29(9)	0.98(8)	0.49(4)	-1.6(1)	-0.47(3)
H17	0.46(2)	0.6(1)	1.38(6)	1.1(2)	2.08(9)	0.41(9)	-3.5(2)	-0.39(9)
H18	0.11(4)	0.8(1)	0.3(1)	1.3(2)	0.5(2)	0.51(9)	-0.8(3)	-0.48(9)
H18'	0.15(4)	0.5(1)	0.5(1)	1.0(2)	0.7(2)	0.36(8)	-1.2(3)	-0.35(8)
H19	0.04(1)	0.25(5)	0.13(4)	0.44(8)	0.19(6)	0.17(3)	-0.3(1)	-0.16(3)
H20	0.194(5)	0.16(4)	0.59(1)	0.28(6)	0.89(2)	0.11(2)	-1.49(3)	-0.10(2)
H21	-0.016(2)	-0.17(2)	-0.047(7)	-0.30(3)	-0.07(1)	-0.11(1)	0.12(2)	0.11(1)
H22	-0.05(2)	-0.67(3)	-0.16(5)	-1.17(5)	-0.24(7)	-0.45(2)	0.4(1)	0.42(2)
H23	-0.3(1)	-3.8(5)	-1.1(4)	-6.6(8)	-1.6(6)	-2.5(3)	2.7(9)	2.4(3)
H24	0.06(1)	0.38(4)	0.19(4)	0.66(7)	0.29(5)	0.25(2)	-0.49(9)	-0.24(2)
H24'	0.045(6)	-0.22(4)	0.14(2)	-0.38(7)	0.21(3)	-0.15(3)	-0.35(5)	0.14(3)
H25	0.024(3)	0.26(3)	0.07(1)	0.45(5)	0.11(1)	0.17(2)	-0.19(3)	-0.16(2)
H26	-0.05(1)	-1.09(6)	-0.16(4)	-1.9(1)	-0.24(6)	-0.73(4)	0.4(1)	0.69(4)
H26'	-0.003(7)	-0.18(1)	-0.01(2)	-0.32(2)	-0.01(3)	-0.123(7)	0.03(5)	0.117(7)
H27	-0.152(6)	-2.74(5)	-0.46(2)	-4.79(8)	-0.69(3)	-1.83(3)	1.17(5)	1.74(3)

Table 51 Contact and pseudo contact terms of Ln_2 complexes of L^{AB3}

	Ce_2		Pr_2		Nd_2		Eu_2	
	Δ_c	Δ_{pc}	Δ_c	Δ_{pc}	Δ_c	Δ_{pc}	Δ_c	Δ_{pc}
H1	0.15(1)	0.81(8)	0.45(4)	1.4(1)	0.68(7)	0.54(5)	-1.1(1)	-0.52(5)
H3	0.26(2)	1.8(1)	0.78(6)	3.2(2)	1.2(1)	1.21(6)	-2.0(2)	-1.15(6)
H4	0.011(3)	0.43(2)	0.034(9)	0.76(4)	0.05(1)	0.29(2)	-0.09(2)	-0.28(1)
H4'	0.005(4)	0.84(2)	0.02(1)	1.46(3)	0.02(2)	0.56(1)	-0.04(3)	-0.53(1)
H5	0.036(9)	1.11(6)	0.11(3)	1.9(1)	0.16(4)	0.74(4)	-0.28(7)	-0.70(4)
H6	0.120(9)	-0.07(3)	0.36(3)	-0.11(5)	0.55(4)	-0.04(2)	-0.93(7)	0.04(2)
H7	-0.0489(8)	-0.460(5)	-0.148(2)	-0.804(8)	-0.224(4)	-0.307(3)	0.377(6)	0.292(3)
H8	-0.24(6)	-7.1(1)	-0.7(2)	-12.4(2)	-1.1(3)	-4.73(7)	1.8(5)	4.50(7)
H9	-0.066(4)	-0.53(2)	-0.20(1)	-0.93(4)	-0.30(2)	-0.36(1)	0.51(3)	0.34(1)
H9'	-0.068(9)	-0.51(4)	-0.21(3)	-0.90(6)	-0.31(4)	-0.34(2)	0.52(7)	0.33(2)
H10	-0.4(2)	-7.1(4)	-1.4(5)	-12.5(7)	-2.0(8)	-4.8(3)	3(1)	4.5(2)
H11	-0.019(1)	-0.218(5)	-0.057(4)	-0.38(1)	-0.087(6)	-0.146(4)	0.15(1)	0.139(3)
H12	0.181(9)	0.07(5)	0.55(3)	0.12(9)	0.83(4)	0.05(3)	-1.39(7)	-0.05(3)
H13	0.16(4)	0.6(2)	0.5(1)	1.0(3)	0.8(2)	0.4(1)	-1.3(3)	-0.4(1)
H13'	0.09(7)	0.8(2)	0.3(2)	1.4(3)	0.4(3)	0.5(1)	-0.7(5)	-0.5(1)
H14	0.07(2)	0.47(7)	0.22(7)	0.8(1)	0.3(1)	0.31(5)	-0.6(2)	-0.30(5)
H15	0.42(3)	0.5(2)	1.27(8)	0.9(3)	1.9(1)	0.3(1)	-3.2(2)	-0.3(1)
H16	0.22(2)	0.73(6)	0.66(6)	1.3(1)	0.99(8)	0.48(4)	-1.7(1)	-0.46(4)
H17	0.46(2)	0.6(1)	1.40(6)	1.1(2)	2.11(9)	0.40(9)	-3.5(2)	-0.38(9)
H18	0.11(4)	0.8(1)	0.3(1)	1.3(2)	0.5(2)	0.51(9)	-0.9(3)	-0.48(9)
H18'	0.16(4)	0.5(1)	0.5(1)	0.9(2)	0.7(2)	0.35(9)	-1.2(3)	-0.34(8)
H19	0.04(1)	0.27(5)	0.13(4)	0.46(8)	0.20(6)	0.18(3)	-0.3(1)	-0.17(3)
H20	0.196(5)	0.16(4)	0.60(1)	0.28(7)	0.90(2)	0.11(3)	-1.51(4)	-0.10(2)
H21	-0.014(3)	-0.16(2)	-0.04(1)	-0.28(3)	-0.06(2)	-0.11(1)	0.11(3)	0.10(1)
H22	-0.05(1)	-0.63(3)	-0.16(4)	-1.11(6)	-0.24(7)	-0.42(2)	0.4(1)	0.40(2)
H23	-0.3(1)	-3.9(4)	-1.0(4)	-6.9(6)	-1.5(6)	-2.6(2)	3(1)	2.5(2)
H24	0.050(4)	0.40(2)	0.15(1)	0.71(3)	0.23(2)	0.27(1)	-0.38(3)	-0.26(1)
H24'	0.045(9)	-0.14(4)	0.14(3)	-0.24(7)	0.21(4)	-0.09(3)	-0.35(7)	0.09(3)
H25	0.033(4)	0.24(3)	0.10(1)	0.41(5)	0.15(2)	0.16(2)	-0.26(3)	-0.15(2)
H26	-0.03(2)	-1.05(6)	-0.10(5)	-1.8(1)	-0.15(8)	-0.70(4)	0.2(1)	0.66(4)
H26'	-0.015(2)	-0.04(2)	-0.046(7)	-0.08(3)	-0.07(1)	-0.03(1)	0.12(2)	0.03(1)
H27	-0.140(4)	-2.47(1)	-0.43(1)	-4.32(2)	-0.64(2)	-1.649(7)	1.08(3)	1.571(7)

Table 52 Contact and pseudo contact terms of Ln_2 complexes of L^{AB4}

	Ce_2		Pr_2		Nd_2		Eu_2	
	Δ_c	Δ_{pc}	Δ_c	Δ_{pc}	Δ_c	Δ_{pc}	Δ_c	Δ_{pc}
H1	0.21(2)	0.87(8)	0.63(5)	1.5(1)	0.94(7)	0.58(5)	-1.6(1)	-0.56(5)
H2	0.11(2)	1.4(1)	0.33(5)	2.4(2)	0.50(7)	0.93(8)	-0.8(1)	-0.88(8)
H3	0.30(3)	1.6(1)	0.92(8)	2.8(2)	1.4(1)	1.08(6)	-2.3(2)	-1.03(6)
H4	0.012(5)	0.333(8)	0.04(1)	0.58(1)	0.06(2)	0.222(5)	-0.09(3)	-0.212(5)
H4'	-0.002(6)	0.68(2)	-0.01(2)	1.18(3)	-0.01(3)	0.45(1)	0.02(5)	-0.43(1)
H5	0.025(6)	0.95(4)	0.07(2)	1.66(8)	0.11(3)	0.63(3)	-0.19(5)	-0.60(3)
H6	0.106(7)	-0.20(1)	0.32(2)	-0.36(2)	0.49(3)	-0.136(8)	-0.82(6)	0.129(8)
H7	-0.055(2)	-0.512(8)	-0.166(7)	-0.89(1)	-0.25(1)	-0.341(6)	0.42(2)	0.325(5)
H8	-0.38(5)	-8.6(1)	-1.1(1)	-15.1(3)	-1.7(2)	-5.8(1)	2.9(4)	5.48(9)
H9	-0.060(4)	-0.60(2)	-0.18(1)	-1.04(4)	-0.28(2)	-0.40(2)	0.46(3)	0.38(1)
H9'	-0.095(5)	-0.72(4)	-0.29(1)	-1.26(7)	-0.43(2)	-0.48(3)	0.73(4)	0.46(2)
H10	-0.8(1)	-10.5(2)	-2.4(3)	-18.3(3)	-3.6(4)	-7.0(1)	6.0(7)	6.7(1)
H11	-0.028(1)	-0.266(9)	-0.084(4)	-0.47(2)	-0.127(5)	-0.178(6)	0.213(9)	0.169(6)
H12	0.189(2)	0.26(1)	0.573(5)	0.46(2)	0.863(8)	0.176(8)	-1.45(1)	-0.168(8)
H13	0.26(1)	1.39(2)	0.77(3)	2.43(4)	1.17(5)	0.93(1)	-1.96(8)	-0.88(1)
H13'	0.20(3)	1.71(8)	0.61(9)	3.0(1)	0.9(1)	1.14(5)	-1.6(2)	-1.09(5)
H14	0.101(6)	0.85(2)	0.31(2)	1.49(3)	0.46(3)	0.57(1)	-0.77(5)	-0.54(1)
H15	0.545(7)	1.81(6)	1.65(2)	3.2(1)	2.49(3)	1.21(4)	-4.20(6)	-1.15(4)
H17	0.55(1)	1.66(4)	1.66(3)	2.90(8)	2.50(5)	1.11(3)	-4.21(9)	-1.05(3)
H18	0.21(3)	1.89(6)	0.6(1)	3.3(1)	1.0(1)	1.26(4)	-1.6(2)	-1.20(4)
H18'	0.24(2)	1.5(1)	0.74(7)	2.5(2)	1.1(1)	0.97(8)	-1.9(2)	-0.92(7)
H19	0.06(1)	0.67(2)	0.19(3)	1.16(3)	0.28(5)	0.44(1)	-0.48(8)	-0.42(1)
H20	0.209(2)	0.540(3)	0.633(6)	0.943(6)	0.954(8)	0.360(2)	-1.61(1)	-0.343(2)
H21	-0.014(4)	-0.028(9)	-0.04(1)	-0.05(2)	-0.07(2)	-0.019(6)	0.11(3)	0.018(6)
H22	-0.081(4)	-0.81(2)	-0.25(1)	-1.41(4)	-0.37(2)	-0.54(2)	0.63(3)	0.51(1)
H23	-0.59(6)	-6.2(1)	-1.8(2)	-10.9(2)	-2.7(3)	-4.15(7)	4.5(5)	3.95(7)
H24	0.050(8)	0.15(6)	0.15(3)	0.3(1)	0.23(4)	0.10(4)	-0.38(6)	-0.09(4)
H24'	0.037(7)	-0.44(5)	0.11(2)	-0.8(1)	0.17(3)	-0.29(4)	-0.28(5)	0.28(3)
H25	0.017(5)	0.07(4)	0.05(1)	0.12(6)	0.08(2)	0.04(2)	-0.13(3)	-0.04(2)
H26	-0.06(1)	-1.35(7)	-0.18(4)	-2.4(1)	-0.27(7)	-0.90(5)	0.5(1)	0.86(4)
H26'	-0.019(4)	-0.48(3)	-0.06(1)	-0.83(5)	-0.09(2)	-0.32(2)	0.15(3)	0.30(2)
H27	-0.154(7)	-2.85(5)	-0.47(2)	-4.97(9)	-0.70(3)	-1.90(4)	1.18(5)	1.81(3)
H28	0.048(5)	0.57(4)	0.15(2)	1.00(7)	0.22(2)	0.38(2)	-0.37(4)	-0.36(2)
H28'	0.062(2)	0.64(2)	0.187(7)	1.12(3)	0.28(1)	0.43(1)	-0.48(2)	-0.41(1)
H29	0.077(3)	0.48(3)	0.23(1)	0.83(4)	0.35(1)	0.32(2)	-0.59(2)	-0.30(2)

Table 53 Contact and pseudo contact terms of Ln_2 complexes of L^{AB5}

	Ce_2		Pr_2		Nd_2		Eu_2	
	Δ_c	Δ_{pc}	Δ_c	Δ_{pc}	Δ_c	Δ_{pc}	Δ_c	Δ_{pc}
H1	0.22(2)	1.0(1)	0.68(7)	1.8(2)	1.0(1)	0.68(7)	-1.7(2)	-0.65(6)
H2	0.13(2)	1.6(1)	0.39(6)	2.7(2)	0.59(9)	1.05(9)	-1.0(1)	-1.00(9)
H3	0.33(3)	2.0(1)	1.01(9)	3.4(2)	1.5(1)	1.31(9)	-2.6(2)	-1.25(8)
H4	0.014(3)	0.49(2)	0.042(9)	0.85(3)	0.06(1)	0.33(1)	-0.11(2)	-0.31(1)
H4'	0.024(3)	0.90(2)	0.07(1)	1.57(3)	0.11(2)	0.60(1)	-0.18(3)	-0.57(1)
H5	0.04(1)	1.12(6)	0.13(3)	2.0(1)	0.20(5)	0.75(4)	-0.34(9)	-0.71(4)
H6	0.120(7)	-0.04(3)	0.36(2)	-0.08(5)	0.55(3)	-0.03(2)	-0.92(5)	0.03(2)
H7	-0.048(3)	-0.473(4)	-0.145(8)	-0.826(7)	-0.22(1)	-0.316(3)	0.37(2)	0.301(3)
H8	-0.27(6)	-7.1(1)	-0.8(2)	-12.3(2)	-1.2(3)	-4.70(8)	2.1(5)	4.48(8)
H9	-0.071(5)	-0.55(1)	-0.22(2)	-0.95(2)	-0.33(3)	-0.364(7)	0.55(4)	0.347(6)
H9'	-0.063(9)	-0.48(3)	-0.19(3)	-0.83(5)	-0.29(4)	-0.32(2)	0.49(7)	0.30(2)
H10	-0.4(2)	-7.2(3)	-1.3(5)	-12.6(5)	-1.9(7)	-4.8(2)	3(1)	4.6(2)
H11	-0.024(3)	-0.236(9)	-0.073(8)	-0.41(2)	-0.11(1)	-0.158(6)	0.19(2)	0.150(6)
H12	0.172(9)	0.03(4)	0.52(3)	0.04(6)	0.79(4)	0.02(2)	-1.32(7)	-0.02(2)
H13	0.11(6)	0.5(2)	0.3(2)	0.9(3)	0.5(3)	0.4(1)	-0.9(4)	-0.3(1)
H13'	0.07(6)	0.7(1)	0.2(2)	1.1(2)	0.3(3)	0.43(9)	-0.6(5)	-0.41(9)
H14	0.06(4)	0.59(8)	0.2(1)	1.0(1)	0.3(2)	0.39(5)	-0.4(3)	-0.37(5)
H15	0.35(3)	0.3(2)	1.0(1)	0.6(3)	1.6(1)	0.2(1)	-2.7(2)	-0.2(1)
H17	0.38(2)	0.4(1)	1.14(7)	0.7(2)	1.7(1)	0.28(9)	-2.9(2)	-0.26(9)
H18	0.12(2)	0.6(1)	0.35(6)	1.0(2)	0.53(9)	0.38(9)	-0.9(1)	-0.36(9)
H18'	0.13(4)	0.5(1)	0.4(1)	0.8(2)	0.6(2)	0.30(9)	-1.0(3)	-0.29(9)
H19	0.04(1)	0.29(5)	0.11(5)	0.51(8)	0.17(7)	0.19(3)	-0.3(1)	-0.18(3)
H20	0.189(5)	0.13(3)	0.57(1)	0.23(5)	0.86(2)	0.09(2)	-1.46(4)	-0.08(2)
H21	-0.016(2)	-0.20(1)	-0.049(6)	-0.34(2)	-0.07(1)	-0.132(7)	0.12(2)	0.125(6)
H22	-0.05(2)	-0.67(4)	-0.14(6)	-1.17(7)	-0.21(9)	-0.45(3)	0.4(1)	0.43(3)
H23	-0.3(1)	-3.7(4)	-1.0(4)	-6.4(7)	-1.5(6)	-2.4(3)	2(1)	2.3(2)
H24	0.06(1)	0.36(4)	0.20(3)	0.63(6)	0.30(5)	0.24(2)	-0.50(8)	-0.23(2)
H24'	0.054(8)	-0.27(4)	0.16(2)	-0.47(6)	0.25(4)	-0.18(2)	-0.41(6)	0.17(2)
H25	0.026(3)	0.24(2)	0.078(8)	0.43(3)	0.12(1)	0.16(1)	-0.20(2)	-0.15(1)
H26	-0.05(2)	-1.07(5)	-0.14(5)	-1.87(8)	-0.21(7)	-0.72(3)	0.4(1)	0.68(3)
H26'	-0.0051(7)	-0.187(1)	-0.016(2)	-0.326(2)	-0.023(3)	-0.1244(8)	0.040(6)	0.1185(8)
H27	-0.146(5)	-2.68(4)	-0.44(1)	-4.69(6)	-0.67(2)	-1.79(2)	1.12(4)	1.70(2)

Table 54 Contact and pseudo contact terms of LaLn complexes of L^{AB}

	LaCe		LaPr		LaNd		LaEu	
	Δ_c	Δ_{pc}	Δ_c	Δ_{pc}	Δ_c	Δ_{pc}	Δ_c	Δ_{pc}
H1	0.25(1)	1.24(8)	0.76(4)	2.2(1)	1.14(6)	0.83(5)	-1.9(1)	-0.79(5)
H2	0.15(2)	1.8(1)	0.46(5)	3.1(2)	0.70(8)	1.20(9)	-1.2(1)	-1.14(8)
H3	0.38(2)	2.3(1)	1.16(6)	4.0(2)	1.74(9)	1.52(6)	-2.9(2)	-1.45(6)
H4	0.064(3)	0.76(1)	0.19(1)	1.33(2)	0.29(1)	0.509(8)	-0.49(3)	-0.484(8)
H4'	0.060(4)	1.158(8)	0.18(1)	2.02(1)	0.28(2)	0.772(5)	-0.46(3)	-0.736(5)
H5	0.067(8)	1.33(6)	0.20(2)	2.3(1)	0.31(3)	0.88(4)	-0.52(6)	-0.84(4)
H6	0.16(1)	0.19(2)	0.49(3)	0.33(3)	0.74(5)	0.13(1)	-1.24(8)	-0.12(1)
H7	-0.023(2)	-0.30(2)	-0.071(7)	-0.53(3)	-0.11(1)	-0.20(1)	0.18(2)	0.19(1)
H8	-0.16(3)	-5.8(2)	-0.47(9)	-10.1(3)	-0.7(1)	-3.9(1)	1.2(2)	3.7(1)
H9	-0.024(2)	-0.48(1)	-0.072(6)	-0.83(2)	-0.108(8)	-0.318(9)	0.18(1)	0.303(9)
H9'	-0.030(5)	-0.10(2)	-0.09(2)	-0.17(3)	-0.13(2)	-0.06(1)	0.23(4)	0.06(1)
H10	-0.13(2)	-2.9(2)	-0.41(6)	-5.1(3)	-0.61(9)	-2.0(1)	1.0(2)	1.9(1)
H11	-0.014(2)	-0.214(4)	-0.041(6)	-0.374(6)	-0.062(9)	-0.143(2)	0.10(2)	0.136(2)
H12	-0.021(2)	-0.348(6)	-0.064(6)	-0.61(1)	-0.096(9)	-0.232(4)	0.16(1)	0.221(4)
H13	-0.018(4)	-0.42(3)	-0.05(1)	-0.73(5)	-0.08(2)	-0.28(2)	0.14(3)	0.27(2)
H13'	-0.021(3)	-0.407(7)	-0.065(8)	-0.71(1)	-0.10(1)	-0.272(5)	0.17(2)	0.259(5)
H14	-0.011(3)	-0.30(2)	-0.034(9)	-0.52(3)	-0.05(1)	-0.20(1)	0.09(2)	0.19(1)
H15	-0.025(1)	-0.47(1)	-0.076(4)	-0.83(2)	-0.114(6)	-0.317(6)	0.19(1)	0.302(6)
H16	-0.016(1)	-0.30(1)	-0.048(4)	-0.53(2)	-0.072(6)	-0.203(7)	0.12(1)	0.193(7)
H17	-0.017(3)	-0.37(2)	-0.052(9)	-0.65(4)	-0.08(1)	-0.25(1)	0.13(2)	0.24(1)
H18	-0.020(3)	-0.34(2)	-0.062(9)	-0.60(3)	-0.09(1)	-0.23(1)	0.16(2)	0.22(1)
H18'	-0.015(2)	-0.30(1)	-0.047(7)	-0.52(2)	-0.07(1)	-0.200(9)	0.12(2)	0.190(9)
H19	-0.013(3)	-0.23(1)	-0.040(8)	-0.41(2)	-0.06(1)	-0.155(9)	0.10(2)	0.148(8)
H20	-0.012(2)	-0.24(1)	-0.038(5)	-0.42(2)	-0.057(7)	-0.161(8)	0.10(1)	0.154(8)
H21	-0.011(1)	-0.21(1)	-0.033(4)	-0.36(2)	-0.049(6)	-0.139(6)	0.08(1)	0.132(6)
H22	-0.013(1)	-0.27(1)	-0.038(4)	-0.47(2)	-0.058(6)	-0.181(7)	0.10(1)	0.172(7)
H23	-0.022(3)	-0.46(3)	-0.07(1)	-0.80(5)	-0.10(1)	-0.31(2)	0.17(3)	0.29(2)
H24	0.084(7)	0.60(5)	0.25(2)	1.06(9)	0.38(3)	0.40(4)	-0.65(5)	-0.38(3)
H24'	0.071(8)	-0.05(6)	0.22(2)	-0.1(1)	0.33(4)	-0.03(4)	-0.55(6)	0.03(4)
H25	0.062(7)	0.37(5)	0.19(2)	0.65(8)	0.28(3)	0.25(3)	-0.47(5)	-0.23(3)
H26	-0.04(3)	-0.82(7)	-0.13(8)	-1.4(1)	-0.2(1)	-0.54(5)	0.3(2)	0.52(4)
H26'	0.01(1)	0.06(4)	0.03(3)	0.11(6)	0.05(5)	0.04(2)	-0.08(9)	-0.04(2)
H27	-0.149(7)	-2.49(6)	-0.45(2)	-4.4(1)	-0.68(3)	-1.66(4)	1.14(6)	1.58(4)

Table 55 Contact and pseudo contact terms of LaLn complexes of L^{AB3}

	LaCe		LaPr		LaNd		LaEu	
	Δ_c	Δ_{pc}	Δ_c	Δ_{pc}	Δ_c	Δ_{pc}	Δ_c	Δ_{pc}
H1	0.17(1)	1.05(7)	0.53(3)	1.8(1)	0.80(4)	0.70(4)	-1.34(7)	-0.66(4)
H3	0.31(2)	2.11(8)	0.95(6)	3.7(1)	1.43(9)	1.40(6)	-2.4(2)	-1.34(5)
H4	0.06(2)	0.65(3)	0.18(5)	1.14(5)	0.26(8)	0.43(2)	-0.4(1)	-0.41(2)
H4'	0.050(5)	1.11(1)	0.15(1)	1.93(2)	0.23(2)	0.738(9)	-0.39(4)	-0.703(9)
H5	0.065(8)	1.30(6)	0.20(2)	2.3(1)	0.30(4)	0.87(4)	-0.50(6)	-0.83(4)
H6	0.17(1)	0.17(2)	0.51(4)	0.29(4)	0.76(6)	0.11(2)	-1.3(1)	-0.11(2)
H7	-0.023(2)	-0.30(1)	-0.069(6)	-0.53(2)	-0.104(9)	-0.202(7)	0.18(2)	0.192(7)
H8	-0.13(2)	-5.5(2)	-0.39(7)	-9.7(3)	-0.6(1)	-3.7(1)	1.0(2)	3.5(1)
H9	-0.027(3)	-0.46(1)	-0.081(9)	-0.80(2)	-0.12(1)	-0.307(8)	0.20(2)	0.292(8)
H9'	-0.026(4)	-0.149(6)	-0.08(1)	-0.26(1)	-0.12(2)	-0.099(4)	0.20(3)	0.094(4)
H10	-0.12(2)	-2.8(1)	-0.36(5)	-4.8(2)	-0.55(8)	-1.85(9)	0.9(1)	1.76(8)
H11	-0.016(3)	-0.215(5)	-0.048(8)	-0.376(8)	-0.07(1)	-0.143(3)	0.12(2)	0.137(3)
H12	-0.021(5)	-0.35(2)	-0.06(2)	-0.62(4)	-0.10(2)	-0.24(2)	0.16(4)	0.22(2)
H13	-0.019(2)	-0.37(2)	-0.058(8)	-0.65(3)	-0.09(1)	-0.25(1)	0.15(2)	0.24(1)
H13'	-0.018(2)	-0.40(1)	-0.053(6)	-0.70(2)	-0.080(9)	-0.266(9)	0.14(2)	0.253(9)
H14	-0.013(3)	-0.28(2)	-0.04(1)	-0.48(3)	-0.06(2)	-0.18(1)	0.10(3)	0.18(1)
H15	-0.021(3)	-0.46(2)	-0.06(1)	-0.81(4)	-0.09(1)	-0.31(2)	0.16(2)	0.30(1)
H16	-0.014(2)	-0.28(1)	-0.044(6)	-0.49(2)	-0.066(8)	-0.187(8)	0.11(1)	0.178(8)
H17	-0.018(3)	-0.34(1)	-0.053(9)	-0.59(3)	-0.08(1)	-0.23(1)	0.14(2)	0.214(9)
H18	-0.020(6)	-0.32(4)	-0.06(2)	-0.56(6)	-0.09(3)	-0.21(2)	0.16(4)	0.20(2)
H18'	-0.014(4)	-0.29(2)	-0.04(1)	-0.51(3)	-0.07(2)	-0.20(1)	0.11(3)	0.19(1)
H19	-0.011(4)	-0.23(1)	-0.03(1)	-0.40(2)	-0.05(2)	-0.153(9)	0.09(3)	0.146(9)
H20	-0.011(4)	-0.25(2)	-0.03(1)	-0.43(4)	-0.05(2)	-0.16(2)	0.09(3)	0.16(2)
H21	-0.010(2)	-0.187(5)	-0.030(7)	-0.327(9)	-0.04(1)	-0.125(4)	0.08(2)	0.119(3)
H22	-0.011(2)	-0.25(1)	-0.035(5)	-0.43(2)	-0.052(8)	-0.165(6)	0.09(1)	0.157(6)
H23	-0.017(2)	-0.44(2)	-0.051(6)	-0.77(3)	-0.077(9)	-0.29(1)	0.13(2)	0.28(1)
H24	0.077(3)	0.65(3)	0.23(1)	1.13(5)	0.35(1)	0.43(2)	-0.59(3)	-0.41(2)
H24'	0.07(1)	0.03(7)	0.20(3)	0.0(1)	0.30(5)	0.02(5)	-0.50(8)	-0.02(5)
H25	0.069(9)	0.40(5)	0.21(3)	0.70(8)	0.31(4)	0.27(3)	-0.53(7)	-0.25(3)
H26	-0.01(1)	-0.79(8)	-0.04(4)	-1.4(1)	-0.06(6)	-0.52(5)	0.1(1)	0.50(5)
H26'	0.007(9)	0.22(2)	0.02(3)	0.39(3)	0.03(4)	0.15(1)	-0.06(7)	-0.14(1)
H27	-0.143(7)	-2.15(1)	-0.43(2)	-3.76(2)	-0.65(3)	-1.435(8)	1.10(5)	1.367(8)

Table 56 Contact and pseudo contact terms of LaLn complexes of L^{AB4}

	LaCe		LaPr		LaNd		LaEu	
	Δ_c	Δ_{pc}	Δ_c	Δ_{pc}	Δ_c	Δ_{pc}	Δ_c	Δ_{pc}
H1	0.25(2)	1.26(8)	0.75(5)	2.2(1)	1.14(7)	0.84(5)	-1.9(1)	-0.80(5)
H2	0.15(2)	1.7(1)	0.45(5)	3.0(2)	0.68(7)	1.15(8)	-1.1(1)	-1.09(8)
H3	0.36(2)	2.2(1)	1.10(7)	3.8(2)	1.7(1)	1.44(7)	-2.8(2)	-1.37(7)
H4	0.05(1)	1.0(1)	0.15(4)	1.8(2)	0.22(7)	0.70(7)	-0.4(1)	-0.67(7)
H4'	0.06(1)	1.07(4)	0.19(3)	1.87(8)	0.29(4)	0.71(3)	-0.48(7)	-0.68(3)
H5	0.082(7)	1.05(5)	0.25(2)	1.83(9)	0.38(3)	0.70(4)	-0.64(5)	-0.66(3)
H6	0.17(1)	0.20(2)	0.51(4)	0.34(4)	0.76(6)	0.13(1)	-1.3(1)	-0.12(1)
H7	-0.014(3)	-0.28(2)	-0.044(9)	-0.49(4)	-0.07(1)	-0.19(1)	0.11(2)	0.18(1)
H8	-0.15(3)	-5.9(2)	-0.45(9)	-10.2(4)	-0.7(1)	-3.9(2)	1.1(2)	3.7(1)
H9	-0.026(4)	-0.50(2)	-0.08(1)	-0.88(4)	-0.12(2)	-0.33(2)	0.20(3)	0.32(2)
H9'	-0.019(2)	-0.13(1)	-0.058(7)	-0.23(2)	-0.09(1)	-0.089(8)	0.15(2)	0.085(8)
H10	-0.12(1)	-2.77(9)	-0.35(4)	-4.8(2)	-0.53(6)	-1.85(6)	0.89(9)	1.76(6)
H11	-0.016(2)	-0.21(1)	-0.049(7)	-0.37(2)	-0.07(1)	-0.140(8)	0.12(2)	0.134(7)
H12	-0.024(4)	-0.35(1)	-0.07(1)	-0.61(2)	-0.11(2)	-0.232(7)	0.19(3)	0.221(7)
H13	-0.020(4)	-0.41(2)	-0.06(1)	-0.71(4)	-0.09(2)	-0.27(2)	0.16(3)	0.26(2)
H13'	-0.018(2)	-0.45(2)	-0.055(7)	-0.79(3)	-0.08(1)	-0.30(1)	0.14(2)	0.29(1)
H14	-0.014(3)	-0.25(1)	-0.04(1)	-0.44(3)	-0.06(1)	-0.17(1)	0.11(3)	0.161(9)
H16	-0.020(3)	-0.48(2)	-0.062(8)	-0.84(4)	-0.09(1)	-0.32(1)	0.16(2)	0.31(1)
H17	-0.015(3)	-0.36(2)	-0.047(8)	-0.63(3)	-0.07(1)	-0.24(1)	0.12(2)	0.23(1)
H18	-0.019(4)	-0.36(3)	-0.06(1)	-0.63(5)	-0.09(2)	-0.24(2)	0.15(3)	0.23(2)
H18'	-0.027(9)	-0.25(1)	-0.08(3)	-0.44(3)	-0.13(4)	-0.17(1)	0.21(7)	0.160(9)
H19	-0.013(2)	-0.221(8)	-0.039(6)	-0.39(1)	-0.058(9)	-0.148(5)	0.10(2)	0.141(5)
H20	-0.011(2)	-0.24(1)	-0.034(6)	-0.42(2)	-0.052(9)	-0.161(7)	0.09(1)	0.153(7)
H21	-0.009(1)	-0.210(9)	-0.028(4)	-0.37(2)	-0.042(6)	-0.140(6)	0.07(1)	0.133(6)
H22	-0.010(2)	-0.27(1)	-0.030(5)	-0.47(2)	-0.045(8)	-0.179(9)	0.08(1)	0.171(8)
H23	-0.016(3)	-0.43(2)	-0.05(1)	-0.76(3)	-0.07(1)	-0.29(1)	0.12(2)	0.27(1)
H24	0.083(8)	0.51(6)	0.25(2)	0.9(1)	0.38(3)	0.34(4)	-0.64(6)	-0.33(4)
H24'	0.069(9)	-0.09(6)	0.21(3)	-0.2(1)	0.31(4)	-0.06(4)	-0.53(7)	0.06(4)
H25	0.051(5)	0.34(4)	0.15(2)	0.59(8)	0.23(2)	0.22(3)	-0.39(4)	-0.21(3)
H26	-0.03(2)	-1.00(8)	-0.09(7)	-1.8(1)	-0.1(1)	-0.67(5)	0.2(2)	0.64(5)
H26'	0.01(1)	-0.06(4)	0.03(3)	-0.11(7)	0.05(5)	-0.04(3)	-0.08(8)	0.04(3)
H27	-0.131(9)	-2.52(7)	-0.40(3)	-4.4(1)	-0.60(4)	-1.68(4)	1.01(7)	1.60(4)
H28	-0.008(9)	-0.23(6)	-0.02(3)	-0.4(1)	-0.03(4)	-0.16(4)	0.06(7)	0.15(4)
H28'	-0.010(5)	-0.15(1)	-0.03(2)	-0.27(2)	-0.04(2)	-0.103(9)	0.07(4)	0.098(9)
H29	-0.006(1)	-0.152(7)	-0.019(3)	-0.27(1)	-0.028(5)	-0.102(5)	0.048(8)	0.097(5)

Table 57 Contact and pseudo contact terms of LaLn complexes of L^{AB5}

	LaCe		LaPr		LaNd		LaEu	
	Δ_c	Δ_{pc}	Δ_c	Δ_{pc}	Δ_c	Δ_{pc}	Δ_c	Δ_{pc}
H1	0.24(2)	1.21(8)	0.74(5)	2.1(1)	1.11(7)	0.81(6)	-1.9(1)	-0.77(5)
H2	0.15(2)	1.8(1)	0.45(5)	3.1(2)	0.67(7)	1.18(8)	-1.1(1)	-1.12(8)
H3	0.37(2)	2.3(1)	1.11(7)	4.0(2)	1.7(1)	1.54(7)	-2.8(2)	-1.46(7)
H4	0.061(2)	0.700(7)	0.184(7)	1.22(1)	0.28(1)	0.467(4)	-0.47(2)	-0.445(4)
H4'	0.053(3)	1.163(9)	0.161(9)	2.03(2)	0.24(1)	0.775(6)	-0.41(2)	-0.739(6)
H5	0.065(8)	1.34(6)	0.20(3)	2.3(1)	0.30(4)	0.89(4)	-0.50(6)	-0.85(4)
H6	0.16(1)	0.16(2)	0.50(3)	0.27(3)	0.75(5)	0.10(1)	-1.26(9)	-0.10(1)
H7	-0.020(3)	-0.33(2)	-0.059(9)	-0.58(3)	-0.09(1)	-0.22(1)	0.15(2)	0.21(1)
H8	-0.13(2)	-5.9(2)	-0.40(7)	-10.3(3)	-0.6(1)	-4.0(1)	1.0(2)	3.8(1)
H9	-0.025(3)	-0.51(2)	-0.077(9)	-0.90(4)	-0.12(1)	-0.34(1)	0.19(2)	0.33(1)
H9'	-0.023(2)	-0.129(3)	-0.069(6)	-0.225(6)	-0.10(1)	-0.086(2)	0.18(2)	0.082(2)
H10	-0.11(3)	-3.1(2)	-0.34(9)	-5.4(4)	-0.5(1)	-2.0(1)	0.9(2)	2.0(1)
H11	-0.014(1)	-0.228(6)	-0.044(4)	-0.40(1)	-0.066(6)	-0.152(4)	0.11(1)	0.144(4)
H12	-0.021(3)	-0.355(7)	-0.063(8)	-0.62(1)	-0.10(1)	-0.237(5)	0.16(2)	0.226(5)
H13	-0.018(2)	-0.41(1)	-0.056(6)	-0.71(2)	-0.084(9)	-0.271(7)	0.14(1)	0.258(7)
H13'	-0.018(2)	-0.399(6)	-0.056(7)	-0.70(1)	-0.08(1)	-0.266(4)	0.14(2)	0.253(4)
H14	-0.011(3)	-0.33(2)	-0.03(1)	-0.57(4)	-0.05(2)	-0.22(2)	0.08(3)	0.21(2)
H16	-0.019(3)	-0.51(2)	-0.059(8)	-0.88(4)	-0.09(1)	-0.34(1)	0.15(2)	0.32(1)
H17	-0.015(2)	-0.38(2)	-0.045(7)	-0.66(3)	-0.07(1)	-0.25(1)	0.12(2)	0.24(1)
H18	-0.0202(7)	-0.285(3)	-0.061(2)	-0.497(6)	-0.092(3)	-0.190(2)	0.155(5)	0.181(2)
H18'	-0.015(3)	-0.28(1)	-0.047(9)	-0.49(2)	-0.07(1)	-0.187(7)	0.12(2)	0.178(7)
H19	-0.010(2)	-0.25(1)	-0.032(6)	-0.43(3)	-0.048(9)	-0.17(1)	0.08(1)	0.157(9)
H20	-0.012(3)	-0.224(8)	-0.037(9)	-0.39(1)	-0.06(1)	-0.149(6)	0.09(2)	0.142(5)
H21	-0.0088(7)	-0.205(6)	-0.027(2)	-0.36(1)	-0.040(3)	-0.137(4)	0.068(5)	0.130(4)
H22	-0.0117(9)	-0.257(7)	-0.036(3)	-0.45(1)	-0.054(4)	-0.172(5)	0.090(7)	0.163(4)
H23	-0.015(3)	-0.47(2)	-0.04(1)	-0.81(4)	-0.07(1)	-0.31(2)	0.11(2)	0.30(2)
H24	0.082(6)	0.60(5)	0.25(2)	1.04(9)	0.38(3)	0.40(3)	-0.63(5)	-0.38(3)
H24'	0.076(9)	-0.11(6)	0.23(3)	-0.2(1)	0.35(4)	-0.07(4)	-0.58(7)	0.07(4)
H25	0.056(7)	0.37(5)	0.17(2)	0.65(9)	0.26(3)	0.25(3)	-0.43(5)	-0.24(3)
H26	-0.03(2)	-0.81(6)	-0.10(7)	-1.4(1)	-0.2(1)	-0.54(4)	0.3(2)	0.51(4)
H26'	0.010(7)	0.09(3)	0.03(2)	0.15(5)	0.05(3)	0.06(2)	-0.08(5)	-0.06(2)
H27	-0.132(8)	-2.48(5)	-0.40(2)	-4.3(1)	-0.60(4)	-1.66(4)	1.02(6)	1.58(3)

Table 58 Contact and pseudo contact terms of LnLu complexes of L^{AB}

	CeLu		PrLu		NdLu		EuLu	
	Δ_c	Δ_{pc}	Δ_c	Δ_{pc}	Δ_c	Δ_{pc}	Δ_c	Δ_{pc}
H1	-0.022(7)	-0.21(2)	-0.07(2)	-0.36(4)	-0.10(3)	-0.14(1)	0.17(5)	0.13(1)
H2	-0.019(5)	-0.19(1)	-0.06(1)	-0.34(2)	-0.09(2)	-0.128(7)	0.14(4)	0.122(7)
H3	-0.030(8)	-0.28(2)	-0.09(3)	-0.48(4)	-0.14(4)	-0.18(2)	0.23(6)	0.18(2)
H4	-0.033(3)	-0.30(1)	-0.100(9)	-0.52(2)	-0.15(1)	-0.199(8)	0.25(2)	0.190(8)
H4'	-0.032(7)	-0.28(2)	-0.10(2)	-0.50(4)	-0.15(3)	-0.19(1)	0.25(5)	0.18(1)
H5	-0.021(5)	-0.20(1)	-0.06(2)	-0.35(2)	-0.10(2)	-0.132(9)	0.16(4)	0.126(8)
H6	-0.0377(7)	-0.300(5)	-0.114(2)	-0.524(9)	-0.172(3)	-0.200(3)	0.290(5)	0.190(3)
H7	-0.028(2)	-0.19(1)	-0.084(5)	-0.34(2)	-0.126(7)	-0.129(7)	0.21(1)	0.123(6)
H8	-0.15(5)	-1.4(1)	-0.4(2)	-2.4(3)	-0.7(2)	-0.9(1)	1.1(4)	0.89(9)
H9	-0.042(3)	-0.083(4)	-0.127(8)	-0.145(8)	-0.19(1)	-0.055(3)	0.32(2)	0.053(3)
H9'	-0.04(1)	-0.34(3)	-0.12(3)	-0.59(6)	-0.19(5)	-0.23(2)	0.31(9)	0.22(2)
H10	-0.4(2)	-4.3(5)	-1.1(5)	-7.5(8)	-1.7(7)	-2.9(3)	3(1)	2.7(3)
H11	-0.007(2)	0.023(5)	-0.021(7)	0.041(8)	-0.03(1)	0.016(3)	0.05(2)	-0.015(3)
H12	0.199(6)	0.42(4)	0.60(2)	0.74(6)	0.91(3)	0.28(2)	-1.53(5)	-0.27(2)
H13	0.19(4)	0.9(1)	0.6(1)	1.6(2)	0.8(2)	0.60(9)	-1.4(3)	-0.58(9)
H13'	0.12(6)	1.1(2)	0.4(2)	1.9(3)	0.5(3)	0.7(1)	-0.9(4)	-0.7(1)
H14	0.08(2)	0.69(6)	0.25(6)	1.2(1)	0.38(8)	0.46(4)	-0.6(1)	-0.44(4)
H15	0.43(3)	1.0(1)	1.31(8)	1.7(2)	2.0(1)	0.65(9)	-3.3(2)	-0.62(9)
H16	0.21(2)	1.07(5)	0.65(8)	1.86(8)	1.0(1)	0.71(3)	-1.7(2)	-0.68(3)
H17	0.46(2)	1.0(1)	1.40(8)	1.7(2)	2.1(1)	0.64(8)	-3.6(2)	-0.61(8)
H18	0.13(4)	1.0(1)	0.4(1)	1.8(2)	0.6(2)	0.67(9)	-1.0(3)	-0.64(9)
H18'	0.18(3)	0.8(1)	0.6(1)	1.4(2)	0.8(2)	0.55(8)	-1.4(3)	-0.52(7)
H19	0.05(1)	0.50(4)	0.15(4)	0.87(6)	0.23(7)	0.33(2)	-0.4(1)	-0.32(2)
H20	0.203(4)	0.42(3)	0.62(1)	0.73(5)	0.93(2)	0.28(2)	-1.56(3)	-0.27(2)
H21	-0.011(6)	0.07(1)	-0.03(2)	0.12(2)	-0.05(3)	0.047(8)	0.09(4)	-0.045(7)
H22	-0.05(1)	-0.33(4)	-0.15(3)	-0.58(7)	-0.22(5)	-0.22(3)	0.37(9)	0.21(3)
H23	-0.4(1)	-3.2(4)	-1.1(4)	-5.7(7)	-1.6(5)	-2.2(3)	2.7(9)	2.1(2)
H24	-0.020(5)	-0.20(1)	-0.06(2)	-0.34(2)	-0.09(2)	-0.131(9)	0.16(4)	0.124(9)
H25	-0.018(4)	-0.15(2)	-0.05(1)	-0.26(3)	-0.08(2)	-0.10(1)	0.14(3)	0.09(1)
H26	-0.027(7)	-0.23(3)	-0.08(2)	-0.40(5)	-0.12(3)	-0.15(2)	0.21(5)	0.15(2)
H26'	-0.021(6)	-0.19(1)	-0.06(2)	-0.34(2)	-0.10(3)	-0.129(7)	0.16(5)	0.123(7)
H27	-0.020(6)	-0.18(2)	-0.06(2)	-0.32(3)	-0.09(3)	-0.12(1)	0.16(4)	0.12(1)

Table 59 Contact and pseudo contact terms of LnLu complexes of L^{AB3}

	CeLu		PrLu		NdLu		EuLu	
	Δ_c	Δ_{pc}	Δ_c	Δ_{pc}	Δ_c	Δ_{pc}	Δ_c	Δ_{pc}
H1	-0.022(7)	-0.19(2)	-0.07(2)	-0.34(4)	-0.10(3)	-0.13(2)	0.17(6)	0.12(1)
H3	-0.030(9)	-0.27(3)	-0.09(3)	-0.47(5)	-0.14(4)	-0.18(2)	0.23(7)	0.17(2)
H4	-0.038(3)	-0.28(2)	-0.115(9)	-0.49(3)	-0.17(1)	-0.19(1)	0.29(2)	0.18(1)
H4'	-0.033(6)	-0.28(3)	-0.10(2)	-0.49(5)	-0.15(3)	-0.19(2)	0.25(5)	0.18(2)
H5	-0.022(4)	-0.19(2)	-0.07(1)	-0.33(3)	-0.10(2)	-0.12(1)	0.17(3)	0.12(1)
H6	-0.037(3)	-0.29(2)	-0.11(1)	-0.50(3)	-0.17(1)	-0.19(1)	0.29(3)	0.18(1)
H7	-0.031(2)	-0.19(2)	-0.095(7)	-0.33(3)	-0.14(1)	-0.13(1)	0.24(2)	0.12(1)
H8	-0.16(4)	-1.4(1)	-0.5(1)	-2.4(2)	-0.7(2)	-0.91(9)	1.2(3)	0.86(8)
H9	-0.044(3)	-0.069(9)	-0.134(8)	-0.12(2)	-0.20(1)	-0.046(6)	0.34(2)	0.044(6)
H9'	-0.04(1)	-0.33(3)	-0.13(4)	-0.58(6)	-0.20(5)	-0.22(2)	0.33(9)	0.21(2)
H10	-0.4(2)	-4.2(5)	-1.2(5)	-7.4(8)	-1.8(7)	-2.8(3)	3(1)	2.7(3)
H11	-0.0075(5)	0.022(1)	-0.023(2)	0.038(2)	-0.034(2)	0.0147(6)	0.058(4)	-0.0140(6)
H12	0.198(4)	0.41(3)	0.60(1)	0.72(4)	0.91(2)	0.28(2)	-1.53(3)	-0.26(2)
H13	0.18(4)	0.9(1)	0.6(1)	1.5(3)	0.8(2)	0.6(1)	-1.4(3)	-0.56(9)
H13'	0.12(5)	1.1(2)	0.4(2)	1.9(3)	0.5(2)	0.7(1)	-0.9(4)	-0.7(1)
H14	0.08(2)	0.68(5)	0.25(5)	1.19(9)	0.38(8)	0.46(3)	-0.6(1)	-0.43(3)
H15	0.43(2)	0.9(1)	1.31(7)	1.6(2)	2.0(1)	0.63(8)	-3.3(2)	-0.60(8)
H16	0.22(2)	1.03(4)	0.66(6)	1.80(7)	1.00(9)	0.69(3)	-1.7(2)	-0.65(2)
H17	0.47(2)	0.9(1)	1.42(5)	1.6(2)	2.13(8)	0.62(8)	-3.6(1)	-0.59(7)
H18	0.14(4)	1.0(1)	0.4(1)	1.7(2)	0.6(2)	0.65(9)	-1.0(3)	-0.62(8)
H18'	0.18(3)	0.8(1)	0.56(9)	1.4(2)	0.8(1)	0.53(8)	-1.4(2)	-0.50(7)
H19	0.05(1)	0.49(3)	0.16(4)	0.85(6)	0.24(6)	0.32(2)	-0.4(1)	-0.31(2)
H20	0.205(3)	0.41(2)	0.622(9)	0.71(4)	0.94(1)	0.27(2)	-1.58(2)	-0.26(1)
H21	-0.009(4)	0.078(7)	-0.03(1)	0.14(1)	-0.04(2)	0.052(5)	0.07(3)	-0.050(5)
H22	-0.05(1)	-0.34(4)	-0.14(4)	-0.59(7)	-0.21(6)	-0.23(3)	0.3(1)	0.21(3)
H23	-0.4(1)	-3.2(4)	-1.1(4)	-5.5(7)	-1.6(6)	-2.1(3)	3(1)	2.0(2)
H24	-0.022(6)	-0.18(3)	-0.07(2)	-0.31(5)	-0.10(3)	-0.12(2)	0.17(4)	0.11(2)
H25	-0.020(3)	-0.15(2)	-0.06(1)	-0.25(3)	-0.09(2)	-0.10(1)	0.16(3)	0.09(1)
H26	-0.024(7)	-0.22(3)	-0.07(2)	-0.39(5)	-0.11(3)	-0.15(2)	0.18(5)	0.14(2)
H26'	-0.021(8)	-0.19(2)	-0.06(3)	-0.34(3)	-0.10(4)	-0.13(1)	0.16(6)	0.12(1)
H27	-0.021(5)	-0.17(2)	-0.07(1)	-0.30(3)	-0.10(2)	-0.11(1)	0.17(4)	0.11(1)

Table 60 Contact and pseudo contact terms of LnLu complexes of L^{AB4}

	CeLu		PrLu		NdLu		EuLu	
	Δ_c	Δ_{pc}	Δ_c	Δ_{pc}	Δ_c	Δ_{pc}	Δ_c	Δ_{pc}
H1	-0.038(2)	-0.380(4)	-0.114(7)	-0.664(7)	-0.17(1)	-0.254(3)	0.29(2)	0.242(3)
H2	-0.034(2)	-0.331(3)	-0.104(6)	-0.579(5)	-0.157(9)	-0.221(2)	0.26(2)	0.210(2)
H3	-0.052(4)	-0.52(1)	-0.16(1)	-0.90(1)	-0.24(2)	-0.345(4)	0.40(3)	0.328(4)
H4	-0.0532(2)	-0.507(2)	-0.1613(6)	-0.884(3)	-0.2429(9)	-0.338(1)	0.409(2)	0.322(1)
H4'	-0.053(2)	-0.508(4)	-0.160(7)	-0.887(7)	-0.24(1)	-0.339(3)	0.41(2)	0.323(3)
H5	-0.035(1)	-0.346(2)	-0.106(4)	-0.605(3)	-0.160(6)	-0.231(1)	0.27(1)	0.220(1)
H6	-0.055(2)	-0.496(6)	-0.168(7)	-0.87(1)	-0.25(1)	-0.331(4)	0.43(2)	0.315(4)
H7	-0.0374(2)	-0.3149(5)	-0.1135(6)	-0.5498(8)	-0.1709(9)	-0.2099(3)	0.288(1)	0.1999(3)
H8	-0.26(2)	-2.62(4)	-0.77(7)	-4.57(7)	-1.2(1)	-1.74(2)	2.0(2)	1.66(2)
H9	-0.040(1)	-0.153(4)	-0.123(4)	-0.266(7)	-0.185(6)	-0.102(3)	0.31(1)	0.097(3)
H9'	-0.068(5)	-0.627(8)	-0.21(2)	-1.10(1)	-0.31(2)	-0.418(5)	0.53(4)	0.398(5)
H10	-0.69(7)	-7.8(2)	-2.1(2)	-13.5(3)	-3.2(3)	-5.2(1)	5.3(6)	4.9(1)
H11	-0.0155(6)	-0.059(4)	-0.047(2)	-0.103(7)	-0.071(3)	-0.039(3)	0.119(5)	0.038(3)
H12	0.210(5)	0.597(9)	0.64(2)	1.04(2)	0.96(2)	0.398(6)	-1.62(4)	-0.379(6)
H13	0.287(7)	1.61(5)	0.87(2)	2.80(8)	1.31(3)	1.07(3)	-2.21(5)	-1.02(3)
H13'	0.24(2)	2.05(4)	0.72(5)	3.58(6)	1.08(7)	1.37(2)	-1.8(1)	-1.30(2)
H14	0.114(5)	1.058(9)	0.35(2)	1.85(2)	0.52(2)	0.705(6)	-0.88(4)	-0.672(6)
H15	0.568(5)	2.24(3)	1.72(2)	3.91(6)	2.60(2)	1.49(2)	-4.38(4)	-1.42(2)
H17	0.56(1)	2.00(3)	1.69(4)	3.49(5)	2.54(6)	1.33(2)	-4.3(1)	-1.27(2)
H18	0.24(2)	2.15(7)	0.74(6)	3.8(1)	1.12(9)	1.43(5)	-1.9(2)	-1.37(4)
H18'	0.26(2)	1.8(1)	0.79(6)	3.1(2)	1.19(9)	1.17(7)	-2.0(1)	-1.12(7)
H19	0.074(9)	0.90(2)	0.22(3)	1.57(3)	0.34(4)	0.60(1)	-0.57(7)	-0.57(1)
H20	0.221(4)	0.784(9)	0.67(1)	1.37(2)	1.01(2)	0.523(6)	-1.70(3)	-0.498(6)
H21	-0.007(5)	0.21(1)	-0.02(2)	0.36(2)	-0.03(2)	0.139(7)	0.05(4)	-0.132(6)
H22	-0.078(2)	-0.48(2)	-0.237(6)	-0.84(3)	-0.36(1)	-0.32(1)	0.60(2)	0.30(1)
H23	-0.61(4)	-5.47(9)	-1.8(1)	-9.6(2)	-2.8(2)	-3.65(6)	4.7(3)	3.47(6)
H24	-0.0357(6)	-0.335(5)	-0.108(2)	-0.585(8)	-0.163(3)	-0.223(3)	0.275(4)	0.213(3)
H24'	-0.0362(3)	-0.3334(9)	-0.1100(8)	-0.582(2)	-0.166(1)	-0.2223(6)	0.279(2)	0.2117(6)
H25	-0.028(2)	-0.268(4)	-0.084(7)	-0.469(7)	-0.13(1)	-0.179(3)	0.21(2)	0.170(3)
H26	-0.044(1)	-0.419(3)	-0.134(4)	-0.732(5)	-0.202(7)	-0.279(2)	0.34(1)	0.266(2)
H26'	-0.033(3)	-0.347(5)	-0.10(1)	-0.606(9)	-0.15(2)	-0.231(3)	0.25(3)	0.220(3)
H27	-0.0358(6)	-0.336(1)	-0.109(2)	-0.587(3)	-0.163(3)	-0.224(1)	0.275(5)	0.2134(9)
H28	0.052(6)	0.75(3)	0.16(2)	1.31(5)	0.24(3)	0.50(2)	-0.40(5)	-0.48(2)
H28'	0.070(2)	0.79(1)	0.212(5)	1.37(2)	0.320(8)	0.525(9)	-0.54(1)	-0.500(8)
H29	0.081(2)	0.649(8)	0.246(5)	1.13(1)	0.371(7)	0.433(5)	-0.63(1)	-0.412(5)

Table 61 Contact and pseudo contact terms of LnLu complexes of L^{AB5}

	CeLu		PrLu		NdLu		EuLu	
	Δ_c	Δ_{pc}	Δ_c	Δ_{pc}	Δ_c	Δ_{pc}	Δ_c	Δ_{pc}
H1	-0.019(8)	-0.19(2)	-0.06(2)	-0.34(4)	-0.09(3)	-0.13(1)	0.15(6)	0.12(1)
H2	-0.018(8)	-0.15(3)	-0.05(3)	-0.26(5)	-0.08(4)	-0.10(2)	0.14(6)	0.09(2)
H3	-0.027(7)	-0.25(3)	-0.08(2)	-0.43(5)	-0.12(3)	-0.17(2)	0.21(6)	0.16(2)
H4	-0.030(5)	-0.30(2)	-0.09(2)	-0.52(3)	-0.14(2)	-0.20(1)	0.23(4)	0.19(1)
H4'	-0.029(7)	-0.26(2)	-0.09(2)	-0.46(4)	-0.13(3)	-0.18(2)	0.22(6)	0.17(2)
H5	-0.019(5)	-0.19(1)	-0.06(1)	-0.33(2)	-0.09(2)	-0.127(9)	0.15(4)	0.121(8)
H6	-0.038(2)	-0.29(1)	-0.115(5)	-0.51(2)	-0.173(7)	-0.194(8)	0.29(1)	0.185(8)
H7	-0.026(3)	-0.22(1)	-0.080(8)	-0.38(2)	-0.12(1)	-0.145(9)	0.20(2)	0.138(9)
H8	-0.12(4)	-1.3(1)	-0.4(1)	-2.3(2)	-0.6(2)	-0.90(9)	1.0(3)	0.85(8)
H9	-0.044(2)	-0.111(3)	-0.132(7)	-0.193(6)	-0.20(1)	-0.074(2)	0.34(2)	0.070(2)
H9'	-0.04(1)	-0.33(4)	-0.12(4)	-0.58(7)	-0.18(6)	-0.22(3)	0.3(1)	0.21(2)
H10	-0.3(2)	-4.0(5)	-1.0(5)	-7.0(8)	-1.5(7)	-2.7(3)	3(1)	2.5(3)
H11	-0.010(1)	-0.016(2)	-0.029(3)	-0.029(3)	-0.044(4)	-0.011(1)	0.074(8)	0.010(1)
H12	0.194(5)	0.36(3)	0.59(1)	0.62(5)	0.89(2)	0.24(2)	-1.49(4)	-0.23(2)
H13	0.15(4)	0.8(1)	0.5(1)	1.4(2)	0.7(2)	0.53(9)	-1.2(3)	-0.51(9)
H13'	0.09(5)	0.9(1)	0.3(2)	1.6(3)	0.4(2)	0.6(1)	-0.7(4)	-0.60(9)
H14	0.08(3)	0.79(6)	0.23(8)	1.4(1)	0.3(1)	0.52(4)	-0.6(2)	-0.50(4)
H15	0.36(3)	0.8(1)	1.10(8)	1.4(2)	1.7(1)	0.53(9)	-2.8(2)	-0.51(9)
H17	0.38(2)	0.8(1)	1.15(6)	1.3(2)	1.7(1)	0.51(8)	-2.9(2)	-0.48(8)
H18	0.14(2)	0.8(1)	0.42(7)	1.5(2)	0.6(1)	0.56(8)	-1.1(2)	-0.53(8)
H18'	0.15(3)	0.7(1)	0.5(1)	1.3(2)	0.7(2)	0.49(7)	-1.2(3)	-0.46(7)
H19	0.05(1)	0.54(3)	0.14(4)	0.94(6)	0.21(6)	0.36(2)	-0.4(1)	-0.34(2)
H20	0.200(2)	0.39(2)	0.606(6)	0.68(3)	0.91(1)	0.26(1)	-1.54(2)	-0.25(1)
H21	-0.009(2)	0.050(4)	-0.029(6)	0.087(7)	-0.04(1)	0.033(3)	0.07(2)	-0.032(2)
H22	-0.04(1)	-0.33(5)	-0.14(4)	-0.57(9)	-0.21(7)	-0.22(3)	0.3(1)	0.21(3)
H23	-0.3(1)	-3.0(4)	-1.0(3)	-5.2(7)	-1.5(5)	-2.0(3)	2.5(9)	1.9(3)
H24	-0.015(7)	-0.21(1)	-0.05(2)	-0.36(2)	-0.07(3)	-0.137(8)	0.12(5)	0.131(8)
H24'	-0.017(7)	-0.19(2)	-0.05(2)	-0.33(3)	-0.08(3)	-0.13(1)	0.13(6)	0.12(1)
H25	-0.015(5)	-0.14(2)	-0.05(1)	-0.24(3)	-0.07(2)	-0.09(1)	0.12(4)	0.09(1)
H26	-0.017(6)	-0.24(1)	-0.05(2)	-0.43(2)	-0.08(3)	-0.163(8)	0.13(5)	0.155(8)
H26'	-0.017(7)	-0.18(2)	-0.05(2)	-0.31(3)	-0.08(3)	-0.12(1)	0.13(5)	0.11(1)
H27	-0.016(7)	-0.17(2)	-0.05(2)	-0.30(3)	-0.07(3)	-0.12(1)	0.13(5)	0.11(1)

5.3.8 Recalculation of lanthanide induced shifts

The calculated contact and pseudo contact terms have been added to give the total lanthanide induced shift. The results have been compared to the experimental lanthanide induced shifts by means of calculating for each proton Hi an agreement factor, AF_i:

$$AF_i = \sqrt{\frac{\sum_j \left(\left(\Delta_{i,j}\right)_{calc} - \left(\Delta_{i,j}\right)_{exp} \right)^2}{\sum_j \left(\left(\Delta_{i,j}\right)_{exp} \right)^2}} \qquad (9)$$

The agreement factors can be used to discriminate whether the separation in contact and pseudo contact contributions has been successful and a low agreement factor can be seen as an expression of good linear correlation according to Equations (3), (4), (7) and (8). Results are shown in Table 62 - Table 73.

Table 62 Re-calculated and observed LIS and AF_i for Ln_2 complexes of L^{AB}

	Ce_2		Pr_2		Nd_2		Eu_2		AF_i
	Calc.	Obs.	Calc.	Obs.	Calc.	Obs	Calc.	Obs.	
H1	1.3(1)	1.28	2.5(2)	2.12	1.7(1)	1.49	-2.4(2)	-2.35	0.126
H2	1.7(1)	1.76	3.2(3)	2.67	1.7(1)	1.51	-2.0(2)	-1.92	0.139
H3	2.4(1)	2.36	4.6(3)	4.02	2.9(2)	2.52	-3.8(3)	-3.80	0.098
H4	0.55(2)	0.56	0.98(4)	0.91	0.42(2)	0.41	-0.45(2)	-0.43	0.065
H4'	0.94(2)	0.94	1.67(4)	1.59	0.72(2)	0.69	-0.76(3)	-0.75	0.039
H5	1.18(7)	1.18	2.1(1)	1.85	0.94(7)	0.83	-1.02(9)	-1.00	0.109
H6	0.08(2)	0.08	0.30(4)	0.21	0.51(3)	0.45	-0.88(5)	-0.88	0.105
H7	-0.50(1)	-0.50	-0.93(2)	-0.89	-0.52(2)	-0.48	0.65(3)	0.65	0.047
H8	-7.7(1)	-7.77	-13.8(3)	-13.64	-6.2(3)	-6.71	6.8(5)	6.73	0.030
H9	-0.60(2)	-0.60	-1.14(4)	-1.06	-0.66(3)	-0.60	0.85(5)	0.85	0.062
H9'	-0.51(3)	-0.52	-0.98(6)	-1.11	-0.60(5)	-0.70	0.80(7)	0.80	0.096
H10	-7.9(4)	-8.04	-14.4(8)	-15.57	-7.1(8)	-8.83	8(1)	8.17	0.100
H11	-0.215(7)	-0.21	-0.40(1)	-0.37	-0.22(1)	-0.18	0.27(2)	0.27	0.076
H12	0.27(4)	0.27	0.70(8)	0.87	0.88(4)	0.95	-1.43(6)	-1.45	0.093
H13	0.7(2)	0.72	1.4(3)	2.13	1.1(2)	1.61	-1.6(4)	-1.65	0.263
H13'	0.9(2)	0.96	1.7(3)	2.32	0.9(3)	1.63	-1.2(5)	-1.16	0.288
H14	0.52(7)	0.53	1.0(1)	1.29	0.6(1)	0.84	-0.8(2)	-0.85	0.193
H15	0.9(2)	0.92	2.1(3)	2.74	2.2(2)	2.49	-3.5(2)	-3.55	0.126
H16	0.95(6)	0.96	1.9(1)	2.15	1.47(9)	1.66	-2.1(1)	-2.12	0.080
H17	1.1(1)	1.06	2.5(2)	2.98	2.5(1)	2.67	-3.9(2)	-3.97	0.096
H18	0.9(1)	0.88	1.7(3)	2.19	1.0(2)	1.44	-1.3(3)	-1.33	0.230
H18'	0.7(1)	0.72	1.4(2)	1.92	1.1(2)	1.48	-1.5(3)	-1.56	0.214
H19	0.29(5)	0.30	0.56(9)	0.75	0.36(7)	0.50	-0.5(1)	-0.49	0.214
H20	0.35(4)	0.35	0.86(6)	1.00	0.99(3)	1.02	-1.59(4)	-1.61	0.062
H21	-0.19(2)	-0.19	-0.35(3)	-0.28	-0.19(2)	-0.17	0.23(2)	0.22	0.161
H22	-0.72(3)	-0.73	-1.33(7)	-1.43	-0.69(8)	-0.85	0.8(1)	0.83	0.098
H23	-4.1(5)	-4.15	-7.6(9)	-9.48	-4.1(6)	-5.41	5(1)	5.20	0.177
H24	0.44(4)	0.43	0.85(7)	0.95	0.54(6)	0.46	-0.73(9)	-0.76	0.096
H24'	-0.18(4)	-0.18	-0.25(7)	-0.11	0.06(4)	0.05	-0.21(5)	-0.23	0.422
H25	0.28(3)	0.28	0.52(5)	0.62	0.28(2)	0.30	-0.35(3)	-0.36	0.119
H26	-1.14(6)	-1.14	-2.1(1)	-1.82	-0.97(7)	-0.82	1.1(1)	1.08	0.111
H26'	-0.19(1)	-0.19	-0.33(3)	-0.35	-0.14(3)	-0.20	0.14(5)	0.14	0.147
H27	-2.90(5)	-2.91	-5.25(9)	-5.09	-2.52(4)	-2.52	2.91(6)	2.89	0.024

Table 63 Re-calculated and observed LIS and AF_i for Ln_2 complexes of L^{AB3}

	Ce_2		Pr_2		Nd_2		Eu_2		AF_i
	Calc.	Obs.	Calc.	Obs.	Calc.	Obs	Calc.	Obs.	
H1	0.96(8)	0.96	1.9(1)	1.57	1.22(8)	1.07	-1.7(1)	-1.64	0.125
H3	2.1(1)	2.07	3.9(2)	3.56	2.4(1)	2.16	-3.1(2)	-3.10	0.080
H4	0.45(2)	0.45	0.79(4)	0.71	0.34(2)	0.33	-0.36(3)	-0.35	0.088
H4'	0.84(2)	0.85	1.48(4)	1.42	0.58(2)	0.60	-0.57(3)	-0.56	0.035
H5	1.14(7)	1.15	2.0(1)	1.80	0.90(6)	0.82	-0.98(8)	-0.95	0.105
H6	0.06(3)	0.05	0.25(6)	0.13	0.51(4)	0.41	-0.88(7)	-0.88	0.155
H7	-0.509(5)	-0.51	-0.952(9)	-0.97	-0.530(5)	-0.53	0.669(7)	0.67	0.012
H8	-7.3(1)	-7.39	-13.1(3)	-13.12	-5.8(3)	-6.40	6.3(5)	6.25	0.034
H9	-0.60(2)	-0.60	-1.13(4)	-1.05	-0.66(2)	-0.62	0.85(3)	0.84	0.057
H9'	-0.58(4)	-0.58	-1.10(7)	-1.24	-0.65(5)	-0.75	0.85(8)	0.86	0.098
H10	-7.6(4)	-7.71	-13.8(8)	-15.24	-6.8(9)	-8.66	8(1)	7.92	0.113
H11	-0.237(6)	-0.24	-0.44(1)	-0.42	-0.232(7)	-0.22	0.28(1)	0.28	0.044
H12	0.25(5)	0.25	0.67(9)	0.87	0.87(5)	0.96	-1.44(7)	-1.46	0.109
H13	0.7(2)	0.75	1.5(3)	2.16	1.1(2)	1.60	-1.6(3)	-1.67	0.248
H13'	0.9(2)	0.92	1.6(3)	2.28	0.9(3)	1.62	-1.2(5)	-1.17	0.296
H14	0.54(8)	0.55	1.0(1)	1.34	0.6(1)	0.88	-0.9(2)	-0.87	0.201
H15	0.9(2)	0.92	2.2(3)	2.77	2.3(2)	2.51	-3.5(2)	-3.61	0.126
H16	0.94(6)	0.95	1.9(1)	2.15	1.48(9)	1.67	-2.1(1)	-2.14	0.083
H17	1.1(1)	1.05	2.5(3)	2.99	2.5(1)	2.69	-3.9(2)	-4.00	0.099
H18	0.9(1)	0.89	1.7(3)	2.21	1.0(2)	1.44	-1.3(3)	-1.36	0.222
H18'	0.7(1)	0.70	1.4(3)	1.94	1.1(2)	1.48	-1.6(3)	-1.62	0.217
H19	0.31(5)	0.31	0.60(9)	0.78	0.38(7)	0.51	-0.5(1)	-0.52	0.207
H20	0.36(4)	0.35	0.88(7)	1.02	1.01(3)	1.03	-1.62(5)	-1.64	0.067
H21	-0.18(2)	-0.18	-0.33(3)	-0.26	-0.17(2)	-0.14	0.21(3)	0.20	0.196
H22	-0.69(4)	-0.70	-1.27(7)	-1.40	-0.67(7)	-0.82	0.8(1)	0.81	0.101
H23	-4.3(4)	-4.34	-7.9(8)	-9.35	-4.2(7)	-5.61	5(1)	5.13	0.160
H24	0.45(2)	0.45	0.86(3)	0.91	0.50(2)	0.47	-0.64(4)	-0.65	0.047
H24'	-0.09(4)	-0.11	-0.11(8)	0.01	0.11(5)	0.06	-0.26(7)	-0.29	0.428
H25	0.27(3)	0.26	0.51(5)	0.61	0.31(3)	0.30	-0.41(4)	-0.43	0.119
H26	-1.08(6)	-1.07	-1.9(1)	-1.67	-0.84(9)	-0.66	0.9(1)	0.90	0.135
H26'	-0.06(2)	-0.06	-0.12(3)	-0.19	-0.10(2)	-0.12	0.14(2)	0.15	0.248
H27	-2.61(1)	-2.62	-4.74(2)	-4.72	-2.29(2)	-2.32	2.65(3)	2.64	0.006

Table 64 Re-calculated and observed LIS and AF_i for Ln_2 complexes of L^{AB4}

	Ce_2		Pr_2		Nd_2		Eu_2		AF_i
	Calc.	Obs.	Calc.	Obs.	Calc.	Obs	Calc.	Obs.	
H1	1.08(8)	1.08	2.2(1)	1.84	1.53(9)	1.36	-2.1(1)	-2.12	0.107
H2	1.5(1)	1.52	2.8(2)	2.32	1.4(1)	1.34	-1.7(1)	-1.67	0.132
H3	1.9(1)	1.92	3.8(2)	3.37	2.5(1)	2.20	-3.4(2)	-3.35	0.085
H4	0.345(9)	0.34	0.62(2)	0.59	0.28(2)	0.23	-0.31(4)	-0.31	0.068
H4'	0.67(2)	0.68	1.17(4)	1.25	0.44(3)	0.51	-0.41(5)	-0.41	0.063
H5	0.97(4)	0.98	1.73(8)	1.57	0.75(4)	0.70	-0.79(5)	-0.77	0.081
H6	-0.10(1)	-0.10	-0.03(3)	-0.07	0.35(3)	0.28	-0.69(6)	-0.69	0.110
H7	-0.567(9)	-0.57	-1.06(2)	-1.03	-0.59(1)	-0.57	0.75(2)	0.74	0.028
H8	-9.0(2)	-9.07	-16.2(3)	-15.86	-7.5(2)	-7.82	8.4(4)	8.26	0.024
H9	-0.66(2)	-0.65	-1.22(4)	-1.30	-0.67(2)	-0.66	0.84(3)	0.86	0.044
H9'	-0.82(4)	-0.82	-1.55(7)	-1.41	-0.91(3)	-0.90	1.19(4)	1.17	0.062
H10	-11.3(2)	-11.35	-20.7(4)	-20.77	-10.6(5)	-11.48	12.7(8)	12.56	0.032
H11	-0.294(9)	-0.29	-0.55(2)	-0.58	-0.304(8)	-0.31	0.38(1)	0.39	0.043
H12	0.45(1)	0.45	1.04(2)	1.08	1.04(1)	1.05	-1.62(2)	-1.63	0.022
H13	1.65(2)	1.66	3.21(5)	3.29	2.09(5)	2.21	-2.85(8)	-2.85	0.026
H13'	1.91(8)	1.93	3.6(2)	3.90	2.1(1)	2.38	-2.6(2)	-2.64	0.078
H14	0.95(2)	0.96	1.79(3)	1.86	1.03(3)	1.10	-1.31(5)	-1.32	0.035
H16	2.36(6)	2.35	4.8(1)	5.03	3.70(5)	3.75	-5.35(7)	-5.38	0.025
H17	2.21(5)	2.19	4.56(9)	4.68	3.61(6)	3.53	-5.27(9)	-5.30	0.018
H18	2.10(7)	2.14	3.9(1)	3.91	2.2(2)	2.51	-2.8(2)	-2.76	0.051
H18'	1.7(1)	1.69	3.3(2)	3.72	2.1(1)	2.32	-2.8(2)	-2.85	0.093
H19	0.73(2)	0.74	1.35(4)	1.40	0.73(5)	0.84	-0.90(8)	-0.89	0.059
H20	0.749(4)	0.75	1.577(8)	1.58	1.314(9)	1.30	-1.95(1)	-1.95	0.006
H21	-0.04(1)	-0.04	-0.09(2)	-0.06	-0.08(2)	-0.04	0.13(3)	0.13	0.363
H22	-0.89(2)	-0.89	-1.66(4)	-1.75	-0.91(2)	-0.95	1.14(3)	1.15	0.040
H23	-6.8(1)	-6.86	-12.7(3)	-13.01	-6.8(3)	-7.50	8.5(5)	8.46	0.040
H24	0.20(6)	0.19	0.4(1)	0.61	0.33(5)	0.32	-0.48(7)	-0.51	0.227
H24'	-0.40(5)	-0.41	-0.7(1)	-0.46	-0.13(5)	-0.10	0.00(6)	-0.03	0.315
H25	0.08(4)	0.08	0.17(6)	0.30	0.12(3)	0.15	-0.17(4)	-0.19	0.345
H26	-1.41(7)	-1.41	-2.5(1)	-2.27	-1.17(8)	-1.02	1.3(1)	1.29	0.099
H26'	-0.49(3)	-0.50	-0.89(5)	-0.78	-0.40(3)	-0.39	0.45(3)	0.43	0.101
H27	-3.00(5)	-3.01	-5.44(9)	-5.25	-2.60(5)	-2.59	2.99(6)	2.96	0.026
H28	0.62(4)	0.62	1.14(7)	1.29	0.60(3)	0.65	-0.74(5)	-0.75	0.086
H28'	0.70(2)	0.70	1.30(3)	1.37	0.71(2)	0.73	-0.88(2)	-0.89	0.036
H29	0.55(3)	0.55	1.07(5)	1.16	0.67(2)	0.69	-0.90(3)	-0.91	0.057

Table 65 Re-calculated and observed LIS and AF_i for Ln_2 complexes of L^{AB5}

	Ce_2		Pr_2		Nd_2		Eu_2		AF_i
	Calc.	Obs.	Calc.	Obs.	Calc.	Obs	Calc.	Obs.	
H1	1.2(1)	1.24	2.5(2)	2.06	1.7(1)	1.46	-2.4(2)	-2.34	0.127
H2	1.7(1)	1.71	3.1(3)	2.60	1.6(1)	1.47	-2.0(2)	-1.92	0.141
H3	2.3(1)	2.30	4.4(2)	3.94	2.8(2)	2.51	-3.8(3)	-3.79	0.095
H4	0.50(2)	0.51	0.89(3)	0.84	0.39(2)	0.40	-0.42(2)	-0.40	0.053
H4'	0.92(2)	0.92	1.64(3)	1.57	0.71(2)	0.67	-0.75(3)	-0.75	0.037
H5	1.16(6)	1.16	2.1(1)	1.84	0.95(7)	0.83	-1.05(9)	-1.03	0.105
H6	0.08(3)	0.08	0.29(5)	0.18	0.52(4)	0.45	-0.89(6)	-0.89	0.133
H7	-0.521(5)	-0.52	-0.97(1)	-0.97	-0.53(1)	-0.51	0.67(2)	0.67	0.019
H8	-7.3(1)	-7.36	-13.1(3)	-13.57	-5.9(3)	-6.56	6.5(5)	6.52	0.043
H9	-0.62(1)	-0.61	-1.17(2)	-1.13	-0.69(3)	-0.63	0.89(4)	0.90	0.039
H9'	-0.54(3)	-0.54	-1.02(6)	-1.14	-0.61(5)	-0.70	0.79(7)	0.80	0.092
H10	-7.6(3)	-7.76	-13.9(7)	-14.72	-6.7(7)	-8.29	8(1)	7.66	0.090
H11	-0.261(9)	-0.26	-0.49(2)	-0.51	-0.27(1)	-0.25	0.34(2)	0.34	0.043
H12	0.20(4)	0.20	0.57(7)	0.71	0.80(5)	0.90	-1.34(7)	-1.35	0.097
H13	0.6(2)	0.67	1.3(3)	1.91	0.9(3)	1.46	-1.2(4)	-1.22	0.314
H13'	0.7(2)	0.76	1.4(3)	1.89	0.8(3)	1.41	-1.0(5)	-0.97	0.314
H14	0.65(9)	0.67	1.2(2)	1.51	0.7(2)	1.03	-0.8(3)	-0.81	0.229
H15	0.7(2)	0.67	1.6(3)	2.27	1.8(2)	2.12	-2.9(3)	-2.93	0.168
H17	0.8(1)	0.78	1.9v(3)	2.41	2.0(1)	2.22	-3.2(2)	-3.22	0.128
H18	0.7(1)	0.67	1.3(2)	1.85	0.9(1)	1.08	-1.3(2)	-1.32	0.207
H18'	0.6(1)	0.60	1.2(3)	1.72	0.9(2)	1.35	-1.3(3)	-1.28	0.276
H19	0.33(5)	0.33	0.62(9)	0.80	0.36(8)	0.52	-0.5(1)	-0.48	0.218
H20	0.32(3)	0.32	0.80(5)	0.91	0.95(3)	1.00	-1.54(4)	-1.55	0.056
H21	-0.21(1)	-0.21	-0.39(2)	-0.35	-0.21(1)	-0.18	0.25(2)	0.25	0.089
H22	-0.72(5)	-0.73	-1.31(9)	-1.47	-0.66(9)	-0.86	0.8(2)	0.78	0.127
H23	-4.0(4)	-4.03	-7.3(8)	-8.87	-3.9(7)	-5.31	5(1)	4.83	0.172
H24	0.43(4)	0.41	0.83(7)	0.92	0.54(5)	0.46	-0.73(8)	-0.76	0.092
H24'	-0.22(4)	-0.23	-0.31(7)	-0.20	0.07(4)	0.02	-0.24(7)	-0.27	0.304
H25	0.27(2)	0.27	0.50(4)	0.58	0.28(2)	0.30	-0.35(2)	-0.36	0.096
H26	-1.12(5)	-1.11	-2.01(9)	-1.82	-0.93(8)	-0.76	1.0(1)	1.03	0.101
H26'	-0.192(1)	-0.19	-0.341(3)	-0.34	-0.148(3)	-0.14	0.158(6)	0.16	0.016
H27	-2.83(4)	-2.84	-5.13(7)	-5.00	-2.45(3)	-2.44	2.83(4)	2.81	0.020

Table 66 Re-calculated and observed LIS and AF_i for LaLn complexes of L^{AB}

	LaCe		LaPr		LaNd		LaEu		AF_i
	Calc.	Obs.	Calc.	Obs.	Calc.	Obs	Calc.	Obs.	
H1	1.49(8)	1.50	2.9(1)	2.62	1.97(8)	1.84	-2.7(1)	-2.67	0.076
H2	1.9(1)	1.97	3.6(2)	3.14	1.9(1)	1.86	-2.3(2)	-2.24	0.098
H3	2.7(1)	2.67	5.1(2)	4.77	3.3(1)	3.06	-4.4(2)	-4.35	0.057
H4	0.83(1)	0.83	1.53(2)	1.48	0.80(2)	0.77	-0.98(3)	-0.97	0.029
H4'	1.219(9)	1.22	2.21(2)	2.23	1.05(2)	1.09	-1.20(3)	-1.20	0.017
H5	1.39(6)	1.40	2.5(1)	2.30	1.19(5)	1.16	-1.36(7)	-1.33	0.069
H6	0.35(2)	0.34	0.82(5)	0.75	0.86(5)	0.75	-1.36(8)	-1.37	0.073
H7	-0.32(2)	-0.33	-0.60(3)	-0.54	-0.31(2)	-0.29	0.37(2)	0.36	0.084
H8	-5.9(2)	-5.94	-10.6(3)	-9.88	-4.6(2)	-4.26	4.9(3)	4.80	0.057
H9	-0.50(1)	-0.50	-0.90(3)	-0.85	-0.43(1)	-0.41	0.48(2)	0.48	0.047
H9'	-0.13(2)	-0.12	-0.26(3)	-0.19	-0.20(3)	-0.14	0.29(4)	0.29	0.215
H10	-3.1(2)	-3.11	-5.6(3)	-5.01	-2.6(1)	-2.54	2.9(2)	2.82	0.079
H11	-0.228(4)	-0.23	-0.416(9)	-0.42	-0.21(1)	-0.19	0.24(2)	0.24	0.035
H12	-0.369(6)	-0.37	-0.67(1)	-0.65	-0.328(9)	-0.31	0.38(1)	0.38	0.034
H13	-0.44(3)	-0.44	-0.79(5)	-0.69	-0.36(2)	-0.36	0.40(3)	0.39	0.097
H13'	-0.429(8)	-0.43	-0.78(1)	-0.76	-0.37(1)	-0.39	0.42(2)	0.42	0.026
H14	-0.31(2)	-0.31	-0.56(4)	-0.48	-0.25(2)	-0.22	0.28(3)	0.27	0.120
H15	-0.50(1)	-0.50	-0.91(2)	-0.87	-0.431(9)	-0.43	0.49(1)	0.49	0.028
H16	-0.32(1)	-0.32	-0.58(2)	-0.54	-0.275(9)	-0.27	0.31(1)	0.31	0.050
H17	-0.39(2)	-0.39	-0.70(4)	-0.62	-0.33(2)	-0.32	0.37(3)	0.36	0.091
H18	-0.36(2)	-0.36	-0.66(4)	-0.58	-0.32(2)	-0.29	0.37(3)	0.37	0.097
H18'	-0.32(1)	-0.32	-0.57(3)	-0.52	-0.27(1)	-0.25	0.31(2)	0.30	0.084
H19	-0.25(1)	-0.25	-0.45(2)	-0.40	-0.21(2)	-0.19	0.25(2)	0.24	0.105
H20	-0.25(1)	-0.26	-0.46(2)	-0.42	-0.22(1)	-0.21	0.25(1)	0.24	0.080
H21	-0.22(1)	-0.22	-0.40(2)	-0.36	-0.188(9)	-0.18	0.22(1)	0.21	0.073
H22	-0.28(1)	-0.29	-0.51(2)	-0.48	-0.239(9)	-0.24	0.27(1)	0.26	0.056
H23	-0.48(3)	-0.49	-0.87(5)	-0.78	-0.41(2)	-0.40	0.46(3)	0.44	0.086
H24	0.69(5)	0.68	1.31(9)	1.50	0.79(5)	0.81	-1.03(6)	-1.06	0.091
H24'	0.02(7)	0.01	0.1(1)	0.36	0.29(6)	0.32	-0.52(8)	-0.55	0.325
H25	0.43(5)	0.42	0.83(9)	1.00	0.53(4)	0.53	-0.71(6)	-0.74	0.121
H26	-0.86(7)	-0.85	-1.6(1)	-1.28	-0.7(1)	-0.48	0.9(2)	0.85	0.214
H26'	0.07(4)	0.08	0.14(7)	0.29	0.09(6)	0.21	-0.12(9)	-0.12	0.497
H27	-2.64(6)	-2.65	-4.8(1)	-4.60	-2.34(5)	-2.29	2.73(7)	2.70	0.034

Table 67 Re-calculated and observed LIS and AF_i for LaLn complexes of L^{AB3}

	LaCe		LaPr		LaNd		LaEu		AF_i
	Calc.	Obs.	Calc.	Obs.	Calc.	Obs	Calc.	Obs.	
H1	1.22(7)	1.22	2.4(1)	2.10	1.49(6)	1.40	-2.01(9)	-1.98	0.077
H3	2.42(9)	2.42	4.6(2)	4.30	2.8(1)	2.62	-3.7(2)	-3.72	0.059
H4	0.71(3)	0.73	1.31(7)	1.31	0.70(8)	0.86	-0.9(1)	-0.83	0.084
H4'	1.16(1)	1.16	2.09(3)	2.05	0.97(2)	1.00	-1.09(4)	-1.08	0.018
H5	1.37(6)	1.37	2.5(1)	2.25	1.16(5)	1.10	-1.33(7)	-1.30	0.072
H6	0.33(3)	0.32	0.80(6)	0.71	0.87(6)	0.73	-1.4(1)	-1.40	0.092
H7	-0.33(1)	-0.33	-0.60(2)	-0.56	-0.31(1)	-0.29	0.37(2)	0.36	0.059
H8	-5.7(2)	-5.69	-10.1(3)	-9.37	-4.3(2)	-4.15	4.5(2)	4.40	0.056
H9	-0.49(1)	-0.49	-0.88(2)	-0.84	-0.43(2)	-0.40	0.50(2)	0.49	0.050
H9'	-0.175(7)	-0.17	-0.34(2)	-0.33	-0.22(2)	-0.18	0.29(3)	0.30	0.074
H10	-2.9(1)	-2.91	-5.2(2)	-4.72	-2.4(1)	-2.29	2.7(2)	2.61	0.076
H11	-0.231(5)	-0.23	-0.42(1)	-0.41	-0.22(1)	-0.19	0.26(2)	0.26	0.055
H12	-0.37(2)	-0.37	-0.68(5)	-0.58	-0.33(3)	-0.27	0.38(4)	0.38	0.134
H13	-0.39(2)	-0.39	-0.71(3)	-0.64	-0.34(2)	-0.31	0.38(2)	0.38	0.078
H13'	-0.42(1)	-0.42	-0.75(2)	-0.70	-0.35(1)	-0.33	0.39(2)	0.38	0.058
H14	-0.29(2)	-0.29	-0.52(3)	-0.45	-0.24(2)	-0.21	0.28(3)	0.27	0.127
H15	-0.49(2)	-0.49	-0.87(4)	-0.79	-0.40(2)	-0.38	0.45(3)	0.44	0.083
H16	-0.30(1)	-0.30	-0.53(2)	-0.49	-0.25(1)	-0.24	0.29(2)	0.28	0.075
H17	-0.36(1)	-0.36	-0.64(3)	-0.59	-0.31(2)	-0.28	0.35(2)	0.34	0.080
H18	-0.34(4)	-0.34	-0.62(7)	-0.48	-0.31(4)	-0.25	0.36(5)	0.35	0.204
H18'	-0.31(2)	-0.31	-0.56(4)	-0.48	-0.26(2)	-0.22	0.30(3)	0.29	0.134
H19	-0.24(1)	-0.24	-0.43(3)	-0.38	-0.21(2)	-0.16	0.23(3)	0.23	0.137
H20	-0.26(2)	-0.26	-0.46(4)	-0.37	-0.21(2)	-0.18	0.24(3)	0.23	0.189
H21	-0.197(6)	-0.20	-0.36(1)	-0.34	-0.17(1)	-0.15	0.19(2)	0.19	0.070
H22	-0.26(1)	-0.26	-0.47(2)	-0.43	-0.22(1)	-0.20	0.24(1)	0.24	0.071
H23	-0.46(2)	-0.46	-0.82(3)	-0.76	-0.37(1)	-0.36	0.41(2)	0.40	0.060
H24	0.73(3)	0.72	1.37(5)	1.46	0.78(2)	0.80	-1.00(3)	-1.02	0.047
H24'	0.09(8)	0.08	0.2(1)	0.51	0.32(7)	0.33	-0.52(9)	-0.56	0.323
H25	0.47(5)	0.45	0.91(9)	1.05	0.58(5)	0.53	-0.78(8)	-0.82	0.106
H26	-0.80(8)	-0.80	-1.4(1)	-1.10	-0.58(8)	-0.44	0.6(1)	0.57	0.222
H26'	0.23(2)	0.23	0.41(4)	0.48	0.18(4)	0.27	-0.20(7)	-0.20	0.189
H27	-2.30(1)	-2.29	-4.19(3)	-4.20	-2.09(3)	-2.03	2.47(5)	2.48	0.011

Table 68 Re-calculated and observed LIS and AF_i for LaLn complexes of L^{AB4}

	LaCe		LaPr		LaNd		LaEu		AF_i
	Calc.	Obs.	Calc.	Obs.	Calc.	Obs	Calc.	Obs.	
H1	1.51(8)	1.51	3.0(1)	2.64	1.97(9)	1.82	-2.7(1)	-2.68	0.079
H2	1.9(1)	1.89	3.5(2)	3.01	1.8(1)	1.75	-2.2(1)	-2.17	0.102
H3	2.5(1)	2.52	4.9(2)	4.46	3.1(1)	2.84	-4.2(2)	-4.12	0.067
H4	1.1(1)	1.11	2.0(2)	1.58	0.9(1)	0.80	-1.0(1)	-0.99	0.183
H4'	1.13(5)	1.13	2.06(8)	2.23	1.00(5)	1.10	-1.16(8)	-1.18	0.068
H5	1.13(5)	1.12	2.1(1)	2.27	1.07(5)	1.10	-1.30(6)	-1.33	0.064
H6	0.36(2)	0.35	0.85(5)	0.83	0.90(6)	0.77	-1.4(1)	-1.43	0.068
H7	-0.30(2)	-0.30	-0.54(4)	-0.46	-0.25(2)	-0.25	0.29(3)	0.28	0.117
H8	-6.0(2)	-6.04	-10.7(4)	-9.84	-4.6(2)	-4.44	4.8(3)	4.72	0.064
H9	-0.53(3)	-0.53	-0.96(5)	-0.86	-0.45(3)	-0.41	0.52(4)	0.51	0.089
H9'	-0.15(1)	-0.15	-0.29(2)	-0.24	-0.18(1)	-0.15	0.23(2)	0.23	0.135
H10	-2.9(1)	-2.90	-5.2(2)	-4.84	-2.38(8)	-2.29	2.6(1)	2.60	0.055
H11	-0.23(1)	-0.22	-0.42(2)	-0.45	-0.21(1)	-0.20	0.26(2)	0.27	0.065
H12	-0.37(1)	-0.37	-0.68(2)	-0.64	-0.34(2)	-0.30	0.41(3)	0.41	0.067
H13	-0.43(2)	-0.43	-0.77(4)	-0.68	-0.36(2)	-0.33	0.41(3)	0.40	0.104
H13'	-0.47(2)	-0.47	-0.84(3)	-0.78	-0.38(2)	-0.38	0.43(2)	0.42	0.057
H14	-0.27(1)	-0.27	-0.49(3)	-0.43	-0.23(2)	-0.20	0.27(3)	0.26	0.112
H16	-0.50(2)	-0.51	-0.91(4)	-0.83	-0.42(2)	-0.40	0.46(3)	0.45	0.072
H17	-0.38(2)	-0.38	-0.68(3)	-0.61	-0.31(2)	-0.29	0.35(2)	0.34	0.088
H18	-0.38(3)	-0.38	-0.69(5)	-0.58	-0.33(3)	-0.29	0.38(4)	0.37	0.135
H18'	-0.28(2)	-0.27	-0.52(4)	-0.48	-0.29(4)	-0.20	0.37(7)	0.38	0.144
H19	-0.234(8)	-0.23	-0.43(2)	-0.39	-0.21(1)	-0.18	0.24(2)	0.24	0.071
H20	-0.25(1)	-0.25	-0.46(2)	-0.41	-0.21(1)	-0.19	0.24(2)	0.24	0.083
H21	-0.219(9)	-0.22	-0.39(2)	-0.36	-0.182(9)	-0.17	0.20(1)	0.20	0.074
H22	-0.28(1)	-0.28	-0.50(2)	-0.45	-0.22(1)	-0.21	0.25(2)	0.24	0.083
H23	-0.45(2)	-0.45	-0.80(3)	-0.74	-0.36(2)	-0.37	0.40(3)	0.39	0.062
H24	0.60(6)	0.59	1.2(1)	1.36	0.72(5)	0.74	-0.97(7)	-1.00	0.108
H24'	-0.02(6)	-0.04	0.0(1)	0.25	0.25(6)	0.24	-0.47(8)	-0.51	0.341
H25	0.39(4)	0.38	0.74(8)	0.90	0.46(4)	0.48	-0.60(5)	-0.63	0.129
H26	-1.03(8)	-1.03	-1.8(2)	-1.53	-0.8(1)	-0.57	0.9(2)	0.84	0.188
H26'	-0.05(4)	-0.05	-0.08(8)	0.08	0.01(6)	0.12	-0.04(9)	-0.05	1.222
H27	-2.65(7)	-2.66	-4.8(1)	-4.55	-2.28(6)	-2.21	2.61(8)	2.58	0.042
H28	-0.24(7)	-0.25	-0.4(1)	-0.20	-0.19(6)	-0.18	0.21(8)	0.17	0.563
H28'	-0.16(1)	-0.17	-0.30(3)	-0.27	-0.15(3)	-0.19	0.17(4)	0.16	0.132
H29	-0.159(7)	-0.16	-0.28(1)	-0.26	-0.130(7)	-0.13	0.144(9)	0.14	0.070

Table 69 Re-calculated and observed LIS and AF_i for LaLn complexes of L^{AB5}

	LaCe		LaPr		LaNd		LaEu		AF_i
	Calc.	Obs.	Calc.	Obs.	Calc.	Obs	Calc.	Obs.	
H1	1.45(8)	1.46	2.8(2)	2.53	1.92(9)	1.76	-2.6(1)	-2.61	0.085
H2	1.9(1)	1.94	3.5(2)	3.08	1.9(1)	1.78	-2.3(1)	-2.19	0.102
H3	2.7(1)	2.67	5.1(2)	4.71	3.2(1)	2.96	-4.3(2)	-4.25	0.066
H4	0.761(7)	0.76	1.41(1)	1.38	0.74(1)	0.72	-0.91(2)	-0.91	0.018
H4'	1.22(1)	1.22	2.19(2)	2.17	1.02(1)	1.04	-1.15(2)	-1.14	0.011
H5	1.40(6)	1.41	2.5(1)	2.31	1.19(5)	1.12	-1.35(7)	-1.32	0.074
H6	0.32(2)	0.31	0.77(5)	0.72	0.85(5)	0.74	-1.36(9)	-1.37	0.071
H7	-0.35(2)	-0.36	-0.64(3)	-0.58	-0.31(2)	-0.29	0.36(2)	0.36	0.090
H8	-6.1(2)	-6.09	-10.8(3)	-10.07	-4.6(2)	-4.46	4.8(2)	4.68	0.052
H9	-0.54(2)	-0.54	-0.97(4)	-0.89	-0.46(2)	-0.43	0.52(3)	0.51	0.070
H9'	-0.152(4)	-0.15	-0.295(9)	-0.29	-0.19(1)	-0.17	0.26(2)	0.26	0.047
H10	-3.2(2)	-3.21	-5.7(4)	-4.90	-2.6(2)	-2.34	2.8(3)	2.71	0.123
H11	-0.242(6)	-0.24	-0.44(1)	-0.46	-0.218(8)	-0.21	0.26(1)	0.26	0.034
H12	-0.376(8)	-0.38	-0.68(1)	-0.65	-0.33(1)	-0.31	0.39(2)	0.39	0.044
H13	-0.42(1)	-0.43	-0.77(2)	-0.73	-0.35(1)	-0.34	0.40(2)	0.40	0.045
H13'	-0.417(7)	-0.42	-0.75(1)	-0.74	-0.35(1)	-0.37	0.40(2)	0.39	0.024
H14	-0.34(3)	-0.34	-0.60(4)	-0.51	-0.27(2)	-0.24	0.29(3)	0.28	0.137
H15	-0.53(2)	-0.53	-0.94(4)	-0.87	-0.43(2)	-0.42	0.47(2)	0.46	0.063
H17	-0.39(2)	-0.40	-0.70(3)	-0.64	-0.32(2)	-0.31	0.35(2)	0.35	0.082
H18	-0.305(3)	-0.31	-0.558(6)	-0.54	-0.282(4)	-0.27	0.336(6)	0.34	0.020
H18'	-0.30(1)	-0.30	-0.54(2)	-0.50	-0.26(2)	-0.23	0.30(2)	0.30	0.078
H19	-0.26(1)	-0.26	-0.46(3)	-0.41	-0.21(1)	-0.20	0.24(2)	0.23	0.098
H20	-0.236(9)	-0.24	-0.43(2)	-0.40	-0.21(1)	-0.18	0.24(2)	0.24	0.082
H21	-0.214(6)	-0.22	-0.39(1)	-0.37	-0.177(5)	-0.18	0.198(7)	0.20	0.041
H22	-0.269(7)	-0.27	-0.48(1)	-0.46	-0.225(6)	-0.22	0.254(8)	0.25	0.041
H23	-0.48(2)	-0.48	-0.86(4)	-0.77	-0.38(2)	-0.38	0.41(3)	0.40	0.079
H24	0.68(5)	0.67	1.29(9)	1.47	0.77(4)	0.80	-1.01(6)	-1.04	0.089
H24'	-0.03(6)	-0.05	0.0(1)	0.27	0.28(6)	0.28	-0.52(6)	-0.56	0.335
H25	0.43(5)	0.42	0.82(9)	1.00	0.51(5)	0.51	-0.67(6)	-0.70	0.129
H26	-0.84(7)	-0.83	-1.5(1)	-1.26	-0.7(1)	-0.46	0.8(2)	0.76	0.194
H26'	0.10(3)	0.10	0.18(5)	0.29	0.10(4)	0.18	-0.13(6)	-0.14	0.340
H27	-2.62(5)	-2.62	-4.7(1)	-4.53	-2.26(5)	-2.19	2.60(7)	2.57	0.035

Table 70 Re-calculated and observed LIS and AF_i for LnLu complexes of L^{AB}

	CeLu		PrLu		NdLu		EuLu		AF_i
	Calc.	Obs.	Calc.	Obs.	Calc.	Obs	Calc.	Obs.	
H1	-0.23(2)	-0.23	-0.42(4)	-0.51	-0.24(3)	-0.31	0.30(6)	0.30	0.161
H2	-0.21(1)	-0.21	-0.39(2)	-0.43	-0.21(2)	-0.26	0.27(4)	0.27	0.106
H3	-0.31(3)	-0.31	-0.57(5)	-0.67	-0.32(4)	-0.41	0.41(7)	0.41	0.140
H4	-0.33(1)	-0.33	-0.62(2)	-0.67	-0.35(2)	-0.38	0.44(2)	0.45	0.063
H4'	-0.32(2)	-0.32	-0.59(4)	-0.68	-0.34(3)	-0.41	0.43(5)	0.43	0.118
H5	-0.22(1)	-0.22	-0.41(3)	-0.46	-0.23(2)	-0.28	0.29(4)	0.29	0.115
H6	-0.338(5)	-0.34	-0.638(9)	-0.66	-0.372(5)	-0.38	0.480(6)	0.48	0.021
H7	-0.22(1)	-0.22	-0.42(2)	-0.46	-0.26(1)	-0.27	0.34(1)	0.34	0.063
H8	-1.5(2)	-1.57	-2.9(3)	-3.48	-1.6(3)	-2.14	2.0(4)	2.02	0.167
H9	-0.125(5)	-0.12	-0.27(1)	-0.27	-0.25(1)	-0.22	0.37(2)	0.38	0.046
H9'	-0.38(4)	-0.39	-0.72(7)	-0.86	-0.41(6)	-0.54	0.53(9)	0.54	0.154
H10	-4.7(5)	-4.75	-8.6(9)	-10.49	-4.6(8)	-6.32	6(1)	5.69	0.177
H11	0.017(5)	0.02	0.02(1)	0.04	-0.02(1)	0.01	0.04(2)	0.04	0.516
H12	0.62(4)	0.62	1.34(7)	1.48	1.19(4)	1.25	-1.80(5)	-1.81	0.056
H13	1.1(1)	1.11	2.1(3)	2.69	1.5(2)	1.88	-2.0(3)	-2.04	0.171
H13'	1.2(2)	1.24	2.3(3)	2.93	1.3(3)	1.87	-1.6(4)	-1.62	0.222
H14	0.77(6)	0.78	1.5(1)	1.68	0.84(9)	1.04	-1.1(1)	-1.09	0.125
H15	1.4(1)	1.40	3.0(3)	3.54	2.6(1)	2.89	-3.9(2)	-3.99	0.097
H16	1.28(5)	1.30	2.5(1)	2.68	1.7(1)	1.95	-2.3(2)	-2.32	0.072
H17	1.4(1)	1.41	3.1(2)	3.54	2.8(1)	2.96	-4.2(2)	-4.22	0.081
H18	1.1(1)	1.15	2.2(3)	2.72	1.3(2)	1.67	-1.6(3)	-1.68	0.182
H18'	1.0(1)	1.02	2.0(2)	2.46	1.4(2)	1.74	-1.9(3)	-1.95	0.157
H19	0.55(4)	0.56	1.02(8)	1.17	0.56(7)	0.72	-0.7(1)	-0.71	0.129
H20	0.62(3)	0.62	1.35(5)	1.45	1.21(3)	1.25	-1.83(4)	-1.84	0.041
H21	0.06(1)	0.06	0.09(3)	0.13	0.00(3)	0.05	0.04(4)	0.04	0.445
H22	-0.38(4)	-0.39	-0.73(8)	-0.90	-0.44(6)	-0.57	0.58(9)	0.60	0.162
H23	-3.6(4)	-3.64	-6.7(8)	-8.32	-3.8(6)	-5.05	4.8(9)	4.88	0.176
H24	-0.22(1)	-0.22	-0.40(3)	-0.46	-0.22(3)	-0.28	0.28(4)	0.28	0.122
H25	-0.16(2)	-0.17	-0.31(3)	-0.38	-0.18(2)	-0.23	0.23(4)	0.23	0.154
H26	-0.26(3)	-0.26	-0.48(5)	-0.60	-0.28(4)	-0.35	0.35(5)	0.36	0.165
H26'	-0.21(1)	-0.22	-0.40(3)	-0.44	-0.22(3)	-0.29	0.28(5)	0.28	0.118
H27	-0.20(2)	-0.21	-0.38(3)	-0.45	-0.21(3)	-0.28	0.27(5)	0.27	0.143

Table 71 Re-calculated and observed LIS and AF_i for LnLu complexes of L^{AB3}

	CeLu		PrLu		NdLu		EuLu		AF_i
	Calc.	Obs.	Calc.	Obs.	Calc.	Obs	Calc.	Obs.	
H1	-0.22(2)	-0.22	-0.41(5)	-0.50	-0.23(4)	-0.31	0.30(6)	0.30	0.173
H3	-0.30(3)	-0.30	-0.56(6)	-0.68	-0.32(5)	-0.41	0.40(7)	0.41	0.164
H4	-0.32(2)	-0.32	-0.61(3)	-0.68	-0.36(2)	-0.39	0.47(3)	0.48	0.078
H4'	-0.31(3)	-0.31	-0.59(5)	-0.69	-0.34(3)	-0.40	0.43(5)	0.44	0.130
H5	-0.21(2)	-0.21	-0.39(3)	-0.46	-0.22(2)	-0.27	0.29(3)	0.29	0.127
H6	-0.33(2)	-0.33	-0.62(3)	-0.69	-0.36(2)	-0.40	0.47(3)	0.48	0.079
H7	-0.22(2)	-0.22	-0.43(3)	-0.49	-0.27(2)	-0.29	0.36(2)	0.37	0.093
H8	-1.5(1)	-1.54	-2.8(3)	-3.39	-1.6(2)	-2.09	2.1(3)	2.09	0.150
H9	-0.11(1)	-0.11	-0.25(2)	-0.28	-0.25(1)	-0.23	0.38(2)	0.39	0.058
H9'	-0.38(4)	-0.38	-0.71(7)	-0.85	-0.42(6)	-0.54	0.54(9)	0.55	0.153
H10	-4.6(5)	-4.67	-8.5(9)	-10.37	-4.6(8)	-6.24	6(1)	5.70	0.176
H11	0.014(1)	0.01	0.016(2)	0.01	-0.020(3)	-0.02	0.044(4)	0.04	0.096
H12	0.61(3)	0.61	1.32(5)	1.42	1.18(2)	1.22	-1.79(3)	-1.80	0.039
H13	1.1(2)	1.08	2.1(3)	2.70	1.4(2)	1.85	-2.0(3)	-2.01	0.183
H13'	1.2(2)	1.21	2.2(3)	2.84	1.2(3)	1.82	-1.6(4)	-1.60	0.215
H14	0.77(5)	0.77	1.4(1)	1.65	0.83(8)	1.01	-1.1(1)	-1.08	0.118
H15	1.4(1)	1.37	3.0(2)	3.45	2.6(1)	2.84	-3.9(2)	-3.98	0.089
H16	1.25(4)	1.26	2.46(9)	2.60	1.7(1)	1.89	-2.3(2)	-2.33	0.060
H17	1.4(1)	1.38	3.0(2)	3.46	2.7(1)	2.90	-4.2(1)	-4.23	0.073
H18	1.1(1)	1.12	2.1(3)	2.64	1.3(2)	1.69	-1.7(3)	-1.69	0.182
H18'	1.0(1)	0.98	1.9(2)	2.39	1.4(2)	1.68	-1.9(2)	-1.95	0.151
H19	0.54(4)	0.55	1.01(7)	1.15	0.56(6)	0.70	-0.7(1)	-0.72	0.118
H20	0.61(2)	0.61	1.34(4)	1.42	1.21(2)	1.22	-1.84(3)	-1.85	0.032
H21	0.069(8)	0.07	0.11(2)	0.13	0.01(2)	0.05	0.02(3)	0.02	0.296
H22	-0.38(4)	-0.39	-0.73(8)	-0.90	-0.43(6)	-0.57	0.6(1)	0.57	0.172
H23	-3.5(4)	-3.56	-6.6(8)	-8.17	-3.7(6)	-5.09	5(1)	4.84	0.183
H24	-0.20(3)	-0.20	-0.38(5)	-0.48	-0.22(3)	-0.28	0.28(5)	0.29	0.183
H25	-0.17(2)	-0.17	-0.31(3)	-0.39	-0.19(2)	-0.23	0.25(3)	0.26	0.146
H26	-0.25(3)	-0.25	-0.46(5)	-0.57	-0.26(3)	-0.33	0.32(5)	0.33	0.165
H26'	-0.21(2)	-0.22	-0.40(4)	-0.46	-0.22(4)	-0.31	0.28(6)	0.28	0.158
H27	-0.19(2)	-0.19	-0.36(3)	-0.43	-0.21(2)	-0.26	0.27(4)	0.28	0.144

Table 72 Re-calculated and observed LIS and AF_i for LnLu complexes of L^{AB4}

	CeLu		PrLu		NdLu		EuLu		AF_i
	Calc.	Obs.	Calc.	Obs.	Calc.	Obs	Calc.	Obs.	
H1	-0.418(5)	-0.42	-0.78(1)	-0.79	-0.43(1)	-0.45	0.53(2)	0.53	0.024
H2	-0.366(4)	-0.37	-0.683(8)	-0.69	-0.38(1)	-0.40	0.47(2)	0.47	0.021
H3	-0.570(8)	-0.57	-1.06(2)	-1.08	-0.58(2)	-0.62	0.73(3)	0.73	0.029
H4	-0.560(2)	-0.56	-1.046(3)	-1.04	-0.581(1)	-0.58	0.731(2)	0.73	0.004
H4'	-0.561(5)	-0.56	-1.05(1)	-1.06	-0.58(1)	-0.60	0.73(2)	0.73	0.018
H5	-0.381(2)	-0.38	-0.711(5)	-0.71	-0.391(6)	-0.40	0.49(1)	0.49	0.012
H6	-0.551(6)	-0.55	-1.03(1)	-1.01	-0.58(1)	-0.56	0.74(2)	0.74	0.022
H7	-0.3523(5)	-0.35	-0.663(1)	-0.66	-0.3809(9)	-0.38	0.488(2)	0.49	0.002
H8	-2.87(4)	-2.89	-5.3(1)	-5.45	-2.9(1)	-3.14	3.6(2)	3.61	0.032
H9	-0.193(4)	-0.19	-0.389(8)	-0.37	-0.287(7)	-0.27	0.41(1)	0.41	0.034
H9'	-0.696(9)	-0.70	-1.30(2)	-1.32	-0.73(2)	-0.78	0.92(4)	0.92	0.027
H10	-8.4(2)	-8.48	-15.6(4)	-16.33	-8.3(4)	-9.09	10.2(6)	10.25	0.045
H11	-0.075(4)	-0.08	-0.150(7)	-0.14	-0.110(4)	-0.11	0.157(5)	0.16	0.067
H12	0.81(1)	0.80	1.68(2)	1.68	1.36(2)	1.31	-2.00(4)	-2.01	0.016
H13	1.89(5)	1.89	3.67(9)	3.86	2.38(4)	2.44	-3.23(6)	-3.25	0.033
H13'	2.29(4)	2.30	4.30(8)	4.44	2.45(8)	2.62	-3.1(1)	-3.12	0.034
H14	1.17(1)	1.18	2.19(2)	2.20	1.23(3)	1.28	-1.55(4)	-1.54	0.016
H15	2.81(3)	2.80	5.64(6)	5.75	4.09(3)	4.08	-5.80(5)	-5.82	0.012
H17	2.55(3)	2.54	5.17(8)	5.21	3.87(6)	3.76	-5.5(1)	-5.57	0.014
H18	2.40(7)	2.42	4.5(1)	4.32	2.6(1)	2.69	-3.3(2)	-3.20	0.036
H18'	2.0(1)	2.02	3.9(2)	4.27	2.4(1)	2.56	-3.1(2)	-3.16	0.072
H19	0.98(2)	0.99	1.80(4)	1.78	0.94(4)	1.02	-1.14(7)	-1.13	0.032
H20	1.00(1)	1.00	2.04(2)	2.00	1.53(2)	1.49	-2.20(3)	-2.20	0.015
H21	0.20(1)	0.21	0.34(2)	0.34	0.11(3)	0.16	-0.08(4)	-0.07	0.116
H22	-0.56(2)	-0.56	-1.07(3)	-1.14	-0.68(1)	-0.69	0.91(2)	0.92	0.036
H23	-6.1(1)	-6.10	-11.4(2)	-11.77	-6.4(2)	-6.84	8.2(3)	8.17	0.032
H24	-0.371(5)	-0.37	-0.693(8)	-0.71	-0.386(4)	-0.39	0.488(5)	0.49	0.017
H24'	-0.3696(9)	-0.37	-0.692(2)	-0.69	-0.388(1)	-0.39	0.491(2)	0.49	0.003
H25	-0.296(5)	-0.30	-0.55(1)	-0.57	-0.31(1)	-0.33	0.38(2)	0.38	0.033
H26	-0.464(3)	-0.47	-0.866(6)	-0.87	-0.482(7)	-0.50	0.61(1)	0.61	0.011
H26'	-0.379(6)	-0.38	-0.70(1)	-0.71	-0.38(2)	-0.41	0.47(3)	0.47	0.033
H27	-0.372(2)	-0.37	-0.695(3)	-0.69	-0.388(3)	-0.39	0.489(5)	0.49	0.006
H28	0.80(3)	0.80	1.47(5)	1.58	0.74(3)	0.80	-0.88(5)	-0.89	0.061
H28'	0.86(1)	0.86	1.59(2)	1.64	0.84(1)	0.86	-1.04(2)	-1.05	0.022
H29	0.730(8)	0.73	1.38(1)	1.41	0.804(9)	0.82	-1.04(1)	-1.04	0.017

Table 73 Re-calculated and observed LIS and AF_i for LnLu complexes of L^{AB5}

	CeLu		PrLu		NdLu		EuLu		AF_i
	Calc.	Obs.	Calc.	Obs.	Calc.	Obs	Calc.	Obs.	
H1	-0.21(2)	-0.22	-0.40(5)	-0.49	-0.22(4)	-0.30	0.27(6)	0.27	0.180
H2	-0.16(3)	-0.17	-0.31(5)	-0.42	-0.18(4)	-0.27	0.23(7)	0.23	0.246
H3	-0.28(3)	-0.28	-0.52(6)	-0.64	-0.29(4)	-0.37	0.36(6)	0.37	0.166
H4	-0.33(2)	-0.33	-0.61(3)	-0.67	-0.33(2)	-0.39	0.42(4)	0.42	0.086
H4'	-0.29(3)	-0.30	-0.55(5)	-0.65	-0.31(4)	-0.39	0.39(6)	0.39	0.139
H5	-0.21(1)	-0.21	-0.39(3)	-0.44	-0.21(2)	-0.26	0.27(4)	0.27	0.114
H6	-0.33(1)	-0.33	-0.62(2)	-0.67	-0.37(1)	-0.38	0.48(1)	0.48	0.048
H7	-0.24(1)	-0.24	-0.46(3)	-0.51	-0.27(2)	-0.29	0.34(2)	0.35	0.084
H8	-1.5(1)	-1.49	-2.7(3)	-3.26	-1.5(2)	-1.93	1.8(3)	1.83	0.158
H9	-0.154(4)	-0.15	-0.325(9)	-0.32	-0.27(1)	-0.25	0.41(2)	0.41	0.035
H9'	-0.37(4)	-0.38	-0.70(8)	-0.85	-0.40(7)	-0.55	0.5(1)	0.51	0.178
H10	-4.3(5)	-4.40	-8.0(9)	-9.81	-4.2(8)	-5.88	5(1)	5.15	0.188
H11	-0.026(2)	-0.02	-0.058(4)	-0.05	-0.055(5)	-0.04	0.084(8)	0.09	0.088
H12	0.55(3)	0.55	1.21(5)	1.32	1.12(3)	1.17	-1.72(4)	-1.73	0.047
H13	1.0(1)	0.96	1.9(3)	2.42	1.2(2)	1.66	-1.7(3)	-1.73	0.200
H13'	1.0(2)	1.06	1.9(3)	2.50	1.0(3)	1.61	-1.3(4)	-1.32	0.235
H14	0.86(6)	0.88	1.6(1)	1.82	0.9(1)	1.14	-1.1(2)	-1.07	0.136
H15	1.2(1)	1.16	2.5(3)	3.05	2.2(2)	2.47	-3.3(2)	-3.34	0.119
H17	1.1(1)	1.14	2.5(2)	2.95	2.2(1)	2.46	-3.4(2)	-3.45	0.097
H18	1.0(1)	0.97	1.9(2)	2.37	1.2(1)	1.42	-1.6(2)	-1.64	0.163
H18'	0.9(1)	0.90	1.7(2)	2.17	1.2(2)	1.54	-1.6(3)	-1.65	0.173
H19	0.58(4)	0.59	1.08(7)	1.21	0.57(7)	0.71	-0.7(1)	-0.70	0.116
H20	0.59(2)	0.59	1.28(3)	1.35	1.17(1)	1.19	-1.79(2)	-1.79	0.024
H21	0.040(4)	0.04	0.058(9)	0.07	-0.01(1)	0.01	0.04(2)	0.04	0.274
H22	-0.37(5)	-0.38	-0.7(1)	-0.91	-0.42(7)	-0.58	0.6(1)	0.56	0.198
H23	-3.3(4)	-3.31	-6.1(8)	-7.74	-3.5(6)	-4.66	4.4(9)	4.47	0.189
H24	-0.22(1)	-0.23	-0.41(3)	-0.45	-0.21(3)	-0.28	0.25(5)	0.24	0.130
H24'	-0.21(2)	-0.21	-0.38(4)	-0.45	-0.20(4)	-0.28	0.25(6)	0.25	0.167
H25	-0.15(2)	-0.15	-0.28(3)	-0.35	-0.16(3)	-0.21	0.20(4)	0.21	0.179
H26	-0.26(1)	-0.27	-0.48(3)	-0.53	-0.24(3)	-0.31	0.29(5)	0.29	0.111
H26'	-0.19(2)	-0.20	-0.36(4)	-0.43	-0.20(3)	-0.27	0.24(5)	0.24	0.166
H27	-0.19(1)	-0.19	-0.35(4)	-0.42	-0.19(3)	-0.26	0.24(5)	0.24	0.174

As can be seen in the tables the re-calculated values of lanthanide induced shift are rather close to the experimental ones. The agreement factors AF_i are satisfactory for most protons. The exceptions are all close to one of the magic angles as mentioned earlier.

Similar to the proton agreement factors AF_i, an agreement factor can be calculated for each lanthanide ion j:

$$AF_j = \sqrt{\frac{\sum_i \left(\left(\Delta_{i,j}\right)_{calc} - \left(\Delta_{i,j}\right)_{exp} \right)^2}{\sum_i \left(\left(\Delta_{i,j}\right)_{exp} \right)^2}} \qquad (10)$$

These agreement factors are given in Table 74 below.

Table 74 Lanthanide agreement factors AF_j

	Ce	Pr	Nd	Eu
$Ln_2(L^{AB})_3$	0.012	0.112	0.182	0.016
$LaLn(L^{AB})_3$	0.005	0.087	0.071	0.018
$LnLu(L^{AB})_3$	0.014	0.176	0.233	0.012
$Ln_2(L^{AB3})_3$	0.013	0.108	0.195	0.012
$LaLn(L^{AB3})_3$	0.006	0.084	0.067	0.020
$LnLu(L^{AB3})_3$	0.014	0.177	0.233	0.012
$Ln_2(L^{AB4})_3$	0.007	0.037	0.075	0.011
$LaLn(L^{AB4})_3$	0.006	0.098	0.072	0.022
$LnLu(L^{AB4})_3$	0.005	0.039	0.067	0.005
$Ln_2(L^{AB5})_3$	0.012	0.104	0.191	0.014
$LaLn(L^{AB5})_3$	0.006	0.097	0.069	0.022
$LnLu(L^{AB5})_3$	0.014	0.190	0.251	0.015

The agreement factors are satisfactory showing that the one proton method of separating contact and pseudo contact terms was successful. The AF_j values for Pr and Nd are one order of magnitude larger than those for Ce and Eu without any simple explanation being evident.

Leaving out the problematic atoms (H11 and H21 for LnLu, H24' and H26' for LaLn and Ln_2) does not improve the agreement factors significantly (a few % at most) even though their individual agreement factors (AF_i) were high. The absolute "disagreement" of these protons is low and it is only the relative "disagreement" which is high. This leads to high values of AF_i, but negligible contributions to the values of AF_j.

5.4 Comparing mono- and bimetallic complexes

One of the purposes of this project is to determine whether the contributions to the chemical shift from two paramagnetic lanthanide ions in the same complex are additive. This will be examined by means of comparing first the lanthanide induced shift of the Ln_2 complexes with the sums of LIS of the LaLn and LnLu complexes. Subsequently a similar comparison will be carried out for the contact and pseudo contact parameters obtained from the one proton analysis.

5.4.1 LIS of mono- and bimetallic complexes

The sums of the contributions from a paramagnetic lanthanide ion in the bpa site (LaLn complexes) and a paramagnetic lanthanide ion in the bpb site (LnLu complexes) are given in Table 75 and Table 76. These values will here be compared to the lanthanide induced shifts of the Ln_2 complexes (Table 32 and Table 33) in which both sites (bpa and bpb) are occupied by a paramagnetic lanthanide ion.

Table 75 Sums of LIS of LaLn and LnLu complexes of L^{AB} and L^{AB3}

	Ce		Pr		Nd		Eu	
	L^{AB}	L^{AB3}	L^{AB}	L^{AB3}	L^{AB}	L^{AB3}	L^{AB}	L^{AB3}
H1	1.27	1.00	2.11	1.60	1.53	1.09	-2.37	-1.68
H2	1.76		2.71		1.60		-1.97	
H3	2.36	2.11	4.10	3.61	2.65	2.20	-3.95	-3.31
H4	0.49	0.41	0.80	0.63	0.38	0.47	-0.53	-0.35
H4'	0.90	0.85	1.55	1.36	0.68	0.60	-0.77	-0.64
H5	1.18	1.16	1.84	1.79	0.88	0.83	-1.04	-1.01
H6	0.01	0.00	0.10	0.03	0.38	0.34	-0.88	-0.92
H7	-0.55	-0.55	-1.00	-1.05	-0.56	-0.58	0.70	0.73
H8	-7.51	-7.23	-13.36	-12.76	-6.40	-6.24	6.82	6.48
H9	-0.62	-0.60	-1.12	-1.12	-0.63	-0.63	0.86	0.88
H9'	-0.51	-0.55	-1.05	-1.18	-0.68	-0.72	0.82	0.85
H10	-7.86	-7.58	-15.50	-15.09	-8.86	-8.53	8.51	8.31
H11	-0.21	-0.21	-0.38	-0.39	-0.18	-0.20	0.28	0.31
H12	0.25	0.24	0.83	0.84	0.94	0.95	-1.43	-1.42
H13	0.66	0.68	1.99	2.05	1.51	1.53	-1.65	-1.64
H13'	0.81	0.79	2.17	2.14	1.48	1.49	-1.20	-1.22
H14	0.47	0.48	1.20	1.20	0.82	0.80	-0.82	-0.81
H15	0.90	0.88	2.67	2.66	2.46	2.46	-3.50	-3.54
H16	0.98	0.97	2.14	2.12	1.68	1.66	-2.01	-2.04
H17	1.02	1.02	2.92	2.87	2.64	2.62	-3.86	-3.89
H18	0.79	0.78	2.14	2.16	1.38	1.44	-1.32	-1.34
H18'	0.70	0.67	1.94	1.91	1.49	1.46	-1.65	-1.66
H19	0.31	0.31	0.77	0.77	0.53	0.54	-0.46	-0.48
H20	0.36	0.35	1.03	1.05	1.04	1.04	-1.60	-1.62
H21	-0.16	-0.12	-0.23	-0.20	-0.13	-0.09	0.25	0.22
H22	-0.67	-0.65	-1.37	-1.33	-0.80	-0.77	0.86	0.81
H23	-4.12	-4.02	-9.09	-8.93	-5.44	-5.45	5.33	5.24
H24	0.46	0.52	1.04	0.98	0.53	0.52	-0.78	-0.73
H24'	-0.21	-0.12	-0.10	0.03	0.04	0.05	-0.27	-0.27
H25	0.26	0.29	0.63	0.67	0.31	0.31	-0.50	-0.56
H26	-1.11	-1.05	-1.88	-1.67	-0.83	-0.77	1.21	0.90
H26'	-0.14	0.01	-0.15	0.02	-0.08	-0.04	0.16	0.08
H27	-2.86	-2.48	-5.05	-4.63	-2.57	-2.29	2.97	2.76

Table 76 Sums of LIS of LaLn and LnLu complexes of L^{AB4} and L^{AB5}

	Ce		Pr		Nd		Eu	
	L^{AB4}	L^{AB5}	L^{AB4}	L^{AB5}	L^{AB4}	L^{AB5}	L^{AB4}	L^{AB5}
H1	1.09	1.24	1.85	2.04	1.37	1.46	-2.15	-2.33
H2	1.52	1.77	2.32	2.66	1.35	1.51	-1.70	-1.95
H3	1.95	2.39	3.38	4.07	2.22	2.59	-3.39	-3.88
H4	0.55	0.43	0.54	0.71	0.22	0.33	-0.26	-0.49
H4'	0.57	0.92	1.17	1.52	0.50	0.65	-0.45	-0.75
H5	0.74	1.20	1.56	1.87	0.70	0.86	-0.84	-1.05
H6	-0.20	-0.02	-0.18	0.05	0.21	0.36	-0.69	-0.89
H7	-0.65	-0.60	-1.12	-1.09	-0.63	-0.58	0.77	0.70
H8	-8.93	-7.58	-15.29	-13.33	-7.58	-6.39	8.33	6.51
H9	-0.72	-0.69	-1.23	-1.21	-0.68	-0.68	0.92	0.92
H9'	-0.85	-0.53	-1.56	-1.14	-0.93	-0.72	1.15	0.77
H10	-11.38	-7.61	-21.17	-14.71	-11.38	-8.22	12.85	7.86
H11	-0.30	-0.26	-0.59	-0.52	-0.31	-0.26	0.42	0.35
H12	0.43	0.18	1.04	0.67	1.01	0.87	-1.60	-1.35
H13	1.46	0.54	3.18	1.70	2.11	1.33	-2.85	-1.33
H13'	1.82	0.64	3.65	1.76	2.23	1.24	-2.71	-0.93
H14	0.91	0.54	1.77	1.31	1.08	0.90	-1.28	-0.79
H15	2.29	0.63	4.92	2.18	3.68	2.05	-5.37	-2.88
H17	2.16	0.74	4.60	2.31	3.47	2.15	-5.23	-3.11
H18	2.04	0.67	3.74	1.83	2.40	1.15	-2.83	-1.30
H18'	1.75	0.60	3.79	1.67	2.36	1.31	-2.78	-1.35
H19	0.75	0.33	1.38	0.80	0.83	0.51	-0.89	-0.47
H20	0.75	0.35	1.59	0.95	1.30	1.01	-1.96	-1.56
H21	-0.01	-0.17	-0.02	-0.29	-0.01	-0.16	0.13	0.24
H22	-0.84	-0.65	-1.59	-1.37	-0.90	-0.80	1.16	0.81
H23	-6.56	-3.80	-12.52	-8.52	-7.22	-5.04	8.55	4.86
H24	0.22	0.44	0.65	1.02	0.35	0.52	-0.51	-0.80
H24'	-0.41	-0.26	-0.44	-0.19	-0.15	-0.01	-0.02	-0.31
H25	0.08	0.27	0.33	0.65	0.15	0.30	-0.25	-0.49
H26	-1.49	-1.10	-2.39	-1.79	-1.06	-0.77	1.45	1.05
H26'	-0.43	-0.10	-0.63	-0.14	-0.29	-0.09	0.42	0.10
H27	-3.03	-2.81	-5.24	-4.95	-2.60	-2.45	3.06	2.81
H28	0.55		1.38		0.62		-0.72	
H28'	0.69		1.37		0.67		-0.89	
H29	0.57		1.15		0.69		-0.90	

The total lanthanide induced shifts for all complexes are visualised in Figure 50 - Figure 65. In the top part of the figures are shown the lanthanide shifts of the LaLn (Table 34 and Table 35) and LnLu (Table 36 and Table 37) (Ln = Ce, Pr, Nd, Eu) complexes, each containing one paramagnetic lanthanide ion. As noted above and seen in the figures, only protons close to the paramagnetic lanthanide ion exhibit significant values of lanthanide induced shift.

In the bottom part of the figures are shown the sums of the lanthanide induced shifts of the LaLn and LnLu complexes (Table 75 and Table 76) compared to the lanthanide induced shifts of the Ln_2 complexes (Table 32 and Table 33).

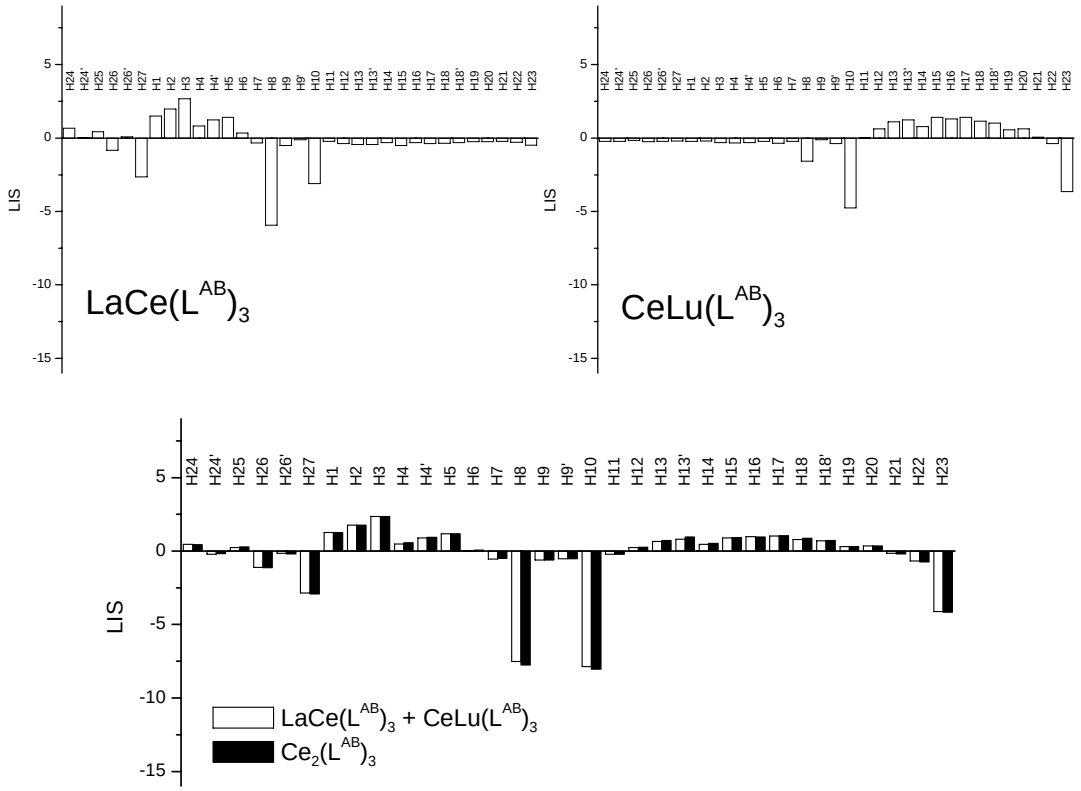

Figure 50 Lanthanide induced shifts of Ce complexes of L^{AB}

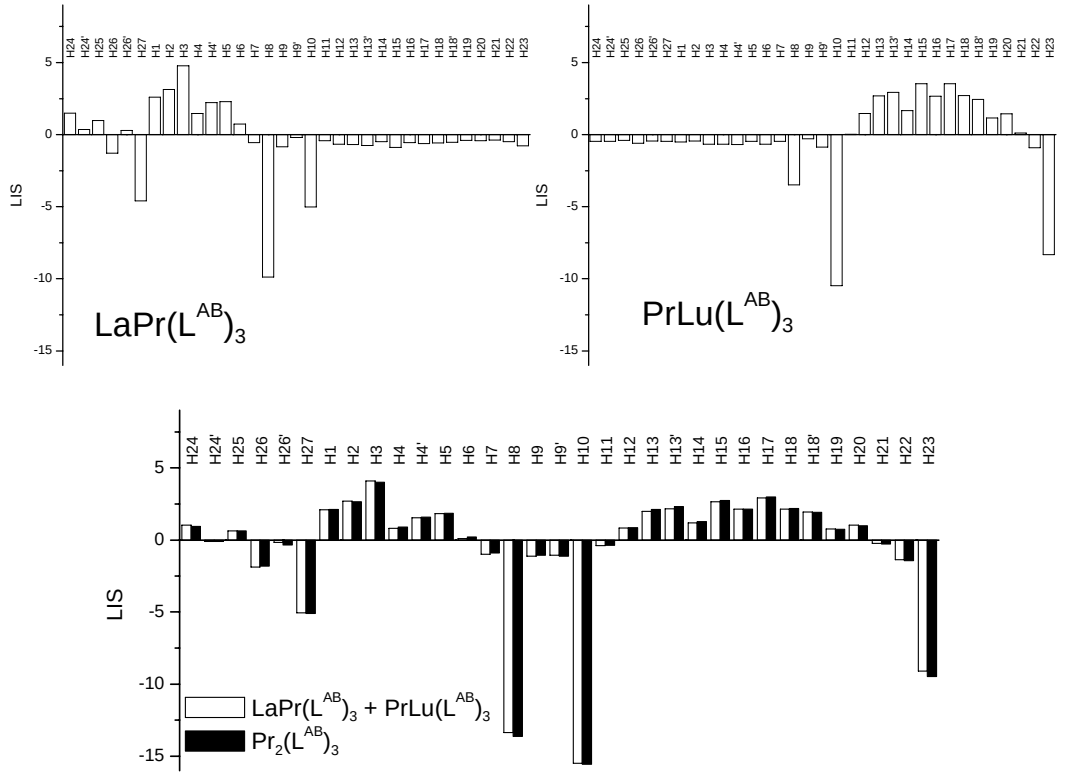

Figure 51 Lanthanide induced shifts of Pr complexes of L^{AB}

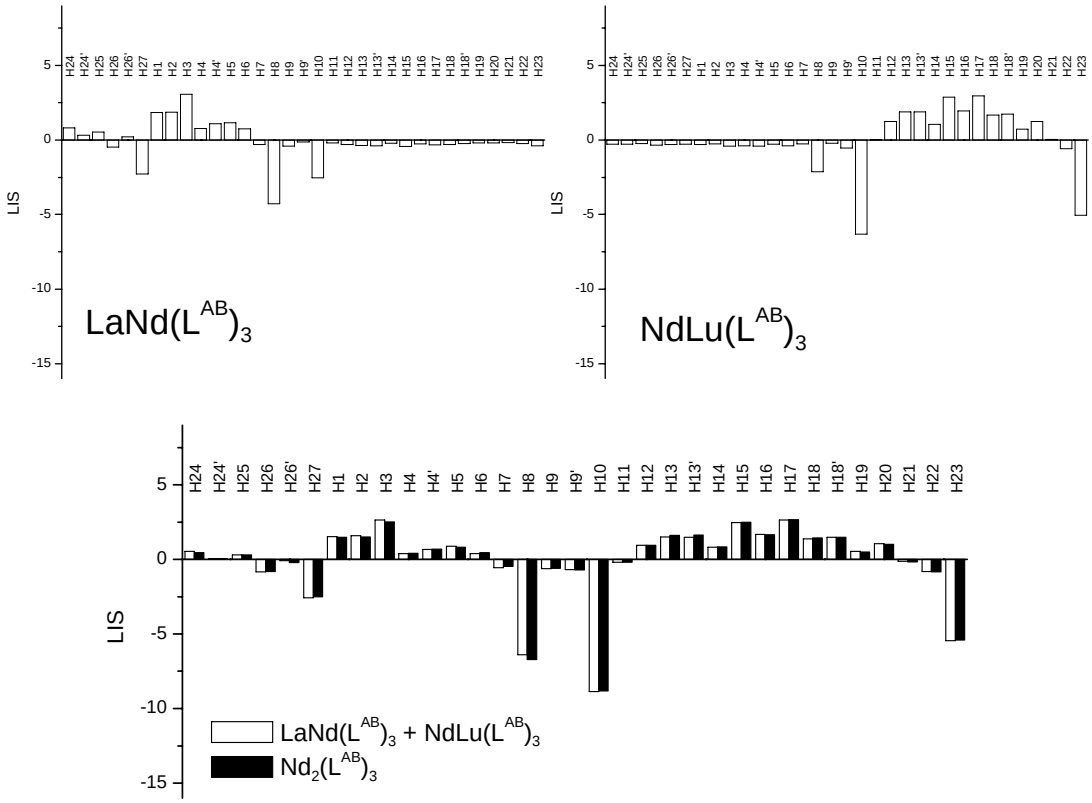

Figure 52 Lanthanide induced shifts of Nd complexes of L^{AB}

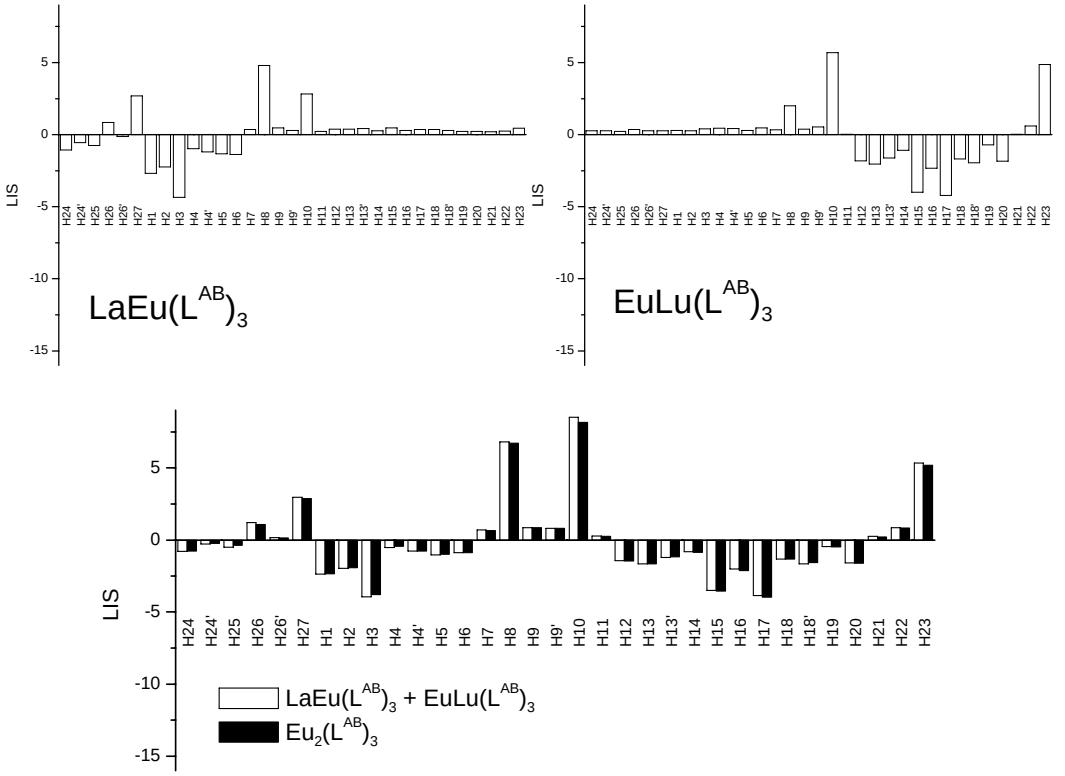

Figure 53 Lanthanide induced shifts of Eu complexes of L^{AB}

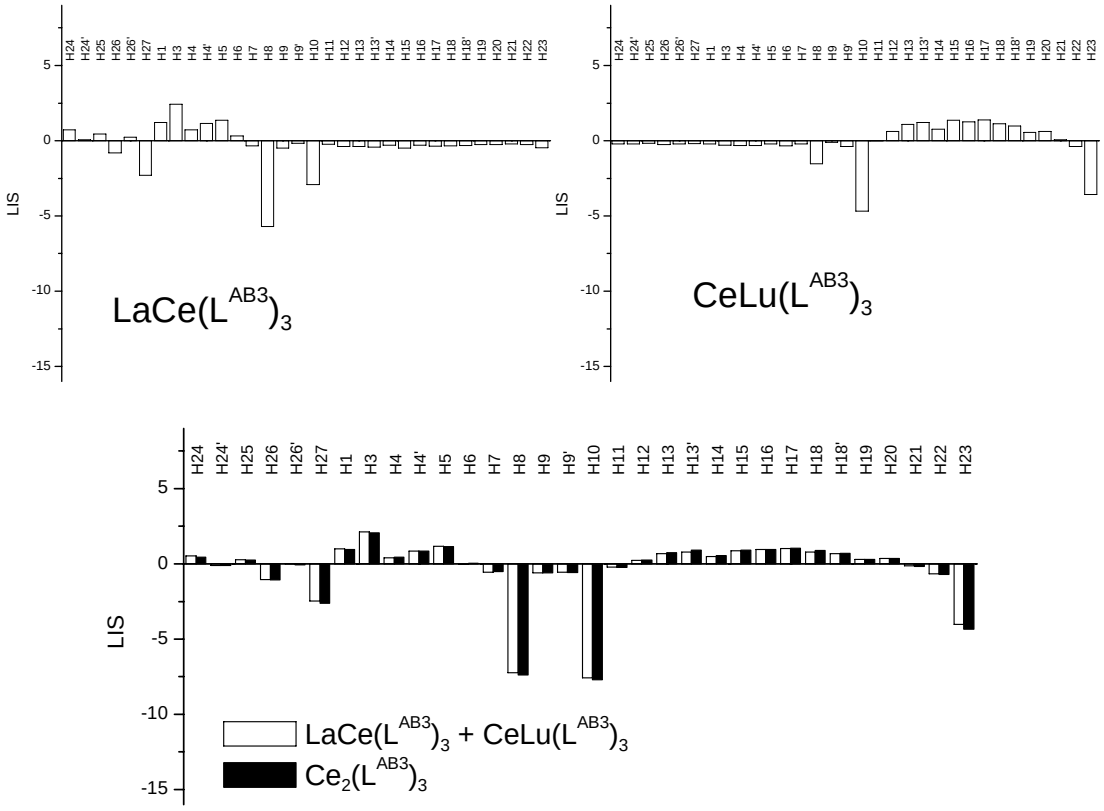

Figure 54 Lanthanide induced shifts of Ce complexes of L^{AB3}

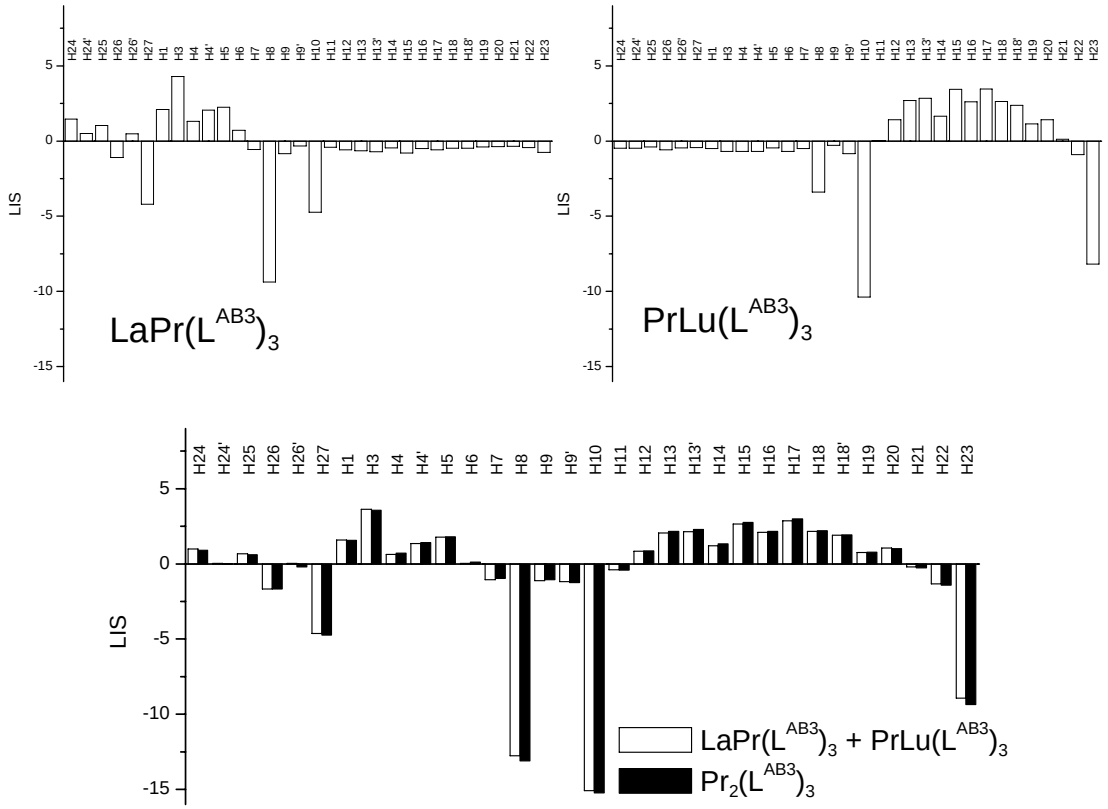

Figure 55 Lanthanide induced shifts of Pr complexes of L^{AB3}

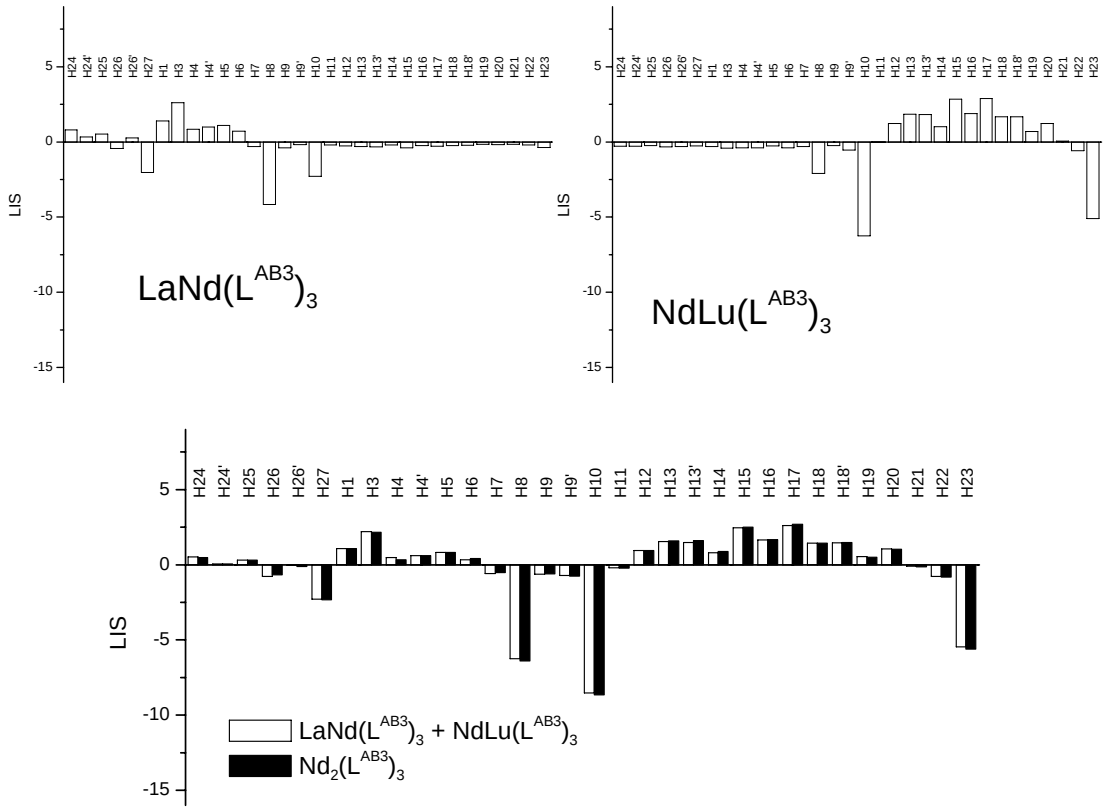

Figure 56 Lanthanide induced shifts of Nd complexes of L^{AB3}

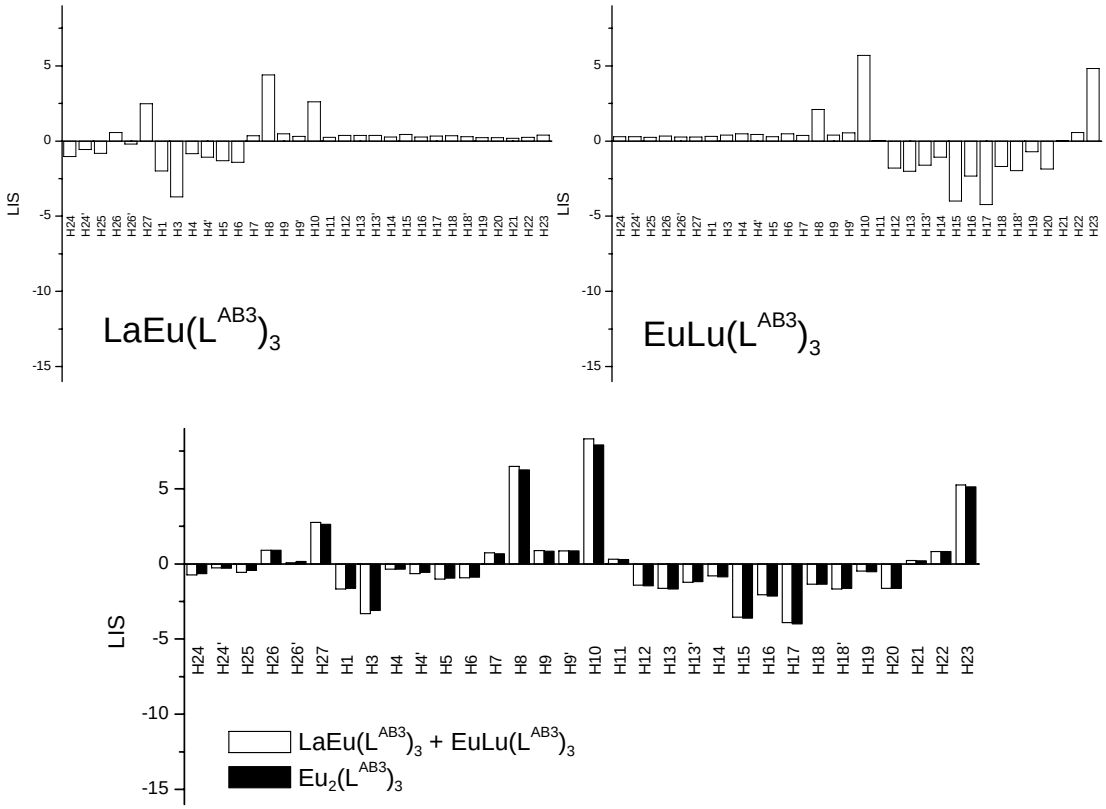

Figure 57 Lanthanide induced shifts of Eu complexes of L^{AB3}

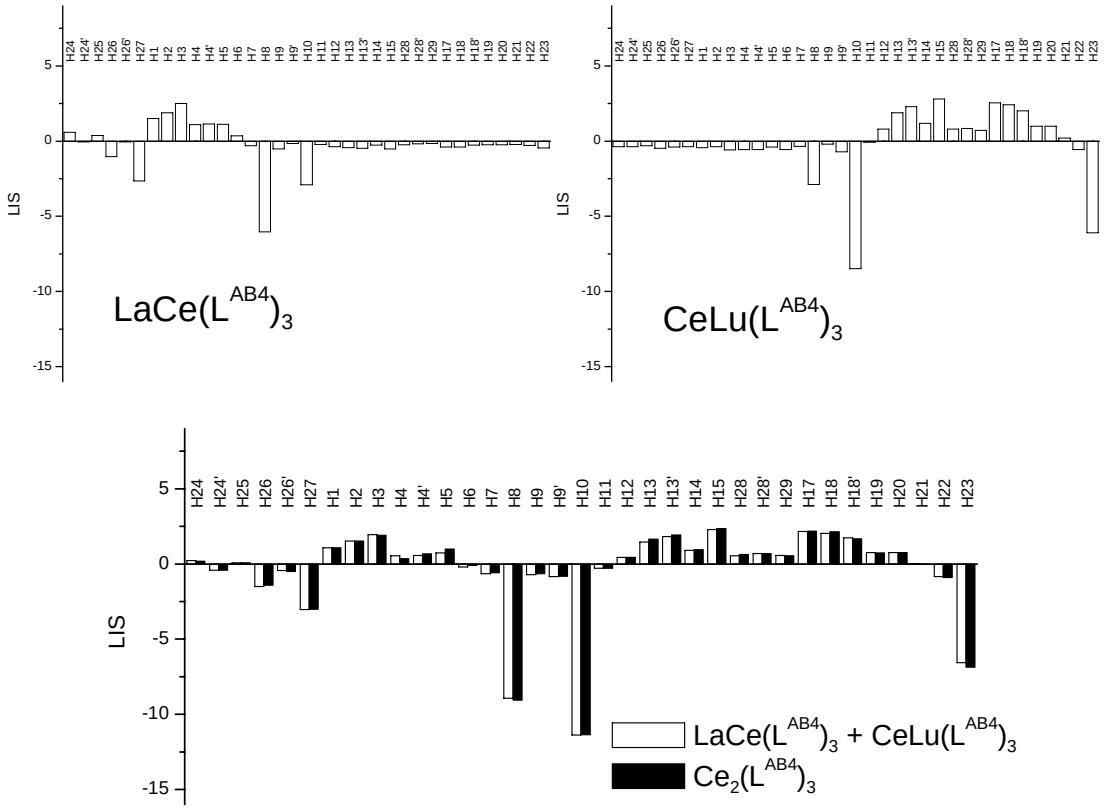

Figure 58 Lanthanide induced shifts of Ce complexes of L^{AB4}

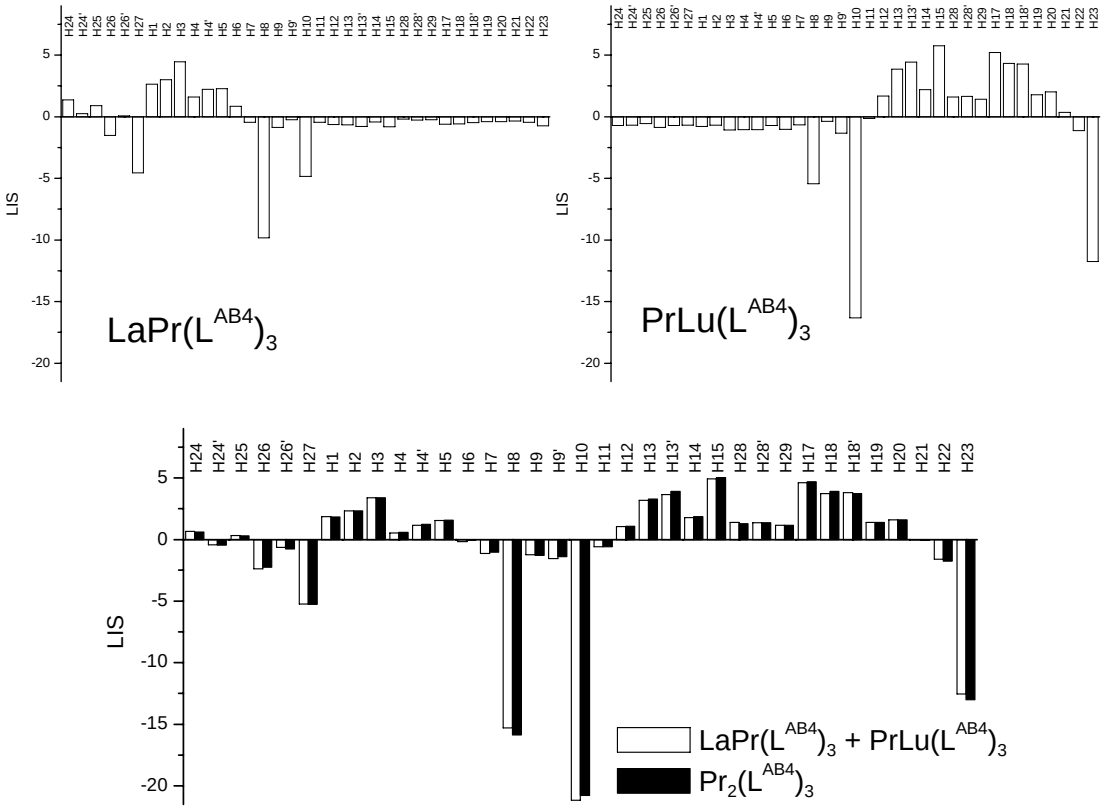

Figure 59 Lanthanide induced shifts of Pr complexes of L^{AB4}

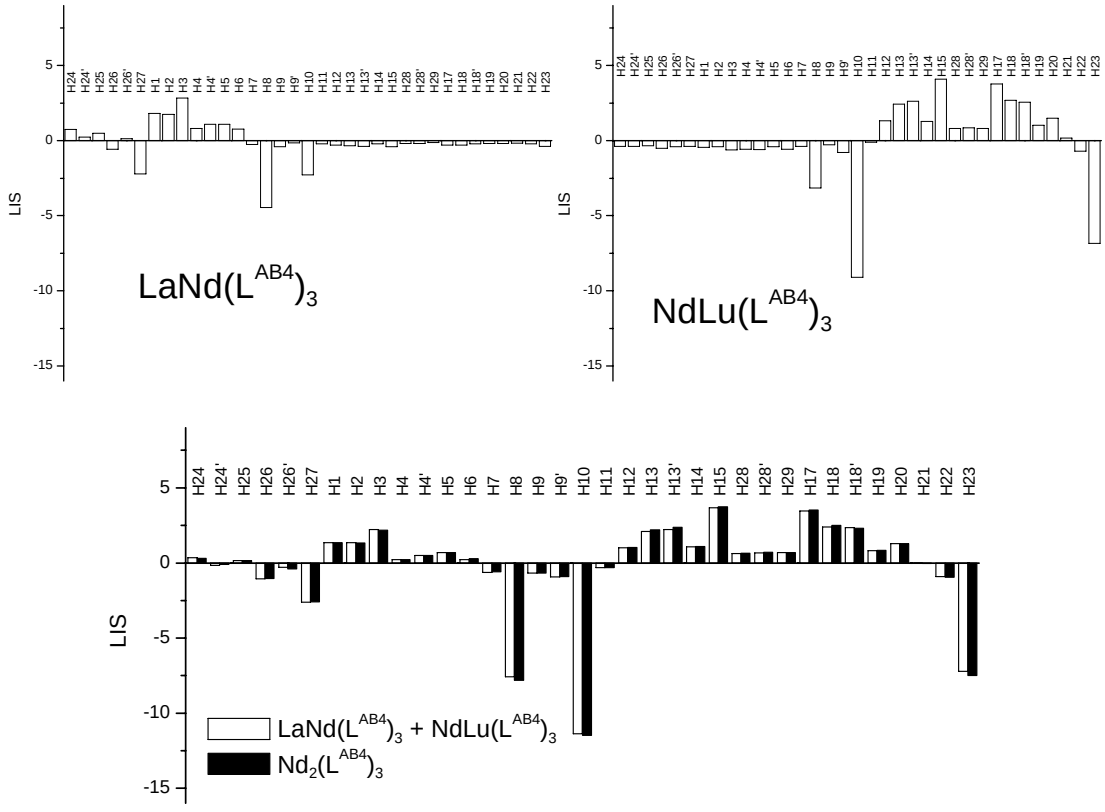

Figure 60 Lanthanide induced shifts of Nd complexes of L^{AB4}

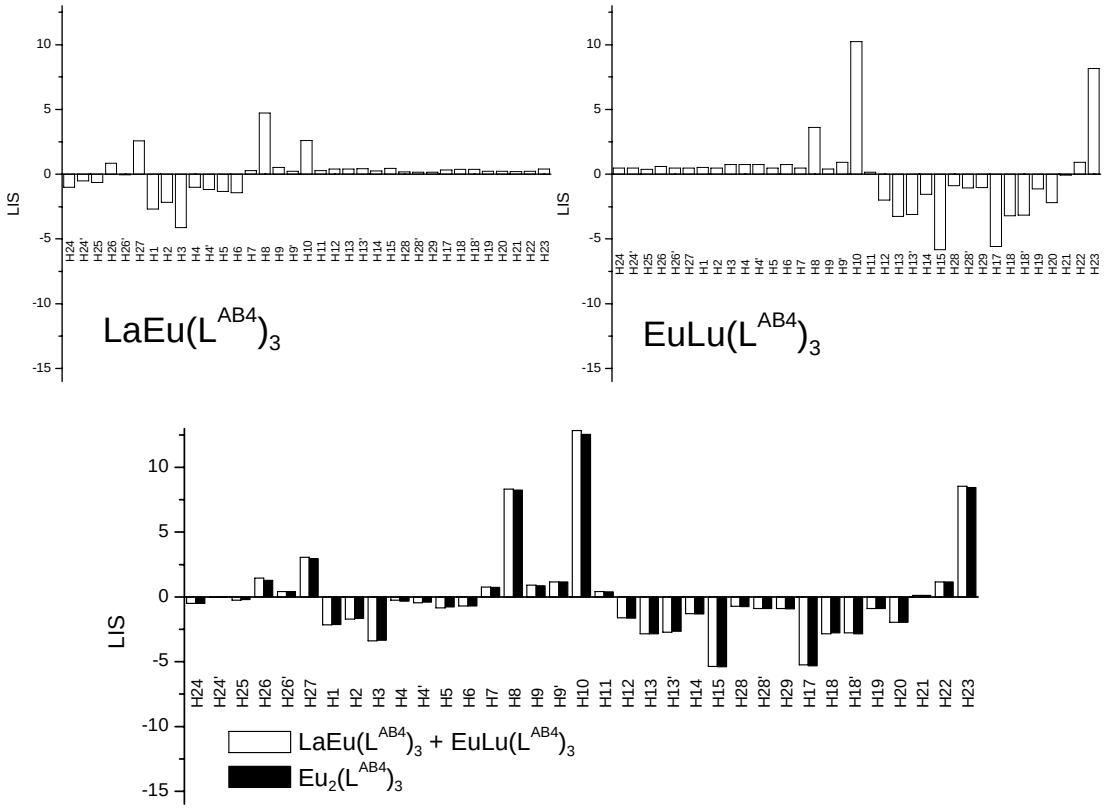

Figure 61 Lanthanide induced shifts of Eu complexes of L^{AB4}

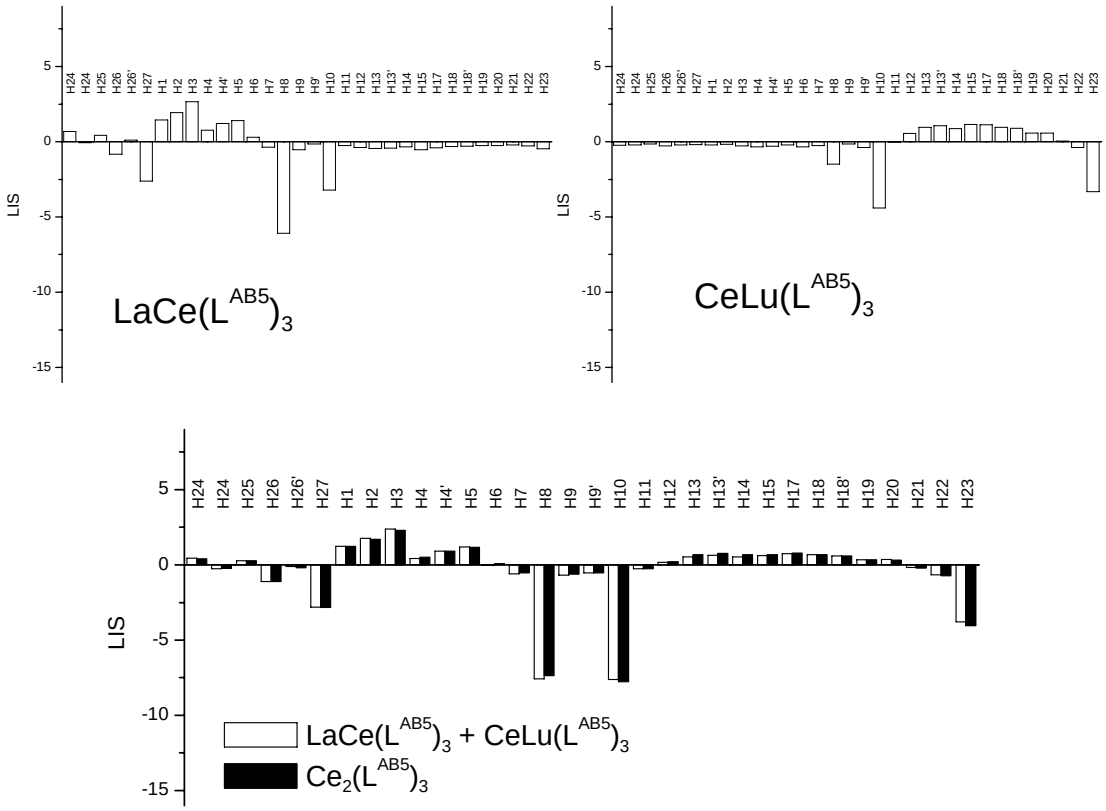

Figure 62 Lanthanide induced shifts of Ce complexes of L^{AB5}

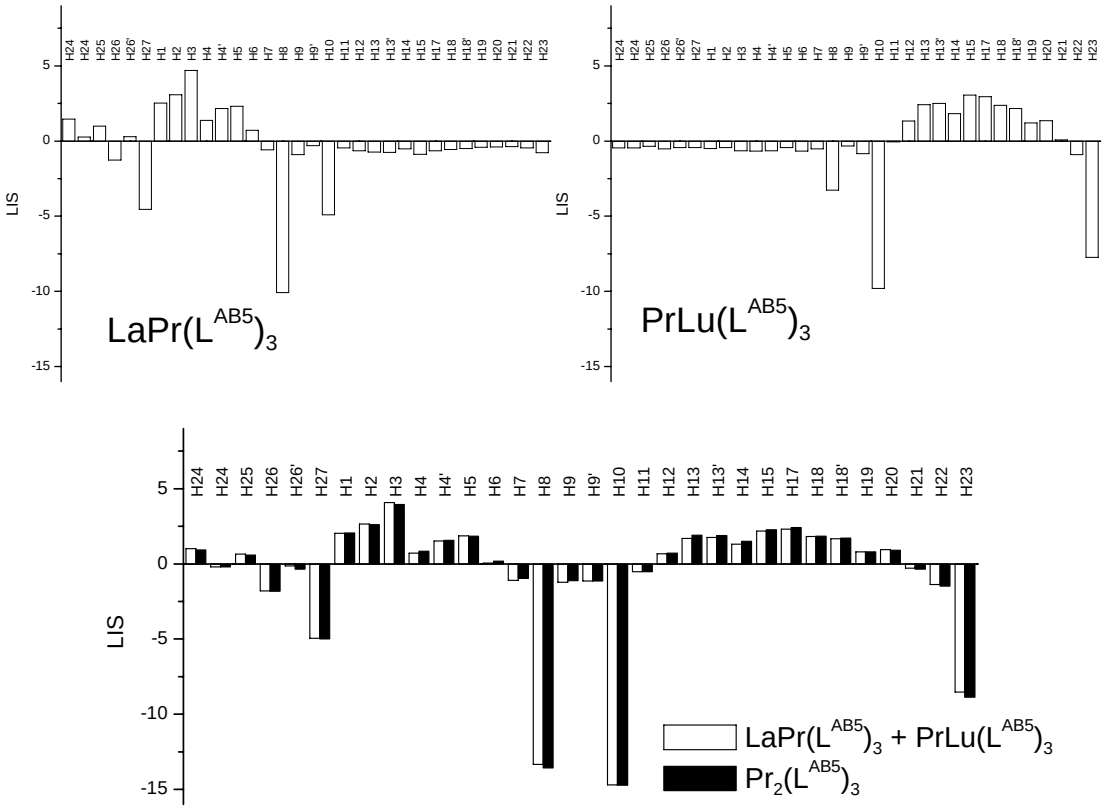

Figure 63 Lanthanide induced shifts of Pr complexes of L^{AB5}

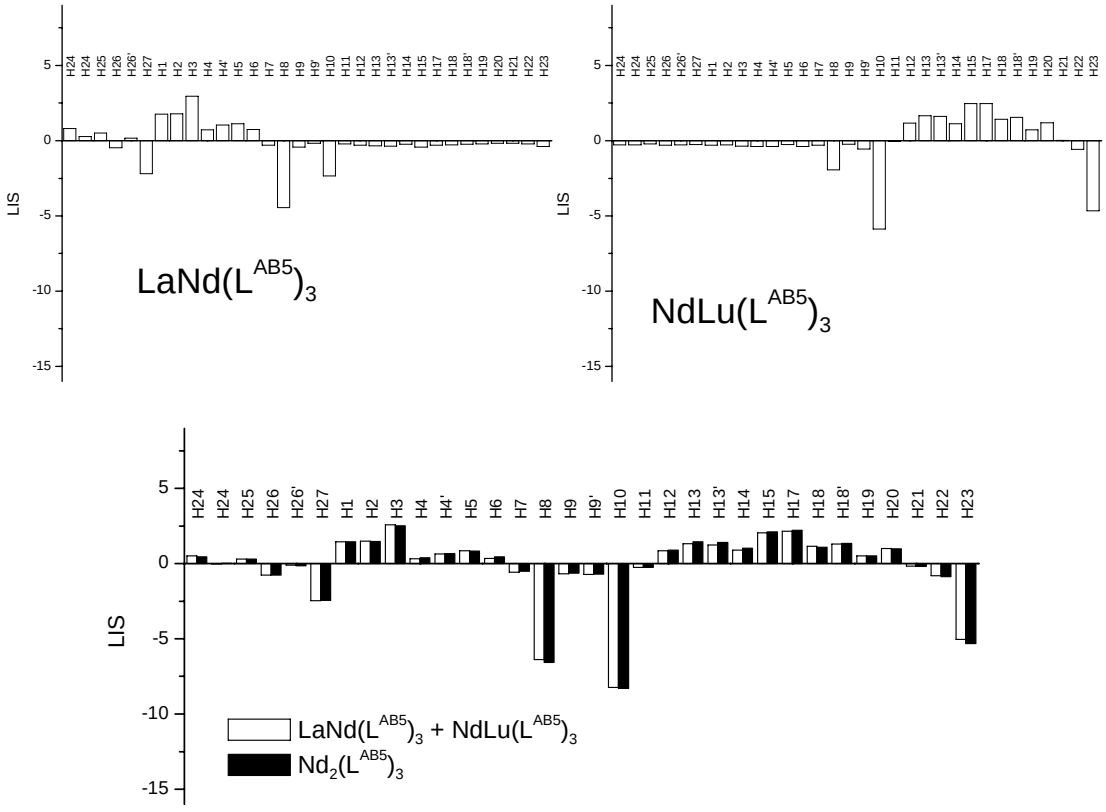

Figure 64 Lanthanide induced shifts of Nd complexes of L^{AB5}

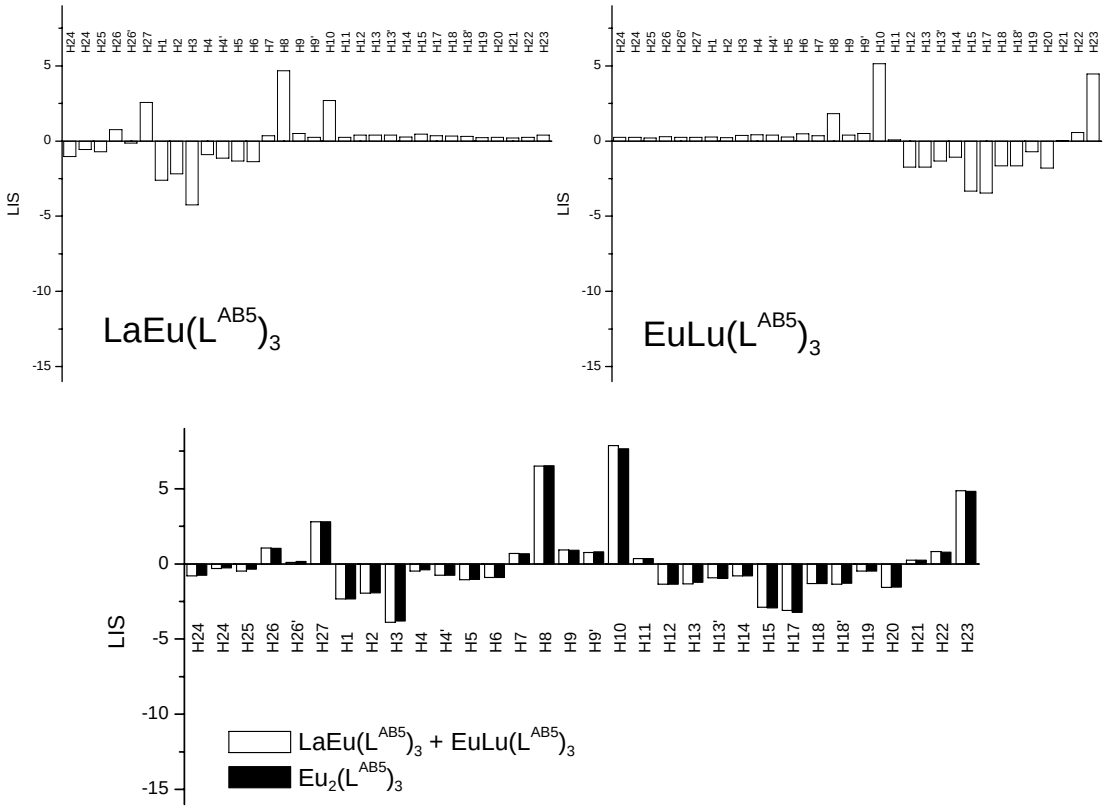

Figure 65 Lanthanide induced shifts of Eu complexes of L^{AB5}

As can be seen from the bottom part of the figures the sums of the contributions of the monometallic complexes (LaLn + LnLu) correspond very well to the lanthanide induced shift of the Ln_2 complexes.

The LIS values have been compared by means of an agreement factor defined for each lanthanide ion as

$$AF_j^{LIS} = \sqrt{\frac{\sum_i \left(\left(\Delta_{i,j}\right)_{LaLn+LnLu} - \left(\Delta_{i,j}\right)_{Ln_2} \right)^2}{\sum_i \left(\left(\Delta_{i,j}\right)_{Ln_2} \right)^2}} \qquad (11)$$

Table 77 LIS agreement factors comparing (LaLn + LnLu) and Ln_2 complexes

	Ce	Pr	Nd	Eu
L^{AB}	0.032	0.026	0.032	0.035
L^{AB3}	0.038	0.030	0.029	0.042
L^{AB4}	0.033	0.031	0.027	0.020
L^{AB5}	0.040	0.029	0.037	0.025

The agreement factors are small indicating that the hypothesis that lanthanide induced shifts from individual lanthanide ions are additive seems valid.

Plots of the sums of lanthanide induced shifts of the LaLn and LnLu complexes compared with that of the Ln_2 complexes are shown in Figure 66 - Figure 69. It is clear from these plots as it was from the agreement factors calculated above that the agreement between the two sets of values is almost perfect.

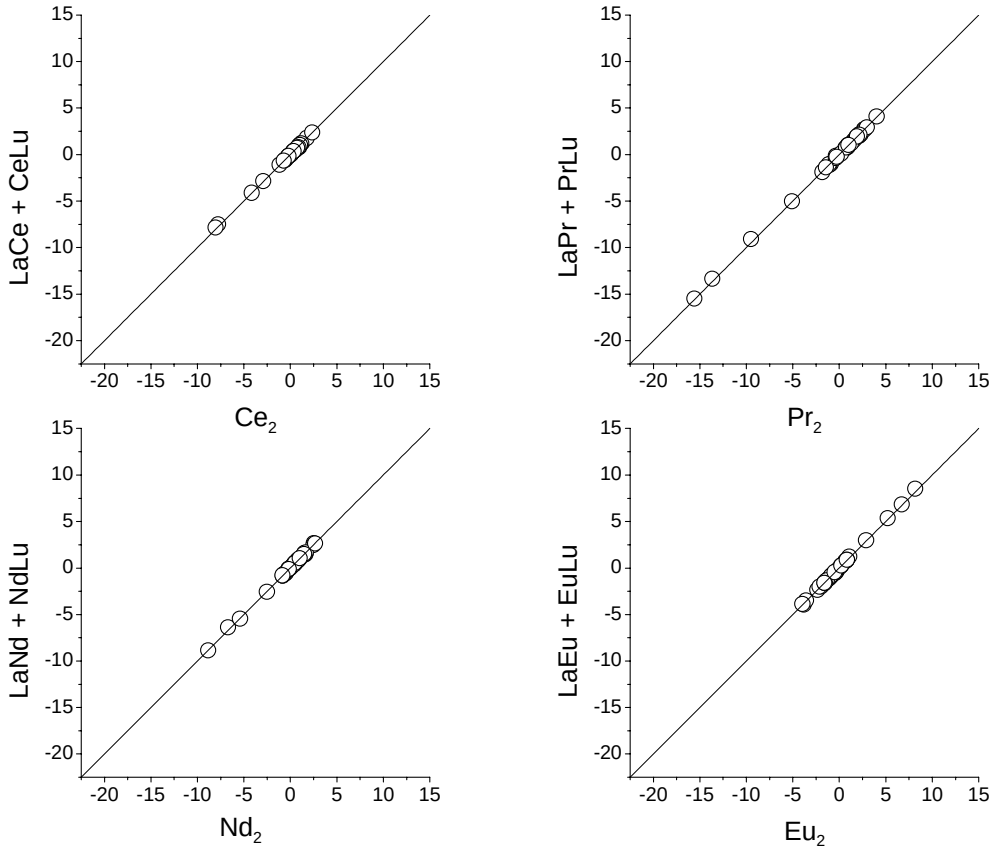

Figure 66 Comparison of (LaLn + LnLu) with Ln_2 LIS for L^{AB} complexes

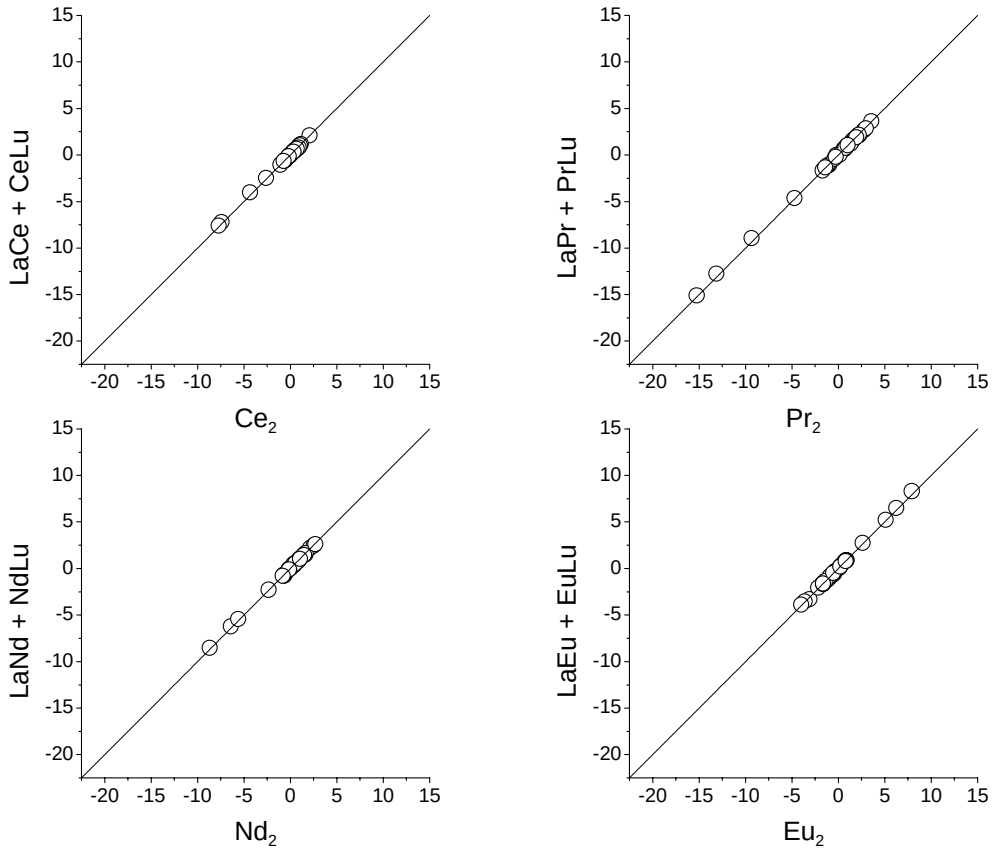

Figure 67 Comparison of (LaLn + LnLu) with Ln_2 LIS for L^{AB3} complexes

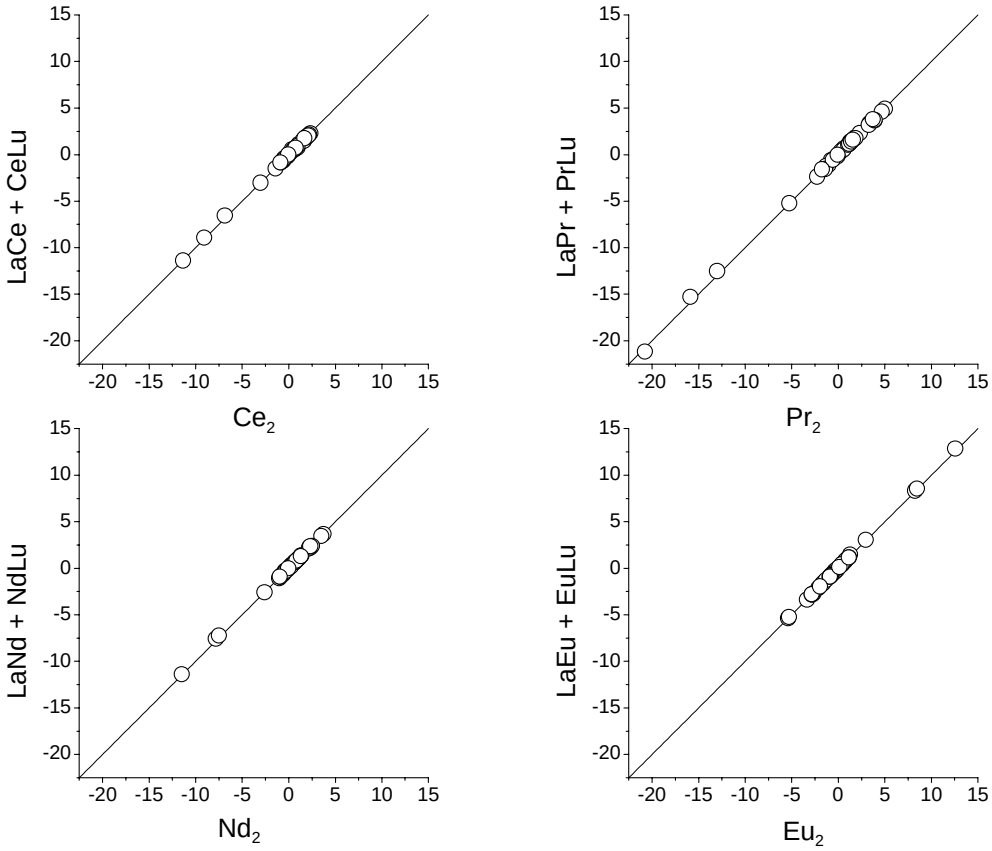

Figure 68 Comparison of (LaLn + LnLu) with Ln_2 LIS for L^{AB4} complexes

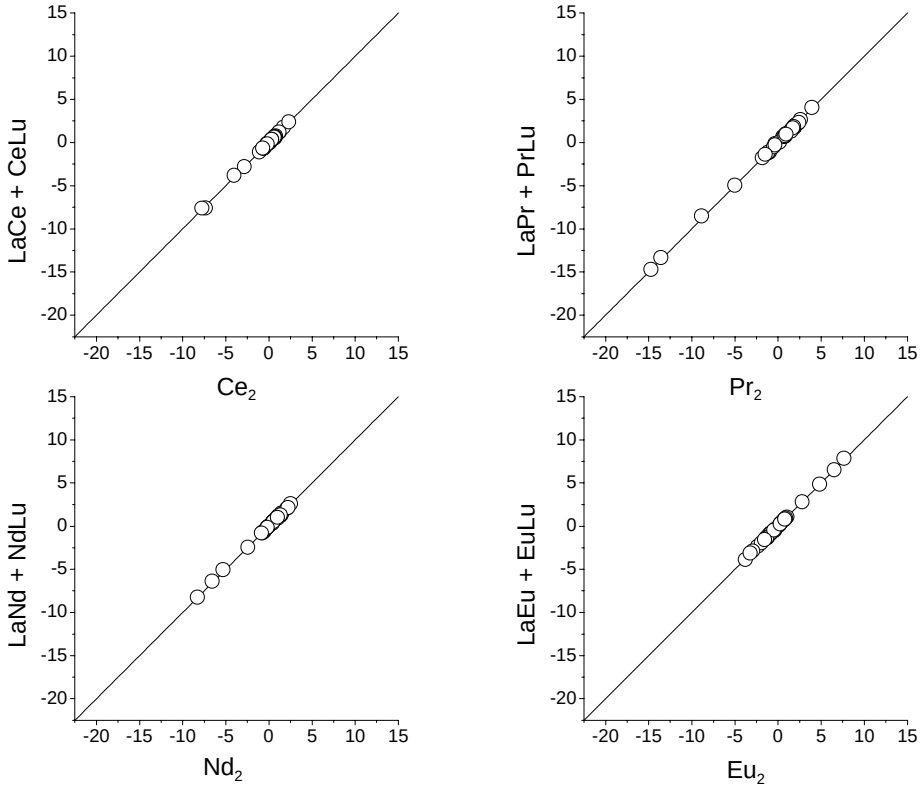

Figure 69 Comparison of (LaLn + LnLu) with Ln_2 LIS for L^{AB5} complexes

5.4.2 Contact and pseudo contact terms of mono- and bimetallic complexes

Sums of contact parameters F_i of a paramagnetic lanthanide ion in the bpa site (LaLn complexes, Table 42 - Table 45) and a paramagnetic lanthanide ion in the bpb site (LnLu complexes, Table 46 - Table 49) have been calculated. Similar sums have been calculated for pseudo contact parameters $B_0^2 G_i$ and the values are given in Table 78. In the following these values will be compared to the contact and pseudo contact parameters of the Ln_2 complexes (Table 38 - Table 41) in which both bpa and bpb sites are occupied by a paramagnetic lanthanide ion.

Table 78 Sums of contact and pseudo contact parameters of LaLn and LnLu complexes

	F_i				$B_0^2 G_i$			
	L^{AB}	L^{AB3}	L^{AB4}	L^{AB5}	L^{AB}	L^{AB3}	L^{AB4}	L^{AB5}
H1	-0.23(2)	-0.16(1)	-0.22(2)	-0.23(2)	-0.16(1)	-0.13(1)	-0.14(1)	-0.16(1)
H2	-0.14(2)		-0.12(2)	-0.13(2)	-0.25(2)		-0.22(2)	-0.26(2)
H3	-0.36(2)	-0.29(2)	-0.32(2)	-0.35(3)	-0.32(2)	-0.29(1)	-0.26(2)	-0.33(2)
H4	-0.032(5)	-0.02(2)	0.00(2)	-0.031(6)	-0.074(3)	-0.058(6)	-0.09(2)	-0.064(3)
H4'	-0.029(8)	-0.018(8)	-0.01(1)	-0.025(8)	-0.139(4)	-0.131(5)	-0.089(7)	-0.143(4)
H5	-0.047(9)	-0.044(9)	-0.049(7)	-0.05(1)	-0.18(1)	-0.18(1)	-0.111(8)	-0.18(1)
H6	-0.13(1)	-0.13(1)	-0.11(1)	-0.13(1)	0.017(3)	0.019(5)	0.048(3)	0.021(3)
H7	0.052(3)	0.056(3)	0.053(3)	0.047(4)	0.078(3)	0.078(3)	0.095(3)	0.088(4)
H8	0.31(6)	0.29(5)	0.41(4)	0.26(5)	1.14(4)	1.10(4)	1.34(4)	1.15(4)
H9	0.067(3)	0.072(4)	0.068(5)	0.071(4)	0.089(2)	0.084(2)	0.104(4)	0.099(3)
H9'	0.07(1)	0.07(1)	0.090(6)	0.06(1)	0.069(6)	0.077(6)	0.121(2)	0.073(6)
H10	0.5(2)	0.5(2)	0.83(8)	0.5(2)	1.15(8)	1.11(8)	1.67(3)	1.12(8)
H11	0.021(3)	0.024(3)	0.033(2)	0.025(2)	0.0303(9)	0.0307(8)	0.043(2)	0.039(1)
H12	-0.182(6)	-0.182(7)	-0.191(7)	-0.177(5)	-0.012(6)	-0.010(6)	-0.039(2)	0.000(5)
H13	-0.17(4)	-0.17(4)	-0.274(8)	-0.14(4)	-0.08(2)	-0.08(2)	-0.190(9)	-0.06(2)
H13'	-0.10(6)	-0.10(5)	-0.22(2)	-0.08(5)	-0.11(3)	-0.11(2)	-0.254(6)	-0.09(2)
H14	-0.07(2)	-0.07(2)	-0.103(6)	-0.07(3)	-0.062(9)	-0.064(9)	-0.128(3)	-0.07(1)
H15	-0.42(3)	-0.42(2)	-0.562(6)	-0.35(3)	-0.08(2)	-0.08(2)	-0.279(6)	-0.05(2)
H16	-0.20(3)	-0.21(2)			-0.121(8)	-0.119(7)		
H17	-0.46(2)	-0.46(2)	-0.56(1)	-0.37(2)	-0.09(2)	-0.09(2)	-0.259(5)	-0.06(2)
H18	-0.11(4)	-0.12(4)	-0.23(2)	-0.12(2)	-0.11(2)	-0.10(2)	-0.28(1)	-0.09(2)
H18'	-0.17(3)	-0.17(3)	-0.24(2)	-0.14(3)	-0.08(2)	-0.08(2)	-0.24(2)	-0.07(2)
H19	-0.04(2)	-0.04(1)	-0.063(9)	-0.04(1)	-0.042(6)	-0.041(6)	-0.108(3)	-0.046(6)
H20	-0.196(5)	-0.199(5)	-0.215(4)	-0.193(4)	-0.028(5)	-0.026(5)	-0.086(2)	-0.026(3)
H21	0.023(6)	0.019(5)	0.016(6)	0.019(2)	0.022(2)	0.017(1)	0.000(2)	0.025(1)
H22	0.06(1)	0.06(1)	0.090(3)	0.06(1)	0.096(7)	0.093(7)	0.119(3)	0.093(8)
H23	0.4(1)	0.4(1)	0.64(4)	0.3(1)	0.59(6)	0.57(6)	0.94(2)	0.54(6)
H24	-0.065(9)	-0.056(7)	-0.049(8)	-0.069(9)	-0.065(9)	-0.075(6)	-0.028(9)	-0.062(8)
H24'	-0.05(1)	-0.04(1)	-0.033(9)	-0.06(1)	0.04(1)	0.02(1)	0.07(1)	0.05(1)
H25	-0.045(8)	-0.05(1)	-0.030(4)	-0.042(9)	-0.035(8)	-0.040(8)	-0.008(3)	-0.038(8)
H26	0.07(3)	0.04(2)	0.08(2)	0.05(2)	0.17(1)	0.16(1)	0.23(1)	0.17(1)
H26'	0.01(1)	0.01(1)	0.02(1)	0.01(1)	0.021(6)	-0.004(4)	0.065(6)	0.014(5)
H27	0.17(1)	0.169(8)	0.171(9)	0.15(1)	0.425(9)	0.369(3)	0.45(1)	0.422(9)
H28			-0.05(1)				-0.08(1)	
H28'			-0.062(6)				-0.100(3)	
H29			-0.077(2)				-0.079(2)	

Contact parameters (F_i) are compared in Figure 70 - Figure 73.

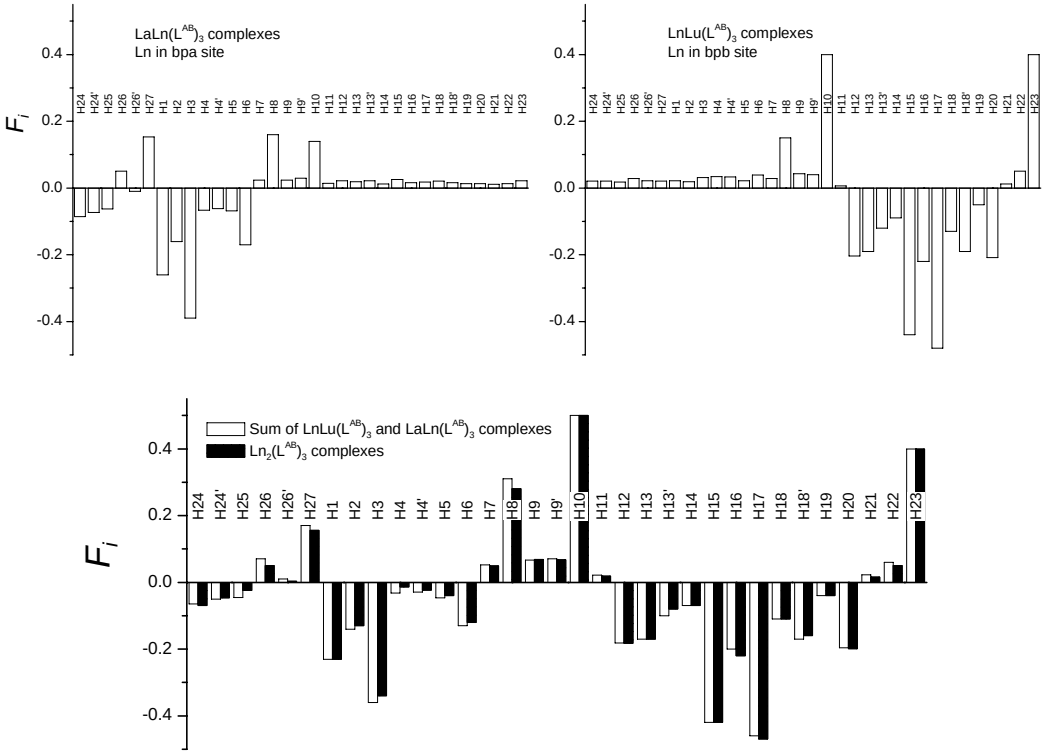

Figure 70 Contact parameters of L^{AB} complexes

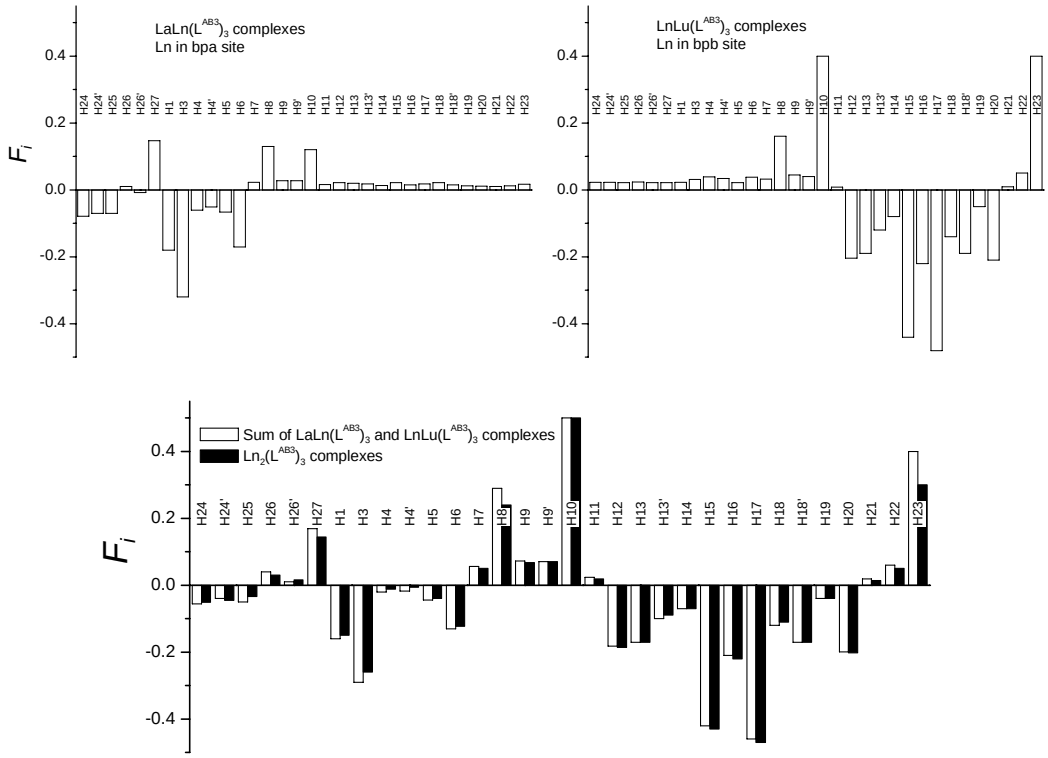

Figure 71 Contact parameters of L^{AB3} complexes

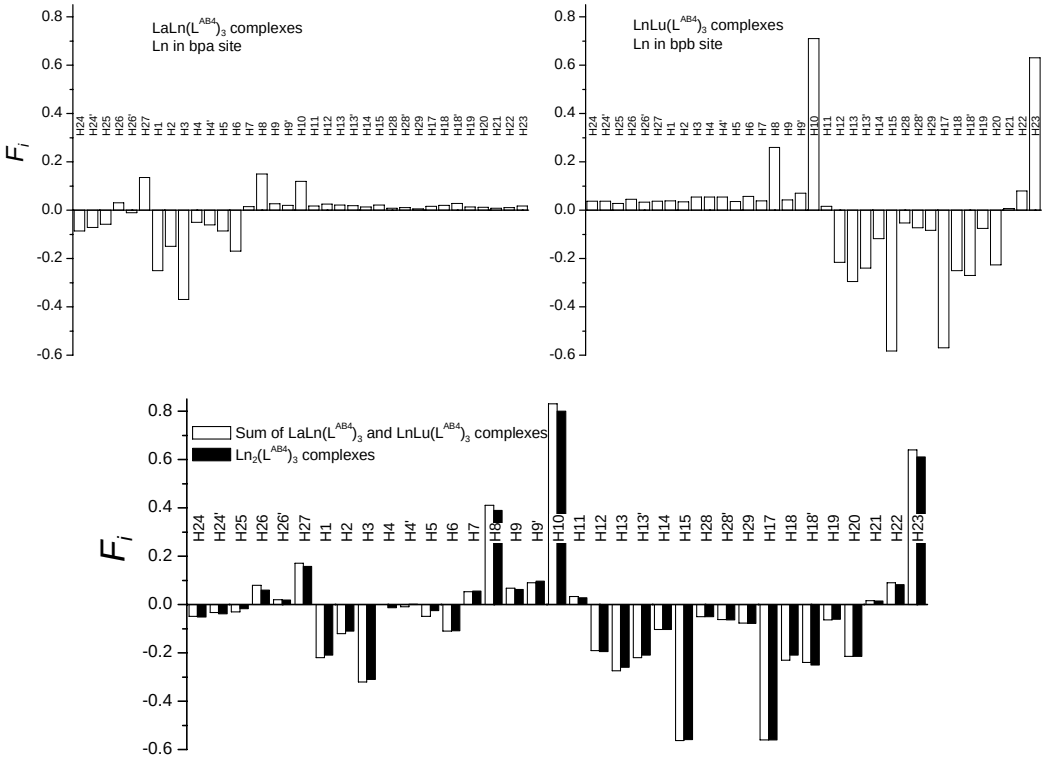

Figure 72 Contact parameters of L^{AB4} complexes

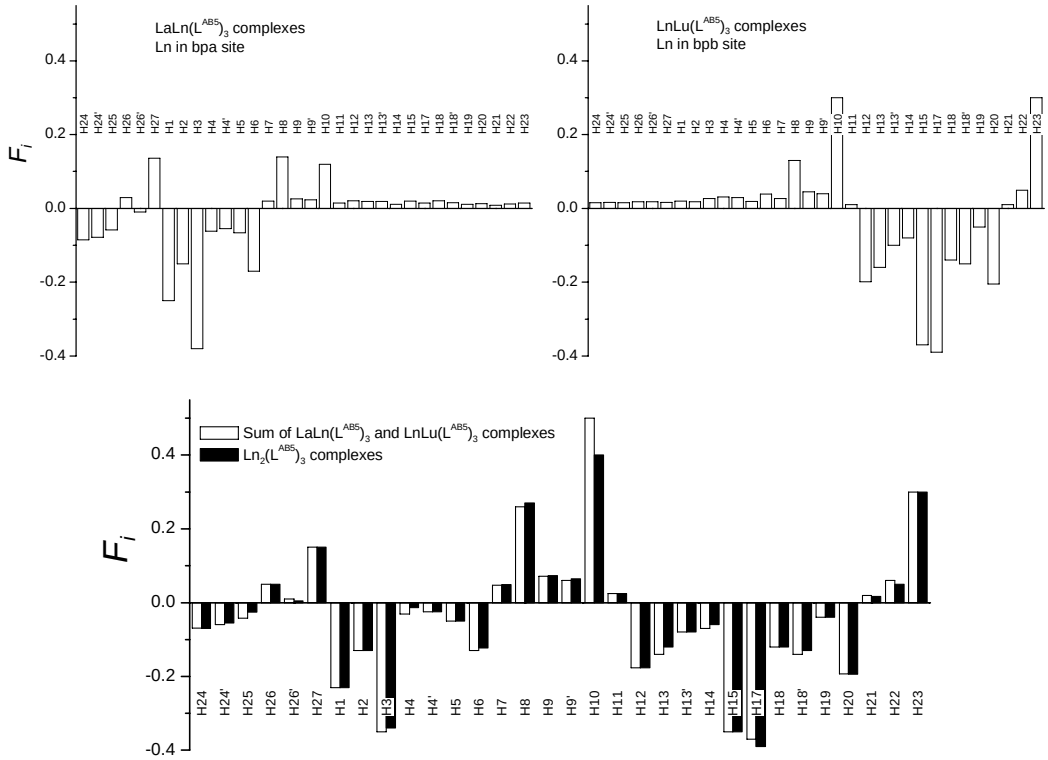

Figure 73 Contact parameters of L^{AB5} complexes

Pseudo contact parameters ($B_0^2 G_i$) are compared in Figure 74 -Figure 77.

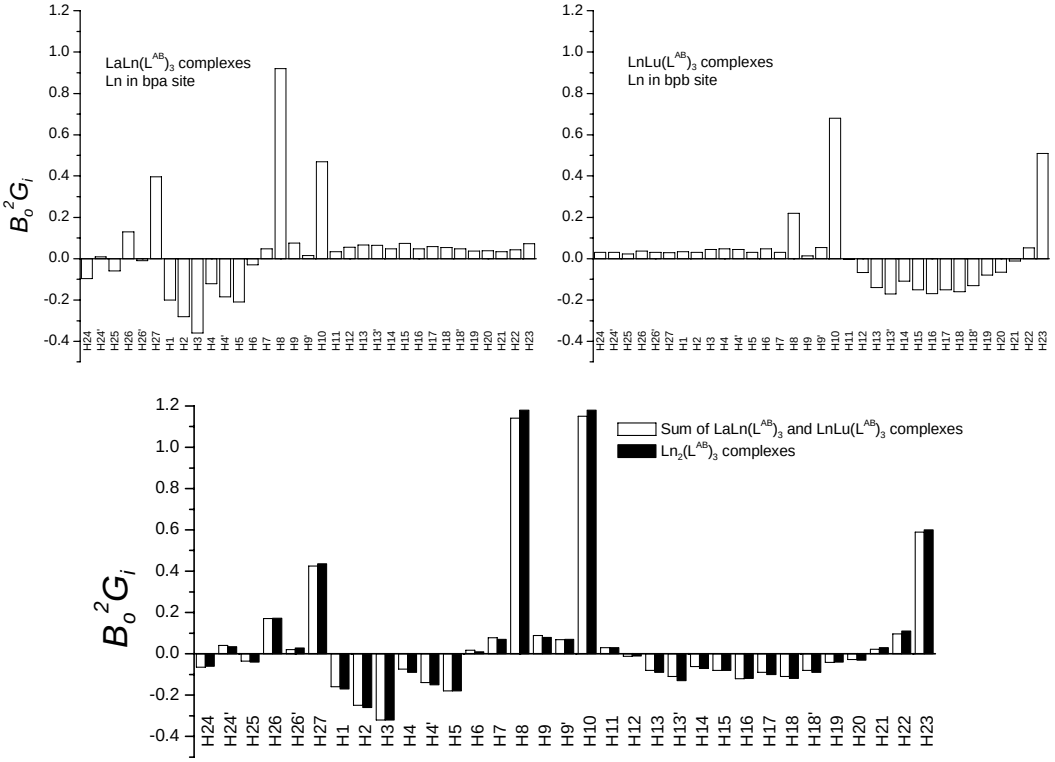

Figure 74 Pseudo contact parameters of L^{AB} complexes

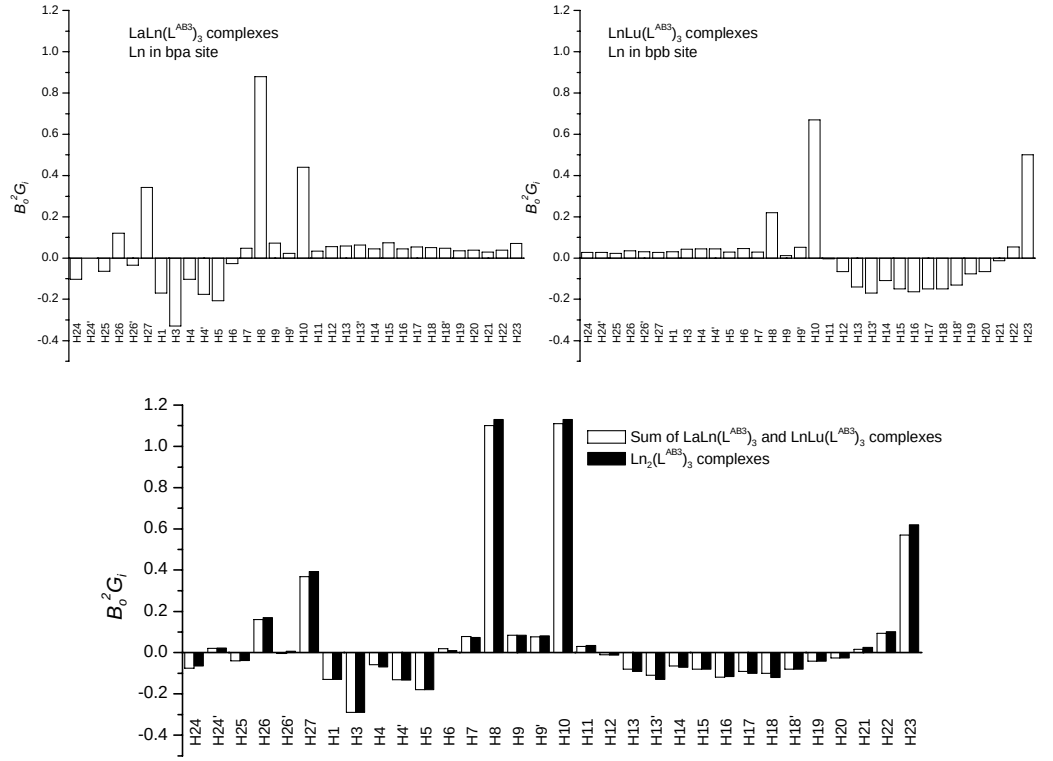

Figure 75 Pseudo contact parameters of L^{AB3} complexes

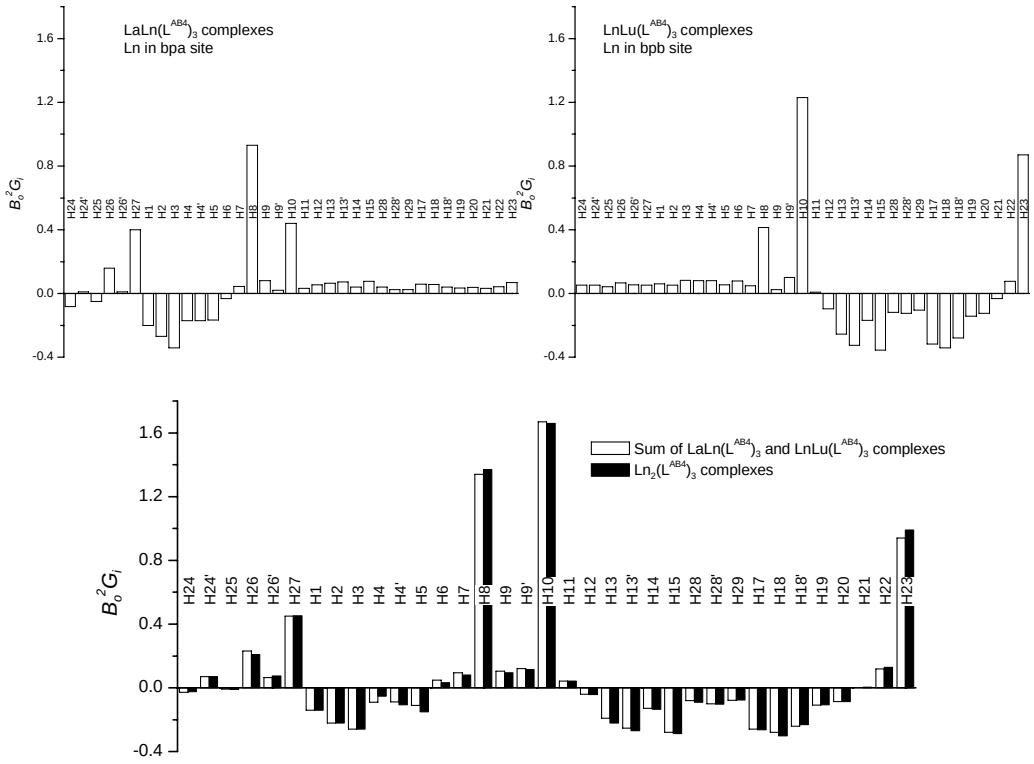

Figure 76 Pseudo contact parameters of L^{AB4} complexes

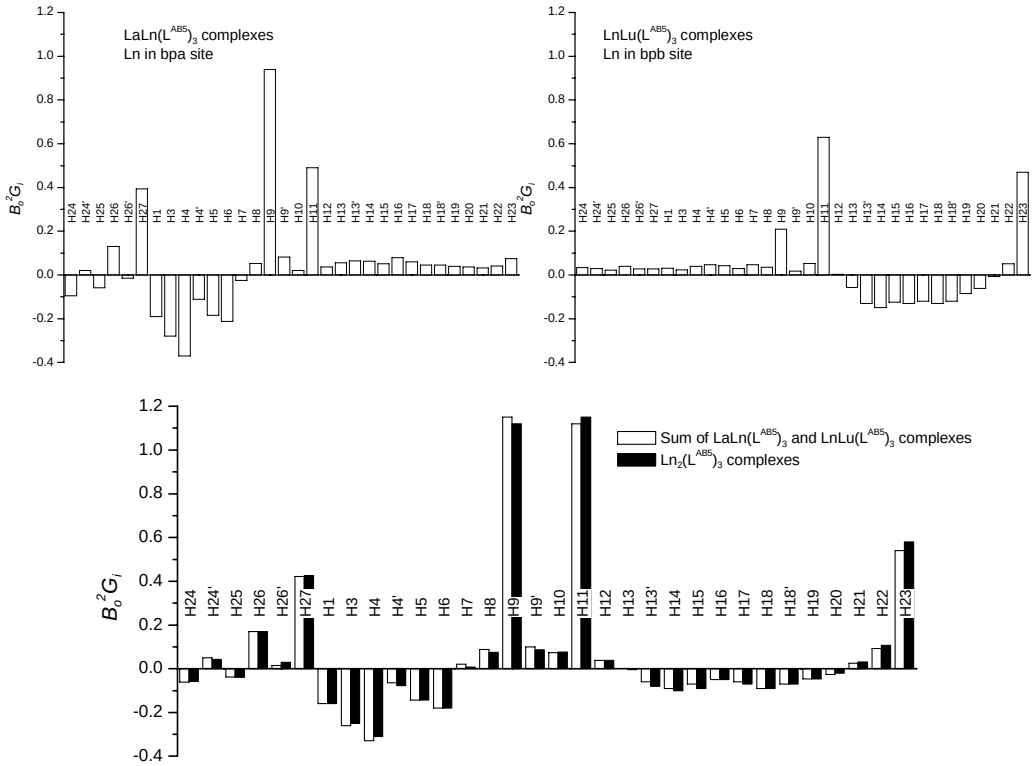

Figure 77 Pseudo contact parameters of L^{AB5} complexes

An alternative way of graphically demonstrating how well the data fit is the plots of (LaLn + LnLu) parameters versus Ln_2 parameters shown in Figure 78 - Figure 81. The straight line in the plots correspond to (LaLn + LnLu) = Ln_2 (a perfect fit).

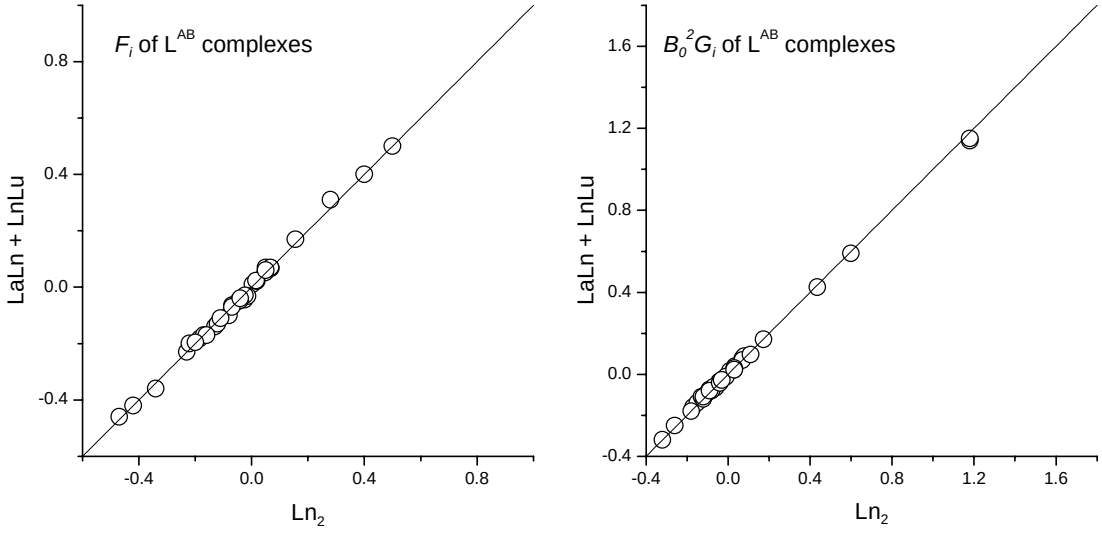

Figure 78 Comparison of (LaLn + LnLu) with Ln_2 parameters for L^{AB} complexes

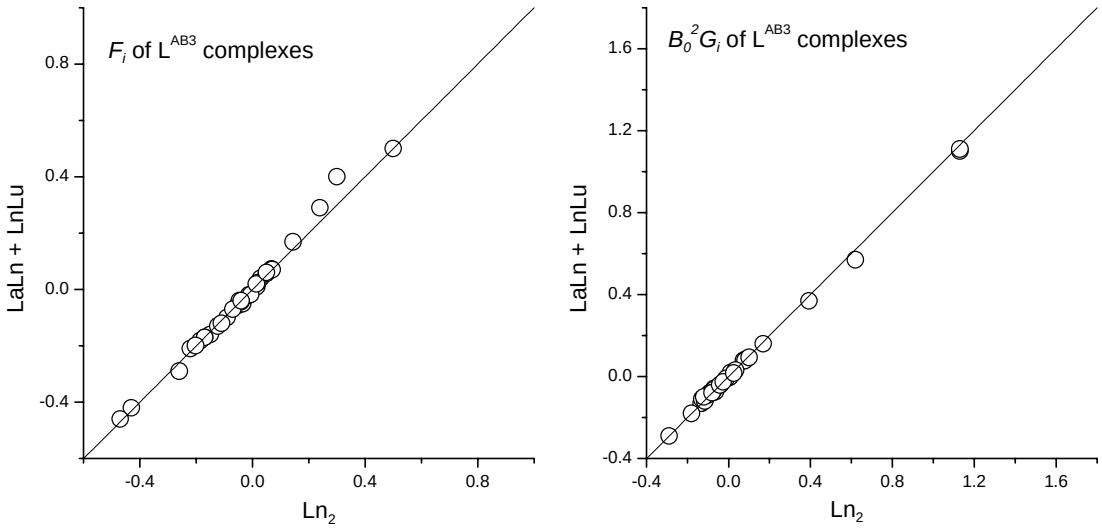

Figure 79 Comparison of (LaLn + LnLu) with Ln_2 parameters for L^{AB3} complexes

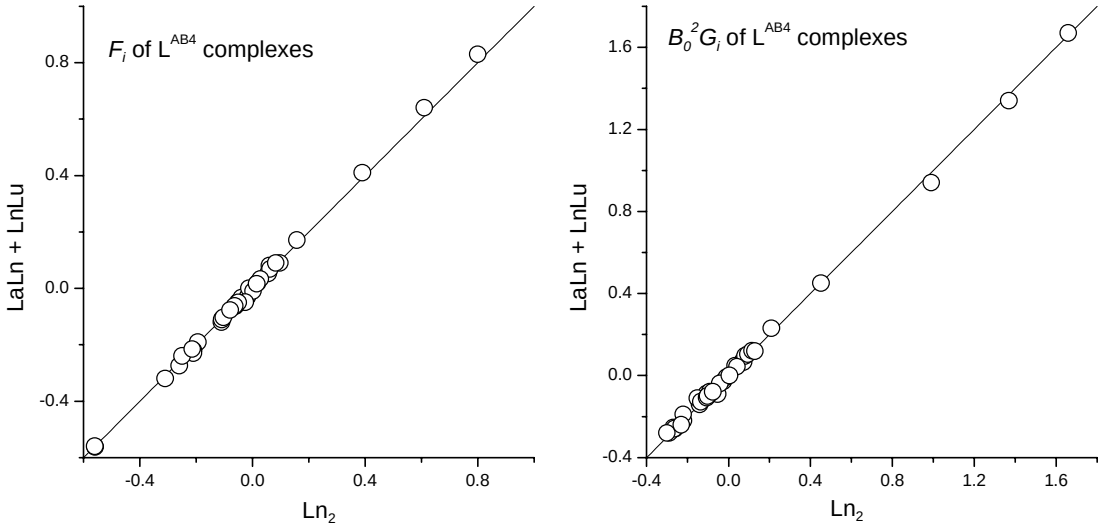

Figure 80 Comparison of (LaLn + LnLu) with Ln_2 parameters for L^{AB4} complexes

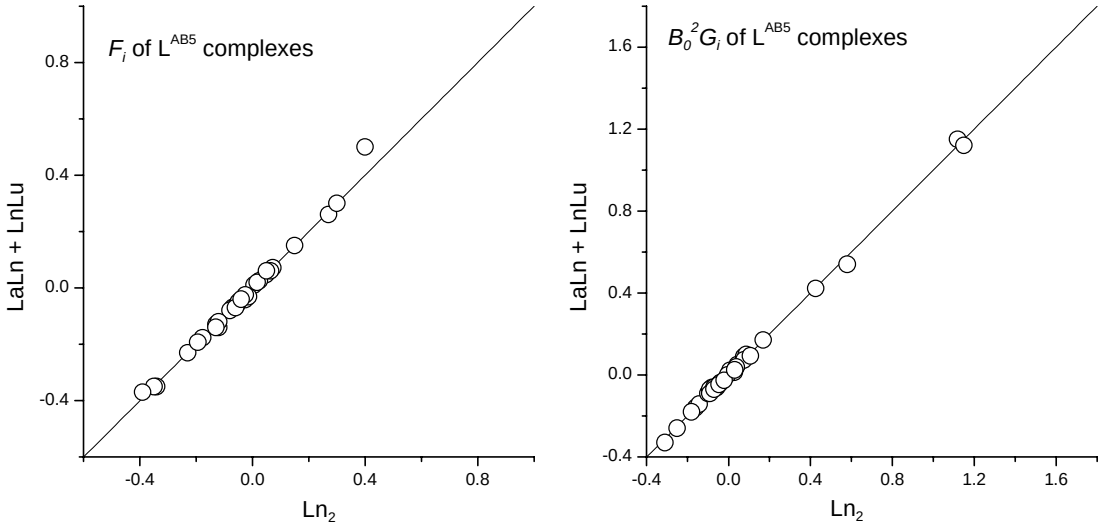

Figure 81 Comparison of (LaLn + LnLu) with Ln_2 parameters for L^{AB5} complexes

Agreement factors as defined below were calculated and are given in Table 79.

$$AF_j^{Fi} = \sqrt{\frac{\sum_i \left((F_i)_{LaLn+LnLu} - (F_i)_{Ln_2}\right)^2}{\sum_i \left((F_i)_{Ln_2}\right)^2}} \qquad (12)$$

$$AF_j^{B_0^2 G_i} = \sqrt{\frac{\sum_i \left(\left(B_0^2 G_i \right)_{LaLn + LnLu} - \left(B_0^2 G_i \right)_{Ln_2} \right)^2}{\sum_i \left(\left(B_0^2 G_i \right)_{Ln_2} \right)^2}} \qquad (13)$$

Table 79 Contact and pseudo contact agreement factors comparing (LaLn + LnLu) with Ln_2 complexes

	F_i	$B_0^2 G_i$
L^{AB}	0.081	0.037
L^{AB3}	0.093	0.045
L^{AB4}	0.048	0.037
L^{AB5}	0.058	0.042

As can be seen the agreement is excellent proving that not only the lanthanide induced shift, but also the individual contributions thereof (contact and pseudo contact parameters) are additive for two paramagnetic lanthanide ions in the same complex. This was expected since the distance between the two lanthanide ions in the complexes studied here is large (> 9 Å), and additionally there is no through-bond electronic relay between them, which rules out any magnetic interaction between the lanthanide ions.

5.5 Two proton (Geraldes) analysis

5.5.1 Theory

As mentioned above the one proton (Reilley) method of separation is based on the assumption that the ligand field parameter B_0^2 does not vary along the lanthanide series for a series of complexes. This assumption is well known to be a rather crude approximation[9] and conclusions regarding isostructurality may be erroneous.[91] To overcome this problem a method has been developed in which two protons in the ligand are being considered simultaneously.[92,93]

Usually the problem arises when studying a series of complexes spanning the whole lanthanide series – it is often observed that two different B_0^2 parameters are needed, one for the early lanthanides and one for the late lanthanides (after the so-called gadolinium break). In the present case (with all the complexes being "pre-Gd") the problem is expected to be less pronounced as is indeed seen in the linearity of the plots in the one proton analysis.

The two proton (Geraldes) analysis consists of combining Eq. (2) for two protons, Hi and Hk, where the latter is the reference proton. Eliminating the crystal field parameter this can then be rearranged to

$$\frac{\Delta_{i,j}}{\langle S_z \rangle_j} = \left[F_i - \left(\frac{G_i}{G_k} \right) \cdot F_k \right] + \left(\frac{G_i}{G_k} \right) \cdot \frac{\Delta_{k,j}}{\langle S_z \rangle_j} \qquad (14)$$

As can be seen, plotting $\Delta_{i,j} / \langle S_z \rangle_j$ as a function of $\Delta_{k,j} / \langle S_z \rangle_j$ yields a straight line if the position of Hi relative to Hk does not change along the series of lanthanide complexes being investigated. Moreover, the slope is the structural ratio G_i/G_k, which is pure structural information without contamination of other parameters. Structural ratios obtained in this manner can then be compared with results for another series of complexes and in this way the structures in solution of complexes of the different ligands can be compared. Similarly, the structure in solution can be compared with the solid state structure as determined by X-ray diffraction, for which structural parameters θ_i and r_i can be measured and structural ratios can easily be calculated.

The application of the two proton (Geraldes) method is unfortunately not feasible for complexes containing two paramagnetic complexes. The presence of two different crystal field parameters makes it impossible to extract pure structural information from the data using the scheme outlined above. An even more sophisticated method has been developed for dealing with complexes containing two non-equivalent lanthanide ions.[51] Three protons are employed simultaneously, two of which serve as reference protons. In this way some rather complicated structural factors can be isolated, each of which are non-linear combinations of the geometric factors G_i^{site1} and G_i^{site2}. These can then be compared with structural factors calculated from a solid state structure. An analysis of this kind has not been carried out in the present project.

5.5.2 Choice of reference proton

The structural information obtained from the two proton analysis of the lanthanide induced shift can be compared to the solid state structures by means of the structural ratios G_i / G_{ref}. Choosing a reference proton for this purpose is not a trivial task. Ideally, any proton of the set could be used, but some candidates had to be discarded for the reasons outlined below.

The G_i values obtained from the X-ray data, which are used to compare with the NMR results are the averages of the values calculated for each of the three ligand strands in a given complex. Therefore a proton must be chosen which has a similar G_i value for all three ligand strands, signifying that this particular solid state G_i value is "well defined". Using an average of three very different values has less physical meaning since such an average does not correspond to any "real" structure. Again, this should hold both for Ln in the bpb and in the bpa coordination cavity and for all three types of structure (L^{AB} complexes, monoclinic L^{AB3} complexes and triclinic L^{AB3} complexes). This condition was investigated by calculating the standard deviation of the mean

$$\sqrt{\frac{\sum_{n=1}^{3}\left(G_i^n - G_i^{mean}\right)^2}{n-1}} \qquad (15)$$

for every proton, each coordination cavity (bpb and bpa) and each of the eight solid state structures (Table 95 - Table 102).

A second quantity has also been calculated, namely the above mentioned standard deviation divided by G_i^{mean} and multiplied by 100 % (the relative standard deviation).

The relative standard deviation is the more useful of the two. Since information from the NMR data is extracted in the form of structural ratios G_i / G_{ref} it is of crucial importance that the reference proton has a low *relative* standard deviation on the structural factor since this will be reflected in the structural ratios calculated for all protons.
The agreement factors as well as the standard deviation do not take into account the fact that the G_i factors span several orders of magnitude. This is due to the r^{-3} factor as well as the angular dependence of the $(3\cos^2\theta - 1)$ term, which can be any value between -1 and +2.

The first quantity (the standard deviation) could be relevant when evaluating agreement factors. A large difference between G_i/G_{ref} values calculated from X-ray and NMR data could originate in the X-ray value not being well-defined due to a large difference between the values calculated for the three individual ligand strands. It could thus be argued that it would be justified to leave this proton out of the calculation of the agreement factor since it compares two values of which one is not well-defined. It should be noted that agreement factors may not be the best way to compare two sets of values.

Total relative standard deviations (the sum of the two values for the paramagnetic lanthanide ion in each of the two coordination sites) lower than 30 % are only achieved for all eight structures for H3, H5, H15, H16 and H17 with H16 being the best candidate having no sums exceeding 7 %. H8 and H10 fulfil the criterion for 7 structures with the eighth having a value of 31 % and 37 %, respectively.

The proton H5 was ruled out since it is a methyl proton of one of the ethyl groups, which are flexible in solution. This flexibility is not reflected in the solid state structures since they are a "frozen picture" of the complex ions.

The two protons H15 and H17 had to be ruled out since they exhibit large differences between X-ray and NMR G_i/G_{ref} structural ratios (≈ 50 %) when any other proton is used as reference. Using any of these two as reference would cause all other structural ratios to show the same kind of deviation (slope of about 1.5 with H17 as reference, agreement factors 3-4 times larger).

Of the two protons left H16 has the lowest total relative standard deviation and was therefore initially chosen as reference proton. However, in the ligands L^{AB4} and L^{AB5} this proton is replaced with either a NEt_2 or a Cl substituent, which rules out the possibility to use H16 as general reference proton.

For these reasons the analysis is carried using H3 as reference proton and then repeated for the complexes of L^{AB} and L^{AB3} utilising H16 to investigate whether the choice of reference proton has any profound influence on the results.

5.5.3 Analysis

The lanthanide induced shifts have been treated according to the theory of Geraldes (two proton treatment). Examples of plots of $\Delta_i / \langle S_z \rangle_j$ as a function of $\Delta_{ref} / \langle S_z \rangle_j$ (Eq. (14)) using either H16 or H3 as reference proton are given in Figure 82 - Figure 85. The complete set of plots can be found in Appendix 2 (pages 353 ff.). It is evident that the plots are linear, which proves that the complexes in each of the series of complexes are all isostructural.

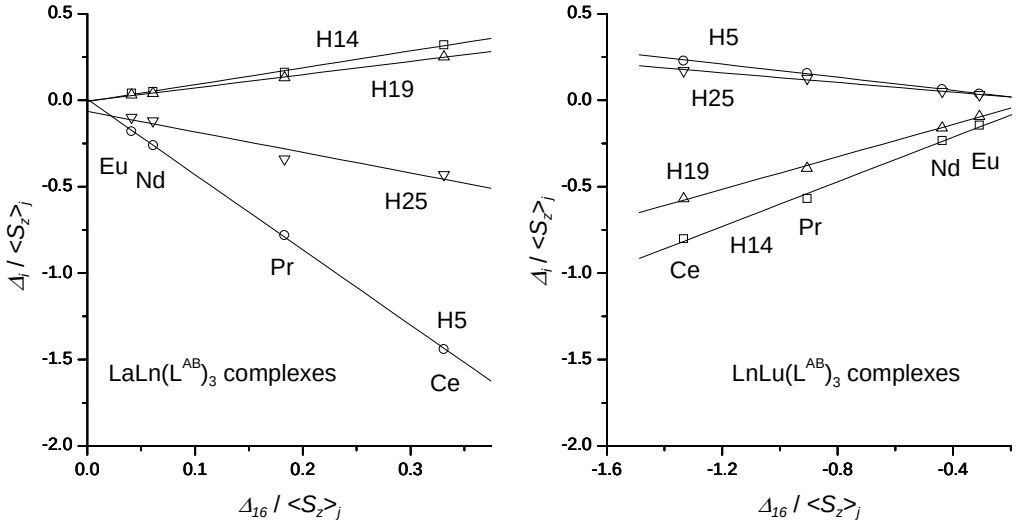

Figure 82 Geraldes plots of L^{AB} complexes using H16 as reference

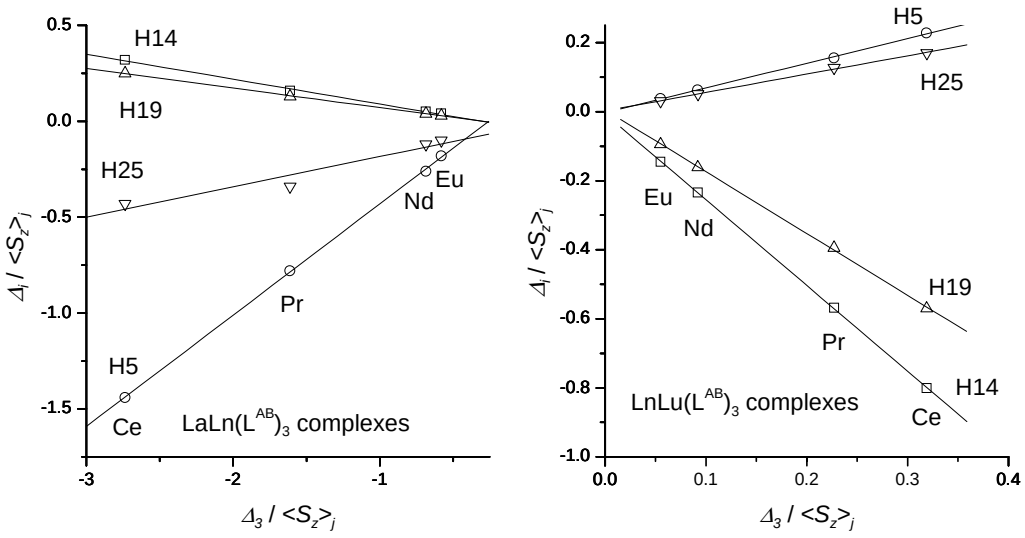

Figure 83 Geraldes plots of L^{AB} complexes using H3 as reference

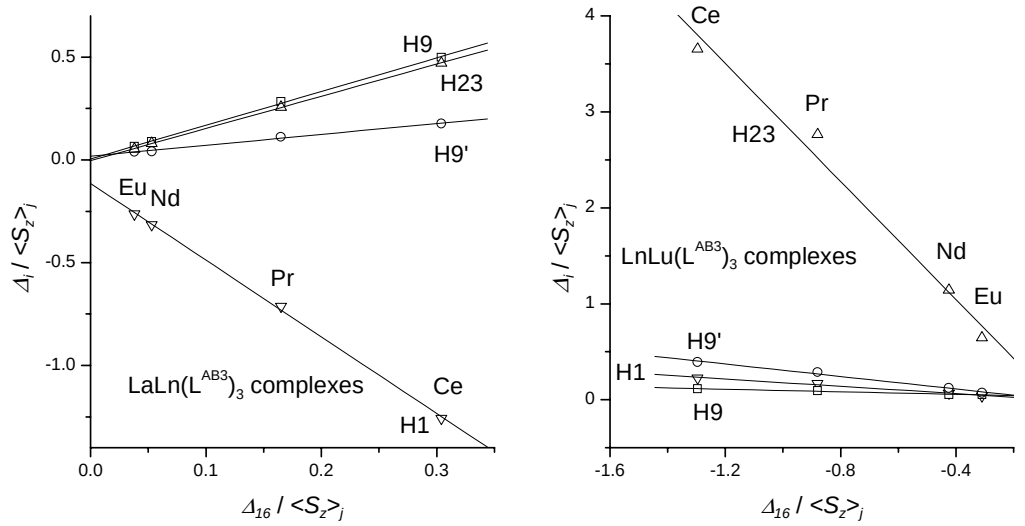

Figure 84 Geraldes plots of L^{AB3} complexes using H16 as reference

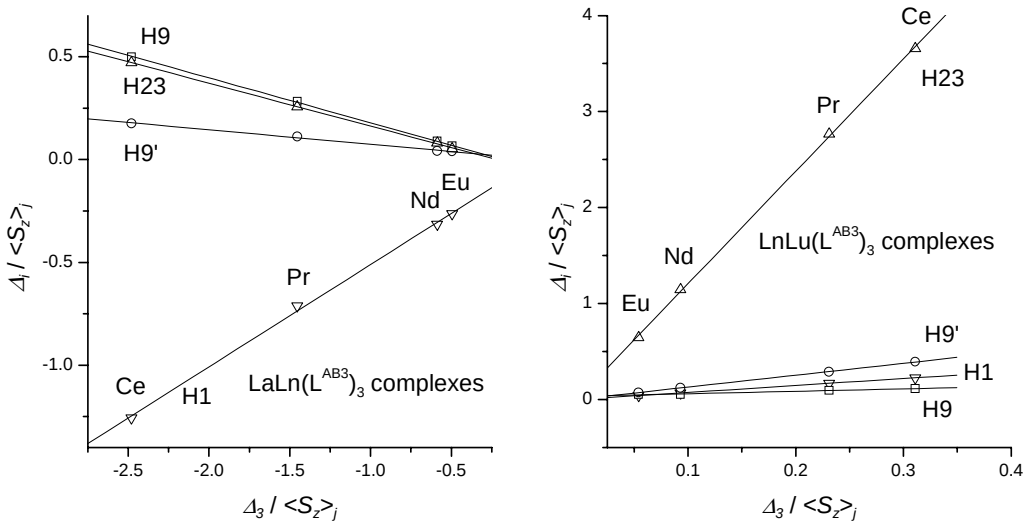

Figure 85 Geraldes plots of L^{AB3} complexes using H3 as reference

Results of the two proton analysis (correlation coefficients, slopes (G_i/G_{ref}) and intercepts ($F_i - (G_i/G_{ref}) \cdot F_{ref}$) are given in Table 80 - Table 85. The correlation coefficients are generally excellent with the only exceptions being two protons close to one of the so-called magic angles (H24' and H26' for the LaLn complexes).

It should be noted that H11 in the $LnLu(L^{AB})_3$ complexes exhibits very good correlation coefficients (0.976 using H16 as reference). This is a marked improvement compared to the published[80] value of 0.490 using the LaLu complex as diamagnetic reference. The average correlation coefficient of all the protons in the $LnLu(L^{AB})_3$ series is 0.994 using the "virtual reference complex" consisting of 70 % $LaLu(L^{AB})_3$ and 30 % $Lu_2(L^{AB})_3$ and 0.978 when only the $LaLu(L^{AB})_3$ is used. Evidently the utilisation of "virtual reference complexes" employed here provides a better diamagnetic reference than using a single complex.

Table 80 Results of two proton analysis of LaLn complexes of L^{AB} and L^{AB3} using H3 as reference

	$LaLn(L^{AB})_3$			$LaLn(L^{AB3})_3$		
	Correlation coefficient	$\frac{G_i}{G_3}$	$\left[F_i-\left(\frac{G_i}{G_3}\right)\cdot F_3\right]$	Correlation coefficient	$\frac{G_i}{G_3}$	$\left[F_i-\left(\frac{G_i}{G_3}\right)\cdot F_3\right]$
H1	0.999	0.54(1)	-0.03(2)	0.999	0.50(1)	-0.01(2)
H2	0.999	0.79(3)	0.15(4)			
H3	1.000	1(0)	0(0)	1.000	1(0)	0(0)
H4	0.999	0.333(9)	0.06(1)	0.997	0.31(2)	0.01(3)
H4'	0.998	0.51(2)	0.11(4)	0.999	0.52(2)	0.09(3)
H5	1.000	0.581(7)	0.15(1)	1.000	0.618(7)	0.13(1)
H6	0.994	0.084(6)	-0.12(1)	0.986	0.080(9)	-0.13(1)
H7	1.000	-0.132(2)	-0.028(3)	1.000	-0.1437(8)	-0.021(1)
H8	1.000	-2.53(3)	-0.79(5)	1.000	-2.63(3)	-0.66(5)
H9	1.000	-0.208(3)	-0.053(5)	1.000	-0.218(3)	-0.039(4)
H9'	0.985	-0.043(5)	0.006(9)	0.997	-0.070(4)	0.004(5)
H10	1.000	-1.29(2)	-0.35(4)	1.000	-1.32(2)	-0.29(3)
H11	0.998	-0.094(5)	-0.020(7)	0.999	-0.102(3)	-0.015(4)
H12	0.999	-0.152(4)	-0.034(7)	0.999	-0.168(5)	-0.038(7)
H13	0.999	-0.183(5)	-0.052(9)	1.000	-0.178(2)	-0.037(3)
H13'	0.999	-0.178(6)	-0.04(1)	1.000	-0.189(2)	-0.040(3)
H14	0.999	-0.131(3)	-0.042(5)	0.999	-0.132(4)	-0.032(6)
H15	0.999	-0.207(5)	-0.048(8)	1.000	-0.221(3)	-0.049(5)
H16	1.000	-0.133(2)	-0.033(3)	1.000	-0.133(1)	-0.027(2)
H17	0.999	-0.163(4)	-0.045(7)	1.000	-0.1604(9)	-0.033(1)
H18	1.000	-0.150(2)	-0.039(4)	0.995	-0.15(1)	-0.04(2)
H18'	1.000	-0.1313(7)	-0.036(1)	0.999	-0.140(4)	-0.034(6)
H19	1.000	-0.102(1)	-0.028(2)	1.000	-0.109(2)	-0.027(4)
H20	1.000	-0.106(1)	-0.028(2)	0.996	-0.117(7)	-0.03(1)
H21	1.000	-0.091(1)	-0.024(2)	1.000	-0.089(1)	-0.018(2)
H22	1.000	-0.119(2)	-0.031(3)	1.000	-0.1174(6)	-0.0252(8)
H23	1.000	-0.201(4)	-0.055(7)	1.000	-0.209(2)	-0.046(4)
H24	0.984	0.26(3)	-0.01(6)	0.994	0.31(2)	0.00(4)
H24'	0.544	-0.03(3)	-0.10(5)	0.194	0.01(4)	-0.09(5)
H25	0.971	0.16(3)	-0.02(5)	0.977	0.19(3)	-0.03(4)
H26	0.998	-0.36(2)	-0.12(3)	0.996	-0.37(2)	-0.13(3)
H26'	0.727	0.03(2)	-0.02(3)	0.984	0.10(1)	0.01(2)
H27	1.000	-1.09(2)	-0.24(4)	0.998	-1.02(4)	-0.14(6)

Table 81 Results of two proton analysis of LaLn complexes of L^{AB4} and L^{AB5} using H3 as reference

	$LaLn(L^{AB4})_3$			$LaLn(L^{AB5})_3$		
	Correlation coefficient	$\frac{G_i}{G_3}$	$\left[Fi-\left(\frac{Gi}{G_3}\right)\cdot F_3\right]$	Correlation coefficient	$\frac{G_i}{G_3}$	$\left[Fi-\left(\frac{Gi}{G_3}\right)\cdot F_3\right]$
H1	1.000	0.58(1)	-0.03(1)	1.000	0.53(1)	-0.04(2)
H2	0.999	0.80(2)	0.15(4)	0.999	0.77(2)	0.14(4)
H3	1.000	1(0)	0(0)	1.000	1(0)	0(0)
H4	0.997	0.49(3)	0.15(4)	0.999	0.30(1)	0.04(2)
H4'	0.992	0.49(4)	0.07(7)	0.998	0.50(2)	0.11(3)
H5	0.991	0.48(5)	0.05(7)	1.000	0.581(5)	0.144(9)
H6	0.988	0.09(1)	-0.13(2)	0.990	0.067(7)	-0.13(1)
H7	0.999	-0.131(5)	-0.034(8)	1.000	-0.145(1)	-0.034(2)
H8	1.000	-2.71(4)	-0.79(7)	1.000	-2.57(5)	-0.75(8)
H9	1.000	-0.233(1)	-0.059(2)	1.000	-0.222(2)	-0.054(3)
H9'	0.998	-0.062(3)	-0.006(4)	0.998	-0.056(3)	0.004(4)
H10	1.000	-1.28(2)	-0.32(3)	0.999	-1.34(4)	-0.40(6)
H11	0.990	-0.10(1)	-0.01(2)	0.995	-0.098(7)	-0.02(1)
H12	1.000	-0.161(3)	-0.033(5)	0.999	-0.154(4)	-0.032(7)
H13	1.000	-0.188(3)	-0.049(4)	1.000	-0.176(4)	-0.042(6)
H13'	1.000	-0.209(4)	-0.053(6)	0.998	-0.172(7)	-0.04(1)
H14	1.000	-0.118(1)	-0.031(2)	0.999	-0.142(4)	-0.044(7)
H15	1.000	-0.224(3)	-0.058(4)	1.000	-0.220(3)	-0.057(5)
H17	1.000	-0.168(2)	-0.045(3)	1.000	-0.164(2)	-0.044(3)
H18	0.999	-0.168(5)	-0.045(8)	0.999	-0.123(4)	-0.020(7)
H18'	0.998	-0.117(6)	-0.019(9)	1.000	-0.122(1)	-0.029(2)
H19	1.000	-0.102(1)	-0.024(2)	1.000	-0.108(2)	-0.029(3)
H20	1.000	-0.1119(6)	-0.029(1)	1.000	-0.097(1)	-0.024(2)
H21	1.000	-0.0972(9)	-0.025(1)	1.000	-0.089(2)	-0.021(3)
H22	1.000	-0.124(1)	-0.035(2)	1.000	-0.111(2)	-0.026(4)
H23	0.999	-0.200(5)	-0.051(7)	1.000	-0.202(4)	-0.057(6)
H24	0.975	0.23(4)	-0.03(6)	0.984	0.26(3)	-0.02(5)
H24'	0.777	-0.05(3)	-0.10(4)	0.802	-0.05(3)	-0.11(4)
H25	0.970	0.15(3)	-0.02(4)	0.968	0.16(3)	-0.02(5)
H26	0.999	-0.47(1)	-0.16(2)	0.999	-0.35(1)	-0.12(2)
H26'	0.794	-0.03(2)	-0.04(3)	0.893	0.04(1)	-0.01(2)
H27	0.999	-1.16(3)	-0.26(4)	0.999	-1.07(3)	-0.23(4)
H28	0.951	-0.11(3)	-0.05(4)			
H28'	0.995	-0.071(5)	-0.012(8)			
H29	1.000	-0.071(1)	-0.018(2)			

Table 82 Results of two proton analysis of LnLu complexes of L^{AB} and L^{AB3} using H3 as reference

	$LnLu(L^{AB})_3$			$LnLu(L^{AB3})_3$		
	Correlation coefficient	$\frac{G_i}{G_3}$	$\left[Fi-\left(\frac{G_i}{G_3}\right)\cdot F_3\right]$	Correlation coefficient	$\frac{G_i}{G_3}$	$\left[Fi-\left(\frac{G_i}{G_3}\right)\cdot F_3\right]$
H1	1.000	0.74(1)	0.001(3)	1.000	0.723(5)	0.002(1)
H2	0.999	0.69(2)	-0.004(5)			
H3	1.000	1(0)	0(0)	1.000	1(0)	0(0)
H4	0.998	1.07(5)	-0.01(1)	0.997	1.04(5)	0.00(1)
H4'	1.000	1.02(1)	-0.001(3)	1.000	1.03(2)	-0.001(4)
H5	1.000	0.71(2)	-0.002(3)	0.999	0.69(2)	-0.001(3)
H6	0.995	1.07(8)	-0.01(2)	0.997	1.06(6)	0.00(1)
H7	0.998	0.69(3)	0.002(6)	0.998	0.70(3)	0.006(6)
H8	1.000	5.1(1)	0.01(2)	1.000	5.04(7)	0.00(1)
H9	0.989	0.29(3)	0.028(6)	0.990	0.26(3)	0.034(5)
H9'	1.000	1.23(2)	0.006(4)	1.000	1.24(1)	0.006(3)
H10	1.000	15.5(3)	-0.04(6)	1.000	15.6(2)	-0.07(3)
H11	0.986	-0.09(1)	0.008(2)	0.984	-0.08(1)	0.011(2)
H12	0.999	-1.52(6)	-0.15(1)	0.997	-1.52(8)	-0.14(2)
H13	0.996	-3.3(2)	-0.11(4)	0.997	-3.3(2)	-0.10(4)
H13'	0.996	-4.0(2)	-0.03(5)	0.999	-4.0(1)	-0.02(3)
H14	1.000	-2.48(2)	-0.007(3)	0.999	-2.52(9)	0.00(2)
H15	0.996	-3.5(2)	-0.34(4)	0.999	-3.5(1)	-0.33(3)
H16	0.998	-3.8(2)	-0.09(4)	0.994	-3.8(3)	-0.08(6)
H17	0.997	-3.5(2)	-0.37(4)	0.999	-3.4(1)	-0.36(3)
H18	0.997	-3.7(2)	-0.04(4)	0.999	-3.62(9)	-0.04(2)
H18'	0.997	-3.0(2)	-0.11(3)	0.999	-2.96(9)	-0.10(2)
H19	1.000	-1.79(3)	0.005(5)	0.998	-1.79(8)	0.01(2)
H20	0.999	-1.50(5)	-0.15(1)	0.996	-1.5(1)	-0.15(2)
H21	0.993	-0.26(2)	0.016(4)	0.996	-0.29(2)	0.018(4)
H22	0.998	1.21(5)	0.02(1)	1.000	1.26(2)	0.010(3)
H23	0.999	11.8(4)	0.05(8)	1.000	11.7(2)	0.03(3)
H24	1.000	0.71(1)	-0.002(2)	0.999	0.66(3)	0.003(5)
H25	0.999	0.53(1)	0.003(3)	0.999	0.54(1)	0.003(3)
H26	0.998	0.84(4)	0.004(7)	1.000	0.83(1)	-0.001(2)
H26'	0.998	0.69(3)	-0.001(6)	0.997	0.71(4)	0.000(7)
H27	1.000	0.660(1)	0.0008(3)	1.000	0.629(6)	0.002(1)

Table 83 Results of two proton analysis of LnLu complexes of L^{AB4} and L^{AB5} using H3 as reference

	$LnLu(L^{AB4})_3$			$LnLu(L^{AB5})_3$		
	Correlation coefficient	$\frac{G_i}{G_3}$	$\left[Fi-\left(\frac{Gi}{G_3}\right)\cdot F_3\right]$	Correlation coefficient	$\frac{G_i}{G_3}$	$\left[Fi-\left(\frac{Gi}{G_3}\right)\cdot F_3\right]$
H1	1.000	0.735(2)	-0.0013(7)	1.000	0.78(2)	-0.001(3)
H2	1.000	0.640(4)	0.000(1)	0.996	0.60(4)	0.007(7)
H3	1.000	1(0)	0(0)	1.000	1(0)	0(0)
H4	1.000	0.98(1)	-0.003(5)	0.995	1.17(8)	-0.01(2)
H4'	1.000	0.982(5)	0.000(2)	0.999	1.05(3)	-0.001(6)
H5	1.000	0.669(6)	-0.002(2)	0.997	0.76(4)	-0.004(8)
H6	0.999	0.96(2)	-0.002(8)	0.993	1.14(9)	0.00(2)
H7	1.000	0.608(8)	0.003(3)	0.997	0.86(5)	-0.002(9)
H8	1.000	5.06(1)	-0.006(4)	0.999	5.4(2)	-0.02(3)
H9	0.999	0.29(1)	0.022(4)	0.984	0.43(6)	0.03(1)
H9'	1.000	1.213(5)	0.005(2)	0.999	1.33(4)	0.006(7)
H10	1.000	15.0(2)	-0.05(7)	0.999	16.0(4)	-0.07(7)
H11	0.994	0.114(9)	0.008(3)	0.970	0.06(1)	0.006(2)
H12	0.999	-1.15(3)	-0.15(1)	0.998	-1.42(7)	-0.15(1)
H13	0.999	-3.10(8)	-0.13(3)	0.997	-3.2(2)	-0.09(3)
H13'	1.000	-3.96(3)	-0.04(1)	0.998	-3.8(2)	-0.02(3)
H14	1.000	-2.05(2)	-0.002(7)	0.996	-3.1(2)	0.01(4)
H15	1.000	-4.33(7)	-0.34(3)	0.997	-3.2(2)	-0.29(3)
H17	1.000	-3.86(8)	-0.34(3)	0.999	-3.1(1)	-0.31(2)
H18	0.999	-4.2(1)	-0.01(5)	0.999	-3.4(1)	-0.05(2)
H18'	0.997	-3.4(2)	-0.11(6)	0.999	-2.95(9)	-0.09(2)
H19	1.000	-1.74(3)	0.02(1)	0.996	-2.1(1)	0.02(3)
H20	0.999	-1.51(4)	-0.13(1)	0.994	-1.5(1)	-0.15(2)
H21	0.998	-0.40(2)	0.027(6)	0.994	-0.20(1)	0.015(3)
H22	0.999	0.93(3)	0.03(1)	0.999	1.32(4)	0.016(8)
H23	1.000	10.58(8)	0.07(3)	1.000	11.9(2)	0.04(4)
H24	1.000	0.647(9)	0.001(3)	0.993	0.81(7)	-0.01(1)
H24'	1.000	0.644(8)	0.000(3)	0.998	0.76(4)	-0.003(7)
H25	1.000	0.519(2)	0.0011(7)	1.000	0.548(6)	0.001(1)
H26	1.000	0.810(9)	-0.001(3)	0.994	0.96(8)	-0.01(1)
H26'	1.000	0.671(5)	-0.002(2)	0.999	0.70(3)	-0.001(5)
H27	1.000	0.649(8)	-0.001(3)	0.999	0.69(2)	-0.001(4)
H28	0.999	-1.45(5)	0.02(2)			
H28'	1.000	-1.52(2)	0.012(8)			
H29	1.000	-1.25(1)	-0.014(5)			

Table 84 Results of two proton analysis of LaLn complexes of L^{AB} and L^{AB3} using H16 as reference

	$LaLn(L^{AB})_3$			$LaLn(L^{AB3})_3$		
	Correlation coefficient	$\frac{G_i}{G_{16}}$	$\left[F_i-\left(\frac{G_i}{G16}\right)\cdot F16\right]$	Correlation coefficient	$\frac{G_i}{G_{16}}$	$\left[F_i-\left(\frac{G_i}{G16}\right)\cdot F16\right]$
H1	0.999	-4.1(1)	-0.17(2)	1.000	-3.72(7)	-0.12(1)
H2	0.999	-5.9(2)	-0.04(4)			
H3	1.000	-7.5(1)	-0.25(2)	1.000	-7.49(8)	-0.21(1)
H4	1.000	-2.50(5)	-0.03(1)	0.997	-2.3(1)	-0.05(2)
H4'	0.999	-3.8(1)	-0.02(3)	0.999	-3.9(1)	-0.01(2)
H5	1.000	-4.36(5)	0.007(9)	1.000	-4.634(9)	0.000(2)
H6	0.992	-0.63(6)	-0.14(1)	0.985	-0.60(7)	-0.15(1)
H7	1.000	0.99(2)	0.005(4)	1.000	1.08(1)	0.008(2)
H8	1.000	19.0(2)	-0.16(3)	1.000	19.7(2)	-0.12(4)
H9	1.000	1.57(1)	-0.001(2)	1.000	1.64(3)	0.005(6)
H9'	0.982	0.32(4)	0.017(8)	0.996	0.53(3)	0.018(6)
H10	1.000	9.7(2)	-0.03(3)	1.000	9.86(5)	-0.020(8)
H11	0.998	0.70(3)	0.004(6)	0.999	0.76(3)	0.006(5)
H12	1.000	1.14(3)	0.004(5)	0.999	1.26(3)	-0.003(6)
H13	0.999	1.38(4)	-0.007(8)	1.000	1.331(3)	-0.0003(4)
H13'	1.000	1.34(3)	0.005(6)	1.000	1.42(1)	-0.001(3)
H14	0.999	0.99(3)	-0.010(6)	0.999	0.99(2)	-0.005(4)
H15	1.000	1.56(2)	0.003(4)	1.000	1.654(8)	-0.004(1)
H16	1.000	1(0)	0(0)	1.000	1(0)	0(0)
H17	0.999	1.23(3)	-0.005(6)	1.000	1.201(7)	0.000(1)
H18	0.999	1.13(3)	-0.002(5)	0.996	1.15(8)	-0.01(1)
H18'	1.000	0.99(2)	-0.003(3)	0.999	1.05(3)	-0.005(4)
H19	0.999	0.77(2)	-0.003(4)	0.999	0.82(2)	-0.004(3)
H20	1.000	0.80(1)	-0.002(2)	0.997	0.88(5)	-0.008(9)
H21	1.000	0.684(9)	-0.001(2)	0.999	0.66(2)	0.000(3)
H22	1.000	0.892(3)	-0.0017(6)	1.000	0.879(6)	-0.001(1)
H23	1.000	1.51(3)	-0.006(6)	1.000	1.56(1)	-0.003(2)
H24	0.985	-2.0(2)	-0.08(5)	0.993	-2.3(2)	-0.07(3)
H24'	0.537	0.2(2)	-0.10(4)	0.184	-0.1(3)	-0.09(5)
H25	0.973	-1.2(2)	-0.06(4)	0.974	-1.4(2)	-0.07(4)
H26	0.996	2.7(2)	-0.03(3)	0.997	2.8(2)	-0.05(3)
H26'	0.738	-0.2(1)	-0.03(2)	0.984	-0.8(1)	-0.01(2)
H27	1.000	8.2(1)	0.03(2)	0.998	7.6(4)	0.07(6)

Table 85 Results of two proton analysis of LnLu complexes of L^{AB} and L^{AB3} using H16 as reference

	$LnLu(L^{AB})_3$			$LnLu(L^{AB3})_3$		
	Correlation coefficient	$\frac{G_i}{G_{16}}$	$\left[Fi-\left(\frac{Gi}{G16}\right)\cdot F16\right]$	Correlation coefficient	$\frac{G_i}{G_{16}}$	$\left[Fi-\left(\frac{Gi}{G16}\right)\cdot F16\right]$
H1	0.996	-0.19(1)	-0.01(1)	0.993	-0.19(2)	-0.01(1)
H2	1.000	-0.181(3)	-0.019(2)			
H3	0.998	-0.26(1)	-0.02(1)	0.994	-0.26(2)	-0.02(2)
H4	0.999	-0.280(7)	-0.030(6)	0.998	-0.28(1)	-0.02(1)
H4'	0.998	-0.27(1)	-0.023(9)	0.996	-0.27(2)	-0.02(2)
H5	0.999	-0.186(5)	-0.018(5)	0.996	-0.18(1)	-0.015(9)
H6	0.999	-0.28(1)	-0.030(8)	0.998	-0.28(1)	-0.025(9)
H7	0.999	-0.181(7)	-0.013(6)	0.996	-0.18(1)	-0.01(1)
H8	0.995	-1.32(9)	-0.10(8)	0.996	-1.33(9)	-0.10(7)
H9	0.993	-0.077(6)	0.022(6)	0.984	-0.067(9)	0.029(7)
H9'	0.996	-0.32(2)	-0.02(2)	0.995	-0.33(2)	-0.02(2)
H10	0.995	-4.0(3)	-0.4(2)	0.994	-4.1(3)	-0.4(3)
H11	0.976	0.022(3)	0.010(3)	0.998	0.021(1)	0.0127(8)
H12	0.996	0.40(2)	-0.12(2)	0.998	0.40(2)	-0.11(1)
H13	0.988	0.9(1)	-0.04(8)	0.982	0.9(1)	0.0(1)
H13'	0.988	1.0(1)	0.0(1)	0.988	1.0(1)	0.05(9)
H14	0.998	0.65(3)	0.05(2)	0.998	0.66(3)	0.05(2)
H15	0.988	0.9(1)	-0.27(9)	0.989	0.9(1)	-0.27(8)
H16	1.000	1(0)	0(0)	1.000	1(0)	0(0)
H17	0.990	0.90(9)	-0.30(8)	0.990	0.90(9)	-0.30(7)
H18	0.989	1.0(1)	0.04(8)	0.989	0.9(1)	0.03(8)
H18'	0.989	0.78(8)	-0.05(7)	0.988	0.77(9)	-0.05(7)
H19	0.999	0.47(2)	0.04(1)	0.999	0.47(2)	0.05(1)
H20	0.998	0.39(2)	-0.12(2)	0.998	0.40(2)	-0.12(1)
H21	0.986	0.067(8)	0.021(7)	0.997	0.076(4)	0.024(3)
H22	0.992	-0.31(3)	-0.01(2)	0.992	-0.33(3)	-0.01(3)
H23	0.993	-3.1(3)	-0.2(2)	0.992	-3.1(3)	-0.2(2)
H24	0.999	-0.184(6)	-0.018(5)	0.987	-0.17(2)	-0.01(2)
H25	0.994	-0.14(1)	-0.009(9)	0.991	-0.14(1)	-0.01(1)
H26	0.992	-0.22(2)	-0.01(2)	0.992	-0.22(2)	-0.02(2)
H26'	1.000	-0.182(3)	-0.017(2)	0.998	-0.188(9)	-0.015(7)
H27	0.997	-0.17(1)	-0.013(7)	0.995	-0.17(1)	-0.01(1)

5.5.4 Comparing G_i factors of the complexes

The results of interest to us here are the structural ratios (G_i / G_{ref}), which contain structural information regarding the position of the proton relative to the paramagnetic lanthanide ion ($G_i = (3\cos^2\theta - 1)/r^3$).

The first question to answer is whether the inclusion of a Cl or NEt_2 substituent in the L^{ABX} ligands (X = 3, 4, or 5) changes the structure of the complexes compared to the structure of the L^{AB} complexes.

For the purpose of comparing the structural ratios of two structures agreement factors defined analogously to the agreement factors utilised in the one proton analysis have been calculated and tabulated in Table 88.

$$AF_j^G = \sqrt{\frac{\sum_i \left(\left(G_i/G_{ref}\right)_{L^{AB}} - \left(G_i/G_{ref}\right)_{L^{ABX}} \right)^2}{\sum_i \left(\left(G_i/G_{ref}\right)_{L^{ABX}} \right)^2}} \qquad (16)$$

An alternative way of comparing the structural ratios is by plotting G_i / G_{ref} of the L^{ABX} complexes as a function of G_i / G_{ref} of the L^{AB} complexes (Figure 86 and Figure 87). The results of the fitting are also listed in Table 86.

Table 86 Comparing structural ratios of L^{ABX} complexes to structural ratios of L^{AB} complexes

	L^{AB3}				L^{AB4}		L^{AB5}	
	Reference H3		Reference H16		Reference H3		Reference H3	
	LaLn	LnLu	LaLn	LnLu	LaLn	LnLu	LaLn	LnLu
AF	0.055	0.008	0.051	0.014	0.090	0.082	0.027	0.052
Correlation coefficient	0.999	1.000	0.999	1.000	0.997	0.997	1.000	0.999
Slope	1.024	1.001	1.019	1.012	1.048	0.996	1.007	1.016

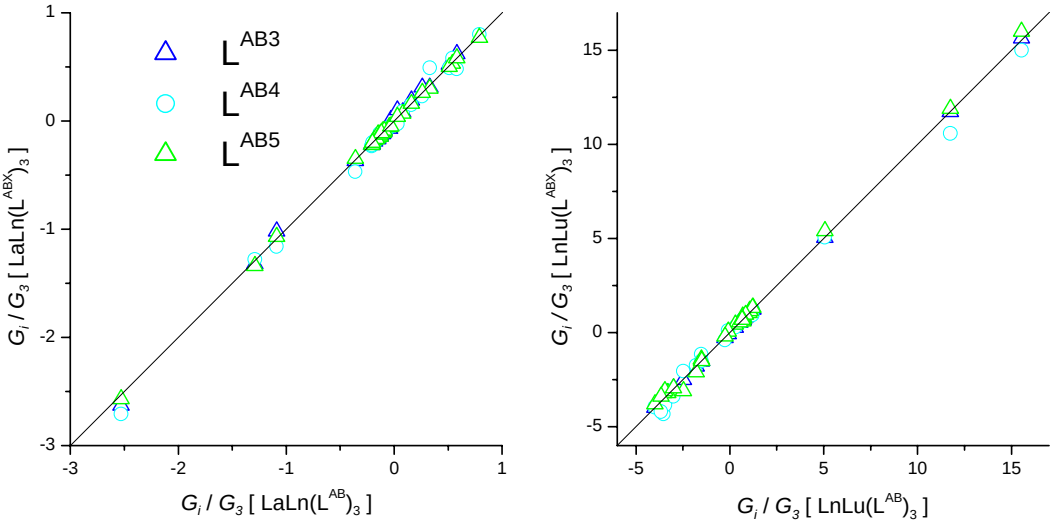

Figure 86 Comparing LIS structural factors using H3 as reference

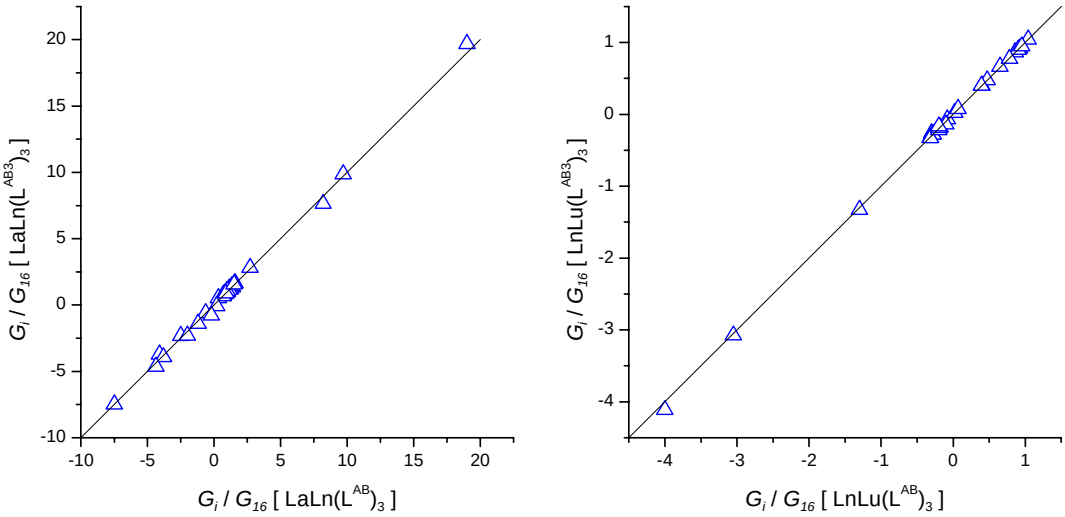

Figure 87 Comparing LIS structural factors using H16 as reference

All results (agreement factors, correlation coefficients and slopes) demonstrate that the complexes of L^{AB3} have the same structure as the L^{AB} complexes in solution. Or to put it another way, that whatever structural difference there might be between the complexes of the two ligands it is not significant enough to manifest itself in the information extracted from the analysis of the lanthanide induced shift.

That the complexes of L^{AB} and L^{AB4} are isostructural is interesting since it was seen in the one proton analysis that the pseudo contact terms $B_0^2 G_i$ were rather different (Chapter 5.3.6; page

124). This means that the difference between the two ligands is mainly in the crystal field parameter. We will return to this point in Chapter 5.6 (page 219).

5.5.5 Parameters of the solid state structures

Eight complexes have been crystallised and their structures (including hydrogen atom positions) have been determined by X-ray diffraction. With the ligand L^{AB} the isostructural LaEu, LaTb and Eu_2 complexes have been characterised this way.[8,80] For L^{AB3} two series of complexes are formed. The complexes Ce_2, NdLu and Sm_2 are monoclinic, whereas Pr_2 and PrLu are triclinic (Chapter 3; page 41).

The only structural information that can be extracted from the analysis of the LIS data are the structural ratios G_i/G_{ref} ($G_i = (3\cos^2\theta_i - 1)/r_i^3$). The relevant numbers to extract from the solid state structure are therefore the distance r_i between the proton and the paramagnetic lanthanide ion and the angle θ_i between the Ln-Hi vector and the molecular axis, which we define as the Ln-Ln' vector. The structural parameters are given in Table 87 - Table 94.

Table 87 Structural parameters θ_i and r_i in the solid state LaEu(L^{AB})$_3$ complex

	Ln ion in bpb site						Ln ion in bpa site					
	Ligand strand 1		Ligand strand 2		Ligand strand 3		Ligand strand 1		Ligand strand 2		Ligand strand 3	
	θ_i	r_i	θ_i	r_i	θ_i	r_i	θ_i	r_i	θ_i	r_i	θ_i	r_i
H1	21.86	12.693	21.09	12.809	23.96	12.311	118.57	5.381	120.77	5.364	112.23	5.401
H2	27.58	12.556	27.42	12.618	30.53	11.990	108.30	6.123	108.94	6.143	100.43	6.193
H3	30.78	10.705	30.39	10.842	32.15	10.268	89.90	5.478	91.52	5.487	84.63	5.488
H4	44.15	8.254	43.76	8.295	44.98	8.168	60.26	6.621	60.73	6.577	59.29	6.715
H4'	38.42	9.197	37.83	9.282	39.52	8.949	70.70	6.056	71.76	5.994	67.97	6.143
H5a	41.35	10.363	41.56	10.372	40.36	10.325	78.22	6.994	78.13	7.031	78.67	6.819
H6	47.29	7.477	47.47	7.405	47.49	7.366	53.03	6.877	52.41	6.887	52.08	6.883
H7	51.90	6.745	52.36	6.621	51.87	6.809	46.45	7.323	45.44	7.359	46.95	7.329
H8	21.68	6.821	23.42	7.063	22.72	6.884	41.30	3.818	45.84	3.913	42.94	3.903
H9	52.63	6.553	53.23	6.703	52.64	6.945	44.88	7.380	45.95	7.471	47.87	7.443
H9'	43.35	7.320	44.31	7.445	43.29	7.496	52.30	6.351	53.28	6.488	53.88	6.363
H10	33.31	3.940	37.36	3.957	35.68	4.093	20.09	6.298	21.61	6.520	22.09	6.348
H11	54.71	7.068	54.81	7.152	57.95	7.248	48.39	7.716	48.98	7.748	48.89	8.153
H12	63.69	6.586	63.40	6.673	68.51	6.669	43.20	8.625	43.81	8.619	42.53	9.179
H13	69.86	6.707	72.88	6.501	86.05	6.183	42.39	9.340	40.43	9.581	35.09	10.731
H13'	72.94	6.335	70.83	6.254	89.52	5.715	39.49	9.523	39.55	9.277	31.96	10.796
H14a	89.48	5.888	92.06	6.021	73.24	7.228	32.75	10.884	32.56	11.181	44.18	9.931
H15	75.31	5.528	73.60	5.562	79.71	5.548	34.41	9.461	34.94	9.316	33.60	9.864
H16	87.12	6.347	83.79	6.383	88.33	6.372	35.50	10.917	36.69	10.621	35.22	11.043
H17	101.17	5.526	95.16	5.615	99.01	5.610	27.81	11.620	29.93	11.207	28.78	11.507
H18	99.76	5.719	92.35	6.003	114.42	6.240	28.98	11.633	32.39	11.195	25.74	13.085
H18'	106.41	6.258	97.93	6.562	119.17	6.796	28.68	12.509	32.73	12.021	25.36	13.855
H19a	116.12	7.171	111.82	6.880	99.45	6.803	27.51	13.940	28.50	13.386	33.02	12.313
H20	125.45	6.730	114.97	6.917	123.45	6.949	22.69	14.210	27.34	13.652	23.98	14.268
H21	135.63	7.188	119.75	7.362	126.30	7.383	19.31	15.200	26.43	14.361	23.66	14.824
H22	146.51	6.146	125.61	6.239	128.42	6.216	13.31	14.728	21.56	13.805	20.44	13.948
H23	153.27	3.955	129.55	3.970	131.74	3.905	7.95	12.863	14.62	12.128	13.86	12.161
H24	25.84	12.319	25.46	12.127	27.29	11.963	109.30	5.689	108.48	5.497	104.56	5.667
H24'	26.73	13.023	23.80	13.470	27.64	12.904	112.48	6.339	119.84	6.266	110.38	6.386
H24a	26.12	12.650	24.53	12.792	27.33	12.417	111.12	5.970	65.41	5.841	107.74	5.986
H25a	31.13	10.869	31.49	12.368	32.76	10.862	90.99	5.620	101.71	6.598	89.29	5.878
H26	16.38	12.329	18.92	11.929	18.41	12.046	127.02	4.354	118.24	4.391	120.29	4.406
H26'	23.22	12.491	24.19	12.707	23.26	12.933	114.77	5.424	114.60	5.727	117.64	5.765
H27a	18.09	14.464	16.59	14.065	14.48	14.056	135.32	6.388	136.77	5.864	141.40	5.633

Table 88 Structural parameters θ_i and r_i in the solid state LaTb(L^{AB})$_3$ complex

	Ln ion in bpb site						Ln ion in bpa site					
	Ligand strand 1		Ligand strand 2		Ligand strand 3		Ligand strand 1		Ligand strand 2		Ligand strand 3	
	θ_i	r_i	θ_i	r_i	θ_i	r_i	θ_i	r_i	θ_i	r_i	θ_i	r_i
H1	21.46	12.669	20.97	12.733	23.90	12.333	119.21	5.310	120.56	5.292	112.57	5.411
H2	28.03	12.572	27.76	12.596	30.63	11.955	107.81	6.205	108.36	6.182	100.13	6.187
H3	30.18	10.763	29.81	10.855	32.07	10.218	91.11	5.412	92.33	5.401	84.31	5.452
H4	45.13	8.381	43.54	8.282	44.91	8.167	61.05	6.788	60.75	6.539	59.36	6.701
H4'	40.01	9.136	37.39	9.288	39.80	8.900	69.45	6.273	72.12	5.926	67.49	6.167
H5a	40.63	10.474	41.37	10.313	40.10	10.302	79.61	6.934	77.91	6.971	78.76	6.766
H6	47.27	7.467	47.03	7.509	46.99	7.251	53.01	6.867	53.40	6.844	51.27	6.797
H7	51.70	6.735	51.69	6.505	51.90	6.799	46.45	7.293	44.65	7.263	46.92	7.326
H8	21.72	6.912	22.78	7.128	22.54	6.916	42.64	3.776	46.41	3.810	43.32	3.864
H9	52.83	6.531	53.34	6.657	52.82	6.902	44.73	7.395	45.63	7.471	47.56	7.451
H9'	43.75	7.309	44.61	7.426	43.51	7.460	52.21	6.396	53.12	6.520	53.59	6.382
H10	33.84	3.964	36.84	3.986	35.32	4.011	20.49	6.306	21.69	6.467	21.37	6.364
H11	54.41	7.055	54.61	7.105	58.02	7.212	48.40	7.672	48.72	7.707	48.67	8.146
H12	64.39	6.595	63.43	6.701	68.45	6.656	43.13	8.699	44.02	8.624	42.51	9.162
H13	69.90	6.709	72.92	6.478	85.79	6.178	42.43	9.339	40.32	9.570	35.17	10.698
H13'	72.54	6.365	71.17	6.239	89.38	5.705	39.79	9.487	39.41	9.300	31.98	10.772
H14a	90.08	5.796	92.17	5.783	73.05	7.223	32.19	10.880	31.53	11.050	44.25	9.902
H15	76.04	5.551	73.19	5.577	80.36	5.546	34.43	9.529	35.14	9.276	33.47	9.914
H16	87.32	6.323	85.02	6.397	89.86	6.415	35.35	10.916	36.40	10.739	34.94	11.202
H17	101.08	5.563	94.66	5.593	100.06	5.537	28.00	11.629	30.01	11.147	28.20	11.536
H18	99.41	5.801	91.60	5.946	113.69	6.262	29.42	11.650	32.40	11.092	26.08	13.043
H18'	105.84	6.336	98.04	6.508	118.22	6.812	29.15	12.513	32.52	11.988	25.79	13.794
H19a	116.01	7.224	110.79	6.932	97.76	6.738	27.70	13.968	29.07	13.339	33.44	12.114
H20	124.35	6.734	115.04	6.954	121.85	6.976	23.16	14.138	27.42	13.680	24.71	14.178
H21	134.29	7.201	120.62	7.290	124.99	7.354	19.92	15.132	25.91	14.355	24.18	14.707
H22	143.17	6.156	126.46	6.188	128.20	6.200	14.64	14.600	21.13	13.805	20.50	13.914
H23	154.50	3.943	131.08	3.874	131.75	3.977	7.58	12.870	13.96	12.102	14.06	12.213
H24	25.67	12.456	25.65	12.183	26.98	12.150	110.60	5.764	108.68	5.567	106.46	5.748
H24'	26.42	13.121	23.97	13.519	27.16	12.935	113.61	6.371	119.87	6.333	111.36	6.340
H24a	25.87	12.767	24.71	12.843	26.90	12.521	112.33	6.022	65.31	5.909	109.15	5.997
H25a	30.93	10.860	31.51	12.373	32.45	10.715	91.20	5.583	101.79	6.606	88.44	5.751
H26	16.13	12.303	18.25	11.984	18.79	12.224	127.47	4.306	120.18	4.341	121.08	4.597
H26'	23.10	12.429	24.05	12.618	22.16	13.251	114.61	5.364	114.32	5.643	121.59	5.867
H27a	17.96	14.452	16.88	14.171	13.34	13.981	135.59	6.368	136.67	5.996	143.78	5.460

Table 89 Structural parameters θ_i and r_i in the solid state $Eu_2(L^{AB})_3$ complex

	Ln ion in bpb site						Ln ion in bpa site					
	Ligand strand 1		Ligand strand 2		Ligand strand 3		Ligand strand 1		Ligand strand 2		Ligand strand 3	
	θ_i	r_i	θ_i	r_i	θ_i	r_i	θ_i	r_i	θ_i	r_i	θ_i	r_i
H1	21.66	12.822	21.08	12.958	23.77	12.434	118.45	5.383	120.44	5.406	112.02	5.406
H2	27.96	12.655	27.31	12.816	29.33	12.260	107.10	6.208	109.09	6.222	102.55	6.152
H3	30.56	10.842	29.79	10.961	31.60	10.486	89.83	5.513	91.69	5.448	85.62	5.511
H4	44.12	8.387	43.50	8.391	44.26	8.322	60.29	6.722	60.52	6.635	59.71	6.726
H4'	38.54	9.298	37.85	9.369	38.85	9.131	70.26	6.155	71.23	6.072	68.63	6.150
H5a	40.85	10.505	40.94	10.451	39.84	10.435	78.44	7.013	77.99	7.002	78.67	6.818
H6	46.74	7.576	46.45	7.456	46.98	7.473	52.98	6.910	52.05	6.853	52.10	6.924
H7	51.40	6.633	51.68	6.648	51.46	6.951	44.83	7.352	44.92	7.386	47.28	7.401
H8	21.68	6.905	22.58	7.135	21.95	6.878	40.99	3.889	44.75	3.892	40.86	3.930
H9	52.17	6.609	52.55	6.722	52.10	6.957	44.57	7.438	45.39	7.496	47.23	7.478
H9'	43.05	7.376	43.69	7.421	43.04	7.546	51.80	6.407	52.13	6.493	53.31	6.422
H10	33.98	4.015	37.42	3.993	36.51	4.117	20.44	6.427	21.43	6.640	22.06	6.521
H11	53.04	7.137	54.55	7.144	57.61	7.264	48.41	7.625	48.17	7.810	48.32	8.212
H12	62.92	6.526	62.38	6.653	67.97	6.785	42.32	8.630	43.24	8.604	42.74	9.268
H13	68.91	6.611	71.94	6.468	85.82	6.227	41.49	9.310	39.93	9.581	34.91	10.851
H13'	70.82	6.239	69.89	6.196	89.34	5.748	38.90	9.383	38.86	9.274	31.76	10.921
H14a	89.49	5.907	91.47	5.948	72.69	7.218	32.42	11.017	32.03	11.211	43.73	9.969
H15	76.23	5.483	74.29	5.513	79.86	5.522	33.50	9.649	34.03	9.483	32.97	9.988
H16	87.31	6.227	83.58	6.326	89.34	6.325	34.47	10.990	36.02	10.689	34.28	11.230
H17	102.31	5.518	94.75	5.475	101.72	5.606	27.11	11.828	29.09	11.221	27.62	11.840
H18	101.66	5.658	92.18	5.989	115.32	6.115	27.83	11.868	31.99	11.296	24.79	13.182
H18'	108.49	6.192	99.59	6.528	121.13	6.764	27.43	12.749	31.66	12.264	24.26	14.093
H19a	118.15	7.101	110.81	6.941	100.97	6.729	26.24	14.161	28.77	13.482	31.85	12.518
H20	127.14	6.661	114.28	6.915	123.51	6.900	21.66	14.389	27.33	13.728	23.61	14.364
H21	138.00	7.297	120.94	7.320	126.86	7.453	18.29	15.561	25.58	14.541	23.34	15.054
H22	147.09	6.275	126.48	6.310	127.17	6.277	13.13	15.012	21.17	14.052	20.83	14.064
H23	156.46	4.147	130.71	3.985	130.82	3.891	7.18	13.258	14.18	12.327	13.90	12.255
H24	25.83	12.447	25.83	12.284	27.03	12.161	108.85	5.731	107.67	5.617	105.00	5.722
H24'	26.69	13.160	23.73	13.667	27.17	13.126	112.15	6.382	119.88	6.343	111.21	6.429
H24a	26.10	12.783	24.69	12.970	26.97	12.626	110.72	6.013	65.82	5.939	108.36	6.033
H25a	31.48	11.012	30.95	12.688	32.94	11.052	90.39	5.751	103.19	6.702	89.27	6.010
H26	15.74	12.543	18.19	12.212	17.94	12.233	128.65	4.357	120.55	4.427	121.25	4.407
H26'	22.67	12.657	23.96	12.767	23.35	12.973	115.50	5.405	114.06	5.678	116.45	5.743
H27a	17.98	14.621	17.09	14.408	15.15	14.287	135.26	6.412	136.23	6.121	139.93	5.800

Table 90 Structural parameters θ_i and r_i in the solid state $Ce_2(L^{AB3})_3$ complex

	Ln ion in bpb site						Ln ion in bpa site					
	Ligand strand 1		Ligand strand 2		Ligand strand 3		Ligand strand 1		Ligand strand 2		Ligand strand 3	
	θ_i	r_i	θ_i	r_i	θ_i	r_i	θ_i	r_i	θ_i	r_i	θ_i	r_i
H1	20.70	12.796	24.77	12.122	24.68	12.126	122.40	5.359	110.60	5.425	110.77	5.416
H3	28.60	11.222	32.87	10.071	35.06	9.325	98.00	5.424	83.33	5.503	74.70	5.553
H4	42.54	9.620	46.37	7.811	45.21	8.383	72.83	6.808	56.74	6.761	61.78	6.752
H4'	35.82	10.597	40.79	8.561	41.03	8.800	85.34	6.223	64.93	6.175	66.94	6.278
H5a	41.70	9.518	41.86	10.022	37.88	10.404	72.54	6.637	76.27	6.885	82.10	6.450
H6	46.86	8.286	49.39	7.005	47.92	7.380	60.42	6.953	49.52	6.991	52.84	6.874
H7	51.69	7.442	53.08	6.547	52.30	6.597	52.48	7.362	45.38	7.354	45.87	7.272
H8	23.20	6.612	23.48	6.895	21.68	6.695	40.77	3.988	44.73	3.904	40.68	3.793
H9	54.73	6.589	53.23	6.870	52.52	6.558	45.46	7.548	47.82	7.426	45.54	7.291
H9'	46.24	7.460	43.45	7.405	42.89	7.257	53.83	6.674	53.84	6.308	52.57	6.220
H10	36.27	4.037	39.20	3.905	30.99	3.918	22.23	6.313	22.12	6.554	19.37	6.083
H11	55.63	7.170	55.68	7.228	57.26	6.962	49.56	7.781	49.92	7.802	47.68	7.920
H12	63.62	6.682	66.24	6.735	65.78	6.529	44.32	8.567	43.99	8.874	42.85	8.755
H13	73.05	6.434	85.27	6.169	84.42	6.001	40.44	9.489	35.60	10.562	31.52	10.526
H13'	71.46	6.175	88.78	5.690	88.70	5.504	39.37	9.230	32.36	10.627	35.05	10.400
H14a	92.77	5.918	72.96	7.192	72.47	7.091	32.21	11.091	44.53	9.805	44.16	9.705
H15	73.10	5.561	77.86	5.540	79.27	5.568	35.42	9.181	34.32	9.606	34.16	9.742
H16	83.08	6.380	86.05	6.333	90.70	6.400	37.25	10.464	36.10	10.721	34.89	11.187
H17	93.46	5.644	97.77	5.593	103.32	5.580	30.83	10.992	29.35	11.306	27.61	11.718
H18	90.13	5.905	116.92	6.076	115.96	6.458	32.94	10.858	23.28	14.053	27.66	13.425
H18'	96.03	6.472	124.46	6.736	114.13	6.829	33.36	11.706	24.57	13.029	25.96	13.263
H19a	108.38	7.102	103.75	7.020	94.01	6.400	30.73	13.190	32.35	12.744	33.78	11.483
H20	112.83	6.840	129.36	6.952	119.17	6.716	28.21	13.336	21.70	14.537	25.36	13.691
H21	122.07	7.271	133.04	7.314	129.49	7.242	25.43	14.349	20.78	15.069	22.19	14.799
H22	130.42	6.135	133.10	6.097	136.61	6.171	19.66	13.885	18.55	13.991	17.34	14.229
H23	138.15	3.898	134.42	3.868	145.68	4.027	12.23	12.280	13.17	12.124	10.36	12.629
H24	26.59	11.976	28.92	11.652	17.87	13.314	106.73	5.597	101.05	5.741	131.17	5.429
H24'	27.89	12.804	30.37	12.246	13.22	14.428	110.32	6.387	103.34	6.363	146.30	5.946
H24a	27.10	12.372	29.48	11.926	15.45	13.861	108.78	5.953	102.34	6.007	139.10	5.638
H25a	32.97	10.661	34.69	10.047	18.93	14.912	88.49	5.803	81.67	5.780	135.99	6.962
H26	21.06	11.586	19.21	11.682	8.92	13.414	112.37	4.503	116.72	4.302	153.39	4.646
H26'	25.82	12.472	26.28	11.936	8.46	14.649	111.40	5.835	106.90	5.523	158.22	5.806
H27a	17.77	13.705	20.33	13.801	1.20	13.862	133.38	5.756	128.71	6.145	176.52	4.770

Table 91 Structural parameters θ_i and r_i in the solid state $Pr_2(L^{AB3})_3$ complex

	Ln ion in bpb site						Ln ion in bpa site					
	Ligand strand 1		Ligand strand 2		Ligand strand 3		Ligand strand 1		Ligand strand 2		Ligand strand 3	
	θ_i	r_i	θ_i	r_i	θ_i	r_i	θ_i	r_i	θ_i	r_i	θ_i	r_i
H1	22.16	12.674	22.25	12.602	23.91	12.416	117.65	5.397	116.99	5.355	112.82	5.460
H3	30.49	10.810	30.79	10.715	34.43	9.841	90.86	5.485	89.70	5.485	78.66	5.675
H4	44.53	8.127	44.15	8.462	45.00	8.329	58.89	6.657	61.79	6.688	60.42	6.772
H4'	38.21	9.232	38.21	9.300	40.47	8.838	70.89	6.044	71.49	6.066	66.37	6.261
H5a	43.10	10.048	40.67	10.560	39.15	10.446	74.56	7.123	79.92	6.990	80.26	6.692
H6	48.43	7.101	46.88	7.711	47.71	7.253	49.60	6.976	54.86	6.883	50.95	6.909
H7	53.62	6.357	51.17	7.196	51.36	6.470	43.14	7.485	49.90	7.329	44.22	7.246
H8	23.68	6.965	21.45	6.940	21.70	6.934	44.42	3.997	42.46	3.760	42.58	3.789
H9	54.50	6.660	51.94	6.963	51.85	6.524	45.30	7.628	47.98	7.380	44.60	7.307
H9'	44.81	7.347	42.85	7.524	42.58	7.333	52.17	6.556	54.01	6.324	52.31	6.270
H10	37.30	3.912	33.17	4.178	36.30	3.809	21.17	6.564	21.73	6.175	20.10	6.563
H11	57.23	7.125	57.40	7.172	50.41	7.152	48.09	8.050	48.38	8.083	49.69	7.227
H12	67.16	6.587	68.39	6.591	58.51	6.738	42.28	9.023	42.00	9.158	45.16	8.103
H13	86.23	6.074	86.22	5.935	67.94	6.594	34.45	10.713	33.81	10.642	42.13	9.110
H13'	89.94	5.611	89.92	5.489	67.81	6.239	31.30	10.799	30.75	10.735	40.03	8.981
H14a	73.96	7.028	74.10	7.124	87.96	6.233	42.81	9.939	43.26	9.998	34.65	10.955
H15	82.03	5.521	80.23	5.522	75.58	5.536	32.85	10.079	33.26	9.922	34.32	9.510
H16	90.77	6.383	88.80	6.344	87.21	6.338	34.41	11.295	34.88	11.092	35.35	10.942
H17	101.21	5.523	99.33	5.584	100.38	5.540	27.73	11.644	28.52	11.539	28.04	11.592
H18	106.23	6.245	98.38	5.946	101.92	5.926	28.64	12.509	30.22	11.688	29.01	11.957
H18'	106.03	6.634	104.79	6.517	108.48	6.475	29.95	12.771	30.04	12.587	28.55	12.848
H19a	86.20	6.288	116.32	7.066	119.61	7.028	35.44	10.821	27.12	13.894	25.68	14.098
H20	113.73	6.810	119.20	6.833	122.89	6.766	27.50	13.499	25.39	13.910	23.76	14.102
H21	120.78	7.331	127.47	7.245	130.46	7.265	25.88	14.432	22.86	14.803	21.62	15.003
H22	126.35	6.108	133.23	6.119	137.34	6.088	20.94	13.763	18.37	14.145	16.75	14.317
H23	134.18	3.962	140.90	3.906	143.55	3.943	13.33	12.326	11.36	12.509	10.69	12.624
H24	27.04	12.223	27.12	12.050	15.10	13.715	106.58	5.798	105.20	5.692	138.29	5.370
H24'	28.39	12.873	28.53	12.681	12.65	14.854	108.87	6.468	107.49	6.350	148.27	6.185
H24a	27.56	12.528	27.66	12.346	13.68	14.274	107.91	6.092	106.54	5.979	143.94	5.735
H25a(1)	33.96	10.844	33.48	10.517	20.97	13.894	87.74	6.062	85.46	5.820	126.95	6.222
H25a(2)					10.82	14.863					152.53	6.048
H26	20.83	11.663	19.42	11.689	9.71	13.115	111.91	4.470	114.74	4.279	149.09	4.306
H26'	25.72	12.538	25.97	12.107	10.71	14.474	110.76	5.819	107.30	5.553	151.67	5.668
H27a(1)	17.29	13.890	19.08	13.836	1.40	14.316	134.31	5.769	130.35	5.935	176.06	5.091
H27a(2)					12.35	15.117					149.70	6.409

Table 92 Structural parameters θ_i and r_i in the solid state $Sm_2(L^{AB3})_3$ complex

	Ln ion in bpb site						Ln ion in bpa site					
	Ligand strand 1		Ligand strand 2		Ligand strand 3		Ligand strand 1		Ligand strand 2		Ligand strand 3	
	θ_i	r_i	θ_i	r_i	θ_i	r_i	θ_i	r_i	θ_i	r_i	θ_i	r_i
H1	20.03	12.871	24.10	12.187	24.19	12.177	123.43	5.283	111.33	5.342	111.10	5.348
H3	27.79	11.337	32.37	10.138	34.31	9.377	99.11	5.353	83.49	5.463	74.79	5.477
H4	42.20	9.718	45.46	7.842	44.67	8.407	73.10	6.822	56.63	6.693	61.54	6.723
H4'	35.62	10.709	40.03	8.612	40.75	8.742	85.63	6.255	64.96	6.114	65.84	6.254
H5a	41.22	9.561	41.38	10.029	37.52	10.456	72.47	6.607	75.97	6.834	82.05	6.430
H6	46.44	8.172	47.99	7.177	47.46	7.357	59.05	6.905	50.61	6.900	52.18	6.862
H7	51.63	7.427	52.55	6.507	51.65	6.719	51.86	7.403	44.67	7.348	46.43	7.273
H8	23.04	6.704	23.04	6.961	21.86	6.783	41.05	3.995	44.46	3.890	41.18	3.836
H9	54.52	6.571	52.81	6.929	52.61	6.569	44.91	7.579	47.87	7.444	45.14	7.363
H9'	46.23	7.435	43.16	7.436	43.22	7.320	53.05	6.718	53.54	6.324	52.49	6.319
H10	36.78	4.056	38.77	3.934	32.63	3.923	22.26	6.411	21.94	6.592	19.79	6.247
H11	55.37	7.159	56.56	7.242	55.70	7.017	49.04	7.801	49.34	7.967	47.95	7.806
H12	62.84	6.662	65.82	6.709	65.67	6.535	43.99	8.535	43.57	8.880	42.54	8.808
H13	72.38	6.401	88.96	5.635	84.07	6.015	40.10	9.471	31.82	10.686	34.95	10.444
H13'	70.63	6.152	85.18	6.114	88.22	5.525	39.10	9.203	35.10	10.595	31.50	10.568
H14a	92.21	5.900	72.57	7.238	72.18	7.099	32.07	11.104	44.55	9.843	43.96	9.737
H15	72.65	5.481	78.42	5.479	78.77	5.523	34.73	9.183	33.59	9.702	33.75	9.750
H16	82.69	6.326	85.84	6.306	90.96	6.363	36.83	10.466	35.79	10.755	34.41	11.259
H17	93.49	5.593	98.60	5.521	104.07	5.523	30.38	11.038	28.61	11.400	26.98	11.810
H18	90.51	5.889	117.46	6.046	113.41	6.739	32.53	10.952	24.14	13.117	27.54	13.375
H18'	97.29	6.465	124.60	6.716	116.54	6.437	32.66	11.882	23.04	14.123	25.53	13.363
H19a	108.51	7.100	103.81	6.983	91.89	6.386	30.49	13.271	32.01	12.794	34.20	11.356
H20	114.15	6.805	128.80	6.914	119.88	6.654	27.43	13.481	21.74	14.549	24.78	13.764
H21	121.85	7.274	134.17	7.291	130.06	7.263	25.39	14.412	20.14	15.191	21.86	14.930
H22	131.58	6.175	135.27	6.123	137.48	6.217	19.18	14.061	17.66	14.202	16.98	14.391
H23	139.04	3.881	135.03	3.895	147.68	4.005	11.86	12.377	12.99	12.251	9.67	12.748
H24	25.95	12.013	28.26	11.826	17.57	13.356	107.13	5.501	102.43	5.734	131.37	5.373
H24'	27.25	12.917	29.73	12.402	12.88	14.416	111.26	6.346	104.47	6.352	146.59	5.836
H24a	26.47	12.447	28.81	12.091	15.12	13.874	109.46	5.884	103.63	5.995	139.33	5.553
H25a	32.41	10.904	34.14	10.174	18.11	15.035	90.23	5.844	82.41	5.760	137.54	6.924
H26	20.81	11.715	18.83	11.781	8.74	13.454	113.02	4.522	117.37	4.282	153.59	4.596
H26'	25.16	12.680	25.90	12.004	8.36	14.717	113.06	5.859	107.13	5.487	158.31	5.789
H27a	16.95	13.798	20.12	13.947	1.25	13.979	134.96	5.685	129.21	6.192	176.36	4.803

Table 93 Structural parameters θ_i and r_i in the solid state PrLu(L^{AB3})$_3$ complex

	Ln ion in bpb site						Ln ion in bpa site					
	Ligand strand 1		Ligand strand 2		Ligand strand 3		Ligand strand 1		Ligand strand 2		Ligand strand 3	
	θ_i	r_i	θ_i	r_i	θ_i	r_i	θ_i	r_i	θ_i	r_i	θ_i	r_i
H1	21.01	12.750	22.30	12.499	23.87	12.255	120.76	5.319	116.67	5.307	112.21	5.357
H3	29.88	10.776	31.36	10.473	33.63	9.763	91.72	5.371	87.49	5.456	78.98	5.509
H4	44.34	8.131	43.86	8.527	44.50	8.308	59.36	6.605	62.82	6.642	60.79	6.672
H4'	38.35	9.178	38.55	9.224	39.89	8.803	70.79	6.030	71.10	6.076	66.73	6.145
H5a	42.12	10.183	39.02	10.656	38.62	10.416	76.59	7.021	82.33	6.769	80.88	6.584
H6	47.94	7.201	46.20	7.848	47.41	7.279	50.82	6.897	56.49	6.793	51.54	6.843
H7	53.25	6.428	50.59	7.147	51.60	6.557	43.99	7.416	49.93	7.216	45.17	7.246
H8	23.47	6.835	21.83	6.883	21.75	6.866	43.07	3.987	42.51	3.788	42.21	3.787
H9	54.34	6.550	51.70	6.974	52.60	6.466	44.78	7.556	48.40	7.319	44.35	7.348
H9'	45.16	7.333	42.67	7.554	43.56	7.315	52.35	6.567	54.68	6.275	52.41	6.362
H10	36.78	3.897	33.62	4.169	38.59	3.808	21.06	6.494	22.01	6.159	20.94	6.645
H11	57.00	7.135	57.11	7.176	50.75	7.216	48.49	7.991	48.75	8.015	50.44	7.248
H12	67.02	6.619	67.60	6.654	58.02	6.746	42.73	8.981	42.79	9.057	45.57	8.013
H13	85.66	6.108	85.59	5.968	67.44	6.638	34.93	10.636	34.30	10.559	42.73	9.034
H13'	90.04	5.605	88.77	5.514	67.28	6.256	31.39	10.761	31.31	10.608	40.46	8.892
H14a	74.19	7.058	73.48	7.150	87.24	6.302	43.09	9.940	43.80	9.904	35.34	10.884
H15	82.13	5.537	78.87	5.518	75.65	5.547	33.07	10.052	33.70	9.757	34.54	9.478
H16	92.65	6.387	88.43	6.363	86.60	6.311	33.95	11.425	35.23	11.027	35.57	10.829
H17	103.03	5.595	98.04	5.564	100.69	5.573	27.56	11.780	28.95	11.382	28.19	11.591
H18	105.37	6.174	98.17	5.953	100.37	5.952	28.82	12.348	30.44	11.631	29.73	11.807
H18'	107.64	6.630	104.60	6.544	107.53	6.494	29.45	12.852	30.31	12.547	29.07	12.744
H19a	87.56	6.361	115.95	7.067	118.85	7.077	35.50	10.945	27.37	13.822	26.20	14.039
H20	114.15	6.854	119.33	6.827	121.63	6.782	27.55	13.520	25.42	13.868	24.39	13.986
H21	119.53	7.240	127.56	7.257	129.19	7.291	26.29	14.222	22.92	14.772	22.28	14.902
H22	126.75	6.173	135.41	6.132	136.24	6.131	21.01	13.793	17.63	14.216	17.31	14.255
H23	134.28	3.933	141.72	3.923	142.89	3.938	13.28	12.256	11.21	12.500	10.91	12.549
H24	25.50	12.518	25.95	12.214	16.88	13.676	111.44	5.790	108.62	5.640	134.52	5.569
H24'	26.99	13.094	26.91	12.925	12.53	14.777	112.70	6.442	111.83	6.302	148.56	6.146
H24a	26.08	12.784	26.26	12.549	14.59	14.215	112.26	6.073	110.46	5.926	141.95	5.809
H25a	32.78	11.090	32.47	10.787	20.09	14.277	91.35	6.006	89.20	5.792	130.75	6.474
H26	19.97	11.774	18.45	11.906	10.70	13.207	115.10	4.441	119.27	4.320	147.13	4.519
H26'	25.11	12.571	24.10	12.600	9.74	14.533	112.42	5.771	114.27	5.644	154.44	5.699
H27a	17.32	13.968	15.85	13.849	1.56	13.840	134.96	5.877	137.59	5.608	175.37	4.668

Table 94 Structural parameters θ_i and r_i in the solid state NdLu(L^{AB3})$_3$ complex

	Ln ion in bpb site						Ln ion in bpa site					
	Ligand strand 1		Ligand strand 2		Ligand strand 3		Ligand strand 1		Ligand strand 2		Ligand strand 3	
	θ_i	r_i	θ_i	r_i	θ_i	r_i	θ_i	r_i	θ_i	r_i	θ_i	r_i
H1	20.18	12.787	24.34	12.174	24.35	12.197	122.99	5.259	111.28	5.385	111.43	5.402
H3	27.71	11.297	32.49	10.072	34.56	9.283	99.33	5.324	83.23	5.448	74.17	5.474
H4	41.75	9.598	45.21	7.795	44.75	8.348	72.81	6.690	56.61	6.626	61.36	6.696
H4'	35.06	10.574	39.36	8.641	40.65	8.731	85.46	6.093	65.85	6.006	66.16	6.218
H5a	41.25	9.572	41.59	9.928	37.48	10.386	72.90	6.603	75.43	6.809	81.93	6.383
H6	46.32	8.191	48.20	7.052	47.36	7.283	59.56	6.871	49.83	6.880	51.88	6.810
H7	51.78	7.343	52.42	6.436	51.56	6.670	51.46	7.375	44.38	7.293	46.31	7.225
H8	22.39	6.612	23.13	6.922	21.45	6.781	39.79	3.936	44.44	3.883	41.26	3.760
H9	54.56	6.630	52.54	6.956	52.45	6.601	45.58	7.563	48.37	7.387	45.66	7.318
H9'	45.94	7.452	42.76	7.422	42.90	7.283	53.55	6.658	53.79	6.245	52.51	6.248
H10	36.17	4.059	37.98	3.889	31.10	3.961	22.23	6.332	21.51	6.527	19.60	6.100
H11	54.77	7.169	56.57	7.232	55.67	7.016	49.49	7.702	49.51	7.937	48.19	7.773
H12	63.44	6.637	65.84	6.721	65.64	6.527	43.89	8.562	43.83	8.854	42.69	8.769
H13	73.49	6.387	88.69	5.711	84.35	6.022	39.90	9.546	32.37	10.665	35.04	10.437
H13'	71.05	6.222	84.25	6.184	88.12	5.528	39.58	9.235	35.84	10.508	31.67	10.524
H14a	92.47	5.879	72.30	7.191	72.34	7.066	32.02	11.077	44.58	9.760	43.91	9.709
H15	72.70	5.496	78.98	5.460	79.62	5.508	34.97	9.156	33.51	9.708	33.63	9.783
H16	83.03	6.332	85.76	6.314	90.45	6.359	36.90	10.467	35.99	10.716	34.69	11.174
H17	93.31	5.588	99.21	5.488	103.41	5.558	30.53	10.983	28.41	11.387	27.41	11.745
H18	90.70	5.882	116.46	6.126	110.98	6.636	32.56	10.928	24.80	13.074	28.29	13.075
H18'	97.43	6.479	123.60	6.758	114.81	6.366	32.78	11.866	23.61	14.054	26.07	13.147
H19a	108.37	7.066	103.77	6.948	92.08	6.439	30.54	13.196	32.02	12.728	34.47	11.368
H20	113.97	6.803	128.06	6.910	120.31	6.700	27.58	13.427	22.10	14.460	24.80	13.791
H21	122.16	7.269	134.55	7.311	129.69	7.211	25.32	14.389	20.06	15.188	21.99	14.821
H22	130.77	6.138	134.74	6.195	137.72	6.147	19.47	13.944	18.06	14.198	16.81	14.297
H23	137.72	3.949	134.33	3.892	146.82	3.984	12.42	12.349	13.21	12.180	9.92	12.662
H24	25.83	12.073	27.95	11.814	17.98	13.201	108.19	5.537	103.19	5.687	129.99	5.319
H24'	26.94	12.920	29.64	12.355	13.56	14.286	112.13	6.319	104.68	6.316	144.81	5.812
H24a	26.24	12.480	28.63	12.061	15.65	13.733	110.44	5.888	104.07	5.958	137.80	5.515
H25a	32.58	10.863	33.91	10.137	18.70	14.999	90.15	5.849	82.69	5.702	136.51	6.987
H26	20.33	11.693	18.82	11.781	8.70	13.407	114.21	4.454	117.91	4.301	153.76	4.587
H26'	25.22	12.533	25.92	11.970	8.25	14.661	112.39	5.776	107.28	5.480	158.61	5.769
H27a	17.37	13.845	20.21	13.935	1.05	13.910	134.60	5.805	129.29	6.220	176.94	4.776

Values of structure factors G_i ($G_i = (3\cos^2\theta_i - 1)/r_i^3$) were calculated for each ligand strand (L^1, L^2 and L^3) of the complex and average G_i values were calculated for each of the eight complexes. The values are given in Table 95 - Table 102.

Note that an alternative way to calculate average structural factors would be to average θ_i and r_i values for Hi in the three ligand strands and then calculate G_i values based on these averaged coordinates. This would be erroneous since the geometrical midpoint cannot be calculated like this with polar coordinates (as opposed to with Cartesian coordinates). Take for example the two points (θ_1, r_1) = (0, 1) and (θ_2, r_2) = (90, 1). The midpoint of these two points is (θ_3, r_3) = (45, 1/ 2) (≈ (45, 0.707)) and not (45, 1) as the result of averaging the polar coordinates would be.

Table 95 G_i **factors (·10^3) calculated for the solid state LaEu(L^{AB})$_3$ complex**

	Ln ion in bpb site					Ln ion in bpa site				
	L^1	L^2	L^3	Mean	St.dev. %	L^1	L^2	L^3	Mean	St.dev. %
H1	0.77	0.77	0.81	0.78(2)	3	-2.01	-1.39	-3.62	-2(1)	49
H2	0.69	0.68	0.71	0.69(2)	2	-3.07	-2.95	-3.80	-3.3(5)	14
H3	0.99	0.97	1.06	1.01(5)	5	-6.08	-6.04	-5.89	-6.0(1)	2
H4	0.97	0.99	0.92	0.96(4)	4	-0.90	-0.99	-0.72	-0.9(1)	16
H4'	1.08	1.09	1.10	1.089(7)	1	-3.03	-3.28	-2.49	-2.9(4)	14
H5a	0.62	0.61	0.67	0.63(3)	5	-2.56	-2.51	-2.79	-2.6(1)	6
H6	0.91	0.91	0.93	0.916(8)	1	0.26	0.36	0.41	0.34(7)	22
H7	0.46	0.41	0.46	0.44(3)	7	1.08	1.20	1.01	1.10(9)	9
H8	5.01	4.33	4.76	4.7(3)	7	12.46	7.61	10.22	10(2)	24
H9	0.37	0.25	0.31	0.31(6)	20	1.26	1.08	0.85	1.1(2)	19
H9'	1.49	1.30	1.40	1.4(1)	7	0.48	0.27	0.16	0.3(2)	53
H10	17.91	14.45	14.28	16(2)	13	6.59	5.75	6.16	6.2(4)	7
H11	0.00	-0.01	-0.41	-0.1(2)	169	0.70	0.63	0.55	0.63(8)	12
H12	-1.44	-1.34	-2.01	-1.6(4)	23	0.93	0.88	0.81	0.87(6)	7
H13	-2.14	-2.69	-4.17	-3(1)	35	0.78	0.84	0.82	0.81(3)	4
H13'	-2.92	-2.77	-5.36	-4(1)	40	0.91	0.98	0.92	0.94(4)	4
H14a	-4.90	-4.56	-1.99	-4(2)	42	0.87	0.81	0.55	0.7(2)	23
H15	-4.78	-4.42	-5.30	-4.8(4)	9	1.23	1.26	1.13	1.20(7)	6
H16	-3.88	-3.71	-3.86	-3.82(9)	2	0.76	0.78	0.74	0.76(2)	2
H17	-5.26	-5.51	-5.25	-5.3(1)	3	0.86	0.89	0.86	0.87(2)	2
H18	-4.89	-4.60	-2.01	-4(2)	41	0.82	0.81	0.64	0.8(1)	14
H18'	-3.10	-3.34	-0.92	-2(1)	54	0.67	0.65	0.55	0.62(7)	11
H19a	-1.13	-1.80	-2.92	-2.0(9)	46	0.50	0.55	0.59	0.55(5)	8
H20	0.03	-1.41	-0.26	-0.5(8)	139	0.54	0.54	0.52	0.53(1)	2
H21	1.44	-0.65	0.13	0(1)	349	0.48	0.47	0.47	0.472(6)	1
H22	4.68	0.07	0.66	2(3)	139	0.58	0.61	0.60	0.59(2)	3
H23	22.52	3.46	5.54	11(10)	100	0.91	1.01	1.02	0.98(6)	6
H24	0.76	0.81	0.80	0.79(2)	3	-3.65	-4.21	-4.45	-4.1(4)	10
H24'	0.63	0.62	0.63	0.626(7)	1	-2.20	-1.05	-2.44	-1.9(7)	39
H24a	0.70	0.71	0.71	0.708(7)	1	-2.87	-2.41	-3.36	-2.9(5)	17
H25a	0.93	0.62	0.88	0.8(2)	20	-5.63	-3.05	-4.92	-5(1)	29
H26	0.94	0.99	0.97	0.97(3)	3	1.06	-3.88	-2.77	-2(3)	139
H26'	0.79	0.73	0.71	0.74(4)	5	-2.97	-2.56	-1.85	-2.5(6)	23
H27a	0.57	0.63	0.65	0.62(5)	7	1.98	2.94	4.66	3(1)	42

Table 96 G_i **factors (·10^3) calculated for the solid state LaTb(L^{AB})$_3$ complex**

	Ln ion in bpb site					Ln ion in bpa site				
	L^1	L^2	L^3	Mean	St.dev. %	L^1	L^2	L^3	Mean	St.dev. %
H1	0.79	0.78	0.80	0.79(1)	1	-1.91	-1.51	-3.52	-2(1)	46
H2	0.67	0.68	0.71	0.69(2)	3	-3.01	-2.97	-3.83	-3.3(5)	15
H3	1.00	0.98	1.08	1.02(5)	5	-6.30	-6.32	-5.99	-6.2(2)	3
H4	0.84	1.01	0.93	0.93(9)	10	-0.95	-1.01	-0.73	-0.9(1)	16
H4'	1.00	1.12	1.09	1.07(6)	6	-2.55	-3.45	-2.39	-2.8(6)	20
H5a	0.63	0.63	0.69	0.65(3)	5	-2.71	-2.56	-2.86	-2.7(1)	5
H6	0.92	0.93	1.04	0.96(7)	7	0.27	0.21	0.56	0.3(2)	54
H7	0.50	0.56	0.45	0.50(5)	10	1.09	1.35	1.02	1.2(2)	15
H8	4.81	4.28	4.71	4.6(3)	6	11.58	7.70	10.19	10(2)	20
H9	0.34	0.24	0.29	0.29(5)	18	1.27	1.12	0.88	1.1(2)	18
H9'	1.45	1.27	1.39	1.37(9)	7	0.48	0.29	0.22	0.3(1)	41
H10	17.17	14.55	15.45	16(1)	8	6.51	5.88	6.21	6.2(3)	5
H11	0.05	0.02	-0.42	-0.1(3)	219	0.71	0.67	0.57	0.65(7)	11
H12	-1.53	-1.33	-2.02	-1.6(4)	22	0.91	0.86	0.82	0.86(4)	5
H13	-2.14	-2.73	-4.17	-3(1)	35	0.78	0.85	0.82	0.82(4)	4
H13'	-2.83	-2.83	-5.38	-4(1)	40	0.90	0.98	0.93	0.94(4)	4
H14a	-5.14	-5.15	-1.98	-4(2)	45	0.89	0.87	0.56	0.8(2)	24
H15	-4.83	-4.32	-5.37	-4.8(5)	11	1.20	1.26	1.12	1.19(7)	6
H16	-3.93	-3.73	-3.79	-3.8(1)	3	0.77	0.76	0.72	0.75(2)	3
H17	-5.17	-5.60	-5.35	-5.4(2)	4	0.85	0.90	0.87	0.87(3)	3
H18	-4.71	-4.75	-2.10	-4(2)	39	0.81	0.83	0.64	0.8(1)	14
H18'	-3.05	-3.42	-1.04	-3(1)	51	0.66	0.66	0.55	0.62(6)	10
H19a	-1.12	-1.87	-3.09	-2(1)	49	0.50	0.54	0.61	0.55(6)	11
H20	-0.15	-1.38	-0.48	-0.7(6)	95	0.54	0.53	0.52	0.53(1)	2
H21	1.24	-0.57	-0.03	0.2(9)	441	0.48	0.48	0.47	0.477(6)	1
H22	3.95	0.25	0.62	2(2)	127	0.58	0.61	0.61	0.60(2)	3
H23	23.55	5.08	5.25	11(11)	94	0.91	1.03	1.00	0.98(6)	6
H24	0.74	0.80	0.77	0.77(3)	3	-3.28	-4.01	-4.00	-3.8(4)	11
H24'	0.62	0.61	0.64	0.62(1)	2	-2.01	-1.01	-2.36	-1.8(7)	39
H24a	0.69	0.70	0.71	0.70(1)	1	-2.59	-2.31	-3.14	-2.7(4)	16
H25a	0.94	0.62	0.92	0.8(2)	22	-5.74	-3.03	-5.24	-5(1)	31
H26	0.95	0.99	0.92	0.96(3)	4	1.38	-2.96	-2.06	-1(2)	189
H26'	0.80	0.75	0.68	0.74(6)	8	-3.11	-2.73	-0.88	-2(1)	53
H27a	0.57	0.61	0.67	0.62(5)	9	2.06	2.72	5.85	4(2)	57

Table 97 G_i **factors (·10^3) calculated for the solid state Eu$_2$(L^{AB})$_3$ complex**

	Ln ion in bpb site					Ln ion in bpa site				
	L^1	L^2	L^3	Mean	St.dev. %	L^1	L^2	L^3	Mean	St.dev. %
H1	0.75	0.74	0.79	0.76(2)	3	-2.05	-1.46	-3.66	-2(1)	48
H2	0.66	0.65	0.69	0.67(2)	3	-3.10	-2.82	-3.69	-3.2(4)	14
H3	0.96	0.96	1.02	0.98(4)	4	-5.97	-6.17	-5.87	-6.0(2)	3
H4	0.93	0.98	0.93	0.95(3)	3	-0.87	-0.94	-0.78	-0.86(8)	9
H4'	1.04	1.06	1.08	1.06(2)	2	-2.82	-3.08	-2.59	-2.8(2)	9
H5a	0.62	0.62	0.68	0.64(3)	5	-2.55	-2.53	-2.79	-2.6(1)	5
H6	0.94	1.02	0.95	0.97(5)	5	0.26	0.42	0.40	0.36(8)	23
H7	0.57	0.52	0.49	0.53(4)	8	1.28	1.25	0.94	1.2(2)	16
H8	4.83	4.29	4.86	4.7(3)	7	12.06	8.71	11.80	11(2)	17
H9	0.45	0.36	0.39	0.40(4)	11	1.27	1.14	0.92	1.1(2)	16
H9'	1.50	1.39	1.40	1.43(6)	4	0.56	0.48	0.27	0.4(2)	35
H10	16.42	14.02	13.44	15(2)	11	6.16	5.46	5.69	5.8(4)	6
H11	0.23	0.03	-0.36	0.0(3)	861	0.73	0.70	0.59	0.67(7)	11
H12	-1.36	-1.21	-1.85	-1.5(3)	23	1.00	0.93	0.78	0.9(1)	12
H13	-2.12	-2.63	-4.08	-3(1)	35	0.85	0.87	0.80	0.84(4)	4
H13'	-2.78	-2.71	-5.26	-4(1)	40	0.99	1.03	0.90	0.97(7)	7
H14a	-4.85	-4.74	-1.95	-4(2)	43	0.85	0.82	0.57	0.7(2)	20
H15	-5.04	-4.66	-5.39	-5.0(4)	7	1.21	1.24	1.12	1.19(7)	6
H16	-4.11	-3.80	-3.95	-4.0(2)	4	0.78	0.79	0.74	0.77(3)	3
H17	-5.14	-5.97	-4.97	-5.4(5)	10	0.83	0.91	0.82	0.85(5)	6
H18	-4.84	-4.63	-1.97	-4(2)	42	0.81	0.80	0.64	0.75(9)	12
H18'	-2.94	-3.30	-0.64	-2(1)	63	0.66	0.64	0.53	0.61(7)	11
H19a	-0.93	-1.86	-2.93	-2(1)	53	0.50	0.53	0.59	0.54(5)	9
H20	0.32	-1.49	-0.26	-0.5(9)	193	0.53	0.53	0.51	0.53(1)	2
H21	1.69	-0.53	0.19	0(1)	251	0.45	0.47	0.45	0.46(1)	2
H22	4.51	0.24	0.38	2(2)	142	0.55	0.58	0.58	0.57(2)	4
H23	21.33	4.36	4.79	10(10)	95	0.84	0.97	0.99	0.93(8)	9
H24	0.74	0.77	0.77	0.76(2)	2	-3.65	-4.08	-4.27	-4.0(3)	8
H24'	0.61	0.59	0.61	0.60(1)	2	-2.21	-1.00	-2.29	-1.8(7)	39
H24a	0.68	0.68	0.69	0.681(5)	1	-2.87	-2.37	-3.20	-2.8(4)	15
H25a	0.89	0.59	0.82	0.8(2)	20	-5.26	-2.80	-4.60	-4(1)	30
H26	0.90	0.94	0.94	0.93(2)	2	2.06	-2.60	-2.25	-1(3)	279
H26'	0.77	0.72	0.70	0.73(3)	5	-2.81	-2.74	-2.14	-2.6(4)	14
H27a	0.55	0.58	0.62	0.58(3)	6	1.95	2.46	3.88	3(1)	36

Table 98 G_i **factors (·10^3) calculated for the solid state $Ce_2(L^{AB3})_3$ complex**

	Ln ion in bpb site					Ln ion in bpa site				
	L^1	L^2	L^3	Mean	St.dev. %	L^1	L^2	L^3	Mean	St.dev. %
H1	0.78	0.83	0.83	0.81(3)	4	-0.90	-3.94	-3.92	-3(2)	60
H3	0.93	1.09	1.25	1.1(2)	15	-5.90	-5.76	-4.62	-5.4(7)	13
H4	0.71	0.90	0.83	0.8(1)	12	-2.34	-0.32	-1.07	-1(1)	82
H4'	0.82	1.15	1.04	1.0(2)	17	-4.07	-1.96	-2.18	-3(1)	42
H5a	0.78	0.66	0.77	0.74(7)	9	-2.50	-2.55	-3.52	-2.9(6)	20
H6	0.71	0.79	0.86	0.79(8)	10	-0.80	0.77	0.29	0.1(8)	914
H7	0.37	0.29	0.42	0.36(7)	18	0.28	1.21	1.18	0.9(5)	59
H8	5.31	4.65	5.30	5.1(4)	7	11.36	8.64	13.29	11(2)	21
H9	0.00	0.23	0.39	0.2(2)	95	1.11	0.86	1.22	1.1(2)	17
H9'	1.05	1.43	1.60	1.4(3)	21	0.15	0.18	0.45	0.3(2)	64
H10	14.44	13.46	20.03	16(4)	22	6.24	5.59	7.42	6.4(9)	14
H11	-0.12	-0.12	-0.36	-0.2(1)	69	0.56	0.51	0.72	0.6(1)	19
H12	-1.37	-1.68	-1.78	-1.6(2)	13	0.85	0.79	0.91	0.85(6)	7
H13	-2.80	-4.17	-4.50	-3.8(9)	24	0.86	0.83	1.01	0.9(1)	11
H13'	-2.96	-5.42	-5.99	-5(2)	34	1.01	0.95	0.90	0.95(6)	6
H14a	-4.79	-2.00	-2.04	-3(2)	54	0.84	0.56	0.60	0.7(2)	23
H15	-4.34	-5.10	-5.19	-4.9(5)	10	1.28	1.18	1.14	1.20(7)	6
H16	-3.68	-3.88	-3.81	-3.8(1)	3	0.79	0.78	0.73	0.76(3)	4
H17	-5.50	-5.40	-4.84	-5.2(4)	7	0.91	0.89	0.84	0.88(4)	4
H18	-4.86	-1.72	-1.58	-3(2)	68	0.87	0.55	0.56	0.7(2)	27
H18'	-3.57	-0.13	-1.57	-2(2)	98	0.68	0.67	0.61	0.65(4)	6
H19a	-1.96	-2.40	-3.76	-2.7(9)	35	0.53	0.55	0.71	0.6(1)	16
H20	-1.71	0.61	-0.95	-1(1)	174	0.56	0.52	0.56	0.55(3)	5
H21	-0.40	1.02	0.56	0.4(7)	185	0.49	0.47	0.49	0.483(8)	2
H22	1.13	1.77	2.49	1.8(7)	38	0.62	0.62	0.60	0.61(1)	2
H23	11.22	8.12	16.02	12(4)	34	1.01	1.03	0.94	1.00(5)	5
H24	0.81	0.82	0.73	0.79(5)	7	-4.29	-4.70	1.88	-2(4)	155
H24'	0.64	0.67	0.61	0.64(3)	5	-2.45	-3.26	5.12	0(5)	2348
H24a	0.73	0.75	0.67	0.72(4)	6	-3.27	-3.98	3.98	-1(4)	405
H25a	0.92	1.01	0.51	0.8(3)	33	-5.11	-4.85	1.64	-3(4)	138
H26	1.04	1.05	0.80	1.0(1)	15	-6.19	-4.94	13.94	1(11)	1206
H26'	0.74	0.83	0.62	0.7(1)	15	-3.02	-4.43	8.11	0(7)	3149
H27a	0.67	0.62	0.75	0.68(6)	9	2.18	0.75	18.33	7(10)	138

Table 99 G_i **factors (·10^3) calculated for the solid state $Pr_2(L^{AB3})_3$ complex**

	Ln ion in bpb site					Ln ion in bpa site				
	L^1	L^2	L^3	Mean	St.dev. %	L^1	L^2	L^3	Mean	St.dev. %
H1	0.77	0.78	0.79	0.782(8)	1	-2.25	-2.49	-3.37	-2.7(6)	22
H3	0.97	0.99	1.09	1.02(7)	6	-6.05	-6.06	-4.84	-5.7(7)	12
H4	0.98	0.90	0.87	0.91(6)	6	-0.68	-1.10	-0.87	-0.9(2)	24
H4'	1.08	1.06	1.07	1.07(1)	1	-3.07	-3.13	-2.11	-2.8(6)	21
H5a	0.59	0.62	0.71	0.64(6)	9	-2.18	-2.66	-3.05	-2.6(4)	17
H6	0.90	0.88	0.94	0.90(3)	4	0.77	-0.02	0.58	0.4(4)	93
H7	0.22	0.48	0.63	0.4(2)	47	1.42	0.62	1.42	1.2(5)	40
H8	4.49	4.78	4.77	4.7(2)	4	8.31	11.91	11.52	11(2)	19
H9	0.04	0.42	0.52	0.3(3)	78	1.09	0.86	1.34	1.1(2)	22
H9'	1.29	1.44	1.59	1.4(2)	11	0.46	0.14	0.49	0.4(2)	53
H10	15.01	15.11	17.16	16(1)	8	5.69	6.75	5.82	6.1(6)	9
H11	-0.33	-0.35	0.60	0.0(5)	1852	0.65	0.61	0.68	0.65(3)	5
H12	-1.92	-2.07	-0.59	-1.5(8)	53	0.87	0.86	0.92	0.88(4)	4
H13	-4.40	-4.72	-2.01	-4(1)	40	0.85	0.89	0.86	0.86(2)	3
H13'	-5.66	-6.05	-2.36	-5(2)	43	0.94	0.98	1.05	0.99(5)	5
H14a	-2.22	-2.14	-4.11	-3(1)	39	0.63	0.59	0.78	0.7(1)	15
H15	-5.60	-5.43	-4.80	-5.3(4)	8	1.09	1.12	1.22	1.14(7)	6
H16	-3.84	-3.91	-3.90	-3.88(4)	1	0.72	0.75	0.76	0.74(2)	3
H17	-5.26	-5.29	-5.31	-5.29(2)	0	0.86	0.86	0.86	0.857(1)	0
H18	-3.14	-4.45	-4.19	-3.9(7)	18	0.67	0.78	0.76	0.73(6)	8
H18'	-2.64	-2.91	-2.57	-2.7(2)	7	0.60	0.63	0.62	0.62(1)	2
H19a	-3.97	-1.16	-0.77	-2(2)	89	0.78	0.51	0.51	0.6(2)	26
H20	-1.63	-0.90	-0.37	-1.0(6)	65	0.55	0.54	0.54	0.544(8)	2
H21	-0.54	0.29	0.69	0.1(6)	436	0.48	0.48	0.47	0.475(3)	1
H22	0.24	1.78	2.76	2(1)	80	0.62	0.60	0.60	0.61(1)	2
H23	7.35	13.54	15.35	12(4)	35	0.98	0.96	0.94	0.96(2)	2
H24	0.76	0.79	0.70	0.75(5)	6	-3.88	-4.30	4.34	-1(5)	380
H24'	0.62	0.65	0.57	0.61(4)	7	-2.54	-2.85	4.95	0(4)	3025
H24a	0.69	0.72	0.63	0.68(5)	7	-3.17	-3.54	5.09	-1(5)	905
H25a(1)	0.83	0.93	0.60	0.7(2)	24	-4.47	-4.98	0.35	-1(5)	705
H25a(2)			0.58					6.15		
H26	1.02	1.04	0.85	1.0(1)	11	-6.52	-6.06	15.14	1(12)	1450
H26'	0.73	0.80	0.63	0.72(9)	12	-3.16	-4.29	7.27	0(6)	10701
H27a(1)	0.65	0.63	0.68	0.63(6)	10	2.42	1.23	15.05	6(6)	108
H27a(2)			0.54					4.70		

Table 100 G_i **factors (·10^3) calculated for the solid state $Sm_2(L^{AB3})_3$ complex**

	Ln ion in bpb site					Ln ion in bpa site				
	L^1	L^2	L^3	Mean	St.dev. %	L^1	L^2	L^3	Mean	St.dev. %
H1	0.77	0.83	0.83	0.81(3)	4	-0.61	-3.96	-3.99	-3(2)	68
H3	0.93	1.09	1.27	1.1(2)	16	-6.03	-5.90	-4.83	-5.6(7)	12
H4	0.70	0.99	0.87	0.9(1)	17	-2.35	-0.31	-1.05	-1(1)	84
H4'	0.80	1.19	1.08	1.0(2)	20	-4.01	-2.02	-2.03	-3(1)	43
H5a	0.80	0.68	0.78	0.75(6)	8	-2.52	-2.58	-3.55	-2.9(6)	20
H6	0.78	0.93	0.93	0.88(9)	10	-0.63	0.63	0.40	0.1(7)	501
H7	0.38	0.40	0.51	0.43(7)	17	0.36	1.30	1.11	0.9(5)	54
H8	5.11	4.57	5.08	4.9(3)	6	11.07	8.98	12.39	11(2)	16
H9	0.04	0.29	0.37	0.2(2)	75	1.16	0.85	1.23	1.1(2)	19
H9'	1.06	1.45	1.51	1.3(2)	18	0.28	0.23	0.44	0.3(1)	35
H10	13.86	13.53	18.68	15(3)	19	5.96	5.52	6.79	6.1(6)	11
H11	-0.09	-0.23	-0.14	-0.15(8)	50	0.61	0.54	0.73	0.63(9)	15
H12	-1.27	-1.64	-1.76	-1.6(3)	16	0.89	0.82	0.92	0.88(5)	6
H13	-2.76	-5.58	-4.45	-4(1)	33	0.89	0.96	0.89	0.91(4)	4
H13'	-2.88	-4.28	-5.91	-4(2)	35	1.04	0.85	1.00	1.0(1)	10
H14a	-4.85	-1.93	-2.01	-3(2)	57	0.84	0.55	0.60	0.7(2)	24
H15	-4.45	-5.34	-5.26	-5.0(5)	10	1.33	1.18	1.16	1.22(9)	7
H16	-3.76	-3.92	-3.88	-3.85(9)	2	0.80	0.78	0.73	0.77(4)	5
H17	-5.65	-5.54	-4.88	-5.4(4)	8	0.92	0.89	0.84	0.88(4)	4
H18	-4.90	-1.64	-1.72	-3(2)	68	0.86	0.66	0.57	0.7(2)	22
H18'	-3.52	-0.11	-1.50	-2(2)	100	0.67	0.55	0.60	0.61(6)	10
H19a	-1.95	-2.43	-3.83	-3(1)	36	0.53	0.55	0.72	0.6(1)	17
H20	-1.58	0.54	-0.87	-1(1)	169	0.56	0.52	0.56	0.55(3)	5
H21	-0.43	1.18	0.63	0.5(8)	177	0.48	0.47	0.48	0.476(7)	2
H22	1.36	2.24	2.62	2.1(6)	31	0.60	0.60	0.59	0.60(1)	2
H23	12.16	8.49	17.78	13(5)	37	0.99	1.01	0.92	0.97(4)	4
H24	0.82	0.80	0.72	0.78(5)	7	-4.45	-4.57	2.00	-2(4)	161
H24'	0.64	0.66	0.62	0.64(2)	3	-2.37	-3.17	5.49	0(5)	26925
H24a	0.73	0.74	0.67	0.71(4)	5	-3.27	-3.87	4.24	-1(5)	467
H25a	0.88	1.00	0.50	0.8(3)	33	-5.01	-4.96	1.91	-3(4)	148
H26	1.01	1.03	0.79	0.9(1)	14	-5.85	-4.66	14.49	1(11)	861
H26'	0.72	0.83	0.61	0.7(1)	15	-2.68	-4.48	8.20	0(7)	1985
H27a	0.66	0.61	0.73	0.67(6)	9	2.71	0.84	17.94	7(9)	131

Table 101 G_i **factors (·10^3) calculated for the solid state PrLu(L^{AB3})$_3$ complex**

	Ln ion in bpb site					Ln ion in bpa site				
	L^1	L^2	L^3	Mean	St.dev. %	L^1	L^2	L^3	Mean	St.dev. %
H1	0.78	0.80	0.82	0.80(2)	3	-1.43	-2.65	-3.72	-3(1)	44
H3	1.00	1.03	1.16	1.07(8)	8	-6.44	-6.12	-5.33	-6.0(6)	10
H4	0.99	0.90	0.92	0.94(5)	5	-0.77	-1.28	-0.96	-1.0(3)	26
H4'	1.09	1.06	1.12	1.09(3)	3	-3.08	-3.05	-2.29	-2.8(4)	16
H5a	0.62	0.67	0.74	0.67(6)	9	-2.42	-3.05	-3.24	-2.9(4)	15
H6	0.93	0.90	0.97	0.93(3)	4	0.60	-0.27	0.50	0.3(5)	173
H7	0.28	0.57	0.56	0.5(2)	35	1.36	0.65	1.29	1.1(4)	36
H8	4.77	4.86	4.91	4.85(7)	1	9.49	11.60	11.89	11(1)	12
H9	0.07	0.45	0.39	0.3(2)	67	1.19	0.82	1.35	1.1(3)	24
H9'	1.25	1.44	1.47	1.4(1)	9	0.42	0.01	0.45	0.3(2)	84
H10	15.62	14.91	15.08	15.2(4)	2	5.89	6.76	5.51	6.1(6)	11
H11	-0.30	-0.31	0.53	0.0(5)	1812	0.62	0.59	0.57	0.59(3)	4
H12	-1.87	-1.92	-0.52	-1.4(8)	55	0.85	0.83	0.91	0.87(4)	5
H13	-4.31	-4.62	-1.91	-4(1)	41	0.84	0.89	0.84	0.86(3)	3
H13'	-5.68	-5.96	-2.26	-5(2)	45	0.95	1.00	1.05	1.00(5)	5
H14a	-2.21	-2.07	-3.97	-3(1)	38	0.61	0.58	0.77	0.7(1)	16
H15	-5.56	-5.29	-4.78	-5.2(4)	8	1.09	1.16	1.22	1.15(6)	5
H16	-3.81	-3.87	-3.94	-3.87(6)	2	0.71	0.75	0.78	0.75(3)	4
H17	-4.84	-5.46	-5.18	-5.2(3)	6	0.83	0.88	0.85	0.85(2)	3
H18	-3.35	-4.45	-4.28	-4.0(6)	15	0.69	0.78	0.77	0.75(5)	6
H18'	-2.49	-2.89	-2.66	-2.7(2)	8	0.60	0.63	0.62	0.62(1)	2
H19a	-3.86	-1.21	-0.85	-2(2)	83	0.75	0.52	0.51	0.6(1)	23
H20	-1.55	-0.88	-0.56	-1.0(5)	50	0.55	0.54	0.54	0.545(4)	1
H21	-0.71	0.30	0.51	0.0(7)	2041	0.49	0.48	0.47	0.481(9)	2
H22	0.31	2.26	2.45	2(1)	71	0.62	0.60	0.60	0.605(9)	1
H23	7.60	14.06	14.87	12(4)	33	1.00	0.97	0.96	0.97(2)	2
H24	0.74	0.78	0.68	0.73(5)	7	-3.09	-3.87	2.75	-1(4)	258
H24'	0.62	0.64	0.58	0.61(3)	5	-2.07	-2.34	5.10	0(4)	1830
H24a	0.68	0.71	0.63	0.67(4)	6	-2.54	-3.04	4.39	0(4)	1040
H25a	0.82	0.90	0.57	0.8(2)	23	-4.61	-5.14	1.03	-3(1)	118
H26	1.01	1.01	0.82	0.9(1)	11	-5.25	-3.51	12.10	1(10)	858
H26'	0.73	0.75	0.62	0.70(7)	10	-2.93	-2.74	7.79	1(6)	872
H27a	0.64	0.67	0.75	0.69(6)	9	2.45	3.60	19.47	9(10)	112

Table 102 G_i **factors (·10^3) calculated for the solid state NdLu(L^{AB3})$_3$ complex**

	Ln ion in bpb site					Ln ion in bpa site				
	L^1	L^2	L^3	Mean	St.dev. %	L^1	L^2	L^3	Mean	St.dev. %
H1	0.79	0.83	0.82	0.81(2)	3	-0.76	-3.88	-3.80	-3(2)	63
H3	0.94	1.11	1.29	1.1(2)	16	-6.11	-5.93	-4.74	-5.6(7)	13
H4	0.76	1.03	0.88	0.9(1)	15	-2.46	-0.31	-1.04	-1(1)	86
H4'	0.85	1.23	1.09	1.1(2)	18	-4.34	-2.30	-2.12	-3(1)	42
H5a	0.79	0.69	0.79	0.76(6)	8	-2.57	-2.57	-3.62	-2.9(6)	21
H6	0.78	0.95	0.97	0.9(1)	11	-0.71	0.76	0.45	0.2(8)	459
H7	0.37	0.43	0.54	0.45(8)	18	0.41	1.37	1.14	1.0(5)	52
H8	5.41	4.63	5.13	5.1(4)	8	12.65	9.04	13.08	12(2)	19
H9	0.03	0.33	0.40	0.3(2)	78	1.09	0.80	1.19	1.0(2)	19
H9'	1.09	1.51	1.58	1.4(3)	19	0.20	0.19	0.46	0.3(2)	53
H10	14.28	14.69	19.30	16(3)	17	6.19	5.74	7.33	6.4(8)	13
H11	0.00	-0.24	-0.13	-0.1(1)	93	0.58	0.53	0.71	0.61(9)	15
H12	-1.37	-1.64	-1.76	-1.6(2)	13	0.89	0.81	0.92	0.87(6)	7
H13	-2.91	-5.36	-4.45	-4(1)	29	0.88	0.94	0.89	0.90(3)	4
H13'	-2.84	-4.10	-5.90	-4(2)	36	0.99	0.84	1.01	0.95(9)	10
H14a	-4.89	-1.94	-2.05	-3(2)	56	0.85	0.56	0.61	0.7(2)	23
H15	-4.43	-5.47	-5.40	-5.1(6)	11	1.32	1.19	1.15	1.22(9)	7
H16	-3.76	-3.91	-3.89	-3.85(8)	2	0.80	0.78	0.74	0.77(3)	4
H17	-5.67	-5.59	-4.88	-5.4(4)	8	0.93	0.89	0.84	0.89(4)	5
H18	-4.91	-1.76	-2.11	-3(2)	59	0.87	0.66	0.59	0.7(1)	20
H18'	-3.49	-0.26	-1.83	-2(2)	87	0.67	0.55	0.63	0.61(6)	10
H19a	-1.99	-2.47	-3.73	-2.7(9)	33	0.53	0.56	0.71	0.60(9)	16
H20	-1.60	0.42	-0.78	-1(1)	156	0.56	0.52	0.56	0.55(2)	4
H21	-0.39	1.22	0.60	0.5(8)	171	0.49	0.47	0.49	0.481(9)	2
H22	1.21	2.05	2.76	2.0(8)	39	0.61	0.60	0.60	0.604(9)	2
H23	10.43	7.89	17.42	12(5)	41	0.99	1.02	0.94	0.98(4)	4
H24	0.81	0.81	0.75	0.79(4)	5	-4.17	-4.59	1.59	-2(3)	144
H24'	0.64	0.67	0.63	0.65(2)	3	-2.28	-3.20	5.11	0(5)	3703
H24a	0.73	0.75	0.69	0.72(3)	4	-3.11	-3.89	3.85	-1(4)	407
H25a	0.88	1.02	0.50	0.8(3)	34	-5.00	-5.13	1.70	-3(4)	139
H26	1.02	1.03	0.80	1.0(1)	14	-5.61	-4.31	14.64	2(11)	719
H26'	0.74	0.83	0.62	0.7(1)	15	-2.93	-4.47	8.34	0(7)	2228
H27a	0.65	0.61	0.74	0.67(7)	10	2.45	0.84	18.27	7(10)	134

To compare the solid state structures with the results extracted from Geraldes analysis of the lanthanide induced shifts the structural factors (G_i, Table 95 - Table 102) have been used to calculate structural ratios (G_i/G_{ref}). This has been done using either H3 (Table 103 and Table 104) or H16 (Table 105 and Table 106) as reference proton.

Table 103 Structural ratios for LaLn complexes using H3 as reference proton (G_i/G_3)

	L^{AB}			L^{AB3}				
	LaEu	LaTb	EuEu	CeCe	PrPr	PrLu	NdLu	SmSm
H1	0.4(2)	0.4(2)	0.4(2)	0.5(3)	0.5(1)	0.4(2)	0.5(3)	0.5(4)
H2	0.54(8)	0.53(8)	0.53(8)					
H3	1.00(2)	1.00(4)	1.00(4)	1.0(2)	1.0(2)	1.0(1)	1.0(2)	1.0(2)
H4	0.15(2)	0.14(2)	0.14(1)	0.2(2)	0.16(4)	0.17(5)	0.2(2)	0.2(2)
H4'	0.49(7)	0.45(9)	0.47(4)	0.5(2)	0.5(1)	0.47(9)	0.5(2)	0.5(2)
H5	0.44(3)	0.44(3)	0.44(3)	0.5(1)	0.5(1)	0.49(9)	0.5(1)	0.5(1)
H6	-0.06(1)	-0.06(3)	-0.06(1)	0.0(1)	-0.08(7)	-0.05(8)	0.0(1)	0.0(1)
H7	-0.18(2)	-0.19(3)	-0.19(3)	-0.2(1)	-0.20(9)	-0.18(7)	-0.17(9)	-0.16(9)
H8	-1.7(4)	-1.6(3)	-1.8(3)	-2.0(5)	-1.9(4)	-1.8(3)	-2.1(5)	-1.9(4)
H9	-0.18(3)	-0.18(3)	-0.18(3)	-0.20(4)	-0.19(5)	-0.19(5)	-0.18(4)	-0.19(4)
H9'	-0.05(3)	-0.05(2)	-0.07(3)	-0.05(3)	-0.06(3)	-0.05(4)	-0.05(3)	-0.06(2)
H10	-1.03(7)	-1.00(6)	-0.96(6)	-1.2(2)	-1.1(2)	-1.0(1)	-1.1(2)	-1.1(2)
H11	-0.10(1)	-0.10(1)	-0.11(1)	-0.11(3)	-0.11(2)	-0.10(1)	-0.11(2)	-0.11(2)
H12	-0.15(1)	-0.139(8)	-0.15(2)	-0.16(2)	-0.16(2)	-0.15(2)	-0.16(2)	-0.16(2)
H13	-0.135(5)	-0.132(7)	-0.139(7)	-0.17(3)	-0.15(2)	-0.14(1)	-0.16(2)	-0.16(2)
H13'	-0.156(7)	-0.151(8)	-0.16(1)	-0.18(2)	-0.18(2)	-0.17(2)	-0.17(3)	-0.17(3)
H14	-0.12(3)	-0.12(3)	-0.12(3)	-0.12(3)	-0.12(2)	-0.11(2)	-0.12(3)	-0.12(3)
H15	-0.20(1)	-0.19(1)	-0.20(1)	-0.22(3)	-0.20(3)	-0.19(2)	-0.22(3)	-0.22(3)
H16	-0.127(3)	-0.121(5)	-0.128(5)	-0.14(2)	-0.13(2)	-0.13(1)	-0.14(2)	-0.14(2)
H17	-0.145(4)	-0.141(6)	-0.142(9)	-0.16(2)	-0.15(2)	-0.14(1)	-0.16(2)	-0.16(2)
H18	-0.13(2)	-0.12(2)	-0.13(2)	-0.12(4)	-0.13(2)	-0.13(1)	-0.13(3)	-0.12(3)
H18'	-0.10(1)	-0.10(1)	-0.10(1)	-0.12(2)	-0.11(1)	-0.10 (1)	-0.11(2)	-0.11(2)
H19	-0.091(8)	-0.09(1)	-0.090(8)	-0.11(2)	-0.11(3)	-0.10(3)	-0.11(2)	-0.11(2)
H20	-0.089(3)	-0.086(3)	-0.087(3)	-0.10(1)	-0.10(1)	-0.091(9)	-0.10(1)	-0.10(1)
H21	-0.079(2)	-0.077(2)	-0.076(3)	-0.09(1)	-0.08(1)	-0.081(8)	-0.09(1)	-0.09(1)
H22	-0.099(3)	-0.097(4)	-0.095(4)	-0.11(1)	-0.11(1)	-0.10(1)	-0.11(1)	-0.11(1)
H23	-0.16(1)	-0.16(1)	-0.16(1)	-0.18(3)	-0.17(2)	-0.16(2)	-0.18(2)	-0.17(2)
H24	0.68(7)	0.61(7)	0.67(6)	0.4(7)	0.2(9)	0.2(6)	0.4(6)	0.4(7)
H24'	0.3(1)	0.3(1)	0.3(1)	0.0(9)	0.0(8)	0.0(7)	0.0(8)	0.0(9)
H25	0.8(2)	0.8(2)	0.7(2)	0.5(7)	0.1(9)	0.5(6)	0.5(7)	0.5(7)
H26	0.3(4)	0.2(4)	0.2(4)	0(2)	0(2)	0(2)	0(2)	0(2)
H26'	0.41(9)	0.4(2)	0.43(6)	0(1)	0(1)	0(1)	0(1)	0(1)
H27	-0.5(2)	-0.6(3)	-0.5(2)	-1(2)	-1(1)	-1(2)	-1(2)	-1(2)

Table 104 Structural ratios for LnLu complexes using H3 as reference proton (G_i/G_3)

	L^{AB}			L^{AB3}				
	LaEu	LaTb	EuEu	CeCe	PrPr	PrLu	NdLu	SmSm
H1	0.78(4)	0.77(4)	0.78(4)					
H2	0.69(4)	0.67(4)	0.68(3)	0.7(1)	0.77(5)	0.75(6)	0.7(1)	0.7(1)
H3	1.00(7)	1.00(7)	1.00(5)	1.0(2)	1.00(9)	1.0(1)	1.0(2)	1.0(2)
H4	0.95(6)	0.9(1)	0.97(5)	0.7(1)	0.90(8)	0.88(8)	0.8(2)	0.8(2)
H4'	1.08(5)	1.05(8)	1.08(4)	0.9(2)	1.05(7)	1.03(8)	1.0(2)	0.9(2)
H5	0.63(5)	0.64(5)	0.65(4)	0.7(1)	0.63(7)	0.63(7)	0.7(1)	0.7(1)
H6	0.91(5)	0.94(8)	0.99(6)	0.7(1)	0.89(7)	0.88(8)	0.8(2)	0.8(1)
H7	0.44(4)	0.49(6)	0.54(5)	0.33(8)	0.4(2)	0.4(2)	0.4(1)	0.39(9)
H8	4.7(4)	4.5(4)	4.8(4)	4.7(8)	4.6(3)	4.5(4)	4.5(8)	4.5(8)
H9	0.31(6)	0.28(5)	0.41(5)	0.2(2)	0.3(2)	0.3(2)	0.2(2)	0.2(2)
H9'	1.4(1)	1.3(1)	1.46(8)	1.2(3)	1.4(2)	1.3(2)	1.3(3)	1.2(3)
H10	15(2)	15(2)	15(2)	15(4)	15(2)	14(1)	14(3)	14(3)
H11	-0.1(2)	-0.1(3)	0.0(3)	-0.2(1)	0.0(5)	0.0(5)	-0.1(1)	-0.14(7)
H12	-1.6(4)	-1.6(4)	-1.5(3)	-1.5(3)	-1.5(8)	-1.3(8)	-1.4(3)	-1.4(3)
H13	-3(1)	-3(1)	-3(1)	-4(1)	-4(1)	-3(1)	-4(1)	-4(1)
H13'	-4(1)	-4(1)	-4(1)	-4(2)	-5(2)	-4(2)	-4(2)	-4(2)
H14	-4(2)	-4(2)	-4(2)	-3(2)	-3(1)	-3(1)	-3(2)	-3(2)
H15	-4.8(5)	-4.7(6)	-5.1(4)	-4.5(8)	-5.2(5)	-4.9(5)	-4.6(9)	-4.6(8)
H16	-3.8(2)	-3.7(2)	-4.0(2)	-3.5(5)	-3.8(2)	-3.6(3)	-3.5(6)	-3.5(6)
H17	-5.3(3)	-5.3(3)	-5.5(6)	-4.8(8)	-5.2(3)	-4.8(5)	-4.8(9)	-4.9(9)
H18	-4(2)	-4(2)	-4(2)	-2(2)	-3.9(7)	-3.8(6)	-3(2)	-3(2)
H18'	-2(1)	-2(1)	-2(1)	-2(2)	-2.7(2)	-2.5(3)	-2(1)	-2(2)
H19	-1.9(9)	-2.0(1)	-2(1)	-2.5(9)	-2(2)	-2(2)	-2.5(9)	-2(1)
H20	-0.5(8)	-0.7(6)	-0.5(9)	-1(1)	-0.9(6)	-0.9(5)	-0.6(9)	-1(1)
H21	0(1)	0.2(9)	0(1)	0.4(7)	0.1(6)	0.0(6)	0.4(7)	0.4(7)
H22	2(2)	2(2)	2(2)	1.6(7)	2(1)	2(1)	1.8(8)	1.9(7)
H23	10(10)	11(10)	10(10)	11(4)	12(4)	11(4)	11(5)	12(5)
H24	0.70(4)	0.68(4)	0.70(3)	0.7(1)	0.67(6)	0.63(6)	0.6(1)	0.7(1)
H25	0.8(2)	0.8(2)	0.8(2)	0.7(3)	0.7(2)	0.7(2)	0.7(3)	0.7(3)
H26	0.96(5)	0.94(6)	0.95(4)	0.9(2)	1.0(1)	0.9(1)	0.9(2)	0.9(2)
H26'	0.74(5)	0.73(7)	0.75(4)	0.7(1)	0.7(1)	0.66(8)	0.7(1)	0.7(1)
H27	0.61(5)	0.61(6)	0.59(4)	0.6(1)	0.62(7)	0.64(8)	0.6(1)	0.6(1)

Table 105 Structural ratios for LaLn complexes using H16 as reference proton (G_i/G_{16})

	L^{AB}			L^{AB3}				
	LaEu	LaTb	EuEu	CeCe	PrPr	PrLu	NdLu	SmSm
H1	-3(2)	-3(1)	-3(1)	-4(2)	-4(8)	-3(2)	-4(2)	-4(3)
H2	-4.3(6)	-4.4(7)	-4.2(6)					
H3	-7.9(2)	-8.3(4)	-7.8(3)	-7(1)	-8(1)	-8.0(8)	-7(1)	-7.2(9)
H4	-1.1(2)	-1.2(2)	-1.1(1)	-2(1)	-1(3)	-1(4)	-2(1)	-2(1)
H4'	-3.9(5)	-3.7(8)	-3.7(3)	-4(2)	-4(8)	-4(6)	-4(2)	-3(1)
H5	-3.4(2)	-3.6(2)	-3.4(2)	-3.7(8)	-3.5(6)	-3.9(6)	-3.8(8)	-3.7(8)
H6	0.4(1)	0.5(2)	0.5(1)	0(1)	0.6(6)	0.4(6)	0(1)	0.2(9)
H7	1.4(1)	1.5(2)	1.5(3)	1.2(7)	1.6(6)	1.5(5)	1.3(7)	1.2(7)
H8	13(3)	13(3)	14(2)	15(3)	14(3)	15(2)	15(3)	14(2)
H9	1.4(3)	1.5(3)	1.4(2)	1.4(2)	1.5(3)	1.5(4)	1.3(3)	1.4(3)
H9'	0.4(2)	0.4(2)	0.6(2)	0.3(2)	0.5(3)	0.4(3)	0.4(2)	0.4(1)
H10	8.1(6)	8.3(5)	7.5(5)	8(1)	8(8)	8(9)	8(1)	8(9)
H11	0.8(1)	0.9(1)	0.9(1)	0.8(1)	0.9(5)	0.8(5)	0.8(1)	0.8(1)
H12	1.15(8)	1.15(7)	1.2(2)	1.12(9)	1.19(6)	1.16(8)	1.13(9)	1.14(9)
H13	1.07(4)	1.09(6)	1.09(6)	1.2(1)	1.2(4)	1.2(6)	1.2(6)	1.2(8)
H13'	1.23(6)	1.25(7)	1.3(1)	1.25(9)	1.33(8)	1.34(8)	1.22(1)	1.24(1)
H14	1.0(2)	1.0(3)	1.0(2)	0.9(2)	0.9(1)	0.9(1)	0.9(2)	0.9(2)
H15	1.6(1)	1.6(1)	1.5(1)	1.6(1)	1.5(1)	1.5(1)	1.6(1)	1.6(1)
H16	1.00(3)	1.00(4)	1.00(5)	1.00(6)	1.00(4)	1.00(6)	1.00(6)	1.00(7)
H17	1.14(3)	1.16(5)	1.11(8)	1.15(7)	1.15(3)	1.15(6)	1.15(7)	1.14(8)
H18	1.0(1)	1.0(1)	1.0(1)	0.9(2)	1.0(8)	1.0(8)	0.9(2)	0.9(2)
H18'	0.82(9)	0.83(9)	0.79(9)	0.86(6)	0.83(3)	0.83(4)	0.79(9)	0.79(9)
H19	0.72(6)	0.73(8)	0.70(7)	0.8(1)	0.8(2)	0.8(2)	0.8(1)	0.8(1)
H20	0.70(2)	0.71(3)	0.68(3)	0.72(5)	0.73(2)	0.73(3)	0.71(4)	0.71(5)
H21	0.62(1)	0.64(2)	0.59(2)	0.63(3)	0.64(2)	0.65(3)	0.62(3)	0.62(3)
H22	0.78(3)	0.80(3)	0.74(4)	0.80(4)	0.82(3)	0.81(4)	0.78(4)	0.77(4)
H23	1.29(8)	1.31(9)	1.2(1)	1.30(8)	1.29(4)	1.31(6)	1.27(7)	1.26(8)
H24	-5.4(6)	-5.0(6)	-5.2(4)	-3(5)	-2(7)	-2(5)	-3(4)	-3(5)
H24'	-2(1)	-2.4(9)	-2.4(9)	0(6)	0(6)	0(6)	0(6)	0(6)
H25	-6(2)	-6(2)	-5(2)	-4(5)	-1(7)	-4(5)	-4(5)	-3(5)
H26	-2(3)	-2(3)	-1(3)	1(15)	1(17)	1(13)	2(15)	2(15)
H26'	-3.2(7)	-3(2)	-3.3(5)	0(9)	0(9)	1(8)	0(9)	0(9)
H27	4(2)	5(3)	4(1)	9(13)	8(8)	11(13)	9(12)	9(12)

Table 106 Structural ratios for LnLu complexes using H16 as reference proton (G_i/G_{16})

	L^{AB}			L^{AB3}				
	LaEu	LaTb	EuEu	CeCe	PrPr	PrLu	NdLu	SmSm
H1	-0.205(7)	-0.207(6)	-0.19(1)	-0.21(1)	-0.201(3)	-0.207(6)	-0.210(7)	-0.21(1)
H2	-0.181(6)	-0.180(8)	-0.169(9)					
H3	-0.26(1)	-0.27(2)	-0.25(1)	-0.29(4)	-0.26(2)	-0.28(2)	-0.29(5)	-0.28(5)
H4	-0.25(1)	-0.24(2)	-0.24(1)	-0.21(3)	-0.24(1)	-0.24(1)	-0.23(3)	-0.22(4)
H4'	-0.285(7)	-0.28(2)	-0.27(1)	-0.26(4)	-0.275(4)	-0.282(9)	-0.27(5)	-0.27(5)
H5a	-0.17(1)	-0.17(1)	-0.16(1)	-0.19(2)	-0.16(2)	-0.17(2)	-0.20(2)	-0.20(2)
H6	-0.240(6)	-0.25(2)	-0.25(2)	-0.21(2)	-0.233(9)	-0.241(9)	-0.23(3)	-0.23(2)
H7	-0.116(8)	-0.13(1)	-0.13(1)	-0.10(2)	-0.11(5)	-0.12(4)	-0.12(2)	-0.11(2)
H8	-1.23(9)	-1.21(8)	-1.18(9)	-1.3(1)	-1.20(4)	-1.25(3)	-1.3(1)	-1.28(8)
H9	-0.08(2)	-0.08(1)	-0.10(1)	-0.05(5)	-0.08(7)	-0.08(5)	-0.07(5)	-0.06(5)
H9'	-0.37(3)	-0.36(3)	-0.36(2)	-0.36(7)	-0.37(4)	-0.36(3)	-0.36(7)	-0.35(6)
H10	-4.1(5)	-4.1(4)	-3.7(4)	-4.2(9)	-4.1(3)	-3.9(1)	-4.2(7)	-4.0(8)
H11	0.04(6)	0.03(7)	0.01(8)	0.05(4)	0.0(1)	0.0(1)	0.03(3)	0.04(2)
H12	0.4(1)	0.43(9)	0.37(9)	0.42(6)	0.4(2)	0.4(2)	0.41(5)	0.40(7)
H13	0.8(3)	0.8(3)	0.7(3)	1.0(2)	1.0(4)	0.9(4)	1.1(3)	1.1(4)
H13'	1.0(4)	1.0(4)	0.9(4)	1.3(44)	1.2(5)	1.2(5)	1.1(4)	1.1(4)
H14a	1.0(4)	1.1(5)	1.0(4)	0.8(4)	0.7(3)	0.7(3)	0.8(4)	0.8(4)
H15	1.3(1)	1.3(1)	1.3(1)	1.3(1)	1.4(1)	1.3(1)	1.3(2)	1.3(1)
H16	1.00(3)	1.00(4)	1.00(6)	1.00(4)	1.00(1)	1.00(2)	1.00(3)	1.00(3)
H17	1.40(5)	1.41(7)	1.4(1)	1.4(1)	1.36(1)	1.33(8)	1.4(1)	1.4(1)
H18	1.0(4)	1.0(4)	1.0(4)	0.7(5)	1.0(2)	1.0(2)	0.8(4)	0.7(5)
H18'	0.6(4)	0.7(3)	0.6(4)	0.5(5)	0.70(5)	0.69(5)	0.5(4)	0.4(4)
H19a	0.5(2)	0.5(3)	0.5(3)	0.7(2)	0.5(4)	0.5(3)	0.7(2)	0.7(3)
H20	0.1(2)	0.2(2)	0.1(2)	0.2(3)	0.2(2)	0.3(1)	0.2(3)	0.2(3)
H21	-0.1(3)	-0.1(2)	-0.1(3)	-0.1(2)	0.0(2)	0.0(2)	-0.1(2)	-0.1(2)
H22	-0.5(7)	-0.4(5)	-0.4(6)	-0.5(2)	-0.4(3)	-0.4(3)	-0.5(2)	-0.5(2)
H23	-3(3)	-3(3)	-3(2)	-3(1)	-3(1)	-3(1)	-3(1)	-3(1)
H24a	-0.186(5)	-0.182(5)	-0.172(7)	-0.19(1)	-0.18(1)	-0.17(1)	-0.187(9)	-0.18(1)
H25a	-0.21(4)	-0.22(5)	-0.19(4)	-0.21(7)	-0.19(5)	-0.20(5)	-0.21(7)	-0.21(7)
H26	-0.254(9)	-0.25(1)	-0.23(1)	-0.25(4)	-0.25(3)	-0.24(3)	-0.25(3)	-0.25(3)
H26'	-0.19(1)	-0.19(2)	-0.18(1)	-0.19(3)	-0.19(2)	-0.18(2)	-0.19(3)	-0.19(3)
H27a	-0.16(1)	-0.16(1)	-0.15(1)	-0.18(2)	-0.16(2)	-0.18(2)	-0.17(2)	-0.17(2)

5.5.6 Comparing solution and solid state parameters

The structural ratios obtained from the analysis of the lanthanide induced shifts were compared with those calculated for the solid state structures by means of linear fitting (yielding correlation coefficients and slopes) as well as agreement factors

$$AF_j^G = \sqrt{\frac{\sum_{i\neq k}\left(\left(G_i/G_{ref}\right)_{LIS} - \left(G_i/G_{ref}\right)_{X-ray}\right)^2}{\sum_{i\neq k}\left(\left(G_i/G_{ref}\right)_{X-ray}\right)^2}} \qquad (17)$$

For the LaLn complexes the calculations of the agreement factors were repeated leaving out H8 since it was found to contribute up to half of the value. The results are given in Table 107 - Table 112. Best values (lowest agreement factors, correlation coefficients closest to 1) for each series of complexes in solution are written in bold.

Table 107 Comparing LIS and X-ray structural ratios of L^{AB} complexes using H3 as reference

	$LaLn(L^{AB})_3$			$LnLu(L^{AB})_3$		
	AF	Correlation coefficient	Slope	*AF*	Correlation coefficient	Slope
$LaEu(L^{AB})_3$	0.608 0.460*	0.903	1.144	0.147	0.990	0.994
$LaTb(L^{AB})_3$	0.627 0.445*	0.912	1.215	0.137	0.991	0.986
$Eu_2(L^{AB})_3$	0.556 0.440*	0.918	1.159	0.166	0.987	0.998
$Ce_2(L^{AB3})_3$	0.239 0.160*	0.977	1.065	0.148	0.990	1.031
$Pr_2(L^{AB3})_3$	0.298 **0.144***	**0.990**	1.254	**0.117**	**0.994**	0.959
$PrLu(L^{AB3})_3$	0.338 0.210*	0.962	1.139	0.119	**0.994**	1.020
$NdLu(L^{AB3})_3$	**0.226** 0.151*	0.980	1.071	0.155	0.990	1.043
$Sm_2(L^{AB3})_3$	0.273 0.161*	0.975	1.117	0.161	0.988	1.029

* calculated without H8

Table 108 Comparing LIS and X-ray structural ratios of L^{AB3} complexes using H3 as reference

	$LaLn(L^{AB3})_3$			$LnLu(L^{AB3})_3$		
	AF	Correlation coefficient	Slope	*AF*	Correlation coefficient	Slope
$LaEu(L^{AB})_3$	0.600 0.427*	0.908	1.161	0.147	0.990	0.995
$LaTb(L^{AB})_3$	0.622 0.409*	0.916	1.233	0.137	0.991	0.987
$Eu_2(L^{AB})_3$	0.551 0.404*	0.926	1.179	0.167	0.987	0.999
$Ce_2(L^{AB3})_3$	0.269 0.169*	0.973	1.087	0.148	0.991	1.032
$Pr_2(L^{AB3})_3$	0.336 **0.154***	**0.987**	1.282	**0.118**	**0.994**	0.960
$PrLu(L^{AB3})_3$	0.380 0.230*	0.954	1.158	0.122	**0.994**	1.021
$NdLu(L^{AB3})_3$	**0.256** 0.160*	0.976	1.094	0.155	0.990	1.044
$Sm_2(L^{AB3})_3$	0.308 0.172*	0.971	1.140	0.161	0.988	1.030

* calculated without H8

Table 109 Comparing LIS and X-ray structural ratios of L^{AB4} complexes using H3 as reference

	$LaLn(L^{AB4})_3$			$LnLu(L^{AB4})_3$		
	AF	Correlation coefficient	Slope	*AF*	Correlation coefficient	Slope
$LaEu(L^{AB})_3$	0.694 0.511*	0.887	1.182	0.137	0.990	0.963
$LaTb(L^{AB})_3$	0.718 0.497*	0.897	1.256	0.138	0.990	0.953
$Eu_2(L^{AB})_3$	0.649 0.489*	0.904	1.201	0.148	0.988	0.970
$Ce_2(L^{AB3})_3$	0.302 0.186*	0.970	1.113	0.151	0.988	0.995
$Pr_2(L^{AB3})_3$	0.386 0.193*	**0.982**	1.309	0.120	**0.994**	0.928
$PrLu(L^{AB3})_3$	0.399 0.227*	0.956	1.192	**0.104**	**0.994**	0.987
$NdLu(L^{AB3})_3$	**0.286** **0.173***	0.974	1.121	0.153	0.988	1.007
$Sm_2(L^{AB3})_3$	0.339 0.185*	0.969	1.169	0.172	0.985	0.992

* calculated without H8

Table 110 Comparing LIS and X-ray structural ratios of L^{AB5} complexes using H3 as reference

	$LaLn(L^{AB5})_3$			$LnLu(L^{AB5})_3$		
	AF	Correlation coefficient	Slope	*AF*	Correlation coefficient	Slope
$LaEu(L^{AB})_3$	0.614 0.458*	0.906	1.157	0.161	0.988	1.008
$LaTb(L^{AB})_3$	0.635 0.442*	0.915	1.228	0.149	0.990	0.999
$Eu_2(L^{AB})_3$	0.571 0.438*	0.920	1.172	0.181	0.985	1.014
$Ce_2(L^{AB3})_3$	0.251 0.164*	0.975	1.073	0.168	0.989	1.044
$Pr_2(L^{AB3})_3$	0.310 **0.144***	**0.990**	1.265	**0.143**	**0.991**	0.970
$PrLu(L^{AB3})_3$	0.352 0.214*	0.960	1.147	0.154	**0.991**	1.031
$NdLu(L^{AB3})_3$	**0.239** 0.156*	0.978	1.079	0.176	0.988	1.056
$Sm_2(L^{AB3})_3$	0.288 0.167*	0.974	1.126	0.181	0.986	1.042

* calculated without H8

Table 111 Comparing LIS and X-ray structural ratios of L^{AB} complexes using H16 as reference

	$LaLn(L^{AB})_3$			$LnLu(L^{AB})_3$		
	AF	Correlation coefficient	Slope	*AF*	Correlation coefficient	Slope
$LaEu(L^{AB})_3$	0.530 0.469*	0.914	1.084	0.148	0.989	0.978
$LaTb(L^{AB})_3$	0.504 0.434*	0.922	1.090	0.140	0.991	0.957
$Eu_2(L^{AB})_3$	0.500 0.454*	0.927	1.111	0.184	0.986	1.049
$Ce_2(L^{AB3})_3$	0.262 0.174*	0.980	1.120	0.148	0.990	0.931
$Pr_2(L^{AB3})_3$	0.266 **0.148***	**0.989**	1.199	0.121	**0.994**	0.950
$PrLu(L^{AB3})_3$	0.281 0.220*	0.966	1.052	**0.118**	**0.994**	0.962
$NdLu(L^{AB3})_3$	**0.239** 0.165*	0.982	1.107	0.149	0.990	0.936
$Sm_2(L^{AB3})_3$	0.287 0.177*	0.978	1.147	0.158	0.988	0.939

* calculated without H8

Table 112 Comparing LIS and X-ray structural ratios of L^{AB3} complexes using H16 as reference

	$LaLn(L^{AB3})_3$			$LnLu(L^{AB3})_3$		
	AF	Correlation coefficient	Slope	*AF*	Correlation coefficient	Slope
$LaEu(L^{AB})_3$	0.519 0.436*	0.919	1.096	0.148	0.989	0.990
$LaTb(L^{AB})_3$	0.495 0.401*	0.926	1.101	0.139	0.991	0.968
$Eu_2(L^{AB})_3$	0.484 0.417*	0.935	1.125	0.191	0.986	1.061
$Ce_2(L^{AB3})_3$	0.293 0.184*	0.976	1.138	0.145	0.990	0.942
$Pr_2(L^{AB3})_3$	0.299 **0.158***	**0.985**	1.219	0.120	**0.994**	0.961
$PrLu(L^{AB3})_3$	0.316 0.241*	0.959	1.065	**0.119**	0.993	0.973
$NdLu(L^{AB3})_3$	**0.268** 0.174*	0.978	1.125	0.146	0.990	0.947
$Sm_2(L^{AB3})_3$	0.320 0.190*	0.973	1.164	0.156	0.988	0.949

* calculated without H8

For the LnLu complexes in solution the $Pr_2(L^{AB3})_3$ and $PrLu(L^{AB3})_3$ solid state complexes are the best structural models. However, all agreement factors and correlation coefficients are very reasonable and the differences between them are maybe not significant.

The situation for the LaLn complexes in solution is markedly different. Agreement factors are larger by a factor of 2-4 than for the LnLu complexes. Also, there is a large difference between utilising solid state L^{AB} and L^{AB3} complexes as structural models; the latter are distinctly better. As for the LnLu complexes, the solid state $Pr_2(L^{AB3})_3$ turns out to be a good structural model, this time together with $NdLu(L^{AB3})_3$.

The large difference between the LaLn and LnLu series of complexes may be related to the fact that in the former, the paramagnetic lanthanide ion is in the bpa site of the complex. This is relatively close to the flexible carboxamide group, which is the main reason (apart from H8) for the larger agreement factors.

Since the three ligand strands in the complexes wrap around the lanthanide ions in a very different way at the ends of the ligands the individual G_i values calculated are very different. The mean values have large standard deviations and may be said to be not very well-defined. This is illustrated in Figure 88 where structural ratios obtained from analysis of the lanthanide induced shift are compared to values calculated from a solid state structure. The straight line corresponds to a perfect match. Note how the inclusion of standard deviations illustrates that the two sets of values do indeed match and that the problem is associated with the calculation and physical meaning of the structural ratios of the solid state structure.

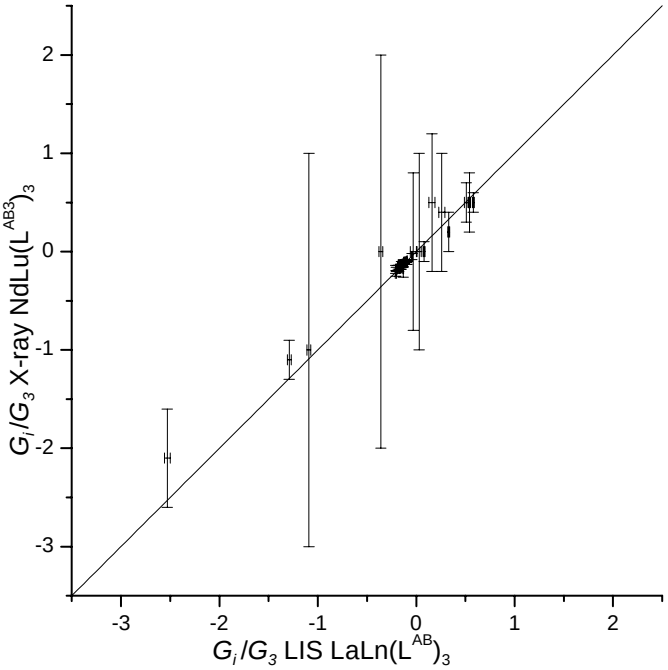

Figure 88 Comparing solution and solid state structural ratios

Leaving out H8 is justified by the fact that the relative errors are less than alarming for this proton. In Figure 89 are shown the relative errors for the comparison of the NdLu(L^{AB3})$_3$ solid state structure with the structural ratios extracted from the lanthanide shift analysis of the LaLn(L^{AB})$_3$ complexes using H3 as reference proton. Contemplating that figure one would be tempted to conclude that H8 does not pose a severe problem since the relative error is less than 10 %, a value that is surpassed by 4 other protons. However, this is at least partially due to the fact that these protons have low absolute values of structural ratios. This just shows that regarding absolute (agreement factors) and relative errors may both lead to hastened conclusions about the significance of an error.

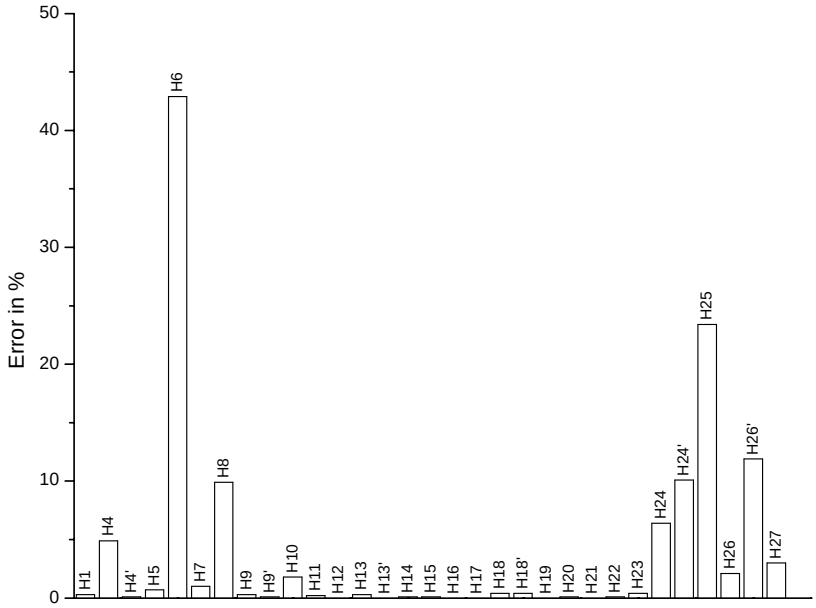

Figure 89 Relative errors comparing solid state and solution structures

Using linear fitting to estimate how similar two structures are is not a much better method than calculating agreement factors. Since the structural ratios span several orders of magnitude a single ("wrong") value much larger than the rest may dominate the fitting and lead to a reasonable correlation coefficient, but on the other hand to a slope different from one.

Returning to the question of whether any of the solid state structures can be used as a model of the structure of the complexes in solution the answer is affirmative. As outlined in Chapter 5.8 (page 267), agreement factors in the 0.1 – 0.2 range are low enough to conclude that two structures are identical. The values found here using the solid state L^{AB} complexes are so high (0.4 – 0.6) that these complexes can be ruled out as good models. Of the two groups of L^{AB3} complexes the triclinic complexes (PrPr and PrLu) have the lowest agreement factors for the two LnLu series of complexes (0.117 – 0.122). Of these two complexes the PrPr eventually emerges as the best candidate based on the agreement factors calculated for the LaLn series (0.144 – 0.158 without H8).

It should be remarked that this complex is the best structural model for all complexes in solution regardless of ligand. The structural changes induced by the Cl and NEt_2 substituents on the L^{AB3}, L^{AB4} and L^{AB5} ligands seem to be small. The differences in the solid state (as evaluated by means of calculation of agreement factors as done here) are larger, but (as

evidenced by the two markedly different types of L^{AB3} complexes) may not be directly related to the change in ligand. Other effects (packing of solvent molecules, etc) may play a decisive role.

5.6 Determination of crystal fields parameters

The pseudo contact terms $B_0^2 G_i$ determined from the one proton (Reilley) analysis (Table 42 - Table 49) will here be used to calculate values of the crystal field parameter B_0^2 for a paramagnetic lanthanide in one of the two coordination sites of the complexes.

It is here supposed that the B_0^2 parameter does not vary along the series of complexes investigated. For series of complexes for which lanthanide induced shift analysis has shown that this is not the case, the change in B_0^2 usually occurs later in the lanthanide series (around Gd) and it would *a priori* be reasonable to assume that the parameter could be regarded as a constant in this case. This is affirmed by the fact that the plots according to one proton (Reilley) method of separation are linear and with good correlation coefficients. To put it another way: two proton analysis shows that the complexes are isostructural and it follows that good Reilley plot leads to the conclusion that the complexes are isostructural *and* have the same B_0^2 parameter. It should be pointed out that this assumption is far from accurate and that variations in B_0^2 of 50 - 100 % have been measured for the lanthanide ions investigated here. The crystal field parameter calculated here is an effective parameter incorporating the values of Ce, Pr, Nd and Eu.

Since the separation of contact and pseudo contact terms according to Reilley yields the crystal field parameters in the form of the products $B_0^2 G_i$ a set of geometric factors G_i must be available for the analysis. Based on the results of the two proton analysis the solid state $Pr_2(L^{AB3})_3$ complex has been chosen as structural model.

B_0^2 can then be determined graphically by plotting for each complex series $B_0^2 G_i$ as obtained from Reilley analysis of the lanthanide induced shifts as a function of G_i calculated from the solid state structure, Table 99 giving the crystal field parameter as the slope. To avoid introducing artificial sources of error protons have been left out of the analysis if the relative standard deviation of the mean G_i value in the solid state is larger than 50 %.

The plots are shown in Figure 90 - Figure 93 and the results of the linear fitting are listed in Table 113.

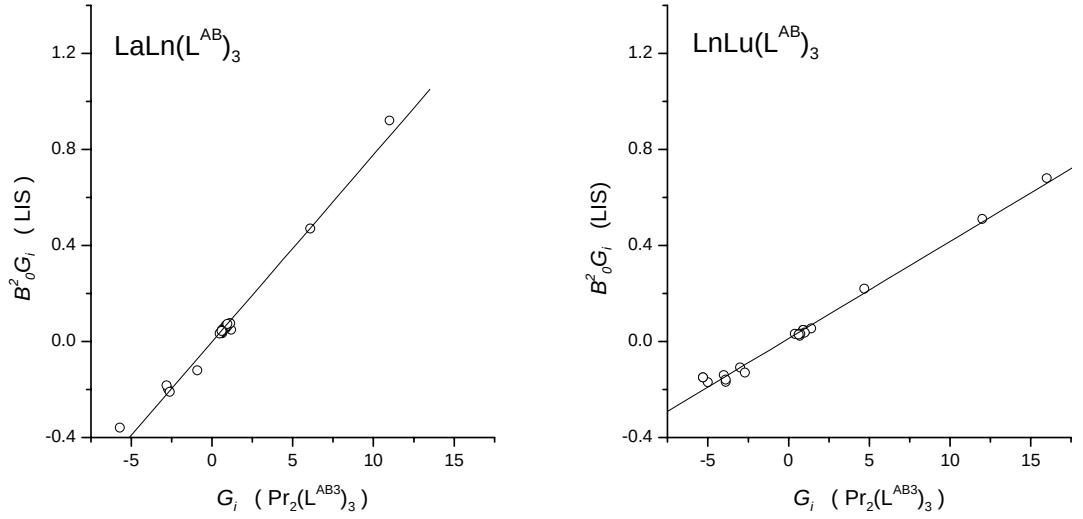

Figure 90 Determination of the crystal field parameter for L^{AB} complexes

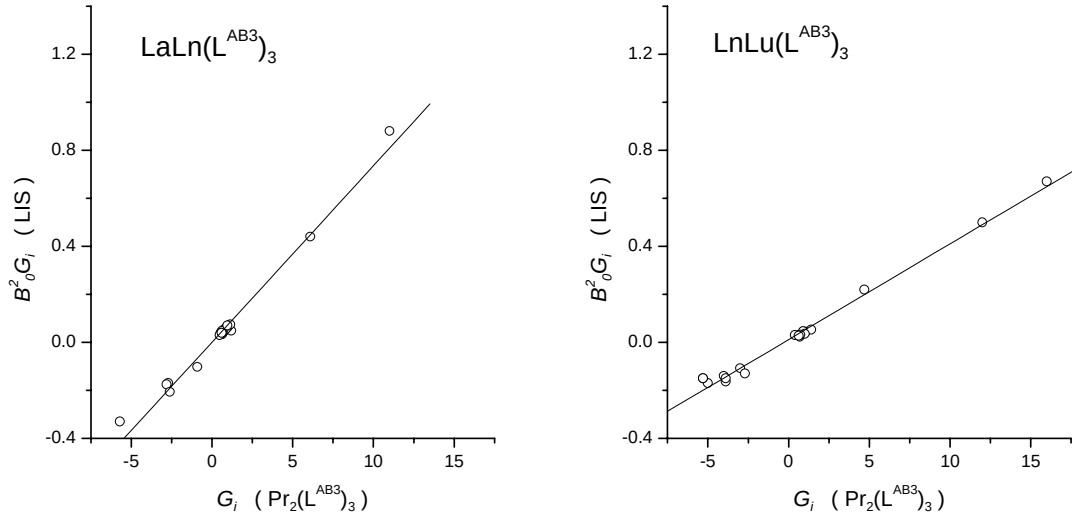

Figure 91 Determination of the crystal field parameter for L^{AB3} complexes

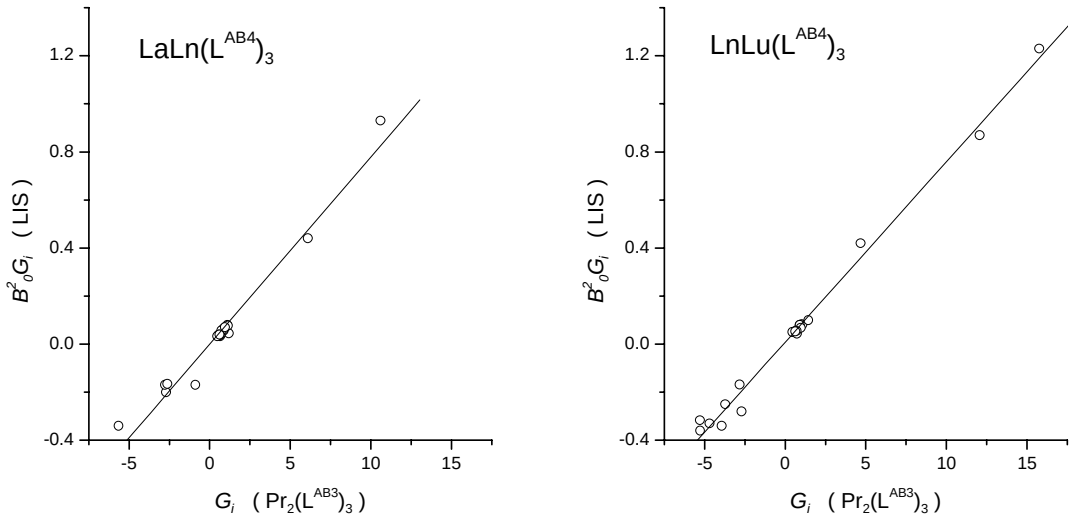

Figure 92 Determination of the crystal field parameter for L^{AB4} complexes

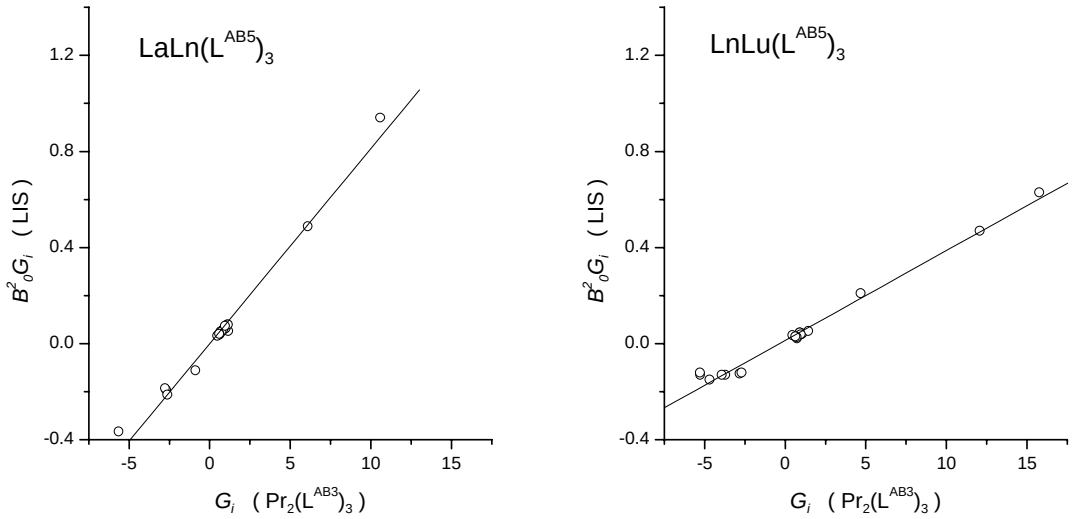

Figure 93 Determination of the crystal field parameter for L^{AB5} complexes

Table 113 Crystal field parameters

	L^{AB}	L^{AB3}	L^{AB4}	L^{AB5}
$\left(B_0^2\right)^{bpa}$ ($LaLn(L)_3$ complexes)	0.079(2)	0.075(2)	0.078(3)	0.081(2)
$\left(B_0^2\right)^{bpb}$ ($LnLu(L)_3$ complexes)	0.0412(9)	0.0402(9)	0.075(2)	0.037(1)
$\left(B_0^2\right)^{bpa} / \left(B_0^2\right)^{bpb}$	1.9(1)	1.9(1)	1.04(5)	2.17(9)

It is seen that that the introduction of a Cl substituent reduces the crystal field parameter of the lanthanide in the corresponding coordination site by less than 10 %. The introduction of the NEt_2 group in the L^{AB4} ligand on the other hand almost doubles the value of the corresponding crystal field parameter.

The crystal field parameters determined in this way are not absolute, but relative since the Bleaney parameters C_j have been (rather arbitrarily) scaled to a value of -100 for Dy.

The value of 1.9(1) found here for the $\left(B_0^2\right)^{bpa} / \left(B_0^2\right)^{bpb}$ ratio of the L^{AB} complexes is comparable to the value of 1.5(1) found for complexes of the related L^{BAB} ligand (Chart 11; page 23).[51]

It should be emphasised again that the crystal field parameters calculated using this approach are mean parameters including the values for all four paramagnetic lanthanide ions in this study. We will see in Chapter 5.7 that this is oversimplified.

It was initially hoped that the crystal field parameters determined from the analysis of the lanthanide induced shift could be compared with values obtained from luminescence measurements of Eu(III) complexes. In the luminescence measurements the splitting of $^7F_1$ into an E and an A component is proportional to the value of B_0^2.[94] If this could be determined for both sites (bpb and bpa) it would be possible to compare the ratio of the two splittings to the ration determined by NMR.

Unfortunately the preliminary measurements of luminescence of the LaEu, Eu_2 and EuLu L^{AB3} complexes are all more or less identical. The conclusion is that the luminescence observed originates from Eu in the bpa site of the complex. This could be expected since measurements of the L^A and L^B complexes showed the latter to be about 50 times more luminescent.[27,30] The introduction of a Cl substituent on the bpa coordination moiety of L^E enhances the luminescence even further.[31] Even in the EuLu complexes, in which the Eu(III) ion formally is in the bpb site, the solution contains some Eu_2 complex, and the luminescence of the Eu(III) ion in the bpa site dominates the spectra.

5.7 Modified one proton analysis

5.7.1 Introduction

As already noted, the above analysis of crystal field parameters as well as the one proton Reilley analysis presumes that the crystal field parameter is the same for all the lanthanides, which is not the case.[90,94]

The one proton analysis resulted in some cases in values of F_i (the contact term parameter) that were too large to be realistic for protons topologically far from the paramagnetic lanthanide ion (see page 124).

Let us as an example re-examine H8 in the LnLu(L^{AB})$_3$ series of complexes. The F_8 parameter is too large: it should be similar to F_7, but it is 5 times bigger. H8 is separated from the paramagnetic lanthanide ion by 8 chemical bonds, which should result in a contact term of zero. The unexpected high value of F_8 is clearly related to the large pseudo contact shift of this proton and evident of a less than perfect separation of contact and pseudo contact contributions to the lanthanide induced shift.

Eq. (3) (p. 106) reduces in the absence of contact shift ($F_i = 0$) to

$$\frac{\Delta_{i,j}}{C_j} = B_0^2 G_i \qquad (18)$$

As was proven in the two proton analysis, all complexes of a given series are isostructural (G_i the same for all j) and values of $_{i,j}/C_j$ should then be identical for all lanthanides for a given proton i if the assumption holds that the crystal field parameter does not vary along the lanthanide series. This can be used to determine relative crystal field parameters of the lanthanide ions as outlined below.

5.7.2 Relative crystal field parameters

In the LnLu(L^{AB})$_3$ complexes the paramagnetic ion is coordinated by the bpb moiety of the ligand and it is safe to assume that the protons on the bpa moiety (H1-H8 and H24-H27) are sufficiently far away to ensure that the contact shift is zero. According to Eq. (18) values of

$_{i,j}/C_j$ should be the same for all lanthanides for a given proton Hi, but examining the left half of Table 116 it is clear that this is not the case; instead an increase of the values is observed going from Ce to Eu.

Values for the Pr, Nd and Eu complexes divided by the values for the Ce complex are shown in the right half of Table 114. For protons with only pseudo contact contribution to the lanthanide induced shift these numbers are relative crystal field parameters with the value for Ce arbitrarily set to 1 (keep in mind that the C_j parameters are scaled to a value of -100 for Dy so no absolute values for the crystal field parameters can be determined).

Table 114 Determining relative crystal field parameters of LnLu L^{AB} complexes

	$\Delta_{i,j}/C_j = B_0^2 G_i$				$(B_0^2)_j/(B_0^2)_{Ce}$		
	CeLu	PrLu	NdLu	EuLu	PrLu	NdLu	EuLu
H1	0.037	0.046	0.074	0.075	1.27	2.02	2.05
H2	0.034	0.039	0.063	0.067	1.16	1.85	1.96
H3	0.049	0.061	0.098	0.102	1.24	1.98	2.07
H4	0.053	0.061	0.091	0.112	1.16	1.73	2.13
H4'	0.051	0.062	0.097	0.108	1.22	1.92	2.13
H5	0.035	0.042	0.067	0.072	1.19	1.91	2.04
H6	0.053	0.060	0.090	0.121	1.12	1.68	2.26
H7	0.035	0.042	0.064	0.085	1.20	1.84	2.43
H8	0.249	0.316	0.509	0.506	1.27	2.05	2.04
H9	0.019	0.025	0.053	0.095	1.28	2.73	4.88
H9'	0.061	0.078	0.127	0.134	1.27	2.08	2.19
H10	0.753	0.953	1.504	1.424	1.27	2.00	1.89
H11	-0.003	-0.003	-0.002	0.009	1.21	0.67	-3.33
H12	-0.098	-0.134	-0.297	-0.453	1.37	3.03	4.62
H13	-0.175	-0.244	-0.446	-0.509	1.39	2.55	2.90
H13'	-0.197	-0.266	-0.445	-0.406	1.35	2.26	2.06
H14	-0.124	-0.153	-0.248	-0.273	1.23	2.00	2.20
H15	-0.222	-0.322	-0.688	-0.998	1.45	3.10	4.49
H16	-0.206	-0.244	-0.464	-0.580	1.18	2.25	2.81
H17	-0.224	-0.322	-0.705	-1.055	1.44	3.15	4.71
H18	-0.182	-0.247	-0.397	-0.420	1.36	2.18	2.30
H18'	-0.161	-0.223	-0.414	-0.488	1.38	2.56	3.02
H19	-0.088	-0.106	-0.170	-0.176	1.20	1.93	2.00
H20	-0.098	-0.132	-0.297	-0.460	1.34	3.03	4.68
H21	-0.010	-0.012	-0.013	0.011	1.21	1.26	-1.08
H22	0.061	0.081	0.135	0.149	1.33	2.20	2.43
H23	0.577	0.756	1.202	1.221	1.31	2.08	2.11
H24	0.035	0.042	0.066	0.070	1.20	1.91	2.02
H25	0.026	0.034	0.054	0.059	1.30	2.04	2.22
H26	0.041	0.054	0.083	0.091	1.33	2.02	2.21
H26'	0.035	0.040	0.069	0.070	1.15	1.98	2.02
H27	0.033	0.041	0.066	0.069	1.24	2.01	2.09

The averages of these values for all protons on the bpa moiety of the ligand (H1-H8 and H24-H27) are 1.22(6), 1.9(1) and 2.1(1) for Pr, Nd and Eu, respectively. Note the relatively small standard deviations. For the other protons (H9-23) the corresponding values are 1.31(8), 2.3(6) and 2(2). While the values are not too different from the other values, the standard

deviations are significantly larger for Nd and especially for Eu. This is no doubt related to the ratio $<S_z>_j/C_j$ (Table 22) which increases going from Ce to Eu and means that the contact contribution increases relative to the pseudo contact contribution. A second contribution to the standard deviation is the inclusion of protons close to the so-called magic angles (H11 and H21).

Relative crystal field parameters have been determined in a similar fashion for the other series of complexes. For all LnLu complexes the calculations are based on the bpa protons (H1-H8 and H24-H27) whereas the bpb protons (H10-H23 as well as H28-H29 for the L^{AB4} series) were used for the LaLn complexes. The results are shown in Table 115.

Table 115 Relative crystal field parameters

	Pr	Nd	Eu
$LaLn(L^{AB})_3$	0.95(5)	1.22(6)	1.50(9)
$LaLn(L^{AB3})_3$	0.92(6)	1.13(7)	1.5(1)
$LaLn(L^{AB4})_3$	0.9(1)	1.2(1)	1.5(2)
$LaLn(L^{AB5})_3$	0.96(6)	1.19(8)	1.5(1)
$LnLu(L^{AB})_3$	1.22(6)	1.9(1)	2.1(1)
$LnLu(L^{AB3})_3$	1.28(5)	2.00(9)	2.2(2)
$LnLu(L^{AB4})_3$	1.07(1)	1.60(3)	2.04(6)
$LnLu(L^{AB5})_3$	1.24(8)	1.9(2)	2.0(2)

Note how the results are similar for the four LaLn series. Among the four LnLu series $LnLu(L^{AB4})_3$ clearly is different from the other three, no doubt a consequence of the NEt_2 substituent situated close to the paramagnetic lanthanide ion in these complexes.

The variation of the crystal field parameter along the lanthanide series has its origin in two different, but related effects.[90,94] The contraction of the f electrons along the lanthanide series

leads to a decrease in interaction between metal f and ligand electrons, causing a decrease in crystal field parameter. The decrease in size, on the other hand, gives smaller Ln-X distances and leads to an increase crystal field parameter. The balance of these two effects gives the variation observed here. The non-monotonous increase and a Eu parameter 50-100 % larger than the Ce one have also been observed in other systems.[90,94]

Note that this interpretation is based on the assumption that the values of the C_j parameters used are accurate. This is known to be correct only to some degree, with the real values of C_j deviating with 10 - 20 % from the tabulated ones. The values in Table 115 contain therefore not only the crystal field parameters, but include an empirical correction to the C_j parameters.A detailed discussion of the C_j parameters can be found in reference 83.

Using these values we can convert Eq. (2) to two linear forms in analogy with Eq. (3) and Eq. (4):

$$\frac{\Delta_{i,j}}{C_j\left(B_0^2\right)_j} = G_i + \left(\frac{< S_z >_j}{C_j\left(B_0^2\right)_j}\right) \cdot F_i \qquad (19)$$

$$\frac{\Delta_{i,j}}{\left\langle S_z \right\rangle_j} = F_i + \left(\frac{C_j\left(B_0^2\right)_j}{\left\langle S_z \right\rangle_j}\right) \cdot G_i \qquad (20)$$

A plot of $\Delta_{i,j} / C_j\left(B_0^2\right)_j$ as a function of $< S_z >_j / C_j\left(B_0^2\right)_j$ will then according to Eq. (19) be linear with F_i as slope and G_i as intercept. Eq. (20) describes a linear plot with F_i as intercept and G_i as slope if $\Delta_{i,j} / \left\langle S_z \right\rangle_j$ is plotted as a function of $C_j\left(B_0^2\right)_j / \left\langle S_z \right\rangle_j$.

5.7.3 Diamagnetic references

"Virtual lanthanide complexes" used as diamagnetic references were determined by the same method that was also utilised in the ordinary one proton analysis (page 93). Average agreement factors were calculated for different La percentages as illustrated in Figure 94 - Figure 97.

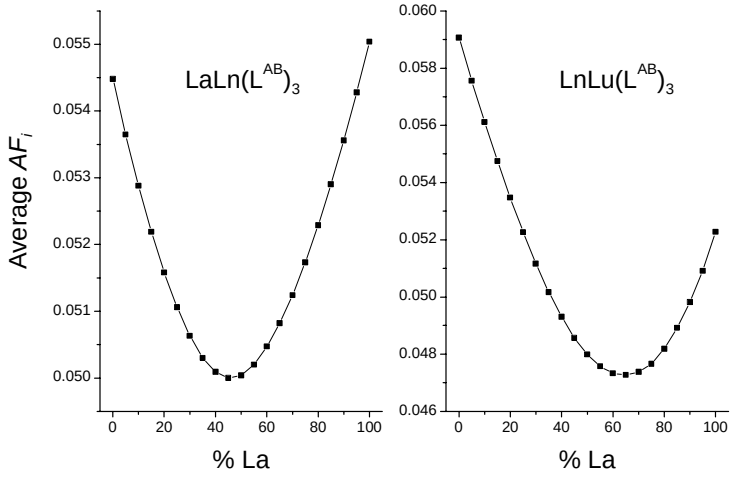

Figure 94 Average AF_i of L^{AB} complexes as function of La percentage

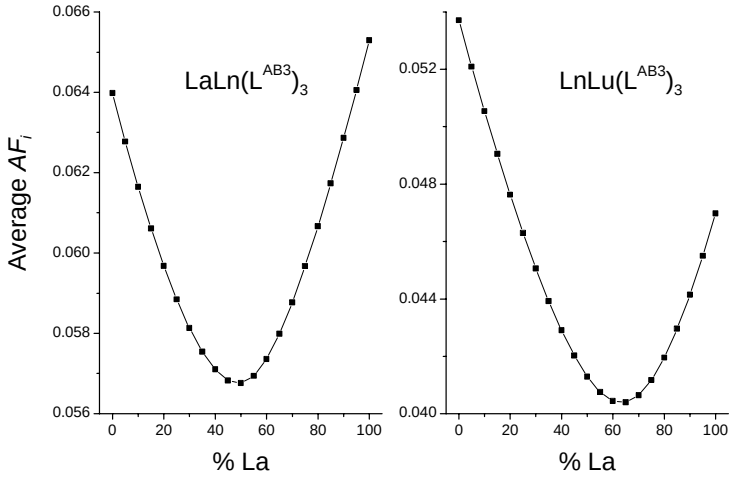

Figure 95 Average AF_i of L^{AB3} complexes as function of La percentage

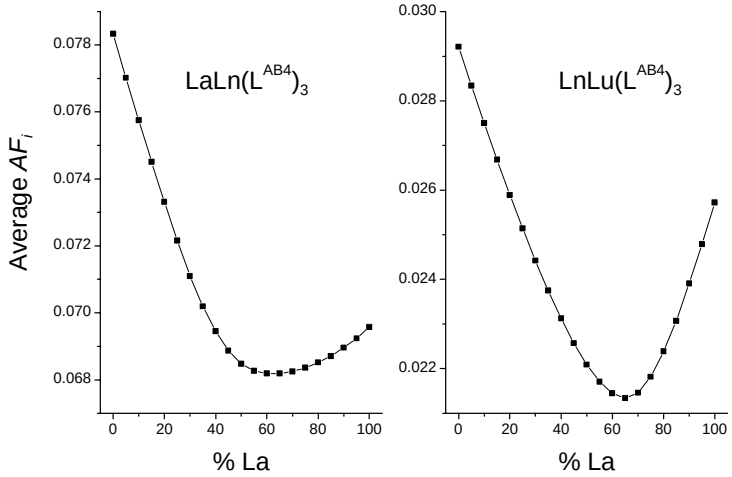

Figure 96 Average AF_i of L^{AB4} complexes as function of La percentage

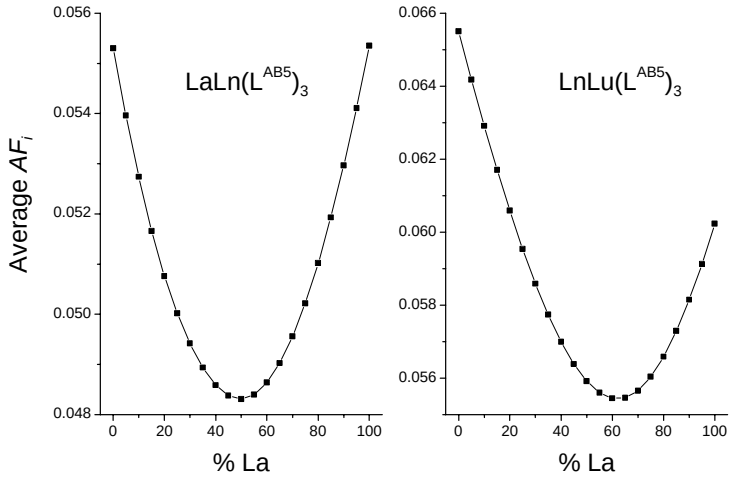

Figure 97 Average AF_i of L^{AB5} complexes as function of La percentage

The best combinations of reference complexes determined this way were:

$LaLn(L^{AB})_3$: 45 % $La_2(L^{AB})_3$ and 55 % $LaLu(L^{AB})_3$
$LnLu(L^{AB})_3$: 65 % $LaLu(L^{AB})_3$ and 35 % $Lu_2(L^{AB})_3$
$LaLn(L^{AB3})_3$: 50 % $La_2(L^{AB3})_3$ and 50 % $LaLu(L^{AB3})_3$
$LnLu(L^{AB3})_3$: 65 % $LaLu(L^{AB3})_3$ and 35 % $Lu_2(L^{AB3})_3$
$LaLn(L^{AB4})_3$: 60 % $La_2(L^{AB4})_3$ and 40 % $LaLu(L^{AB4})_3$
$LnLu(L^{AB4})_3$: 65 % $LaLu(L^{AB4})_3$ and 35 % $Lu_2(L^{AB4})_3$
$LaLn(L^{AB5})_3$: 50 % $La_2(L^{AB5})_3$ and 50 % $LaLu(L^{AB5})_3$
$LnLu(L^{AB5})_3$: 60 % $LaLu(L^{AB5})_3$ and 40 % $Lu_2(L^{AB5})_3$

These percentages are similar to the ones used in the ordinary one proton analysis and have been used to calculate chemical shift values as weighted averages (Table 116).

Table 116 Chemical shift of virtual reference complexes

	L^{AB}		L^{AB3}		L^{AB4}		L^{AB5}	
	LaLn	LnLu	LnLn	LnLu	LnLn	LnLu	LnLn	LnLu
	40 % La_2 60 % LaLu	70 % LaLu 30 % Lu_2	55 % La_2 45 % LaLu	75 % LaLu 25 % Lu_2	65 % La_2 35 % LaLu	75 % LaLu 25 % Lu_2	50 % La_2 50 % LaLu	70 % LaLu 30 % Lu_2
H1	7.71	7.73	7.68	7.67	7.69	7.73	7.74	7.76
H2	8.25	8.24			8.24	8.24	8.28	8.27
H3	8.31	8.34	8.15	8.20	8.29	8.35	8.33	8.38
H4	4.44	4.51	4.46	4.51	4.48	4.55	4.49	4.57
H4'	4.66	4.71	4.70	4.75	4.67	4.72	4.72	4.77
H5	1.48	1.47	1.48	1.47	1.48	1.48	1.49	1.49
H6	7.07	7.10	7.11	7.13	7.10	7.11	7.11	7.14
H7	6.83	6.83	6.88	6.86	6.77	6.75	6.89	6.87
H8	5.76	5.54	5.72	5.47	5.87	5.60	5.76	5.49
H9	3.43	3.43	3.48	3.47	3.40	3.38	3.46	3.47
H9'	3.64	3.62	3.67	3.65	3.68	3.66	3.71	3.68
H10	5.97	5.76	5.93	5.71	6.08	5.88	5.91	5.71
H11	7.31	7.29	7.32	7.31	7.26	7.25	7.39	7.38
H12	7.65	7.64	7.66	7.66	7.56	7.58	7.69	7.70
H13	4.27	4.33	4.29	4.35	4.28	4.33	4.28	4.38
H13'	3.70	3.84	3.74	3.87	3.66	3.77	3.91	4.04
H14	1.58	1.58	1.58	1.59	1.66	1.65	1.37	1.43
H15	7.58	7.57	7.62	7.59	6.22	6.21	7.53	7.50
H16	8.03	7.97	8.05	7.98				
H17	7.64	7.62	7.66	7.64	6.44	6.40	7.54	7.51
H18	4.10	4.16	4.13	4.19	3.88	3.96	4.27	4.30
H18'	4.55	4.55	4.55	4.57	4.35	4.36	4.53	4.55
H19	1.55	1.53	1.55	1.54	1.53	1.53	1.50	1.49
H20	7.68	7.67	7.68	7.68	7.65	7.64	7.71	7.71
H21	7.29	7.29	7.30	7.29	7.29	7.28	7.39	7.37
H22	6.75	6.73	6.75	6.74	6.82	6.80	6.88	6.85
H23	6.75	6.57	6.74	6.57	6.98	6.81	6.65	6.48
H24	3.32	3.31	3.39	3.36	3.34	3.33	3.35	3.34
H24'	3.27	3.31	3.34	0.96	3.28	3.33	3.33	3.37
H25	0.94	1.03	0.86	2.69	0.98	1.06	0.96	1.05
H26	2.63	2.55	2.75	2.74	2.71	2.58	2.66	2.57
H26'	2.75	2.69	2.84	0.68	2.81	2.71	2.77	2.71
H27	0.65	0.61	0.73	7.67	0.67	0.61	0.67	0.62
H28					3.50	3.46		
H28'					3.42	3.41		
H29					1.18	1.15		

5.7.4 LIS values

Using these "virtual lanthanide complexes" as references values the lanthanide induced shifts have been calculated. The values are given in Table 117 - Table 120.

Table 117 LIS of LaLn complexes of L^{AB} and L^{AB3}

	L^{AB}				L^{AB3}			
	LaCe	LaPr	LaNd	LaEu	LaCe	LaPr	LaNd	LaEu
H1	1.50	2.62	1.84	-2.67	1.23	2.11	1.41	-1.98
H2	1.97	3.14	1.86	-2.24				
H3	2.67	4.77	3.06	-4.35	2.41	4.29	2.61	-3.72
H4	0.83	1.48	0.77	-0.97	0.73	1.31	0.86	-0.84
H4'	1.23	2.24	1.10	-1.19	1.16	2.05	1.00	-1.08
H5	1.40	2.30	1.16	-1.33	1.38	2.26	1.11	-1.30
H6	0.34	0.75	0.75	-1.37	0.33	0.72	0.74	-1.39
H7	-0.33	-0.54	-0.29	0.36	-0.32	-0.55	-0.28	0.37
H8	-5.96	-9.90	-4.28	4.78	-5.68	-9.36	-4.14	4.42
H9	-0.50	-0.85	-0.41	0.48	-0.49	-0.84	-0.40	0.50
H9'	-0.12	-0.19	-0.14	0.29	-0.17	-0.33	-0.18	0.30
H10	-3.12	-5.02	-2.55	2.81	-2.91	-4.72	-2.29	2.62
H11	-0.23	-0.42	-0.19	0.24	-0.23	-0.41	-0.19	0.26
H12	-0.37	-0.65	-0.31	0.38	-0.38	-0.59	-0.28	0.37
H13	-0.44	-0.69	-0.36	0.39	-0.40	-0.65	-0.32	0.38
H13'	-0.43	-0.76	-0.39	0.42	-0.42	-0.70	-0.33	0.39
H14	-0.31	-0.48	-0.22	0.27	-0.30	-0.46	-0.22	0.27
H15	-0.50	-0.87	-0.43	0.49	-0.49	-0.79	-0.38	0.45
H16	-0.32	-0.54	-0.27	0.31	-0.30	-0.49	-0.24	0.29
H17	-0.39	-0.62	-0.32	0.36	-0.36	-0.59	-0.28	0.35
H18	-0.36	-0.58	-0.29	0.37	-0.35	-0.49	-0.26	0.35
H18'	-0.32	-0.52	-0.25	0.30	-0.31	-0.48	-0.22	0.29
H19	-0.25	-0.40	-0.19	0.24	-0.24	-0.38	-0.16	0.23
H20	-0.26	-0.42	-0.21	0.24	-0.26	-0.37	-0.18	0.23
H21	-0.22	-0.36	-0.18	0.21	-0.20	-0.34	-0.15	0.20
H22	-0.29	-0.48	-0.24	0.26	-0.26	-0.43	-0.20	0.24
H23	-0.49	-0.78	-0.40	0.44	-0.46	-0.76	-0.36	0.40
H24	0.68	1.50	0.81	-1.06	0.73	1.47	0.81	-1.02
H24'	0.01	0.36	0.32	-0.55	0.08	0.51	0.33	-0.57
H25	0.43	1.01	0.54	-0.73	0.45	1.05	0.53	-0.83
H26	-0.86	-1.29	-0.49	0.84	-0.80	-1.10	-0.44	0.58
H26'	0.07	0.28	0.20	-0.13	0.25	0.50	0.29	-0.19
H27	-2.66	-4.61	-2.30	2.70	-2.29	-4.20	-2.03	2.49

Table 118 LIS of LaLn complexes of L^{AB4} and L^{AB5}

	L^{AB4}				L^{AB5}			
	LaCe	LaPr	LaNd	LaEu	LaCe	LaPr	LaNd	LaEu
H1	1.51	2.64	1.82	-2.68	1.46	2.53	1.76	-2.61
H2	1.89	3.01	1.75	-2.17	1.94	3.08	1.78	-2.19
H3	2.51	4.45	2.83	-4.13	2.67	4.71	2.96	-4.25
H4	1.11	1.58	0.80	-0.99	0.76	1.38	0.72	-0.91
H4'	1.13	2.23	1.10	-1.18	1.22	2.17	1.04	-1.14
H5	1.12	2.27	1.10	-1.33	1.41	2.31	1.12	-1.32
H6	0.36	0.84	0.78	-1.42	0.31	0.72	0.74	-1.37
H7	-0.30	-0.46	-0.25	0.28	-0.36	-0.58	-0.29	0.36
H8	-6.02	-9.82	-4.42	4.74	-6.09	-10.07	-4.46	4.68
H9	-0.53	-0.86	-0.41	0.51	-0.54	-0.89	-0.43	0.51
H9'	-0.15	-0.24	-0.15	0.23	-0.15	-0.29	-0.17	0.26
H10	-2.89	-4.83	-2.28	2.61	-3.21	-4.90	-2.34	2.71
H11	-0.22	-0.45	-0.20	0.27	-0.24	-0.46	-0.21	0.26
H12	-0.37	-0.64	-0.30	0.41	-0.38	-0.65	-0.31	0.39
H13	-0.43	-0.68	-0.33	0.40	-0.43	-0.73	-0.34	0.40
H13'	-0.47	-0.78	-0.38	0.42	-0.42	-0.74	-0.37	0.39
H14	-0.27	-0.43	-0.20	0.26	-0.34	-0.51	-0.24	0.28
H15	-0.51	-0.83	-0.40	0.45	-0.53	-0.87	-0.42	0.46
H17	-0.38	-0.61	-0.29	0.34	-0.40	-0.64	-0.31	0.35
H18	-0.38	-0.58	-0.29	0.37	-0.31	-0.54	-0.27	0.34
H18'	-0.27	-0.48	-0.20	0.38	-0.30	-0.50	-0.23	0.30
H19	-0.23	-0.39	-0.18	0.24	-0.26	-0.41	-0.20	0.23
H20	-0.25	-0.41	-0.19	0.24	-0.24	-0.40	-0.18	0.24
H21	-0.22	-0.36	-0.17	0.20	-0.22	-0.37	-0.18	0.20
H22	-0.28	-0.45	-0.21	0.24	-0.27	-0.46	-0.22	0.25
H23	-0.45	-0.74	-0.37	0.39	-0.48	-0.77	-0.38	0.40
H24	0.59	1.36	0.74	-1.00	0.67	1.47	0.80	-1.04
H24'	-0.04	0.25	0.24	-0.51	-0.05	0.27	0.28	-0.56
H25	0.37	0.89	0.47	-0.64	0.42	1.00	0.51	-0.70
H26	-1.01	-1.51	-0.55	0.86	-0.83	-1.26	-0.46	0.76
H26'	-0.04	0.09	0.13	-0.04	0.10	0.29	0.18	-0.14
H27	-2.65	-4.54	-2.20	2.58	-2.62	-4.53	-2.19	2.57
H28	-0.25	-0.20	-0.18	0.17				
H28'	-0.17	-0.27	-0.19	0.16				
H29	-0.16	-0.26	-0.13	0.14				

Table 119 LIS of LnLu complexes of L^{AB} and L^{AB3}

	L^{AB}				L^{AB3}			
	CeLu	PrLu	NdLu	EuLu	CeLu	PrLu	NdLu	EuLu
H1	-0.23	-0.51	-0.31	0.30	-0.22	-0.50	-0.31	0.30
H2	-0.21	-0.43	-0.26	0.27				
H3	-0.31	-0.67	-0.41	0.41	-0.30	-0.68	-0.41	0.41
H4	-0.34	-0.68	-0.39	0.44	-0.33	-0.69	-0.40	0.47
H4'	-0.32	-0.68	-0.41	0.43	-0.32	-0.70	-0.41	0.43
H5	-0.22	-0.46	-0.28	0.29	-0.21	-0.46	-0.27	0.29
H6	-0.35	-0.67	-0.39	0.47	-0.35	-0.71	-0.42	0.45
H7	-0.23	-0.47	-0.28	0.34	-0.23	-0.50	-0.30	0.36
H8	-1.56	-3.47	-2.13	2.03	-1.52	-3.37	-2.07	2.10
H9	-0.12	-0.27	-0.22	0.38	-0.11	-0.28	-0.23	0.39
H9'	-0.38	-0.85	-0.53	0.54	-0.38	-0.85	-0.54	0.55
H10	-4.72	-10.46	-6.29	5.72	-4.62	-10.32	-6.19	5.75
H11	0.02	0.04	0.01	0.04	0.02	0.02	-0.01	0.05
H12	0.62	1.48	1.25	-1.81	0.61	1.42	1.22	-1.80
H13	1.10	2.68	1.87	-2.04	1.06	2.68	1.83	-2.03
H13'	1.22	2.91	1.85	-1.64	1.16	2.79	1.77	-1.65
H14	0.79	1.69	1.05	-1.09	0.78	1.66	1.02	-1.07
H15	1.40	3.54	2.89	-3.99	1.37	3.45	2.84	-3.98
H16	1.31	2.69	1.96	-2.31	1.28	2.62	1.91	-2.31
H17	1.41	3.54	2.96	-4.22	1.38	3.46	2.90	-4.23
H18	1.14	2.71	1.66	-1.69	1.10	2.62	1.67	-1.71
H18'	1.02	2.46	1.74	-1.95	0.98	2.39	1.68	-1.95
H19	0.56	1.17	0.72	-0.70	0.55	1.15	0.70	-0.71
H20	0.62	1.45	1.25	-1.84	0.61	1.42	1.22	-1.85
H21	0.06	0.13	0.05	0.04	0.07	0.13	0.05	0.02
H22	-0.38	-0.89	-0.56	0.60	-0.38	-0.89	-0.56	0.58
H23	-3.61	-8.29	-5.02	4.91	-3.51	-8.12	-5.04	4.89
H24	-0.22	-0.46	-0.28	0.28	-0.20	-0.48	-0.28	0.29
H25	-0.17	-0.38	-0.23	0.23	-0.17	-0.39	-0.23	0.25
H26	-0.26	-0.60	-0.35	0.36	-0.25	-0.57	-0.33	0.33
H26'	-0.22	-0.44	-0.29	0.28	-0.22	-0.46	-0.31	0.28
H27	-0.21	-0.45	-0.28	0.27	-0.19	-0.43	-0.26	0.28

Table 120 LIS of LnLu complexes of L^{AB4} and L^{AB5}

	L^{AB4}				L^{AB5}			
	CeLu	PrLu	NdLu	EuLu	CeLu	PrLu	NdLu	EuLu
H1	-0.42	-0.79	-0.45	0.53	-0.22	-0.49	-0.30	0.27
H2	-0.37	-0.69	-0.40	0.47	-0.17	-0.42	-0.27	0.23
H3	-0.57	-1.08	-0.62	0.73	-0.28	-0.64	-0.37	0.37
H4	-0.57	-1.05	-0.59	0.72	-0.34	-0.68	-0.40	0.41
H4'	-0.56	-1.06	-0.60	0.73	-0.30	-0.65	-0.39	0.39
H5	-0.39	-0.72	-0.41	0.48	-0.22	-0.45	-0.27	0.26
H6	-0.57	-1.03	-0.58	0.72	-0.35	-0.69	-0.40	0.46
H7	-0.36	-0.67	-0.39	0.48	-0.25	-0.52	-0.30	0.34
H8	-2.88	-5.44	-3.13	3.62	-1.47	-3.24	-1.91	1.85
H9	-0.19	-0.37	-0.27	0.41	-0.16	-0.33	-0.26	0.40
H9'	-0.70	-1.32	-0.78	0.92	-0.37	-0.84	-0.54	0.52
H10	-8.44	-16.29	-9.05	10.29	-4.35	-9.76	-5.83	5.20
H11	-0.07	-0.13	-0.10	0.16	-0.02	-0.05	-0.04	0.09
H12	0.81	1.69	1.32	-2.00	0.55	1.32	1.17	-1.73
H13	1.88	3.85	2.43	-3.26	0.94	2.40	1.64	-1.75
H13'	2.27	4.41	2.59	-3.15	1.02	2.46	1.57	-1.36
H14	1.19	2.21	1.29	-1.53	0.88	1.82	1.14	-1.07
H15	2.80	5.75	4.08	-5.82	1.16	3.05	2.47	-3.34
H17	2.55	5.22	3.77	-5.56	1.14	2.95	2.46	-3.45
H18	2.40	4.30	2.67	-3.22	0.96	2.36	1.41	-1.65
H18'	2.00	4.25	2.54	-3.18	0.89	2.16	1.53	-1.65
H19	0.99	1.78	1.02	-1.12	0.60	1.22	0.72	-0.69
H20	1.01	2.01	1.50	-2.19	0.59	1.35	1.19	-1.79
H21	0.21	0.34	0.16	-0.07	0.05	0.08	0.02	0.05
H22	-0.55	-1.13	-0.68	0.92	-0.37	-0.90	-0.57	0.57
H23	-6.05	-11.72	-6.79	8.22	-3.26	-7.69	-4.61	4.52
H24	-0.37	-0.71	-0.39	0.49	-0.23	-0.45	-0.28	0.24
H24'	-0.37	-0.69	-0.39	0.49	-0.21	-0.45	-0.28	0.25
H25	-0.30	-0.57	-0.33	0.38	-0.15	-0.35	-0.21	0.21
H26	-0.47	-0.87	-0.50	0.60	-0.27	-0.53	-0.31	0.28
H26'	-0.38	-0.71	-0.41	0.47	-0.20	-0.43	-0.27	0.24
H27	-0.37	-0.69	-0.39	0.49	-0.19	-0.42	-0.26	0.24
H28	0.81	1.59	0.81	-0.88				
H28'	0.86	1.64	0.86	-1.04				
H29	0.74	1.42	0.83	-1.03				

5.7.5 Separation of contact and pseudo contact parameters

These lanthanide induced shift values have then been used to carry out the analysis. The results are given in Table 121 - Table 128. The plots are shown in Appendix 3 (pages 365 ff.).

Table 121 Modified one proton analysis of LaLn complexes of L^{AB}

	Plots of $\Delta_{i,j}/\langle S_z \rangle_j$ vs. $C_j\left(B_0^2\right)_j/\langle S_z \rangle_j$			Plots of $\Delta_{i,j}/C_j\left(B_0^2\right)_j$ vs. $< S_z >_j /C_j\left(B_0^2\right)_j$		
	G_i (slope)	F_i (intercept)	Correlation coefficient	G_i (intercept)	F_i (slope)	Correlation coefficient
H1	-0.209(5)	-0.17(2)	0.999	-0.201(8)	-0.19(1)	0.997
H2	-0.30(2)	-0.05(4)	0.999	-0.29(1)	-0.07(2)	0.953
H3	-0.384(3)	-0.26(1)	1.000	-0.38(1)	-0.27(1)	0.997
H4	-0.128(3)	-0.03(1)	0.999	-0.130(3)	-0.025(4)	0.971
H4'	-0.194(8)	-0.03(3)	0.998	-0.21(1)	0.00(1)	0.014
H5	-0.222(1)	-0.001(5)	1.000	-0.222(3)	-0.001(4)	0.237
H6	-0.031(3)	-0.15(1)	0.992	-0.03(1)	-0.15(1)	0.992
H7	0.0513(7)	0.005(3)	1.000	0.0505(8)	0.007(1)	0.983
H8	0.97(1)	-0.13(4)	1.000	0.98(1)	-0.15(2)	0.989
H9	0.0800(8)	0.001(3)	1.000	0.0810(9)	-0.001(1)	0.498
H9'	0.016(2)	0.017(8)	0.984	0.013(5)	0.025(6)	0.939
H10	0.495(7)	-0.02(3)	1.000	0.49(1)	-0.01(2)	0.493
H11	0.036(2)	0.005(7)	0.998	0.037(2)	0.002(3)	0.445
H12	0.058(2)	0.006(6)	0.999	0.059(2)	0.003(3)	0.671
H13	0.070(2)	-0.004(7)	0.999	0.069(3)	-0.002(4)	0.389
H13'	0.068(2)	0.008(7)	0.999	0.071(4)	0.001(5)	0.122
H14	0.050(1)	-0.007(5)	0.999	0.048(2)	-0.003(3)	0.649
H15	0.080(2)	0.006(6)	1.000	0.082(2)	0.001(3)	0.144
H16	0.0512(4)	0.001(1)	1.000	0.052(1)	0.000(1)	0.043
H17	0.063(1)	-0.003(5)	1.000	0.062(2)	-0.001(3)	0.280
H18	0.057(1)	0.000(4)	1.000	0.056(1)	0.003(2)	0.769
H18'	0.0502(4)	-0.001(2)	1.000	0.049(1)	0.000(2)	0.095
H19	0.0390(7)	-0.002(3)	1.000	0.038(2)	0.001(3)	0.290
H20	0.0405(4)	-0.001(1)	1.000	0.0401(4)	0.0004(6)	0.436
H21	0.0348(2)	-0.0001(9)	1.000	0.0347(3)	0.0003(3)	0.580
H22	0.0454(2)	-0.0001(8)	1.000	0.0458(7)	-0.0009(9)	0.545
H23	0.077(1)	-0.003(5)	1.000	0.076(2)	-0.001(2)	0.293
H24	-0.10(1)	-0.08(5)	0.984	-0.11(1)	-0.05(2)	0.914
H24'	0.01(1)	-0.10(4)	0.520	0.00(1)	-0.07(1)	0.968
H25	-0.06(1)	-0.06(4)	0.974	-0.07(1)	-0.04(1)	0.902
H26	0.139(7)	-0.03(3)	0.997	0.13(2)	0.00(3)	0.078
H26'	-0.008(7)	-0.03(2)	0.674	-0.02(1)	-0.01(1)	0.430
H27	0.418(7)	0.04(3)	1.000	0.427(8)	0.02(1)	0.822

Table 122 Modified one proton analysis of LaLn complexes of L^{AB3}

	Plots of $\Delta_{i,j}/\langle S_z \rangle_j$ vs. $C_j\left(B_0^2\right)_j/\langle S_z \rangle_j$			Plots of $\Delta_{i,j}/C_j\left(B_0^2\right)_j$ vs. $< S_z >_j /C_j\left(B_0^2\right)_j$		
	G_i (slope)	F_i (intercept)	Correlation coefficient	G_i (intercept)	F_i (slope)	Correlation coefficient
H1	-0.175(2)	-0.124(7)	1.000	-0.174(3)	-0.126(4)	0.999
H3	-0.350(5)	-0.22(2)	1.000	-0.355(6)	-0.211(7)	0.999
H4	-0.108(6)	-0.06(2)	0.996	-0.12(2)	-0.03(3)	0.624
H4'	-0.183(8)	-0.02(3)	0.998	-0.20(2)	0.00(2)	0.077
H5	-0.217(3)	-0.010(9)	1.000	-0.222(8)	0.00(1)	0.082
H6	-0.029(3)	-0.15(1)	0.989	-0.02(1)	-0.16(2)	0.991
H7	0.049(1)	0.012(4)	1.000	0.050(1)	0.009(1)	0.981
H8	0.92(2)	-0.07(7)	1.000	0.95(5)	-0.14(6)	0.867
H9	0.076(2)	0.009(8)	0.999	0.079(2)	0.004(3)	0.657
H9'	0.024(2)	0.020(6)	0.996	0.025(3)	0.018(4)	0.950
H10	0.462(5)	0.00(2)	1.000	0.47(2)	-0.01(2)	0.372
H11	0.036(2)	0.007(6)	0.998	0.037(2)	0.004(2)	0.811
H12	0.0593(9)	-0.001(3)	1.000	0.058(2)	0.002(2)	0.571
H13	0.0624(6)	0.003(2)	1.000	0.063(2)	0.001(2)	0.190
H13'	0.066(1)	0.002(5)	1.000	0.068(2)	-0.002(3)	0.385
H14	0.0470(7)	-0.003(3)	1.000	0.0464(8)	-0.002(1)	0.754
H15	0.0771(6)	0.000(2)	1.000	0.078(2)	-0.002(3)	0.413
H16	0.0466(5)	0.002(2)	1.000	0.047(1)	0.001(1)	0.418
H17	0.0562(6)	0.002(2)	1.000	0.0569(7)	0.0007(8)	0.522
H18	0.054(3)	0.00(1)	0.997	0.050(3)	0.005(4)	0.608
H18'	0.0494(7)	-0.003(3)	1.000	0.048(1)	-0.001(2)	0.346
H19	0.0385(6)	-0.003(2)	1.000	0.038(2)	-0.001(3)	0.261
H20	0.041(2)	-0.006(7)	0.998	0.039(2)	-0.001(3)	0.304
H21	0.031(1)	0.002(4)	0.999	0.032(1)	0.000(2)	0.008
H22	0.0414(6)	0.001(2)	1.000	0.042(1)	-0.001(1)	0.550
H23	0.073(1)	0.000(5)	1.000	0.076(4)	-0.005(5)	0.571
H24	-0.11(1)	-0.07(4)	0.991	-0.12(1)	-0.04(2)	0.900
H24'	0.00(1)	-0.09(5)	0.149	-0.02(1)	-0.06(2)	0.933
H25	-0.06(1)	-0.07(4)	0.970	-0.07(1)	-0.05(2)	0.900
H26	0.131(6)	-0.04(2)	0.998	0.122(8)	-0.03(1)	0.866
H26'	-0.038(5)	-0.01(2)	0.983	-0.05(1)	0.00(2)	0.128
H27	0.36(2)	0.09(7)	0.997	0.38(2)	0.04(3)	0.658

Table 123 Modified one proton analysis of LaLn complexes of L^{AB4}

	Plots of $\Delta_{i,j}/\langle S_z \rangle_j$ vs. $C_j\left(B_0^2\right)_j/\langle S_z \rangle_j$			Plots of $\Delta_{i,j}/C_j\left(B_0^2\right)_j$ vs. $< S_z >_j /C_j\left(B_0^2\right)_j$		
	G_i (slope)	F_i (intercept)	Correlation coefficient	G_i (intercept)	F_i (slope)	Correlation coefficient
H1	-0.211(2)	-0.180(9)	1.000	-0.209(9)	-0.18(1)	0.996
H2	-0.290(2)	-0.057(8)	1.000	-0.289(4)	-0.060(5)	0.992
H3	-0.362(8)	-0.26(3)	1.000	-0.36(2)	-0.25(2)	0.992
H4	-0.177(6)	0.03(2)	0.999	-0.168(8)	0.01(1)	0.360
H4'	-0.18(2)	-0.06(7)	0.989	-0.20(2)	-0.01(3)	0.125
H5	-0.17(2)	-0.08(7)	0.987	-0.20(2)	-0.02(3)	0.505
H6	-0.034(4)	-0.15(2)	0.985	-0.03(1)	-0.16(2)	0.990
H7	0.0471(6)	0.000(2)	1.000	0.047(1)	0.001(2)	0.328
H8	0.98(3)	-0.10(9)	0.999	1.01(3)	-0.17(4)	0.954
H9	0.084(1)	0.001(5)	1.000	0.085(3)	-0.001(3)	0.200
H9'	0.0224(7)	0.010(3)	0.999	0.021(2)	0.012(2)	0.972
H10	0.46(1)	0.00(5)	0.999	0.48(2)	-0.03(2)	0.777
H11	0.035(4)	0.01(2)	0.986	0.039(5)	0.004(6)	0.408
H12	0.059(2)	0.008(9)	0.998	0.060(4)	0.004(5)	0.540
H13	0.0687(4)	-0.002(2)	1.000	0.069(1)	-0.002(1)	0.779
H13'	0.076(2)	0.000(7)	0.999	0.079(3)	-0.006(4)	0.745
H14	0.0432(6)	-0.001(2)	1.000	0.043(2)	-0.001(2)	0.244
H15	0.081(2)	-0.001(6)	1.000	0.083(2)	-0.005(2)	0.864
H17	0.0610(8)	-0.002(3)	1.000	0.0618(9)	-0.004(1)	0.931
H18	0.0611(8)	-0.003(3)	1.000	0.060(1)	0.000(2)	0.044
H18'	0.041(3)	0.01(1)	0.995	0.040(9)	0.01(1)	0.602
H19	0.037(1)	0.002(4)	0.999	0.038(2)	0.000(2)	0.100
H20	0.0407(8)	-0.001(3)	1.000	0.041(1)	-0.002(1)	0.707
H21	0.0353(8)	0.000(3)	1.000	0.0360(8)	-0.002(1)	0.834
H22	0.0452(7)	-0.003(3)	1.000	0.0459(8)	-0.005(1)	0.961
H23	0.073(2)	0.000(7)	0.999	0.076(4)	-0.007(5)	0.695
H24	-0.08(2)	-0.09(6)	0.969	-0.10(2)	-0.05(2)	0.877
H24'	0.018(9)	-0.09(3)	0.804	0.01(1)	-0.07(1)	0.965
H25	-0.05(1)	-0.06(4)	0.961	-0.07(1)	-0.03(1)	0.840
H26	0.167(5)	-0.04(2)	0.999	0.16(2)	-0.03(3)	0.591
H26'	0.010(6)	-0.03(2)	0.762	0.00(1)	-0.01(2)	0.517
H27	0.42(2)	0.04(6)	0.999	0.44(2)	0.00(2)	0.154
H28	0.040(8)	-0.02(3)	0.959	0.032(9)	0.00(1)	0.100
H28'	0.026(1)	0.006(5)	0.997	0.028(6)	0.003(7)	0.273
H29	0.0256(5)	0.000(2)	1.000	0.026(1)	-0.002(1)	0.734

Table 124 Modified one proton analysis of LaLn complexes of L^{AB5}

	Plots of $\Delta_{i,j}/\langle S_z \rangle_j$ vs. $C_j\left(B_0^2\right)_j/\langle S_z \rangle_j$			Plots of $\Delta_{i,j}/C_j\left(B_0^2\right)_j$ vs. $< S_z >_j /C_j\left(B_0^2\right)_j$		
	G_i (slope)	F_i (intercept)	Correlation coefficient	G_i (intercept)	F_i (slope)	Correlation coefficient
H1	-0.202(7)	-0.17(3)	0.999	-0.19(1)	-0.19(1)	0.996
H2	-0.30(1)	-0.04(4)	0.999	-0.29(1)	-0.07(2)	0.944
H3	-0.385(5)	-0.24(2)	1.000	-0.38(1)	-0.26(1)	0.997
H4	-0.117(3)	-0.03(1)	0.999	-0.120(3)	-0.026(4)	0.978
H4'	-0.194(6)	-0.01(2)	0.999	-0.202(9)	0.00(1)	0.216
H5	-0.224(2)	0.005(9)	1.000	-0.222(3)	0.000(4)	0.096
H6	-0.026(3)	-0.15(1)	0.989	-0.02(1)	-0.16(1)	0.992
H7	0.056(1)	0.001(4)	1.000	0.055(1)	0.003(1)	0.851
H8	0.989(7)	-0.14(3)	1.000	1.00(3)	-0.16(3)	0.960
H9	0.0856(7)	-0.001(3)	1.000	0.0851(8)	0.000(1)	0.139
H9'	0.0215(9)	0.017(3)	0.998	0.022(2)	0.016(2)	0.982
H10	0.51(2)	-0.08(7)	0.999	0.50(2)	-0.04(2)	0.738
H11	0.038(2)	0.008(9)	0.996	0.040(2)	0.003(3)	0.550
H12	0.059(1)	0.004(4)	1.000	0.060(1)	0.003(2)	0.754
H13	0.0678(6)	0.000(2)	1.000	0.0685(7)	-0.0019(9)	0.846
H13'	0.066(2)	0.006(7)	0.999	0.069(4)	-0.001(5)	0.070
H14	0.055(2)	-0.010(8)	0.998	0.052(2)	-0.005(3)	0.765
H16	0.0846(9)	-0.004(3)	1.000	0.085(3)	-0.005(3)	0.718
H17	0.063(1)	-0.005(4)	1.000	0.062(1)	-0.003(2)	0.782
H18	0.047(1)	0.009(4)	0.999	0.049(1)	0.006(2)	0.942
H18'	0.0468(4)	0.000(2)	1.000	0.046(2)	0.001(2)	0.363
H19	0.041(1)	-0.004(4)	0.999	0.041(1)	-0.001(1)	0.590
H20	0.0374(5)	0.000(2)	1.000	0.037(2)	0.001(2)	0.200
H21	0.0342(3)	0.000(1)	1.000	0.035(1)	-0.001(1)	0.546
H22	0.0429(4)	0.001(2)	1.000	0.044(1)	-0.001(1)	0.436
H23	0.078(1)	-0.008(6)	1.000	0.078(3)	-0.007(4)	0.785
H24	-0.10(1)	-0.08(4)	0.986	-0.11(1)	-0.05(2)	0.927
H24'	0.02(1)	-0.10(4)	0.793	0.01(1)	-0.08(1)	0.972
H25	-0.06(1)	-0.06(4)	0.972	-0.07(1)	-0.04(1)	0.887
H26	0.135(6)	-0.03(2)	0.998	0.12(2)	-0.01(2)	0.305
H26'	-0.014(5)	-0.02(2)	0.901	-0.021(8)	-0.01(1)	0.406
H27	0.414(5)	0.03(2)	1.000	0.421(8)	0.01(1)	0.584

Table 125 Modified one proton analysis of LnLu complexes of L^{AB}

	Plots of $\Delta_{i,j}/\langle S_z\rangle_j$ vs. $C_j\left(B_0^2\right)_j/\langle S_z\rangle_j$			Plots of $\Delta_{i,j}/C_j\left(B_0^2\right)_j$ vs. $<S_z>_j/C_j\left(B_0^2\right)_j$		
	G_i (slope)	F_i (intercept)	Correlation coefficient	G_i (intercept)	F_i (slope)	Correlation coefficient
H1	0.037(1)	0.002(4)	0.999	0.038(2)	-0.001(3)	0.319
H2	0.0338(9)	-0.003(4)	0.999	0.0335(7)	-0.002(1)	0.674
H3	0.0490(6)	0.002(3)	1.000	0.050(1)	0.000(2)	0.063
H4	0.054(2)	-0.007(8)	0.999	0.052(2)	-0.001(5)	0.144
H4'	0.0507(2)	0.0007(7)	1.000	0.0508(3)	0.0006(5)	0.640
H5	0.0355(6)	-0.001(2)	1.000	0.0355(7)	-0.001(1)	0.546
H6	0.054(3)	-0.01(1)	0.996	0.051(4)	0.003(8)	0.299
H7	0.035(1)	0.002(4)	0.999	0.034(2)	0.006(3)	0.752
H8	0.248(8)	0.02(3)	0.999	0.26(1)	-0.01(2)	0.258
H9	0.015(1)	0.028(5)	0.992	0.013(3)	0.033(5)	0.977
H9'	0.060(2)	0.009(7)	0.999	0.062(2)	0.004(4)	0.547
H10	0.76(2)	0.0(1)	0.999	0.79(4)	-0.10(8)	0.665
H11	-0.0048(6)	0.008(2)	0.986	-0.006(1)	0.011(2)	0.950
H12	-0.075(2)	-0.153(7)	0.999	-0.074(3)	-0.156(6)	0.998
H13	-0.16(1)	-0.12(5)	0.995	-0.17(1)	-0.09(2)	0.929
H13'	-0.19(1)	-0.05(6)	0.994	-0.21(2)	0.00(4)	0.026
H14	-0.1232(9)	-0.010(4)	1.000	-0.124(2)	-0.007(4)	0.789
H15	-0.17(1)	-0.35(5)	0.995	-0.180(9)	-0.33(2)	0.997
H16	-0.189(8)	-0.09(3)	0.998	-0.186(7)	-0.10(1)	0.986
H17	-0.17(1)	-0.37(4)	0.997	-0.174(9)	-0.36(2)	0.998
H18	-0.18(1)	-0.05(5)	0.996	-0.19(1)	-0.02(2)	0.547
H18'	-0.148(9)	-0.12(4)	0.996	-0.16(1)	-0.09(2)	0.958
H19	-0.089(1)	0.003(5)	1.000	-0.089(2)	0.005(5)	0.590
H20	-0.074(2)	-0.155(7)	0.999	-0.072(4)	-0.162(8)	0.998
H21	-0.013(1)	0.015(5)	0.991	-0.015(3)	0.020(5)	0.946
H22	0.059(3)	0.02(1)	0.998	0.062(3)	0.012(5)	0.853
H23	0.57(3)	0.1(1)	0.998	0.60(3)	0.00(6)	0.000
H24	0.0350(5)	-0.001(2)	1.000	0.0352(7)	-0.002(1)	0.660
H25	0.0264(9)	0.003(4)	0.999	0.0272(9)	0.001(2)	0.417
H26	0.042(2)	0.004(8)	0.998	0.043(2)	0.000(3)	0.026
H26'	0.034(1)	0.000(6)	0.998	0.035(2)	0.000(3)	0.058
H27	0.0327(5)	0.002(2)	1.000	0.033(1)	0.000(2)	0.075

Table 126 Modified one proton analysis of LnLu complexes of L^{AB3}

	Plots of $\Delta_{i,j}/\langle S_z \rangle_j$ vs. $C_j\left(B_0^2\right)_j/\langle S_z \rangle_j$			Plots of $\Delta_{i,j}/C_j\left(B_0^2\right)_j$ vs. $< S_z >_j /C_j\left(B_0^2\right)_j$		
	G_i (slope)	F_i (intercept)	Correlation coefficient	G_i (intercept)	F_i (slope)	Correlation coefficient
H1	0.0350(4)	0.001(3)	1.000	0.036(2)	-0.002(3)	0.412
H3	0.0486(4)	-0.001(3)	1.000	0.050(1)	-0.004(3)	0.701
H4	0.053(3)	-0.006(9)	0.998	0.050(3)	0.000(5)	0.015
H4'	0.0509(8)	-0.004(1)	1.000	0.0506(4)	-0.0032(7)	0.954
H5	0.0343(7)	-0.003(2)	1.000	0.0340(4)	-0.0027(7)	0.936
H6	0.055(2)	-0.01(1)	0.998	0.053(2)	-0.005(5)	0.580
H7	0.0362(1)	0.002(4)	0.999	0.035(1)	0.005(3)	0.768
H8	0.241(4)	0.00(1)	1.000	0.244(6)	-0.01(1)	0.460
H9	0.013(3)	0.032(4)	0.995	0.012(2)	0.035(4)	0.985
H9'	0.0595(5)	0.005(3)	1.000	0.060(2)	0.002(4)	0.421
H10	0.75(7)	-0.08(6)	1.000	0.77(3)	-0.13(6)	0.832
H11	-0.0049(1)	0.013(3)	0.978	-0.0048(7)	0.012(1)	0.987
H12	-0.074(2)	-0.14(1)	0.998	-0.071(5)	-0.151(9)	0.997
H13	-0.16(7)	-0.11(5)	0.995	-0.17(1)	-0.08(2)	0.923
H13'	-0.18(5)	-0.03(4)	0.997	-0.20(2)	0.00(3)	0.086
H14	-0.124(6)	0.01(1)	0.999	-0.122(3)	0.004(5)	0.418
H15	-0.169(4)	-0.33(3)	0.998	-0.171(6)	-0.32(1)	0.999
H16	-0.18(5)	-0.07(5)	0.995	-0.18(1)	-0.09(2)	0.959
H17	-0.167(3)	-0.36(2)	0.999	-0.165(8)	-0.36(2)	0.998
H18	-0.172(4)	-0.04(3)	0.998	-0.180(9)	-0.02(2)	0.597
H18'	-0.143(5)	-0.10(3)	0.998	-0.148(7)	-0.09(1)	0.979
H19	-0.088(4)	0.01(1)	0.999	-0.087(3)	0.009(5)	0.778
H20	-0.073(5)	-0.15(2)	0.997	-0.069(6)	-0.16(1)	0.994
H21	-0.014(7)	0.018(4)	0.995	-0.015(2)	0.019(3)	0.973
H22	0.060(5)	0.010(7)	0.999	0.062(2)	0.005(5)	0.573
H23	0.56(1)	0.04(7)	0.999	0.58(3)	-0.02(5)	0.250
H24	0.032(1)	0.002(6)	0.998	0.033(1)	-0.001(2)	0.170
H25	0.0265(2)	0.002(3)	0.999	0.0266(6)	0.002(1)	0.718
H26	0.0406(4)	-0.003(3)	1.000	0.0413(8)	-0.005(2)	0.911
H26'	0.035(8)	-0.002(8)	0.997	0.036(3)	-0.004(3)	0.438
H27	0.0306(6)	0.0008(7)	1.000	0.0309(4)	0.0002(7)	0.166

Table 127 Modified one proton analysis of LnLu complexes of L^{AB4}

	Plots of $\Delta_{i,j}/\langle S_z \rangle_j$ vs. $C_j\left(B_0^2\right)_j/\langle S_z \rangle_j$			Plots of $\Delta_{i,j}/C_j\left(B_0^2\right)_j$ vs. $< S_z >_j /C_j\left(B_0^2\right)_j$		
	G_i (slope)	F_i (intercept)	Correlation coefficient	G_i (intercept)	F_i (slope)	Correlation coefficient
H1	0.0669(4)	-0.001(2)	1.000	0.0674(8)	-0.002(1)	0.733
H2	0.0581(2)	0.0007(7)	1.000	0.0583(5)	0.0001(9)	0.081
H3	0.0905(8)	0.002(3)	1.000	0.091(1)	-0.001(2)	0.303
H4	0.0906(5)	-0.004(2)	1.000	0.0899(9)	-0.002(1)	0.735
H4'	0.0896(5)	0.000(2)	1.000	0.0901(5)	-0.0009(9)	0.561
H5	0.0618(2)	-0.0026(9)	1.000	0.0619(4)	-0.0026(7)	0.928
H6	0.090(1)	-0.006(5)	1.000	0.089(2)	-0.001(3)	0.258
H7	0.0570(3)	0.001(1)	1.000	0.0569(3)	0.0020(4)	0.954
H8	0.458(4)	0.00(2)	1.000	0.464(9)	-0.01(2)	0.523
H9	0.0270(8)	0.022(3)	0.999	0.026(1)	0.025(3)	0.989
H9'	0.1096(7)	0.007(3)	1.000	0.111(2)	0.004(3)	0.726
H10	1.36(3)	0.0(1)	1.000	1.39(4)	-0.11(6)	0.775
H11	0.0093(6)	0.009(2)	0.996	0.008(1)	0.011(2)	0.971
H12	-0.106(2)	-0.145(8)	1.000	-0.104(6)	-0.149(9)	0.996
H13	-0.281(9)	-0.14(4)	0.999	-0.287(9)	-0.12(2)	0.985
H13'	-0.355(6)	-0.05(2)	1.000	-0.361(6)	-0.03(1)	0.893
H14	-0.188(1)	-0.001(4)	1.000	-0.188(2)	-0.001(4)	0.170
H15	-0.394(7)	-0.34(3)	1.000	-0.40(1)	-0.34(2)	0.997
H17	-0.353(6)	-0.34(2)	1.000	-0.35(2)	-0.35(3)	0.994
H18	-0.38(1)	-0.01(4)	0.999	-0.37(1)	-0.03(2)	0.766
H18'	-0.31(2)	-0.12(7)	0.996	-0.32(2)	-0.08(3)	0.878
H19	-0.159(3)	0.02(1)	1.000	-0.159(5)	0.020(8)	0.865
H20	-0.139(2)	-0.133(8)	1.000	-0.136(5)	-0.140(9)	0.996
H21	-0.037(2)	0.027(7)	0.998	-0.038(4)	0.029(7)	0.946
H22	0.083(3)	0.03(1)	0.998	0.085(4)	0.029(6)	0.956
H23	0.95(2)	0.09(6)	1.000	0.97(2)	0.05(3)	0.786
H24	0.0589(9)	0.001(4)	1.000	0.059(1)	0.000(2)	0.043
H24'	0.0586(3)	0.000(1)	1.000	0.0583(8)	0.001(1)	0.514
H25	0.0470(6)	0.002(2)	1.000	0.0477(9)	0.000(2)	0.045
H26	0.0741(2)	-0.0005(9)	1.000	0.0739(2)	0.0000(4)	0.052
H26'	0.0612(6)	-0.002(2)	1.000	0.062(2)	-0.004(3)	0.663
H27	0.0593(2)	-0.001(1)	1.000	0.0590(5)	0.0003(9)	0.223
H28	-0.134(5)	0.02(2)	0.999	-0.138(5)	0.031(9)	0.929
H28'	-0.139(2)	0.01(1)	1.000	-0.140(3)	0.015(5)	0.898
H29	-0.116(1)	-0.013(5)	1.000	-0.116(1)	-0.011(2)	0.969

Table 128 Modified one proton analysis of LnLu complexes of L^{AB5}

	Plots of $\Delta_{i,j}/\langle S_z \rangle_j$ vs. $C_j\left(B_0^2\right)_j/\langle S_z \rangle_j$			Plots of $\Delta_{i,j}/C_j\left(B_0^2\right)_j$ vs. $< S_z >_j /C_j\left(B_0^2\right)_j$		
	G_i (slope)	F_i (intercept)	Correlation coefficient	G_i (intercept)	F_i (slope)	Correlation coefficient
H1	0.0342(9)	0.003(4)	0.999	0.035(1)	0.000(3)	0.066
H2	0.026(2)	0.01(1)	0.991	0.029(3)	0.002(5)	0.308
H3	0.044(2)	0.005(6)	0.999	0.045(1)	0.002(2)	0.590
H4	0.055(3)	-0.01(1)	0.998	0.053(2)	-0.003(4)	0.476
H4'	0.0469(1)	0.0026(4)	1.000	0.0471(2)	0.0022(4)	0.967
H5	0.0342(9)	-0.002(4)	0.999	0.0337(7)	-0.001(1)	0.397
H6	0.054(3)	0.00(1)	0.997	0.051(4)	0.005(7)	0.495
H7	0.040(1)	-0.001(5)	0.999	0.038(2)	0.003(3)	0.598
H8	0.235(3)	0.00(1)	1.000	0.238(4)	-0.005(7)	0.444
H9	0.020(2)	0.026(8)	0.990	0.017(3)	0.033(6)	0.973
H9'	0.058(2)	0.013(7)	0.999	0.060(3)	0.007(6)	0.637
H10	0.70(2)	0.02(8)	0.999	0.72(3)	-0.06(6)	0.569
H11	0.0019(5)	0.008(2)	0.936	0.001(1)	0.010(2)	0.953
H12	-0.063(2)	-0.157(6)	0.999	-0.060(4)	-0.164(7)	0.998
H13	-0.14(1)	-0.11(5)	0.992	-0.15(1)	-0.08(2)	0.926
H13'	-0.16(1)	-0.05(5)	0.995	-0.17(2)	-0.01(3)	0.176
H14	-0.138(4)	0.00(2)	0.999	-0.138(5)	0.001(8)	0.103
H15	-0.14(1)	-0.31(5)	0.992	-0.15(1)	-0.29(2)	0.996
H17	-0.14(1)	-0.32(4)	0.995	-0.141(8)	-0.31(1)	0.998
H18	-0.15(1)	-0.07(4)	0.995	-0.151(9)	-0.06(2)	0.935
H18'	-0.129(8)	-0.10(3)	0.997	-0.137(9)	-0.08(2)	0.959
H19	-0.095(3)	0.01(1)	0.999	-0.093(2)	0.007(4)	0.780
H20	-0.068(4)	-0.15(1)	0.997	-0.063(6)	-0.17(1)	0.996
H21	-0.0095(6)	0.015(2)	0.996	-0.0097(9)	0.016(2)	0.989
H22	0.057(4)	0.02(2)	0.995	0.060(4)	0.014(7)	0.826
H23	0.51(3)	0.1(1)	0.998	0.54(2)	0.04(4)	0.558
H24	0.036(2)	-0.006(8)	0.997	0.036(2)	-0.005(3)	0.746
H24'	0.0329(6)	0.001(2)	1.000	0.034(1)	-0.001(3)	0.340
H25	0.0243(9)	0.004(4)	0.999	0.025(1)	0.001(2)	0.428
H26	0.043(2)	-0.011(9)	0.998	0.043(2)	-0.008(3)	0.883
H26'	0.0312(6)	0.001(3)	1.000	0.032(1)	-0.001(3)	0.229
H27	0.0307(7)	0.001(3)	1.000	0.032(2)	-0.001(3)	0.295

The correlation coefficients are seen to be very good for plots according to Eq. (20). Even the protons close to the so-called magic angles (H11 and H21) in the LnLu series of complexes are almost perfect, although H24' and H26' continue to be problematic in the LaLn series, as was also seen in the ordinary one proton analysis.

The plots according to Eq. (19) are generally less good, some of them very much less. Protons having a substantial contact term ($F_i > 0.1$) and large slopes have a good correlation coefficient.

But even more satisfying is that the problem with too large contact term parameters have been solved. As was pointed out, this was particularly evident for H8 in the LnLu series and for H10 in the LaLn series. Both are characterised by having large pseudo contact shifts due to their proximity to the paramagnetic lanthanide ion and the insufficient separation leads to contact terms too large to be plausible in light of their topological distance (number of bonds) to the paramagnetic center. All this is gone in this modified one proton analysis. All contact terms are of reasonable magnitude and the two problematic protons mentioned above have F_i values close to zero.

5.7.6 Comparing contact and pseudo contact parameters

Contact and pseudo contact parameters of complexes of the four different ligands are shown in Figure 98 (compare Figure 49 (page 124) where similar data for the traditional one proton analysis are shown). In the upper half the contact parameters F_i are compared and it is seen that the values are now very similar for all four ligands. In the previous analysis L^{AB4} deviated from the other three ligands and it was suspected that this was a result of insufficient separation of contact and pseudo contact shifts, a problem that appears to be solved with the present approach.

The lower part of the figure seems at first glance not to encourage the use of this new method; structural factors G_i indicate that the LnLu series of L^{AB4} complexes are structurally different from the complexes of the other three ligands. This contradicts what was found in the two proton (Geraldes) analysis, namely that the complexes of all the ligands are isostructural. However, it should not be forgotten that the structural factors will always be scaled due to the (rather arbitrary) scaling of C_j. In the new analysis there is a second scaling factor since the

crystal field parameter has been set to 1 for each Ce complex. This time the scaling factors are not the same for all four ligands (see Table 115), meaning that the values of the structural factors can no longer be compared between complexes of different ligands. The lower part of Figure 98 is therefore, strictly speaking, not of any use and is only included here as a reminder that relative crystal field parameters have been used as scaling factors in the modified one proton analysis.

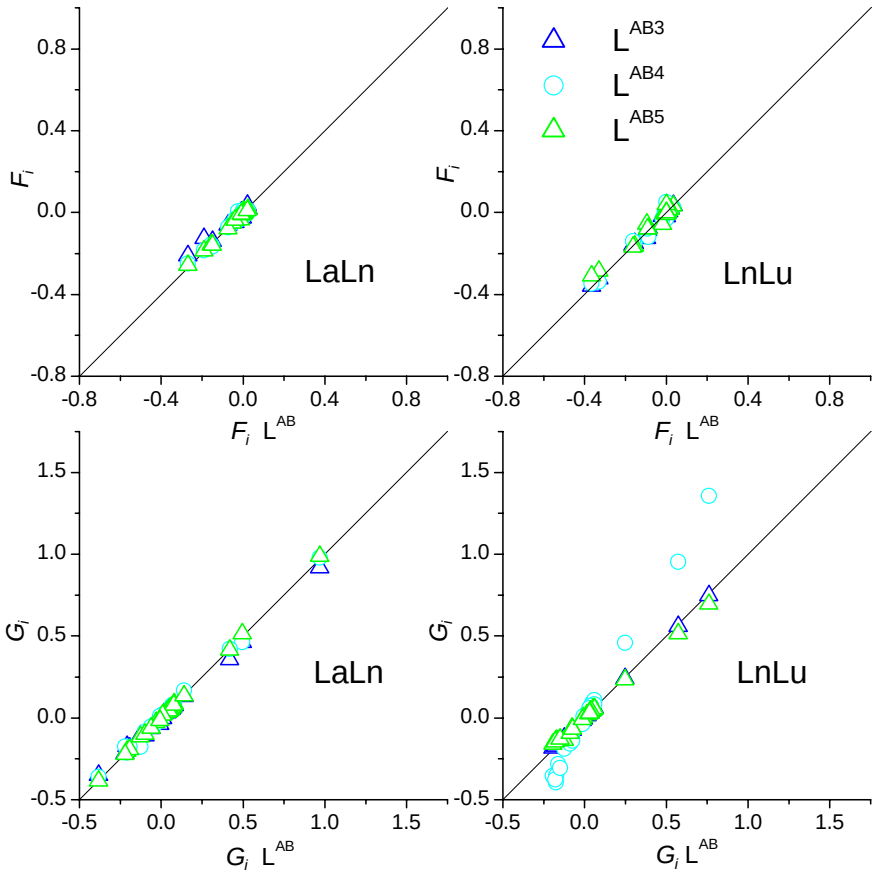

Figure 98 Comparing contact and pseudo contact parameters

The contact (F_i) and pseudo contact (G_i) parameters of the two series of L^{AB} complexes are illustrated in Figure 99 - Figure 102. The radii of the hydrogen atoms in the figures are proportional to the absolute values of the corresponding parameter. It is clearly seen how the contact term is negligible for protons not topologically close to the paramagnetic lanthanide ion. The pseudo contact term, while obviously being largest for close protons, is seen to induce shifts even in protons in the other end of the complex.

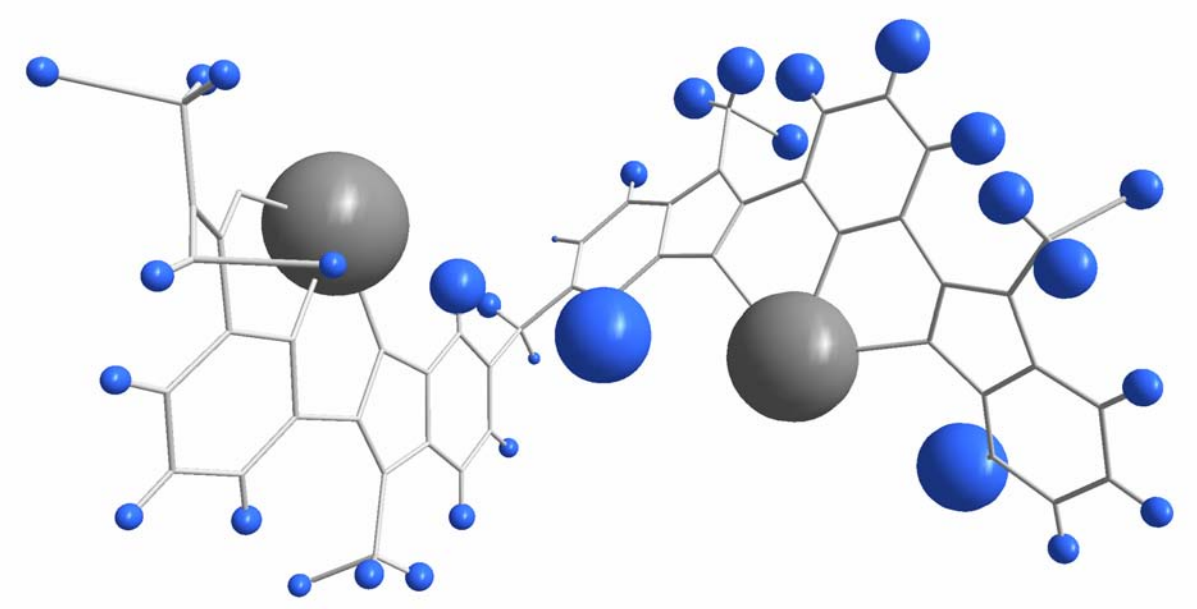

Figure 99 G_i **parameters for LnLu(L^{AB})$_3$ complexes (paramagnetic ion in bpb site, right)**

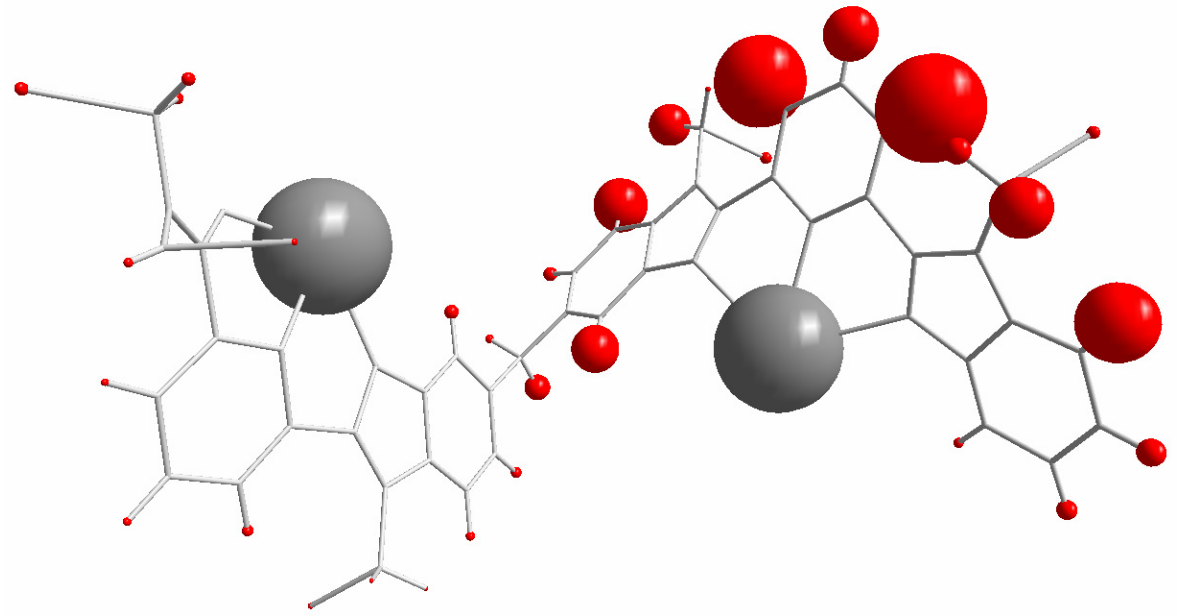

Figure 100 F_i **parameters for LnLu(L^{AB})$_3$ complexes (paramagnetic ion in bpb site, right)**

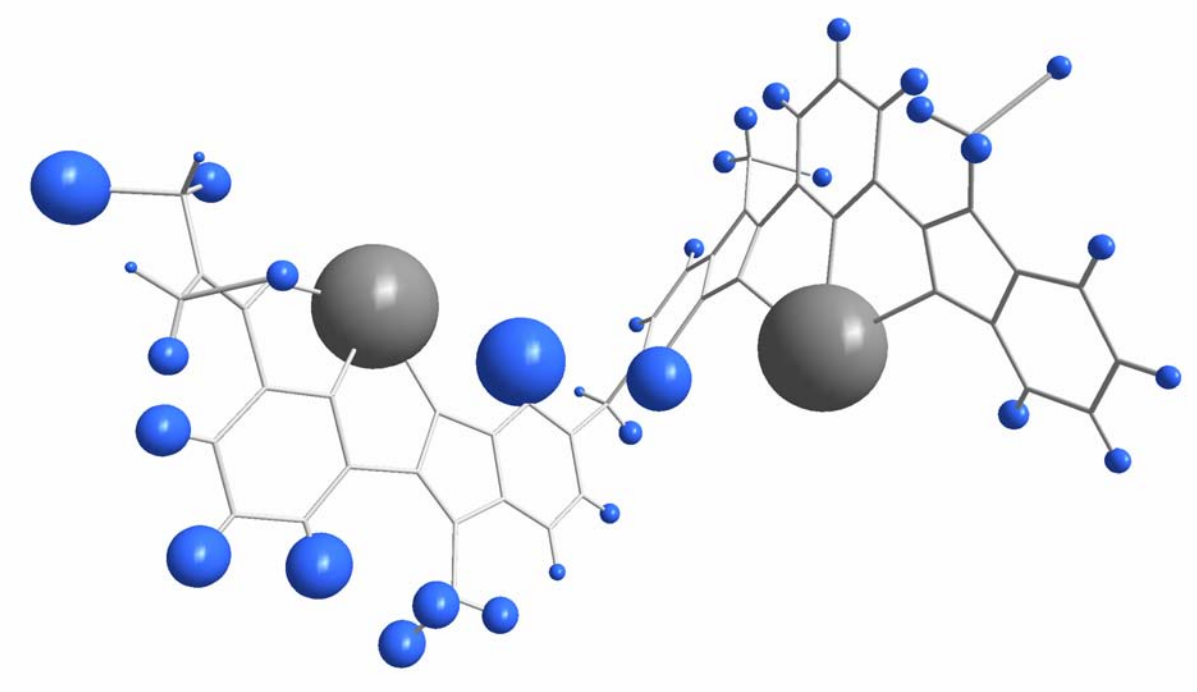

Figure 101 G_i **parameters for LaLn(L^{AB})$_3$ complexes (paramagnetic ion in bpa site, left)**

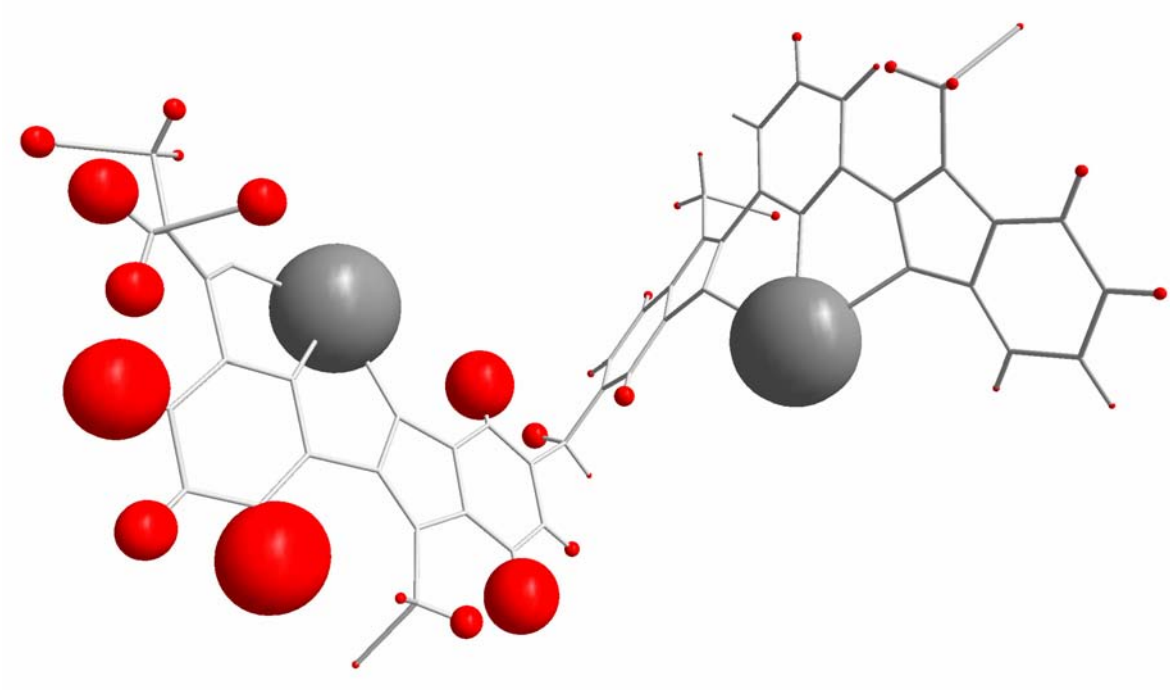

Figure 102 F_i **parameters for LaLn(L^{AB})$_3$ complexes (paramagnetic ion in bpa site, left)**

5.7.7 Recalculation of contact and pseudo contact shifts

Contact and pseudo contact terms have been calculated by multiplying the results of the modified one proton analysis (Table 121 - Table 128) with the parameters of Table 22. They are listed in Table 129 - Table 136.

Table 129 Contact and pseudo contact terms of LaLn complexes of L^{AB}

	LaCe		LaPr		LaNd		LaEu	
	Δ_c	Δ_{pc}	Δ_c	Δ_{pc}	Δ_c	Δ_{pc}	Δ_c	Δ_{pc}
H1	0.19(1)	1.32(3)	0.56(3)	2.18(5)	0.85(5)	1.07(3)	-1.43(8)	-1.25(3)
H2	0.07(1)	1.90(6)	0.20(4)	3.1(1)	0.30(7)	1.54(5)	-0.5(1)	-1.81(6)
H3	0.26(1)	2.42(2)	0.80(4)	4.01(3)	1.20(7)	1.97(2)	-2.0(1)	-2.30(2)
H4	0.024(4)	0.81(2)	0.07(1)	1.34(3)	0.11(2)	0.66(2)	-0.18(3)	-0.77(2)
H4'	0.00(1)	1.22(5)	0.00(4)	2.03(9)	0.00(6)	0.99(4)	0.0(1)	-1.16(5)
H5	0.001(4)	1.399(9)	0.00(1)	2.32(1)	0.01(2)	1.138(7)	-0.01(3)	-1.332(8)
H6	0.15(1)	0.20(2)	0.46(4)	0.33(3)	0.69(6)	0.16(1)	-1.2(1)	-0.19(2)
H7	-0.007(1)	-0.323(5)	-0.022(3)	-0.536(8)	-0.033(4)	-0.263(4)	0.055(7)	0.308(4)
H8	0.15(2)	-6.11(6)	0.44(5)	-10.1(1)	0.66(7)	-4.97(5)	-1.1(1)	5.82(6)
H9	0.001(1)	-0.504(5)	0.003(3)	-0.837(9)	0.004(5)	-0.410(4)	-0.007(9)	0.480(5)
H9'	-0.024(6)	-0.10(1)	-0.07(2)	-0.17(2)	-0.11(3)	-0.08(1)	0.18(5)	0.10(1)
H10	0.01(2)	-3.12(4)	0.04(5)	-5.17(7)	0.06(7)	-2.54(3)	-0.1(1)	2.97(4)
H11	-0.002(3)	-0.22(1)	-0.006(9)	-0.37(2)	-0.01(1)	-0.183(9)	0.02(2)	0.21(1)
H12	-0.003(2)	-0.36(1)	-0.010(8)	-0.60(2)	-0.01(1)	-0.296(8)	0.02(2)	0.347(9)
H13	0.002(3)	-0.44(1)	0.01(1)	-0.73(2)	0.01(2)	-0.359(9)	-0.02(3)	0.42(1)
H13'	-0.001(5)	-0.43(1)	0.00(1)	-0.71(2)	0.00(2)	-0.35(1)	0.01(4)	0.41(1)
H14	0.003(3)	-0.313(8)	0.010(8)	-0.52(1)	0.01(1)	-0.254(6)	-0.02(2)	0.298(7)
H15	-0.001(3)	-0.50(1)	-0.002(9)	-0.83(2)	0.00(1)	-0.408(8)	0.00(2)	0.48(1)
H16	0.000(1)	-0.323(2)	0.000(4)	-0.535(4)	0.000(6)	-0.262(2)	0.00(1)	0.307(2)
H17	0.001(3)	-0.394(8)	0.003(8)	-0.65(1)	0.00(1)	-0.321(7)	-0.01(2)	0.375(8)
H18	-0.003(2)	-0.362(6)	-0.009(5)	-0.60(1)	-0.014(8)	-0.294(5)	0.02(1)	0.345(6)
H18'	0.000(2)	-0.316(3)	-0.001(5)	-0.524(5)	-0.001(7)	-0.257(2)	0.00(1)	0.301(3)
H19	-0.001(2)	-0.246(4)	-0.003(7)	-0.408(7)	0.00(1)	-0.200(4)	0.01(2)	0.234(4)
H20	-0.0004(5)	-0.255(2)	-0.001(2)	-0.423(4)	-0.002(2)	-0.208(2)	0.003(4)	0.243(2)
H21	-0.0003(3)	-0.220(1)	-0.001(1)	-0.364(2)	-0.001(1)	-0.179(1)	0.003(2)	0.209(1)
H22	0.0008(9)	-0.286(1)	0.003(3)	-0.474(2)	0.004(4)	-0.232(1)	-0.006(7)	0.272(1)
H23	0.001(2)	-0.485(8)	0.003(7)	-0.81(1)	0.00(1)	-0.395(7)	-0.01(2)	0.462(8)
H24	0.05(2)	0.63(8)	0.15(5)	1.0(1)	0.23(7)	0.51(7)	-0.4(1)	-0.60(8)
H24'	0.07()(1)	-0.06(7)	0.21(4)	-0.1(1)	0.32(6)	-0.05(5)	-0.5(1)	0.05(6)
H25	0.04(1)	0.40(7)	0.12(4)	0.7(1)	0.17(6)	0.32(5)	-0.3(1)	-0.38(6)
H26	0.00(3)	-0.88(5)	0.01(8)	-1.45(8)	0.0(1)	-0.71(4)	0.0(2)	0.83(4)
H26'	0.01(1)	0.05(4)	0.03(4)	0.09(7)	0.04(6)	0.04(3)	-0.1(1)	-0.05(4)
H27	-0.02(1)	-2.63(5)	-0.06(3)	-4.37(8)	-0.09(4)	-2.14(4)	0.15(8)	2.51(4)

Table 130 Contact and pseudo contact terms of LaLn complexes of L^{AB3}

	LaCe		LaPr		LaNd		LaEu	
	Δ_c	Δ_{pc}	Δ_c	Δ_{pc}	Δ_c	Δ_{pc}	Δ_c	Δ_{pc}
H1	0.123(4)	1.10(1)	0.37(1)	1.77(2)	0.56(2)	0.829(9)	-0.95(3)	-1.05(1)
H3	0.205(7)	2.21(3)	0.62(2)	3.54(5)	0.94(3)	1.66(3)	-1.58(6)	-2.10(3)
H4	0.03(3)	0.68(4)	0.10(9)	1.09(7)	0.1(1)	0.51(3)	-0.3(2)	-0.65(4)
H4'	0.00(2)	1.16(5)	-0.01(6)	1.86(8)	-0.01(9)	0.87(4)	0.0(1)	-1.10(5)
H5	0.00(1)	1.37(2)	0.00(3)	2.20(3)	0.01(5)	1.03(1)	-0.01(8)	-1.30(2)
H6	0.15(1)	0.18(2)	0.46(5)	0.30(3)	0.70(7)	0.14(1)	-1.2(1)	-0.17(2)
H7	-0.009(1)	-0.311(6)	-0.027(4)	-0.50(1)	-0.040(6)	-0.234(5)	0.07(1)	0.296(6)
H8	0.14(6)	-5.8(1)	0.4(2)	-9.3(2)	0.6(3)	-4.36(9)	-1.1(4)	5.5(1)
H9	-0.004(3)	-0.48(1)	-0.011(9)	-0.77(2)	-0.02(1)	-0.36(1)	0.03(2)	0.46(1)
H9'	-0.017(4)	-0.15(1)	-0.05(1)	-0.25(2)	-0.08(2)	-0.116(8)	0.13(3)	0.15(1)
H10	0.01(2)	-2.91(3)	0.04(7)	-4.67(5)	0.1(1)	-2.19(2)	-0.1(2)	2.77(3)
H11	-0.004(2)	-0.226(9)	-0.013(7)	-0.36(2)	-0.02(1)	-0.171(7)	0.03(2)	0.216(9)
H12	-0.002(2)	-0.374(6)	-0.007(7)	-0.600(9)	-0.01(1)	-0.281(4)	0.02(2)	0.356(6)
H13	-0.001(2)	-0.393(4)	-0.002(7)	-0.632(6)	0.00(1)	-0.296(3)	0.00(2)	0.375(3)
H13'	0.002(3)	-0.416(8)	0.005(8)	-0.67(1)	0.01(1)	-0.313(6)	-0.01(2)	0.396(8)
H14	0.002(1)	-0.296(5)	0.005(3)	-0.476(7)	0.007(4)	-0.223(3)	-0.012(7)	0.282(4)
H15	0.002(2)	-0.486(3)	0.005(7)	-0.780(6)	0.01(1)	-0.366(3)	-0.01(2)	0.462(3)
H16	-0.001(1)	-0.294(3)	-0.003(4)	-0.472(5)	-0.004(6)	-0.221(2)	0.01(1)	0.280(3)
H17	-0.0007(8)	-0.354(4)	-0.002(2)	-0.569(6)	-0.003(4)	-0.267(3)	0.005(6)	0.337(3)
H18	-0.005(4)	-0.34(2)	-0.01(1)	-0.55(3)	-0.02(2)	-0.26(2)	0.04(3)	0.32(2)
H18'	0.001(2)	-0.311(5)	0.002(5)	-0.500(7)	0.004(7)	-0.235(3)	-0.01(1)	0.296(4)
H19	0.001(3)	-0.242(3)	0.003(8)	-0.389(6)	0.00(1)	-0.182(3)	-0.01(2)	0.231(3)
H20	0.001(2)	-0.26(1)	0.003(8)	-0.42(2)	0.01(1)	-0.197(9)	-0.01(2)	0.25(1)
H21	0.000(2)	-0.196(6)	0.000(5)	-0.31(1)	0.000(7)	-0.147(5)	0.00(1)	0.186(6)
H22	0.001(1)	-0.261(4)	0.003(4)	-0.42(1)	0.005(6)	-0.196(3)	-0.009(9)	0.248(4)
H23	0.004(5)	-0.463(9)	0.01(1)	-0.74(1)	0.02(2)	-0.349(6)	-0.03(3)	0.441(8)
H24	0.04(1)	0.68(6)	0.13(5)	1.1(1)	0.20(7)	0.51(5)	-0.3(1)	-0.65(6)
H24'	0.06(2)	0.02(8)	0.18(5)	0.0(1)	0.28(8)	0.01(6)	-0.5(1)	-0.02(8)
H25	0.05(2)	0.40(7)	0.14(5)	0.6(1)	0.21(7)	0.30(5)	-0.4(1)	-0.38(7)
H26	0.03(1)	-0.82(4)	0.08(3)	-1.32(6)	0.11(5)	-0.62(3)	-0.19(8)	0.78(4)
H26'	0.00(2)	0.24(3)	-0.01(5)	0.39(5)	-0.01(8)	0.18(2)	0.0(1)	-0.23(3)
H27	-0.03(3)	-2.2(1)	-0.11(9)	-3.6(2)	-0.2(1)	-1.69(9)	0.3(2)	2.1(1)

Table 131 Contact and pseudo contact terms of LaLn complexes of L^{AB4}

	LaCe		LaPr		LaNd		LaEu	
	Δ_c	Δ_{pc}	Δ_c	Δ_{pc}	Δ_c	Δ_{pc}	Δ_c	Δ_{pc}
H1	0.18(1)	1.33(1)	0.55(3)	2.09(2)	0.82(5)	1.07(1)	-1.39(9)	-1.27(1)
H2	0.058(5)	1.83(1)	0.18(2)	2.87(2)	0.27(2)	1.46(1)	-0.45(4)	-1.74(1)
H3	0.24(2)	2.28(5)	0.74(7)	3.58(8)	1.1(1)	1.82(4)	-1.9(2)	-2.17(5)
H4	-0.01(1)	1.12(4)	-0.02(3)	1.75(6)	-0.03(5)	0.89(3)	0.04(8)	-1.06(4)
H4'	0.00(3)	1.1(1)	0.02(8)	1.8(2)	0.0(1)	0.89(9)	0.0(2)	-1.1(1)
H5	0.02(3)	1.1(1)	0.07(8)	1.7(2)	0.1(1)	0.9(1)	-0.2(2)	-1.0(1)
H6	0.15(2)	0.21(3)	0.46(5)	0.33(4)	0.70(7)	0.17(2)	-1.2(1)	-0.20(2)
H7	-0.001(2)	-0.297(4)	-0.002(5)	-0.466(6)	-0.004(7)	-0.237(3)	0.01(1)	0.282(4)
H8	0.16(4)	-6.2(2)	0.5(1)	-9.7(2)	0.7(2)	-4.9(1)	-1.3(3)	5.9(2)
H9	0.001(3)	-0.530(9)	0.00(1)	-0.83(1)	0.00(1)	-0.424(7)	-0.01(2)	0.505(9)
H9'	-0.012(2)	-0.141(4)	-0.037(6)	-0.222(7)	-0.055(9)	-0.113(3)	0.09(2)	0.134(4)
H10	0.03(2)	-2.92(9)	0.10(6)	-4.6(1)	0.15(9)	-2.34(7)	-0.3(1)	2.78(8)
H11	-0.004(6)	-0.22(3)	-0.01(2)	-0.35(4)	-0.02(3)	-0.18(2)	0.03(4)	0.21(3)
H12	-0.004(4)	-0.37(1)	-0.01(1)	-0.58(2)	-0.02(2)	-0.30(1)	0.03(3)	0.35(1)
H13	0.002(1)	-0.433(3)	0.007(4)	-0.680(4)	0.010(6)	-0.346(2)	-0.02(1)	0.412(3)
H13'	0.006(4)	-0.48(1)	0.02(1)	-0.75(2)	0.03(2)	-0.38(1)	-0.05(3)	0.46(1)
H14	0.001(2)	-0.272(4)	0.00(1)	-0.427(6)	0.00(1)	-0.218(3)	-0.01(2)	0.259(4)
H16	0.005(2)	-0.51(1)	0.016(7)	-0.80(2)	0.02(1)	-0.409(8)	-0.04(2)	0.49(1)
H17	0.004(1)	-0.384(5)	0.012(3)	-0.604(8)	0.019(5)	-0.307(4)	-0.032(9)	0.366(5)
H18	0.000(2)	-0.385(5)	0.000(6)	-0.605(8)	-0.001(8)	-0.308(4)	0.00(1)	0.366(5)
H18'	-0.01(1)	-0.26(2)	-0.04(4)	-0.41(3)	-0.06(5)	-0.21(2)	0.10(9)	0.25(2)
H19	0.000(2)	-0.234(7)	-0.001(7)	-0.37(1)	0.00(1)	-0.187(6)	0.00(2)	0.223(7)
H20	0.002(1)	-0.256(5)	0.006(4)	-0.403(8)	0.009(6)	-0.205(4)	-0.01(1)	0.244(5)
H21	0.002(1)	-0.222(5)	0.007(3)	-0.349(7)	0.010(5)	-0.178(4)	-0.017(8)	0.212(5)
H22	0.0046(9)	-0.285(4)	0.014(3)	-0.447(7)	0.021(4)	-0.228(4)	-0.035(7)	0.271(4)
H23	0.007(5)	-0.46(1)	0.02(1)	-0.72(2)	0.03(2)	-0.366(9)	-0.05(4)	0.44(1)
H24	0.05(2)	0.5(1)	0.16(6)	0.8(2)	0.24(9)	0.43(8)	-0.4(2)	-0.51(9)
H24'	0.07(1)	-0.11(6)	0.22(4)	-0.17(9)	0.33(6)	-0.09(5)	-0.5(1)	0.11(6)
H25	0.03(1)	0.34(7)	0.10(4)	0.5(1)	0.15(7)	0.27(6)	-0.2(1)	-0.32(7)
H26	0.03(2)	-1.05(3)	0.08(7)	-1.65(5)	0.1(1)	-0.84(3)	-0.2(2)	1.00(3)
H26'	0.01(2)	-0.06(4)	0.04(5)	-0.10(6)	0.06(7)	-0.05(3)	-0.1(1)	0.06(4)
H27	0.00(2)	-2.7(1)	0.01(7)	-4.2(2)	0.0(1)	-2.12(8)	0.0(2)	2.5(1)
H28	0.00(1)	-0.25(5)	0.01(4)	-0.40(8)	0.01(5)	-0.20(4)	-0.01(9)	0.24(5)
H28'	-0.003(7)	-0.164(9)	-0.01(2)	-0.26(1)	-0.01(3)	-0.131(7)	0.02(5)	0.156(9)
H29	0.002(1)	-0.161(3)	0.005(4)	-0.253(5)	0.008(5)	-0.129(2)	-0.014(9)	0.154(3)

Table 132 Contact and pseudo contact terms of LaLn complexes of L^{AB5}

	LaCe		LaPr		LaNd		LaEu	
	Δ_c	Δ_{pc}	Δ_c	Δ_{pc}	Δ_c	Δ_{pc}	Δ_c	Δ_{pc}
H1	0.18(1)	1.28(4)	0.55(4)	2.14(7)	0.83(6)	1.01(3)	-1.40(9)	-1.21(4)
H2	0.06(2)	1.86(7)	0.19(5)	3.1(1)	0.29(7)	1.48(6)	-0.5(1)	-1.78(7)
H3	0.25(1)	2.43(3)	0.76(4)	4.06(5)	1.15(7)	1.92(2)	-1.9(1)	-2.31(3)
H4	0.025(4)	0.73(2)	0.08(1)	1.23(3)	0.12(2)	0.58(2)	-0.20(3)	-0.70(2)
H4'	0.00(1)	1.22(4)	-0.01(3)	2.05(6)	-0.02(5)	0.97(3)	0.03(9)	-1.16(3)
H5	0.000(4)	1.41(1)	0.00(1)	2.36(2)	0.00(2)	1.12(1)	0.00(3)	-1.34(1)
H6	0.15(1)	0.16(2)	0.47(4)	0.27(3)	0.70(6)	0.13(1)	-1.2(1)	-0.16(2)
H7	-0.003(1)	-0.352(6)	-0.009(4)	-0.59(1)	-0.01(1)	-0.279(5)	0.02(1)	0.335(6)
H8	0.15(3)	-6.23(4)	0.5(1)	-10.44(7)	0.7(1)	-4.94(3)	-1.2(2)	5.93(4)
H9	0.000(1)	-0.539(4)	-0.001(3)	-0.904(7)	-0.001(5)	-0.428(3)	0.002(8)	0.514(4)
H9'	-0.016(2)	-0.135(6)	-0.048(7)	-0.227(9)	-0.07(1)	-0.107(4)	0.12(2)	0.129(5)
H10	0.03(2)	-3.2(1)	0.11(7)	-5.4(2)	0.2(1)	-2.57(9)	-0.3(2)	3.1(1)
H11	-0.003(3)	-0.24(1)	-0.008(9)	-0.40(2)	-0.01(1)	-0.19(1)	0.02(2)	0.23(1)
H12	-0.003(2)	-0.373(6)	-0.008(5)	-0.63(1)	-0.013(8)	-0.296(5)	0.02(1)	0.355(6)
H13	0.0019(8)	-0.427(4)	0.006(3)	-0.716(7)	0.009(4)	-0.339(3)	-0.014(6)	0.407(4)
H13'	0.001(5)	-0.42(1)	0.00(2)	-0.70(2)	0.00(2)	-0.332(9)	0.00(4)	0.40(1)
H14	0.005(3)	-0.34(1)	0.014(8)	-0.58(2)	0.02(1)	-0.27(1)	-0.04(2)	0.33(1)
H16	0.005(3)	-0.533(4)	0.01(1)	-0.893(9)	0.02(1)	-0.423(4)	-0.04(3)	0.508(5)
H17	0.003(2)	-0.397(7)	0.010(5)	-0.67(1)	0.015(8)	-0.315(5)	-0.02(1)	0.378(6)
H18	-0.006(2)	-0.299(7)	-0.018(5)	-0.50(1)	-0.028(7)	-0.237(5)	0.05(1)	0.285(6)
H18'	-0.001(2)	-0.295(3)	-0.004(6)	-0.494(5)	-0.01(1)	-0.234(2)	0.01(2)	0.281(3)
H19	0.001(1)	-0.261(7)	0.004(4)	-0.44(1)	0.007(6)	-0.207(5)	-0.01(1)	0.248(6)
H20	-0.001(2)	-0.236(3)	-0.002(7)	-0.395(5)	0.00(1)	-0.187(2)	0.00(2)	0.224(3)
H21	0.001(1)	-0.216(2)	0.003(4)	-0.361(4)	0.005(6)	-0.171(2)	-0.009(9)	0.205(2)
H22	0.001(1)	-0.270(3)	0.003(4)	-0.453(4)	0.004(6)	-0.214(2)	-0.006(9)	0.257(2)
H23	0.007(4)	-0.490(9)	0.02(1)	-0.82(2)	0.03(2)	-0.389(7)	-0.06(3)	0.467(9)
H24	0.05(1)	0.62(7)	0.15(4)	1.0(1)	0.23(7)	0.49(6)	-0.4(1)	-0.59(7)
H24'	0.08(1)	-0.12(6)	0.24(4)	-0.2(1)	0.36(6)	-0.09(5)	-0.6(1)	0.11(6)
H25	0.04(1)	0.39(7)	0.11(4)	0.7(1)	0.16(6)	0.31(5)	-0.3(1)	-0.37(6)
H26	0.01(2)	-0.85(4)	0.03(7)	-1.43(7)	0.0(4)	-0.67(3)	-0.1(2)	0.81(4)
H26'	0.01(1)	0.09(3)	0.02(3)	0.15(5)	0.03(5)	0.07(1)	-0.05(8)	-0.09(3)
H27	-0.01(1)	-2.61(3)	-0.03(3)	-4.37(6)	-0.05(5)	-2.07(3)	0.08(8)	2.48(3)

Table 133 Contact and pseudo contact terms of LnLu complexes of L^{AB}

	CeLu		PrLu		NdLu		EuLu	
	Δ_c	Δ_{pc}	Δ_c	Δ_{pc}	Δ_c	Δ_{pc}	Δ_c	Δ_{pc}
H1	0.001(3)	-0.231(6)	0.004(8)	-0.49(1)	0.01(1)	-0.292(8)	-0.01(2)	0.308(9)
H2	0.002(1)	-0.213(5)	0.005(4)	-0.45(1)	0.008(6)	-0.270(7)	-0.01(1)	0.284(7)
H3	0.000(2)	-0.309(4)	0.001(7)	-0.658(8)	0.00(1)	-0.391(5)	0.00(2)	0.412(5)
H4	0.001(4)	-0.34(1)	0.00(1)	-0.72(3)	0.00(2)	-0.43(2)	-0.01(3)	0.45(2)
H4'	-0.0006(5)	-0.319(1)	-0.002(2)	-0.680(2)	-0.003(2)	-0.405(1)	0.005(4)	0.426(1)
H5	0.001(1)	-0.224(4)	0.004(4)	-0.477(8)	0.005(6)	-0.283(5)	-0.01(1)	0.298(5)
H6	-0.003(8)	-0.34(2)	-0.01(2)	-0.73(5)	-0.02(3)	-0.43(3)	0.03(6)	0.46(3)
H7	-0.005(3)	-0.221(7)	-0.02(1)	-0.47(1)	-0.02(2)	-0.280(8)	0.04(3)	0.294(9)
H8	0.01(2)	-1.56(5)	0.02(7)	-3.3(1)	0.0(1)	-1.98(6)	-0.1(2)	2.08(7)
H9	-0.033(5)	-0.094(8)	-0.10(2)	-0.20(2)	-0.15(2)	-0.12(1)	0.25(4)	0.13(1)
H9'	-0.004(4)	-0.38(1)	-0.01(1)	-0.81(2)	-0.02(2)	-0.48(1)	0.03(3)	0.50(1)
H10	0.09(7)	-4.8(4)	0.3(2)	-10.2(3)	0.4(3)	-6.1(2)	-0.7(6)	6.4(2)
H11	-0.010(2)	0.030(4)	-0.032(7)	0.064(8)	-0.05(1)	0.038(5)	0.08(2)	-0.040(5)
H12	0.152(6)	0.47(1)	0.46(2)	1.01(2)	0.69(3)	0.60(1)	-1.17(5)	-0.63(1)
H13	0.08(2)	1.02(7)	0.26(7)	2.2(2)	0.4(1)	1.29(9)	-0.7(2)	-1.4(1)
H13'	0.00(4)	1.21(9)	0.0(1)	2.6(2)	0.0(2)	1.5(1)	0.0(3)	-1.6(1)
H14	0.007(4)	0.776(5)	0.02(1)	1.65(1)	0.03(2)	0.983(7)	-0.05(3)	-1.035(7)
H15	0.32(2)	1.10(7)	0.98(5)	2.3(2)	1.47(8)	1.39(9)	-2.5(1)	-1.5(1)
H16	0.10(1)	1.19(5)	0.30(4)	2.5(1)	0.45(5)	1.51(7)	-0.76(9)	-1.59(7)
H17	0.35(2)	1.08(6)	1.08(5)	2.3(1)	1.62(7)	1.37(8)	-2.7(1)	-1.44(8)
H18	0.02(2)	1.13(7)	0.06(6)	2.4(2)	0.08(9)	1.43(9)	-0.1(2)	-1.5(1)
H18'	0.09(2)	0.93(6)	0.27(6)	2.0(1)	0.41(9)	1.18(8)	-0.7(1)	-1.24(8)
H19	-0.005(4)	0.558(8)	-0.01(1)	1.19(2)	-0.02(2)	0.71(1)	0.04(3)	-0.74(1)
H20	0.158(7)	0.47(1)	0.48(2)	1.00(2)	0.72(3)	0.59(1)	-1.21(6)	-0.62(1)
H21	-0.020(5)	0.081(8)	-0.06(1)	0.17(2)	-0.09(2)	0.10(1)	0.15(4)	-0.11(1)
H22	-0.012(5)	-0.37(2)	-0.04(2)	-0.79(4)	-0.05(2)	-0.47(2)	0.09(4)	0.50(2)
H23	0.00(5)	-3.6(2)	0.0(2)	-7.7(4)	0.0(2)	-4.6(2)	0.0(4)	4.8(2)
H24	0.002(1)	-0.221(3)	0.005(4)	-0.470(6)	0.007(6)	-0.280(4)	-0.01(1)	0.294(4)
H25	-0.001(2)	-0.166(6)	-0.003(5)	-0.35(1)	-0.005(7)	-0.211(7)	0.01(1)	0.222(7)
H26	0.000(3)	-0.26(1)	0.000(9)	-0.56(3)	0.00(1)	-0.33(2)	0.00(2)	0.35(2)
H26'	0.000(3)	-0.217(9)	0.00(1)	-0.46(2)	0.00(2)	-0.27(1)	0.00(3)	0.29(1)
H27	0.000(2)	-0.206(3)	0.001(6)	-0.439(7)	0.001(9)	-0.261(4)	0.00(2)	0.275(4)

Table 134 Contact and pseudo contact terms of LnLu complexes of L^{AB3}

	CeLu		PrLu		NdLu		EuLu	
	Δ_c	Δ_{pc}	Δ_c	Δ_{pc}	Δ_c	Δ_{pc}	Δ_c	Δ_{pc}
H1	0.002(3)	-0.221(5)	0.006(9)	-0.49(1)	0.01(1)	-0.294(6)	-0.01(2)	0.315(7)
H3	0.004(3)	-0.306(5)	0.012(9)	-0.68(1)	0.02(1)	-0.408(6)	-0.03(2)	0.437(7)
H4	0.000(5)	-0.33(1)	0.00(2)	-0.74(3)	0.00(2)	-0.44(2)	0.00(4)	0.47(2)
H4'	0.0031(7)	-0.320(2)	0.009(2)	-0.714(5)	0.014(3)	-0.427(3)	-0.024(5)	0.457(3)
H5	0.0026(7)	-0.216(3)	0.008(2)	-0.481(7)	0.012(3)	-0.287(4)	-0.020(5)	0.308(4)
H6	0.004(4)	-0.35(2)	0.01(1)	-0.78(4)	0.02(2)	-0.46(2)	-0.03(3)	0.50(2)
H7	-0.004(3)	-0.228(6)	-0.014(8)	-0.51(1)	-0.02(1)	-0.304(8)	0.03(2)	0.325(8)
H8	0.01(1)	-1.52(2)	0.02(3)	-3.39(3)	0.04(5)	-2.03(2)	-0.06(8)	2.17(2)
H9	-0.034(4)	-0.083(6)	-0.10(1)	-0.18(1)	-0.16(2)	-0.110(8)	0.26(3)	0.118(9)
H9'	-0.002(4)	-0.375(5)	-0.01(1)	-0.83(1)	-0.01(2)	-0.499(7)	0.02(3)	0.534(7)
H10	0.12(6)	-4.71(9)	0.4(2)	-10.5(2)	0.6(3)	-6.3(1)	-1.0(4)	6.7(1)
H11	-0.012(1)	0.031(5)	-0.036(4)	0.07(1)	-0.055(6)	0.042(6)	0.09(1)	-0.044(7)
H12	0.147(9)	0.47(2)	0.45(3)	1.04(4)	0.67(4)	0.62(3)	-1.13(7)	-0.67(3)
H13	0.08(2)	0.99(7)	0.23(7)	2.2(2)	0.3(1)	1.3(1)	-0.6(2)	-1.4(1)
H13'	0.00(3)	1.16(6)	-0.01(9)	2.6(1)	0.0(1)	1.55(9)	0.0(2)	-1.66(9)
H14	-0.003(5)	0.78(2)	-0.01(2)	1.73(5)	-0.02(2)	1.04(3)	0.03(4)	-1.11(3)
H15	0.32(1)	1.07(4)	0.96(4)	2.37(9)	1.44(5)	1.42(6)	-2.43(9)	-1.52(6)
H16	0.09(2)	1.16(8)	0.28(6)	2.6(2)	0.42(9)	1.5(1)	-0.7(1)	-1.7(1)
H17	0.35(2)	1.05(4)	1.06(5)	2.34(8)	1.60(7)	1.40(5)	-2.7(1)	-1.50(5)
H18	0.02(2)	1.09(4)	0.06(5)	2.4(1)	0.08(8)	1.45(6)	-0.1(1)	-1.55(6)
H18'	0.08(1)	0.90(4)	0.26(4)	2.00(9)	0.39(6)	1.20(5)	-0.7(1)	-1.28(6)
H19	-0.009(5)	0.55(2)	-0.03(1)	1.23(4)	-0.04(2)	0.74(3)	0.07(4)	-0.79(3)
H20	0.15(1)	0.46(2)	0.47(4)	1.03(5)	0.71(5)	0.62(3)	-1.19(9)	-0.66(3)
H21	-0.019(3)	0.089(6)	-0.06(1)	0.20(1)	-0.09(1)	0.119(8)	0.15(2)	-0.127(9)
H22	-0.005(5)	-0.38(1)	-0.01(1)	-0.84(2)	-0.02(2)	-0.50(1)	0.04(4)	0.54(2)
H23	0.02(5)	-3.5(1)	0.1(2)	-7.8(2)	0.1(2)	-4.7(1)	-0.1(4)	5.0(1)
H24	0.001(2)	-0.20(1)	0.002(7)	-0.45(2)	0.00(1)	-0.27(1)	0.00(2)	0.29(1)
H25	-0.002(1)	-0.167(4)	-0.005(3)	-0.372(9)	-0.007(5)	-0.222(5)	0.012(8)	0.238(6)
H26	0.005(2)	-0.256(5)	0.015(5)	-0.57(1)	0.022(7)	-0.341(6)	-0.04(1)	0.365(7)
H26'	0.004(6)	-0.22(1)	0.01(2)	-0.49(3)	0.02(3)	-0.30(2)	-0.03(4)	0.32(2)
H27	-0.0002(7)	-0.193(1)	0.000(2)	-0.430(2)	-0.001(3)	-0.257(1)	0.001(5)	0.275(2)

Table 135 Contact and pseudo contact terms of LnLu complexes of L^{AB4}

	CeLu		PrLu		NdLu		EuLu	
	Δ_c	Δ_{pc}	Δ_c	Δ_{pc}	Δ_c	Δ_{pc}	Δ_c	Δ_{pc}
H1	0.18(1)	1.33(1)	0.55(3)	2.09(2)	0.82(5)	1.07(1)	-1.39(9)	-1.27(1)
H2	0.058(5)	1.83(1)	0.18(2)	2.87(2)	0.27(2)	1.46(1)	-0.45(4)	-1.74(1)
H3	0.24(2)	2.28(5)	0.74(7)	3.58(8)	1.1(1)	1.82(4)	-1.9(2)	-2.17(5)
H4	-0.01(1)	1.12(4)	-0.02(3)	1.75(6)	-0.03(5)	0.89(3)	0.04(8)	-1.06(4)
H4'	0.00(3)	1.1(1)	0.02(8)	1.8(2)	0.0(1)	0.89(9)	0.0(2)	-1.1(1)
H5	0.02(3)	1.1(1)	0.07(8)	1.7(2)	0.1(1)	0.9(1)	-0.2(2)	-1.0(1)
H6	0.15(2)	0.21(3)	0.46(5)	0.33(4)	0.70(7)	0.17(2)	-1.2(1)	-0.20(2)
H7	-0.001(2)	-0.297(4)	-0.002(5)	-0.466(6)	-0.004(7)	-0.237(3)	0.01(1)	0.282(4)
H8	0.16(4)	-6.2(2)	0.5(1)	-9.7(2)	0.7(2)	-4.9(1)	-1.3(3)	5.9(2)
H9	0.001(3)	-0.530(9)	0.00(1)	-0.83(1)	0.00(1)	-0.424(4)	-0.01(2)	0.505(9)
H9'	-0.012(2)	-0.141(4)	-0.037(6)	-0.222(7)	-0.055(9)	-0.113(3)	0.09(2)	0.134(4)
H10	0.03(2)	-2.92(9)	0.10(6)	-4.6(1)	0.15(9)	-2.34(7)	-0.3(1)	2.78(8)
H11	-0.004(6)	-0.22(3)	-0.01(2)	-0.35(4)	-0.02(3)	-0.18(2)	0.03(4)	0.21(3)
H12	-0.004(4)	-0.37(1)	-0.01(1)	-0.58(2)	-0.02(2)	-0.30(1)	0.03(3)	0.35(1)
H13	0.002(1)	-0.433(3)	0.007(4)	-0.680(4)	0.010(6)	-0.346(2)	-0.02(1)	0.412(3)
H13'	0.006(4)	-0.48(1)	0.02(1)	-0.75(2)	0.03(2)	-0.38(1)	-0.05(3)	0.46(1)
H14	0.001(2)	-0.272(4)	0.00(1)	-0.427(6)	0.00(1)	-0.218(3)	-0.01(2)	0.259(4)
H15	0.005(2)	-0.51(1)	0.016(7)	-0.80(2)	0.02(1)	-0.409(8)	-0.04(2)	0.49(1)
H17	0.004(1)	-0.384(5)	0.012(3)	-0.604(8)	0.019(5)	-0.307(4)	-0.032(9)	0.366(5)
H18	0.000(2)	-0.385(5)	0.000(6)	-0.605(8)	-0.001(8)	-0.308(4)	0.00(1)	0.366(5)
H18'	-0.01(1)	-0.26(2)	-0.04(4)	-0.41(3)	-0.06(5)	-0.21(2)	0.10(9)	0.25(2)
H19	0.000(2)	-0.234(7)	-0.001(7)	-0.37(1)	0.00(1)	-0.187(6)	0.00(2)	0.223(7)
H20	0.002(1)	-0.256(5)	0.006(4)	-0.403(8)	0.009(6)	-0.205(4)	-0.01(1)	0.244(5)
H21	0.002(1)	-0.222(5)	0.007(3)	-0.349(7)	0.010(5)	-0.178(4)	-0.017(8)	0.212(5)
H22	0.0046(9)	-0.285(4)	0.014(3)	-0.447(7)	0.021(4)	-0.228(4)	-0.035(7)	0.271(4)
H23	0.007(5)	-0.46(1)	0.02(1)	-0.72(2)	0.03(2)	-0.366(9)	-0.05(4)	0.44(1)
H24	0.05(2)	0.5(1)	0.16(6)	0.8(2)	0.24(9)	0.43(8)	-0.4(2)	-0.51(9)
H24'	0.07(1)	-0.11(6)	0.22(4)	-0.17(9)	0.33(6)	-0.09(5)	-0.5(1)	0.11(6)
H25	0.03(1)	0.34(7)	0.10(4)	0.5(1)	0.15(7)	0.27(6)	-0.2(1)	-0.32(7)
H26	0.03(2)	-1.05(3)	0.08(7)	-1.65(5)	0.1(1)	-0.84(3)	-0.2(2)	1.00(3)
H26'	0.01(2)	-0.06(4)	0.04(5)	-0.10(6)	0.06(7)	-0.05(3)	-0.1(1)	0.06(4)
H27	0.00(2)	-2.7(1)	0.01(7)	-4.2(2)	0.0(1)	-2.12(8)	0.0(2)	2.5(1)
H28	0.00(1)	-0.25(5)	0.01(4)	-0.40(8)	0.01(5)	-0.20(4)	-0.01(9)	0.24(5)
H28'	-0.003(7)	-0.164(9)	-0.01(2)	-0.26(1)	-0.01(3)	-0.131(7)	0.02(5)	0.156(9)
H29	0.002(1)	-0.161(3)	0.005(4)	-0.253(5)	0.008(5)	-0.129(2)	-0.014(9)	0.154(3)

Table 136 Contact and pseudo contact terms of LnLu complexes of L^{AB5}

	CeLu		PrLu		NdLu		EuLu	
	Δ_c	Δ_{pc}	Δ_c	Δ_{pc}	Δ_c	Δ_{pc}	Δ_c	Δ_{pc}
H1	0.000(3)	-0.216(6)	0.001(8)	-0.47(1)	0.00(1)	-0.273(7)	0.00(2)	0.274(7)
H2	-0.002(5)	-0.16(2)	-0.01(2)	-0.35(3)	-0.01(2)	-0.21(2)	0.02(4)	0.21(2)
H3	-0.002(2)	-0.28(1)	-0.007(6)	-0.60(2)	-0.01(1)	-0.35(1)	0.02(2)	0.35(1)
H4	0.003(3)	-0.34(2)	0.01(1)	-0.74(3)	0.01(2)	-0.44(2)	-0.02(3)	0.44(2)
H4'	-0.0022(4)	-0.2956(6)	-0.007(1)	-0.640(1)	-0.010(2)	-0.3744(8)	0.017(3)	0.3753(8)
H5	0.001(1)	-0.215(6)	0.002(4)	-0.47(1)	0.003(6)	-0.273(7)	-0.006(9)	0.273(7)
H6	-0.005(7)	-0.34(2)	-0.02(2)	-0.74(4)	-0.02(3)	-0.43(2)	0.04(5)	0.43(2)
H7	-0.003(3)	-0.249(8)	-0.010(9)	-0.54(2)	-0.01(1)	-0.32(1)	0.02(2)	0.32(1)
H8	0.005(7)	-1.48(2)	0.01(2)	-3.20(4)	0.02(3)	-1.87(2)	-0.04(5)	1.88(2)
H9	-0.032(5)	-0.12(1)	-0.10(2)	-0.27(3)	-0.15(2)	-0.16(2)	0.25(4)	0.16(2)
H9'	-0.006(6)	-0.37(1)	-0.02(2)	-0.79(2)	-0.03(3)	-0.46(1)	0.05(4)	0.46(1)
H10	0.05(6)	-4.4(1)	0.2(2)	-9.5(3)	0.2(3)	-5.6(2)	-0.4(4)	5.6(2)
H11	-0.010(2)	-0.012(3)	-0.029(7)	-0.026(7)	-0.04(1)	-0.015(4)	0.07(2)	0.015(4)
H12	0.159(7)	0.40(1)	0.48(2)	0.86(2)	0.73(3)	0.50(1)	-1.23(5)	-0.50(1)
H13	0.08(2)	0.87(8)	0.23(7)	1.9(2)	0.4(1)	1.1(1)	-0.6(2)	-1.1(1)
H13'	0.01(3)	1.01(7)	0.02(9)	2.2(2)	0.0(1)	1.27(9)	-0.1(2)	-1.28(9)
H14	-0.001(8)	0.87(2)	0.00(2)	1.88(5)	-0.01(4)	1.10(3)	0.01(6)	-1.10(3)
H15	0.28(2)	0.90(8)	0.85(5)	1.9(2)	1.28(8)	1.1(1)	-2.2(1)	-1.1(1)
H17	0.30(1)	0.86(6)	0.91(4)	1.9(1)	1.37(6)	1.09(8)	-2.3(1)	-1.09(8)
H18	0.06(1)	0.93(6)	0.17(5)	2.0(1)	0.25(7)	1.17(8)	-0.4(1)	-1.18(8)
H18'	0.08(2)	0.81(5)	0.23(5)	1.8(1)	0.35(7)	1.03(6)	-0.6(1)	-1.03(6)
H19	-0.007(4)	0.60(2)	-0.02(1)	1.30(4)	-0.03(2)	0.76(2)	0.05(3)	-0.76(2)
H20	0.16(1)	0.43(2)	0.49(3)	0.93(5)	0.74(5)	0.54(3)	-1.25(8)	-0.54(3)
H21	-0.015(2)	0.060(4)	-0.047(5)	0.129(8)	-0.071(7)	0.075(5)	0.12(1)	-0.076(5)
H22	-0.014(7)	-0.36(2)	-0.04(2)	-0.77(5)	-0.06(3)	-0.45(3)	0.11(5)	0.45(3)
H23	-0.04(4)	-3.2(2)	-0.1(1)	-7.0(3)	-0.2(2)	-4.1(2)	0.3(3)	4.1(2)
H24	0.005(3)	-0.23(1)	0.02(1)	-0.50(3)	0.02(2)	-0.29(2)	-0.04(3)	0.29(2)
H24'	0.001(2)	-0.207(4)	0.004(7)	-0.449(8)	0.01(1)	-0.262(5)	-0.01(2)	0.263(5)
H25	-0.001(2)	-0.153(5)	-0.003(5)	-0.33(1)	-0.005(8)	-0.194(7)	0.01(1)	0.194(7)
H26	0.008(3)	-0.27(1)	0.023(9)	-0.59(3)	0.04(1)	-0.35(2)	-0.06(2)	0.35(2)
H26'	0.001(3)	-0.197(4)	0.003(8)	-0.426(8)	0.00(1)	-0.249(5)	-0.01(2)	0.250(5)
H27	0.001(3)	-0.193(4)	0.004(8)	-0.419(9)	0.01(1)	-0.245(5)	-0.01(2)	0.245(5)

5.7.8 Recalculation of lanthanide induced shifts

These contact and pseudo contact terms have then been used to re-calculate the lanthanide induced shift. These are compared to the experimental shifts in Table 137 - Table 144. Agreement factors have also been calculated.

Table 137 Re-calculated and observed LIS and AF_i for LaLn complexes of L^{AB}

	LaCe		LaPr		LaNd		LaEu		AF_i
	Calc.	Obs.	Calc.	Obs.	Calc.	Obs	Calc.	Obs.	
H1	1.50(3)	1.50	2.75(6)	2.62	1.92(5)	1.84	-2.68(8)	-2.67	0.034
H2	1.96(6)	1.97	3.3(1)	3.14	1.84(8)	1.86	-2.3(1)	-2.24	0.047
H3	2.68(2)	2.67	4.80(5)	4.77	3.16(7)	3.06	-4.3(1)	-4.35	0.015
H4	0.83(2)	0.83	1.41(3)	1.48	0.76(2)	0.77	-0.95(4)	-0.97	0.034
H4'	1.22(6)	1.23	2.0(1)	2.24	1.00(8)	1.10	-1.2(1)	-1.19	0.077
H5	1.400(9)	1.40	2.32(2)	2.30	1.14(2)	1.16	-1.34(3)	-1.33	0.010
H6	0.35(2)	0.34	0.78(5)	0.75	0.85(6)	0.75	-1.3(1)	-1.37	0.060
H7	-0.330(5)	-0.33	-0.558(8)	-0.54	-0.296(6)	-0.29	0.363(9)	0.36	0.024
H8	-5.97(6)	-5.96	-9.7(1)	-9.90	-4.31(9)	-4.28	4.7(1)	4.78	0.016
H9	-0.503(5)	-0.50	-0.834(9)	-0.85	-0.406(7)	-0.41	0.47(1)	0.48	0.018
H9'	-0.13(1)	-0.12	-0.24(3)	-0.19	-0.19(3)	-0.14	0.28(5)	0.29	0.177
H10	-3.11(5)	-3.12	-5.14(8)	-5.02	-2.48(8)	-2.55	2.9(1)	2.81	0.022
H11	-0.23(1)	-0.23	-0.38(2)	-0.42	-0.19(2)	-0.19	0.23(3)	0.24	0.070
H12	-0.37(1)	-0.37	-0.61(2)	-0.65	-0.31(1)	-0.31	0.37(2)	0.38	0.039
H13	-0.44(1)	-0.44	-0.73(2)	-0.69	-0.35(2)	-0.36	0.40(3)	0.39	0.040
H13'	-0.43(1)	-0.43	-0.72(3)	-0.76	-0.35(2)	-0.39	0.42(4)	0.42	0.058
H14	-0.310(8)	-0.31	-0.51(2)	-0.48	-0.24(1)	-0.22	0.27(2)	0.27	0.056
H15	-0.50(1)	-0.50	-0.83(2)	-0.87	-0.41(2)	-0.43	0.48(2)	0.49	0.038
H16	-0.323(3)	-0.32	-0.536(6)	-0.54	-0.263(7)	-0.27	0.31(1)	0.31	0.018
H17	-0.393(9)	-0.39	-0.65(2)	-0.62	-0.32(1)	-0.32	0.37(2)	0.36	0.034
H18	-0.365(7)	-0.36	-0.61(1)	-0.58	-0.31(1)	-0.29	0.37(2)	0.37	0.035
H18'	-0.316(3)	-0.32	-0.525(7)	-0.52	-0.258(8)	-0.25	0.30(1)	0.30	0.022
H19	-0.247(5)	-0.25	-0.41(1)	-0.40	-0.20(1)	-0.19	0.24(2)	0.24	0.044
H20	-0.256(2)	-0.26	-0.424(4)	-0.42	-0.209(3)	-0.21	0.246(5)	0.24	0.017
H21	-0.220(2)	-0.22	-0.365(3)	-0.36	-0.180(2)	-0.18	0.212(3)	0.21	0.011
H22	-0.285(2)	-0.29	-0.472(4)	-0.48	-0.229(4)	-0.24	0.266(7)	0.26	0.012
H23	-0.484(8)	-0.49	-0.80(2)	-0.78	-0.39(1)	-0.40	0.45(2)	0.44	0.027
H24	0.68(8)	0.68	1.2(1)	1.50	0.7(1)	0.81	-1.0(1)	-1.06	0.148
H24'	0.01(7)	0.01	0.1(1)	0.36	0.28(8)	0.32	-0.5(1)	-0.55	0.345
H25	0.43(7)	0.43	0.8(1)	1.01	0.50(8)	0.54	-0.7(1)	-0.73	0.176
H26	-0.87(5)	-0.86	-1.4(1)	-1.29	-0.7(1)	-0.49	0.8(2)	0.84	0.143
H26'	0.06(4)	0.07	0.12(8)	0.28	0.09(7)	0.20	-0.1(1)	-0.13	0.527
H27	-2.65(5)	-2.66	-4.43(8)	-4.61	-2.23(6)	-2.30	2.66(9)	2.70	0.029

Table 138 Re-calculated and observed LIS and AF_i for LaLn complexes of L^{AB3}

	LaCe		LaPr		LaNd		LaEu		AF_i
	Calc.	Obs.	Calc.	Obs.	Calc.	Obs	Calc.	Obs.	
H1	1.22(1)	1.23	2.14(2)	2.11	1.39(2)	1.41	-2.00(3)	-1.98	0.013
H3	2.41(3)	2.41	4.17(6)	4.29	2.60(4)	2.61	-3.68(6)	-3.72	0.019
H4	0.71(5)	0.73	1.2(1)	1.31	0.7(1)	0.86	-0.9(2)	-0.84	0.122
H4'	1.15(6)	1.16	1.8(1)	2.05	0.9(1)	1.00	-1.1(2)	-1.08	0.088
H5	1.37(2)	1.38	2.20(4)	2.26	1.04(5)	1.11	-1.31(8)	-1.30	0.028
H6	0.34(2)	0.33	0.76(5)	0.72	0.84(7)	0.74	-1.4(1)	-1.39	0.063
H7	-0.320(6)	-0.32	-0.53(1)	-0.55	-0.275(7)	-0.28	0.36(1)	0.37	0.031
H8	-5.7(1)	-5.68	-8.9(3)	-9.36	-3.7(3)	-4.14	4.5(4)	4.42	0.049
H9	-0.48(1)	-0.49	-0.78(2)	-0.84	-0.38(2)	-0.40	0.49(3)	0.50	0.047
H9'	-0.17(1)	-0.17	-0.30(2)	-0.33	-0.20(2)	-0.18	0.28(3)	0.30	0.075
H10	-2.90(4)	-2.91	-4.63(9)	-4.72	-2.1(1)	-2.29	2.7(2)	2.62	0.028
H11	-0.23(1)	-0.23	-0.38(2)	-0.41	-0.19(1)	-0.19	0.25(2)	0.26	0.062
H12	-0.376(6)	-0.38	-0.61(1)	-0.59	-0.29(1)	-0.28	0.37(2)	0.37	0.033
H13	-0.394(4)	-0.40	-0.634(9)	-0.65	-0.30(1)	-0.32	0.38(2)	0.38	0.022
H13'	-0.414(9)	-0.42	-0.66(2)	-0.70	-0.31(1)	-0.33	0.38(2)	0.39	0.039
H14	-0.295(5)	-0.30	-0.471(8)	-0.46	-0.216(6)	-0.22	0.270(9)	0.27	0.027
H15	-0.484(4)	-0.49	-0.775(9)	-0.79	-0.36(1)	-0.38	0.45(2)	0.45	0.018
H16	-0.294(3)	-0.30	-0.474(6)	-0.49	-0.225(7)	-0.24	0.29(1)	0.29	0.022
H17	-0.355(4)	-0.36	-0.571(6)	-0.59	-0.270(5)	-0.28	0.343(7)	0.35	0.018
H18	-0.35(2)	-0.35	-0.56(3)	-0.49	-0.28(2)	-0.26	0.36(4)	0.35	0.110
H18'	-0.310(5)	-0.31	-0.498(9)	-0.48	-0.231(8)	-0.22	0.29(1)	0.29	0.031
H19	-0.241(4)	-0.24	-0.39(1)	-0.38	-0.18(1)	-0.16	0.22(2)	0.23	0.038
H20	-0.26(1)	-0.26	-0.42(2)	-0.37	-0.19(1)	-0.18	0.24(2)	0.23	0.090
H21	-0.196(6)	-0.20	-0.31(1)	-0.34	-0.147(9)	-0.15	0.19(1)	0.20	0.050
H22	-0.260(4)	-0.26	-0.415(7)	-0.43	-0.191(6)	-0.20	0.24(1)	0.24	0.029
H23	-0.46(1)	-0.46	-0.73(2)	-0.76	-0.33(2)	-0.36	0.41(4)	0.40	0.043
H24	0.72(6)	0.73	1.2(1)	1.47	0.71(8)	0.81	-1.0(1)	-1.02	0.126
H24'	0.08(8)	0.08	0.2(1)	0.51	0.3(1)	0.33	-0.5(1)	-0.57	0.373
H25	0.45(7)	0.45	0.8(1)	1.05	0.51(9)	0.53	-0.7(1)	-0.83	0.182
H26	-0.80(4)	-0.80	-1.25(7)	-1.10	-0.51(6)	-0.44	0.59(9)	0.58	0.109
H26'	0.24(4)	0.25	0.38(7)	0.50	0.17(8)	0.29	-0.2(1)	-0.19	0.257
H27	-2.3(1)	-2.29	-3.7(2)	-4.20	-1.9(2)	-2.03	2.4(2)	2.49	0.090

Table 139 Re-calculated and observed LIS and AF_i for LaLn complexes of L^{AB4}

	LaCe		LaPr		LaNd		LaEu		AF_i
	Calc.	Obs.	Calc.	Obs.	Calc.	Obs	Calc.	Obs.	
H1	1.51(2)	1.51	2.64(4)	2.64	1.89(5)	1.82	-2.66(9)	-2.68	0.018
H2	1.89(2)	1.89	3.05(3)	3.01	1.73(3)	1.75	-2.19(4)	-2.17	0.011
H3	2.52(6)	2.51	4.3(1)	4.45	2.9(1)	2.83	-4.0(2)	-4.13	0.026
H4	1.11(4)	1.11	1.74(7)	1.58	0.87(6)	0.80	-1.02(9)	-0.99	0.077
H4'	1.1(1)	1.13	1.8(2)	2.23	0.9(2)	1.10	-1.1(2)	-1.18	0.170
H5	1.1(1)	1.12	1.8(2)	2.27	1.0(2)	1.10	-1.2(2)	-1.33	0.167
H6	0.36(3)	0.36	0.79(6)	0.84	0.87(7)	0.78	-1.4(1)	-1.42	0.060
H7	-0.297(4)	-0.30	-0.468(8)	-0.46	-0.241(8)	-0.25	0.29(1)	0.28	0.021
H8	-6.0(2)	-6.02	-9.2(3)	-9.82	-4.2(2)	-4.42	4.6(3)	4.74	0.050
H9	-0.53(1)	-0.53	-0.83(2)	-0.86	-0.42(2)	-0.41	0.50(3)	0.51	0.028
H9'	-0.153(5)	-0.15	-0.258(9)	-0.24	-0.17(1)	-0.15	0.23(2)	0.23	0.057
H10	-2.89(9)	-2.89	-4.5(2)	-4.83	-2.2(1)	-2.28	2.5(2)	2.61	0.055
H11	-0.22(3)	-0.22	-0.36(4)	-0.45	-0.19(3)	-0.20	0.24(5)	0.27	0.166
H12	-0.38(2)	-0.37	-0.60(3)	-0.64	-0.32(2)	-0.30	0.38(4)	0.41	0.060
H13	-0.431(3)	-0.43	-0.673(6)	-0.68	-0.336(6)	-0.33	0.40(1)	0.40	0.011
H13'	-0.47(1)	-0.47	-0.73(2)	-0.78	-0.36(2)	-0.38	0.41(3)	0.42	0.054
H14	-0.271(4)	-0.27	-0.425(9)	-0.43	-0.21(1)	-0.20	0.25(2)	0.26	0.027
H16	-0.51(1)	-0.51	-0.79(2)	-0.83	-0.38(1)	-0.40	0.45(2)	0.45	0.037
H17	-0.380(5)	-0.38	-0.591(9)	-0.61	-0.289(7)	-0.29	0.33(1)	0.34	0.023
H18	-0.385(6)	-0.38	-0.61(1)	-0.58	-0.308(9)	-0.29	0.37(2)	0.37	0.030
H18'	-0.27(2)	-0.27	-0.45(5)	-0.48	-0.27(6)	-0.20	0.34(9)	0.38	0.119
H19	-0.235(8)	-0.23	-0.37(1)	-0.39	-0.19(1)	-0.18	0.23(2)	0.24	0.050
H20	-0.254(5)	-0.25	-0.397(9)	-0.41	-0.196(7)	-0.19	0.23(1)	0.24	0.032
H21	-0.220(5)	-0.22	-0.343(8)	-0.36	-0.168(6)	-0.17	0.195(9)	0.20	0.037
H22	-0.280(5)	-0.28	-0.433(8)	-0.45	-0.207(6)	-0.21	0.236(8)	0.24	0.029
H23	-0.45(1)	-0.45	-0.70(2)	-0.74	-0.34(2)	-0.37	0.39(4)	0.39	0.056
H24	0.6(1)	0.59	1.0(2)	1.36	0.7(1)	0.74	-0.9(2)	-1.00	0.196
H24'	-0.04(6)	-0.04	0.0(1)	0.25	0.24(8)	0.24	-0.4(1)	-0.51	0.352
H25	0.37(7)	0.37	0.6(1)	0.89	0.42(9)	0.47	-0.6(1)	-0.64	0.220
H26	-1.03(4)	-1.01	-1.58(9)	-1.51	-0.7(1)	-0.55	0.8(2)	0.86	0.091
H26'	-0.05(4)	-0.04	-0.06(7)	0.09	0.01(8)	0.13	0.0(1)	-0.04	1.140
H27	-2.6(1)	-2.65	-4.2(2)	-4.54	-2.1(1)	-2.20	2.5(2)	2.58	0.066
H28	-0.25(5)	-0.25	-0.39(9)	-0.20	-0.19(7)	-0.18	0.2(1)	0.17	0.489
H28'	-0.17(1)	-0.17	-0.27(3)	-0.27	-0.14(3)	-0.19	0.18(5)	0.16	0.123
H29	-0.159(3)	-0.16	-0.248(6)	-0.26	-0.121(6)	-0.13	0.14(1)	0.14	0.043

Table 140 Re-calculated and observed LIS and AF_i for LaLn complexes of L^{AB5}

	LaCe		LaPr		LaNd		LaEu		AF_i
	Calc.	Obs.	Calc.	Obs.	Calc.	Obs	Calc.	Obs.	
H1	1.46(4)	1.46	2.69(8)	2.53	1.85(6)	1.76	-2.6(1)	-2.61	0.044
H2	1.93(7)	1.94	3.3(1)	3.08	1.77(9)	1.78	-2.3(1)	-2.19	0.056
H3	2.68(3)	2.67	4.83(7)	4.71	3.07(7)	2.96	-4.2(1)	-4.25	0.021
H4	0.76(2)	0.76	1.31(3)	1.38	0.70(2)	0.72	-0.90(3)	-0.91	0.038
H4'	1.22(4)	1.22	2.03(7)	2.17	0.95(6)	1.04	-1.13(9)	-1.14	0.055
H5	1.41(2)	1.41	2.36(3)	2.31	1.12(2)	1.12	-1.34(3)	-1.32	0.017
H6	0.32(2)	0.31	0.74(5)	0.72	0.83(6)	0.74	-1.3(1)	-1.37	0.057
H7	-0.355(7)	-0.36	-0.60(1)	-0.58	-0.293(8)	-0.29	0.36(1)	0.36	0.032
H8	-6.07(5)	-6.09	-10.0(1)	-10.07	-4.2(1)	-4.46	4.7(2)	4.68	0.019
H9	-0.539(4)	-0.54	-0.905(8)	-0.89	-0.429(6)	-0.43	0.515(9)	0.51	0.013
H9'	-0.151(6)	-0.15	-0.28(1)	-0.29	-0.18(1)	-0.17	0.25(2)	0.26	0.045
H10	-3.2(1)	-3.21	-5.3(2)	-4.90	-2.4(1)	-2.34	2.8(2)	2.71	0.064
H11	-0.24(1)	-0.24	-0.41(3)	-0.46	-0.20(2)	-0.21	0.25(3)	0.26	0.089
H12	-0.376(7)	-0.38	-0.63(1)	-0.65	-0.309(9)	-0.31	0.38(1)	0.39	0.026
H13	-0.425(4)	-0.43	-0.710(7)	-0.73	-0.330(5)	-0.34	0.392(7)	0.40	0.016
H13'	-0.42(1)	-0.42	-0.70(2)	-0.74	-0.33(3)	-0.37	0.39(4)	0.39	0.057
H14	-0.34(1)	-0.34	-0.56(3)	-0.51	-0.25(2)	-0.24	0.29(3)	0.28	0.077
H15	-0.528(6)	-0.53	-0.88(1)	-0.87	-0.40(2)	-0.42	0.47(3)	0.46	0.020
H17	-0.394(7)	-0.40	-0.66(1)	-0.64	-0.30(1)	-0.31	0.35(2)	0.35	0.026
H18	-0.305(7)	-0.31	-0.52(1)	-0.54	-0.265(9)	-0.27	0.33(1)	0.34	0.037
H18'	-0.296(3)	-0.30	-0.498(8)	-0.50	-0.24(1)	-0.23	0.29(2)	0.30	0.023
H19	-0.259(7)	-0.26	-0.43(1)	-0.41	-0.200(8)	-0.20	0.24(1)	0.23	0.042
H20	-0.236(4)	-0.24	-0.397(8)	-0.40	-0.19(1)	-0.18	0.23(2)	0.24	0.029
H21	-0.214(2)	-0.22	-0.358(5)	-0.37	-0.166(6)	-0.18	0.20(1)	0.20	0.023
H22	-0.269(3)	-0.27	-0.451(6)	-0.46	-0.211(6)	-0.22	0.25(1)	0.25	0.021
H23	-0.48(1)	-0.48	-0.80(2)	-0.77	-0.36(2)	-0.38	0.41(3)	0.40	0.033
H24	0.67(8)	0.67	1.2(1)	1.47	0.73(9)	0.80	-1.0(1)	-1.04	0.139
H24'	-0.04(7)	-0.05	0.0(1)	0.27	0.26(8)	0.28	-0.5(1)	-0.56	0.348
H25	0.42(7)	0.42	0.8(1)	1.00	0.47(8)	0.51	-0.6(1)	-0.70	0.182
H26	-0.84(5)	-0.83	-1.39(9)	-1.26	-0.6(1)	-0.46	0.7(2)	0.76	0.124
H26'	0.10(3)	0.10	0.17(6)	0.29	0.10(5)	0.18	-0.14(8)	-0.14	0.373
H27	-2.62(3)	-2.62	-4.40(6)	-4.53	-2.11(5)	-2.19	2.56(8)	2.57	0.024

Table 141 Re-calculated and observed LIS and AF_i for LnLu complexes of L^{AB}

	CeLu		PrLu		NdLu		EuLu		AF_i
	Calc.	Obs.	Calc.	Obs.	Calc.	Obs	Calc.	Obs.	
H1	-0.229(7)	-0.23	-0.49(2)	-0.51	-0.29(1)	-0.31	0.30(2)	0.30	0.046
H2	-0.211(6)	-0.21	-0.45(1)	-0.43	-0.262(9)	-0.26	0.27(1)	0.27	0.027
H3	-0.309(5)	-0.31	-0.66(1)	-0.67	-0.39(1)	-0.41	0.41(2)	0.41	0.025
H4	-0.34(1)	-0.34	-0.72(3)	-0.68	-0.43(3)	-0.39	0.45(4)	0.44	0.060
H4'	-0.320(1)	-0.32	-0.682(3)	-0.68	-0.407(3)	-0.41	0.430(4)	0.43	0.004
H5	-0.223(4)	-0.22	-0.473(9)	-0.46	-0.278(8)	-0.28	0.29(1)	0.29	0.017
H6	-0.35(2)	-0.35	-0.74(5)	-0.67	-0.45(4)	-0.39	0.48(6)	0.47	0.102
H7	-0.226(7)	-0.23	-0.49(2)	-0.47	-0.30(2)	-0.28	0.34(3)	0.34	0.055
H8	-1.55(5)	-1.56	-3.3(1)	-3.47	-1.9(1)	-2.13	2.0(2)	2.03	0.053
H9	-0.13(1)	-0.12	-0.30(2)	-0.27	-0.27(3)	-0.22	0.38(4)	0.38	0.095
H9'	-0.38(1)	-0.38	-0.82(3)	-0.85	-0.50(2)	-0.53	0.53(3)	0.54	0.042
H10	-4.7(2)	-4.72	-9.9(4)	-10.46	-5.6(4)	-6.29	5.7(6)	5.72	0.059
H11	0.020(4)	0.02	0.03(1)	0.04	-0.01(1)	0.01	0.04(2)	0.04	0.359
H12	0.63(1)	0.62	1.47(3)	1.48	1.29(3)	1.25	-1.80(5)	-1.81	0.017
H13	1.10(8)	1.10	2.4(2)	2.68	1.7(1)	1.87	-2.0(2)	-2.04	0.081
H13'	1.2(1)	1.22	2.6(2)	2.91	1.5(2)	1.85	-1.6(3)	-1.64	0.114
H14	0.783(7)	0.79	1.67(2)	1.69	1.01(2)	1.05	-1.09(3)	-1.09	0.014
H15	1.42(8)	1.40	3.3(2)	3.54	2.9(1)	2.89	-3.9(2)	-3.99	0.038
H16	1.29(5)	1.31	2.8(1)	2.69	1.96(9)	1.96	-2.4(1)	-2.31	0.038
H17	1.43(6)	1.41	3.4(1)	3.54	3.0(1)	2.96	-4.2(1)	-4.22	0.028
H18	1.15(8)	1.14	2.5(2)	2.71	1.5(1)	1.66	-1.6(2)	-1.69	0.078
H18'	1.02(6)	1.02	2.2(1)	2.46	1.6(1)	1.74	-1.9(2)	-1.95	0.069
H19	0.553(9)	0.56	1.17(2)	1.17	0.69(2)	0.72	-0.71(4)	-0.70	0.020
H20	0.63(1)	0.62	1.47(3)	1.45	1.31(4)	1.25	-1.84(6)	-1.84	0.024
H21	0.061(9)	0.06	0.11(2)	0.13	0.01(2)	0.05	0.04(4)	0.04	0.282
H22	-0.38(2)	-0.38	-0.83(4)	-0.89	-0.53(3)	-0.56	0.59(5)	0.60	0.059
H23	-3.6(2)	-3.61	-7.7(4)	-8.29	-4.6(3)	-5.02	4.8(5)	4.91	0.065
H24	-0.219(3)	-0.22	-0.465(7)	-0.46	-0.272(7)	-0.28	0.28(1)	0.28	0.015
H25	-0.167(6)	-0.17	-0.36(1)	-0.38	-0.22(1)	-0.23	0.23(1)	0.23	0.043
H26	-0.26(1)	-0.26	-0.56(3)	-0.60	-0.33(2)	-0.35	0.35(3)	0.36	0.055
H26'	-0.22(1)	-0.22	-0.46(2)	-0.44	-0.27(2)	-0.29	0.29(3)	0.28	0.044
H27	-0.206(4)	-0.21	-0.438(9)	-0.45	-0.26(1)	-0.28	0.27(2)	0.27	0.030

Table 142 Re-calculated and observed LIS and AF_i for LnLu complexes of L^{AB3}

	CeLu		PrLu		NdLu		EuLu		AF_i
	Calc.	Obs.	Calc.	Obs.	Calc.	Obs	Calc.	Obs.	
H1	-0.219(6)	-0.22	-0.49(1)	-0.50	-0.29(1)	-0.31	0.30(2)	0.30	0.041
H3	-0.302(5)	-0.30	-0.67(1)	-0.68	-0.39(1)	-0.41	0.41(2)	0.41	0.028
H4	-0.33(1)	-0.33	-0.74(3)	-0.69	-0.44(3)	-0.40	0.47(4)	0.47	0.063
H4'	-0.317(2)	-0.32	-0.705(5)	-0.70	-0.413(4)	-0.41	0.433(6)	0.43	0.009
H5	-0.213(3)	-0.21	-0.473(7)	-0.46	-0.276(5)	-0.27	0.288(7)	0.29	0.014
H6	-0.34(2)	-0.35	-0.76(4)	-0.71	-0.44(3)	-0.42	0.46(4)	0.45	0.063
H7	-0.232(6)	-0.23	-0.52(2)	-0.50	-0.32(1)	-0.30	0.36(2)	0.36	0.040
H8	-1.51(2)	-1.52	-3.36(5)	-3.37	-1.99(5)	-2.07	2.11(8)	2.10	0.017
H9	-0.117(7)	-0.11	-0.29(2)	-0.28	-0.27(2)	-0.23	0.38(3)	0.39	0.062
H9'	-0.377(6)	-0.38	-0.84(2)	-0.85	-0.51(2)	-0.54	0.55(3)	0.55	0.025
H10	-4.6(1)	-4.62	-10.1(3)	-10.32	-5.7(3)	-6.19	5.8(5)	5.75	0.037
H11	0.019(5)	0.02	0.03(1)	0.02	-0.013(9)	-0.01	0.05(1)	0.05	0.226
H12	0.62(2)	0.61	1.49(5)	1.42	1.30(5)	1.22	-1.80(7)	-1.80	0.037
H13	1.07(8)	1.06	2.4(2)	2.68	1.7(1)	1.83	-2.0(2)	-2.03	0.074
H13'	1.16(7)	1.16	2.6(2)	2.79	1.5(2)	1.77	-1.6(2)	-1.65	0.083
H14	0.77(2)	0.78	1.72(5)	1.66	1.02(4)	1.02	-1.08(5)	-1.07	0.027
H15	1.38(4)	1.37	3.3(1)	3.45	2.86(8)	2.84	-4.0(1)	-3.98	0.020
H16	1.26(8)	1.28	2.9(2)	2.62	2.0(1)	1.91	-2.4(2)	-2.31	0.065
H17	1.40(4)	1.38	3.40(9)	3.46	3.00(9)	2.90	-4.2(1)	-4.23	0.019
H18	1.10(5)	1.10	2.5(1)	2.62	1.5(1)	1.67	-1.7(1)	-1.71	0.056
H18'	0.98(4)	0.98	2.3(1)	2.39	1.58(8)	1.68	-1.9(1)	-1.95	0.045
H19	0.54(2)	0.55	1.21(5)	1.15	0.70(3)	0.70	-0.72(5)	-0.71	0.036
H20	0.62(3)	0.61	1.50(6)	1.42	1.32(6)	1.22	-1.8(1)	-1.85	0.046
H21	0.070(7)	0.07	0.14(2)	0.13	0.03(2)	0.05	0.02(3)	0.02	0.143
H22	-0.38(1)	-0.38	-0.86(3)	-0.89	-0.52(3)	-0.56	0.57(4)	0.58	0.043
H23	-3.5(1)	-3.51	-7.8(3)	-8.12	-4.6(3)	-5.04	4.9(4)	4.89	0.050
H24	-0.20(1)	-0.20	-0.45(2)	-0.48	-0.27(2)	-0.28	0.28(2)	0.29	0.052
H25	-0.168(4)	-0.17	-0.376(9)	-0.39	-0.229(7)	-0.23	0.25(1)	0.25	0.021
H26	-0.251(5)	-0.25	-0.55(1)	-0.57	-0.318(9)	-0.33	0.33(1)	0.33	0.025
H26'	-0.22(1)	-0.22	-0.48(3)	-0.46	-0.28(3)	-0.31	0.29(5)	0.28	0.064
H27	-0.193(1)	-0.19	-0.431(3)	-0.43	-0.258(3)	-0.26	0.277(5)	0.28	0.010

Table 143 Re-calculated and observed LIS and AF_i for LnLu complexes of L^{AB4}

	CeLu		PrLu		NdLu		EuLu		AF_i
	Calc.	Obs.	Calc.	Obs.	Calc.	Obs	Calc.	Obs.	
H1	-0.420(3)	-0.42	-0.781(6)	-0.79	-0.441(7)	-0.45	0.53(1)	0.53	0.011
H2	-0.366(1)	-0.37	-0.684(3)	-0.69	-0.391(4)	-0.40	0.475(7)	0.47	0.006
H3	-0.569(5)	-0.57	-1.06(1)	-1.08	-0.60(1)	-0.62	0.73(2)	0.73	0.016
H4	-0.568(4)	-0.57	-1.059(7)	-1.05	-0.599(7)	-0.59	0.72(1)	0.72	0.010
H4'	-0.564(3)	-0.56	-1.052(7)	-1.06	-0.598(5)	-0.60	0.724(8)	0.73	0.009
H5	-0.387(2)	-0.39	-0.720(3)	-0.72	-0.404(4)	-0.41	0.485(6)	0.48	0.005
H6	-0.567(9)	-0.57	-1.06(2)	-1.03	-0.60(2)	-0.58	0.73(3)	0.72	0.026
H7	-0.361(2)	-0.36	-0.677(3)	-0.67	-0.392(3)	-0.39	0.480(4)	0.48	0.006
H8	-2.87(3)	-2.88	-5.35(7)	-5.44	-3.02(8)	-3.13	3.6(1)	3.62	0.018
H9	-0.194(6)	-0.19	-0.39(1)	-0.37	-0.29(1)	-0.27	0.41(2)	0.41	0.039
H9'	-0.695(5)	-0.70	-1.30(1)	-1.32	-0.76(1)	-0.78	0.93(2)	0.92	0.013
H10	-8.4(2)	-8.44	-15.6(4)	-16.29	-8.6(3)	-9.05	10.2(5)	10.29	0.035
H11	-0.070(4)	-0.07	-0.143(9)	-0.13	-0.11(1)	-0.10	0.16(2)	0.16	0.082
H12	0.81(2)	0.81	1.69(4)	1.69	1.37(4)	1.32	-1.98(7)	-2.00	0.020
H13	1.89(6)	1.88	3.7(1)	3.85	2.42(9)	2.43	-3.2(1)	-3.26	0.033
H13'	2.27(4)	2.27	4.27(8)	4.41	2.52(6)	2.59	-3.13(9)	-3.15	0.024
H14	1.186(7)	1.19	2.22(2)	2.21	1.27(2)	1.29	-1.54(3)	-1.53	0.008
H15	2.81(5)	2.80	5.6(1)	5.75	4.2(1)	4.08	-5.8(2)	-5.82	0.016
H17	2.56(5)	2.55	5.2(1)	5.22	3.9(1)	3.77	-5.5(2)	-5.56	0.019
H18	2.39(7)	2.40	4.5(1)	4.30	2.7(1)	2.67	-3.3(2)	-3.22	0.034
H18'	2.0(1)	2.00	3.8(2)	4.25	2.4(2)	2.54	-3.1(3)	-3.18	0.072
H19	0.98(2)	0.99	1.81(4)	1.78	0.98(4)	1.02	-1.15(6)	-1.12	0.023
H20	1.01(2)	1.01	2.05(4)	2.01	1.56(4)	1.50	-2.18(7)	-2.19	0.021
H21	0.21(1)	0.21	0.35(3)	0.34	0.12(3)	0.16	-0.09(5)	-0.07	0.102
H22	-0.55(2)	-0.55	-1.06(4)	-1.13	-0.69(4)	-0.68	0.89(5)	0.92	0.041
H23	-6.1(1)	-6.05	-11.4(2)	-11.72	-6.6(2)	-6.79	8.2(2)	8.22	0.023
H24	-0.371(6)	-0.37	-0.69(1)	-0.71	-0.40(1)	-0.39	0.48(2)	0.49	0.019
H24'	-0.371(2)	-0.37	-0.694(5)	-0.69	-0.400(7)	-0.39	0.49(1)	0.49	0.011
H25	-0.296(4)	-0.30	-0.553(8)	-0.57	-0.316(8)	-0.33	0.38(1)	0.38	0.021
H26	-0.467(2)	-0.47	-0.872(3)	-0.87	-0.498(2)	-0.50	0.605(3)	0.60	0.004
H26'	-0.382(5)	-0.38	-0.71(1)	-0.71	-0.40(1)	-0.41	0.47(2)	0.47	0.019
H27	-0.374(2)	-0.37	-0.699(4)	-0.69	-0.400(4)	-0.39	0.486(7)	0.49	0.008
H28	0.81(3)	0.81	1.48(6)	1.59	0.76(5)	0.81	-0.86(8)	-0.88	0.057
H28'	0.86(2)	0.86	1.59(3)	1.64	0.87(3)	0.86	-1.02(4)	-1.04	0.023
H29	0.739(8)	0.74	1.39(2)	1.42	0.82(1)	0.83	-1.02(2)	-1.03	0.013

Table 144 Re-calculated and observed LIS and AF_i for LnLu complexes of L^{AB5}

	CeLu		PrLu		NdLu		EuLu		AF_i
	Calc.	Obs.	Calc.	Obs.	Calc.	Obs	Calc.	Obs.	
H1	-0.215(6)	-0.22	-0.47(1)	-0.49	-0.27(1)	-0.30	0.27(2)	0.27	0.047
H2	-0.17(2)	-0.17	-0.36(4)	-0.42	-0.22(3)	-0.27	0.23(5)	0.23	0.127
H3	-0.28(1)	-0.28	-0.60(2)	-0.64	-0.36(2)	-0.37	0.37(2)	0.37	0.038
H4	-0.34(2)	-0.34	-0.74(4)	-0.68	-0.42(3)	-0.40	0.42(3)	0.41	0.059
H4'	-0.2977(7)	-0.30	-0.646(2)	-0.65	-0.384(2)	-0.39	0.392(3)	0.39	0.004
H5	-0.215(6)	-0.22	-0.46(1)	-0.45	-0.269(9)	-0.27	0.27(1)	0.26	0.030
H6	-0.35(2)	-0.35	-0.75(5)	-0.69	-0.46(4)	-0.40	0.47(6)	0.46	0.093
H7	-0.252(8)	-0.25	-0.55(2)	-0.52	-0.33(2)	-0.30	0.34(3)	0.34	0.054
H8	-1.47(2)	-1.47	-3.18(4)	-3.24	-1.85(4)	-1.91	1.84(6)	1.85	0.020
H9	-0.16(1)	-0.16	-0.37(3)	-0.33	-0.31(3)	-0.26	0.41(4)	0.40	0.111
H9'	-0.37(1)	-0.37	-0.81(3)	-0.84	-0.49(3)	-0.54	0.51(4)	0.52	0.052
H10	-4.3(1)	-4.35	-9.3(3)	-9.76	-5.3(3)	-5.83	5.2(5)	5.20	0.051
H11	-0.022(4)	-0.02	-0.06(1)	-0.05	-0.06(1)	-0.04	0.09(2)	0.09	0.178
H12	0.55(1)	0.55	1.34(3)	1.32	1.23(3)	1.17	-1.73(5)	-1.73	0.025
H13	0.95(8)	0.94	2.1(2)	2.40	1.5(1)	1.64	-1.7(2)	-1.75	0.096
H13'	1.01(8)	1.02	2.2(2)	2.46	1.3(2)	1.57	-1.3(2)	-1.36	0.109
H14	0.87(3)	0.88	1.87(6)	1.82	1.09(5)	1.14	-1.09(7)	-1.07	0.029
H15	1.18(8)	1.16	2.8(2)	3.05	2.4(1)	2.47	-3.3(2)	-3.34	0.051
H17	1.16(6)	1.14	2.8(1)	2.95	2.5(1)	2.46	-3.4(1)	-3.45	0.035
H18	0.98(7)	0.96	2.2(1)	2.36	1.4(1)	1.41	-1.6(1)	-1.65	0.058
H18'	0.89(5)	0.89	2.0(1)	2.16	1.4(1)	1.53	-1.6(1)	-1.65	0.069
H19	0.59(2)	0.60	1.27(4)	1.22	0.73(3)	0.72	-0.71(4)	-0.69	0.036
H20	0.59(2)	0.59	1.42(6)	1.35	1.29(6)	1.19	-1.80(9)	-1.79	0.048
H21	0.044(4)	0.05	0.082(9)	0.08	0.005(9)	0.02	0.04(1)	0.05	0.130
H22	-0.37(3)	-0.37	-0.81(6)	-0.90	-0.51(4)	-0.57	0.56(6)	0.57	0.080
H23	-3.3(2)	-3.26	-7.1(4)	-7.69	-4.3(3)	-4.61	4.4(4)	4.52	0.061
H24	-0.22(1)	-0.23	-0.48(3)	-0.45	-0.27(2)	-0.28	0.25(3)	0.24	0.056
H24'	-0.206(4)	-0.21	-0.44(1)	-0.45	-0.26(1)	-0.28	0.25(2)	0.25	0.035
H25	-0.154(6)	-0.15	-0.33(1)	-0.35	-0.20(1)	-0.21	0.20(1)	0.21	0.050
H26	-0.27(1)	-0.27	-0.57(3)	-0.53	-0.31(2)	-0.31	0.29(3)	0.28	0.056
H26'	-0.196(5)	-0.20	-0.42(1)	-0.43	-0.25(1)	-0.27	0.24(2)	0.24	0.039
H27	-0.192(5)	-0.19	-0.41(1)	-0.42	-0.24(1)	-0.26	0.24(2)	0.24	0.045

The agreement factors are markedly smaller than those calculated for the ordinary one proton method, although there are still some problems with protons close to the so-called magic angles.

Lanthanide agreement factors as defined in Eq. (10) are given in Table 145 below.

Table 145 Lanthanide agreement factors AF_j

	Ce	Pr	Nd	Eu
$LaLn(L^{AB})_3$	0.003	0.047	0.047	0.020
$LnLu(L^{AB})_3$	0.005	0.063	0.088	0.013
$LaLn(L^{AB3})_3$	0.004	0.068	0.088	0.025
$LnLu(L^{AB3})_3$	0.007	0.040	0.074	0.008
$LaLn(L^{AB4})_3$	0.003	0.086	0.065	0.034
$LnLu(L^{AB4})_3$	0.002	0.038	0.038	0.012
$LaLn(L^{AB5})_3$	0.007	0.062	0.079	0.015
$LnLu(L^{AB5})_3$	0.007	0.062	0.079	0.015

Most agreement factors (23 out of 32) are better than the ones calculated for the Reilley analysis (Table 74).

5.8 Evaluation of agreement factors

The application of agreement factors is an often used method for determining whether a structure obtained by X-ray diffraction or molecular modelling is a good model for the structure of a complex in solution. The method has its strength when two or more structural models are compared with the solution data, in which case it can easily be concluded which model is the better one (lowest *AF*). In this way the method has been used with considerable success over the last more than 30 years.

While the concept of "better" is thus well-defined, the question arises how low an *AF* has to be in order to be "good" or at least "good enough to conclude that the proposed structure is a good model for the solution structure". No single answer can be given since it depends on the nature of the structure. Short lanthanide-proton distances means that small absolute errors in the distance can result in large relative errors and large *AF*. Similarly, the position of a proton (or rather all of the protons of a given molecule) close to the so-called magic angle results in a low pseudo contact shift and a small absolute error would give a large relative error. These considerations have to be taken into account when evaluating agreement factors.

One possibility is the use of weighing factors for the individual elements of the sums in the *AF*. While this would get rid of the problem with the domination of one or two protons it would also introduce the unfortunate complication that small absolute, but large relative errors of the protons close to the so-called magic angle would be scaled up and out of proportions. It is evident that the choice of definition of the weighing factors is tricky and no attempt to apply weighing factors has been carried out here.

To investigate how low an agreement factor has to be to constitute "good agreement" for the present complexes, two sets of agreement factors have been calculated. First the individual ligand strands of the three available solid state structures of L^{AB} complexes (LaEu, LaTb, and EuEu) have been compared. Then the structural ratios G_i/G_{ref} (averaged over the three strands in a complex) of all eight solid state structures have been compared.
The agreement factors calculated have been defined analogously to the ones used for comparing solid state (X-ray) and solution (LIS) structures.

$$AF_j^{S1,S2} = \sqrt{\frac{\sum_{i\neq k}\left(\left(G_i/G_{ref}\right)_{S1}-\left(G_i/G_{ref}\right)_{S2}\right)^2}{\sum_{i\neq k}\left(\left(G_i/G_{ref}\right)_{S2}\right)^2}} \qquad (21)$$

Here S1 and S2 signify two different structures.

For the comparison of ligand strands in the same complex H16 has been chosen as reference proton (k = 16) and it is assumed the (hypothetical) paramagnetic lanthanide ion is placed in the coordination cavity defined by the bpb moiety of L^{AB}.

Given in Table 146 are the calculated agreement factors for ligands in the same complex.

Table 146 Agreement factors comparing individual ligand strands

	$LaEu(L^{AB})_3$			$LaTb(L^{AB})_3$			$Eu_2(L^{AB})_3$		
S2= / S1=	1	2	3	1	2	3	1	2	3
1		0.980	0.942		0.896	0.908		0.834	0.924
2	0.624		0.316	0.590		0.295	0.584		0.333
3	0.591	0.311		0.609	0.301		0.605	0.311	

It is evident that two of the ligand strands (L^2 and L^3) constitute a pair of similar ligands with a significant deviation from L^1.

Note the large difference in *AF* when changing the choice of reference (interchanging S1 and S2). This can be traced back to H23, the position of which close to the paramagnetic ion makes the calculated G_{23} very sensitive to structural variations. The difference is particularly remarkable when it is considered that the sum of squared errors is the same in $AF^{1,2}$ and $AF^{2,1}$. All *AF*s are large compared to those calculated for comparing solid state and solution structures. This serves to illustrate that even an agreement factor of close to 1 cannot rule out that two structures compared display the same structural motif (in this case a helical wrapping of a ligand strand around two lanthanide ions).

The agreement factors calculated for comparison of different structures are given in Table 147 - Table 150.

Table 147 Agreement factors comparing different structures

Ln in bpa site		Reference proton H3							
		L^{AB}			L^{AB3}				
	S2= / S1=	LaEu	LaTb	Eu_2	Ce_2	Pr_2	PrLu	NdLu	Sm_2
L^{AB}	LaEu		0.077	0.089	0.398	0.443	0.474	0.415	0.417
	LaTb	0.073		0.073	0.398	0.443	0.474	0.415	0.417
	Eu_2	0.090	0.077		0.387	0.421	0.468	0.397	0.403
L^{AB3}	Ce_2	0.459	0.482	0.444		0.217	0.142	0.044	0.060
	Pr_2	0.447	0.470	0.423	0.190		0.200	0.190	0.175
	PrLu	0.509	0.534	0.499	0.132	0.213		0.133	0.104
	NdLu	0.478	0.502	0.456	0.044	0.216	0.142		0.058
	Sm_2	0.459	0.481	0.441	0.058	0.191	0.107	0.055	

Table 148 Agreement factors comparing different structures

Ln in bpa site		Reference proton H16							
		L^{AB}			L^{AB3}				
	S2= / S1=	LaEu	LaTb	Eu_2	Ce_2	Pr_2	PrLu	NdLu	Sm_2
L^{AB}	LaEu		0.056	0.084	0.374	0.422	0.446	0.391	0.399
	LaTb	0.056		0.057	0.374	0.422	0.446	0.391	0.399
	Eu_2	0.084	0.056		0.362	0.398	0.440	0.373	0.384
L^{AB3}	Ce_2	0.382	0.381	0.373		0.163	0.122	0.044	0.045
	Pr_2	0.409	0.408	0.390	0.155		0.203	0.159	0.154
	PrLu	0.481	0.479	0.478	0.129	0.225		0.122	0.129
	NdLu	0.405	0.404	0.390	0.045	0.170	0.118		0.053
	Sm_2	0.397	0.396	0.386	0.044	0.158	0.120	0.051	

Table 149 Agreement factors comparing different structures

Ln in bpb site		Reference proton H3							
		L^{AB}			L^{AB3}				
	S2= / S1=	LaEu	LaTb	Eu_2	Ce_2	Pr_2	PrLu	NdLu	Sm_2
L^{AB}	LaEu		0.033	0.034	0.113	0.095	0.102	0.112	0.138
	LaTb	0.033		0.033	0.113	0.095	0.102	0.112	0.138
	Eu_2	0.034	0.033		0.120	0.103	0.103	0.116	0.139
L^{AB3}	Ce_2	0.109	0.108	0.117		0.106	0.090	0.035	0.059
	Pr_2	0.098	0.098	0.108	0.114		0.068	0.122	0.122
	PrLu	0.100	0.099	0.102	0.091	0.064		0.091	0.092
	NdLu	0.107	0.106	0.112	0.035	0.112	0.089		0.051
	Sm_2	0.133	0.132	0.135	0.059	0.113	0.091	0.052	

Table 150 Agreement factors comparing different structures

Ln in bpb site		Reference proton H16							
		L^{AB}			L^{AB3}				
	S2= / S1=	LaEu	LaTb	Eu_2	Ce_2	Pr_2	PrLu	NdLu	Sm_2
L^{AB}	LaEu		0.039	0.082	0.115	0.093	0.101	0.108	0.136
	LaTb	0.040		0.043	0.115	0.093	0.101	0.108	0.136
	Eu_2	0.076	0.039		0.159	0.134	0.132	0.150	0.167
L^{AB3}	Ce_2	0.121	0.119	0.180		0.084	0.097	0.034	0.061
	Pr_2	0.096	0.094	0.149	0.083		0.027	0.080	0.092
	PrLu	0.104	0.101	0.145	0.094	0.027		0.090	0.093
	NdLu	0.113	0.110	0.169	0.034	0.081	0.092		0.051
	Sm_2	0.142	0.139	0.187	0.060	0.093	0.095	0.051	

The choice of reference the proton (H3 or H16) typically changes the agreement factors by less than 30 % although some changes are larger. For example, the $Pr_2(L^{AB3})_3$/PrLu$(L^{AB3})_3$

agreement factor with Ln in the bpb site changes from 0.027 to 0.068, which corresponds to 150 %. The overall pattern is, however, not seriously influenced and low agreement factors remain low when the reference proton is changed.

It is evident that the eight structures are divided into three distinct groups: the three L^{AB} complexes, the monoclinic L^{AB3} complexes (Ce_2, NdLu and Sm_2) and the triclinic L^{AB3} complexes (Pr_2 and PrLu). Within each group the agreement factors are lower than when structures from different groups are compared.

The choice of the reference lanthanide (that is whether the paramagnetic lanthanide ion is situated in the bpa or bpa site of the complex) has a large influence on the agreement factors.

With the paramagnetic ion in the bpb site (corresponding to the analysis of the LnLu series of complexes in solution) all agreement factors are low. Within the groups the values are between 0.027 and 0.082 and even when complexes from different groups are compared the agreement factors range from 0.080 to 0.187. This is not surprising since ligands L^{AB} and L^{AB3} are identical in this end and it seems reasonable that any structural difference does not occur close to the bpb lanthanide ion.

A different picture emerges when the paramagnetic ion is situated in the bpa site (as in the LaLn series of complexes investigated in solution by NMR). Here the intergroup agreement factors involving a L^{AB} complex as one of the two structures compared fall in the range 0.362 – 0.534, indicative of an appreciable difference between the structures. When the two groups of L^{AB3} complexes are compared the range is 0.107 – 0.217, which is significantly smaller. The intragroup agreement factors remain small (0.044 – 0.090) with the exception of the $PrPr(L^{AB3})_3$/ $PrLu(L^{AB3})_3$ group for which the values lie between 0.200 and 0.225.

The larger agreement factor calculated for complexes with the paramagnetic lanthanide ion in the bpa site is no doubt related to the vicinity of the flexible ethyl groups of the carboxamide function.

In conclusion it can be said that agreement factors of 0.1 – 0.2 as found in the comparison of the solid state complexes with values of structural ratios extracted from analysis of the lanthanide induced shift are low enough to safely conclude that the structures are identical.

Given the imperfections involved in the calculation of the solid state G_i/G_{ref} values (averaging over three ligand strands) it could even be said that the agreement is quite good. Values of up to 0.5 would still lead to the conclusion that the complexes have the same overall structure as seen in the agreement factors calculated for comparison of the solid state L^{AB} and L^{AB3} complexes.

Finally, the analysis of AF between ligand strands in the same complex shows that *for complexes of this type* even an AF as high as 1 does not make it possible to rule out that two structures compared have the same overall structure (that is, helical wrapping of three ligand strands around two lanthanide ions). Of course, in the event of such a large *AF*, nothing can be conclusively said regarding the finer details of the solution structure.

5.9 Lanthanide induced shift: Summary and conclusion

The lanthanide induced shifts of homobimetallic $Ln_2(L)_3$ and heterobimetallic $LaLn(L)_3$ and $LnLu(L)_3$ (Ln = Ce, Pr, Nd, Eu) complexes of the heterobitopic ligands L^{AB}, L^{AB3}, L^{AB4} and L^{AB5} have been analysed.

Instead of using a single compound as a diamagnetic reference complex, the reference chemical shifts have been calculated as weighed averages of chemical shifts of La and Lu containing complexes. The best weighing has been determined by evaluation of proton agreement factors, which indicate whether the separation of contact and pseudo contact terms has been successful. In 11 out of 12 cases investigated the diamagnetic reference complex thus obtained were assembled of more La than Lu containing complex. This is in perfect agreement with what would be expected from considerations of relative ionic size, since the paramagnetic complexes studied were all from the first half of the lanthanide series.

The lanthanide induced shifts obtained by subtracting the chemical shifts of the diamagnetic reference complexes from the experimental chemical shifts of the complexes containing paramagnetic lanthanide ions have been analysed by means of the so-called Reilley (one proton) method. This yielded separate contact and pseudo contact terms.

The effect of two paramagnetic lanthanide ions in the same complex has been examined by comparing data from the heterobimetallic LaLn and LnLu complexes with what was extracted from the analysis of the homobimetallic Ln_2 complexes. It was demonstrated that not only the total lanthanide induced shift, but also the contact and pseudo contact parts thereof are additive.

Using the Geraldes (two proton) method of analysis structural ratios G_i/G_{ref} have been extracted from the lanthanide induced shift of the LaLn and LnLu series of complexes. The values thus obtained have been used to compare the solution structures of the complexes. It was shown that the complexes of all four ligands are isostructural in solution.

The same structural ratios have also been compared to values calculated from eight different solid state structures of complexes. Agreement factors indicate that the solid state L^{AB3} complexes are better than their L^{AB} counterparts as models for the complexes in solution as

studied by analysis of the lanthanide induced shift. Of all the solid state structures $Pr_2(L^{AB3})_3$ turns out to be the best structural model.

Choosing the $Pr_2(L^{AB3})_3$ solid state complex as structural model, values of the crystal field parameter B_0^2 have been calculated from the pseudo contact parameters extracted with the one proton analysis. It is shown that the Cl substituent in the L^{AB3} and L^{AB5} ligands only induces a small reduction of the crystal field parameter, whereas the NEt_2 substituent in L^{AB4} almost doubles the value for the lanthanide ion in the bpb site.

In the standard one proton (Reilley) treatment of contact and pseudo contact terms it was found that the separation was far from perfect for protons whose total lanthanide shifts were dominated by pseudo contact contributions. It was believed that the problem originated in the assumption that the crystal field parameter does not vary along the lanthanide series. This assumption is known to be erroneous and has been the reason for the development of the two proton (Geraldes) method of analysis in which the crystal field parameter is eliminated by including two protons simultaneously in the calculations. The drawback of the two proton method is that only structural information can be extracted; information about the contact shift and the crystal field parameter is lost in the data reduction.

Here we have instead developed a modified one proton analysis. In a first step only protons with no contact shift (i.e. protons topologically far from the paramagnetic lanthanide ion) were considered. This allowed for the determination of relative crystal field parameters, which were in good agreement with values found in the literature.[90,94] These parameters were then utilised in a slightly modified Reilley analysis to give separate contact and pseudo contact terms. The separation was seen to be significantly improved with contact terms now being close to zero for protons removed from the paramagnetic lanthanide ion by more than five chemical bonds.

The new method is not generally applicable to any system; it requires that there is at least one proton which can be safely assigned as having no contact shift. In the present work at least 12 protons were used for each series to determine the relative crystal field parameters, all resulting in similar values.

It could be argued that the lower agreement factors compared to the ones found in the Reilley analysis is a result of the introduction of additional variables. However, the relative crystal field parameters are not free variables, but rather parameters determined experimentally.

Another potential objection would be that the satisfying results (i.e. small contact terms for protons topologically removed from the paramagnetic lanthanide ion) is a direct consequence of the underlying assumption: that these same protons have negligible contact shifts. Considered this way, the model gives as output what we have applied as input. However, only protons at least eight chemical bonds from the paramagnetic lanthanide ions have been used to determine the relative crystal field parameters meaning that the assumption must be valid.

Lastly, the modified one proton method has the drawback that it shares with the two proton method. It cannot be applied to complexes containing more than one paramagnetic lanthanide ion.

To get an estimate of how small an agreement factor has to be in order for one to be able to conclude that two series of complexes are isostructural, the eight available solid state structures have been compared. The calculations demonstrate that agreement factors as low as 0.1 correspond to isostructurality as this value was reached for two structures differing only in the lanthanide ions incorporated. Values up to 1 were reached when comparing individual ligand strands in the same complex leading to the conclusion that even such high values can not rule out that two complexes display the same structural motif.

6 Lanthanide induced relaxation

As a complement to the structural information obtained by lanthanide induced shift analysis longitudinal (spin-lattice) relaxation times (T_1) have been measured and analysed for the $LnLu(L^{AB})_3$ series of complexes (Ln = Ce, Pr, Nd, Sm, Eu) in which the paramagnetic ion is in the bpb site of the complex.

The T_1 data reported in Table 151 were determined by means of an inversion-recovery pulse sequence (180°-τ-90°)[95] with 20 values of τ ranging from 10 ms to 10 s.

Table 151 Measured T_1 values (in ms) [a]

	LaLu	CeLu	PrLu	NdLu	SmLu	EuLu
H1	630(12)	623(4)	642(6)	605(4)	*	582(11)
H2	1026(13)	*	1006(3)	*	1009(8)	1018(9)
H3	534(13)	*	522(6)	*	633(12)	505(10)
H4	265(15)	243(6)	224(11)	213(11)	*	231(9)
H4'	258(9)	239(6)	227(5)	218(11)	*	232(11)
H5	517(15)	497(8)	485(9)	448(9)	495(6)	498(10)
H6	649(10)	526(8)	413(9)	383(5)	619(9)	*
H7	*	511(5)	376(5)	293(2)	*	430(14)
H8	1659(14)	791(3)	541(30)	318(3)	1288(6)	*
H9	263(9)	*	176(12)	*	*	181(6)
H9'	269(14)	*	*	190(6)	*	236(13)
H10	2005(12)	88(31)	27(2)	11(65)	227(7)	42(9)
H11	*	604(2)	462(2)	*	*	*
H12+H20	747(9)	522(5)	365(2)	268(1)	*	453(9)
H13	252(12)	210(12)	175(18)	*	*	*
H13'	256(16)	171(5)	133(14)	75(29)	223(19)	*
H14	418(12)	334(3)	*	230(23)	*	328(8)
H15	513(18)	233(9)	139(4)	95(7)	*	259(10)
H16	1046(7)	578(4)	306(3)	214(3)	856(9)	487(10)
H17	637(12)	246(8)	144(3)	96(5)	*	201(12)
H18	254(12)	173(5)	131(7)	100(13)	*	*
H18'	257(9)	210(6)	175(18)	126(8)	238(13)	152(43)
H19	532(13)	447(16)	313(4)	*	495(7)	411(11)
H21	*	772(5)	549(9)	*	*	*

	LaLu	CeLu	PrLu	NdLu	SmLu	EuLu
H22	*	541(4)	306(3)	*	940(7)	*
H23	*	55(17)	25(10)	29(72)	207(8)	42(9)
H24	290(12)	271(4)	*	*	298(13)	259(10)
H25	575(10)	565(7)	571(8)	556(7)	559(6)	563(12)
H26	350(18)	340(3)	*	*	322(28)	*
H26'	317(19)	289(16)	*	*	280(32)	*
H27	555(14)	558(7)	566(9)	552(8)	565(6)	567(12)

[a] In all spectra, the H12 and H20 signals overlapped, the values given in the table are for the double signal.
* indicates value not determined due to overlap of lines
PrLu: H13 and H18' 100 % overlap; EuLu: H10 and H23 100 % overlap

The relaxation times were corrected for diamagnetic effects by subtracting the values measured for the LaLu complex:

$$\frac{1}{T_{1i}^{para}} = \frac{1}{T_{1i}^{meas}} - \frac{1}{T_{1i}^{dia}} \qquad (22)$$

As the LIS, the paramagnetic contribution to the spin-lattice relaxation time (often termed lanthanide induced relaxation, LIR) has two components, through bond and through space. Due to the limited delocalization of the 4f unpaired electron density, the contact term can be ignored for all (weakly covalent) lanthanide complexes.

The remaining paramagnetic contributions can be treated by using that the relaxation times are proportional to the sixth power of the Ln-proton distance:

$$T_{1i}^{para} \propto r^6 \qquad (23)$$

This can be re-arranged to the simple expression (24)[96,97] and used to yield relative Ln-H distances (Table 152); as previously, proton H16 was chosen as reference.

$$\frac{T_{1i}^{para}}{T_{1ref}^{para}} = \left(\frac{r_i}{r_{ref}} \right)^6 \qquad (24)$$

Only protons closer than 8 Å from the paramagnetic lanthanide ion yield reliable distances since diamagnetic contributions dominate for more distant protons, leading to unsatisfactory separation of the paramagnetic contribution.

Table 152 Relative Ln-H distances as determined by LIR analysis

			r/r_{16}			$Pr_2(L^{AB3})_3$, X-ray	
	CeLu	PrLu	NdLu	SmLu	EuLu	Mean *r* / Å	r/r_{16}
H6	1.14	1.17	1.23	1.19	*b*	7.36	1.16
H8	1.03	1.11	1.07	1.03	*b*	6.95	1.09
H9	*b*	1.04	*b*	*b*	0.93	6.72	1.06
H9'	*b*	*b*	1.16	*b*	1.13	7.40	1.16
H10	0.64	0.63	0.59	0.62	0.60	3.97	0.62
H12+H20	1.05	1.09	1.08	*b*	1.04	6.72	1.06
H13	1.00	1.05	*b*	*b*	*b*	6.20	0.98
H13'	0.86	0.93	0.86	0.85	*b*	5.78	0.91
H14	1.04	*b*	1.11	*b*	1.09	6.80	1.07
H15	0.83	0.87	0.87	*b*	0.91	5.53	0.87
H16	1.00	1.00	1.00	1.00	1.00	6.36	1.00
H17	0.82	0.87	0.87	*b*	0.83	5.55	0.87
H18	0.87	0.92	0.92	*b*	*b*	6.04	0.95
H18'	0.98	1.04	0.99	0.94	0.86	6.54	1.03
H19	1.14	1.10	*b*	1.07	1.12	6.79	1.07

[a] Values for H7, H11, H21, H22, and H23 not calculated due to lack of reference value for the LaLu complex. [b] Not measured due to overlap of lines.

The agreement between relative distances determined by means of LIR analysis in solution and distances determined by X-ray diffraction in the solid state of the $Pr_2(L^{AB3})_3$ complex is quite good as can be seen in Table 152 and Figure 103, the differences being less than 10 % for all protons except two.

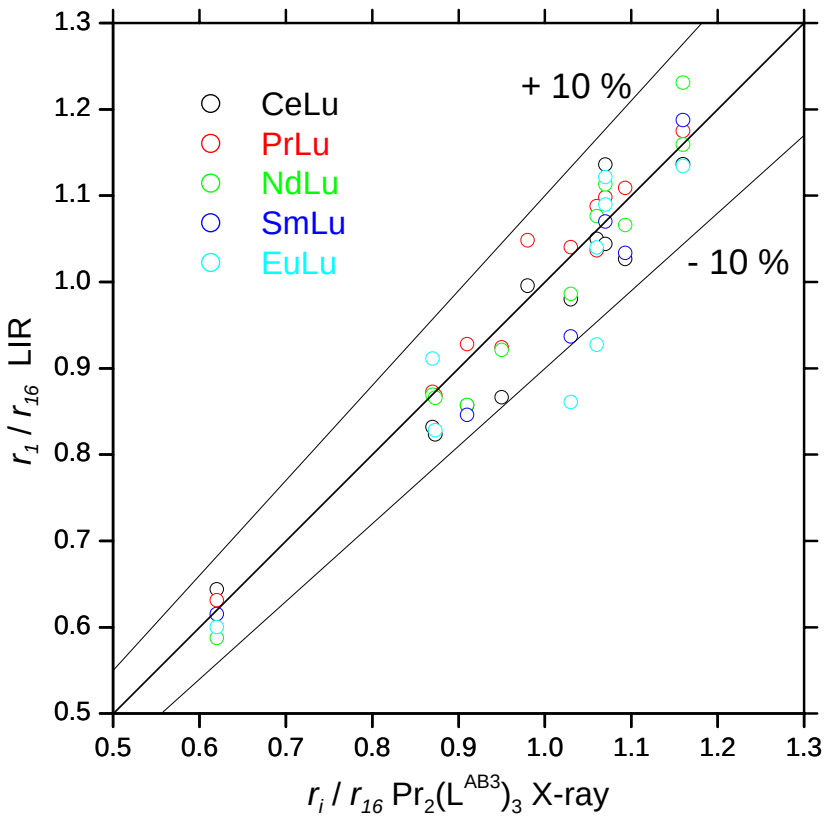

Figure 103 Comparing LIR with X-ray data

This result not only confirms the assignment of the ^{1}H NMR spectra, but also the conclusion drawn from the lanthanide induced shift analysis, that the structure of the helicates is the same in solution and in the solid state and that the solid state $Pr_2(L^{AB3})_3$ structure is a reasonable structural model for the investigated $LnLu(L^{AB})_3$ series (Ln = La, Ce, Pr, Nd, Sm, Eu).

7 Variable temperature measurements

7.1 Introduction

The determination of the speciation in solution (Chapter 4; page 59) demonstrated the importance of the *HHH*/*HHT* equilibrium for the selectivity of a ligand towards a pair of different lanthanide ions. The *HHT* isomer is expected to be less selective than the *HHH* one. In the latter, one coordination cavity is formed by three identical bpb coordination units, all coding for large and midsize lanthanide ions, and the other cavity is formed by three bpa units, preferring the smaller lanthanide ions. In the *HHT* isomer the coordination cavities are both mixed bpb/bpa and most of the selectivity is lost.

This is indeed what was observed for complexes with L^{AB2}, which only forms 6 - 20 % *HHH* isomer of the homobimetallic complexes. Even with the LaLu couple of ligands only 65 % heterobimetallic complexes are formed, significantly less than the 96 % measured for the L^{AB} ligand. For the EuLu couple, L^{AB} still gives 73 % heterobimetallic complexes while the percentage for L^{AB2} falls to 21 %.

The purpose of this study is to gain insight into the energetics of the *HHH*/*HHT* equilibrium of homobimetallic complexes of the five ligands. It is hoped that that a deeper understanding of the reasons for the different behaviour of the five ligands studied here will be helpful when designing future ligands. For this purpose the complexes have been studied with variable temperature ^{1}H NMR with the aim of extracting values of H and S for the *HHH*/*HHT* equilibrium.

Complexes of L^{AB4} are not included since the low concentration of *HHT* complexes precludes a reliable determination of their concentration by means of integration of their lines in the NMR spectra.

7.2 Method

^{1}H NMR spectra were recorded for $Ln_2(L)_3$ samples in CD_3CN with Ln = La, Pr, Sm, Eu, Y and Lu to represent ion sizes spanning the entire lanthanide series. The total Ln concentrations were $\approx 10^{-2}$ M. The $Ce_2(L)_3$ complexes of L^{AB2} and L^{AB5} were also measured.

Although not formally a lanthanide, Y was included since it displays similar chemical properties and has a size comparable to that of Ho.

The spectra were measured in the temperature range -40 °C to +50 °C with temperature intervals of 10 degrees. The samples were allowed to equilibrate at each temperature prior to recording of the spectrum. Preliminary experiments had shown that thermal equilibrium was reached within a few minutes. Since the time it takes for the sample to reach chemical equilibrium depends on the temperature the equilibration times differed for measurements carried out at different temperatures. Typical equilibration times were 10 - 15 minutes at 50 ºC, 30 minutes at 10 ºC and 2 hours at -20 ºC. At the lowest temperature in each series of measurements the sample was allowed to equilibrate overnight. Preliminary measurements had showed the kinetics of the La samples to be slow, equilibrium being reached only after 2 hours at -10 ºC and 6 - 8 hours at -20 º for the L^{AB} sample. For this reason, no results recorded at lower temperatures are reported here for the La complexes of L^{AB}, L^{AB2} and L^{AB3}. For L^{AB5} the La sample was measured down to -40 ºC. All other samples exhibited faster kinetics and it was in many cases possible to measure down to -40 ºC provided the samples were allowed sufficient equilibration time (6 - 14 hours).

For the diamagnetic La, Y and Lu complexes signals of the benzimidazole H8 and H10 protons were used to determine the concentration of the *HHH* and *HHT* species. The wrapping of the ligand strands in the helicate causes the signals of these aromatic protons to be shifted out of the usual aromatic region of the spectrum and they can be found as the only signals in the spectrum between 5.2 and 6.4 ppm. This ensures that the lines do not overlap with other lines, leading to reliable intensities by integration. Spectra of the $La_2(L^{AB})_3$ sample at two different temperatures are given in Figure 104.

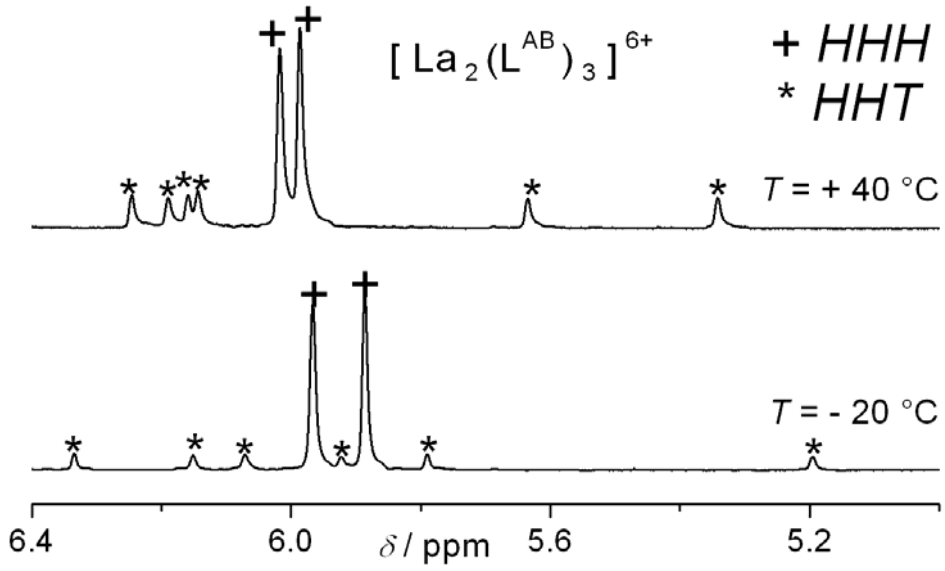

Figure 104 Partial NMR spectra of $La_2(L^{AB})_3$ in CD_3CN. $c_{La\ total} \approx 10^{-2}$ M.

For the Ce, Pr and Eu (Figure 105) complexes paramagnetic effects induces appreciable shifts of lines ensuring that non-overlapping lines could always be found. However, line broadening was a problem in some cases (especially at low temperature) meaning that not all measurements could be included in the final treatment of the data.

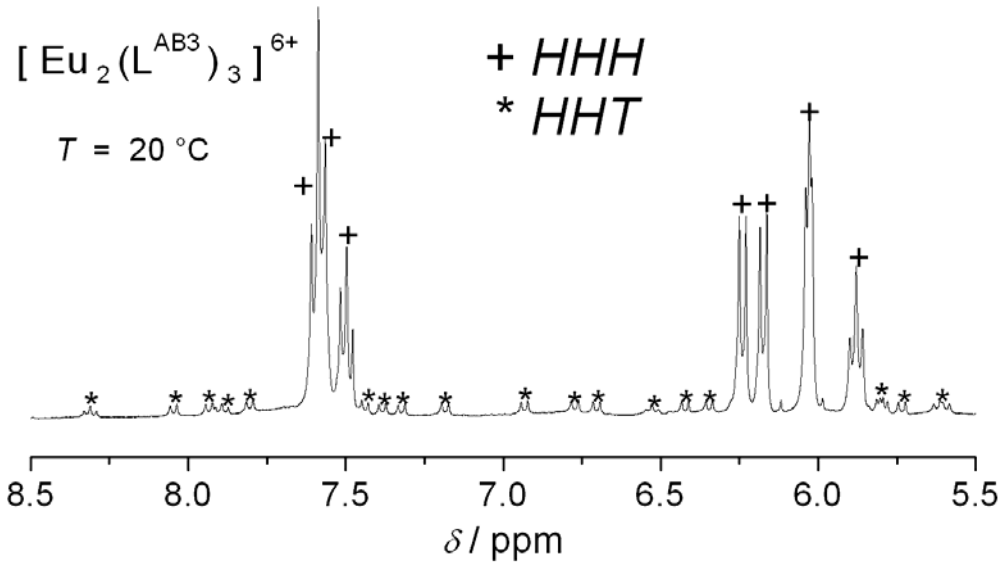

Figure 105 Partial NMR spectrum of $Eu_2(L^{AB3})_3$ in CD_3CN. $c_{Eu\ total} \approx 10^{-2}$ M.

The weak paramagnetism of the Sm complexes (Figure 106) shifts the H8 and H10 signals in a manner that makes it impossible to follow the same strategy as for the diamagnetic complexes, but results on the other hand in some signals being shifted towards the edges of

the spectra, where they are sufficiently isolated to be reliably integrated. No disturbing line broadening was observed as a result of paramagnetic effects.

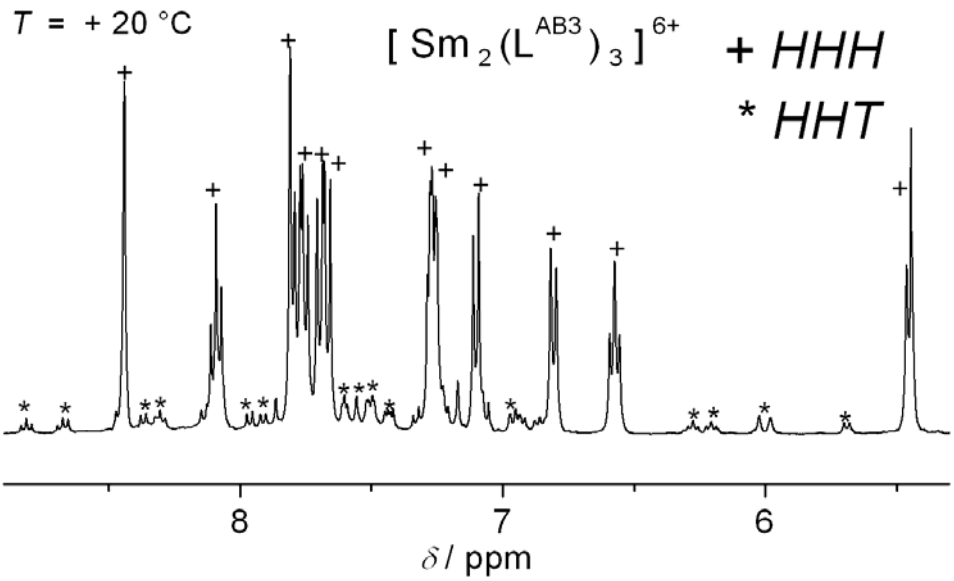

Figure 106 Partial NMR spectrum of $Sm_2(L^{AB3})_3$ in CD_3CN. $c_{Sm\ total} \approx 10^{-2}$ M.

Concentrations of the *HHH* and *HHT* isomers were determined by integration of their respective signals in the NMR spectrum as detailed below. The assignment of the *HHH* isomers of complexes of the ligands L^{AB}, L^{AB3} and L^{AB5} is given in Table 23 - Table 26 (page 85 ff.). No signals of the *HHT* isomers were assigned, nor of the L^{AB2} complexes. The chemical shifts are at T = 20 °C unless otherwise noted. Due to overlap of signals, not all resonances were used at all temperatures. All measurements were done twice.

$La_2(L^{AB})_3$: *HHH:* H8 and H10 at 5.8 - 6.1 ppm
HHT: 4 signals (H8 and H10) at 5.2 - 6.5 ppm

$Pr_2(L^{AB})_3$: *HHH:* H1, H12 and H20 at 8-10 ppm
HHT: 3 - 10 signals at each temperature (δ = -2 - 16 ppm)

$Sm_2(L^{AB})_3$: *HHH:* H23 at 5.4 ppm
HHT: 4 signals between 5.6 and 5.9 ppm

$Eu_2(L^{AB})_3$: *HHH:* H1 at 5 - 5.5 ppm
HHT: 6 - 8 signals at each temperature (δ = -1.5 - 9 ppm)

$Y_2(L^{AB})_3$: *HHH:* H8 and H10 (between 5.4 and 5.6 ppm)
HHT: 4 signals (H8 and H10) at 5.7 - 6.0 ppm

$Lu_2(L^{AB})_3$: *HHH:* H8 and H10 at 5.2 - 6.0 ppm

HHT: H8 and H10 at 5.2 - 6.0 ppm

$La_2(L^{AB2})_3$: *HHH*: H10 at ≈ 5.9 and H27 at 0.2 ppm

HHT: 3 signals at about 8.4, 5.9 and 5.2 ppm

$Ce_2(L^{AB2})_3$: *HHH*: Various signals from 6.5 to 11 ppm

HHT: Various signals from 6.5 to 11 ppm

$Pr_2(L^{AB2})_3$: *HHH*: All signals are in the region 6 - 10.5 ppm

HHT: All signals are in the region 6 - 10.5 ppm

$Sm_2(L^{AB2})_3$: *HHH*: 3 signals at 5.3 - 6.6 ppm and two triplets at 0.1-0.9 ppm

HHT: 4 signals in the 5.5 - 6.4 ppm region and two triplets at 0.4 - 0.8 ppm

$Eu_2(L^{AB2})_3$: *HHH*: 10 signals from -1.4 to 7.8 ppm

HHT: doublet at 8.8 (T = 50 º C) to 9.4 (-40 º C) ppm

$Y_2(L^{AB2})_3$: *HHH:* H8 and H10 at 5.3 to 5.6 ppm

HHT: singlet at 5.15 ppm

$Lu_2(L^{AB2})_3$: *HHH*: H8 and H10

HHT: 3 H8 and H10 signals between 5.3 and 5.9 ppm

$La_2(L^{AB3})_3$: *HHH:* H8 and H10

HHT: H8 and H10 signals from 5.6 to 6.3 ppm

$Pr_2(L^{AB3})_3$: *HHH*: H15, H16 and H17 at 10 to 12 ppm.

HHT: 1-3 methyl triplets (depending on the temperature) 0 to 1 ppm

$Sm_2(L^{AB3})_3$: *HHH*: H27 at 0.2 ppm and H22 at 6.6 ppm

HHT: triplet at 8.8 ppm and two singlets at ~6 ppm.

$Eu_2(L^{AB3})_3$: *HHH:* H3 at 5.0 ppm, H9' at 4.5 ppm, H16 at 5.9 ppm and H21 at 7.5 ppm

HHT: various signals between 4 and 9 ppm

$Y_2(L^{AB3})_3$: *HHH:* H8 and H10 at 5.4 to 5.5 ppm

HHT: singlet at 4.9 to 5 ppm and triplet (intensity 3H) at 0.6 ppm

$Lu_2(L^{AB3})_3$: *HHH:* H8 or H10 between 5.3 and 5.4 ppm

HHT: 4 H8 or H10 signals between 5.6 and 5.9 ppm.

$La_2(L^{AB5})_3$: *HHH:* H8 and H10 at 5.8-6.0 ppm and H23 at 6.6 ppm

HHT: H8 and H10 signals are at 5.2-6.5 ppm

$Pr_2(L^{AB5})_3$: *HHH*: H3 at 12.2 ppm, H6 at 7.3 ppm, H11 at 6.9 ppm, H12 at 8.4 ppm and H20 at 8.6 ppm

HHT: various signals between 5 and 12 ppm

$Sm_2(L^{AB5})_3$: *HHH*: H3 at 8.7 ppm, H22 at 6.7 ppm and H23 at 5.5 ppm
HHT: various signals from the whole spectrum

$Y_2(L^{AB5})_3$: *HHH*: H8 and H10 at 5.4-5.6 ppm
HHT: H8 and H10 at 4.9-6.0 ppm

$Eu_2(L^{AB5})_3$: *HHH:* H1 at 5.4 ppm, H6 at 6.2 ppm, H7 at 7.6 ppm, H9 at 6.2 ppm, H9' at 4.5 ppm, H17 at 4.3 ppm and H20 at 6.2 ppm
HHT: various signals between 4 and 9 ppm

$Lu_2(L^{AB5})_3$: *HHH:* two doublets at 8.4 and 6.2 ppm and H8 and H10 at 5.2-5.4 ppm
HHT: various signals in the region 5.6-6.7 ppm.

When calculating concentrations of the *HHH* and *HHT* isomers from the intensities of their respective lines in the NMR spectrum it has been taken into account that the three ligand strands in the *HHH* complexes are equivalent.

Especially for the L^{AB3} complexes (and less so for the L^{AB} ones) the low concentration of the *HHT* isomer resulted in low intensities in the spectra and therefore large relative uncertainties in the concentrations. This is eventually seen in the standard errors of the calculated thermodynamic parameters. The low intensity at low temperatures also made it impossible to obtain reliable intensities some of the complexes at low temperatures - for the *HHT*-$Lu_2(L^{AB3})_3$ complex below 20 ºC. To obtain more data the $Lu_2(L^{AB3})_3$ sample was measured in temperature intervals of 5 degrees.

To exclude solvent effects as a major contribution to the results the La and Lu complexes of L^{AB} were also measured using acetone-d_6 as solvent.

7.3 Results

The equilibrium examined here is

$$HHT-Ln_2(L)_3 \quad \rightleftarrows \quad HHH-Ln_2(L)_3$$

with the associated equilibrium constant

$$K = \frac{[HHH\text{-}Ln_2(L)_3]}{[HHT\text{-}Ln_2(L)_3]}$$

The values of K and ln$K$ obtained in this manner are given in Table 153 - Table 156. Based on the differences of intensities of different resonances of the same isomer in the same spectrum the relative errors are estimated to be ≈ 5 - 10 %.

Table 153 Equilibrium constants for L^{AB} complexes in CD_3CN

	La_2		Pr_2		Sm_2		Eu_2		Y_2		Lu_2	
T (ºC)	K	ln$K$	K	ln$K$	K	ln$K$	K	ln$K$	K	ln$K$	K	ln$K$
50	1.93	0.66	1.62	0.48	1.70	0.53	2.22	0.75	1.67	0.51	2.18	0.78
40	2.16	0.77	2.04	0.71	1.79	0.58	2.19	0.74	1.70	0.53	2.26	0.81
30	2.47	0.90	2.04	0.71	1.79	0.58	2.09	0.71	1.74	0.56	2.14	0.76
20	2.81	1.03	1.91	0.65	1.86	0.62	2.55	0.94	1.73	0.55	2.07	0.73
10	3.27	1.18	2.30	0.83	1.90	0.64	2.37	0.85	1.77	0.57	2.01	0.70
0			2.24	0.81	2.01	0.70	2.37	0.85	1.77	0.57	2.03	0.71
-10	4.61	1.53	2.59	0.95	1.99	0.69	2.27	0.82	1.77	0.57	2.03	0.71
-20	5.44	1.69	2.73	1.00	1.90	0.64	2.43	0.88	1.79	0.58	1.89	0.64
-30			3.04	1.11	2.11	0.74	3.13	1.14	1.79	0.58	1.77	0.57
-40			3.69	1.31	2.18	0.77			1.80	0.59	1.65	0.50

Table 154 Equilibrium constants for L^{AB2} complexes in CD_3CN

	La_2		Ce_2		Pr_2		Sm_2		Eu_2		Y_2		Lu_2	
T (ºC)	K	ln$K$	K	ln$K$	K	ln$K$	K	ln$K$	K	ln$K$	K	ln$K$	K	ln$K$
50	0.19	-1.66			0.11	-2.23	0.13	-2.03	0.08	-2.50	0.09	-2.46	0.07	-2.60
40	0.21	-1.58	0.15	-1.91	0.13	-2.07	0.13	-2.03	0.09	-2.45	0.09	-2.47	0.07	-2.69
30	0.23	-1.46	0.16	-1.86	0.13	-2.04	0.13	-2.03	0.10	-2.29	0.08	-2.50	0.07	-2.66
20	0.26	-1.34	0.16	-1.84	0.14	-1.96	0.13	-2.06	0.09	-2.40	0.08	-2.50	0.07	-2.64
10	0.30	-1.20	0.16	-1.85	0.14	-2.00	0.13	-2.06	0.09	-2.37	0.08	-2.49	0.07	-2.66
0	0.38	-0.98	0.17	-1.76			0.13	-2.08	0.08	-2.59	0.08	-2.48	0.07	-2.70
-10	0.47	-0.76	0.19	-1.67			0.13	-2.08	0.09	-2.40	0.08	-2.49	0.06	-2.82
-20	0.55	-0.59					0.12	-2.10	0.08	-2.51	0.08	-2.46	0.06	-2.75
-30							0.12	-2.08					0.06	-2.84
-40													0.07	-2.70

Table 155 Equilibrium constants for L^{AB3} complexes in CD_3CN

	La_2		Pr_2		Sm_2		Eu_2		Y_2			Lu_2	
T (ºC)	*K*	ln*K*	*K*	ln*K*	*K*	ln*K*	*K*	ln*K*	*K*	ln*K*	T (ºC)	*K*	ln*K*
50	3.41	1.23	5.86	1.77	4.71	1.55	4.35	1.47	3.96	1.38	50	4.13	1.42
40	3.67	1.30	5.66	1.73	5.11	1.63	4.75	1.56	4.04	1.40	45	4.76	1.56
30	3.78	1.34	6.48	1.87	5.30	1.67	5.25	1.66	3.95	1.37	40	4.87	1.58
20	3.80	1.34	6.55	1.88	5.63	1.73	6.15	1.82	4.70	1.55	35	5.32	1.67
10	4.20	1.43	7.68	2.04	6.43	1.86	6.64	1.89	4.69	1.55	30	5.07	1.60
0	4.30	1.46	8.29	2.11	7.17	1.97	8.48	2.13	5.27	1.66	25	6.57	1.89
-10	4.58	1.52	9.63	2.26	8.13	2.10	9.95	2.30	5.94	1.78	20	5.79	1.89
-20					9.18	2.21			7.48	2.01			
-30									9.93	2.30			

Table 156 Equilibrium constants for L^{AB5} complexes in CD_3CN

	La_2		Ce_2		Pr_2		Sm_2		Eu_2		Y_2		Lu_2	
T (ºC)	*K*	ln*K*	*K*	ln*K*	*K*	ln*K*	*K*	ln*K*	*K*	ln*K*	*K*	ln*K*	*K*	ln*K*
50	1.26	0.23	0.97	-0.03	1.01	0.01	1.09	0.08	0.99	-0.01	1.19	0.17	1.30	0.26
40	1.34	0.29	1.08	0.08	1.03	0.03	1.12	0.11	1.05	0.05	1.33	0.28	1.37	0.31
30	1.40	0.34	1.10	0.10	1.14	0.13	1.23	0.21	1.13	0.12	1.58	0.46	1.49	0.40
20	1.60	0.47	1.17	0.15	1.10	0.09	1.32	0.28	1.18	0.17	1.67	0.51	1.60	0.47
10	1.75	0.56	1.30	0.26	1.22	0.20	1.37	0.31	1.22	0.20	1.86	0.62	1.62	0.48
0	1.86	0.62	1.34	0.29	1.33	0.29	1.42	0.35	1.39	0.33	2.02	0.70	1.79	0.58
-10	2.12	0.75	1.52	0.42	1.47	0.38	1.55	0.44	1.55	0.44	2.08	0.73	1.83	0.60
-20	2.40	0.88	1.78	0.58	1.50	0.40	1.71	0.54	1.61	0.48	2.22	0.80	1.92	0.65
-30	3.16	1.15	1.85	0.62	1.68	0.52	1.85	0.61	1.77	0.57	2.37	0.86	1.94	0.66
-40	3.97	1.37	2.35	0.85	1.92	0.65	1.90	0.64	1.84	0.60	2.53	0.93		

Values of ln*K* were plotted (Figure 107) against T^{-1} (van't Hoff plot), yielding straight lines with slopes of $-\Delta H/R$ and intercepts of $\Delta S/R$.

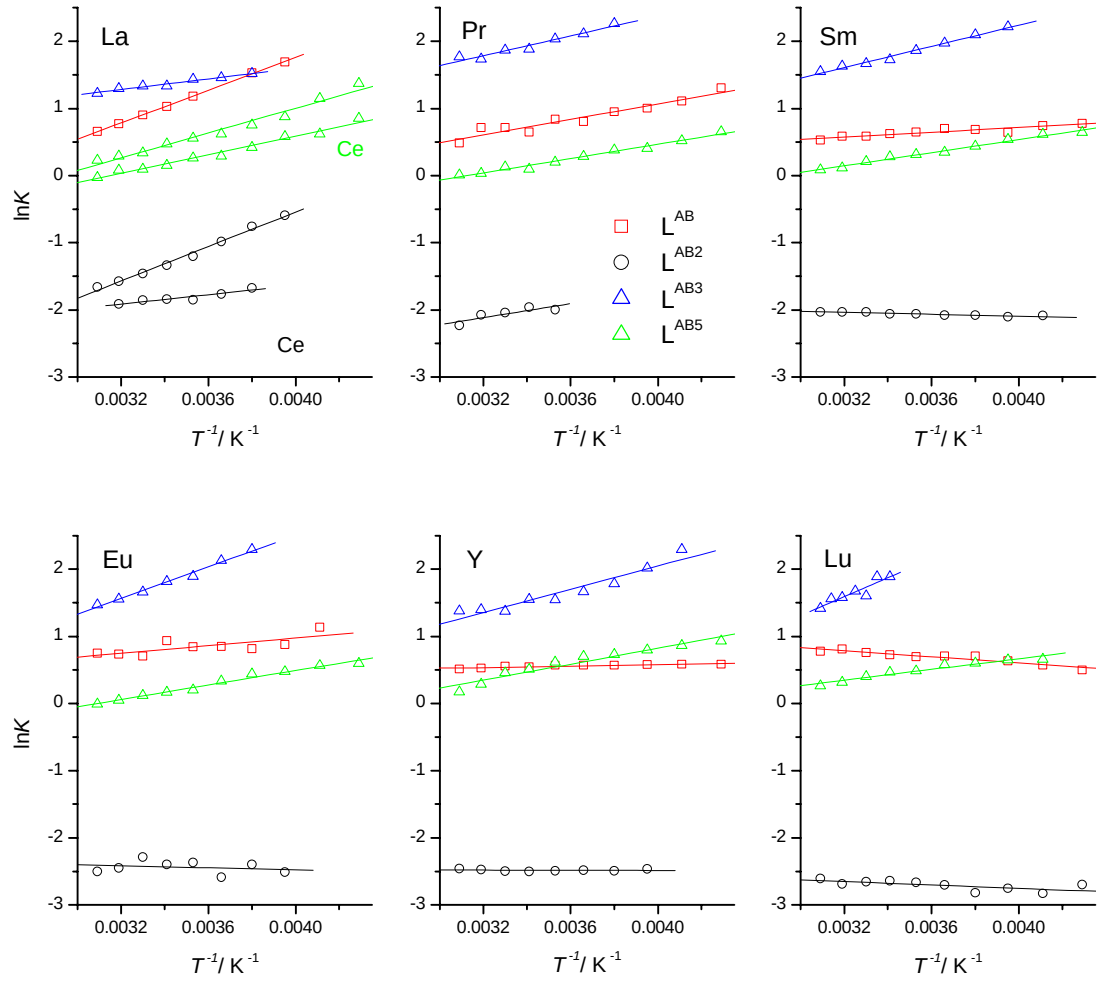

Figure 107 van't Hoff plots

As can be seen the correlation is generally good, especially for the L^{AB}, L^{AB2} and L^{AB5} complexes. The slightly lower quality of the data for the L^{AB3} complexes is due to the low concentration of the *HHT* isomers as mentioned above.

The values of H and S obtained from the slopes and intercepts of the plots are given in Table 157 - Table 160 together with calculated values of $-TS$, G, K and percentages of *HHH* isomer (all at 298 K).

Table 157 Thermodynamic parameters for L^{AB} complexes in CD_3CN

	La_2	Pr_2	Sm_2	Eu_2	Y_2	Lu_2
H [kJ·mol^{-1}]	-10.18(8)	-4.8(5)	-1.5(2)	-2.4(8)	-0.46(8)	1.9(2)
S [J· mol^{-1}·K^{-1}]	-26.1(3)	-10(2)	0.1(7)	-1(3)	3.0(3)	12.6(8)
$-T\ S$ (298 K) [kJ·mol^{-1}]	7.78(9)	3.1(5)	0.0(2)	0.4(8)	-0.89(9)	-3.8(2)
G (298 K) [kJ·mol^{-1}]	-2.4(1)	-1.7(7)	-1.5(3)	-2(1)	-1.3(1)	-1.9(3)
K (298 K)	2.6	2.0	1.8	2.2	1.7	2.1
% *HHH* (298 K)	73	67	65	69	63	68

Table 158 Thermodynamic parameters for L^{AB2} complexes in CD_3CN

	La_2	Ce_2	Pr_2	Sm_2	Eu_2	Y_2	Lu_2
H [kJ·mol^{-1}]	-10.7(4)	-2.9(5)	-4(1)	0.60(9)	1(1)	0.1(2)	1.1(4)
S [J· mol^{-1}·K^{-1}]	-47(1)	-25(2)	-31(5)	-15.0(3)	-18(4)	-20.4(6)	-19(1)
$-T\ S$ (298 K) [kJ·mol^{-1}]	14.1(4)	7.5(6)	9(1)	4.47(9)	5(1)	6.1(2)	5.5(4)
G (298 K) [kJ·mol^{-1}]	3.4(6)	4.6(8)	5(2)	5.1(1)	6(2)	6.1(3)	6.6(6)
K (298 K)	0.25	0.16	0.13	0.13	0.09	0.08	0.07
% *HHH* (298 K)	20	13	12	11	8	8	6

Table 159 Thermodynamic parameters for L^{AB3} complexes in CD_3CN

	La_2	Pr_2	Sm_2	Eu_2	Y_2	Lu_2
H [kJ·mol^{-1}]	-3.3(3)	-6.2(6)	-6.6(3)	-9.8(5)	-7.2(8)	-12(2)
S [J· mol^{-1}·K^{-1}]	0(1)	-5(2)	-8(1)	-18(2)	-12(3)	-25(7)
$-T\ S$ (298 K) [kJ·mol^{-1}]	0.0(3)	1.5(6)	2.3(3)	5.5(5)	3.5(9)	7(2)
G (298 K) [kJ·mol^{-1}]	-3.3(4)	-4.7(9)	-4.3(4)	-4.3(7)	-4(1)	-4(3)
K (298 K)	3.8	6.7	5.6	5.7	4.4	6.1
% *HHH* (298 K)	79	87	85	85	82	86

Table 160 Thermodynamic parameters for L^{AB5} complexes in CD_3CN

	La_2	Ce_2	Pr_2	Sm_2	Eu_2	Y_2	Lu_2
H [kJ·mol^{-1}]	-7.7(5)	-5.7(3)	-4.4(2)	-4.1(2)	-4.5(2)	-5.0(5)	-3.4(3)
S [J· mol^{-1}·K^{-1}]	-23(2)	-18(1)	-13.8(8)	-11.8(6)	-13.9(8)	-13(2)	-8(1)
$-T\ S$ (298 K) [kJ·mol^{-1}]	6.7(5)	5.4(3)	4.1(2)	3.5(2)	4.2(2)	3.9(5)	2.4(3)
G (298 K) [kJ·mol^{-1}]	-1.0(7)	-0.3(4)	-0.3(3)	-0.5(3)	-0.4(3)	-1.1(7)	-1.0(5)
K (298 K)	1.5	1.1	1.1	1.2	1.2	1.6	1.5
% *HHH* (298 K)	60	53	53	56	54	61	60

The values of H, S and G at 298 K are plotted in Figure 108.

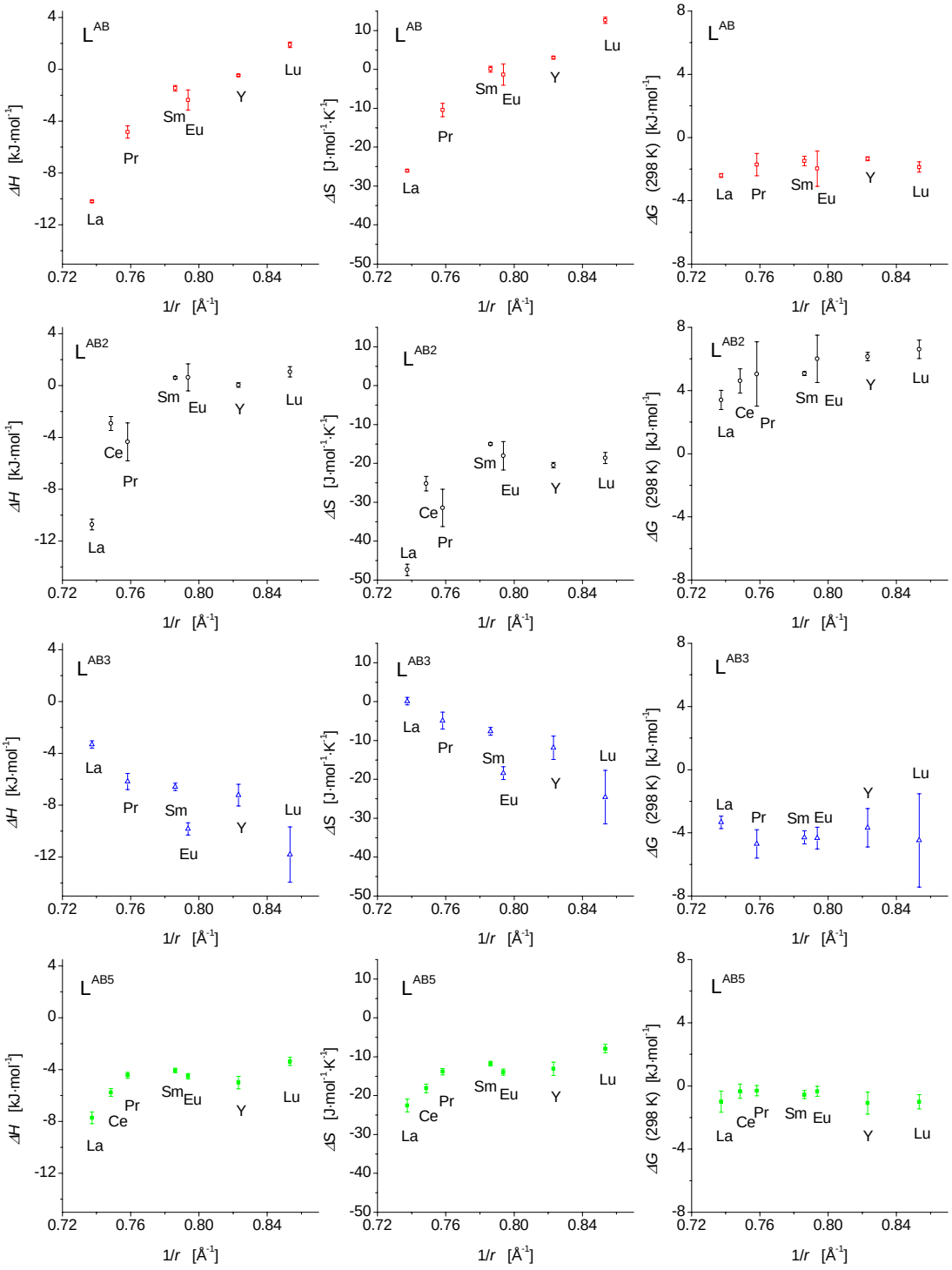

Figure 108 Thermodynamic parameters for $Ln_2(L)_3$ complexes in CD_3CN

To make sure that the parameters determined were not solvent effects the measurements of the La_2 and Lu_2 L^{AB} complexes were repeated using acetone-d_6 as solvent. The results are given in Table 161 and Table 162.

Table 161 Equilibrium constants for L^{AB} complexes in acetone-d_6

	La_2		Lu_2	
T (ºC)	*K*	ln*K*	*K*	ln*K*
40	1.75	0.56		
30	2.08	0.73	2.21	0.79
20	2.13	0.75	2.34	0.85
10	2.55	0.93	3.06	1.12
0	2.83	1.04	2.97	1.09
-10	2.96	1.08	3.16	1.15
-20	3.58	1.27	2.16	0.77
-30			2.37	0.86
-40			2.63	0.97

Table 162 Thermodynamic parameters for L^{AB} complexes in acetone-d_6

	La_2	Lu_2
H [kJ·mol^{-1}]	-7.4(5)	0(1)
S [J· mol^{-1}·K^{-1}]	-19(2)	8(6)
-*T S* (298 K) [kJ·mol^{-1}]	5.5(6)	-2(2)
G (298 K) [kJ·mol^{-1}]	-1.8(8)	-2(2)
K (298 K)	2.1	2.6
% *HHH* (298 K)	68	72

The higher standard errors compared to the results of the CD_3CN solutions are a result of the lower solubility (especially of the Lu complex).

As can be seen by comparison with the thermodynamic parameters of the CD_3CN solutions (Table 157) the results are similar in the two solvents. We therefore conclude that solvent effects only play a minor role in the *HHH/HHT* equilibrium.

7.4 Discussion

The thermodynamic parameters H and $-T S$ are shown in Figure 109.

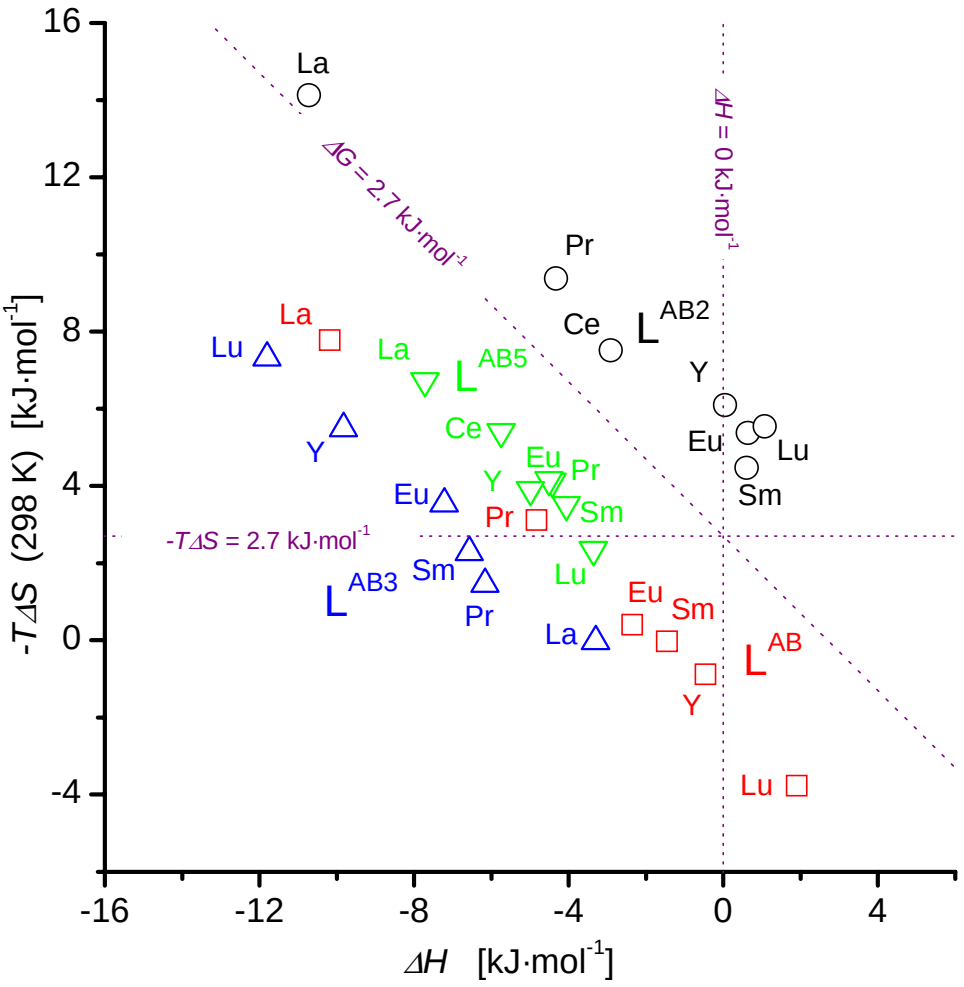

Figure 109 Thermodynamical parameters for the *HHT*/*HHH* equilibrium. Purple lines correspond to parameters calculated for a statistical distribution of *HHT* and *HHH* isomers.

Before discussing the results in terms of stabilisation it is helpful to examine a hypothetical statistical distribution of *HHH* and *HHT* complexes (see Chapter 4.1; page 59). In such a mixture of 25 % *HHH* and 75 % *HHT* complexes K equals 1/3 and G equals 2.7 kJ·mol^{-1} at 298 K (as indicated by a purple line in Figure 109). Only entropy (-9.1 J·mol^{-1}·K^{-1}) contributes to this G value since it is assumed that there is no enthalpy contribution. These values of H and $-T S$ for a statistical mixture are also indicated in Figure 109 by means of dotted purple lines.

The domain below the purple line indicating the statistical value of ΔG corresponds to stabilisation of the *HHH* isomer with respect to the statistical distribution. Similarly, the domain below the purple $-T\Delta S$ line corresponds to entropic and the domain to the left of the purple ΔH line corresponds to enthalpic stabilisation of the *HHH* isomer. This gives four quadrants in Figure 109 corresponding to the four possible combinations of stabilisation and destabilisation of the *HHH* isomer by enthalpy and entropy, respectively.

The enthalpy increases along the lanthanide series for the complexes of L^{AB}, L^{AB2} and L^{AB5}, signifying that the *HHH* isomer is less enthalpy stabilised for the smaller lanthanide ions. This can be assigned to the bpb cavity of the *HHH* conformation of the ligands, which is not well adapted for the smaller ions. In the *HHT* isomer this is not the case and this isomer is favoured by enthalpy over the *HHH* one for the lightest lanthanides. Interestingly, a decrease in stabilisation by enthalpy of the *HHH* isomer is observed for the L^{AB3} complexes.

Similarly, the entropy term $-T\Delta S$ decreases along the lanthanide series for complexes of L^{AB}, L^{AB2} and L^{AB5}, meaning that the *HHH* isomer smaller lanthanide ions are more stabilised by entropy than the larger ones. For the L^{AB3} complexes an increase is observed.

It is noteworthy that the ΔG (and K) values are so similar for complexes with the same ligand despite the variation of enthalpy and entropy. This observation points to the *HHT/HHH* equilibrium being characterised by a subtle interplay of entropic and enthalpic effects. Indeed, none of the ligands gives results in only one quadrant of Figure 109.

Generally speaking the extracted values of enthalpy and entropy are rather low in accordance with what is expected for an equilibrium between two isomers that are overall similar (same number of Ln-X bonds). This could indicate that the relative stability of the *HHH* and *HHT* complexes stems from weak interactions such as stacking interactions. It is however also possible that this is a manifestation of small differences between the strong ion-dipole interactions, which are the strongest interactions in the complexes.

The low values of ΔG should be compared to the values for the homobimetallic / heterobimetallic equilibrium. For the equilibrium $Ln_2(L)_3 + Ln'_2(L)_3 \leftrightarrows 2\ LnLn'(L)_3$ a statistical distribution (50 % of the heterobimetallic LnLn' and 25 % of each of the two homobimetallic species) gives $K = 4$ and $\Delta G = -3.4\ kJ{\cdot}mol^{-1}$. A distribution of 96 % hetero-

and 2 % of the two homobimetallic complexes (as found for $[LaLu(L^{AB})_3]^{6+}$) corresponds to G = -19.2 kJ·mol^{-1}, a difference of only 15.8 kJ·mol^{-1}. The 21 % heterobimetallic complexes found in $EuLu(L^{AB2})_3$ gives G = 3.1 kJ·mol^{-1}, also not far from the statistical value. This serves to illustrate the small energy differences associated with the selection process, comparable in size to the energy of a single hydrogen bond. It is evident from this consideration of the relative sizes of the G values that the stabilisation of the *HHH* isomer can contribute significantly to the formation of high yields of heterobimetallic complexes. The stabilisation of the *HHT* isomer would have the opposite effect, as evidenced by the L^{AB2} complexes. In this case the low proportion of *HHH* isomers seems to be the main reason for the reluctance of this ligand to give high yields of heterobimetallic complexes when reacted with a pair of lanthanide ions.

From the reported[80] value of β_{23} = 23.9 for the formation of the $Eu_2(L^{AB})_3$ complex in CH_3CN a G value of 136 kJ·mol^{-1} can be calculated. This serves to illustrate the small size of the energies discussed here, one order of magnitude smaller.

It is important to emphasise that the selectivity of these ligands when forming heterobimetallic complexes is of a purely supramolecular nature. Whereas the individual ligands contain two coordination sites of different character (type and hardness of ligator atoms), it is the coordination *cavities* of the final triple stranded helicate that exhibits selectivity towards pairs of ions of different sizes. Should a ligand only reluctantly form *HHH* complexes would it lead to a low proportion of these desired coordination cavities and thus a low yield of heterobimetallic species.

A difficulty in the discussion of the relative stability of the *HHH* and *HHT* isomers is the lack of detailed information on the structure of the latter. NMR data does however provide some degree of insight into the structure. In the partial NMR spectra of the $La_2(L)_3$ complexes presented in (Figure 14 and Figure 104) the aromatic protons H8 and H10 of the two bridging benzimidazole groups of the *HHH* isomer are seen to be shifted from the usual aromatic region (δ = 7.70 - 7.77 ppm in the free ligands) to δ values of 5.8 - 6.2 ppm. This is a consequence of the helical wrapping of the three ligand strands in the complexes, which places these two protons in the vicinity of neighbouring aromatic groups. In the region between 5.2 and 6.4 ppm, six signals of the *HHT* isomer can be counted, although these are weak in the $La_2(L^{AB4})_3$ spectrum and overlapping with signals of H1 and H3 for the

$La_2(L^{AB2})_3$. These signals are assigned to H8 and H10 of the three non-equivalent ligand strands in the *HHT* isomer. Their appearance in this region of the spectrum is taken as an indication of the structure in the vicinity of these protons being very similar in the two isomers. In other words, it is concluded that in the *HHT* isomer the two bridging benzimidazole groups of the three ligand strands are arranged in a manner similar to what was found for the *HHH* isomer. Note that the signals fall in two groups with four signals at ≈ 6.0 - 6.3 ppm and two signals at ≈ 5.2 - 5.7 ppm; this corresponds to two of the ligand strands (the "*Head"* strands) having similar structures.

Three intramolecular interactions are foreseen to influence the stability of the complexes: ion-dipole interactions between the ligands and the lanthanide ions, interactions between the three ligand strands and the Ln-Ln' repulsion. These three contributions can be parametrised as outlined in Chapter 4.1 (page 59). The number of parameters needed to do so (eight) is too large to make it possible to extract them from our experimental data. Reducing the number of parameters by simplifying the model would require the making of assumptions regarding some of the parameters being equal. This corresponds to *a priori* ruling out one or two of the three intramolecular interactions as playing a part in the description of the *HHH* ⇆ *HHT* equilibrium. While this could be a good method of approaching the problem under other circumstances, it is not felt to be justified here considering the small energy differences involved. For this reason no quantitative treatment will be carried out here and what follows is instead a qualitative discussion of the three interactions.

The ion-dipole interactions are by far the strongest of the three, approximately 100 – 200 $kJ \cdot mol^{-1}$ per bond, which amounts to several thousand $kJ \cdot mol^{-1}$ for the 18 ion-dipole interactions in the molecule. Differences of a few percent in the Ln-X distances in the two isomers could lead to the energy differences observed here.

The interligand interactions are weaker, probably comparable in energy to hydrogen bonds. In the *HHH* complexes whose structures have been determined in the solid state the distances between the aromatic groups of the bpb moieties of the ligands are rather long (3.5 – 4 Å) and the planes defined by them are not exactly parallel, the angles being ≈ 10 °; this indicates very weak stacking interactions. Unfortunately, no *HHT* complexes have been crystallised, and their exact structure are therefore open for speculation. In the *HHT* isomer interactions are only possible between two bpb units, which *a priori* could lead to the conclusion that the total

stacking interactions are smaller. However, it is possible that these two units are closer and more parallel than in the *HHH* isomer and that this single interaction is stronger than the sum of the three interactions in the *HHH* isomer.

The Ln-Ln' repulsion E_{rep} is the last factor to consider. This can be calculated (as a Coulomb interaction taking into account the relative dielectric constant ≈ 30 of the medium separating the two Ln^{3+} ions) to be $E_{rep} \approx 45$ kJ·mol^{-1} for a Ln-Ln' distance of 9.2 Å.[53,71] Based on the above arguments on the structure of the *HHT* isomer the Ln-Ln' distance is not estimated to be different in the two isomers by more than 0.5 Å. This gives a difference in E_{rep} of 2 - 3 kJ·mol^{-1}. This can be taken as the maximal influence this effect can have on the *HHH*/*HHT* equilibrium, not enough to account for the H values observed, but enough to make a contribution.

Speaking against the Ln-Ln' repulsion as a decisive influence is the fact that it does not explain the difference in H observed for complexes of the same ligand with different lanthanide ions (up to 12 kJ·mol^{-1} upon replacing La with Lu; Table 157 - Table 160). The Ln-Ln' distances determined in the solid state for the *HHH* complexes are all equal within +/- 0.1 Å (ref table 12) corresponding to differences in E_{rep} of ≈ 0.5 kJ·mol^{-1}. If an equally small difference is assumed for the LnLn' distances in the *HHT* isomers the effect of E_{rep} on the variation of H along the lanthanide series is ≈ 1 kJ·mol^{-1}.

7.5 Conclusion

The *HHH*/*HHT* equilibrium has been investigated for a series of complexes of the heterobitopic ligands L^{AB}, L^{AB2}, L^{AB3} and L^{AB5}. For the complexes of L^{AB2} the *HHT* isomer is stabilised with respect to the *HHH* isomer, whereas the opposite is observed for the complexes of L^{AB}, L^{AB3} and L^{AB5}.

Whereas the equilibrium constants for all complexes of each ligand are similar, the thermodynamic parameters characteristic of the equilibria are less straightforward to interpret. In some cases a stabilisation of the *HHH* isomer can be traced back to an enthalpic stabilisation, in other cases the stabilisation originates in entropy. In all cases there is a fine balance between entropy and enthalpy.

Given the small free energies of stabilisation ($|G| < 16$ kJ·mol^{-1}) of the heterobimetallic complexes compared to the statistical value, it is evident that the energy differences between *HHH* and *HHT* isomers (which have the same order of magnitude) can contribute significantly to the formation of heterobimetallic complexes. Indeed this was observed (although as a negative effect) in the complexes of L^{AB2} for which the low stability of the *HHH* isomer leads to low proportions of heterobimetallic complexes, in contrast to what was expected when designing the ligand.

The introduction of different substituents has been a success in the sense that they influence the hardness of the ligands in the predicted manner. Less successful was the occurrence of an unforeseen complication: the *HHH*/*HHT* equilibrium. In previous work with the ligand L^{AC} it was assumed that the high proportion of *HHT* complexes was a result of interstrand repulsion between negatively charged carboxylate groups[80]. With the observation of similar behaviour of the L^{AB2} and L^{AB5} complexes, which contain no carboxylate groups, it has to be concluded that the explanation may not be that simple and that weaker interactions could be responsible.

While this seems to be a reasonable solution, it also carries with it further complications. Indeed this is not specific to the present project, but can be said to be generally relevant in the field of supramolecular chemistry. Strong interactions (ion-ion, ion-dipole and even hydrogen bonding) are well understood and they are fairly easily programmed when designing a supramolecular system. Weaker interactions ($\pi\cdots\pi$, $CH\cdots\pi$) are not yet understood at a similar level, but it is becoming increasingly clear that they contribute in a significant way to structure and stability not only of man-made supramolecular assemblies, but also to biomolecules.

The problem in the present interpretation of the experimental data lies in the lack of structural information available for the *HHT* isomer, which leaves the conclusions drawn to be speculative in nature. It is, however, possible that molecular modelling could shed light on the energetics of the *HHH/HHT* equilibrium as it has successfully done with a series of *fac* and *mer* isomers of monometallic complexes.[47]

8 Conclusion

The new heterobitopic ligands L^{AB2}, L^{AB3}, L^{AB4} and L^{AB5} have been synthesised for two purposes. Firstly for trying to understand the origin of the selectivity displayed by L^{AB} towards heteropairs of Ln(III) ions and secondly in order to, if possible, improve this selectivity.

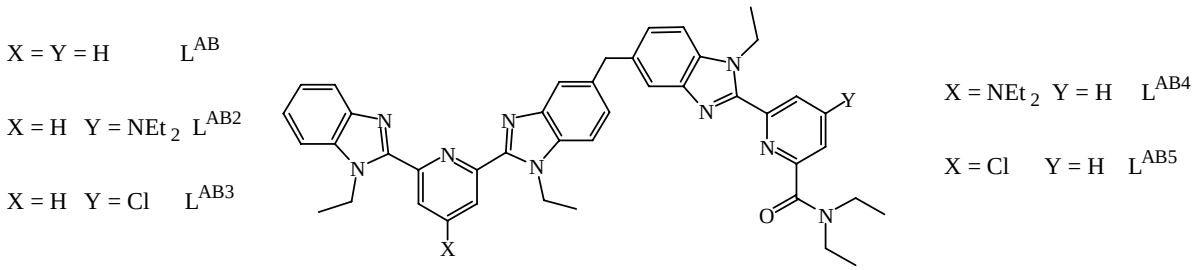

Chart 16 Heterobitopic ligands

In L^{AB}, the bpa (benzimidazole-pyridine-amide) unit has a preference for the smaller lanthanide ions. The bpb (benzimidazole-pyridine-benzimidazole) unit, on the other hand, prefers the larger ions from the first half on the lanthanide series.

Introducing a substituent in the *para* position of a pyridine group was done to modify the electron density of the nitrogen donor atom of the pyridine. The electron donating NEt_2 group increases the electron density whereas the electron withdrawing Cl substituent decreases it. The ligands L^{AB2} (increased electron density on the bpa pyridine) and L^{AB5} (reduced electron density on the bpb pyridine) were thus expected to improve the selectivity compared to L^{AB}. L^{AB3} and L^{AB4} were, based on the same arguments, not expected to be an improvement.

The goal of the project has been to:

- Determine the structure in the solid state of the complexes
- Determine the speciation in solution of homo- and heterobimetallic complexes of the ligands in solution.
- Gain insight into the structure in solution by means of analysis of lanthanide induced paramagnetic shift.
- Estimate the thermodynamic contributions (enthalpy and entropy) to the *HHH* ⇆ *HHT* equilibrium by means of variable temperature NMR.

8.1 Solid state structure

Five complexes of the ligand L^{AB3} have been crystallised and their structures in the solid state have been determined by means of X-ray diffraction. The structures consist of isolated molecular ions $[LnLn'(L^{AB3})_3]^{6+}$, ClO_4^- ions and solvent molecules. The molecular ions contain three ligand strands wrapped around the Ln-Ln' axis in a helical fashion.

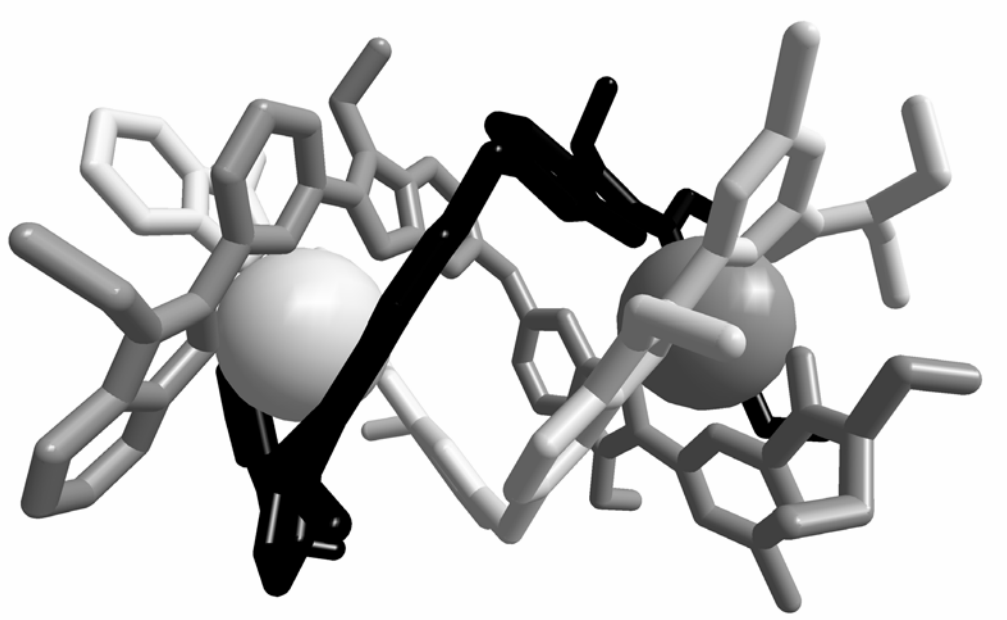

Figure 110 The $[PrLu(L^{AB3})_3]^{6+}$ molecular ion

Very weak interstrand π-π interactions have been observed between aromatic groups of the bpb moiety of the L^{AB3} ligand and it is thought that they contribute to some degree to the stability of the complexes.

The coordination polyhedra around the lanthanide ions are slightly distorted tricapped trigonal prisms. The Ln-X bond lengths are in line with what is usually observed for similar bonds.

The helical pitch does not change significantly upon changing the LnLn' couple; values of 13.2 - 13.4 Å were found for the five L^{AB3} complexes. Little variation is also observed for the Ln-Ln' distances, which are 9.1 - 9.2 Å. Interestingly, this is very similar to what was found for complexes with L^{AB} (13.2 - 13.5 Å and 9.2 - 9.4 Å), meaning the the Cl substituent in L^{AB3} has little influence on the structure in the solid state.

8.2 Speciation in solution

When reacted with 2/3 equivalents of Ln(III) ions in CD_3CN solution the ligands form complexes of overall composition $[Ln_2(L)_3]^{6+}$. Two isomers of this complex are possible, *HHH* (*Head-Head-Head*) in which the three ligand strands are oriented in the same direction and *HHT (Head-Head-Tail*) in which one of the ligands points in the opposite direction of the two others.

The percentages of *HHH* isomer depend on the ligand and lie within the ranges 6 - 20 % for L^{AB2}, 53 - 61 % for L^{AB5}, 63 - 73 % for L^{AB}, 79 - 86 % for L^{AB3} and 93 - 96 % for L^{AB4}. As can be seen, the *HHH* percentages are not very dependent on the lanthanide ion, the absolute variation being less than 15 % along the lanthanide series for complexes of a given ligand. The Cl substituent in L^{AB3} and L^{AB5} only changes the percentages by 10 - 20 %, whereas the NEt_2 substituent in L^{AB2} and L^{AB4} pushes the equilibrium towards high proportions of either the *HHH* or the *HHT* isomer. This means that fine-tuning of the ligand structure has made it possible to maximise the proportions of *HHH* complexes.

In the presence of a LnLn' pair of different lanthanide ions the ligands form a mixture of homobimetallic ($Ln_2(L)_3$ and $Ln'_2(L)_3$) and heterobimetallic ($LnLn'(L)_3$) complexes. For the original L^{AB} ligand the proportion of heterobimetallic complexes reaches 96 % for the LaLu pair with the percentage being lower and approaching statistical values (50 %) for pairs of lanthanide ions closer in size.

In the design of the ligands it was planned that the modification of the hardness of the pyridyl nitrogen atom induced by the substituents would lead to improved selectivities for the ligands L^{AB2} and L^{AB5}. Unfortunately, the selectivities of these two ligands are altered by the higher proportions of *HHT* isomers formed. For the LaLu couple L^{AB2} yielded only 65 % $LaLu(L^{AB2})_3$; L^{AB5} reached 92 % with the percentages for other LnLn' couples in general being lower or equal to the values determined for L^{AB}.

For the ligands L^{AB3} and L^{AB4} no improvement is observed; the proportions of heterobimetallic $LaLu(L)_3$ complexes are 87 % for L^{AB3} and 79 % for L^{AB4}. These results are gratifying since they demonstrate that the idea behind the addition of the substituents is good. Furthermore it is evident that NEt_2 has a larger influence that Cl, as was also seen for the percentages of *HHH* isomer above.

8.3 Analysis of lanthanide induced shift

The complexes have also been investigated in solution by means of analysis of lanthanide induced shift of the $LaLn(L)_3$, $LnLu(L)_3$ and $Ln_2(L)_3$ series of complexes with the ligands L^{AB}, L^{AB3}, L^{AB4} and L^{AB5}.

Application of the two proton (Geraldes) method yielded structural ratios containing information about the geometry of the individual protons relative to the paramagnetic lanthanide ions. In a first step, this was used to demonstrate that all the complexes are isostructural in solution, regardless of the ligand. Comparison with structural ratios calculated from the solid state structures gave as result that the helical structure is maintained in solution. The solid state $Pr_2(L^{AB3})_3$ complex emerged as the best structural model for the solution structure. This result was confirmed by measurement of the lanthanide induced relaxation of the $LnLu(L^{AB})_3$ (Ln = Ce, Pr, Nd, Sm, Eu) series of complexes which yielded relative Ln···H distances similar to those measured in the solid state complex.

Combining the lanthanide induced shift data with the structural data of the $Pr_2(L^{AB3})_3$ complex allowed for the determination of crystal field parameters for lanthanide ions in the two compartments of the complexes. For complexes of L^{AB} it was found that B_0^2 is 1.9(1) times larger for the lanthanide ion in the bpa cavity than for the bpb lanthanide ion. This is probably related to the Ln-X distance being shorter for the O donor than for the N one and is in good agreement with what was reported in the literature for a closely related complex.[51] Again it was found that a Cl substituent has only minor influence on the properties of a complex, resulting in a reduction of B_0^2 of only a few percent for lanthanide ions coordinated by a Cl substituted pyridine. The NEt_2 substituent, on the other hand, induces a doubling of the crystal field parameter, due to the increased electron density on the N donor atom.

To overcome the potential problems associated with the variation of the crystal field parameter along the lanthanide series a modified one proton analysis method was developed. It yields improved separation of contact and pseudo contact shifts, in particular for protons whose lanthanide induced shift is dominated by the pseudo contact shift. As an additional feature it also provides a simple NMR based method for determining relative crystal field parameters for different ions of the lanthanide series. A non-monotonous increase in B_0^2 was observedfor the series Ce, Pr, Nd and Eu. The value for Eu was 50 - 100 % larger than the Ce

value, depending on the ligand and the site, in accordance with what has been reported in the literature.[90,94] Again, the NEt_2 substituted L^{AB4} deviated in behaviour from the other ligands.

8.4 Energetics of the HHH/HHT equilibrium

As was demonstrated by the speciation of complexes in solution the ability of a ligand to form high proportions of *HHH* isomer is vital for the selectivity towards a pair of different lanthanide ions.

To gain insight in the energetics of the *HHH/HHT* equilibrium a variable temperature NMR study was carried out. This yielded values of H and S for this equilibrium for 26 complexes of the ligands L^{AB}, L^{AB2}, L^{AB3} and L^{AB5}.

The results demonstrated that the *HHH/HHT* equilibrium is governed by a subtle interplay of enthalpic and entropic effects with the differences between the two isomers being in the order of a few $kJ \cdot mol^{-1}$. In fact, for complexes with the same ligand the percentage of *HHH* isomer and hence the value of G varies little along the lanthanide series. The values of H, on the other hand, changes with up to 12 $kJ \cdot mol^{-1}$ in going from La to Lu and this change is counterbalanced by a change in S.

Three effects are presumed to participate to the energetics of the equilibrium. Weak interstrand stacking interactions between aromatic groups are known to play a role and could stabilise one of the two isomers. Small differences in the strong ion-dipole interactions are another possible explanation. And finally, differences in the Ln-Ln' Coulomb repulsion could contribute. Based on the experimental data it has not been possible to conclude with certainty on the origin of the markedly different behaviour of the 26 complexes.

8.5 Outlook

The results presented here have shown that the introduction of Cl and, in particular, NEt_2 substituents changes the properties of L^{AB} remarkably. This is evident in all the quantities measured, from crystal field parameters to selectivities towards hetero pairs of lanthanide ions. There is potential in this concept for the fine-tuning of ligand systems.

The problems in fully comprehending the *HHH/HHT* equilibrium demonstrate where the present understanding is still incomplete. More work is needed to elucidate the effects of weak interactions in supramolecular chemistry. It is anticipated that molecular modelling will emerge as a valuable tool in this respect in the future, but this method is not yet mature enough to accurately calculate the diminutive energy differences encountered here. Meanwhile, the simple empirically based model developed by Piguet and coworkers[57] appears to be the method of choice for rationalising the self-assembly of heteropolymetallic helicates.

It is hoped that, with the aid of a combination of experiment and theory, future projects in this fascinating field can make the leap from description to prediction.

9 Experimental

Solvents and starting materials were purchased from Acros, Merck and Fluka and used without further purification, unless otherwise stated. Dichloromethane (CH_2Cl_2) was distilled from CaH_2; thionyl chloride ($SOCl_2$) was distilled from elemental sulfur; triethylamine (NEt_3) was distilled from KOH. Silicagel (Merck 60, 0.04-0.06 mm) was used for preparative column chromatography.

Duplicate elemental analyses were performed by Dr. H. Eder at the Microchemical Laboratory of the University of Geneva.

NMR spectra were measured on Bruker Avance 400 (400 MHz) and Bruker Avance 600 (600 MHz) spectrometers.

MS spectra used for the characterization of organic compounds were recorded in MeOH or CH_3CN with a Finnigan SSQ-710C spectrometer.

9.1 Synthesis of ligands

See Scheme 1 - Scheme 7 (page 28 - 34).

9.1.1 Synthesis of 2

1 (15.0 g; 95 mmol) was stirred overnight in an autoclave at 130°C with 150 ml (1.87 mol) of a 70 % solution of ethylamine in water. After cooling to room temperature, the reaction mixture was poured into 75 ml cold H_2O, followed by extraction with CH_2Cl_2 (2 x 225 ml). The combined organic phases were dried over $MgSO_4$, filtered and the CH_2Cl_2 was removed on rotavapor to give an orange oil. Yield: 15.25 g (97 %).

^{1}H NMR ($CDCl_3$): δ 8.17 (dd, 1H, ^3J = 8.6 Hz, ^4J = 1.6 Hz), 7.97 (br s, 1H), 7.43 (t, 1H, ^3J = 7.8 Hz), 6.84 (d, 1H, ^3J = 8.7 Hz),6.63 (t, 1H, ^3J = 7.7 Hz), 3.36 (q, 1H, ^3J = 7.2 Hz), 3.34 (q, 1H, ^3J = 7.2 Hz), 1.37 (t, 3H, ^3J = 7.2 Hz).

9.1.2 Synthesis of 3

A solution of **2** (8.64 g; 52.0 mmol) and $(CH_2O)_n$ (0.78 g; 26.0 mmol) in 100 ml 37 % HCl was stirred at room temperature for 2 h, after which the temperature was raised to 120°C and stirring was continued overnight. The reaction mixture was poured into 700 ml H_2O and slowly neutralised with 25 % NH_3. The resulting orange precipitate was filtered off and recrystallised from 350 ml EtOH. Yield: 6.96 g (78 %).

^{1}H NMR ($CDCl_3$): δ 7.99 (d, 2H, ^4J = 2.1 Hz), 7.94 (br s, 2H), 7.25 (dd, 2H, ^3J = 9 Hz, ^4J = 2.1 Hz), 6.80 (d, 2H, ^3J = 8.9 Hz), 3.79 (s, 2H), 3.34 (q, 2H, ^3J = 7.2 Hz), 3.33 (q, 2H, ^3J = 7.2 Hz), 1.36 (t, 6 H, ^3J = 7.2 Hz).

9.1.3 Synthesis of 5

4 (20.22 g; 121 mmol) in a mixture of CH_3OH (100 ml), H_2O (100 ml) and fuming H_2SO_4 (10 ml) was refluxed for 15 min, stirred overnight and then poured into a saturated solution of $NaHCO_3$ (500 ml). The solution was extracted with $CHCl_3$ (4 x 150 ml), acidified to pH = 2 with 25 % HCl and extracted with CH_2Cl_2 (3 x 200 ml). The combined CH_2Cl_2 phases were dried over Na_2SO_4, filtered and evaporated. The product was dried in vacuum. Yield: 7.256 g (33 %).

^{1}H NMR ($CDCl_3$): δ 8.42 (dd, 1H, ^3J = 7.8 Hz, ^4J = 1.3 Hz), 8.36 (dd, 1H, ^3J = 7.8 Hz, ^4J = 1.3 Hz), 8.13 (t, 1H, ^3J = 7.8 Hz), 4.04 (s, 3H).

9.1.4 Synthesis of 6 and 7

A solution of **5** (7.246 g; 40 mmol), $SOCl_2$ (100 ml; 1.39 mol) and DMF (0.1 ml) in 200 ml dry CH_2Cl_2 was refluxed under an atmosphere of N_2 for 90 min. After solvent removal on rotavapor, removal of excess $SOCl_2$ in vacuum and drying in vacuum for 30 min, the residue was redisolved in 200 ml dry CH_2Cl_2 and $HNEt_2$ (27.73 g; 0.38 mol) was added dropwise. The reaction mixture was refluxed for 60 min under N_2, the solvent was removed and the residue was partitioned between 250 ml CH_2Cl_2 and 300 ml half-saturated NH_4Cl. The aqueous phase was then extracted with CH_2Cl_2 (3 x 150 ml). The combined organic phases were washed with a saturated solution of $NaHCO_3$ (2 x 200 ml) and evaporated to dryness. The resulting residue of **6** was stirred in 200 ml 1 M KOH for 10 min and extracted with 200

ml $CHCl_3$. After adjusting the pH to 2 with 25 % HCl, a precipitate formed. The solution was kept in the fridge overnight and the precipitate was collected by filtration, washed with 0.01 M HCl and dried in vacuum. Yield: 8.287 g of **7** (93 %).

^{1}H NMR (CD_3OD): δ 8.21 (dd, 1H, ^3J = 7.9 Hz, ^4J = 1.1 Hz), 8.10 (t, 1H, ^3J = 7.8 Hz), 7.76 (dd, 1H, ^3J = 7.8 Hz, ^4J = 1.1 Hz), 3.59 (q, 2H, ^3J = 7.1 Hz), 3.34 (q, 2H, ^3J = 7.1 Hz), 1.29 (t, 3H, ^3J = 7.1 Hz), 1.20 (t, 3H, ^3J = 7.1 Hz).

9.1.5 Synthesis of 8

A solution of **7** (8.282 g; 37 mmol), $SOCl_2$ (40 ml; 0.56 mol) and DMF (0.1 ml) in 150 ml dry CH_2Cl_2 was refluxed under an atmosphere of N_2 for 70 min. After solvent removal on rotavapor, removal of excess $SOCl_2$ in vacuum and drying in vacuum for 45 min, the residue was redisolved in 100 ml dry CH_2Cl_2. After adding a solution of **2** (6.19 g; 37 mmol) and NEt_3 (50 ml) in 50 ml dry CH_2Cl_2, the reaction mixture was refluxed under N_2 for 2 h. Following solvent removal, the residue was partitioned between 200 ml CH_2Cl_2 and 200 ml half-saturated NH_4Cl. The aqueous phase was then extracted with CH_2Cl_2 (5 x 120 ml). The combined organic phases were dried over Na_2SO_4, filtrated and evaporated to dryness. The crude product was purified by column chromatography (silica gel, CH_2Cl_2/CH_3OH = 100/0 $\rightarrow$ 98/2). Yield: 9.939 g (73 %).

9.1.6 Synthesis of 9

A mixture of **8** (9.939 g; 27.0 mmol), Fe powder (25 g; 0.45 mol), 150 ml EtOH, 400 ml H_20 and 150 ml 25 % HCl was refluxed overnight under an atmosphere of N_2. After filtering off excess Fe and removing EtOH on rotavapor, the reaction mixture was poured into a mixture of H_4-EDTA (200 g; 0.68 mol), NaOH (100 g; 2.5 mol), H_2O (350 ml) and CH_2Cl_2 (300 ml). The solution was neutralised with 5 M KOH, 17 ml 30 % H_2O_2 was added slowly, the pH was adjusted to 8.5 with 5 M KOH and the mixture was stirred for 30 min. The organic phase was separated and the aqueous phase was extracted with CH_2Cl_2 (3 x 200 ml). The combined organic phases were washed with H_2O (2 x 200 ml), dried over Na_2SO_4, filtrated and evaporated to dryness. The crude product was purified by column chromatography (silica gel, CH_2Cl_2/CH_3OH = 100/0 $\rightarrow$ 98/2). Yield: 5.890 g (68 %).

^{1}H NMR ($CDCl_3$): δ 8.40 (d, 1H, ^3J = 8.1 Hz), 7.95 (t, 1H, ^3J = 7.9 Hz), 7.84 (d, 1H, ^3J = 7.0 Hz), 7.56 (d, 1H, ^3J = 7.7 Hz), 7.47 (d, 1H, ^3J = 7.7 Hz), 7.34 (m, 2H), 4.78 (q, 2H, ^3J = 7.1 Hz), 3.62 (q, 2H, ^3J = 7.1 Hz), 3.36 (q, 2H, ^3J = 7.1 Hz), 1.48 (t, 3H, ^3J = 7.1 Hz), 1.29 (t, 3H, ^3J = 7.1 Hz), 1.08 (t, 3H, ^3J = 7.1 Hz).

9.1.7 Synthesis of 10

A mixture of **9** (5.890 g; 18.3 mmol), KOH (200 g; 3.5 mol), H_2O (400 ml) and EtOH (200 ml) was refluxed for 14 h. After cooling to room temperature the pH was adjusted to 2 with 25 % HCl. The resulting white precipitate was filtered off, washed with 0.01 M HCl and dried in vacuum. Yield: 4.170 g (85 %).

^{1}H NMR (DMSO-d_6): δ 8.64 (d, 1H, ^3J = 7.7 Hz), 8.34 (t, 1H, ^3J = 7.8 Hz), 8.28 (d, 1H, ^3J = 7.8 Hz), 7.99 (d, 1H, ^3J = 7.7 Hz), 7.89 (d, 1H, ^3J = 7.8 Hz), 7.57 (m, 2H), 4.94 (q, 2H, ^3J = 7.1 Hz), 1.52 (t, 3H, ^3J = 7.0 Hz).

9.1.8 Synthesis of 13 from 11 via 12

A mixture of **11** (25 g; 0.137 mol) and 65 ml *P*,*P*-dichlorophenylphosphine oxide (0.464 mol) was stirred at 120 °C for 2 h during which the colour changed from pale yellow to brown. After cooling down to room temperature, 300 ml MeOH were added slowly. The mixture was stirred for 3 h and 400 ml H_2O was added. The solution was extracted with CH_2Cl_2 (3 x 200 ml) and the combined extracts were washed with H_2O (2 x 200 ml) and evaporated to give **12**. The residue was refluxed in 200 ml 1 M NaOH for 60 min. After cooling to rt, pH was adjusted to 2 with 37 % HCl and the precipitate formed was filtered off and washed with cold aqueous HCl (pH = 2) and dried in vacuum. Yield: 23.9 g (87 %).

^{1}H NMR (CD_3OD): **12:** δ 8.32 (s).
^{1}H NMR (CD_3OD): **13:** δ 8.35 (s).

9.1.9 Synthesis of 13 from 11

A mixture of **11** (6.225 g; 34.0 mmol) and *P*,*P*-dichlorophenylphosphine oxide (20 ml; 143 mmol) was stirred at 130 °C for 2 h. During the reaction, the colour changed from yellow over red to dark brown. After cooling, 100 ml water was added slowly and the solution was

neutralised with concentrated KOH. The pH was then adjusted to 4 with 25 % HCl. The precipitate was collected by filtration, washed with 10^{-4} M HCl and air dried. Yield: 6.254 g (91 %).

^{1}H NMR (CD_3OD): δ 8.35 (s).

9.1.10 Synthesis of 14

13 (4.493 g; 22.3 mmol), $HNEt_2$ (25 ml; 238 mmol) and 25 ml H_2O was placed in an autoclave and stirred at 145°C overnight (P = 8 bar). After evaporation of $HNEt_2$ and H_2O on rotavapor, KOH (10 g; 175 mmol) and 50 ml H_2O was added and the solution was refluxed for 23 h. The solution was neutralised with 25 % HCl, filtrated and the pH was adjusted to 1 with 25 % HCl. The resulting precipitate was filtered off, washed with 0.1 M HCl and dried. Yield: 3.731 g (70 %).

^{1}H NMR (CD_3OD): δ 7.53 (s, 2H), 3.72 (q, 4H, ^3J = 7.3 Hz), 1.32 (t, 6H, ^3J = 7.2 Hz).

9.1.11 Synthesis of 15

A mixture of **14** (4.76 g; 20.0 mmol), 10 ml H_2O, 50 ml CH_3OH and 2 ml 97 % H_2SO_4 was refluxed for 4 h, cooled to rt and poured slowly into 160 ml of saturated $NaHCO_3$ solution. The solution was extracted with CH_2Cl_2 (3 x 50 ml). The aqueous phase was then acidified to pH = 3 with 25 % HCl and extracted with CH_2Cl_2 (12 x 50 ml) over the next 24 h. The extracts were dried over Na_2SO_4, filtered and evaporated. Yield: 2.100 g (39 %) of **15**.

^{1}H NMR (CD_3OD): δ 7.55 (d, 1H, ^4J = 2.9 Hz), 7.50 (d, 1H, ^4J = 2.9 Hz), 4.07 (s, 3H), 3.72 (q, 4H, ^3J = 7.2 Hz), 1.31 (t, 6H, ^3J = 7.2 Hz).
TLC (CH_2Cl_2/CH_3OH = 95/5): *Rf* = 0.05.
MS (CH_3CN) m/z: 253.4 ($[M + H]^+$, calc. 253.3).

9.1.12 Synthesis of 16 and 17

After refluxing a solution of **15** (4.203 g; 16.66 mmol), $SOCl_2$ (30 ml, 412 mmol) and 0.1 ml DMF in 100 ml dry CH_2Cl_2 under an atmosphere of N_2 for 2 h, the solvent was removed on

rotavapor, excess $SOCl_2$ was removed in vacuum and the residue was dried in vacuum for 1 h. The pale yellow solid was redisolved in 100 ml dry CH_2Cl_2, $HNEt_2$ (16 ml; 153 mmol) was added dropwise and the reaction mixture was refluxed under N_2 for 2 h. Following removal of solvent, the residue was partitioned between 150 ml CH_2Cl_2 and 150 ml half-saturated NH_4Cl. The aqueous phase was extracted with CH_2Cl_2 (2 x 150 ml) and the combined organic phases were then washed with saturated $NaHCO_3$ (2 x 100 ml) and evaporated to yield crude **16**. This was dissolved in a mixture of 50 ml CH_3OH and 50 ml 1 M KOH and stirred overnight. Following removal of CH_3OH on rotavapor, the solution was extracted with CH_2Cl_2 (3 x 50 ml) and acidified to pH = 1.6 with 25 % HCl. The solution was then extracted with CH_2Cl_2 (13 x 50 ml) over the next 3 days. The combined extracts were dried over Na_2SO_4, filtered and evaporated to yield 2.834 g (58 %) of **17**.

^{1}H NMR (CD_3OD): **17**: δ 7.48 (d, 1H, ^4J = 2.8 Hz), 7.00 (d, 1H, ^4J = 2.8 Hz), 3.67 (q, 4H, ^3J = 7.2 Hz), 3.58 (q, 2H, ^3J = 7.2 Hz), 1.29 (t, 9H, ^3J = 7.2 Hz), 1.20 (t, 3H, ^3J = 7.2 Hz).
^{1}H NMR ($CDCl_3$): **17**: δ 7.44 (d, 1H, ^4J = 2.6 Hz), 6.82 (d, 1H, ^4J = 2.6 Hz), 3.57 (q, 2H, ^3J = 7.3 Hz), 3.49 (q, 4H, ^3J = 7.3 Hz), 3.33 (q, 2H, ^3J = 7.3 Hz), 1.29 (t, 3H, ^3J = 6.9 Hz), 1.24 (t, 6H, ^3J = 7.1 Hz), 1.20 (t, 3H, ^3J = 6.8 Hz).
MS (CH_3CN) **17**: m/z: 293.8 ($[M + H]^+$, calc. 294.2).
Elemental analysis: calculated (found) for $C_{15}H_{23}N_3O_3 \cdot 0.5H_2O$: C 59.58 (59.83); H 8.00 (7.80); N 13.90 (13.91)

9.1.13 Synthesis of 18

A solution of **17** (3.18 g; 10.8 mmol), 25 ml $SOCl_2$ and 5 drops of DMF in 100 ml dry CH_2Cl_2 was refluxed under N_2 for 2 h. The solvents were evaporated and the residue was dried in vacuum for 1 h and re-dissolved in 50 ml dry CH_2Cl_2. A solution of **2** (3.09 g; 18.6 mmol) and 10 ml NEt_3 in 50 ml dry CH_2Cl_2 was added dropwise. The solution was refluxed for 1 h, evaporated to dryness and partitioned between 120 ml half saturated aqueous NH_4Cl solution and 120 ml CH_2Cl_2. The aqueous phase was extracted with CH_2Cl_2 (3 x 100 ml) and the combined organic phases were dried over Na_2SO_4, filtered and evaporated to dryness. The crude product was purified on column (silica gel, CH_2Cl_2/CH_3OH = 100/0 $\rightarrow$ 96/4). Yield: 1.79 g (37 %).

^{1}H NMR ($CDCl_3$): δ 7.94 (dd, 1H, ^3J = 8.3 Hz, ^4J = 1.5 Hz), 7.46 (td, 1H, ^3J = 7.7 Hz, ^4J = 1.5 Hz), 7.35 (td, 1H, ^3J = 7.8 Hz, ^4J = 1.3 Hz), 7.19 (dd, 1H, ^3J = 8.0 Hz, ^4J = 1.2 Hz), 6.88 (d, 1H, ^4J = 2.7 Hz), 6.44 (d, 1H, ^4J = 2.6 Hz), 4.35 (sextet, 1H, J = 7.1 Hz), 3.55 (sextet, 1H, J = 7.1 Hz), 3.41 (sextet, 1H, J = 7.1 Hz), 3.32 (q, 4H, J = 7.1 Hz), 3.25 (sextet, 1H, J = 7.1 Hz), 3.13 (sextet, 1H, J = 7.3 Hz), 2.97 (sextet, 1H, J = 7.3 Hz), 1.25 (t, 3H, ^3J = 7.2 Hz), 1.19 (t, 3H, ^3J = 7.2 Hz), 1.11 (t, 6H, ^3J = 7.0 Hz), 0.91 (t, 3H, ^3J = 7.0 Hz).
MS (CH_3CN): m/z: 442.4 ($[M + H]^+$ calc. 442.2)

9.1.14 Synthesis of 19

0.99 g **18** (2.24 mmol), 1.8 g Fe powder, 5 ml 25 % HCl, 10 ml H_2O and 45 ml EtOH was refluxed under N_2 overnight. Excess Fe was filtered off and EtOH was removed by evaporation. The solution was mixed with 100 ml CH_2Cl_2 and 70 g $Na_2H_2EDTA{\cdot}2H_2O$ in 200 ml H_2O. Solid KOH was added to a pH value of 7. 10 ml 30 % H_2O_2 was added dropwise and the pH was adjusted to 8.5 with solid KOH. After stirring for 30 min the phases were separated and the aqueous phase was extracted with CH_2Cl_2 (4 x 75 ml). The combined organic phases were dried over Na_2SO_4, filtered and evaporated to dryness. The crude product was purified on column (silica gel, CH_2Cl_2/CH_3OH = 100/0 → 97/3). Yield: 407 mg (46 %).

^{1}H NMR ($CDCl_3$): δ 7.82 (dd, 1H, ^3J = 7.0 Hz, ^4J = 2.2 Hz), 7.50 (d, 1H, ^4J = 2.7 Hz), 7.44 (dd, 1H, ^3J = 7.0 Hz, ^4J = 2.0 Hz), 7.31 (td, 1H, ^3J = 7.3 Hz, ^4J = 1.6 Hz), 7.28 (td, 1H, ^3J = 7.2 Hz, ^4J = 1.6 Hz), 6.73 (d, 1H, ^4J = 2.7 Hz), 4.74 (q, 2H, ^3J = 7.1 Hz), 3.58 (q, 2H, ^3J = 7.1 Hz), 3.48 (q, 4H, ^3J = 7.1 Hz), 3.39 (q, 2H, ^3J = 7.1 Hz), 1.44 (t, 3H, ^3J = 7.1 Hz), 1.27 (t, 3H, ^3J = 7.1 Hz), 1.22 (t, 6H, ^3J = 7.1 Hz), 1.08 (t, 3H, ^3J = 7.1 Hz).

MS (CH_3CN): m/z: 394.3 ($[M + H]^+$ calc. 394.3)

9.1.15 Synthesis of 20 from 19

A mixture of **19** (248 mg; 0.63 mmol), 20 g KOH, 20 ml EtOH and 30 ml H_2O was refluxed for 2 days. The EtOH was evaporated and the solution was extracted with CH_2Cl_2 (2 x 50 ml). The pH value was adjusted to 2 with 25 % HCl and a white precipitate formed. This was filtered of, washed with aqueous HCl (pH = 2) and dried in vacuum. Yield: 150 mg (70 %).

9.1.16 Synthesis of 20 from 28

28 (1.59 g; 5.27 mmol), 30 ml $HNEt_2$ and 5 ml H_2O were heated in an autoclave at 145 ° C and p = 9 bar for 24 h. After cooling the reaction mixture was evaporated to dryness, mixed with 100 ml H_2O and 10 g NaOH and refluxed for 6 h. After extraction with 2 x 50 ml CH_2Cl_2 the solution was acidified to pH = 1.5 with 25 % HCl and extracted with 12 x 50 ml CH_2Cl_2. The extracts were dried over Na_2SO_4, filtered and evaporated. Yield: 611 mg (34 %).

^{1}H NMR ($CDCl_3$): δ 8.12 (d, 1H, ^3J = 7.3 Hz), 8.00 (s, 1H), 7.61 (d, 1H, ^3J = 7.9 Hz), 7.53 (t, 1H, ^3J = 7.5 Hz), 7.52 (t, 1H, ^3J = 7.4 Hz), 7.47 (s, 1H), 4.90 (q, 2H, ^3J = 7.0 Hz), 3.62 (q, 4H, ^3J = 7.0 Hz), 1.62 (t, 3H, ^3J = 6.9 Hz), 1.28 (t, 3H, ^3J = 7.0 Hz).
MS (CH_3CN): m/z: 339.3 ($[M + H]^+$ calc. 339.2)

9.1.17 Synthesis of 21

A solution of **13** (16 g; 0.79 mol) and 4 ml concentrated H_2SO_4 in 125 ml H_2O and 125 ml MeOH was refluxed for 30 min and then left stirring overnight. The solution was slowly added to 800 ml half saturated aqueous $NaHCO_3$ solution. The solution was extracted with CH_2Cl_2 (2 x 500 ml) and then acidified to pH = 1.5 with 25 % HCl. The resulting solution was then extracted with CH_2Cl_2 (7 x 300 ml). The extracts were dried over Na_2SO_4, filtrated and evaporated to yield 4.74 g (28 %) of **13**.

^{1}H NMR (CD_3OD): δ 8.34 (d, 1H, ^4J = 1.8 Hz), 8.32 (d, 1H, ^4J = 1.8 Hz), 4.01 (s, 3H).

9.1.18 Synthesis of 22 and 23

A solution of **21** (1.04 g; 4.81 mmol), 15 ml $SOCl_2$ and 0.1 ml DMF in 40 ml dry CH_2Cl_2 was refluxed under N_2 for 60 min. The solvent was evaporated and the residue dried in vacuum for 75 min and re-dissolved in 50 ml dry CH_2Cl_2. Distilled $HNEt_2$ (10 ml) was added dropwise and the solution was refluxed for 90 min. After cooling, 300 ml half saturated aqueous NH_4Cl solution was added. The phases were separated and the aqueous phase was extracted with CH_2Cl_2 (2 x 75 ml). The combined organic phases were washed with 2 x 75 ml saturated aqueous $NaHCO_3$ solution and evaporated. The residue of **22** was dissolved in 5 ml EtOH, mixed with 50 ml 1 M KOH and stirred for 15 min at rt. The solution was extracted with 2 x 35 ml CH_2Cl_2 and the pH value subsequently adjusted to 2 with 25 % HCl. The white

precipitate was filtered off, washed 3 times with cold aqueous HCl (pH = 2) and dried in dessicator. Yield of **23**: 987 mg (80 %).

^{1}H NMR (CD_3OD): δ 8.21 (d, 1H, ^4J = 2.0 Hz), 7.86(d, 1H, ^4J = 1.9 Hz), 3.57 (q, 2H, ^3J = 7.1 Hz), 3.36 (q, 2H, ^3J = 7.1 Hz), 1.28 (t, 3H, ^3J = 7.1 Hz), 1.22 (t, 3H, ^3J = 7.0 Hz).
^{1}H NMR ($CDCl_3$): δ 8.26 (d, 1H, ^4J = 2.0 Hz), 7.84 (d, 1H, ^4J = 2.0 Hz), 3.60 (q, 2H, ^3J = 7.2 Hz), 3.32 (q, 2H, ^3J = 7.1 Hz), 1.30 (t, 3H, ^3J = 7.2 Hz), 1.23 (t, 3H, ^3J = 7.1 Hz).

9.1.19 Synthesis of 24

A solution of **23** (3.52 g; 13.7 mmol), 30 ml $SOCl_2$ and 0.05 ml DMF in 100 ml dry CH_2Cl_2 was refluxed under N_2 for 45 min. The solvent was evaporated and after drying in vacuum for 1 h the residue was re-dissolved in 50 ml dry CH_2Cl_2. A solution of **2** (3.25 g; 19.5 mmol) and 10 ml distilled NEt_3 in 50 ml dry CH_2Cl_2 was added dropwise and the solution was refluxed for 2 h. After evaporation of the solvent, the residue was partitioned between 150 ml half saturated aqueous NH_4Cl solution and 150 ml CH_2Cl_2. The aqueous phase was extracted with CH_2Cl_2 (3 x 100 ml) and the combined organic phases were dried over Na_2SO_4, filtrated and evaporated to dryness. The crude product was purified by column chromatography (silica gel, CH_2Cl_2/CH_3OH = 100/0 $\rightarrow$ 97/3) to yield 4.44 g (80 %) of **24**.

^{1}H NMR ($CDCl_3$): δ 7.98 (dd, 1H, ^3J = 8.2 Hz, ^4J = 1.5 Hz), 7.86 (d, 1H, ^4J = 2.0 Hz), 7.48 (td, 1H, ^3J = 7.6 Hz, ^4J = 1.6 Hz), 7.40 (td, 1H, ^3J = 7.8 Hz, ^4J = 1.5 Hz), 7.32 (d, 1H, ^4J = 1.9 Hz), 7.14 (dd, 1H, ^3J = 7.8 Hz, ^4J = 1.3 Hz), 4.34 (sextet, 1H, , J = 7.1 Hz), 3.60 (sextet, 1H, , J = 7.2 Hz), 3.54 (sextet, 1H, , J = 7.1 Hz), 3.30 (sextet, 1H, , J = 7.0 Hz), 3.09 (sextet, 1H, , J = 7.3 Hz), 2.95 (sextet, 1H, , J = 7.2 Hz), 1.25 (t, 3H, ^3J = 7.2 Hz), 1.19 (t, 3H, ^3J = 7.1 Hz), 0.92 (t, 3H, ^3J = 7.2 Hz).
MS (CH_3CN): m/z: 405.4 ($[M + H]^+$ calc. 405.2)

9.1.20 Synthesis of 25

A mixture of **24** (4.43 g; 10.9 mmol), 10 g Fe powder, 100 ml EtOH, 25 ml 25 % HCl and 25 ml H_2O was refluxed under N_2 for 15 h. Excess Fe was filtered off, EtOH was evaporated and the solution was mixed with 100 ml CH_2Cl_2 and 50 g $Na_2H_2EDTA{\cdot}2H_2O$ in 150 ml H_2O. The pH value was adjusted to 9 with solid KOH and 10 ml 30 % H_2O_2 was added dropwise. After

stirring for 30 min the phases were separated and the aqueous phase was extracted with 3 x 100 ml CH_2Cl_2. The combined organic phases were dried over Na_2SO_4, filtrated and evaporated. The crude product was purified on column (silica gel, CH_2Cl_2/CH_3OH = 100/0 → 97/3). Yield: 2.99 g (77 %).

^{1}H NMR ($CDCl_3$): δ 8.46 (d, 1H, ^4J = 1.8 Hz), 7.84 (dd, 1H, ^3J = 7.0 Hz, ^4J = 1.2 Hz), 7.54 (d, 1H, ^4J = 1.8 Hz), 7.46 (dd, 1H, ^3J = 7.4 Hz, ^4J = 1.3 Hz), 7.37 (td, 1H, ^3J = 7.2 Hz, ^4J = 1.5 Hz), 7.33 (td, 1H, ^3J = 7.0 Hz, ^4J = 1.3 Hz), 4.76 (q, 2H, ^3J = 7.1 Hz), 3.61 (q, 2H, ^3J = 7.1 Hz), 3.36 (q, 2H, ^3J = 7.1 Hz), 1.46 (t, 3H, ^3J = 7.1 Hz), 1.28 (t, 3H, ^3J = 7.2 Hz), 1.10 (t, 3H, ^3J = 7.2 Hz).
MS (CH_3CN): m/z: 357.3 ($[M + H]^+$ calc. 357.1)

9.1.21 Synthesis of 26

A mixture of **25** (2.33 g; 6.53 mmol), 120 g KOH, 50 ml EtOH and 200 ml H_2O was refluxed for 10 days. After evaporation of EtOH, 400 ml H_2O was added and the solution was extracted with 3 x 100 ml CH_2Cl_2. The solution was acidified to pH = 1 with 25 % HCl and a white precipitate formed. This was filtered off, washed with cold aqueous HCl (pH = 1) and dried. Yield: 1.68 g (91 %).

^{1}H NMR (DMSO-d_6): δ 7.84 (d, 1H, ^4J = 2.1 Hz), 7.78 (m, 2H), 7.56 (d, 1H, ^4J = 1.9 Hz), 7.41 (m, 2H), 4.88 (q, 2H, ^3J = 7.1 Hz), 1.43 (t, 3H, ^3J = 7.0 Hz).
^{1}H NMR (CD_3OD): δ 8.06 (m, 1H), 7.90 (m, 1H), 7.82 (d, 1H, ^4J = 2.0 Hz), 7.76 (d, 1H, ^4J = 2.2 Hz), 7.74 (m, 2H), 4.97 (q, 2H, ^3J = 7.5 Hz), 1.67 (t, 3H, ^3J = 7.2 Hz).
MS (CH_3CN): m/z: 284.3 ($[M + H]^+$ calc. 284.1)

9.1.22 Synthesis of 27 and 28

A mixture of **26** (1.68 g; 5.93 mmol) and *P*,*P*-dichlorophenylphosphine oxide (15 ml) was heated under N_2 atmosphere at 130 ° C for 2 h. After cooling to rt 75 ml H_2O was added slowly and pH was adjusted to 8 with concentrated aqueous NaOH solution. After stirring for 15 min, 25 % HCl was added to pH = 3.5. The mixture was cooled down to 5 ° C and the precipitate was filtered off, washed with cold HCl (pH = 4) and dried in air. Yield: 1.53 g (86 %).

^{1}H NMR (DMSO-d_6): δ 8.52 (d, 1H, ^4J = 2.0 Hz), 8.13 (d, 1H, ^4J = 1.9 Hz), 7.75 (d, 1H, ^3J = 8.0 Hz), 7.70 (d, 1H, ^3J = 8.1 Hz), 7.36 (td, 1H, ^3J = 7.6 Hz, ^4J = 1.2 Hz), 7.29 (td, 1H, ^3J = 7.6 Hz, ^4J = 1.2 Hz), 4.89 (q, 2H, ^3J = 7.1 Hz), 1.41 (t, 3H, ^3J = 7.0 Hz).
^{1}H NMR (CD_3OD): δ 8.50 (d, 1H, ^4J = 1.8 Hz), 8.28 (d, 1H, ^4J = 1.8 Hz), 7.75 (m, 2H), 7.50 (t, 1H, ^3J = 7.4 Hz), 7.45 (t, 1H, ^3J = 7.8 Hz), 4.96 (q, 2H, ^3J = 7.2 Hz), 1.57 (t, 3H, ^3J = 7.0 Hz).
^{1}H NMR (CD_3CN): δ 8.58 (d, 1H, ^4J = 1.6 Hz), 8.24 (d, 1H, ^4J = 1.8 Hz), 7.83 (d, 1H, ^3J = 7.8 Hz), 7.71 (d, 1H, ^3J = 8.0 Hz), 7.48 (t, 1H, ^3J = 7.7 Hz), 7.42 (t, 1H, ^3J = 7.5 Hz), 4.87 (q, 2H, ^3J = 7.1 Hz), 1.51 (t, 3H, ^3J = 7.2 Hz).
MS (CH_3CN): **28**: m/z: 302.4 ($[M + H]^+$ calc. 302.1)
Elemental analysis (**28**): Calculated (found) for $C_{15}H_{12}ClN_3O_2 \cdot 1.5H_2O$: C 54.80 (55.13); H 4.60 (4.12); N 12.78 (12.64).

9.1.23 Synthesis of 29

A solution of **21** (1.50 g; 6.96 mmol), 20 ml $SOCl_2$ and 0.1 ml DMF in 75 ml freshly distilled CH_2Cl_2 was refluxed under N_2 for 75 min. After evaporation of the solvent, the residue was dried in vacuum for 25 min and then re-dissolved in 75 ml dry CH_2Cl_2. To this solution was added a solution of **2** (1.16 g; 6.96 mmol) and 8 ml NEt_3 in 75 ml dry CH_2Cl_2 before refluxing for 60 min. The solvent was evaporated and the residue partitioned between 100 ml CH_2Cl_2 and 100 ml half saturated aqueous NH_4Cl. The aqueous phase was extracted with CH_2Cl_2 (2 x 100 ml) and the combined organic extracts were dried over Na_2SO_4, filtrated and evaporated to dryness. The product was purified on column (silica gel, CH_2Cl_2/CH_3OH = 100/0 $\rightarrow$ 98/2). Yield: 2.18 g (86 %).

^{1}H NMR ($CDCl_3$): δ 8.10 (d, 1H, ^4J = 1.8 Hz), 8.04 (dd, 1H, ^3J = 8.2 Hz, ^4J = 1.5 Hz), 7.91 (d, 1H, ^4J = 1.9 Hz), 7.57 (td, 1H, ^3J = 7.7 Hz, ^4J = 1.5 Hz), 7.41 (td, 1H, ^3J = 7.9 Hz, ^4J = 1.5 Hz), 7.35 (dd, 1H, ^3J = 7.8 Hz, ^4J = 1.4 Hz), 4.23 (sextet, J = 7.1 Hz), 3.80 (s, 3H), 3.72 (sextet, J = 7.1 Hz), 1.25 (t, 3H, ^3J = 7.2 Hz).
MS (CH_3CN): m/z: 364.3 ($[M + H]^+$ calc. 364.1)

9.1.24 Synthesis of 30

A mixture of **29** (1.84 g; 5.02 mmol), 6 g Fe powder, 150 ml EtOH, 40 ml H_2O and 30 ml 25 % HCl was refluxed overnight under N_2. Excess Fe was filtered off and EtOH was evaporated on rotavapor. The solution was added to a mixture of 100 ml CH_2Cl_2 and 40 g Na_2H_2EDTA in 150 H_2O and pH was adjusted to 7 with 5 M KOH. After addition of 3 ml 30 % H_2O_2, 5 M KOH was added to pH = 9 and the mixture was stirred for 40 min. After filtration, the phases were separated and the aqueous phase was extracted with CH_2Cl_2 (6 x 100 ml). The combined organic extracts were washed with 150 ml H_2O, dried over Na_2SO_4, filtrated and evaporated to dryness. The crude product was purified on column (silica gel, CH_2Cl_2/CH_3OH = 100/0 → 98/2) to yield 429 g (26 %).

^{1}H NMR ($CDCl_3$): δ 8.68 (d, 1H, ^4J = 1.7 Hz), 8.12 (d, 1H, ^4J = 1.7 Hz), 7.84 (d, 1H, ^3J = 7.9 Hz), 7.49 (d, 1H, ^3J = 7.8 Hz), 7.38 (t, 1H, ^3J = 7.0 Hz), 7.33 (t, 1H, ^3J = 7.2 Hz), 4.92 (q, 2H, ^3J = 7.1 Hz), 4.48 (q, 2H, ^3J = 7.1 Hz), 1.58 (t, 3H, ^3J = 7.1 Hz), 1.46 (t, 3H, ^3J = 7.1 Hz).
MS (CH_3CN): m/z: 330.3 ($[M + H]^+$ calc. 330.1)

9.1.25 Synthesis of 28 from 30

A solution of **30** (429 mg; 1.30 mmol) in 30 ml 1 M KOH was refluxed overnight. After cooling down, the solution was extracted with 2 x 50 ml CH_2Cl_2 and pH was adjusted to 1 with 25 % HCl. A white precipitate formed and was filtered off, washed with aqueous HCl (pH = 2) and dried in vacuum. Yield: 257 mg (66 %).

9.1.26 Synthesis of 31

A solution of **7** (1.32 g; 5.96 mmol), 20 ml $SOCl_2$ and 0.1 ml DMF in 100 ml dry CH_2Cl_2 was refluxed under N_2 for 50 min. After evaporation of the solvent and drying in vacuum for 45 min, the residue was re-dissolved in 75 ml dry CH_2Cl_2. A solution of **3** (2.05 g; 5.96 mmol) and 8 ml distilled NEt_3 in 75 ml dry CH_2Cl_2 was added dropwise and the resulting solution was refluxed for 65 min. The solvent was evaporated and the residue partitioned between 200 ml half saturated aqueous NH_4Cl solution and 200 ml CH_2Cl_2. The aqueous phase was extracted with CH_2Cl_2 (2 x 200 ml) and the combined organic phases were dried over

Na_2SO_4, filtrated and evaporated to dryness. The crude product was purified by column chromatography (silica gel, CH_2Cl_2/CH_3OH = 100/0 → 98/2) to yield 1.82 g (56 %) of **31**.

MS (CH_3CN): m/z: 549.4 ($[M + H]^+$ calc. 549.3)

9.1.27 Synthesis of 32

A mixture of **10** (293 mg; 1.10 mmol), 3.2 ml $SOCl_2$, 0.1 ml DMF and 30 ml freshly distilled CH_2Cl_2 was refluxed under N_2 for 90 min. The solvent was evaporated and the residue dried in vacuum for 2 h. After redissolving of the residue in 30 ml dry CH_2Cl_2, a solution of **31** (603 mg; 1.10 mmol) and 1.1 g NEt_3 in 30 ml CH_2Cl_2 was added dropwise. The reaction mixture was refluxed for 90 min and evaporated. The residue was partitioned between 50 ml half saturated aqueous NH_4Cl solution and 50 ml CH_2Cl_2. The phases were separated and the aqueous phase was extracted with CH_2Cl_2 (4 x 50 ml). The combined organic extracts were dried over Na_2SO_4, filtrated and evaporated to dryness. The crude product was purified by column chromatography (silica gel, CH_2Cl_2/CH_3OH = 100/0 → 97/3) to yield 746 mg (85 %) of **32**.

MS (CH_3CN): m/z: 797.9 ($[M + H]^+$ calc. 798.3)

9.1.28 Synthesis of L^{AB}

A mixture of **32** (270 mg; 0.34 mmol), Fe powder (420 mg), 5 ml EtOH, 15 ml H_2O and 2.5 ml 25 % HCl was refluxed overnight under N_2. Unreacted Fe was removed by filtration and EtOH was evaporated. The solution was added to a mixture of 40 ml CH_2Cl_2, 15 g H_4EDTA and 90 ml H_2O and the pH was adjusted to 7 with 5 M KOH. After slow addition of 2 ml 30 % H_2O_2, 5 M KOH was added to pH = 9 and the solution was stirred for 30 min. The phases were separated and the aqueous phase was extracted with CH_2Cl_2 (4 x 40 ml). The combined organic extracts were dried over Na_2SO_4, filtered and evaporated to dryness. The crude product was purified by column chromatography (silica gel, CH_2Cl_2/CH_3OH = 100/0 → 96/4) to yield 146 mg (62 %) of L^{AB}.[80]

9.1.29 Synthesis of 33

A solution of **17** (549 mg; 1.87 mmol), $SOCl_2$ (5 ml, 69 mmol) and DMF (0.1 ml) in 50 ml dry CH_2Cl_2 was refluxed under N_2 for 60 min. After removal of solvent on rotavapor and removal of excess $SOCl_2$ in vacuum, the residue was dried in vacuum for 90 min and suspended in 30 ml dry CH_2Cl_2. A solution of **3** (645 mg; 1.87 mmol) and NEt_3 (3 ml, 22 mmol) in 30 ml dry CH_2Cl_2 was added slowly, and the reaction mixture was refluxed for 90 min. After evaporation to dryness, the residue was partitioned between 30 ml CH_2Cl_2 and 30 ml half-saturated NH_4Cl solution. The aqueous phase was then extracted with CH_2Cl_2 (2 x 30 ml) and the combined organic phases were dried over Na_2SO_4, filtrated and evaporated to dryness. The crude product was purified on column (silica gel, CH_2Cl_2/CH_3OH = 100/0 → 97/3). Yield: 465 mg (40 %).

^{1}H NMR ($CDCl_3$): δ 8.00 (d, 1H, ^4J = 1.9 Hz), 7.95 (s, 1H), 7.71 (d, 1H, ^4J = 1.7 Hz), 7.23 (m, 2H), 7.07 (d, 1H, ^3J = 8.0 Hz), 6.97 (d, 1H, ^4J = 2.4 Hz), 6.87 (d, 1H, ^3J = 8.9 Hz), 6.44 (d, 1H, ^4J = 2.5 Hz), 4.33 (sextet, 1H, ^3J = 7.1 Hz), 3.90 (s, 2H), 3.35-3.60 (m, 4H), 3.31 (q, 4H, ^3J = 7.3 Hz), 3.24 (sextet, 1H, ^3J = 6.9 Hz), 3.16 (sextet, 1H, ^3J = 7.2 Hz), 2.99 (sextet, 1H, ^3J = 7.2 Hz), 1.35 (t, 3H, ^3J = 7.2 Hz), 1.23 (t, 3H, ^3J = 7.2 Hz), 1.15 (t, 3H, ^3J = 7.2 Hz), 1.10 (t, 6H, ^3J = 7.1 Hz), 0.90 (t, 3H, ^3J = 7.1 Hz).
MS (CH_3OH) m/z: 620.4 ($[M + H]^+$, Calc. 620.4).

9.1.30 Synthesis of 34

A solution of **10** (267 mg; 1.00 mmol), $SOCl_2$ (3 ml, 41 mmol) and DMF (0.1 ml) in 50 ml dry CH_2Cl_2 was refluxed under N_2 for 60 min. After removal of solvent on rotavapor and removal of excess $SOCl_2$ in vacuum, the residue was dried in vacuum for 40 min and suspended in 30 ml dry CH_2Cl_2. A solution of **33** (553 mg; 0.89 mmol) and NEt_3 (2 ml, 14 mmol) in 30 ml dry CH_2Cl_2 was added slowly, and the reaction mixture was refluxed for 90 min. After evaporation to dryness, the residue was partitioned between 25 ml CH_2Cl_2 and 25 ml half-saturated NH_4Cl solution. The aqueous phase was then extracted with CH_2Cl_2 (2 x 25 ml) and the combined organic phases were dried over Na_2SO_4, filtrated and evaporated to dryness. The crude product was purified on column (silica gel, CH_2Cl_2/CH_3OH = 100/0 → 97/3). Yield: 424 mg (49 %).

MS (CH_3OH) m/z: 868.8 ($[M + H]^+$ calc. 869.0), 435.2 ($[M + 2H]^{2+}$ calc. 435.0)

9.1.31 Synthesis of L^{AB2}

A mixture of **34** (403 mg; 0.46 mmol), Fe powder (0.80 g; 14 mmol), EtOH (30 ml), H_2O (10 ml) and 25 % HCl (5 ml) was refluxed under N_2 for 18 h. After removal of EtOH on rotavapor, the solution was mixed with 60 ml CH_2Cl_2 and a solution of H_4-EDTA (35 g; 120 mmol) and NaOH (16 g; 0.4 mol) in 150 ml H_2O was added. The solution was neutralised with 5 M KOH and 4 ml 30 % H_2O_2 was added after which the pH was adjusted to 8.5 with 5 M KOH. After stirring for 30 min, the organic phase was separated and the aqueous phase was extracted with CH_2Cl_2 (3 x 50 ml). The combined organic phases were dried over Na_2SO_4, filtrated and evaporated to dryness. The crude product was purified on column (silica gel, CH_2Cl_2/CH_3OH = 100/0 → 95/5). The product was washed with pentane and dried in vacuum. Yield: 240 mg (67 %).

MS (CH_3OH) m/z: 773.3 ($[M + H]^+$ calc. 773.4)
Elemental analysis: Calculated (found) for $C_{47}H_{52}N_{10}O{\cdot}0.5H_2O$: C 72.19 (72.02); H 6.83 (6.72); N 17.91 (17.90).

9.1.32 Synthesis of 35

A solution of **23** (1.40 g; 5.45 mmol), 10 ml $SOCl_2$ and 0.1 ml DMF in 40 ml dry CH_2Cl_2 was refluxed under nitrogen for 60 min. After evaporation the residue was dried in vacuum at 40 º C for 75 min and then re-dissolved in 30 ml dry CH_2Cl_2. A solution of **3** (1.87 g; 5.43 mmol) and 5 ml NEt_3 in 30 ml dry CH_2Cl_2 was added. The solution was then stirred at room temperature for 40 min and refluxed for 70 min under nitrogen. After evaporation of the solvent the residue was partitioned between 50 ml half-saturated aqueous NH_4Cl and 50 ml CH_2Cl_2. The aqueous phase was extracted twice with 50 ml CH_2Cl_2 and the combined organic phases were dried over Na_2SO_4, filtrated and evaporated to dryness. The resulting residue was purified on column (silica; CH_2Cl_2/CH_3OH= 100/0 → 98/2) to yield 2.089 g of **35** (66 %).

MS: *m/z* = (583.3 $[M + H]^+$ calc. 583.2)
^{1}H NMR ($CDCl_3$): δ 8.02 (d, 1H, ^4J = 2.1 Hz), 7.97 (s br, 1H), 7.83 (d, 1H, ^4J = 1.8 Hz), 7.76 (d, 1H, ^4J = 2.0 Hz), 7.35 (d, 1H, ^4J = 2.0 Hz), 7.25 (dd, 1H, ^3J = 8.4 Hz, ^4J = 2.0 Hz), 7.22 (dd, 1H, ^3J = 9.2 Hz, ^4J = 2.1 Hz), 7.03 (d, 1H, ^3J = 8.1 Hz), 6.89 (d, 1H, ^3J = 8.8 Hz), 4.34

(sextet, 1H, ^3J = 7.1 Hz), 3.92 (s, 2H), 3.56 (sextet, 1H, ^3J = 7.1 Hz), 3.55 (sextet, 1H, ^3J = 7.1 Hz), 3.37 (sextet, 1H, ^3J = 7.1 Hz), 3.35 (sextet, 1H, ^3J = 7.1 Hz), 3.29 (sextet, 1H, ^3J = 6.9 Hz), 3.14 (sextet, 1H, ^3J = 7.3 Hz), 2.98 (sextet, 1H, ^3J = 7.3 Hz), 1.38 (t, 3H, ^3J = 7.2 Hz), 1.25 (t, 3H, ^3J = 7.3 Hz), 1.17 (t, 3H, ^3J = 7.2 Hz), 0.93 (t, 3H, ^3J = 7.1 Hz).

9.1.33 Synthesis of 36

A solution of **10** (1.036 g; 3.87 mmol), 10 ml $SOCl_2$ and 0.1 ml DMF in 40 ml dry CH_2Cl_2 was refluxed under nitrogen for 55 min. After evaporation the residue was dried in vacuum at 40 ° C for 80 min and then suspended in 25 ml dry CH_2Cl_2. A solution of **35** (2.26 g; 3.87 mmol) and 5 ml NEt_3 in 30 ml dry CH_2Cl_2 was added dropwise. The solution was then refluxed for 2 h under nitrogen. After evaporation the residue was partitioned between 50 ml half-saturated aqueous NH_4Cl and 50 ml CH_2Cl_2. The aqueous phase was extracted twice with 35 ml CH_2Cl_2 and the combined organic phases were dried over Na_2SO_4, filtrated and evaporated to dryness. The resulting residue was purified on column (silica; CH_2Cl_2/CH_3OH= 100/0 → 98/2) to yield 1.508 g of **36** (47 %).

MS: *m/z* = 832.3 ($[M + H]^+$ calc. 832.3)

9.1.34 Synthesis of L^{AB3}

A mixture of **36** (1.453 g; 1.75 mmol), Fe powder (3.00 g; 53.7 mmol), 20 ml 25 % HCl, 20 ml water and 90 ml ethanol was refluxed under nitrogen overnight. After removal of ethanol on rotavapor the reaction mixture was poured into a solution of 70 g H_4-EDTA and 30 g NaOH in 200 ml water. To this was added 20 ml 30 % H_2O_2, the pH was adjusted to 8.5 with 5 M KOH, 75 ml CH_2Cl_2 was added and the mixture was stirred for 30 min. The two phases were separated and the red aqueous phase was extracted three times with 75 ml CH_2Cl_2. The combined organic phases were dried over Na_2SO_4, filtrated and evaporated to dryness. The crude product was purified on column (silica; CH_2Cl_2/CH_3OH= 100/0 → 96/4) to yield 945 mg of L^{AB3} (73 %).

MS: *m/z* = 736.4 ($[M + H]^+$ calc. 736.3)
Elemental analysis: calculated (found) for $C_{43}H_{42}ClN_9O \cdot 0.5H_2O$: C 69.29 (69.17); H 5.82 (5.80); N 16.91 (16.84)

9.1.35 Synthesis of 37

A solution of **20** (150 mg; 0.443 mmol), 5 ml $SOCl_2$ and 0.05 ml DMF in 50 ml dry CH_2Cl_2 was refluxed under N_2 for 1 h. The solvent was evaporated and the residue was dried in vacuum for 30 min and re-dissolved in 20 ml dry CH_2Cl_2. A solution of **31** (550 mg; 1.00 mmol) and 1 ml NEt_3 in 30 ml dry CH_2Cl_2 was added dropwise and the reaction mixture was refluxed for 30 min and then left stirring overnight at rt. After evaporation of the solvent the residue was partitioned between 100 ml CH_2Cl_2 and 100 ml half saturated aqueous NH_4Cl. The phases were separated and the aqueous phase was extracted with 3 x 30 ml CH_2Cl_2. The combined organic phases were dried over Na_2SO_4, filtrated and evaporated to dryness. The residue was purified on column (silica; CH_2Cl_2/CH_3OH= 100/0 → 97/3). Yield: 153 mg of **37** (40 %).

MS (CH_3CN): m/z: 869.3 ($[M + H]^+$ calc. 869.4); 435.2 ($[M + 2H]^{2+}$ calc. 435.2)

9.1.36 Synthesis of L^{AB4}

A mixture of **37** (147 mg; 0.169 mmol), 0.6 g Fe powder, 30 ml EtOH, 10 ml H_2O and 5 ml 25 % HCl was refluxed under N_2 for 8 h. The EtOH was evaporated after removal of excess Fe. The solution was mixed with 15 g $Na_2H_2EDTA{\cdot}2H2O$, 100 ml H_2O and 75 ml CH_2Cl_2 and pH was adjusted to 7 with solid KOH. Following addition of 4 ml 30 % H_2O_2, solid KOH was added to pH = 8.5 and the mixture was stirred for 2 h. The phases were separated and the aqueous phase was extracted with 3 x 40 ml CH_2Cl_2. The organic extracts were dried over Na_2SO_4, filtered and evaporated to dryness. The crude product was purified on column (silica; CH_2Cl_2/CH_3OH= 100/0 → 96/4). Yield: 58 mg of L^{AB5} (44 %).

MS (CH_3CN): m/z: 387.4 ($[M + 2H]^{2+}$ calc. 387.2); 773.3 ($[M + H]^+$ calc. 773.4)
Elemental analysis: calculated (found) for $C_{47}H_{52}N_{10}O{\cdot}H_2O$: C 73.03 (73.16); H 6.78 (6.72); N 18.12 (18.24)

9.1.37 Synthesis of 38

A solution of **28** (291 mg; 0.964 mmol), 5 ml distilled $SOCl_2$ and 0.05 ml DMF in 50 dry CH_2Cl_2 was refluxed for 80 min. The solvent was evaporated and the residue was dried in

vacuum for 60 min and dissolved in 20 ml dry CH_2Cl_2. To this solution was added a solution of **31** (1.00 g; 1.82 mmol) and 1.5 ml distilled NEt_3 in 30 ml dry CH_2Cl_2. The reaction mixture was refluxed for 2 h and evaporated to dryness. The residue was partitioned between 75 ml CH_2Cl_2 and 75 ml half saturated aqueous NH_4Cl solution. After separation of the phases, the aqueous phase was extracted with CH_2Cl_2 (3 x 75 ml) and the combined organic phases were dried over Na_2SO_4, filtrated and evaporated to dryness. The residue was purified on column (silica; CH_2Cl_2/CH_3OH= 100/0 → 97/3) to yield 357 mg of **38** (44 %).

MS: *m/z* = 832.3 ($[M + H]^+$ calc. 832.3)

9.1.38 Synthesis of L^{AB5}

A mixture of **38** (350 mg; 0.421 mmol), 0.6 g Fe powder , 30 ml EtOH, 10 ml H_2O and 5 ml 25 % HCl was refluxed under N_2 for 7 h. After removal of excess Fe, EtOH was removed by evaporation. The solution was mixed with 16.7 g $Na_2H_2EDTA{\cdot}2H_2O$, 150 ml H_2O and 75 ml CH_2Cl_2 and the pH value was adjusted to 7 with solid KOH. Following addition of 4 ml 30 % H_2O_2, solid KOH was added to pH = 9 and the solution was stirred for 30 min. The phases were separated and the aqueous phase was extracted with CH_2Cl_2 (3 x 75 ml). The combined organic extracts were dried over Na_2SO_4, filtrated and evaporated to dryness. The crude product was purified on column (silica; CH_2Cl_2/CH_3OH= 100/0 → 96/4). Yield: 154 mg of L^{AB5} (50 %).

MS: *m/z* = 736.3 ($[M + H]^+$ calc. 736.3)
Elemental analysis: calculated (found) for $C_{43}H_{42}ClN_9O{\cdot}H_2O$: C 68.47 (68.80); H 5.88 (5.94); N 16.71 (16.69)

9.2 Preparation of complexes

The perchlorate salts $Ln(ClO_4)_3 \cdot xH_2O$ (Ln = La-Lu, x = 2-4) were prepared from the corresponding oxides (Rhône-Poulenc, 99.99%) in the usual way.[98] ***Caution!*** *Perchlorate salts combined with organic ligands are potentially explosive and should be handled in small quantities and with adequate precautions.*[99,100] Stock solutions of $Ln(ClO_4)_3 \cdot xH_2O$ in CH_3CN were prepared by weighting. The concentrations of the solutions were determined by complexometric titrations with $Na_2(H_2EDTA)$ in presence of urotropine using xylene orange as indicator.

9.2.1 Samples for NMR measurements

NMR samples of homobimetallic $[Ln_2(L)_3](ClO_4)_6$ complexes were prepared by reacting a weighed amount of L (3-15 mg) dissolved in CH_2Cl_2 with 2/3 equivalents of $Ln(ClO_4)_3 \cdot xH_20$ in the form of a CH_3CN solution (see above). After stirring for 1-3 h the solution was evaporated to dryness, dried in vacuum at 50 °C and redisolved in 0.6 ml CD_3CN. Samples of heterobimetallic $[LnLn'(L)_3](ClO_4)_6$ complexes were prepared in an analogous way using 1/3 equivalent $Ln(ClO_4)_3$ and 1/3 equivalent $Ln'(ClO_4)_3$ and stirring the sample overnight before evaporation.

9.2.2 Solid samples

Solid samples of homobimetallic triple helicate complexes of L^{AB3} were obtained by reacting 2/3 equivalents of $Ln(ClO_4)_3$ with L^{AB3} (5-15 mg) in acetonitrile solution. In a similar way, heterobimetallic complexes were obtained by reacting 1/3 equivalent of $Ln(ClO_4)_3$ and 1/3 equivalent of $Ln'(ClO_4)_3$ with the ligand. After evaporation to dryness and drying in vacuum the solid residues were redisolved in a 1:1 CH_3CN:CH_3CH_2CN mixture (≈ 0.5 ml) and precipitated by slow diffusion of ^tBuOMe at -18 °C.

Table 163 Elemental analysis of $[LnLn'(L^{AB3})_3](ClO_4)_6 \cdot nH_2O$ complexes.

Ln Ln'	n	Formula	*M* g/mol	C (calculated)	H (calculated)	N (calculated)
CeCe	9	$C_{129}Ce_2Cl_9H_{144}N_{27}O_{36}$	3133.41	47.65 (47.70)	4.27 (4.47)	11.41 (11.64)
PrPr	4	$C_{129}Cl_9H_{134}N_{27}O_{31}Pr_2$	3239.04	49.18 (49.04)	4.37 (4.27)	11.94 (11.97)
SmSm	2	$C_{129}Cl_9H_{130}N_{27}O_{29}Sm_2$	3150.54	49.87 (49.31)	4.43 (4.17)	11.53 (12.03)
PrLu	4	$C_{129}Cl_9H_{134}LuN_{27}O_{31}Pr$	3184.60	48.49 (48.52)	4.72 (4.23)	10.96 (11.84)
NdLu	0	$C_{129}Cl_9H_{126}LuN_{27}NdO_{27}$	3115.87	50.31 (49.58)	4.37 (4.06)	11.94 (12.10)

Appendix 1 One proton plots

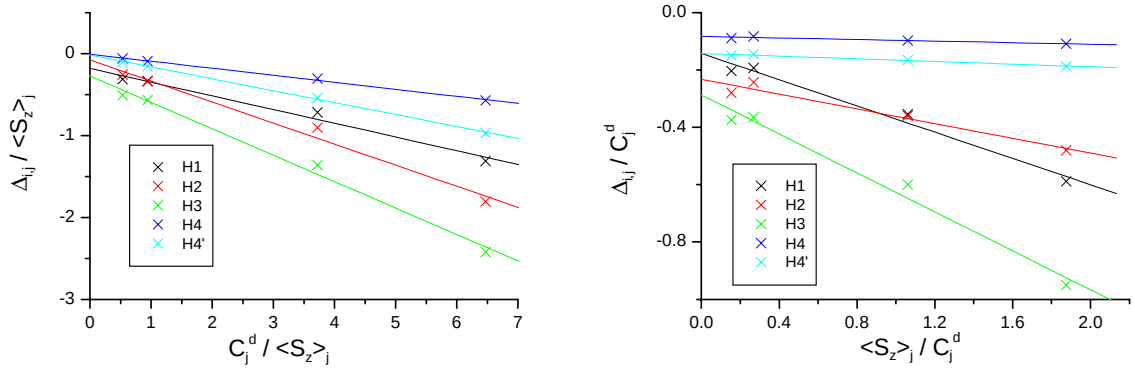

Figure 111 One proton plots of $Ln_2(L^{AB})_3$ complexes

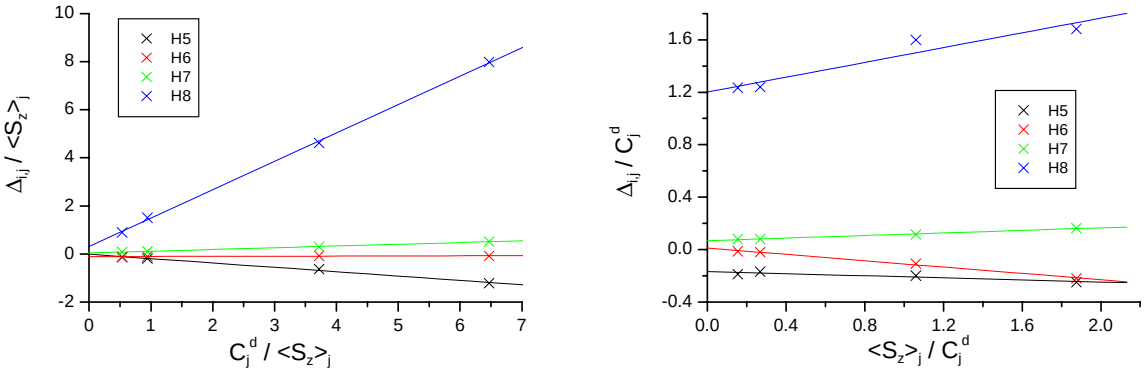

Figure 112 One proton plots of $Ln_2(L^{AB})_3$ complexes

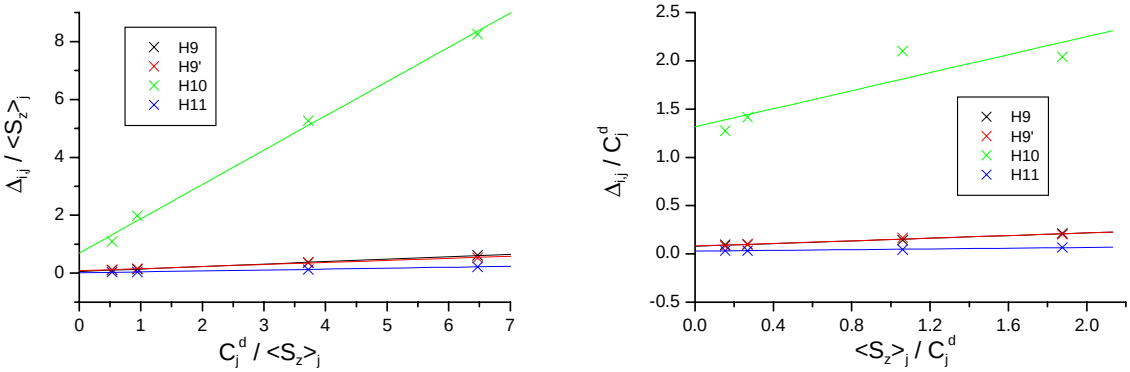

Figure 113 One proton plots of $Ln_2(L^{AB})_3$ complexes

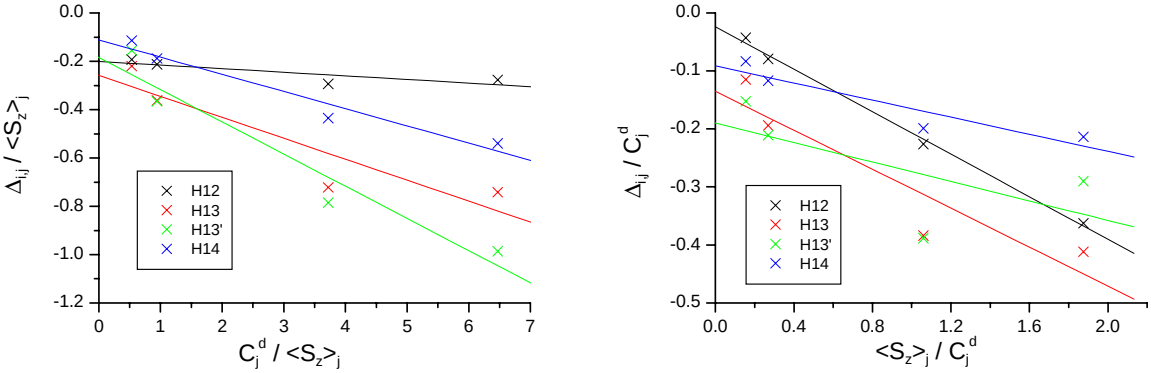

Figure 114 One proton plots of $Ln_2(L^{AB})_3$ complexes

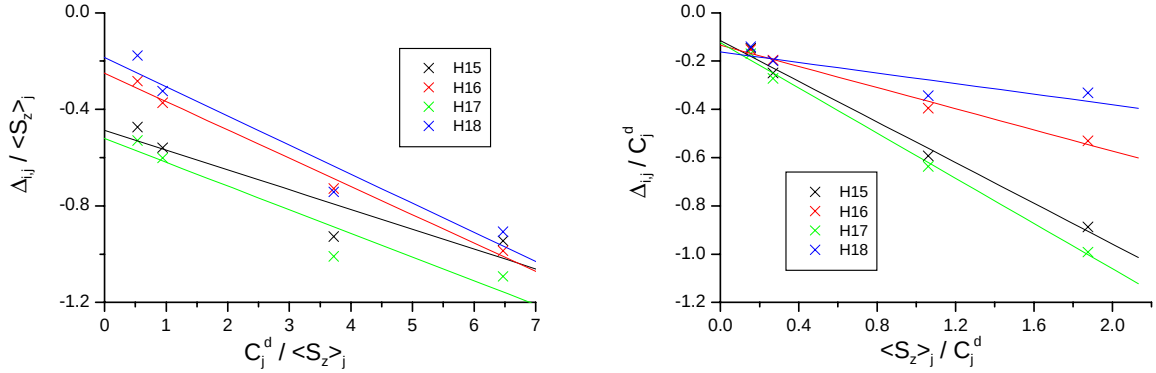

Figure 115 One proton plots of $Ln_2(L^{AB})_3$ complexes

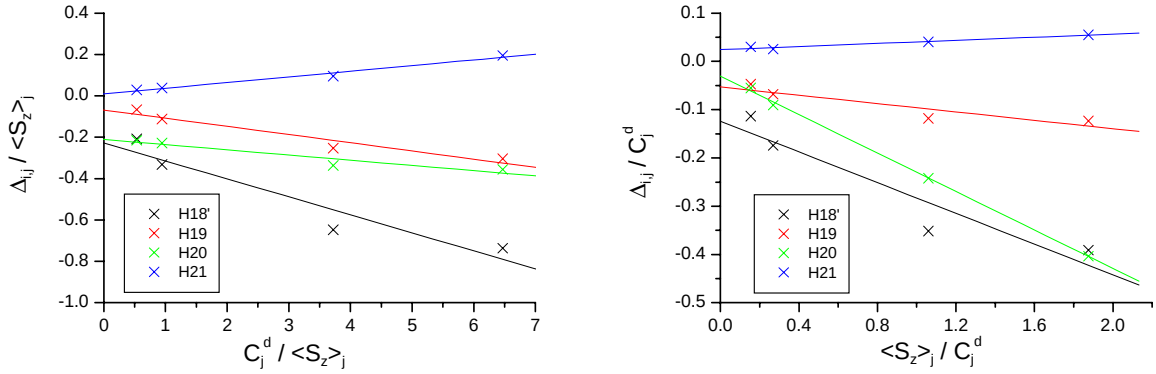

Figure 116 One proton plots of $Ln_2(L^{AB})_3$ complexes

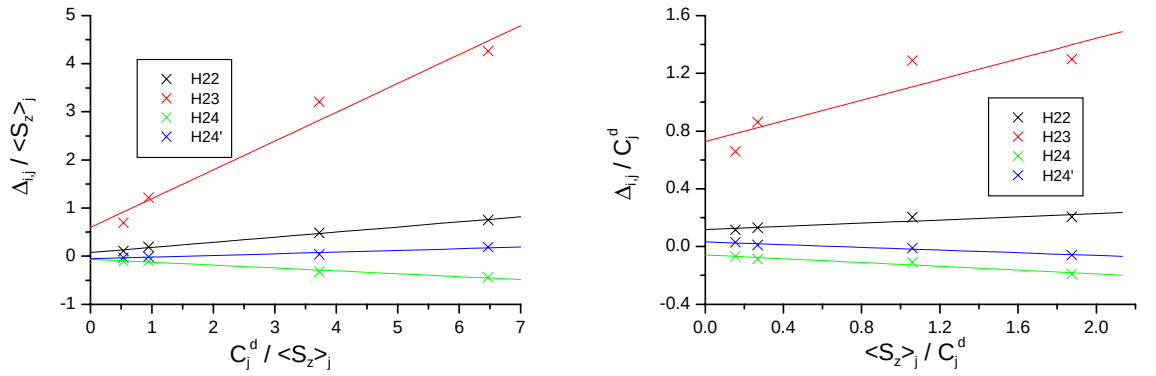

Figure 117 One proton plots of $Ln_2(L^{AB})_3$ complexes

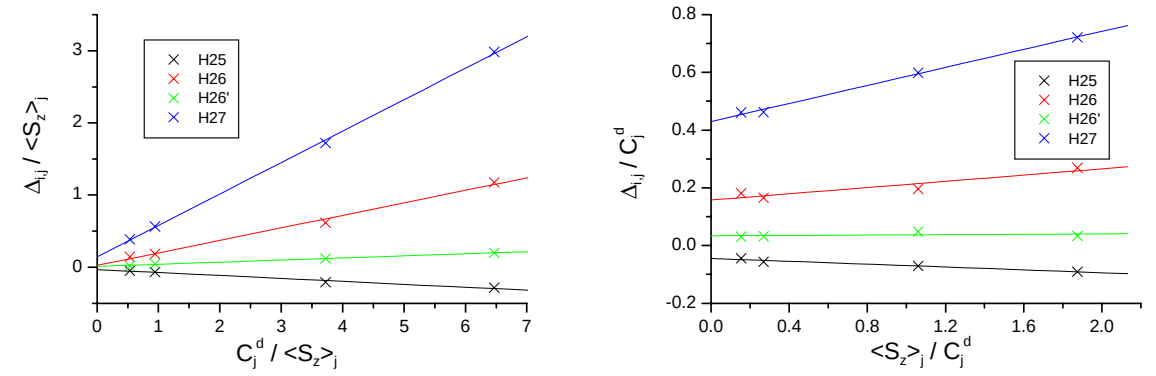

Figure 118 One proton plots of $Ln_2(L^{AB})_3$ complexes

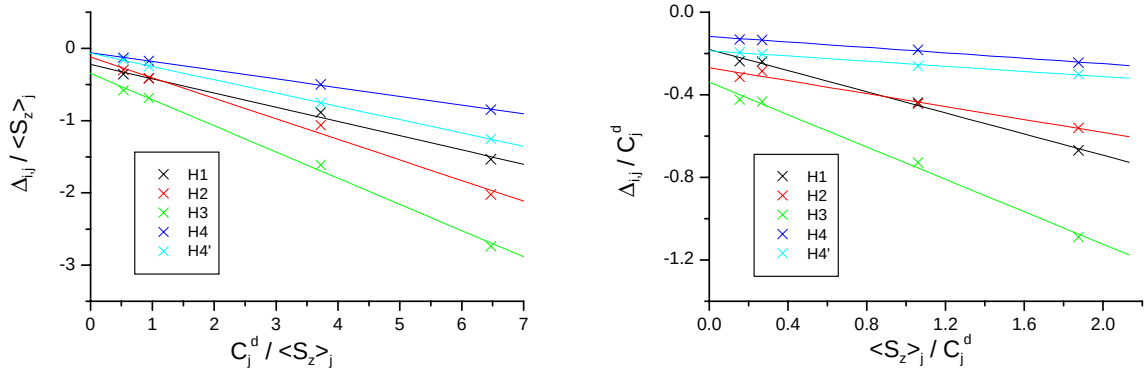

Figure 119 One proton plots of LaLn(L^{AB})$_3$ complexes

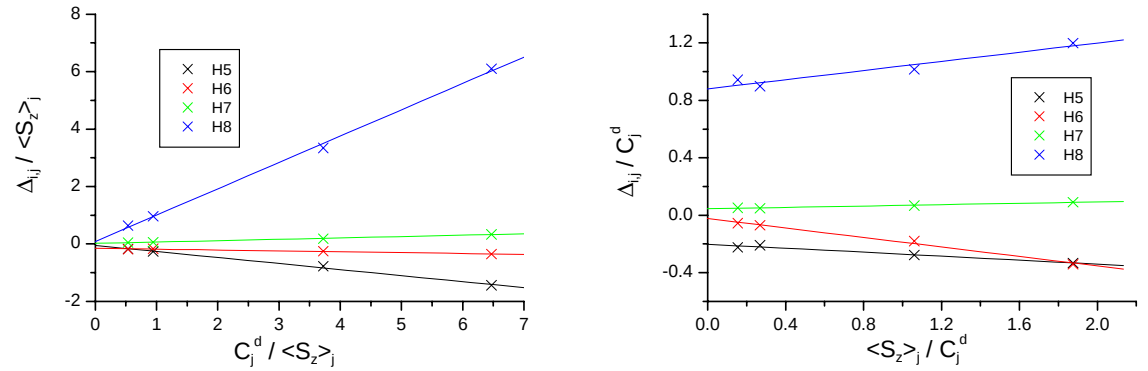

Figure 120 One proton plots of LaLn(L^{AB})$_3$ complexes

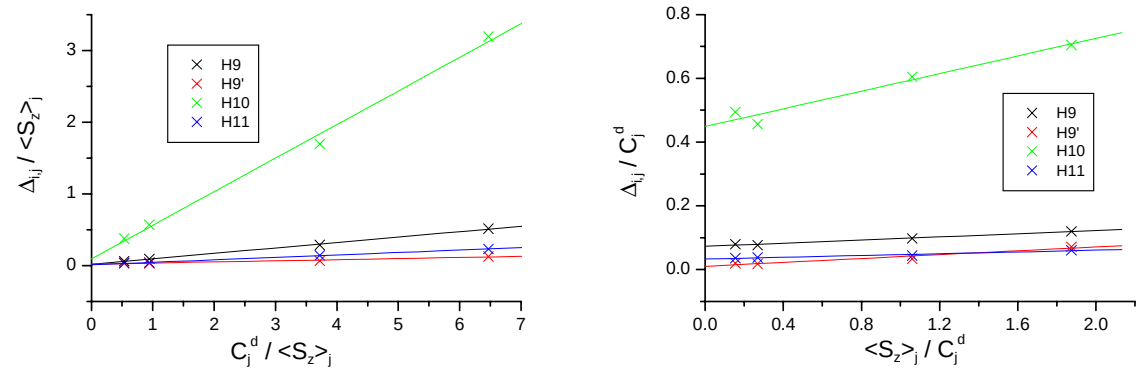

Figure 121 One proton plots of LaLn(L^{AB})$_3$ complexes

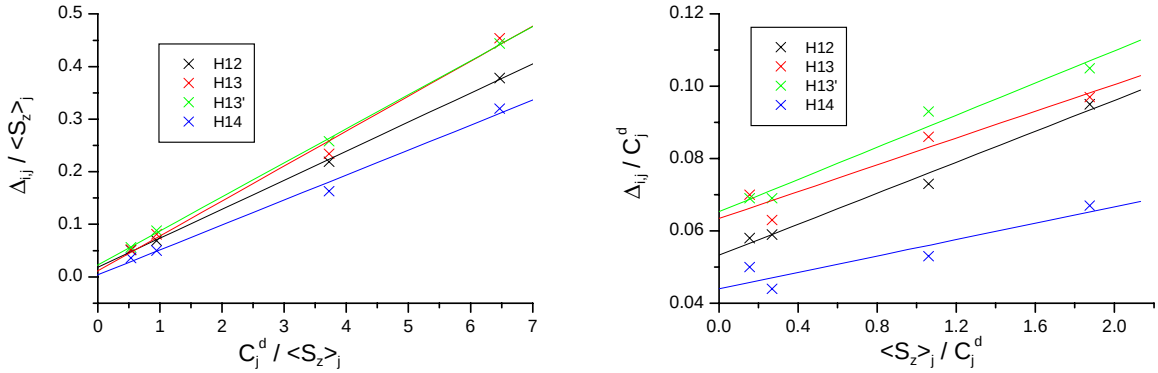

Figure 122 One proton plots of LaLn(L^{AB})$_3$ complexes

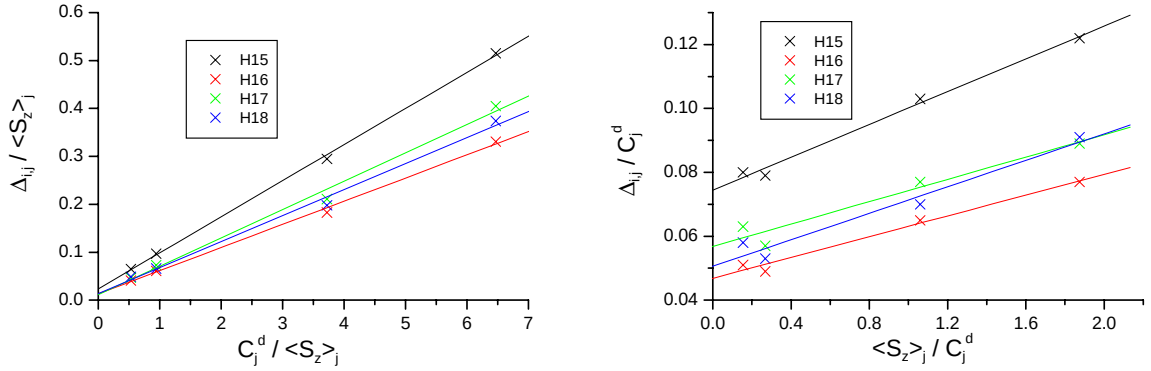

Figure 123 One proton plots of LaLn(L^{AB})$_3$ complexes

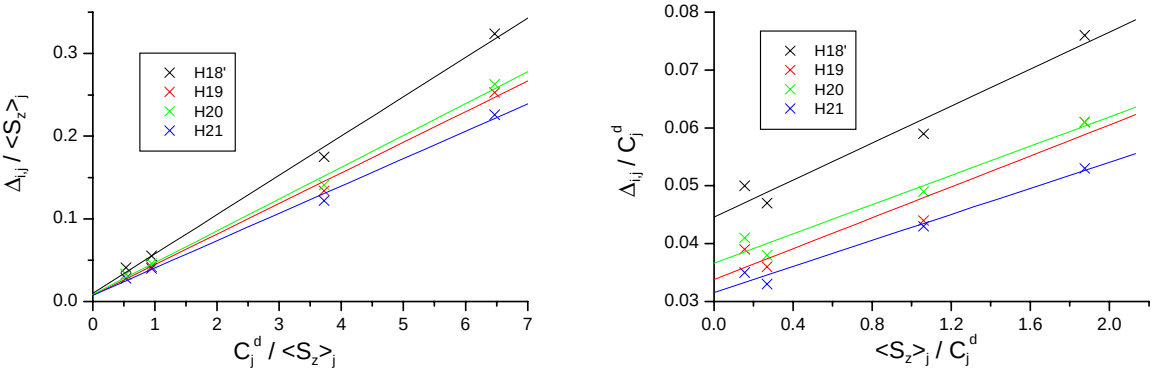

Figure 124 One proton plots of LaLn(L^{AB})$_3$ complexes

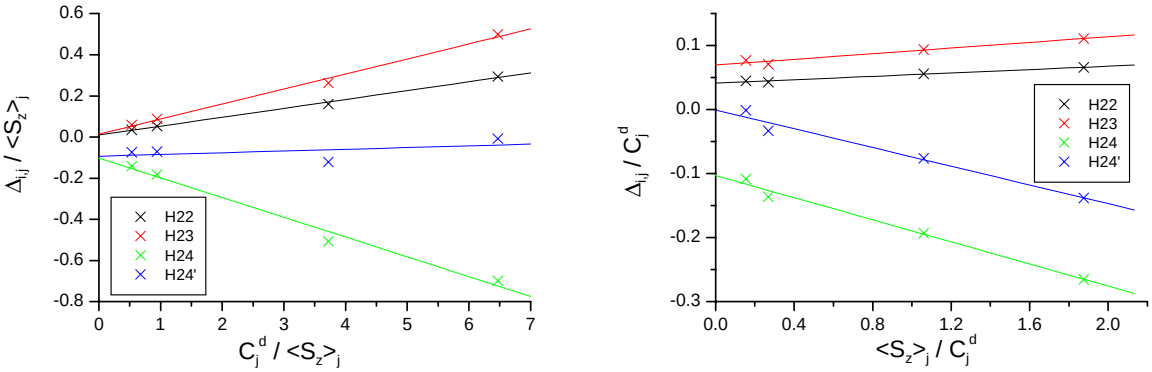

Figure 125 One proton plots of LaLn(L^{AB})$_3$ complexes

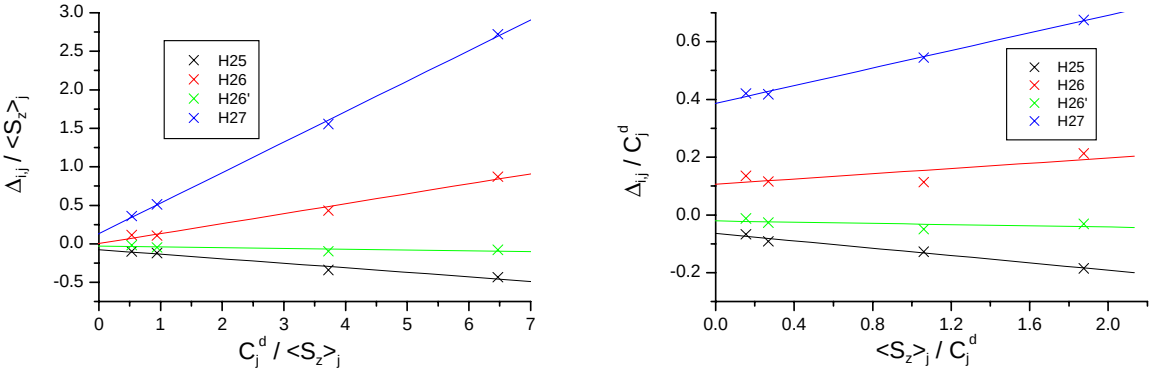

Figure 126 One proton plots of LaLn(L^{AB})$_3$ complexes

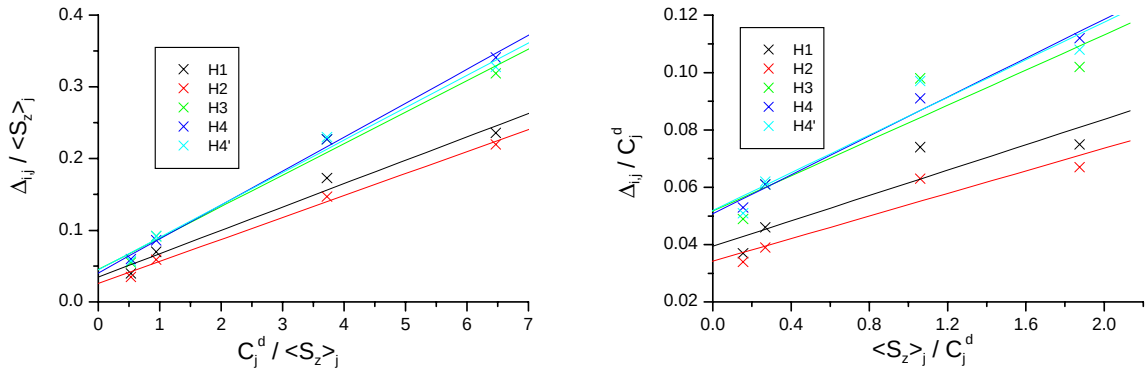

Figure 127 One proton plots of LnLu(L^{AB})$_3$ complexes

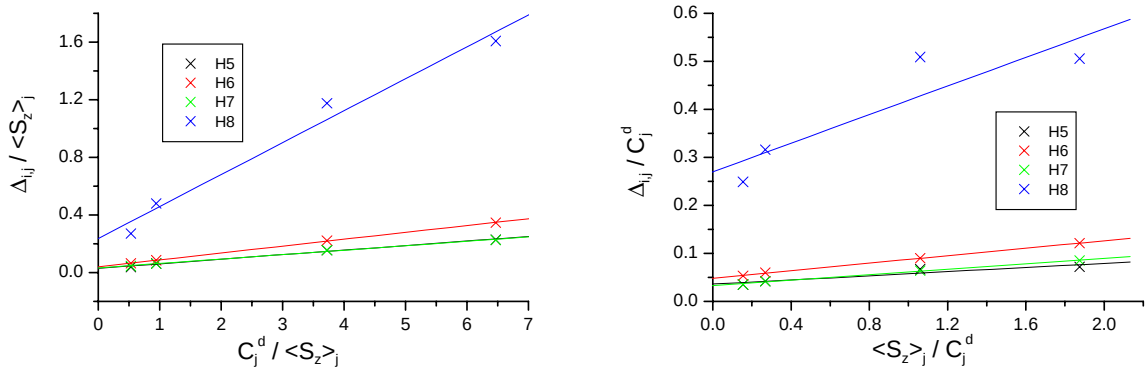

Figure 128 One proton plots of LnLu(L^{AB})$_3$ complexes

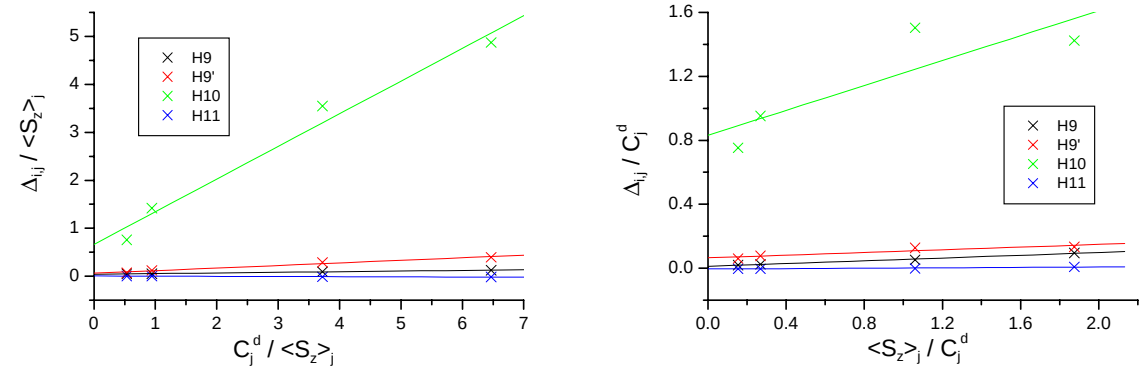

Figure 129 One proton plots of LnLu(L^{AB})$_3$ complexes

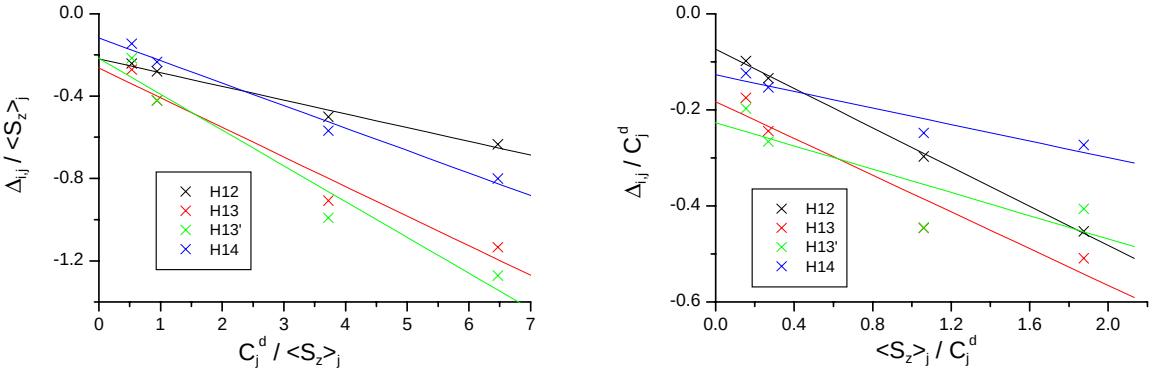

Figure 130 One proton plots of LnLu(L^{AB})$_3$ complexes

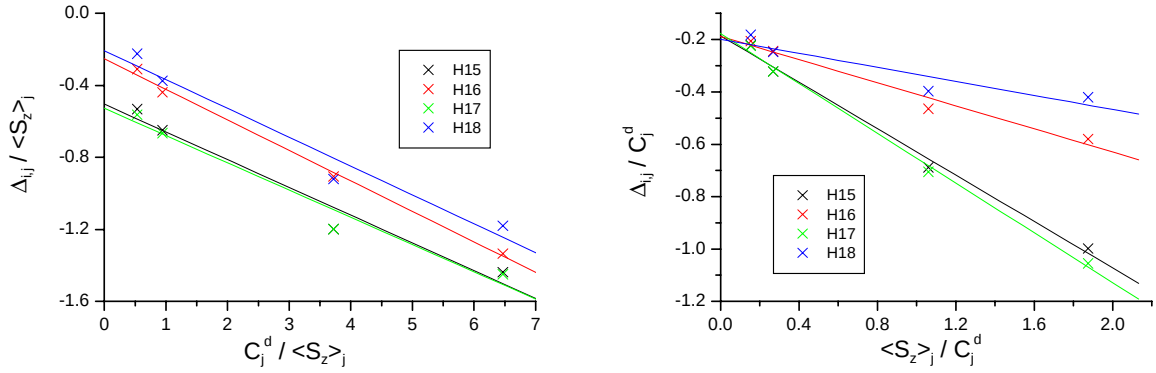

Figure 131 One proton plots of LnLu(L^{AB})$_3$ complexes

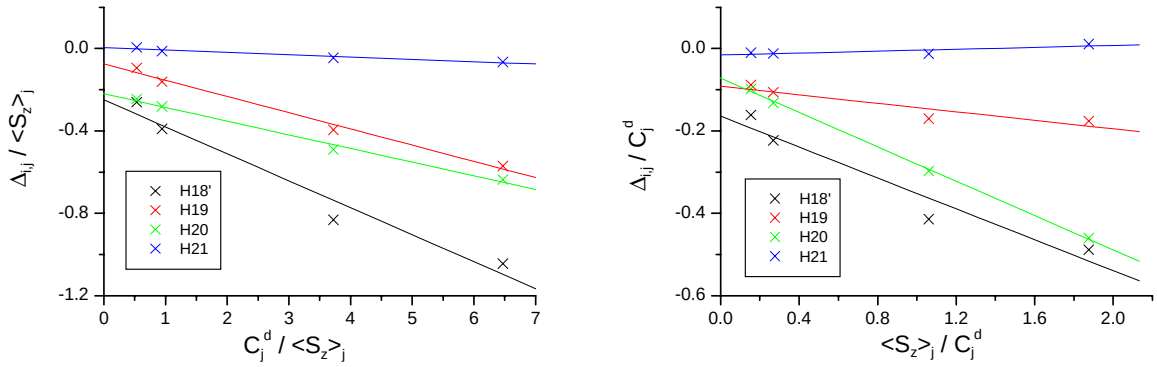

Figure 132 One proton plots of LnLu(L^{AB})$_3$ complexes

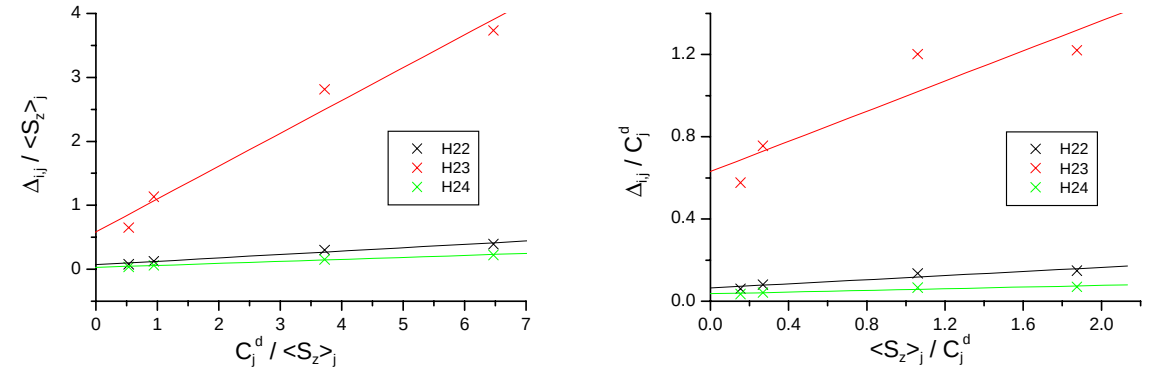

Figure 133 One proton plots of LnLu(L^{AB})$_3$ complexes

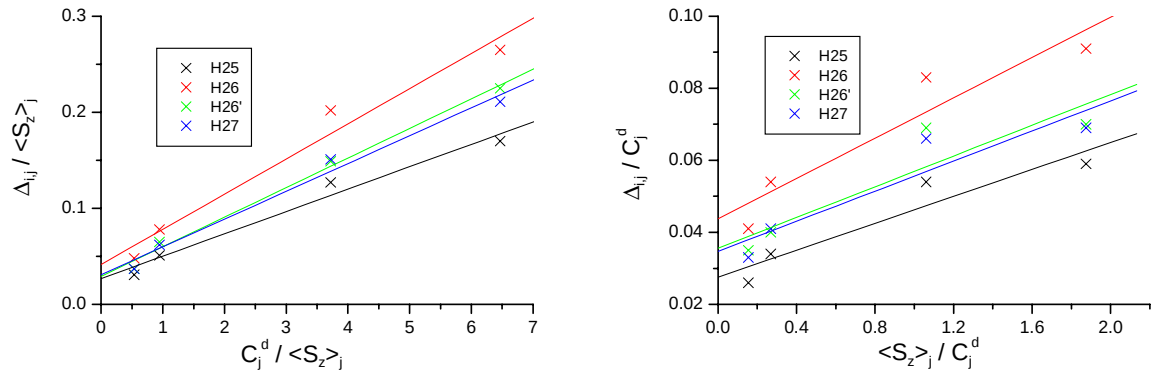

Figure 134 One proton plots of LnLu(L^{AB})$_3$ complexes

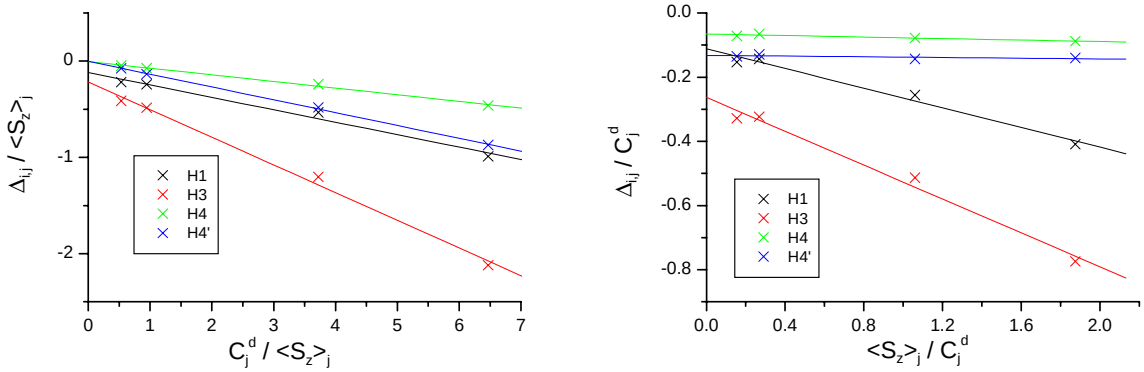

Figure 135 One proton plots of $Ln_2(L^{AB3})_3$ complexes

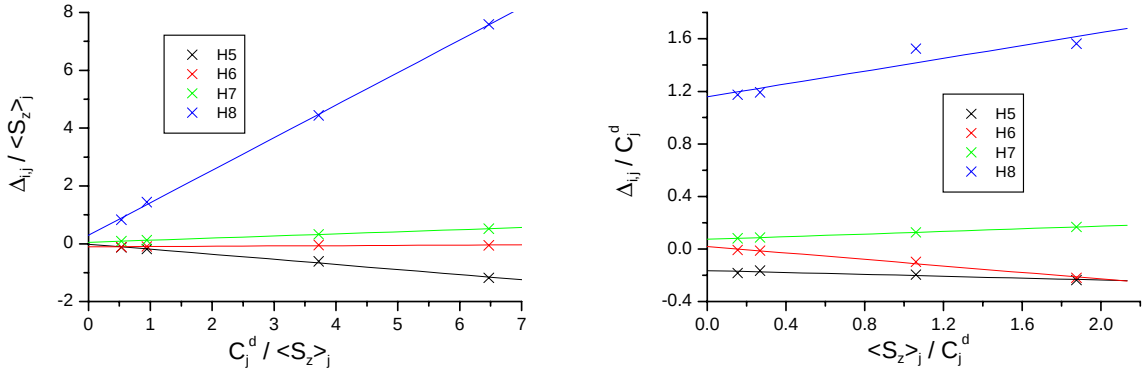

Figure 136 One proton plots of $Ln_2(L^{AB3})_3$ complexes

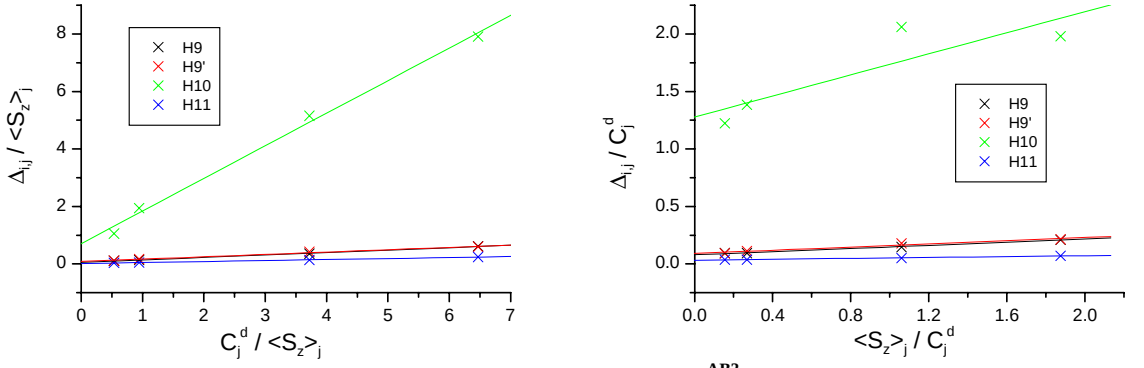

Figure 137 One proton plots of $Ln_2(L^{AB3})_3$ complexes

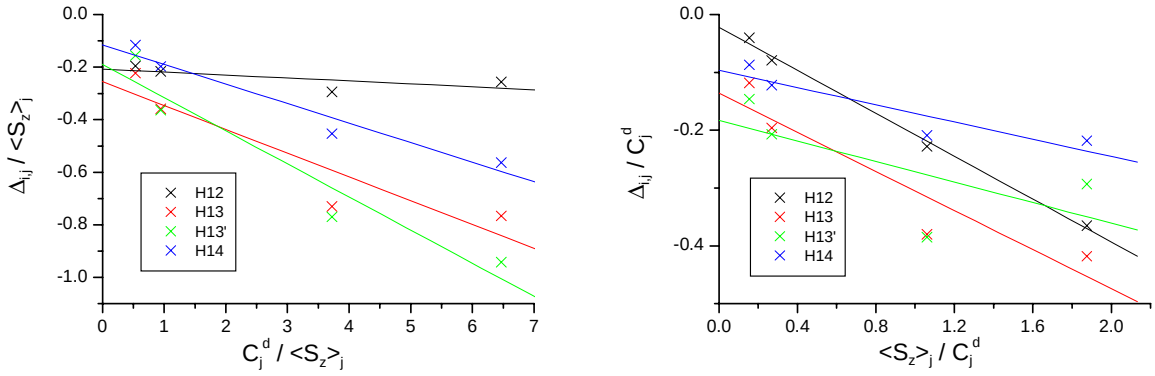

Figure 138 One proton plots of $Ln_2(L^{AB3})_3$ complexes

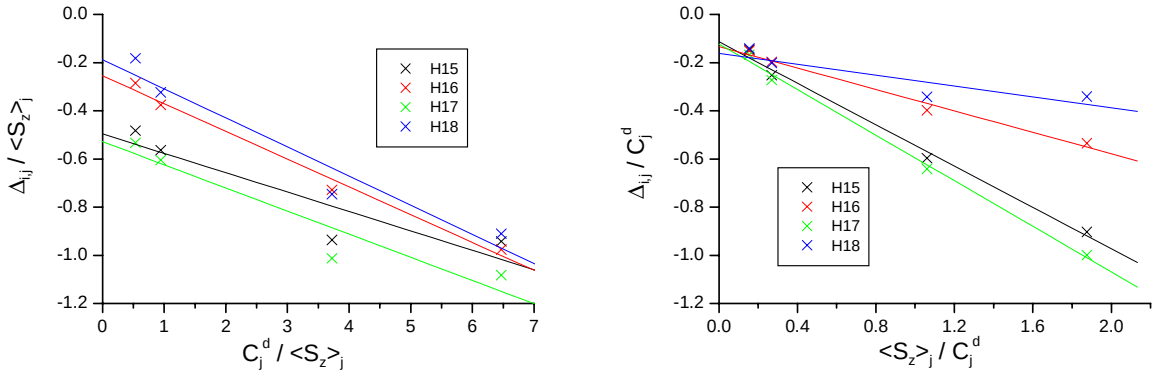

Figure 139 One proton plots of $Ln_2(L^{AB3})_3$ complexes

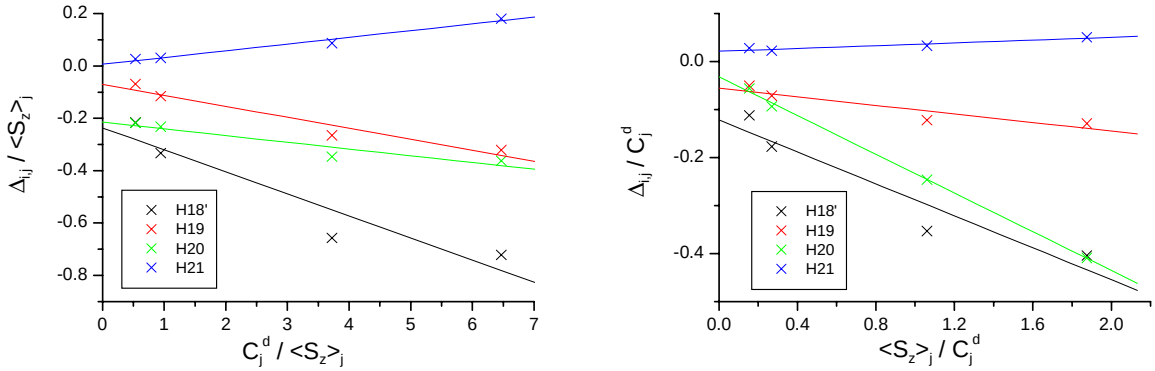

Figure 140 One proton plots of $Ln_2(L^{AB3})_3$ complexes

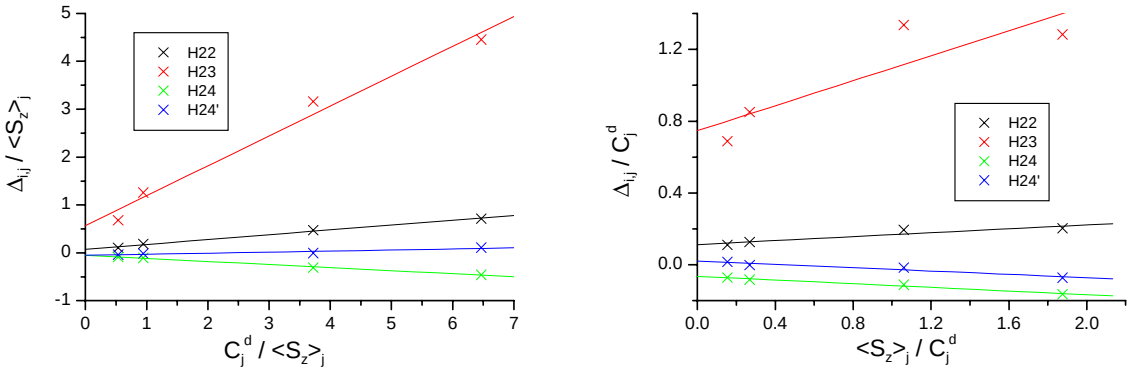

Figure 141 One proton plots of $Ln_2(L^{AB3})_3$ complexes

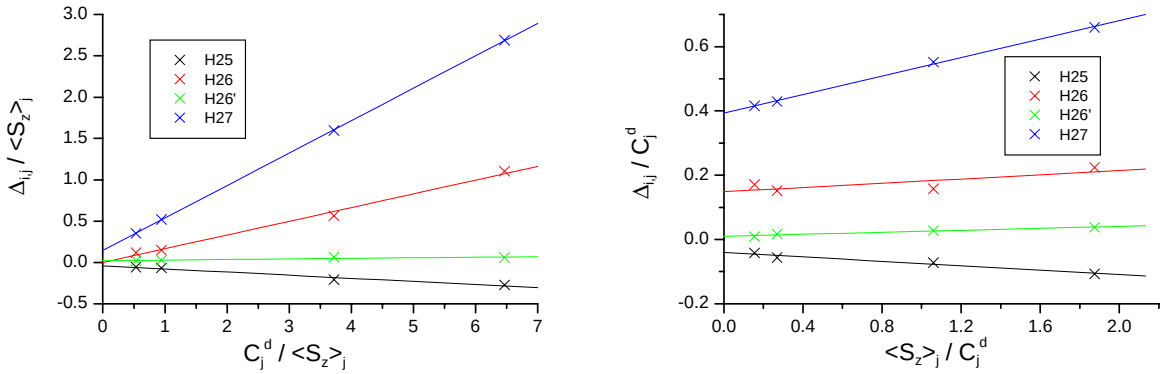

Figure 142 One proton plots of $Ln_2(L^{AB3})_3$ complexes

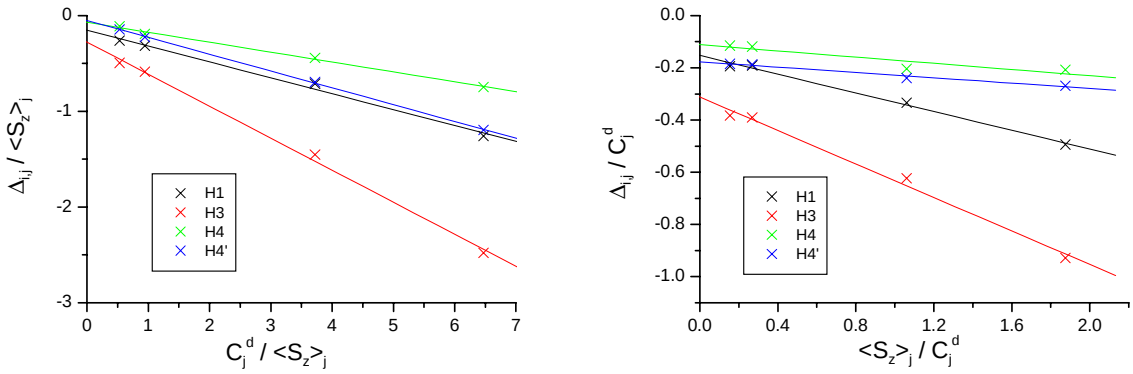

Figure 143 One proton plots of LaLn(L^{AB3})$_3$ complexes

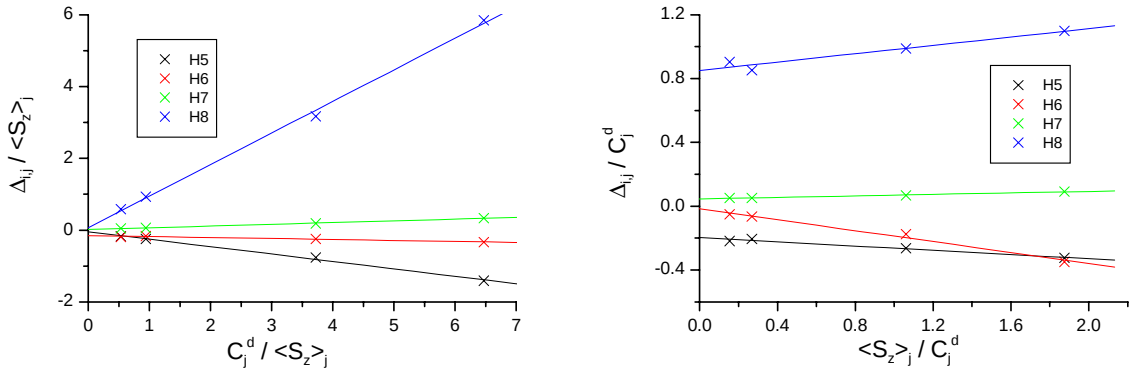

Figure 144 One proton plots of LaLn(L^{AB3})$_3$ complexes

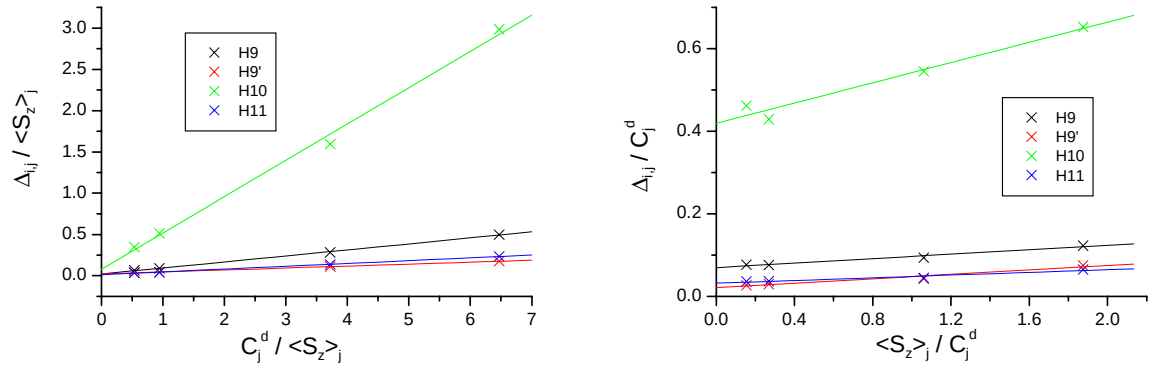

Figure 145 One proton plots of LaLn(L^{AB3})$_3$ complexes

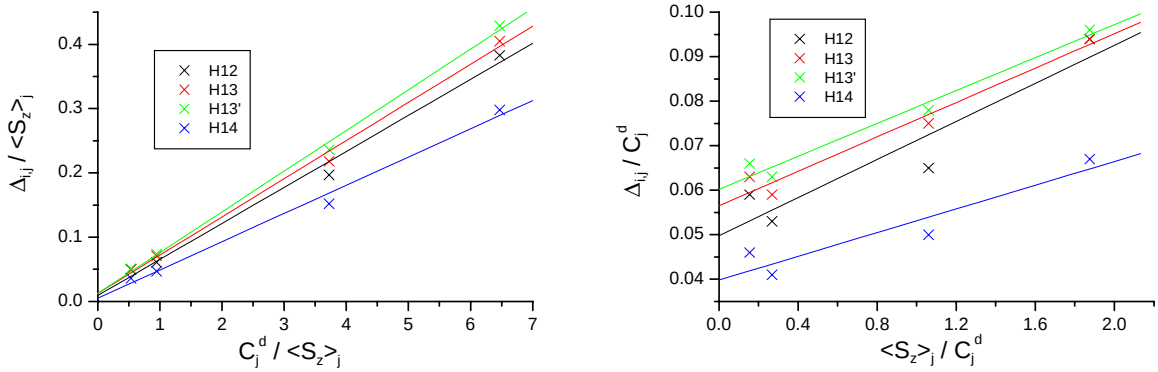

Figure 146 One proton plots of LaLn(L^{AB3})$_3$ complexes

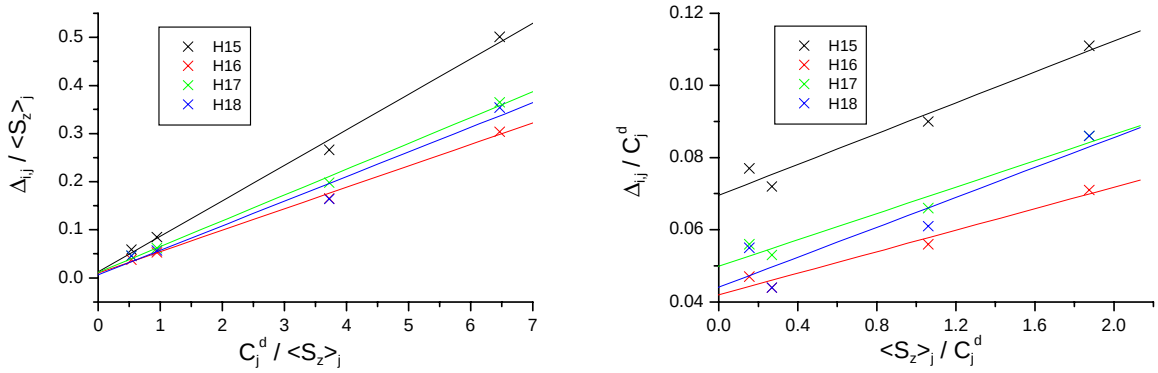

Figure 147 One proton plots of LaLn(L^{AB3})$_3$ complexes

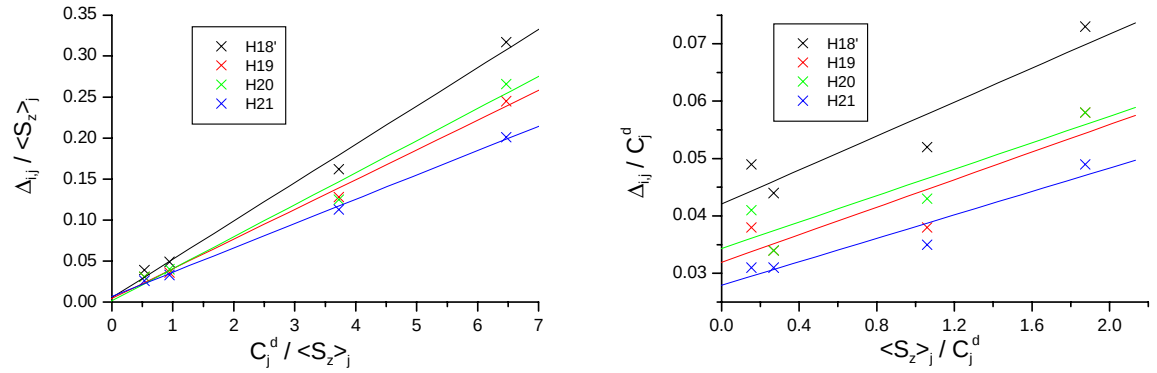

Figure 148 One proton plots of LaLn(L^{AB3})$_3$ complexes

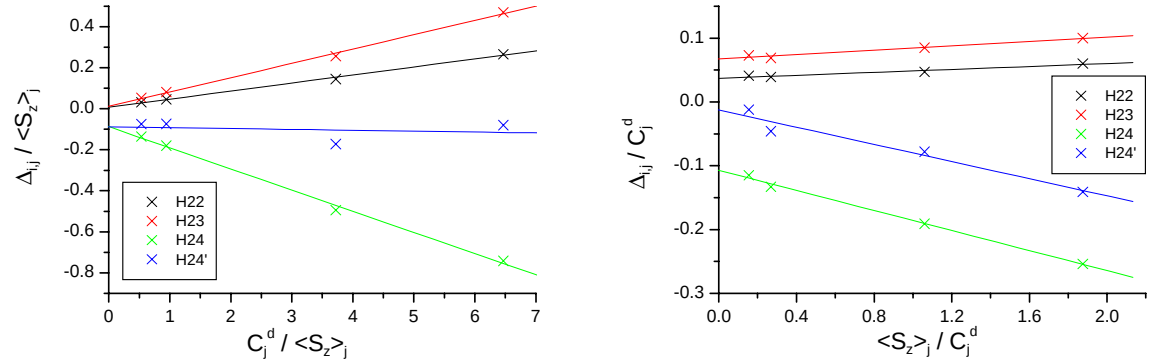

Figure 149 One proton plots of LaLn(L^{AB3})$_3$ complexes

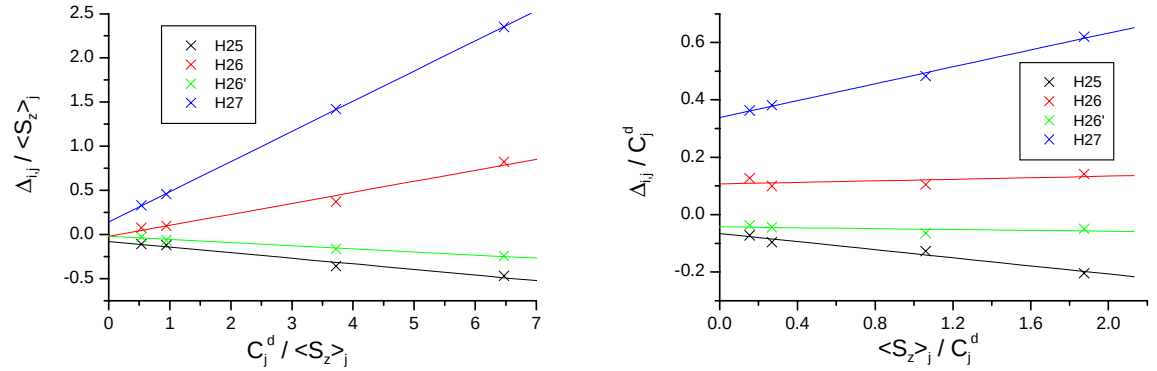

Figure 150 One proton plots of LaLn(L^{AB3})$_3$ complexes

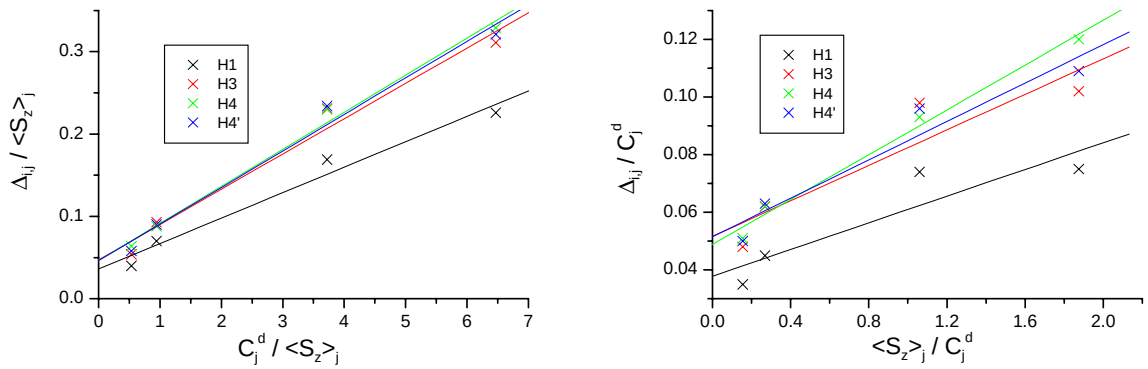

Figure 151 One proton plots of LnLu(L^{AB3})$_3$ complexes

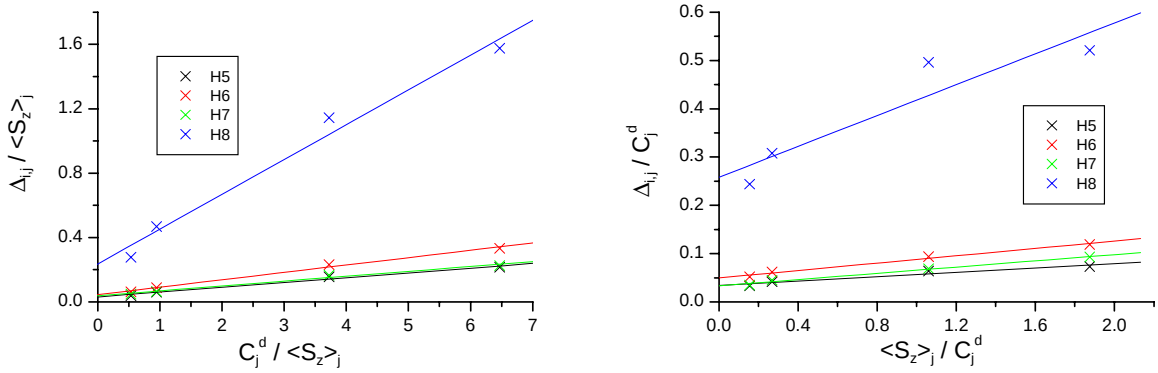

Figure 152 One proton plots of LnLu(L^{AB3})$_3$ complexes

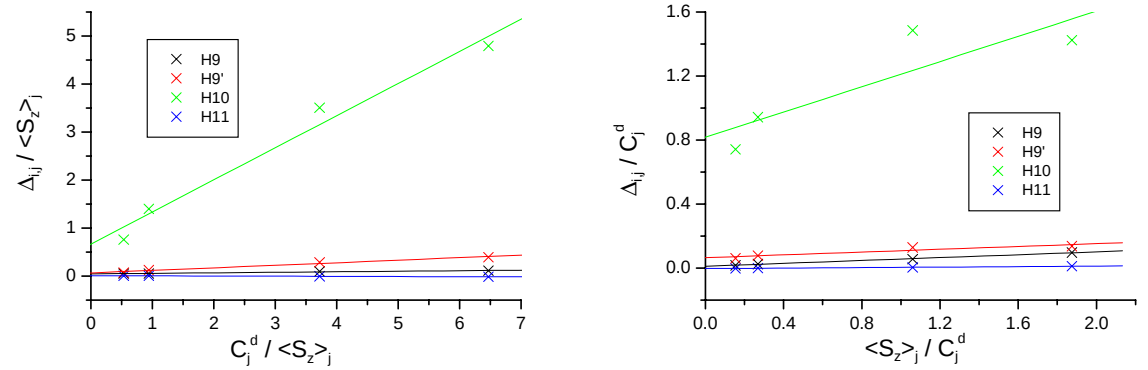

Figure 153 One proton plots of LnLu(L^{AB3})$_3$ complexes

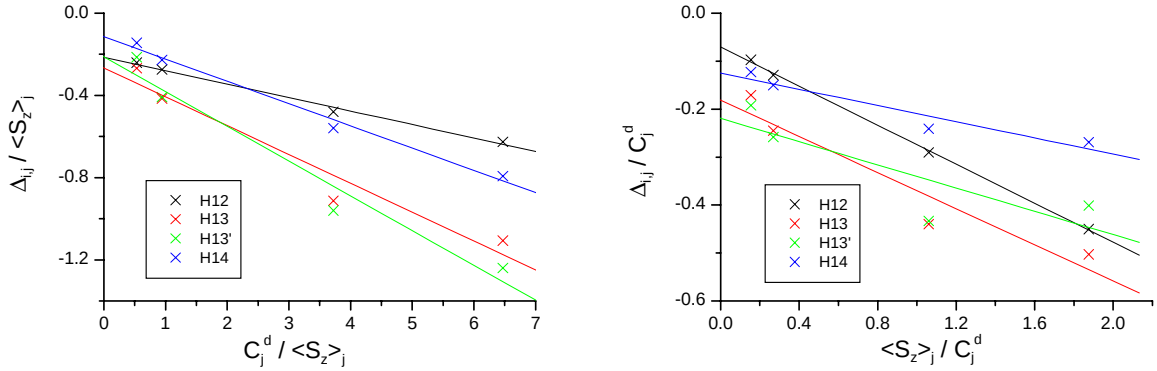

Figure 154 One proton plots of LnLu(L^{AB3})$_3$ complexes

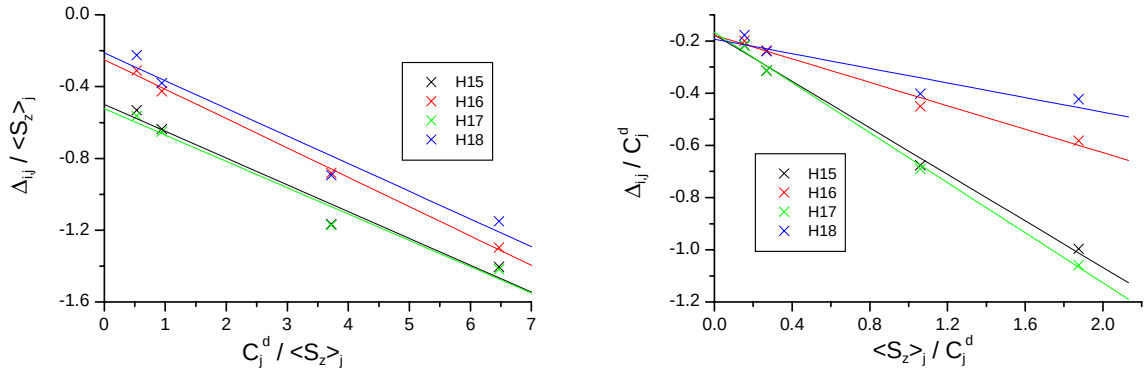

Figure 155 One proton plots of LnLu(L^{AB3})$_3$ complexes

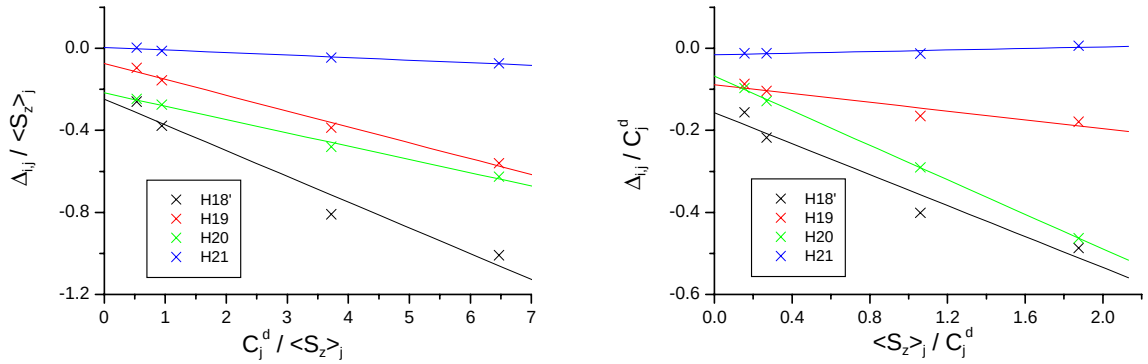

Figure 156 One proton plots of LnLu(L^{AB3})$_3$ complexes

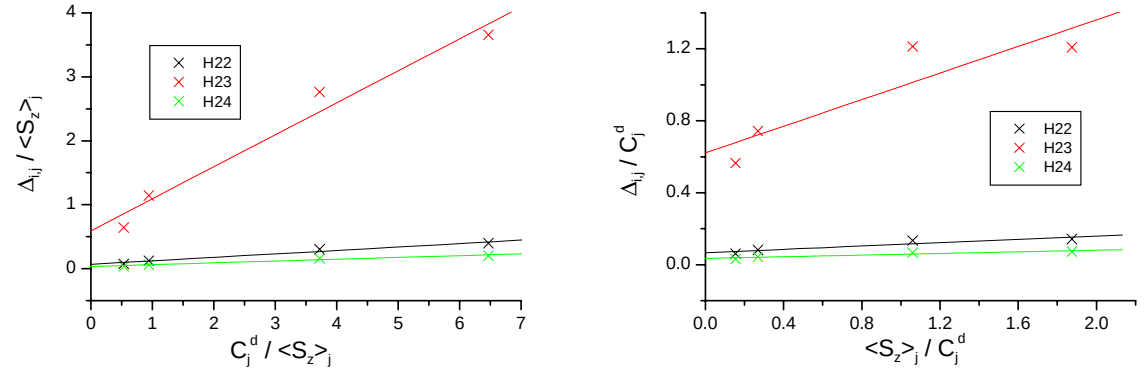

Figure 157 One proton plots of LnLu(L^{AB3})$_3$ complexes

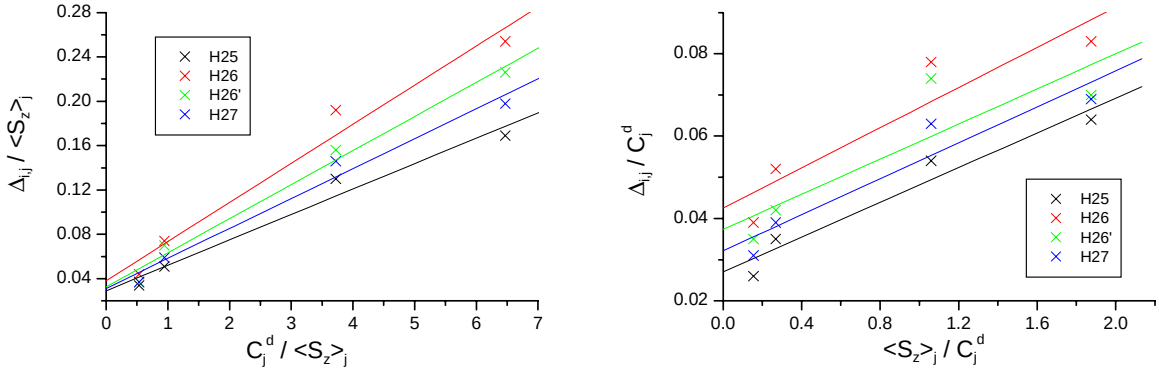

Figure 158 One proton plots of LnLu(L^{AB3})$_3$ complexes

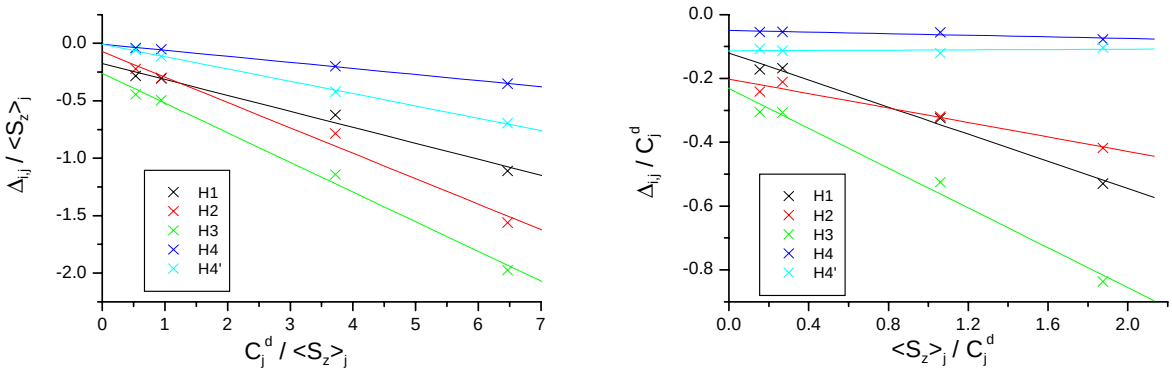

Figure 159 One proton plots of $Ln_2(L^{AB4})_3$ complexes

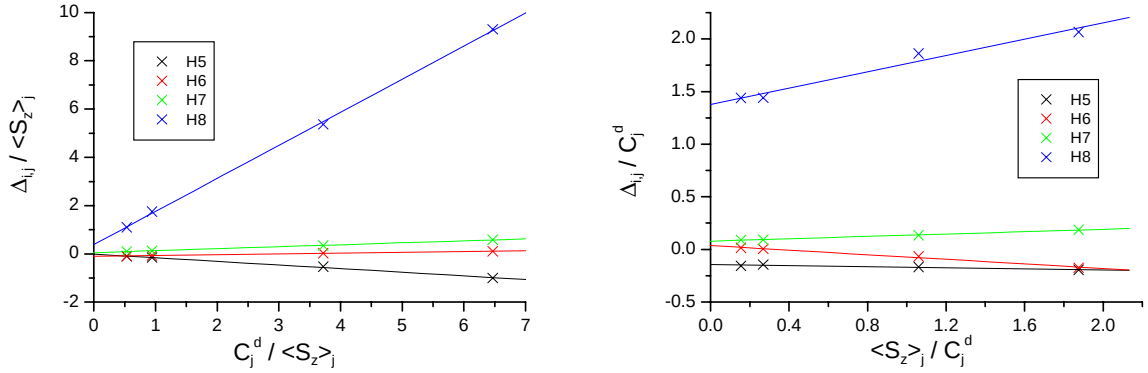

Figure 160 One proton plots of $Ln_2(L^{AB4})_3$ complexes

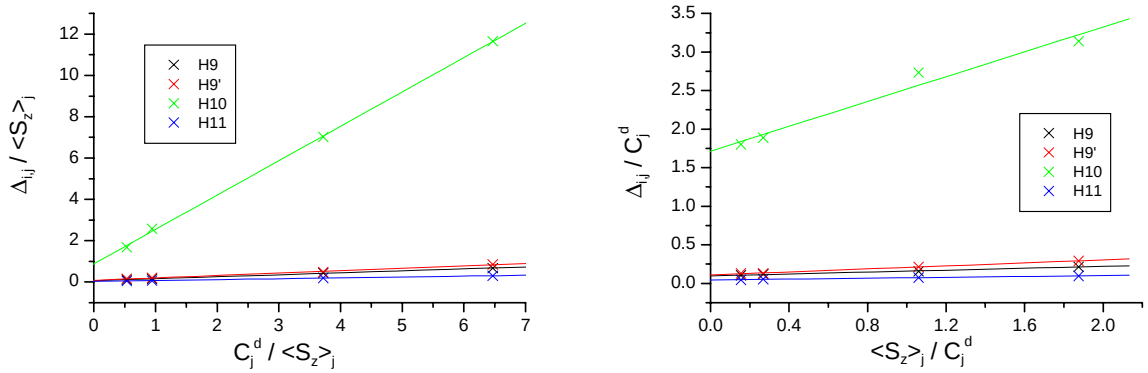

Figure 161 One proton plots of $Ln_2(L^{AB4})_3$ complexes

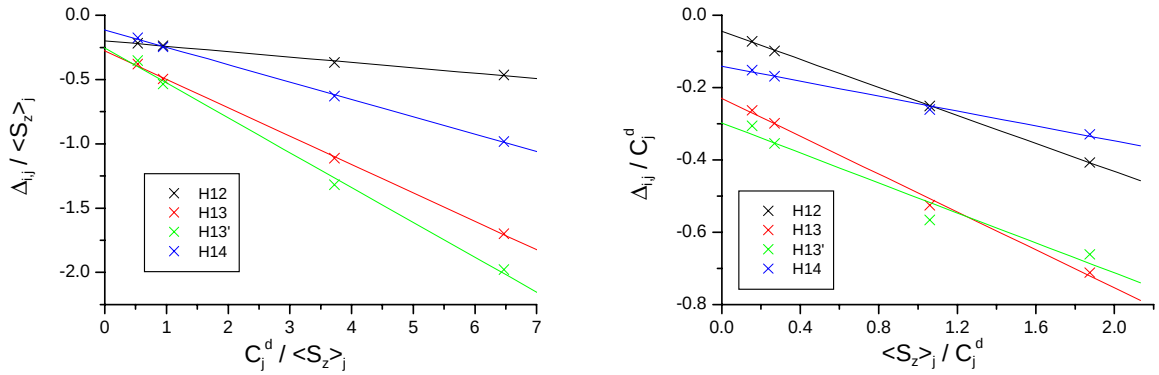

Figure 162 One proton plots of $Ln_2(L^{AB4})_3$ complexes

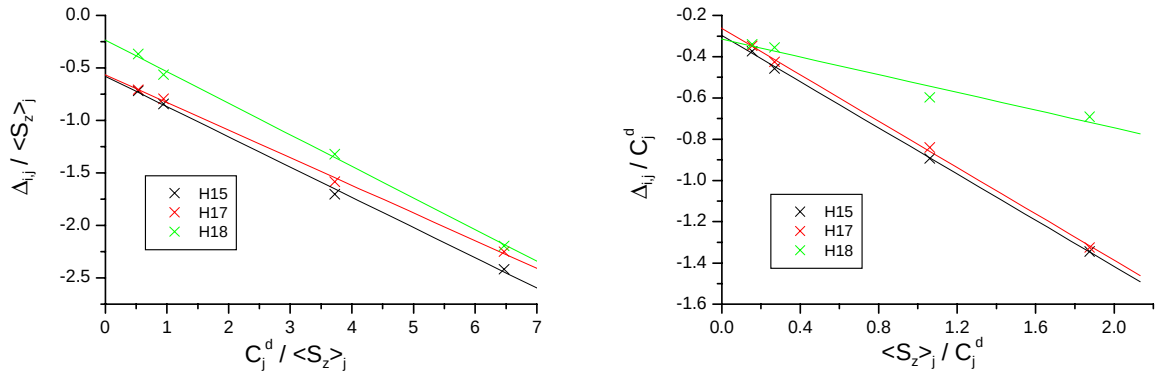

Figure 163 One proton plots of $Ln_2(L^{AB4})_3$ complexes

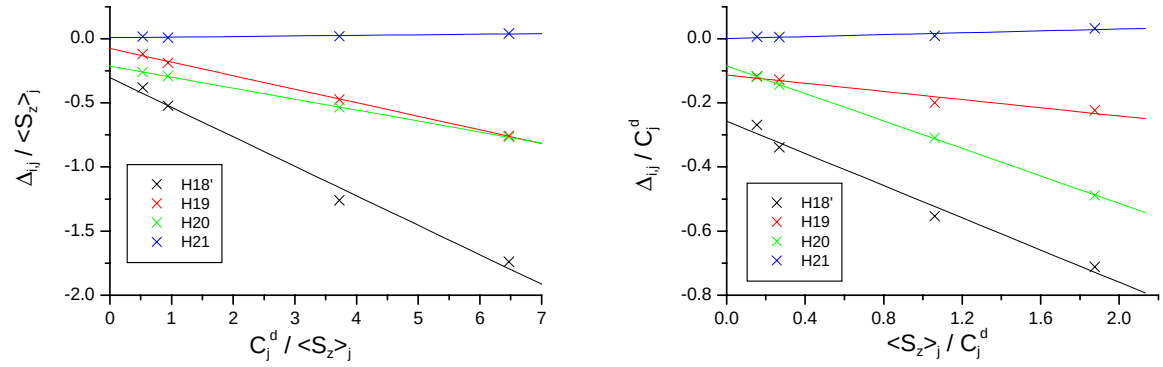

Figure 164 One proton plots of $Ln_2(L^{AB4})_3$ complexes

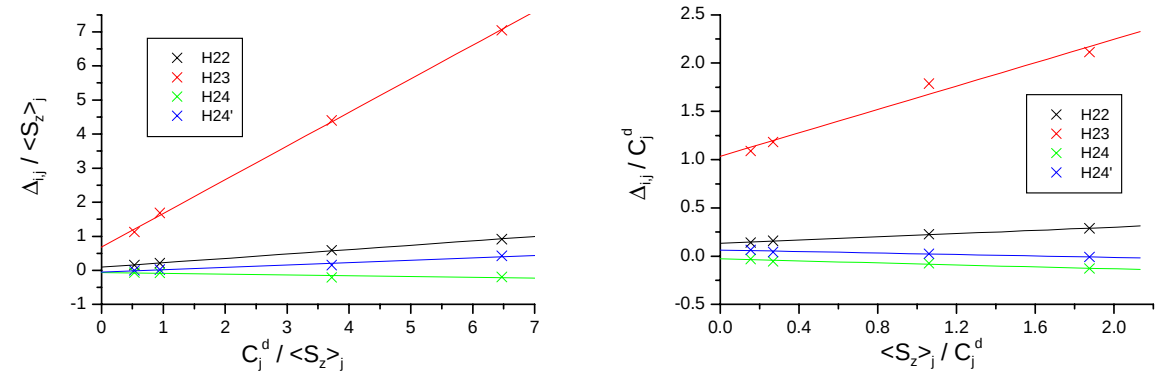

Figure 165 One proton plots of $Ln_2(L^{AB4})_3$ complexes

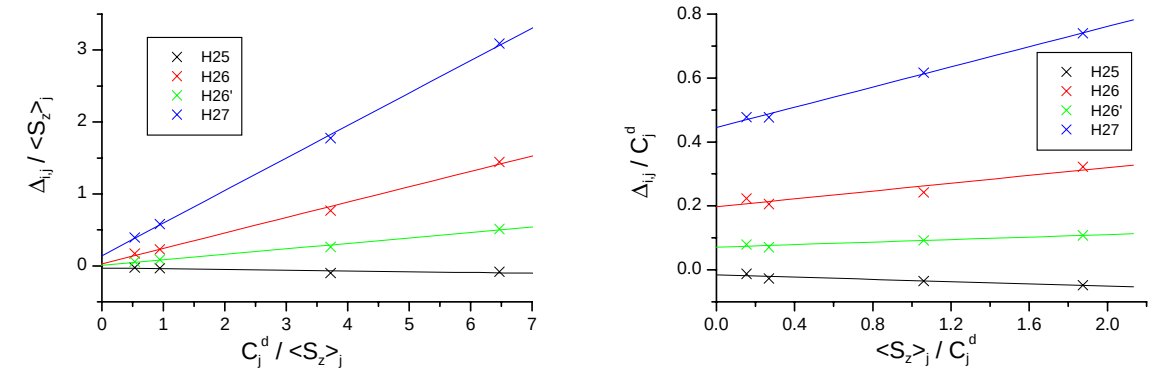

Figure 166 One proton plots $Ln_2(L^{AB4})_3$ complexes

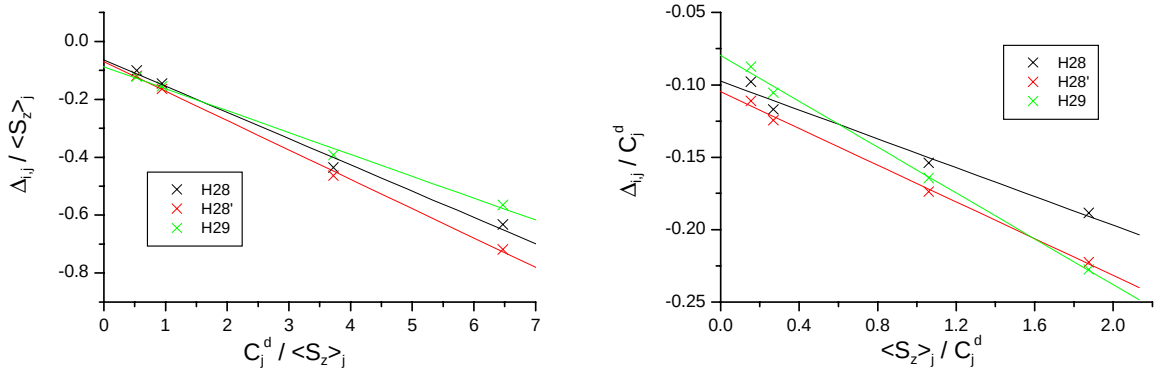

Figure 167 One proton plots of $Ln_2(L^{AB4})_3$ complexes

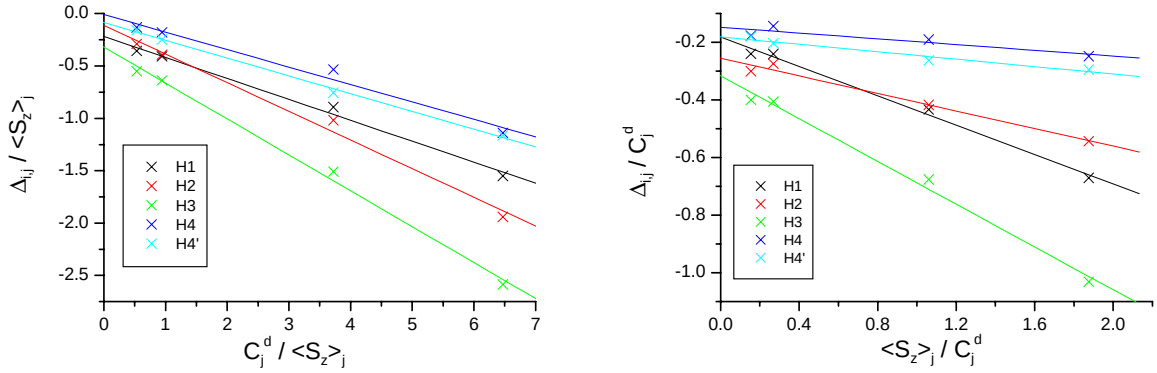

Figure 168 One proton plots of $LaLn(L^{AB4})_3$ complexes

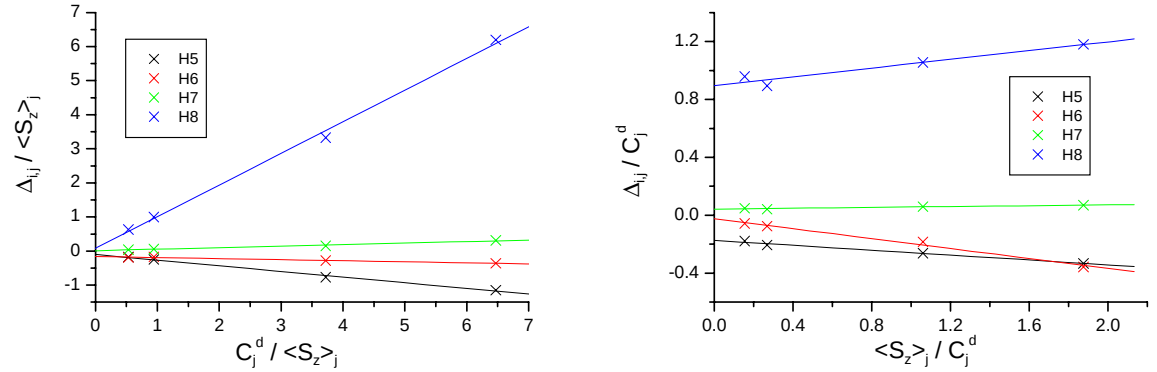

Figure 169 One proton plots of $LaLn(L^{AB4})_3$ complexes

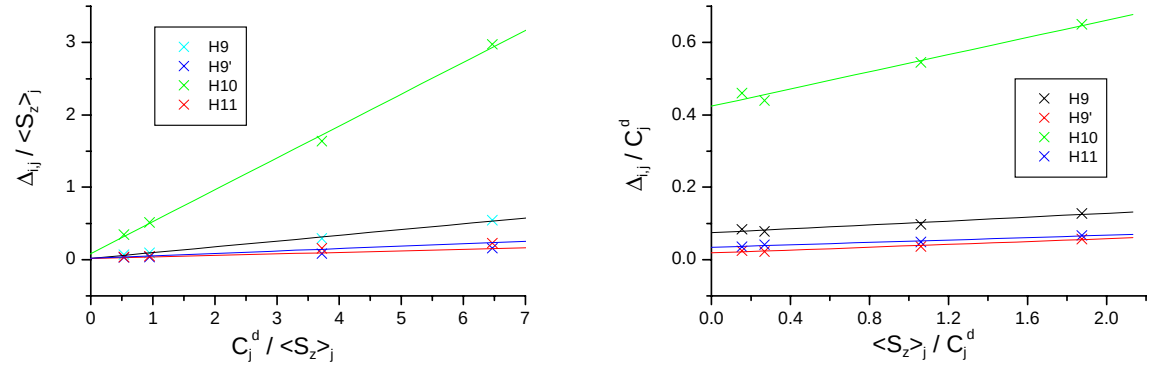

Figure 170 One proton plots of $LaLn(L^{AB4})_3$ complexes

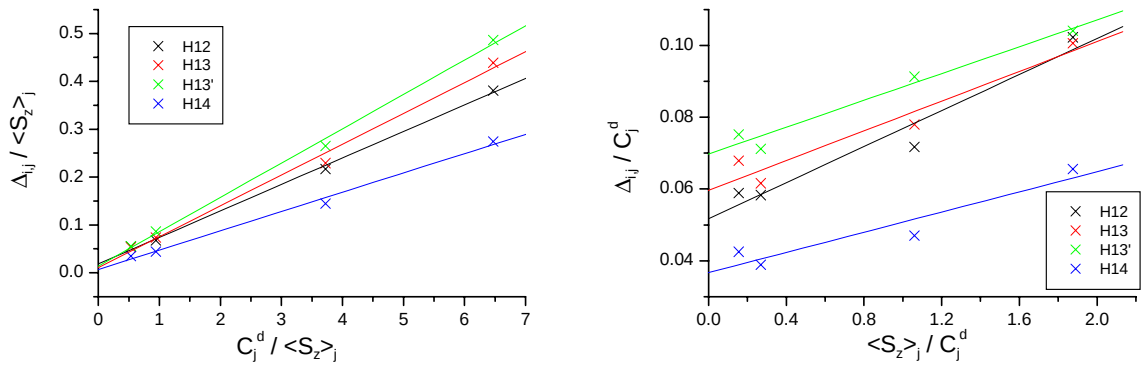

Figure 171 One proton plots of LaLn(L^{AB4})$_3$ complexes

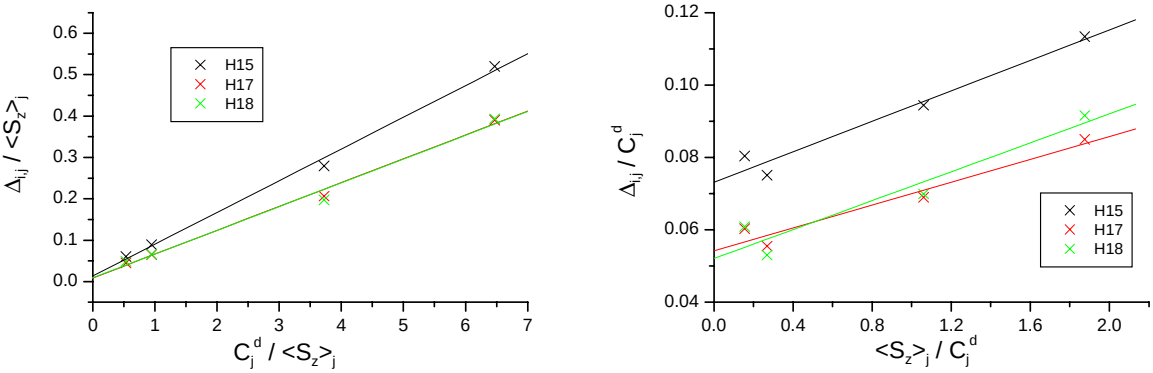

Figure 172 One proton plots of LaLn(L^{AB4})$_3$ complexes

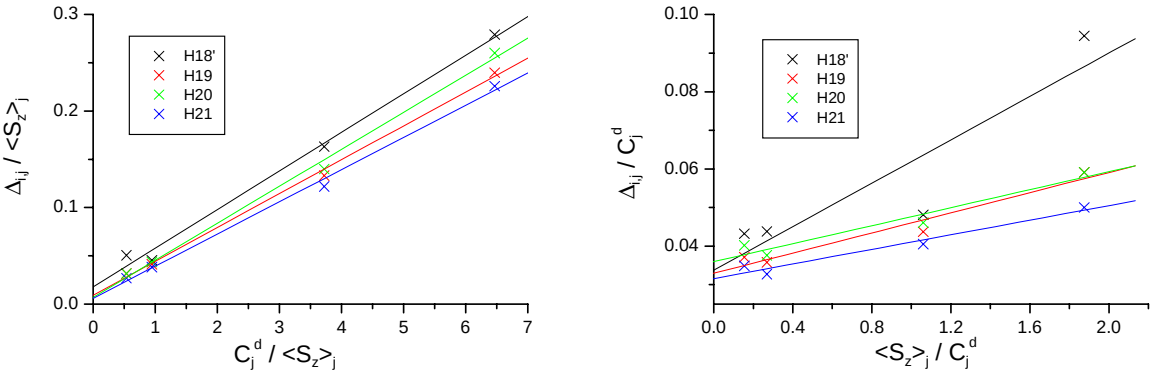

Figure 173 One proton plots of LaLn(L^{AB4})$_3$ complexes

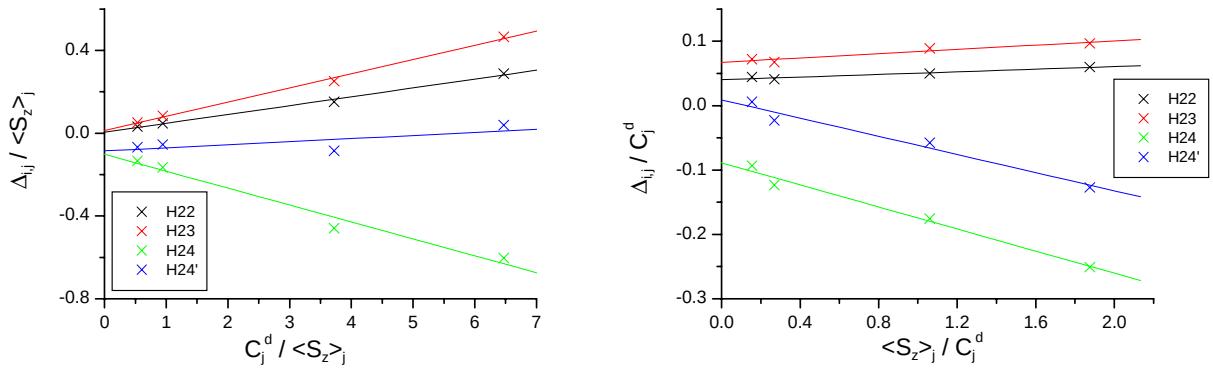

Figure 174 One proton plots of LaLn(L^{AB4})$_3$ complexes

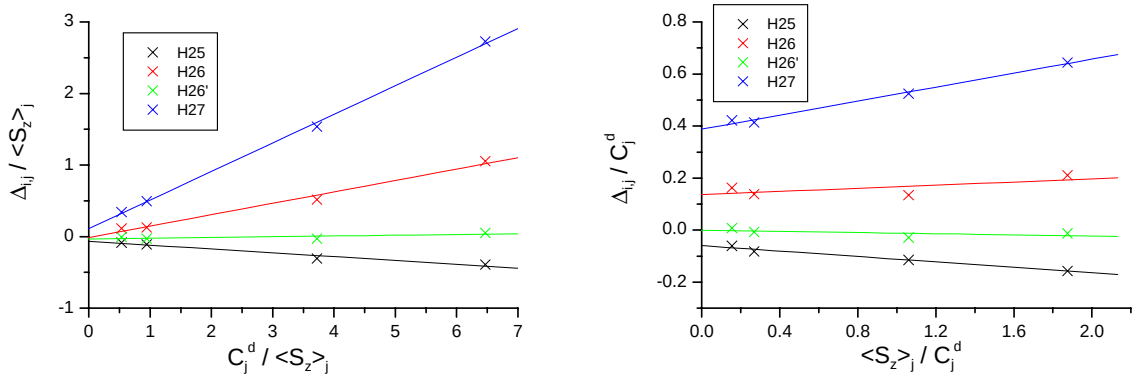

Figure 175 One proton plots of LaLn(L^{AB4})$_3$ complexes

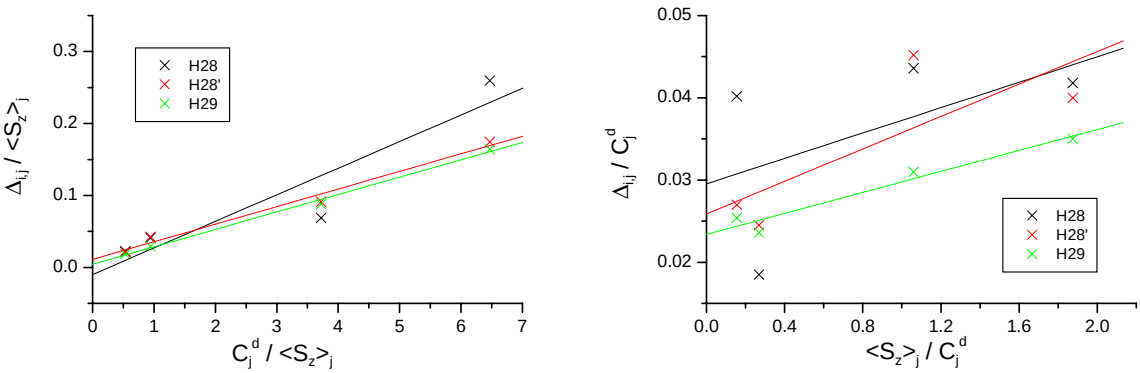

Figure 176 One proton plots of LaLn(L^{AB4})$_3$ complexes

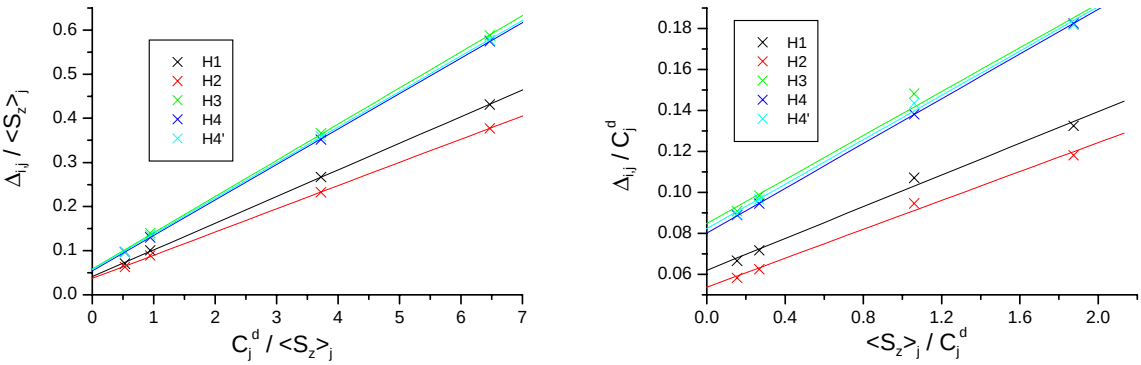

Figure 177 One proton plots of LnLu(L^{AB4})$_3$ complexes

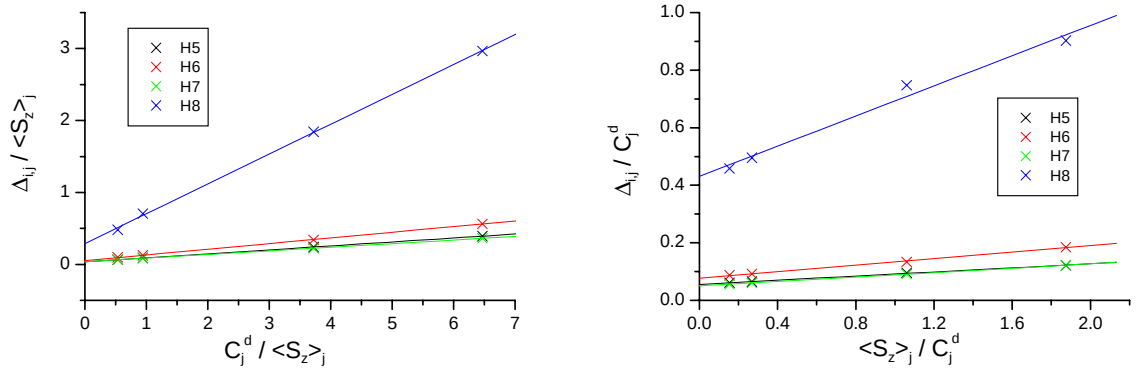

Figure 178 One proton plots of LnLu(L^{AB4})$_3$ complexes

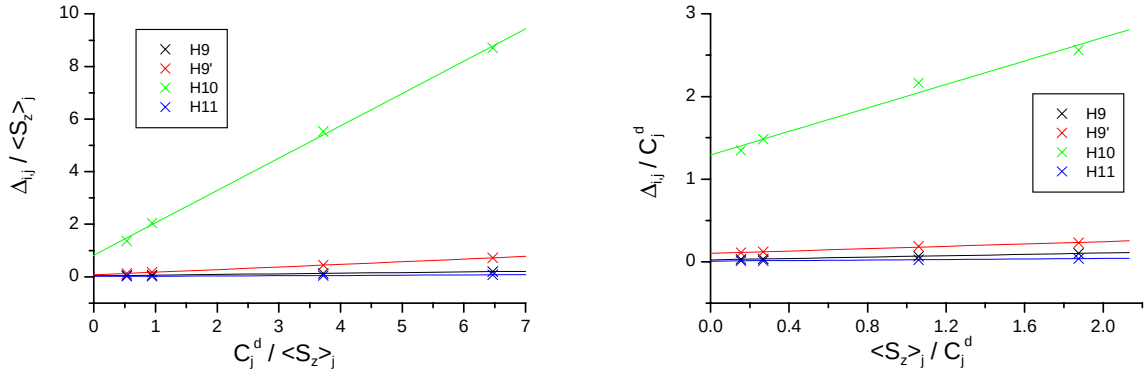

Figure 179 One proton plots of LnLu(L^{AB4})$_3$ complexes

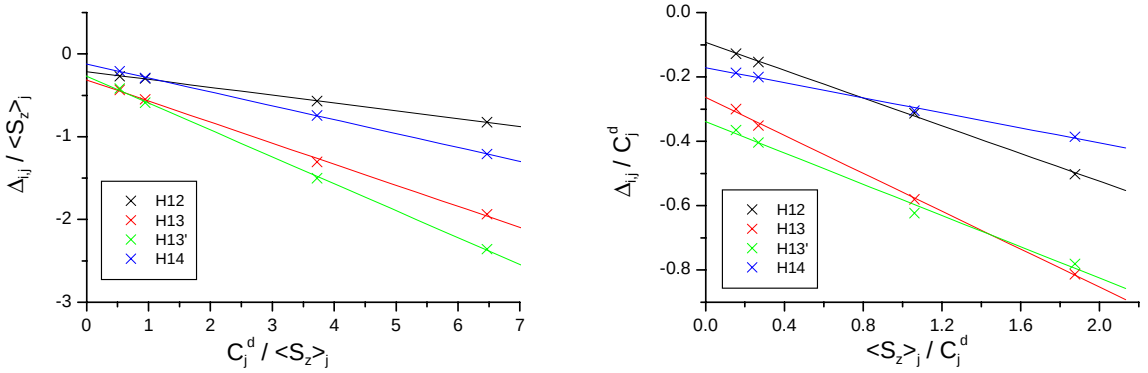

Figure 180 One proton plots of LnLu(L^{AB4})$_3$ complexes

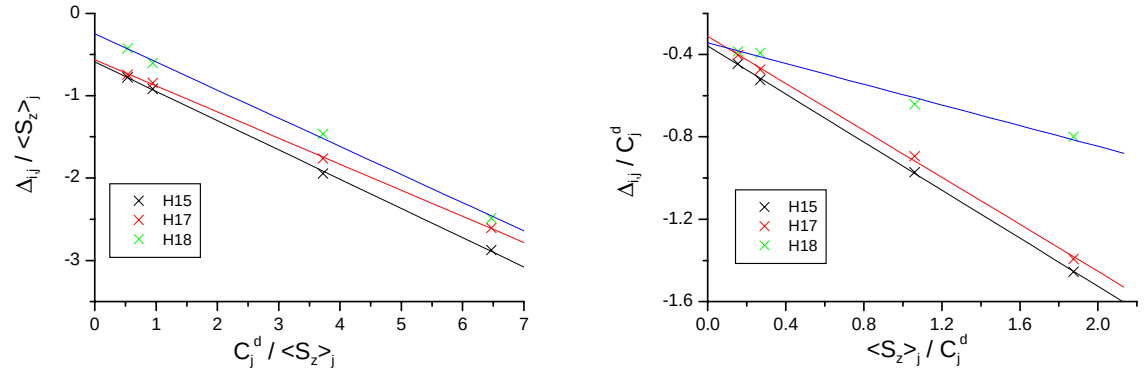

Figure 181 One proton plots of LnLu(L^{AB4})$_3$ complexes

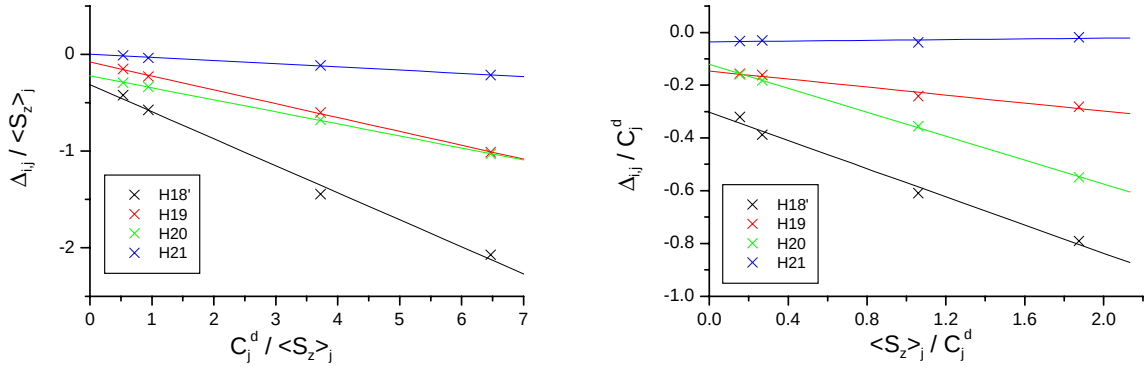

Figure 182 One proton plots of LnLu(L^{AB4})$_3$ complexes

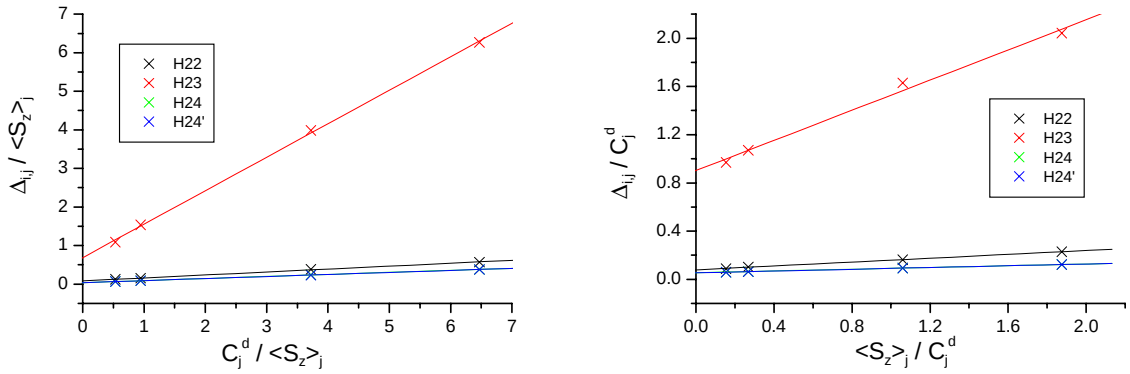

Figure 183 One proton plots of LnLu(L^{AB4})$_3$ complexes

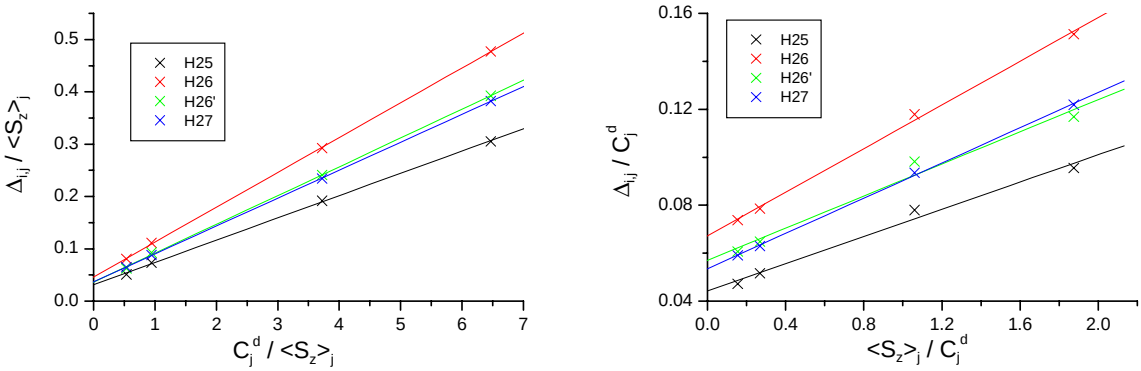

Figure 184 One proton plots of LnLu(L^{AB4})$_3$ complexes

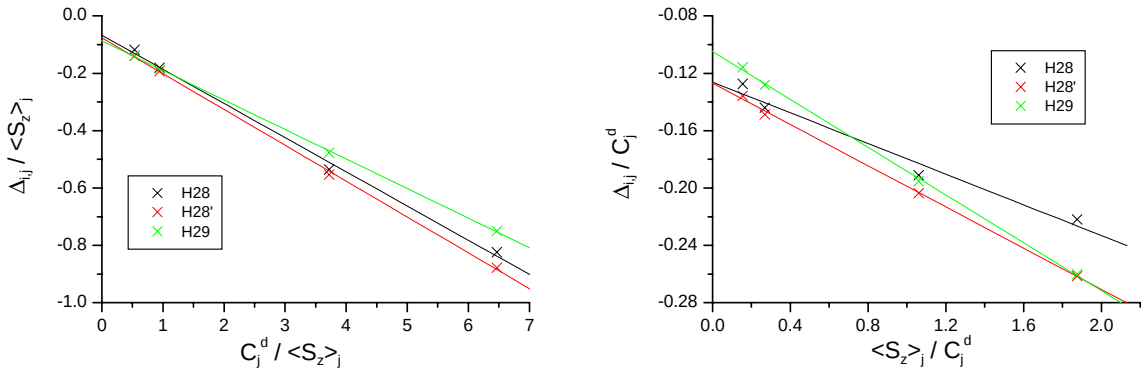

Figure 185 One proton plots of LnLu(L^{AB4})$_3$ complexes

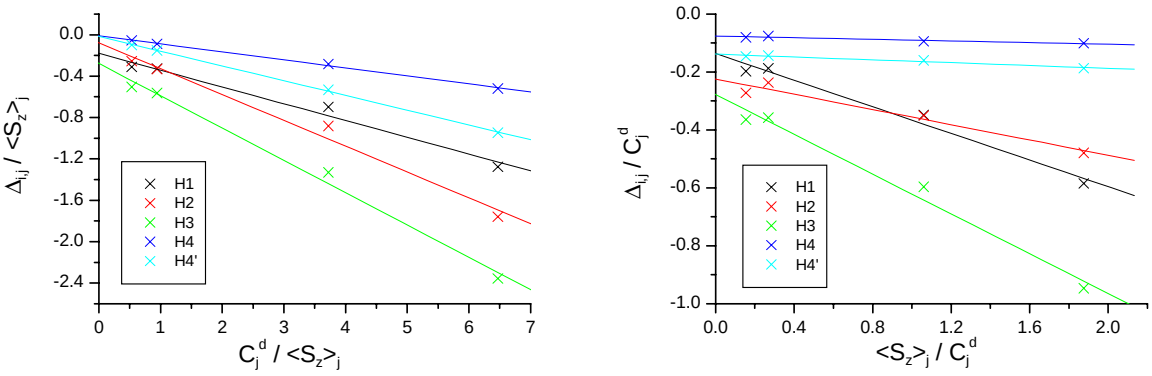

Figure 186 One proton plots of $Ln_2(L^{AB5})_3$ complexes

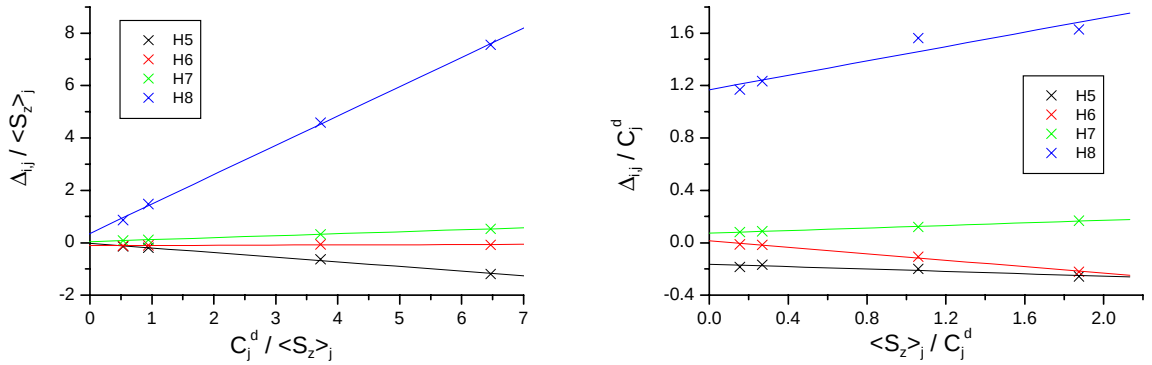

Figure 187 One proton plots of $Ln_2(L^{AB5})_3$ complexes

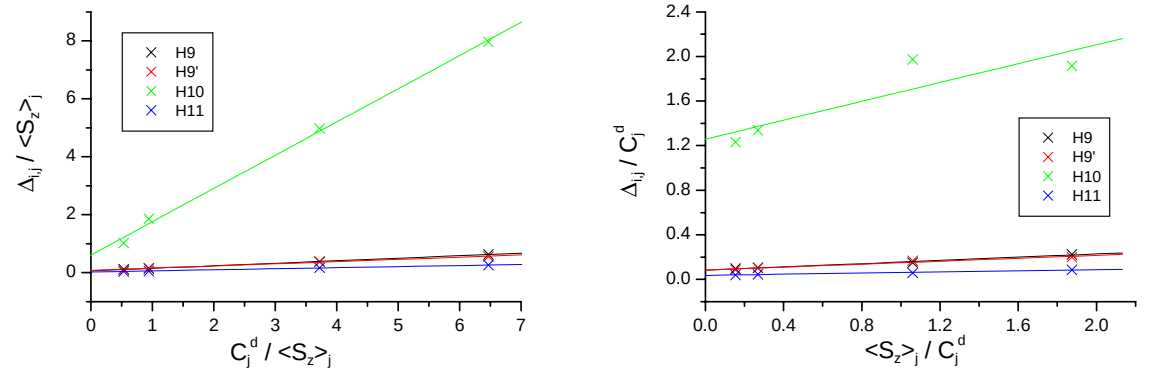

Figure 188 One proton plots of $Ln_2(L^{AB5})_3$ complexes

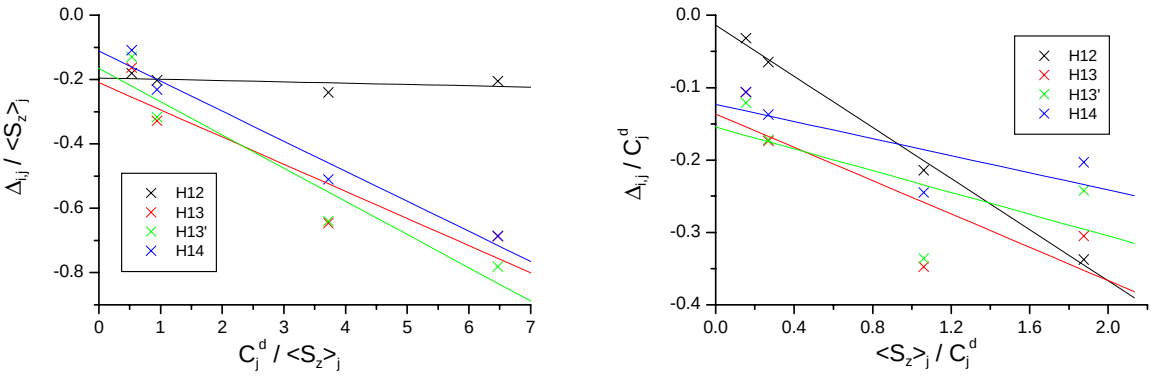

Figure 189 One proton plots of $Ln_2(L^{AB5})_3$ complexes

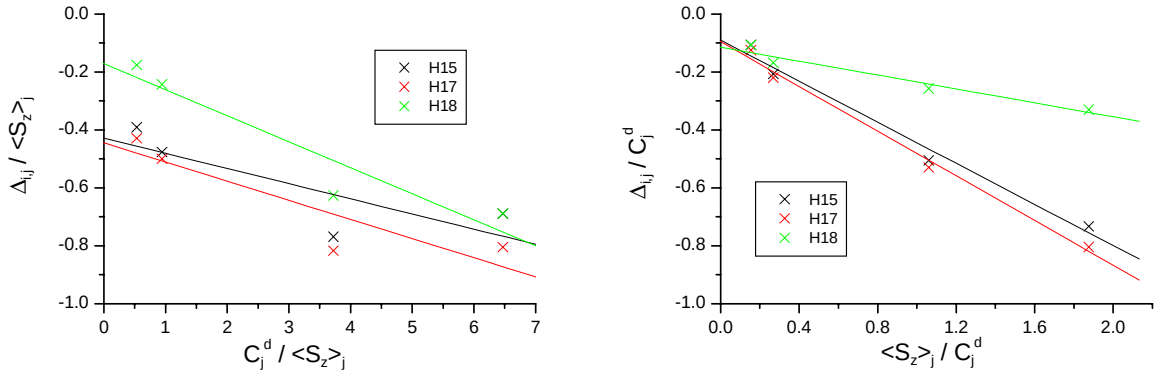

Figure 190 One proton plots of $Ln_2(L^{AB5})_3$ complexes

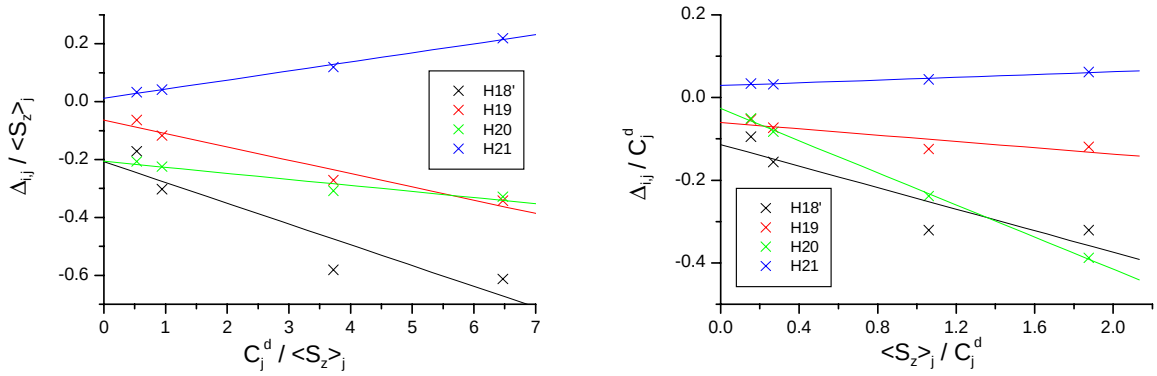

Figure 191 One proton plots of $Ln_2(L^{AB5})_3$ complexes

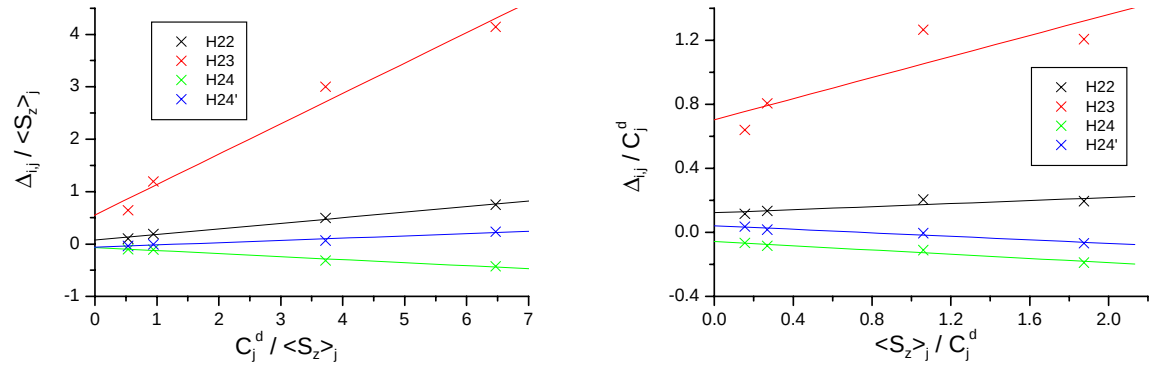

Figure 192 One proton plots of $Ln_2(L^{AB5})_3$ complexes

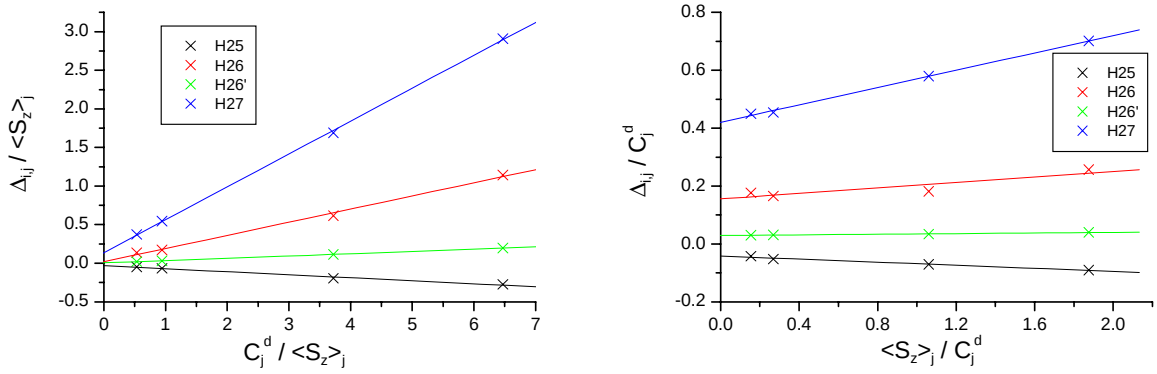

Figure 193 One proton plots of $Ln_2(L^{AB5})_3$ complexes

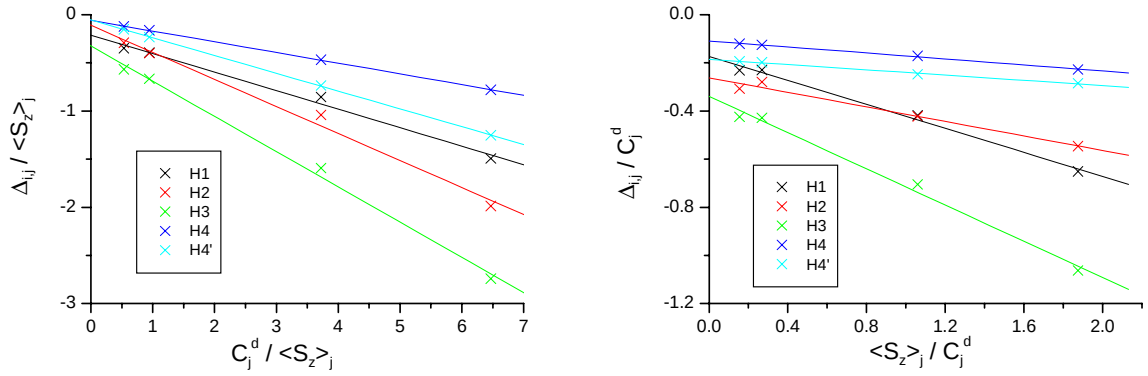

Figure 194 One proton plots of LaLn(L^{AB5})$_3$ complexes

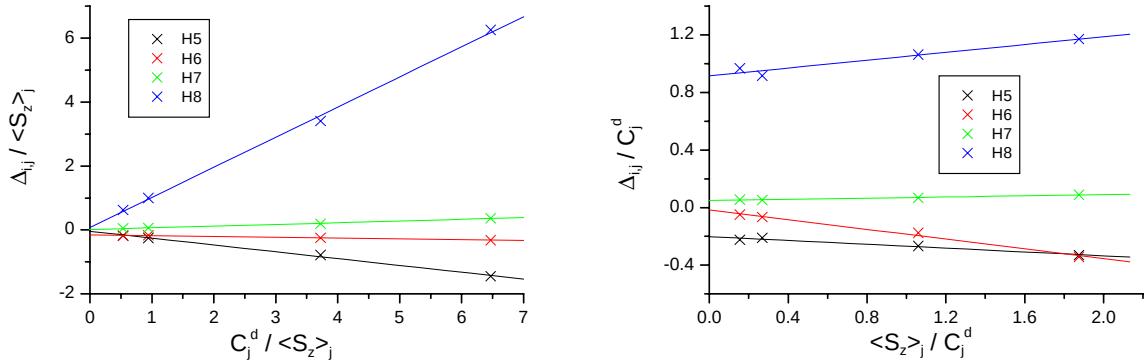

Figure 195 One proton plots of LaLn(L^{AB5})$_3$ complexes

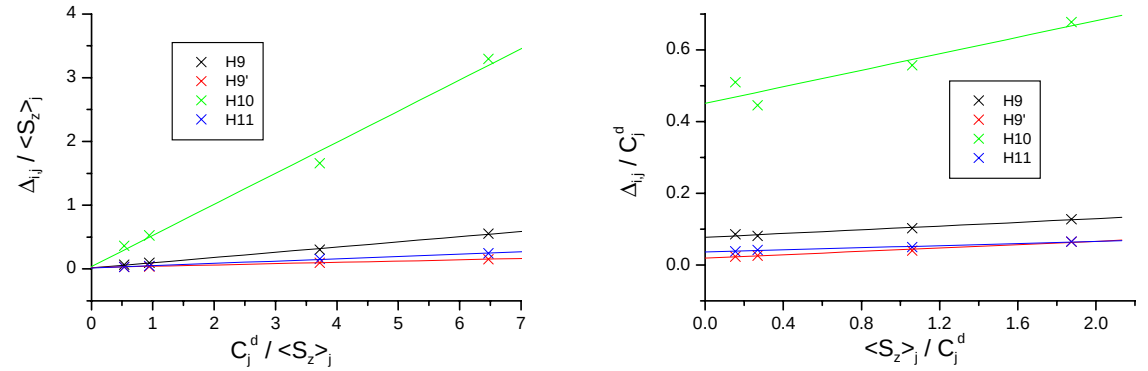

Figure 196 One proton plots of LaLn(L^{AB5})$_3$ complexes

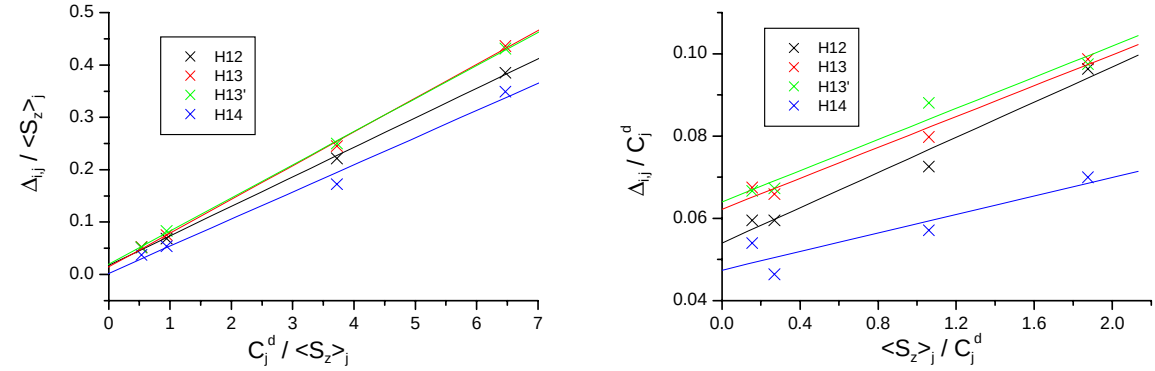

Figure 197 One proton plots of LaLn(L^{AB5})$_3$ complexes

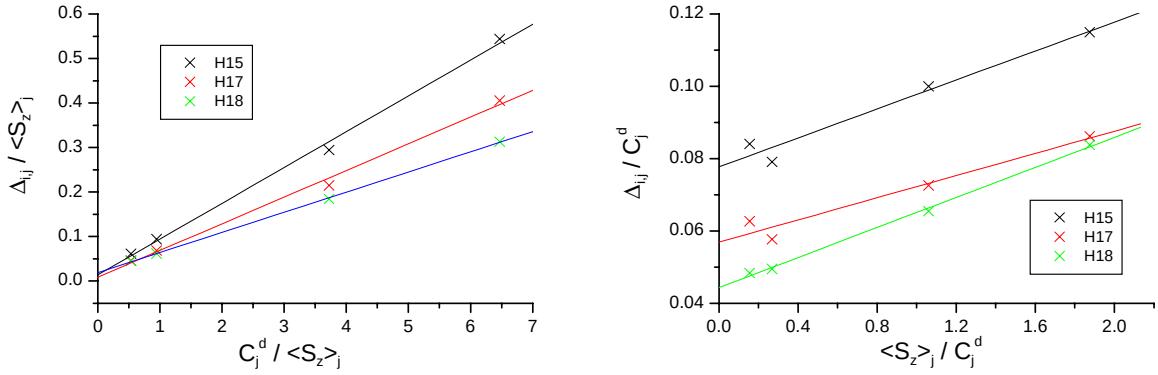

Figure 198 One proton plots of LaLn(L^{AB5})$_3$ complexes

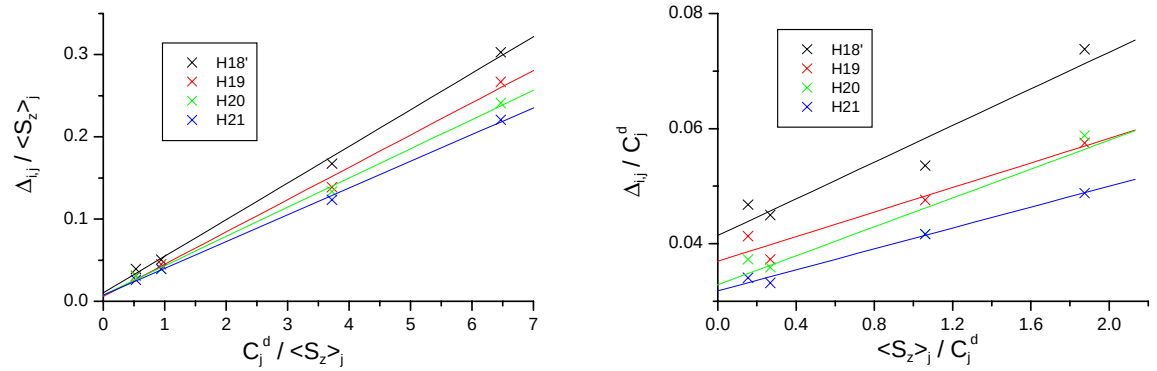

Figure 199 One proton plots of LaLn(L^{AB5})$_3$ complexes

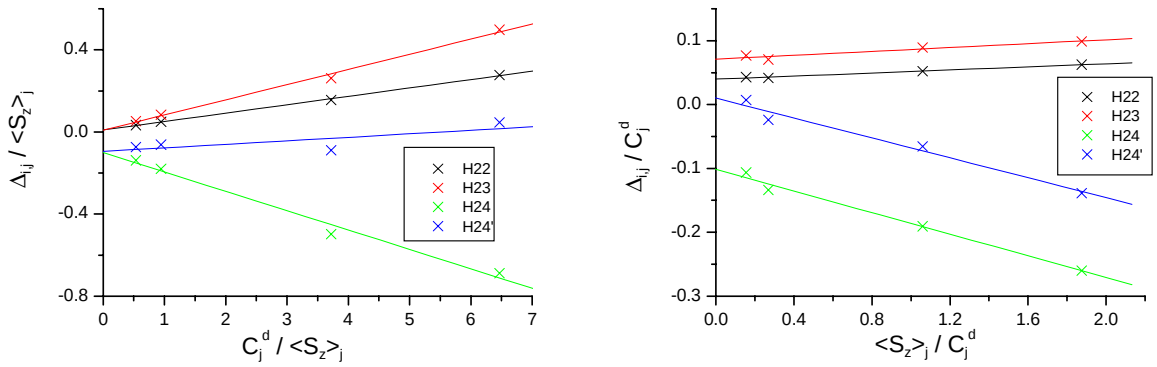

Figure 200 One proton plots of LaLn(L^{AB5})$_3$ complexes

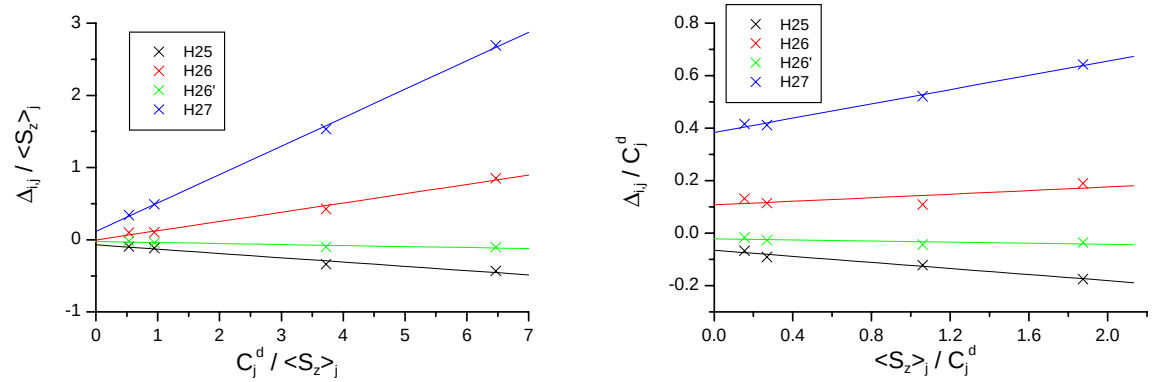

Figure 201 One proton plots of LaLn(L^{AB5})$_3$ complexes

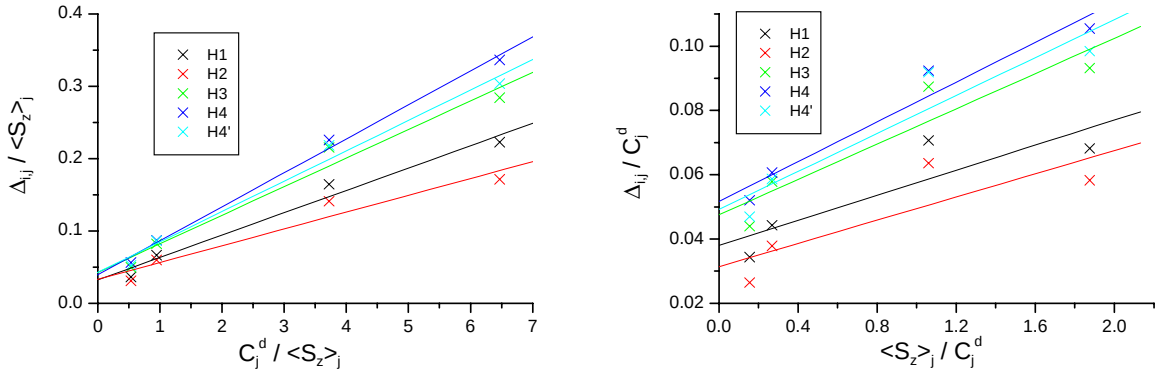

Figure 202 One proton plots of LnLu(L^{AB5})$_3$ complexes

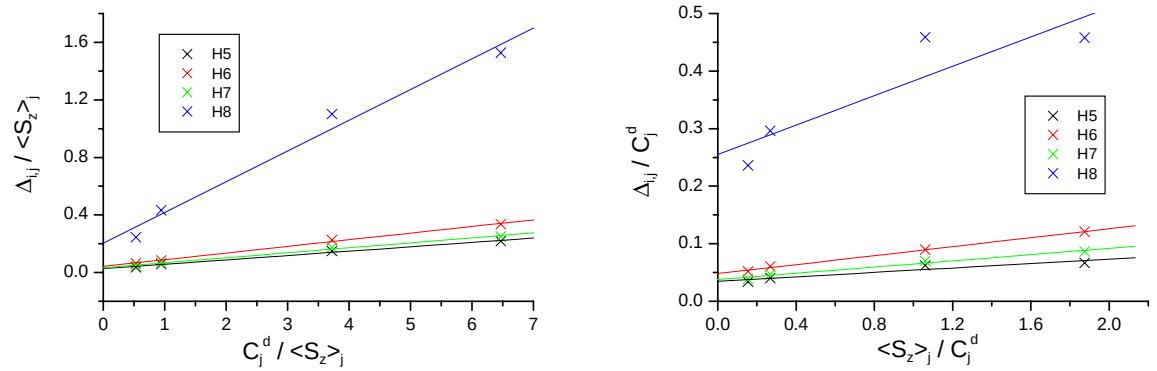

Figure 203 One proton plots of LnLu(L^{AB5})$_3$ complexes

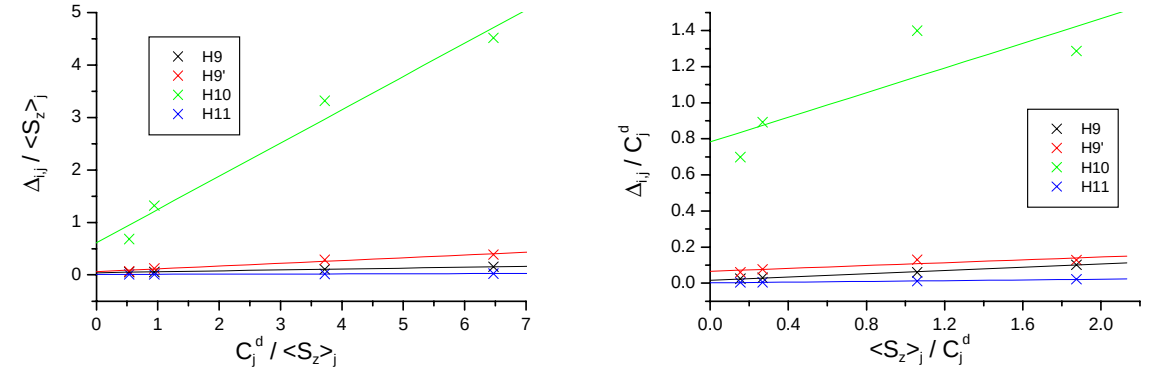

Figure 204 One proton plots of LnLu(L^{AB5})$_3$ complexes

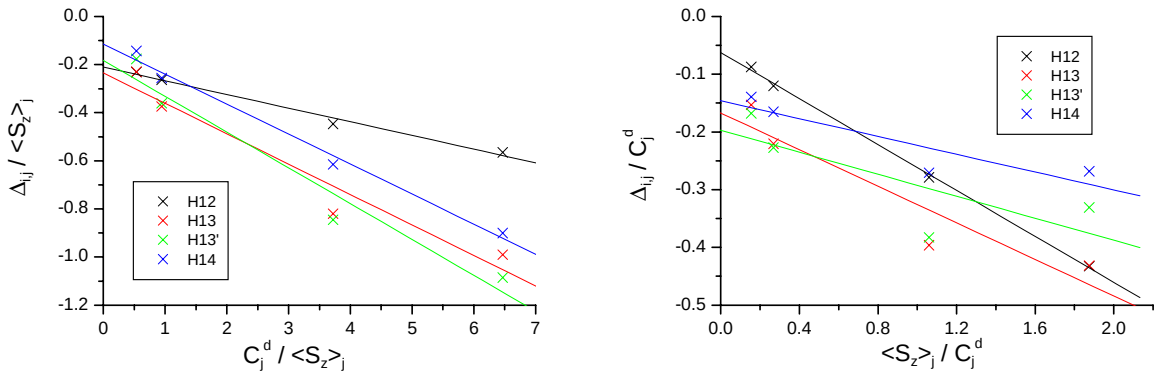

Figure 205 One proton plots of LnLu(L^{AB5})$_3$ complexes

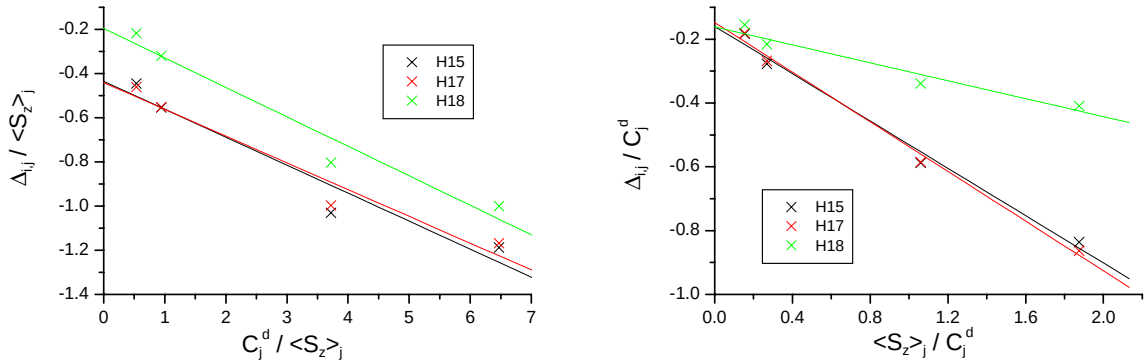

Figure 206 One proton plots of LnLu(L^{AB5})$_3$ complexes

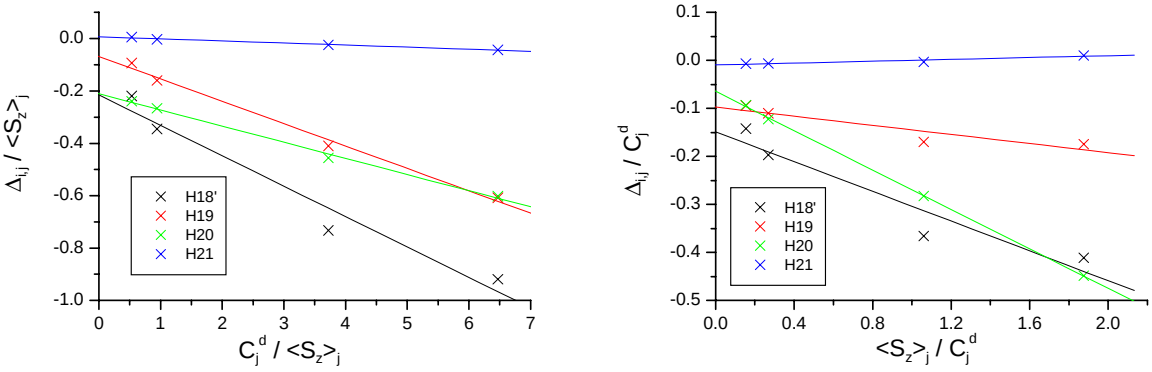

Figure 207 One proton plots of LnLu(L^{AB5})$_3$ complexes

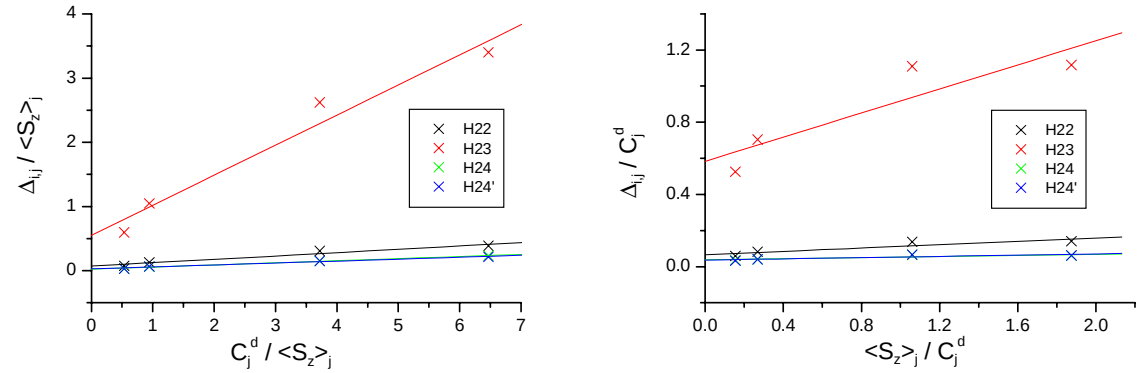

Figure 208 One proton plots of LnLu(L^{AB5})$_3$ complexes

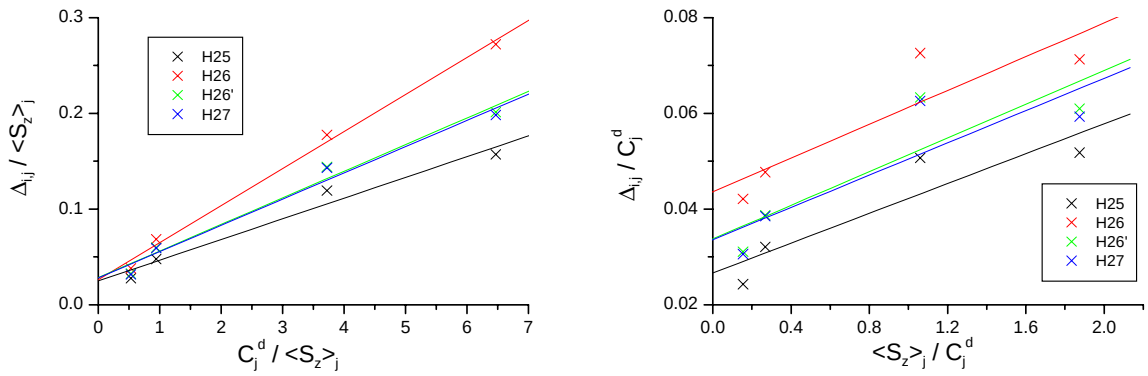

Figure 209 One proton plots of LnLu(L^{AB5})$_3$ complexes

Appendix 2 Two proton plots

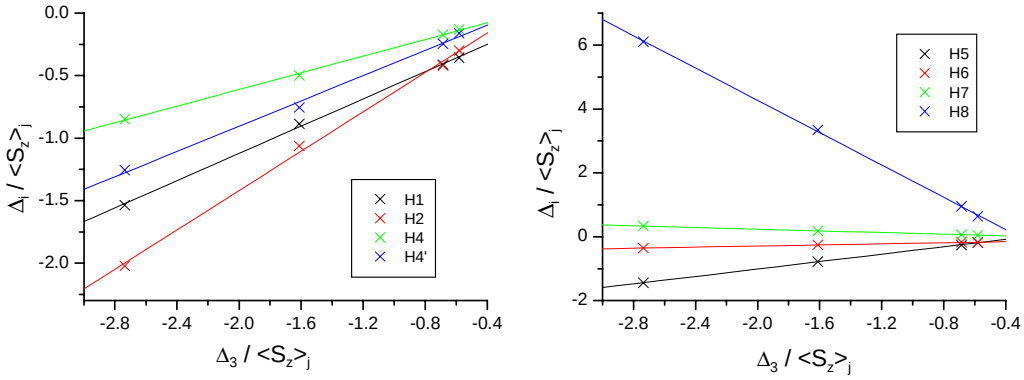

Figure 210 Two proton plots of LaLn(L^{AB})$_3$ complexes using H3 as reference

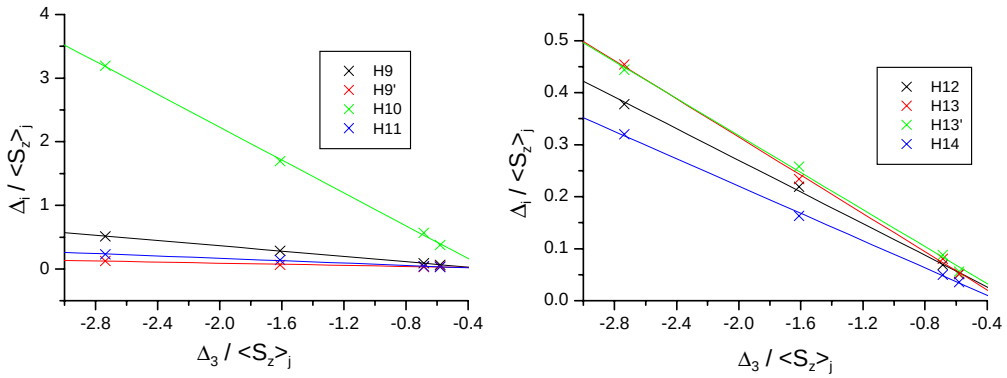

Figure 211 Two proton plots of LaLn(L^{AB})$_3$ complexes using H3 as reference

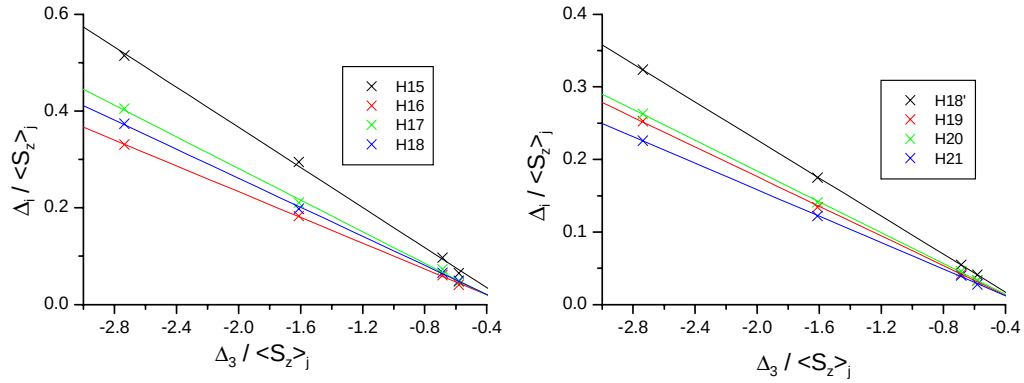

Figure 212 Two proton plots of LaLn(L^{AB})$_3$ complexes using H3 as reference

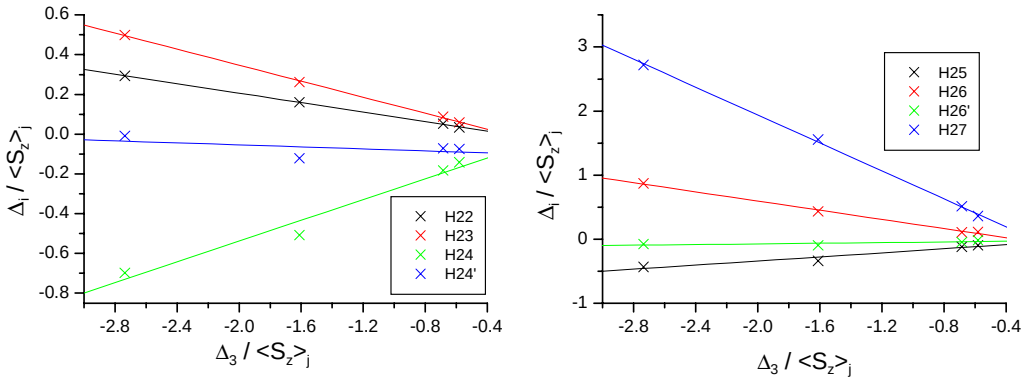

Figure 213 Two proton plots of LaLn(L^{AB})$_3$ complexes using H3 as reference

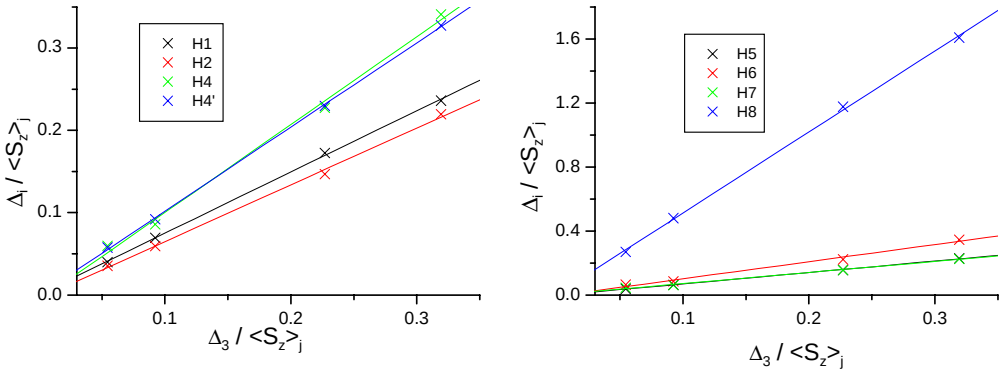

Figure 214 Two proton plots of LnLu(L^{AB})$_3$ complexes using H3 as reference

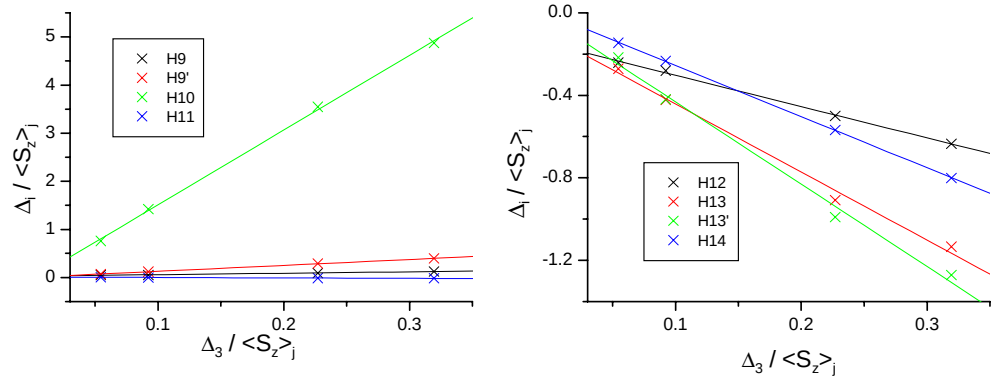

Figure 215 Two proton plots of LnLu(L^{AB})$_3$ complexes using H3 as reference

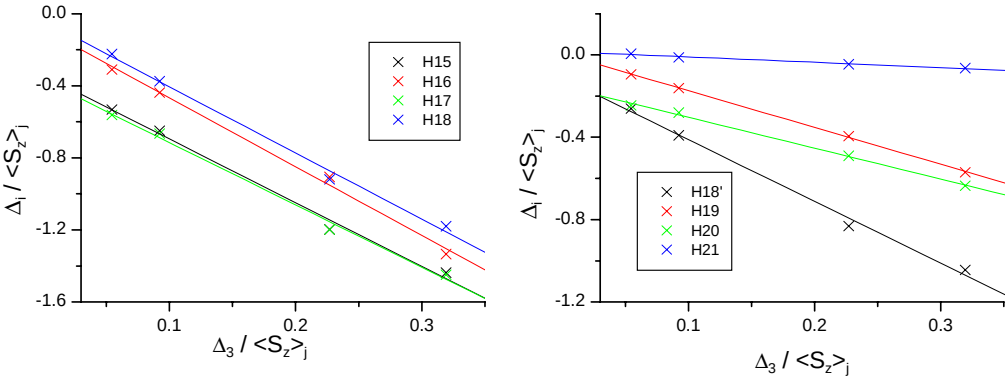

Figure 216 Two proton plots of LnLu(L^{AB})$_3$ complexes using H3 as reference

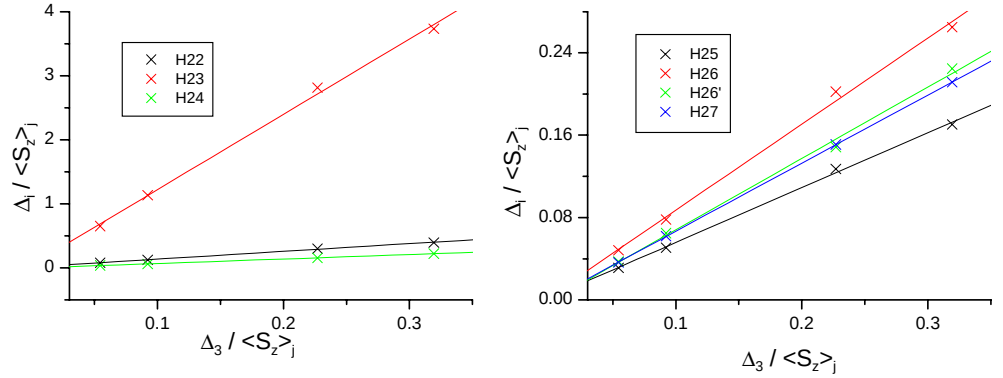

Figure 217 Two proton plots of LnLu(L^{AB})$_3$ complexes using H3 as reference

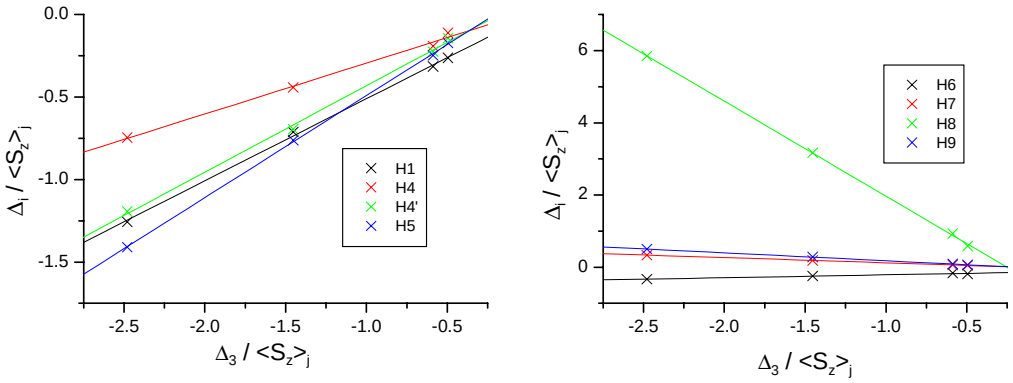

Figure 218 Two proton plots of LaLn(L^{AB3})$_3$ complexes using H3 as reference

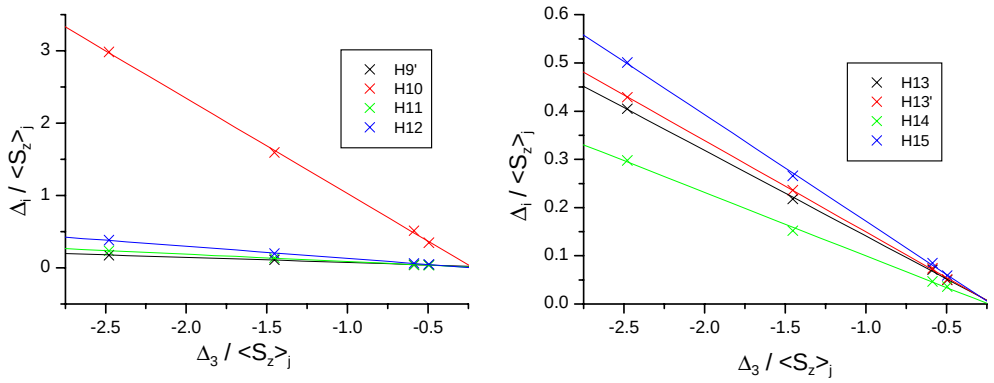

Figure 219 Two proton plots of LaLn(L^{AB3})$_3$ complexes using H3 as reference

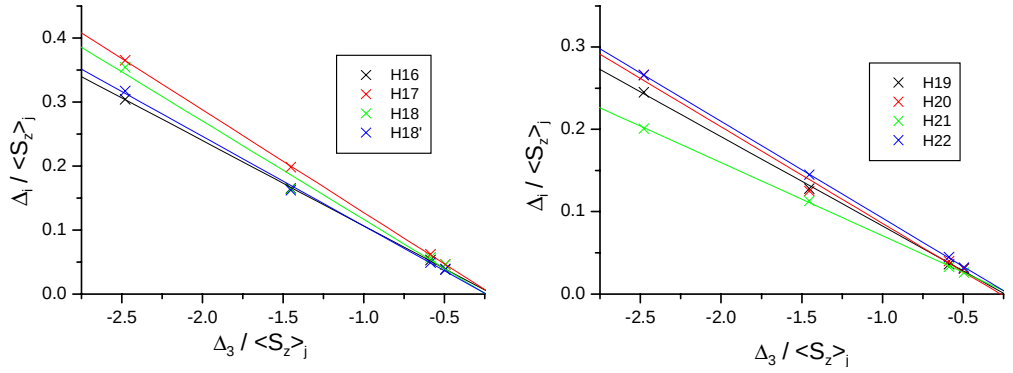

Figure 220 Two proton plots of LaLn(L^{AB3})$_3$ complexes using H3 as reference

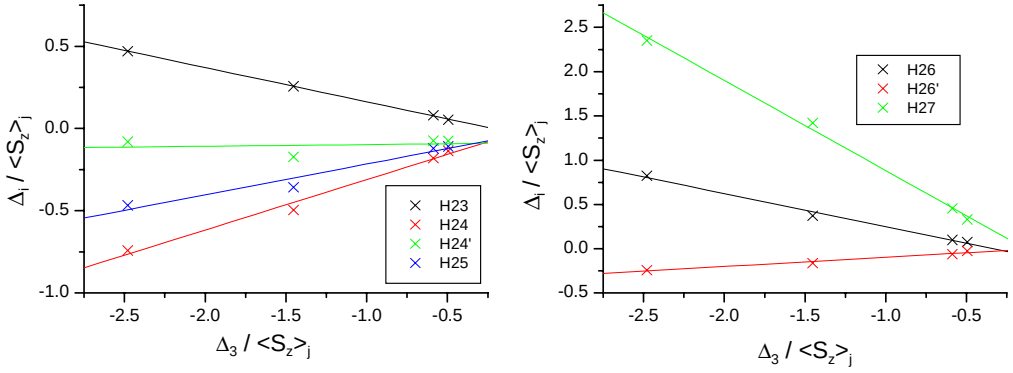

Figure 221 Two proton plots of LaLn(L^{AB3})$_3$ complexes using H3 as reference

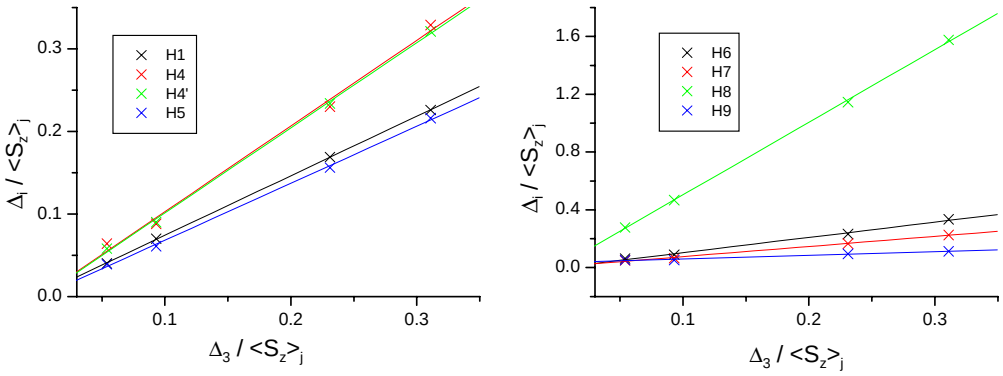

Figure 222 Two proton plots of LnLu(L^{AB3})$_3$ complexes using H3 as reference

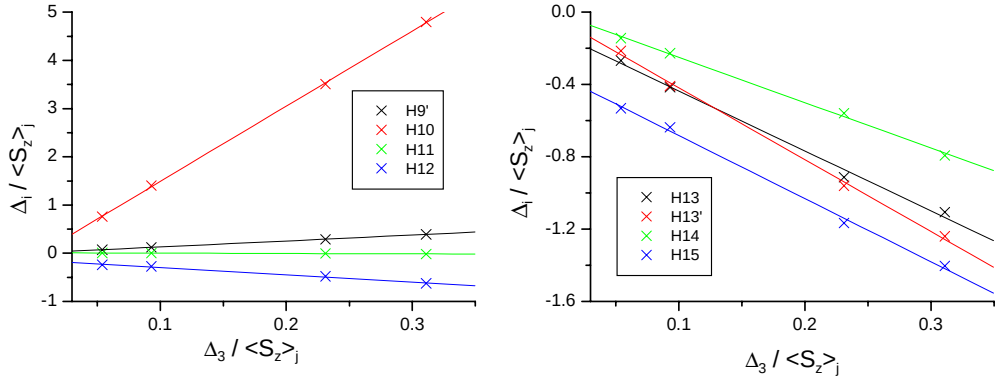

Figure 223 Two proton plots of LnLu(L^{AB3})$_3$ complexes using H3 as reference

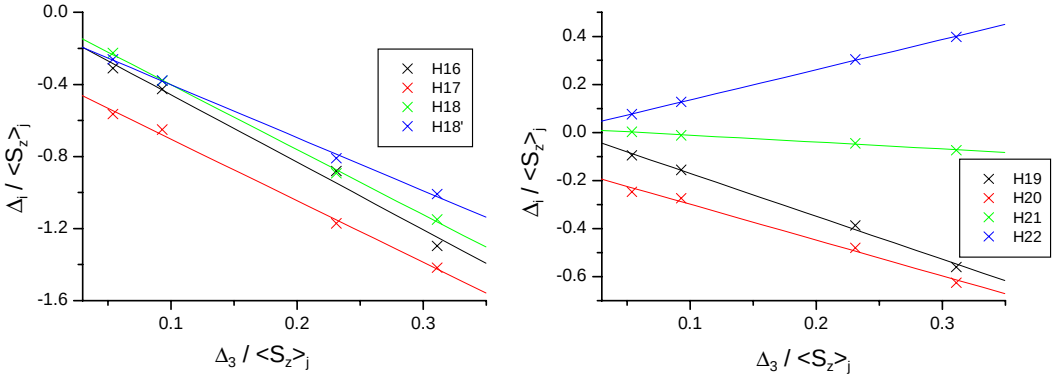

Figure 224 Two proton plots of LnLu(L^{AB3})$_3$ complexes using H3 as reference

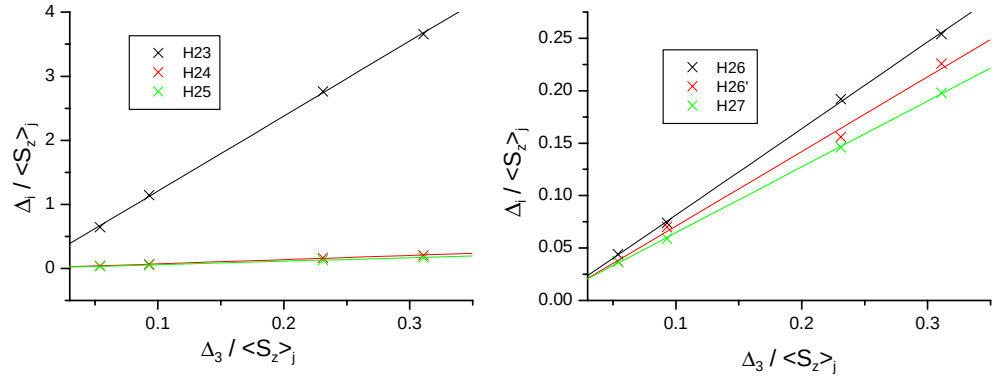

Figure 225 Two proton plots of LnLu(L^{AB3})$_3$ complexes using H3 as reference

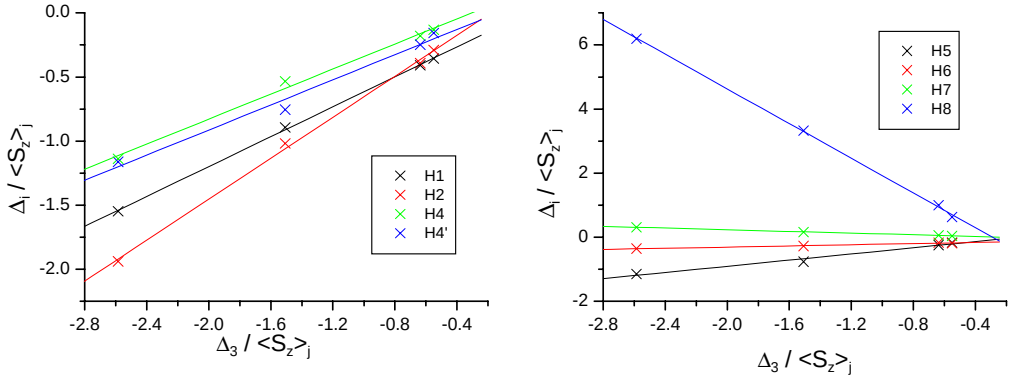

Figure 226 Two proton plots of LaLn(L^{AB4})$_3$ complexes using H3 as reference

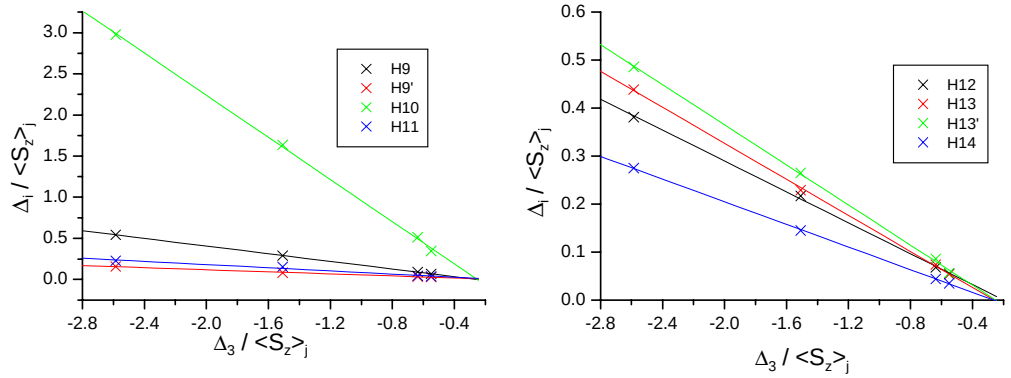

Figure 227 Two proton plots of LaLn(L^{AB4})$_3$ complexes using H3 as reference

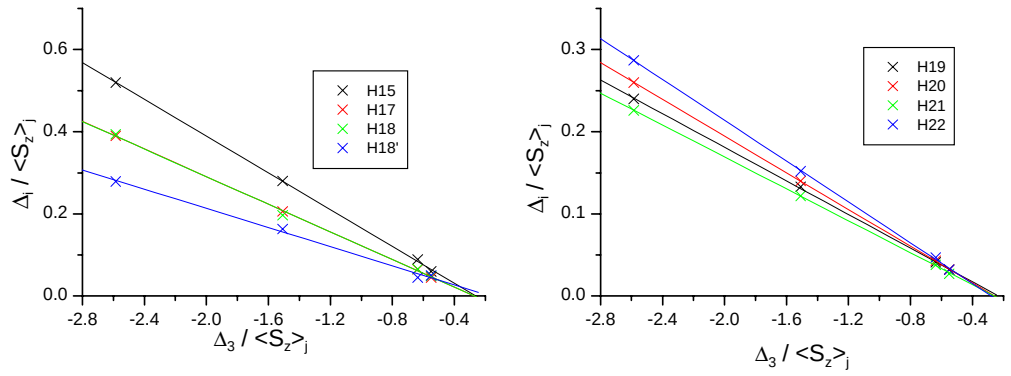

Figure 228 Two proton plots of LaLn(L^{AB4})$_3$ complexes using H3 as reference

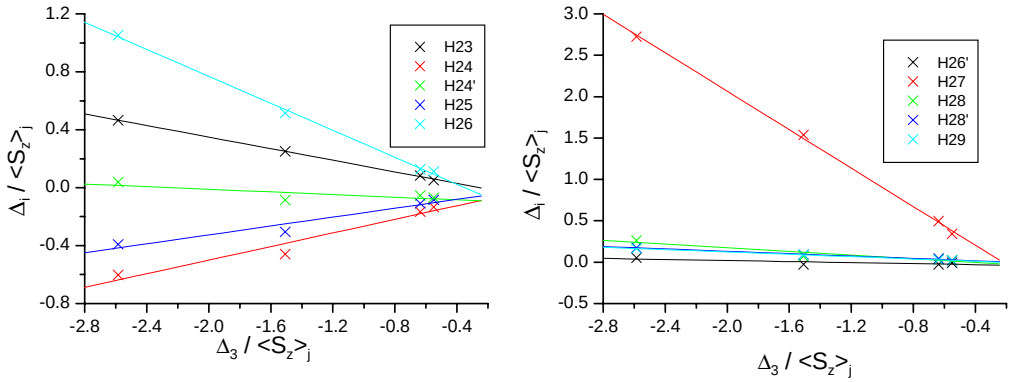

Figure 229 Two proton plots of LaLn(L^{AB4})$_3$ complexes using H3 as reference

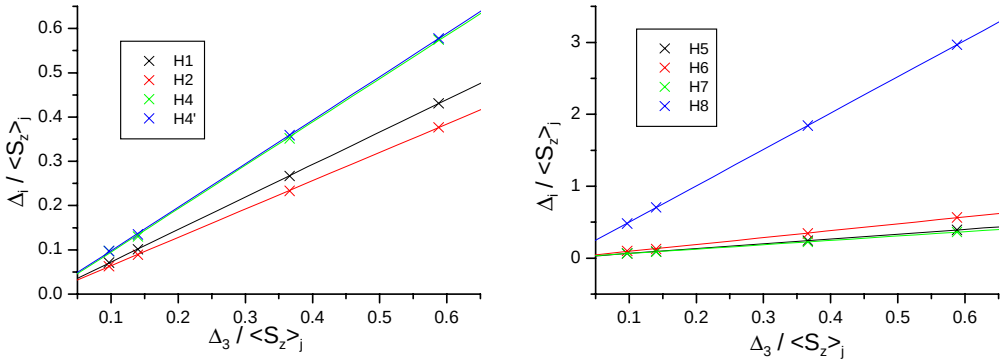

Figure 230 Two proton plots of LnLu(L^{AB4})$_3$ complexes using H3 as reference

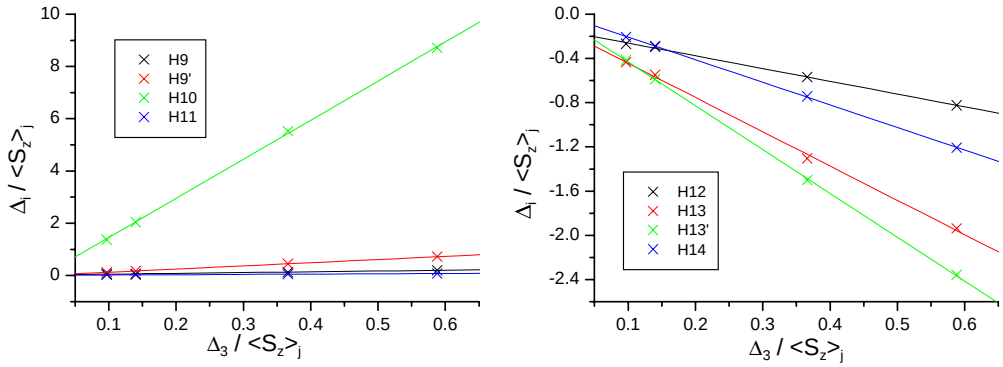

Figure 231 Two proton plots of LnLu(L^{AB4})$_3$ complexes using H3 as reference

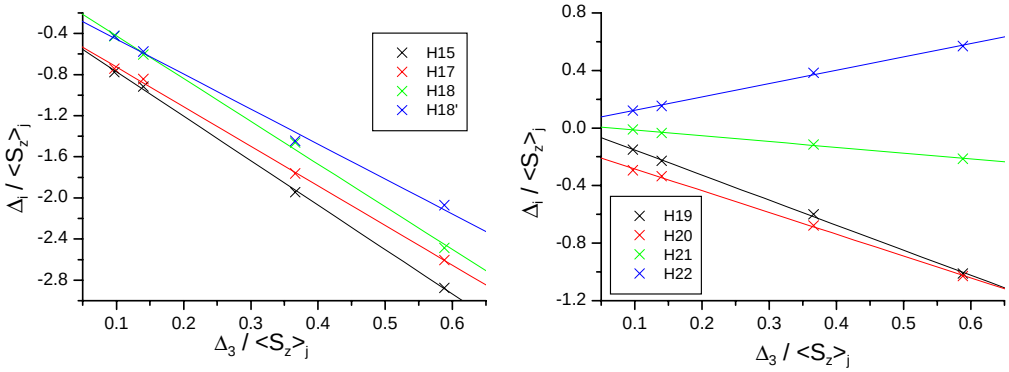

Figure 232 Two proton plots of LnLu(L^{AB4})$_3$ complexes using H3 as reference

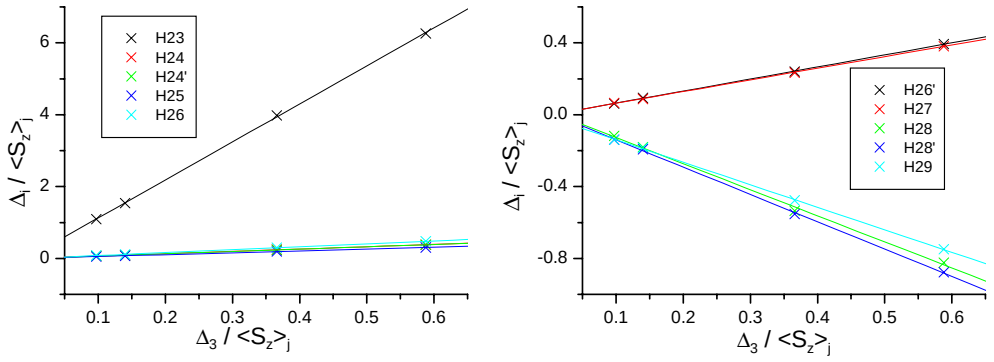

Figure 233 Two proton plots of LnLu(L^{AB4})$_3$ complexes using H3 as reference

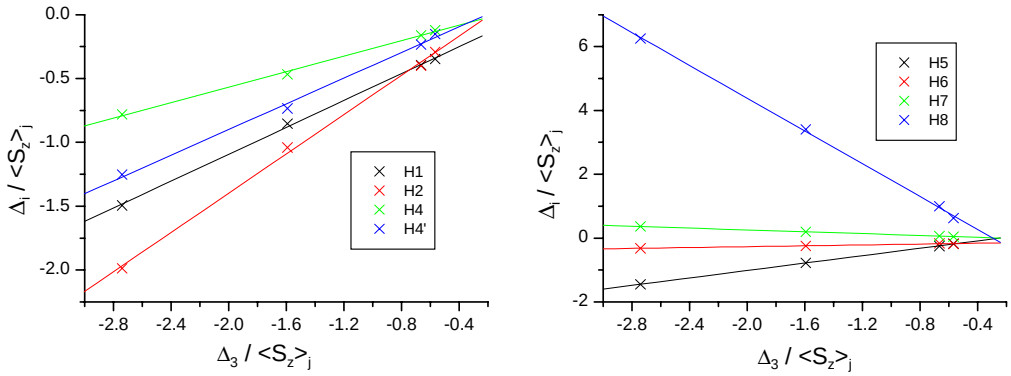

Figure 234 Two proton plots of LaLn(L^{AB5})$_3$ complexes using H3 as reference

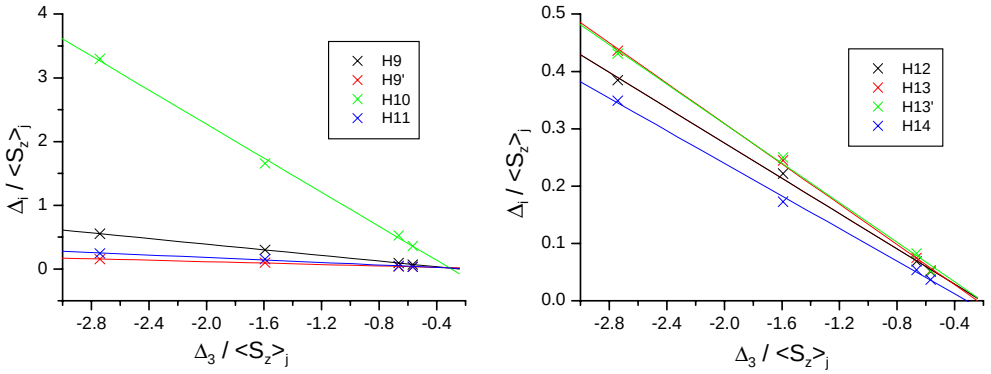

Figure 235 Two proton plots of LaLn(L^{AB5})$_3$ complexes using H3 as reference

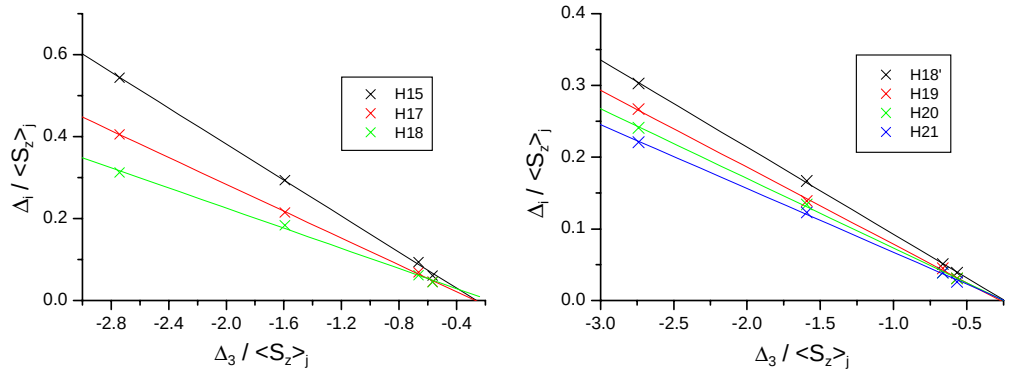

Figure 236 Two proton plots of LaLn(L^{AB5})$_3$ complexes using H3 as reference

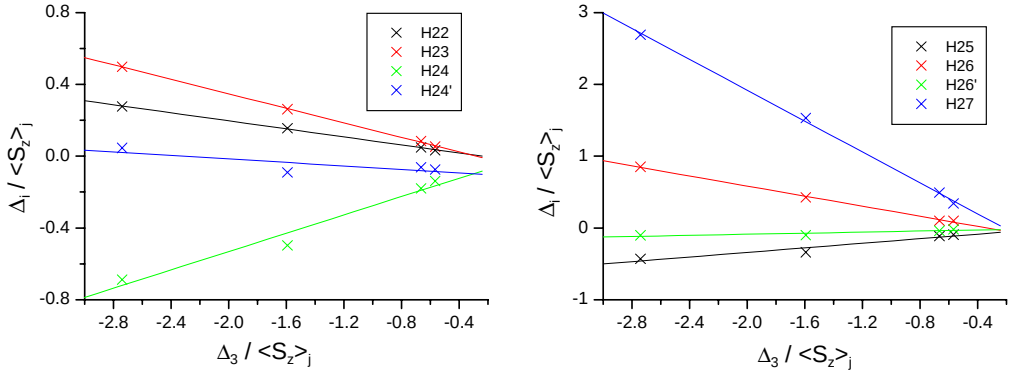

Figure 237 Two proton plots of LaLn(L^{AB5})$_3$ complexes using H3 as reference

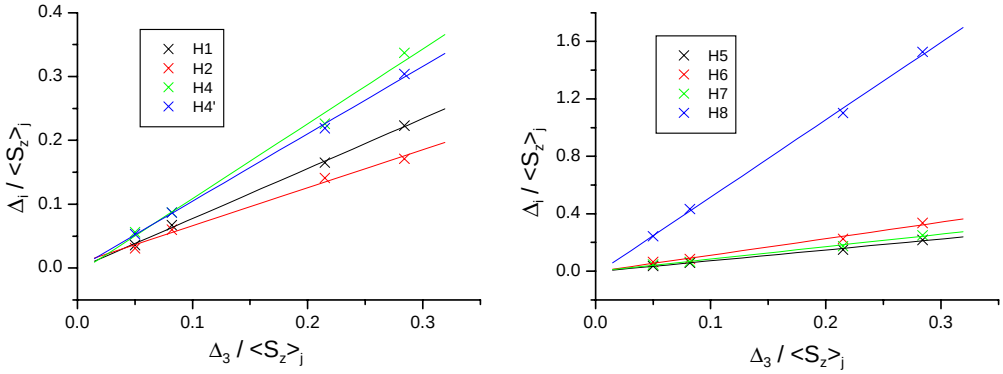

Figure 238 Two proton plots of LnLu(L^{AB5})$_3$ complexes using H3 as reference

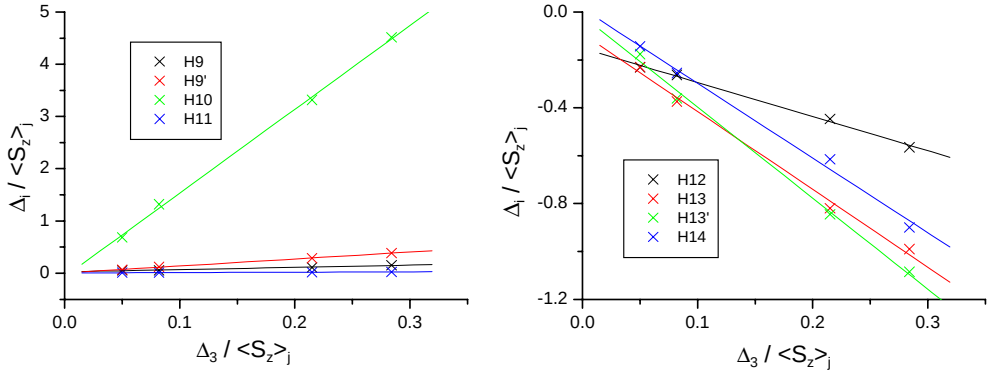

Figure 239 Two proton plots of LnLu(L^{AB5})$_3$ complexes using H3 as reference

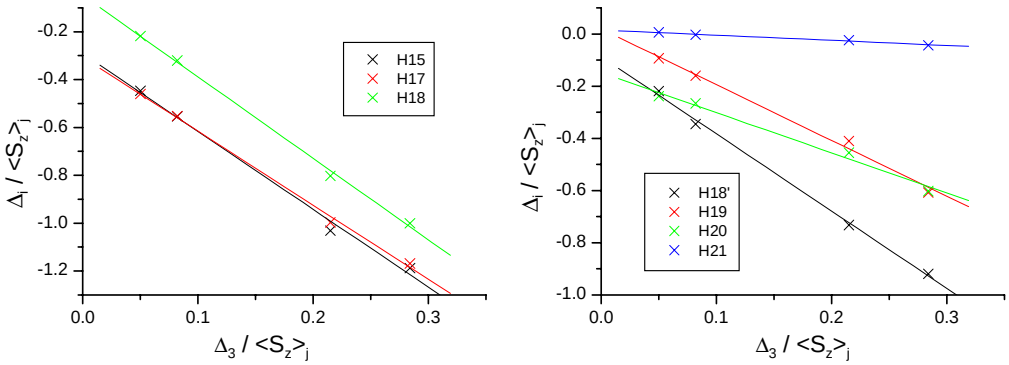

Figure 240 Two proton plots of LnLu(L^{AB5})$_3$ complexes using H3 as reference

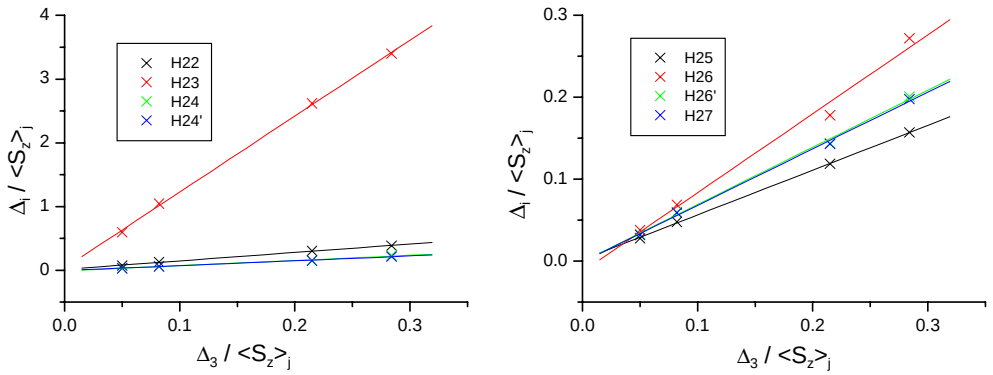

Figure 241 Two proton plots of LnLu(L^{AB5})$_3$ complexes using H3 as reference

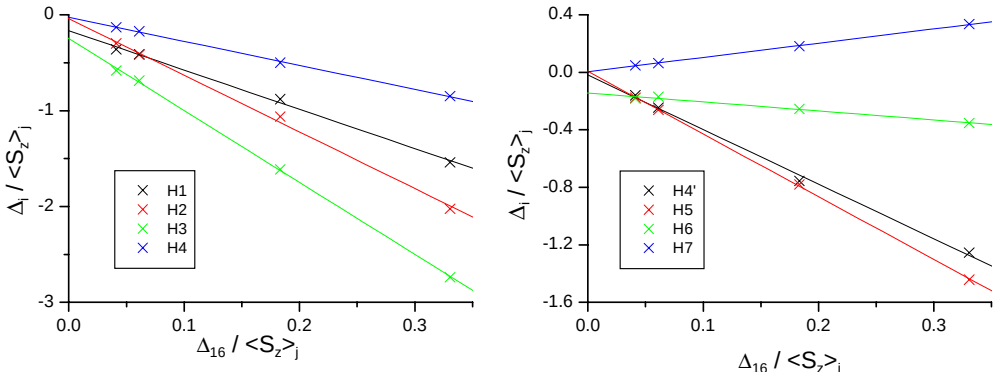

Figure 242 Two proton plots of LaLn(L^{AB})$_3$ complexes using H16 as reference

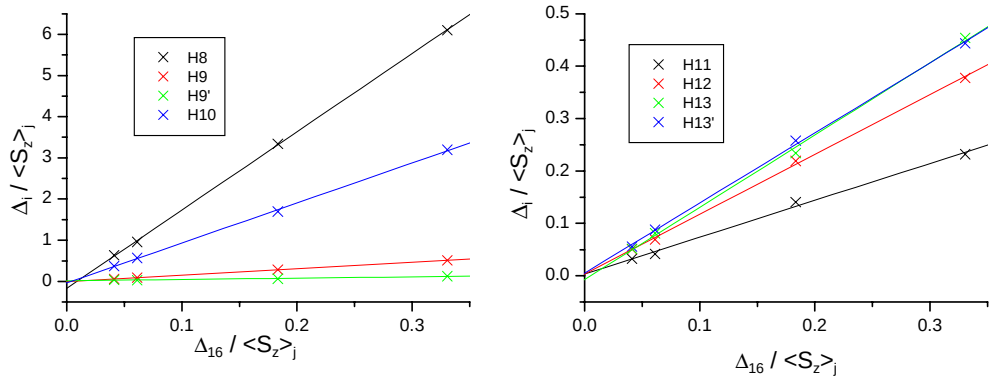

Figure 243 Two proton plots of LaLn(L^{AB})$_3$ complexes using H16 as reference

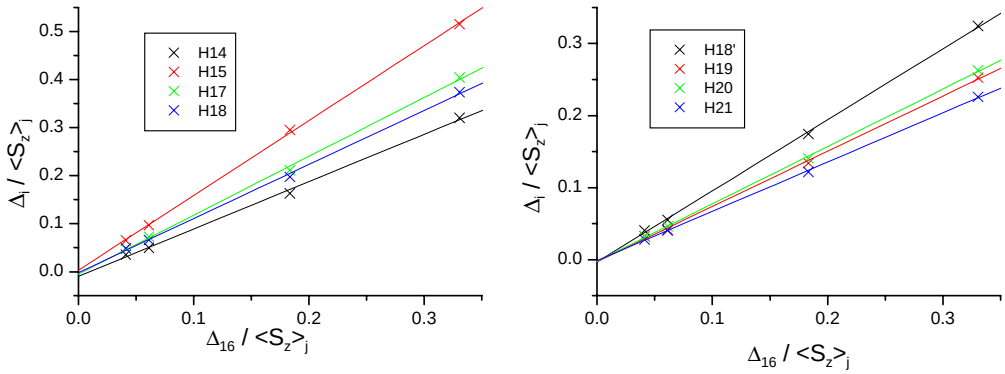

Figure 244 Two proton plots of LaLn(L^{AB})$_3$ complexes using H16 as reference

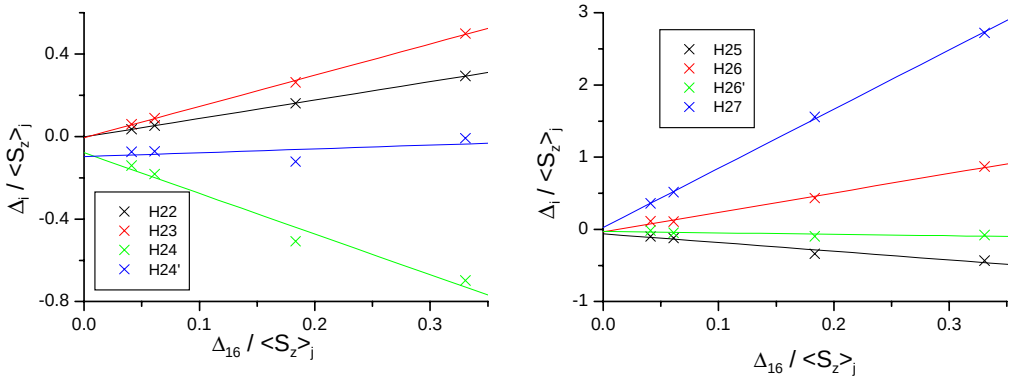

Figure 245 Two proton plots of LaLn(L^{AB})$_3$ complexes using H16 as reference

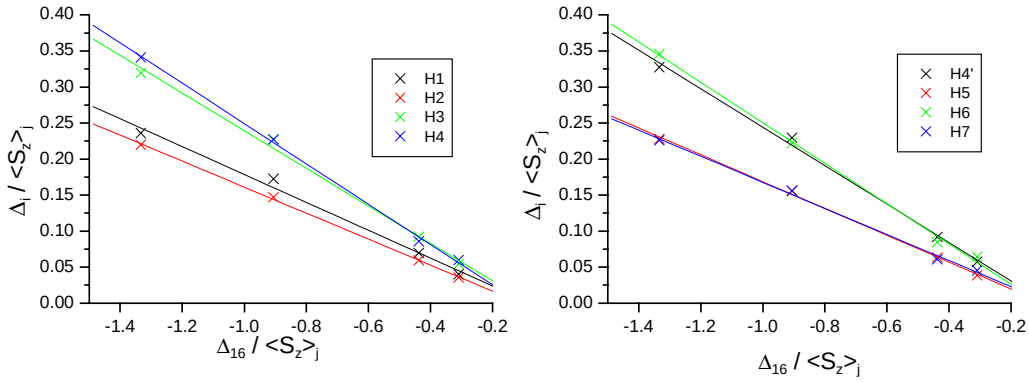

Figure 246 Two proton plots of LnLu(L^{AB})$_3$ complexes using H16 as reference

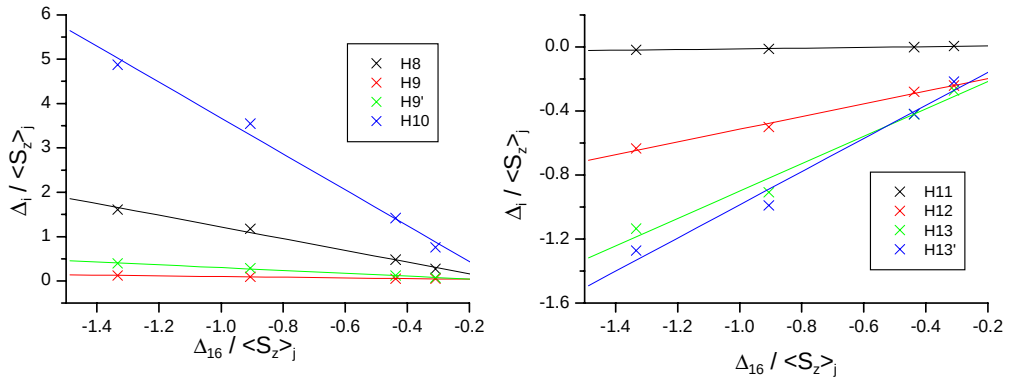

Figure 247 Two proton plots of LnLu(L^{AB})$_3$ complexes using H16 as reference

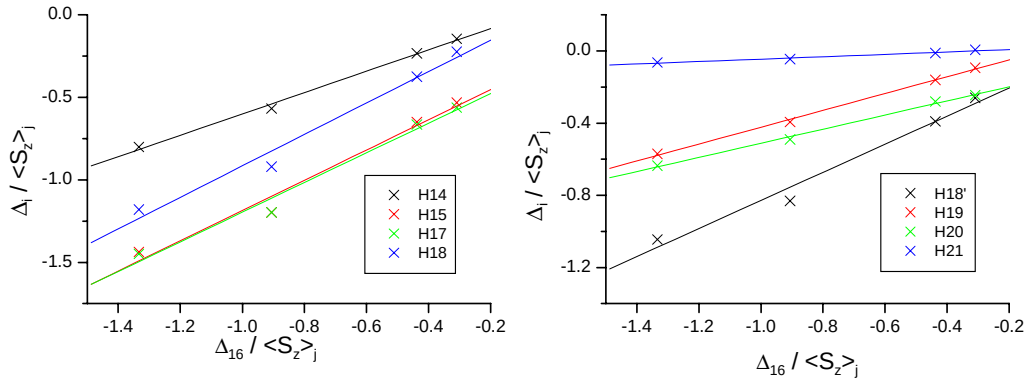

Figure 248 Two proton plots of LnLu(L^{AB})$_3$ complexes using H16 as reference

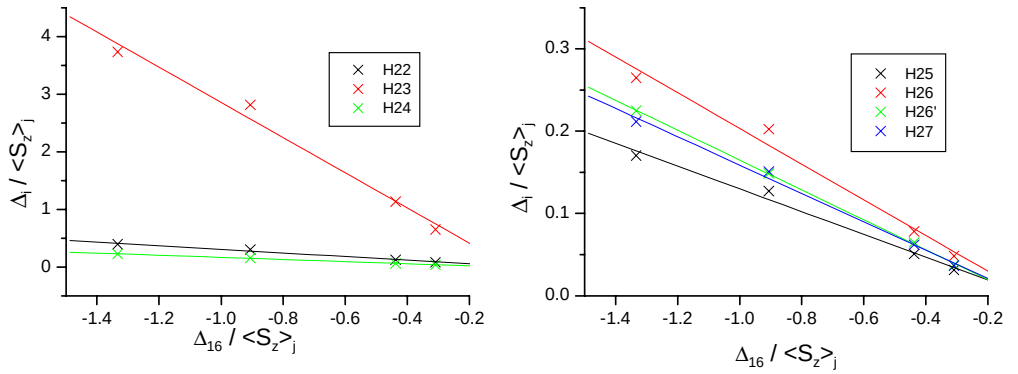

Figure 249 Two proton plots of LnLu(L^{AB})$_3$ complexes using H16 as reference

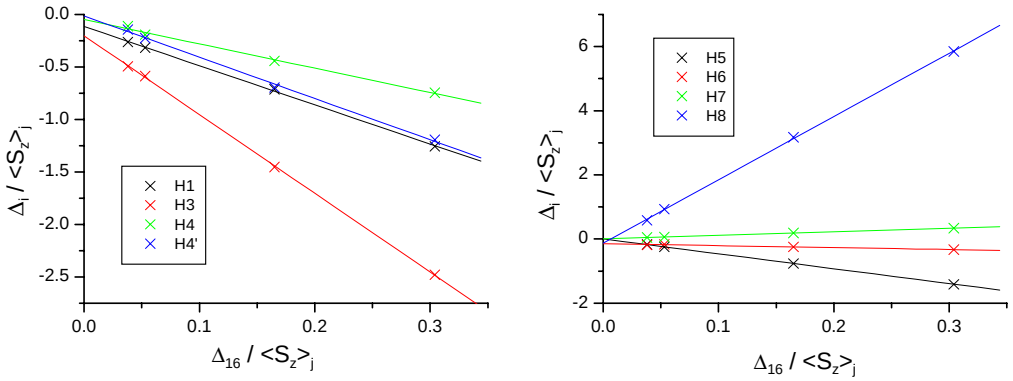

Figure 250 Two proton plots of LaLn(L^{AB3})$_3$ complexes using H16 as reference

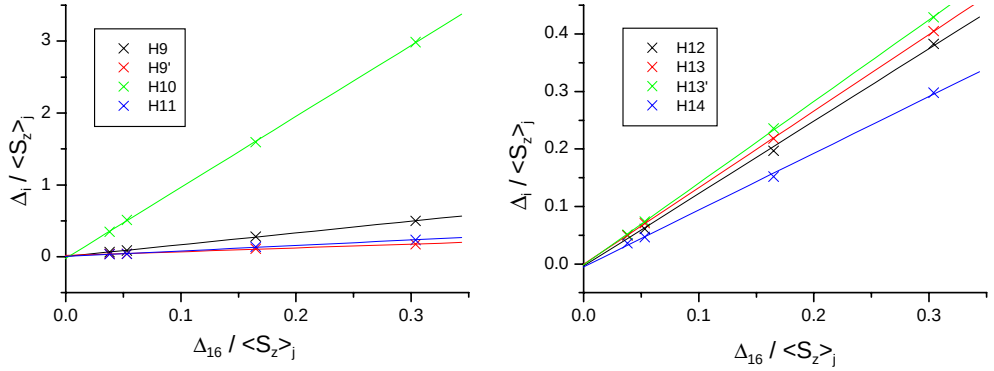

Figure 251 Two proton plots of LaLn(L^{AB3})$_3$ complexes using H16 as reference

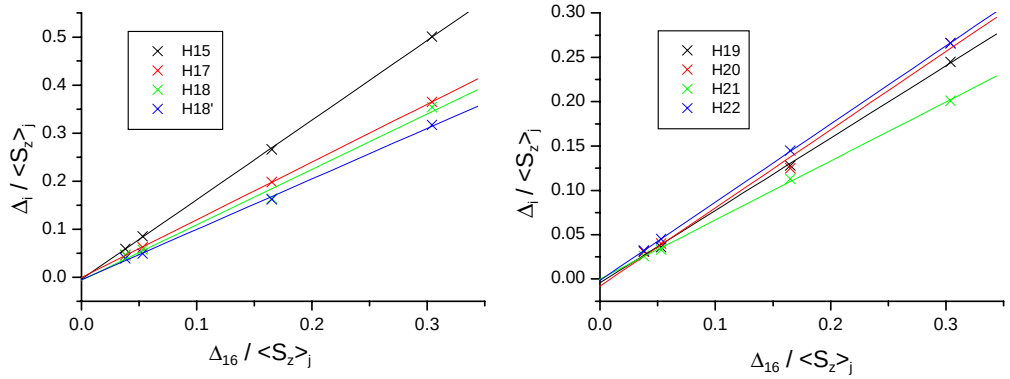

Figure 252 Two proton plots of LaLn(L^{AB3})$_3$ complexes using H16 as reference

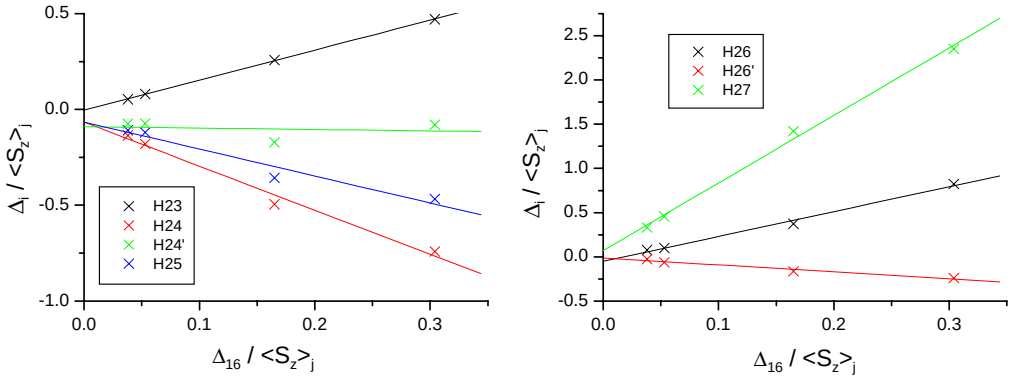

Figure 253 Two proton plots of LaLn(L^{AB3})$_3$ complexes using H16 as reference

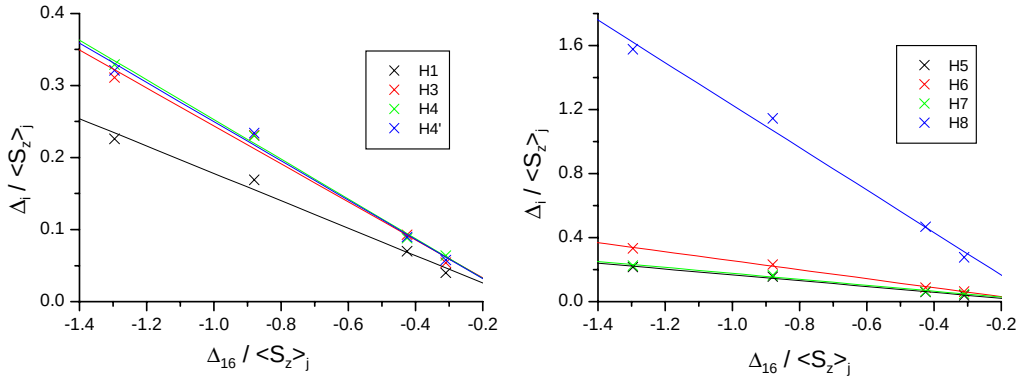

Figure 254 Two proton plots of LnLu(L^{AB3})$_3$ complexes using H16 as reference

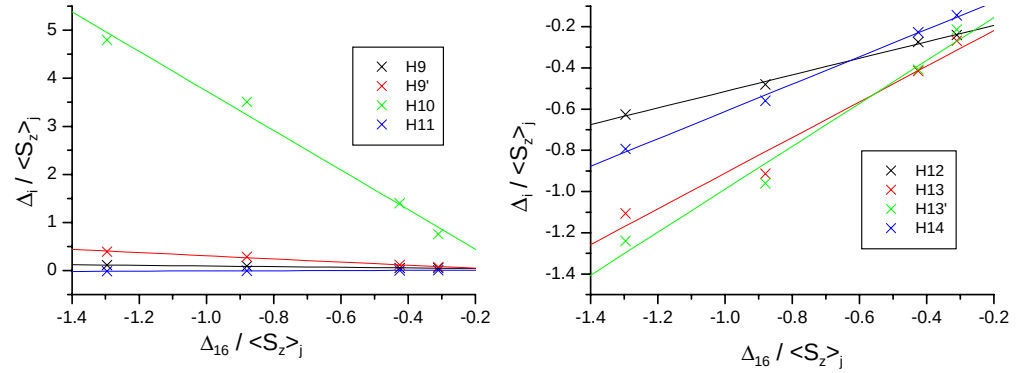

Figure 255 Two proton plots of LnLu(L^{AB3})$_3$ complexes using H16 as reference

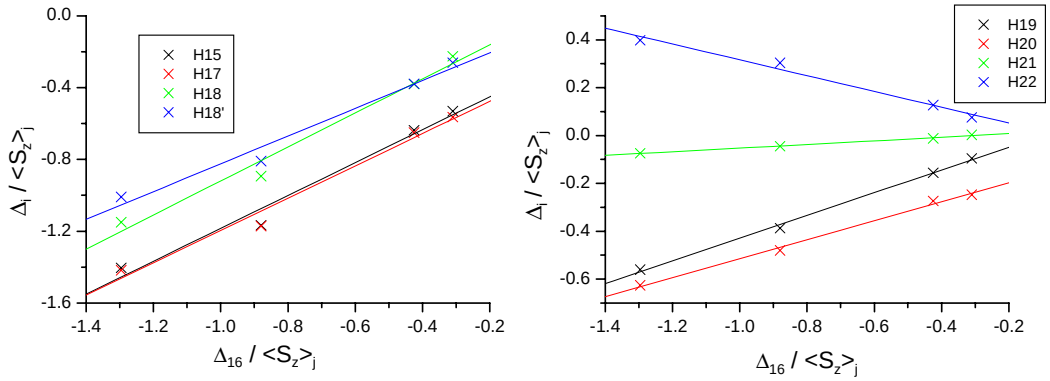

Figure 256 Two proton plots of LnLu(L^{AB3})$_3$ complexes using H16 as reference

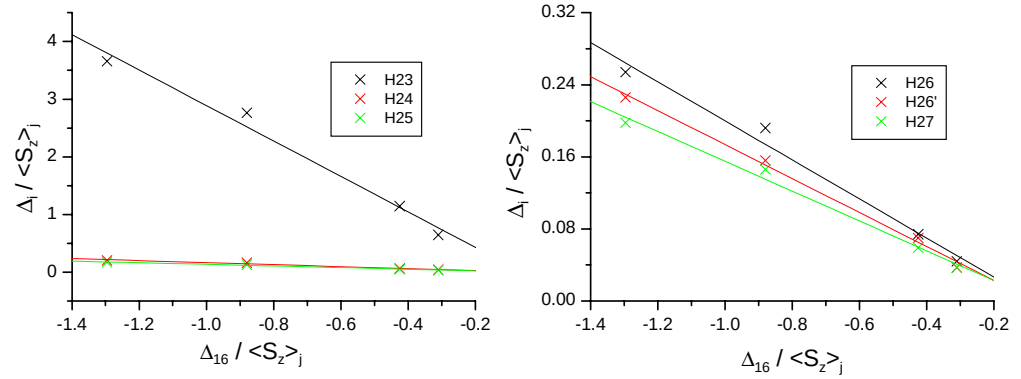

Figure 257 Two proton plots of LnLu(L^{AB3})$_3$ complexes using H16 as reference

Appendix 3 Modified one proton plots

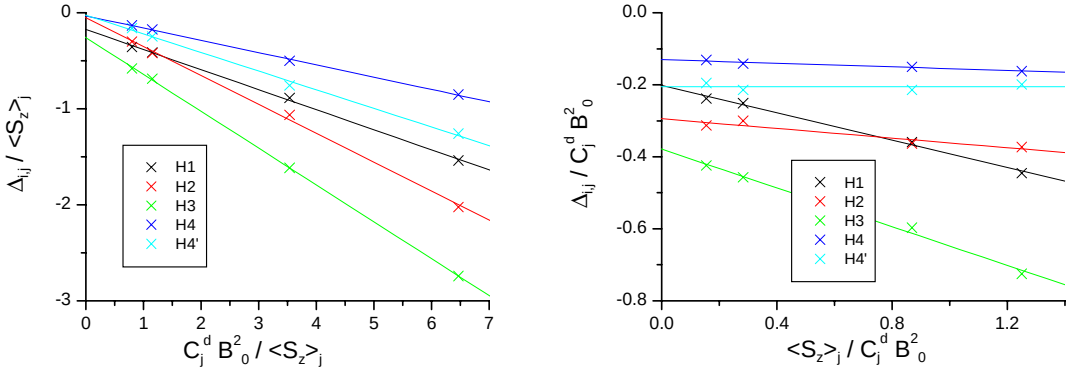

Figure 258 Modified one proton plots of LaLn(L^{AB})$_3$ complexes

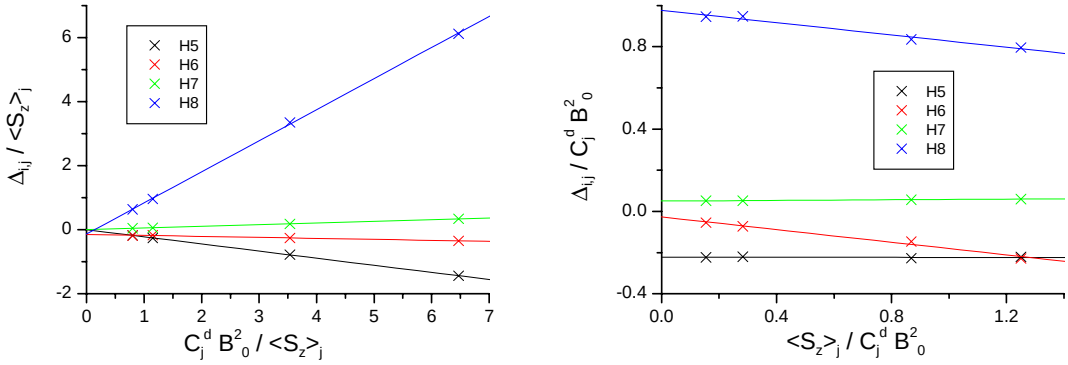

Figure 259 Modified one proton plots of LaLn(L^{AB})$_3$ complexes

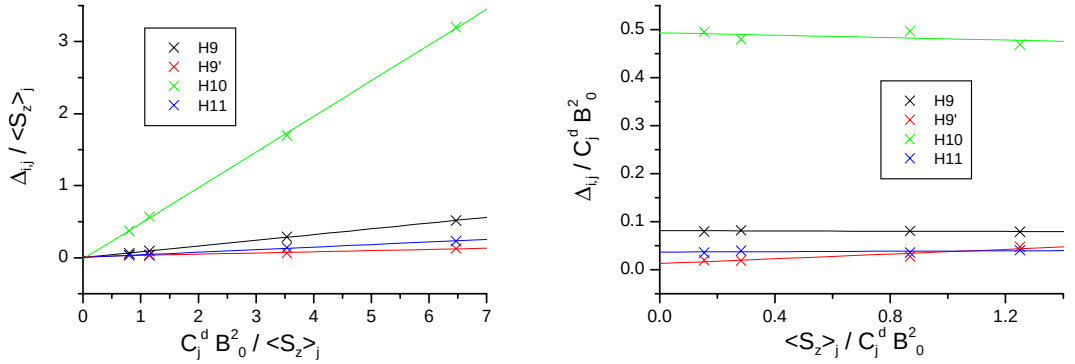

Figure 260 Modified one proton plots of LaLn(L^{AB})$_3$ complexes

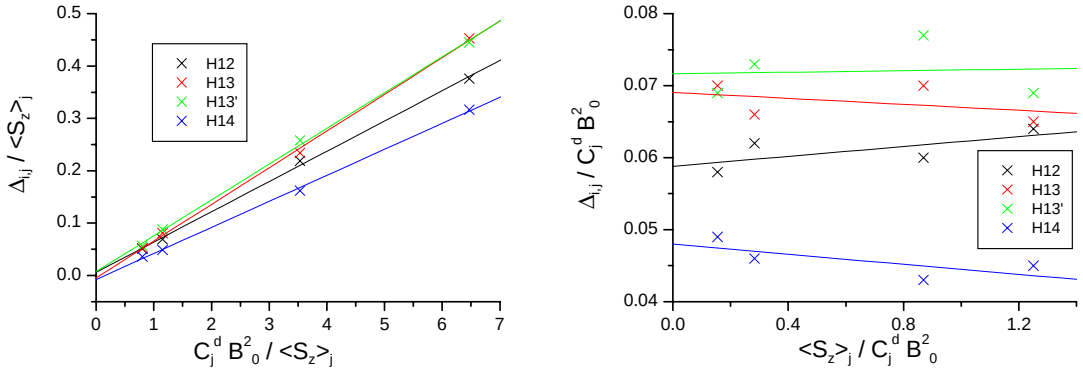

Figure 261 Modified one proton plots of LaLn(L^{AB})$_3$ complexes

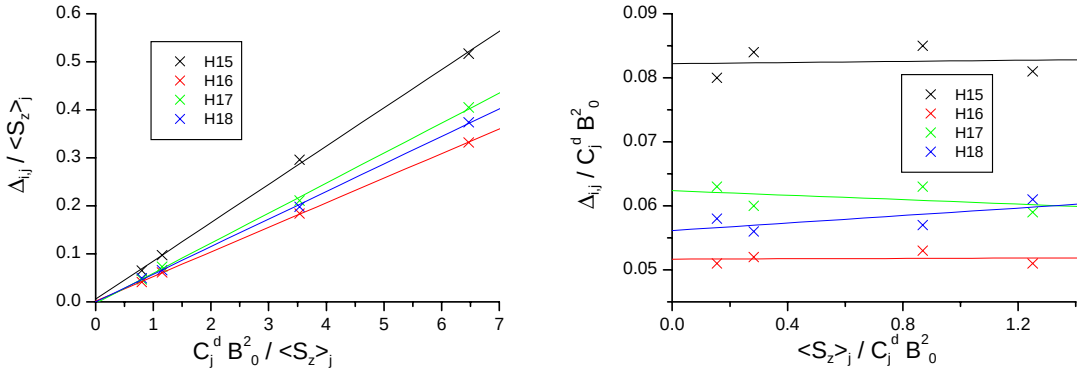

Figure 262 Modified one proton plots of LaLn(L^{AB})$_3$ complexes

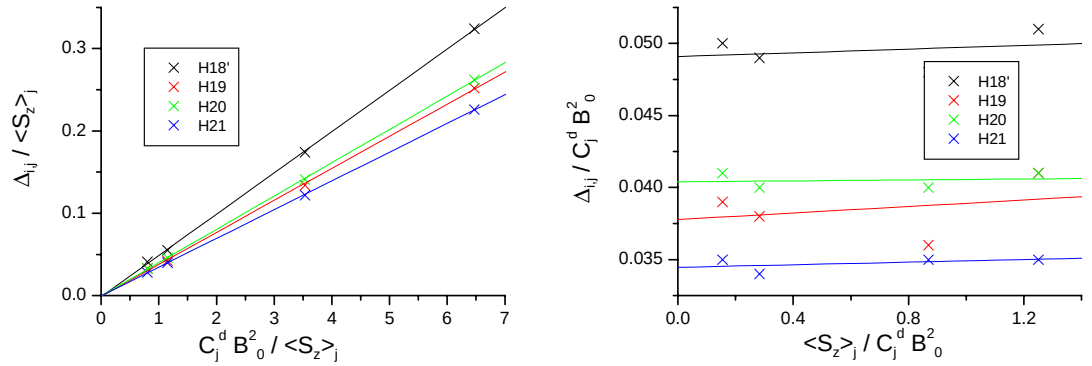

Figure 263 Modified one proton plots of LaLn(L^{AB})$_3$ complexes

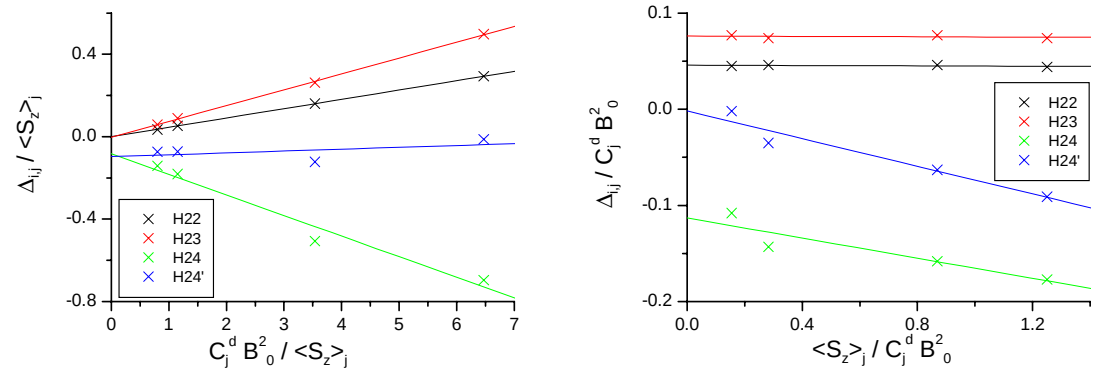

Figure 264 Modified one proton plots of LaLn(L^{AB})$_3$ complexes

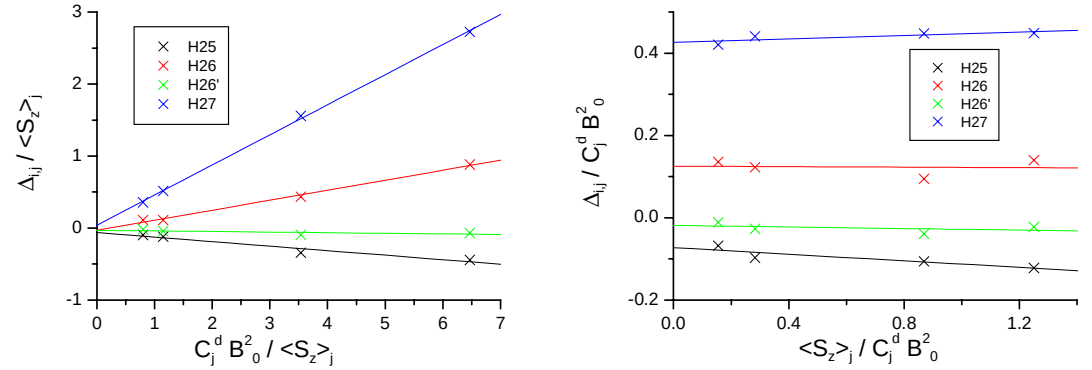

Figure 265 Modified one proton plots of LaLn(L^{AB})$_3$ complexes

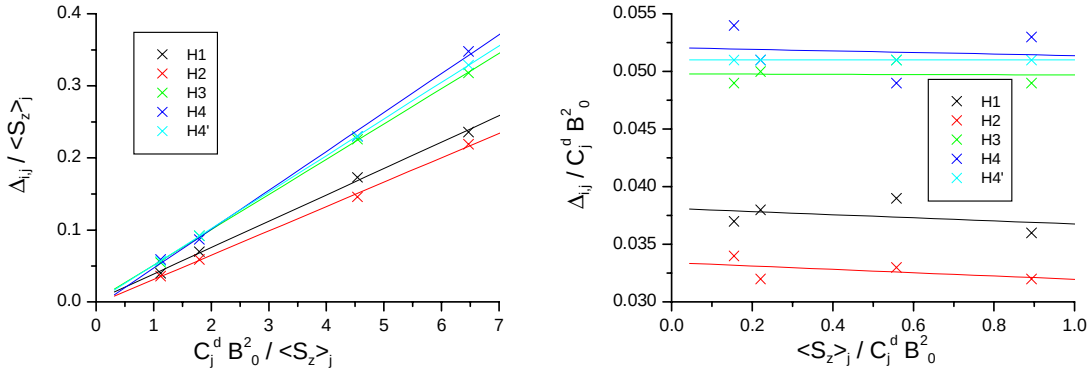

Figure 266 Modified one proton plots of LnLu(L^{AB})$_3$ complexes

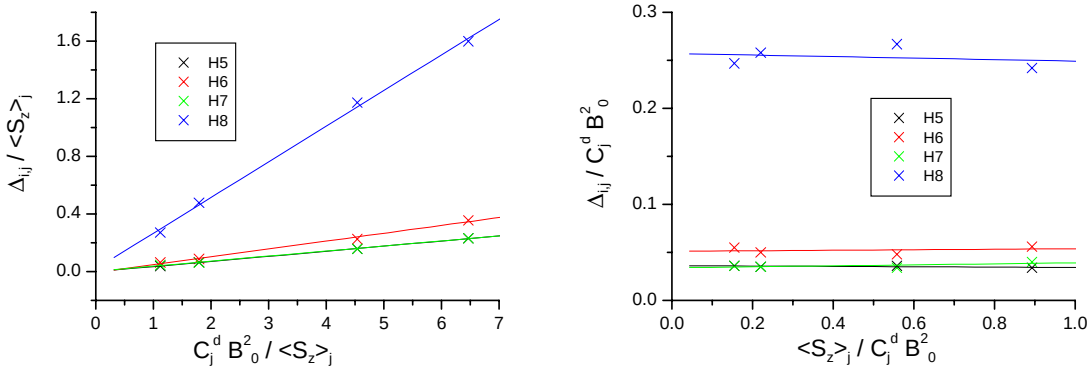

Figure 267 Modified one proton plots of LnLu(L^{AB})$_3$ complexes

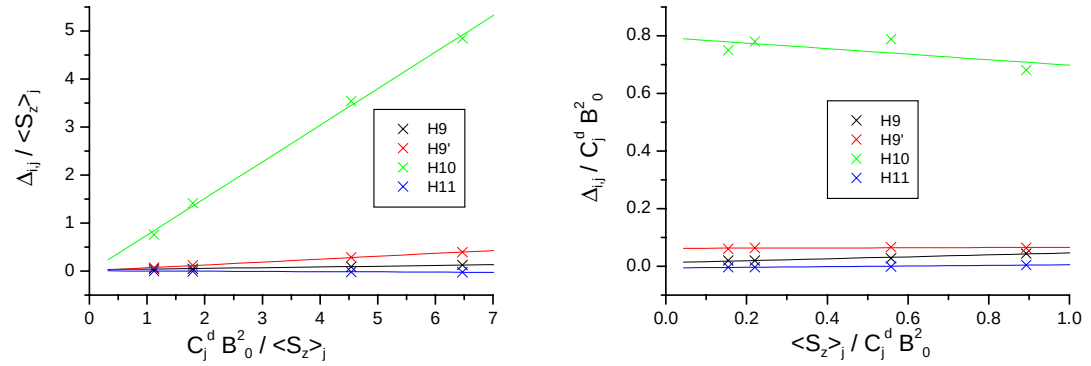

Figure 268 Modified one proton plots of LnLu(L^{AB})$_3$ complexes

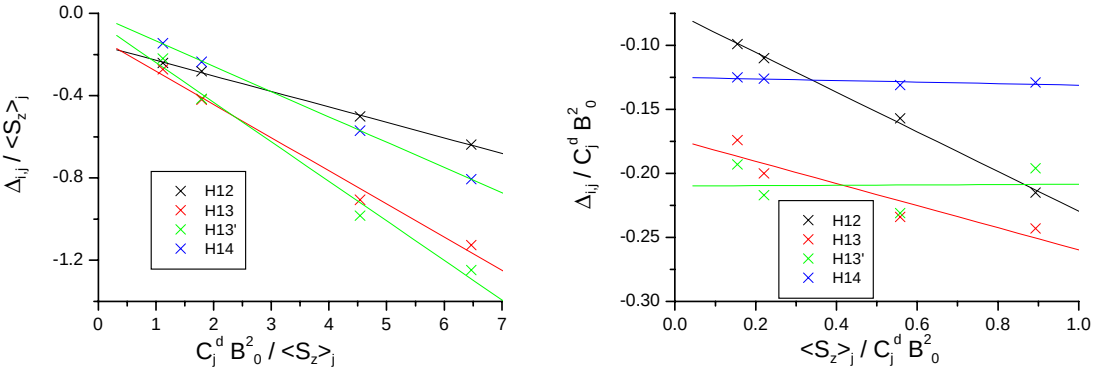

Figure 269 Modified one proton plots of LnLu(L^{AB})$_3$ complexes

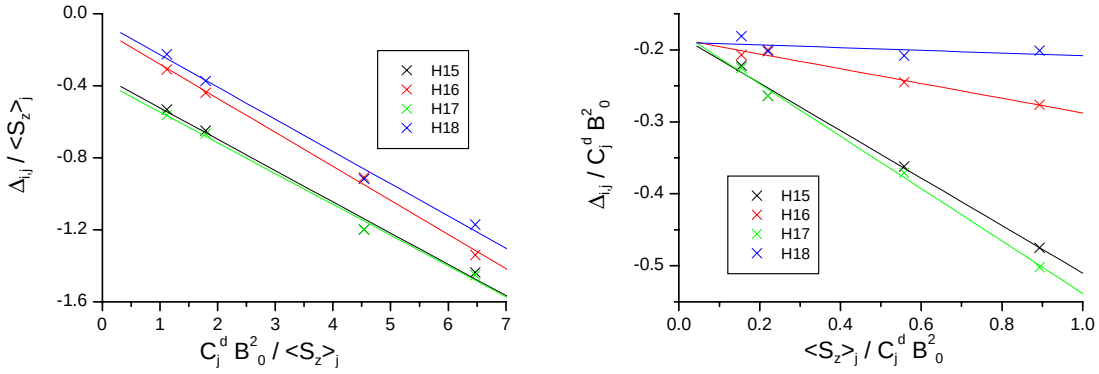

Figure 270 Modified one proton plots of LnLu(L^{AB})$_3$ complexes

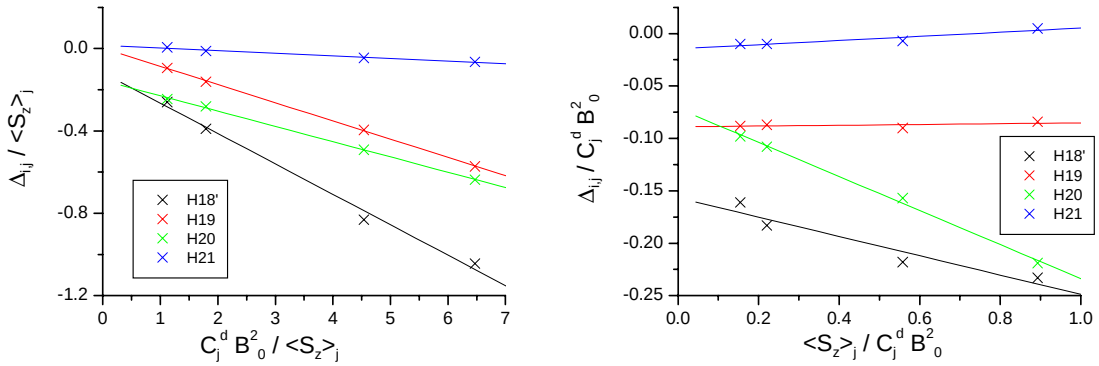

Figure 271 Modified one proton plots of LnLu(L^{AB})$_3$ complexes

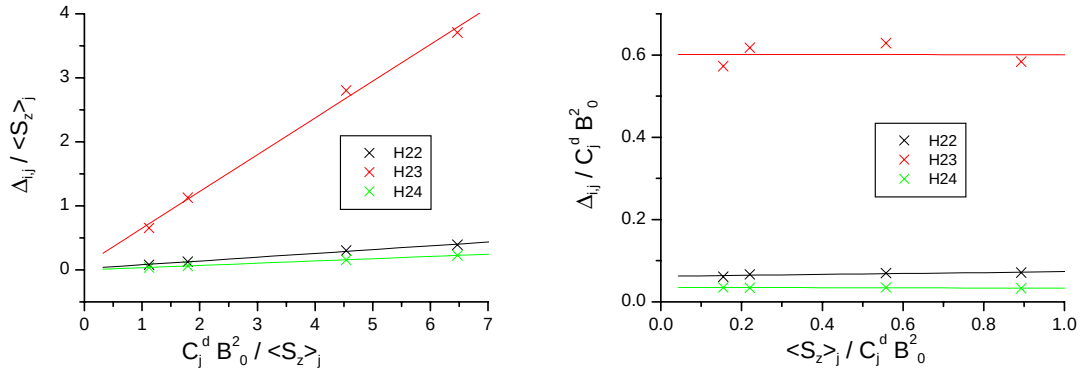

Figure 272 Modified one proton plots of LnLu(L^{AB})$_3$ complexes

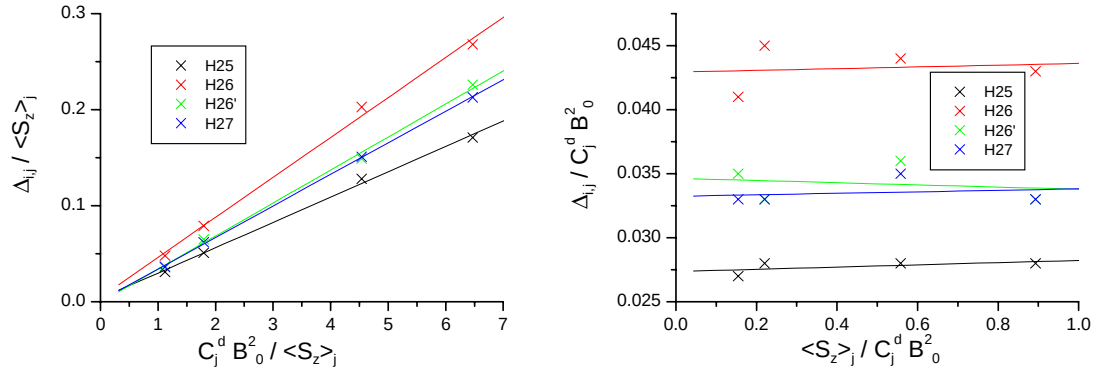

Figure 273 Modified one proton plots of LnLu(L^{AB})$_3$ complexes

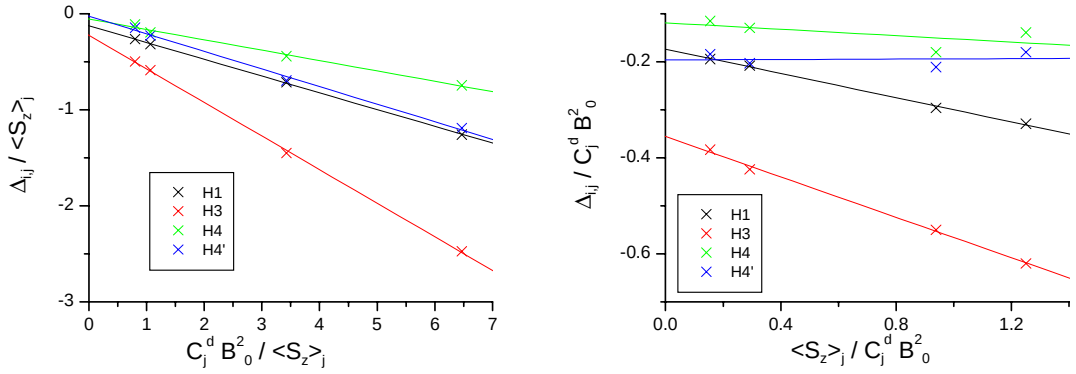

Figure 274 Modified one proton plots of LaLn(L^{AB3})$_3$ complexes

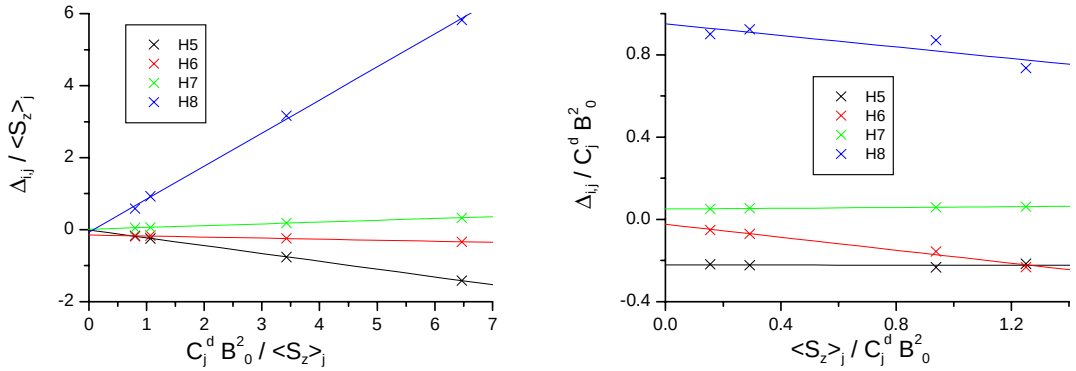

Figure 275 Modified one proton plots of LaLn(L^{AB3})$_3$ complexes

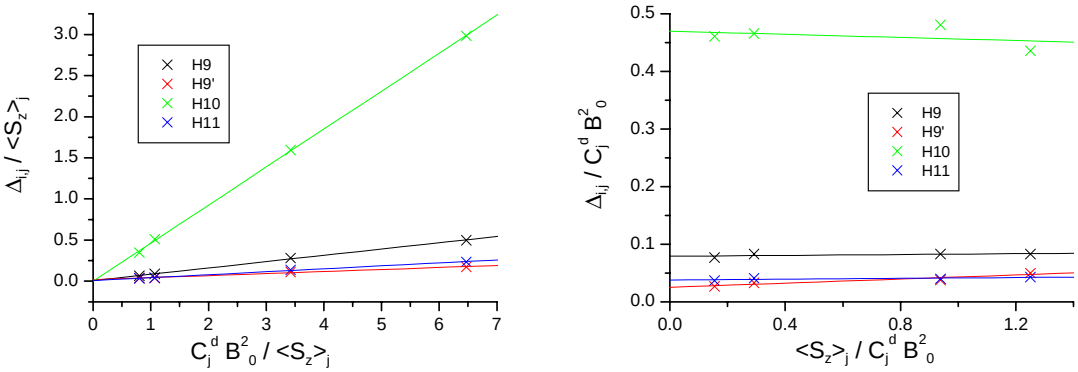

Figure 276 Modified one proton plots of LaLn(L^{AB3})$_3$ complexes

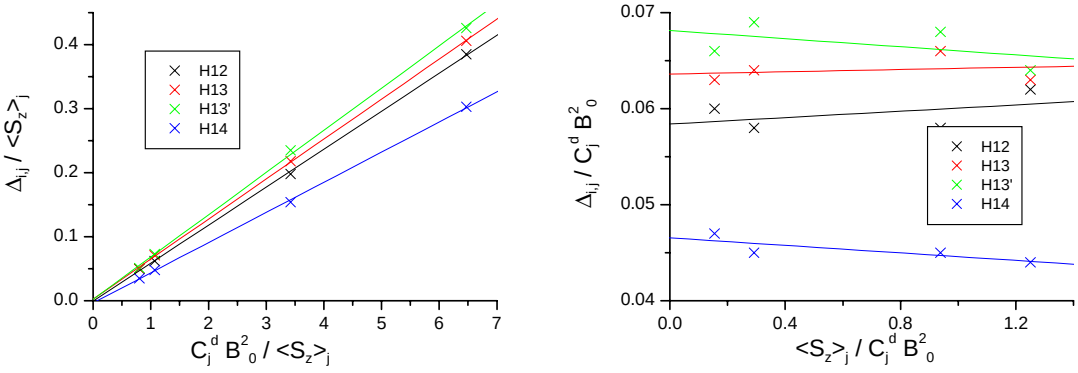

Figure 277 Modified one proton plots of LaLn(L^{AB3})$_3$ complexes

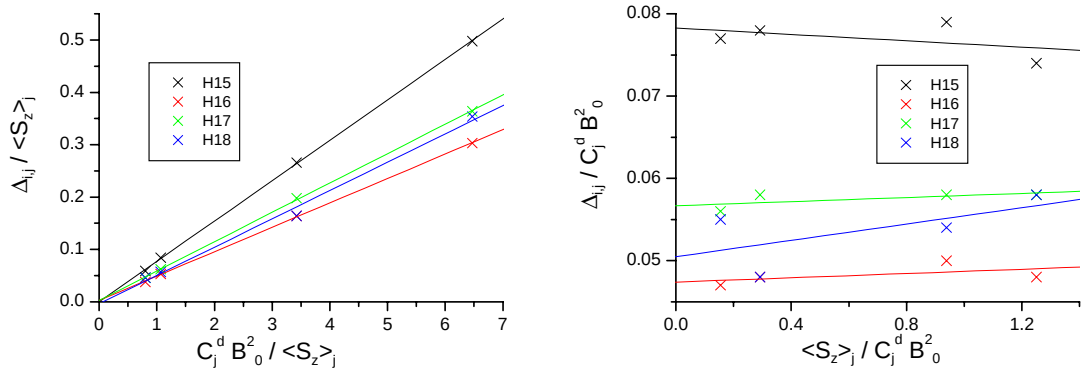

Figure 278 Modified one proton plots of LaLn(L^{AB3})$_3$ complexes

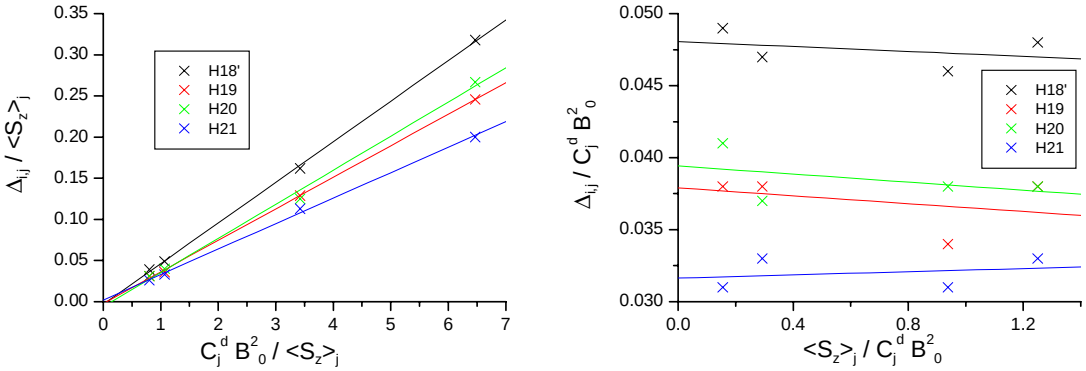

Figure 279 Modified one proton plots of LaLn(L^{AB3})$_3$ complexes

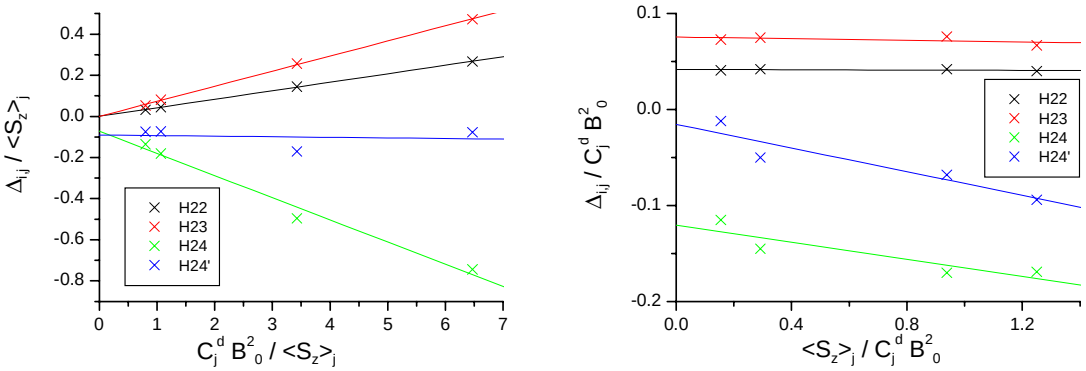

Figure 280 Modified one proton plots of LaLn(L^{AB3})$_3$ complexes

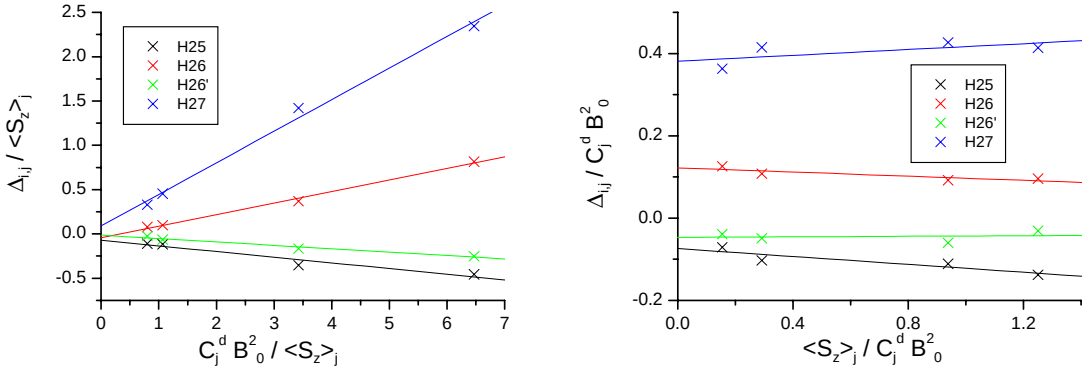

Figure 281 Modified one proton plots of LaLn(L^{AB3})$_3$ complexes

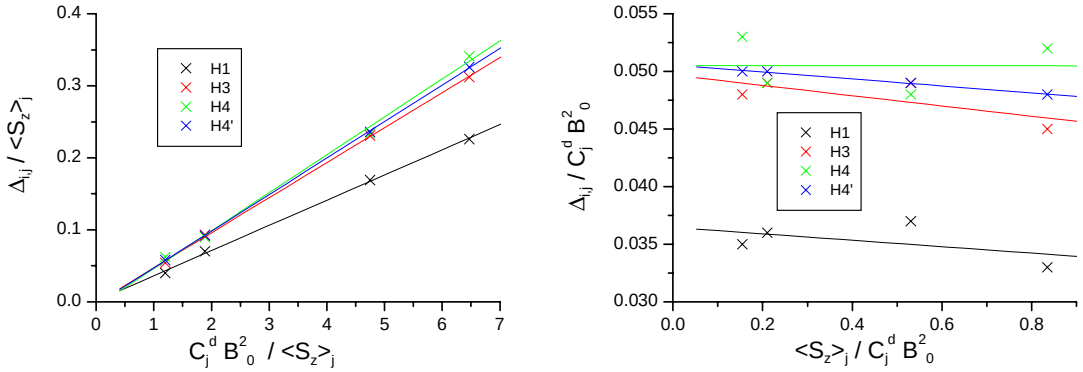

Figure 282 Modified one proton plots of LnLu(L^{AB3})$_3$ complexes

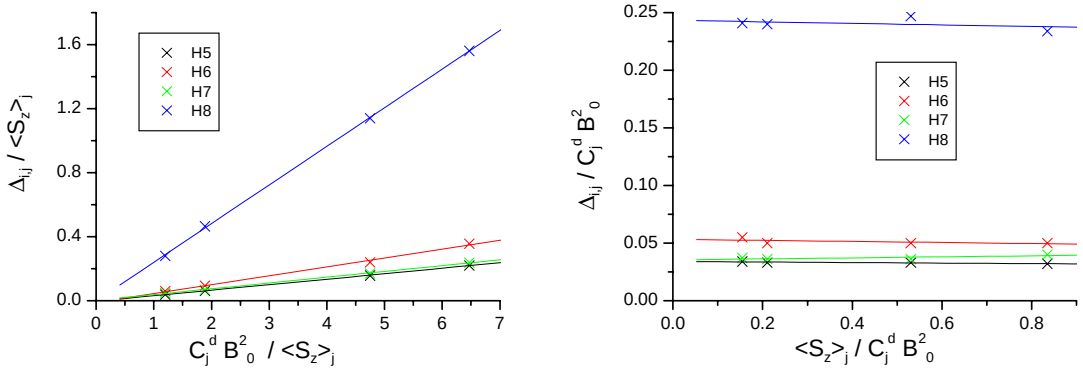

Figure 283 Modified one proton plots of LnLu(L^{AB3})$_3$ complexes

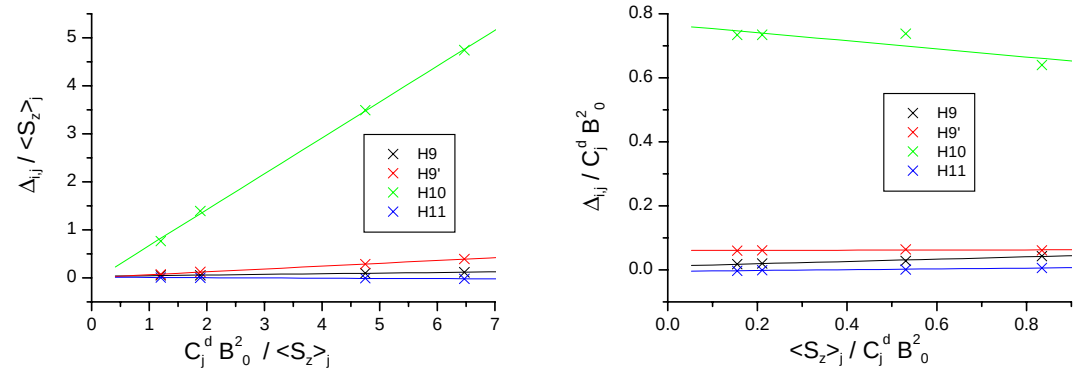

Figure 284 Modified one proton plots of LnLu(L^{AB3})$_3$ complexes

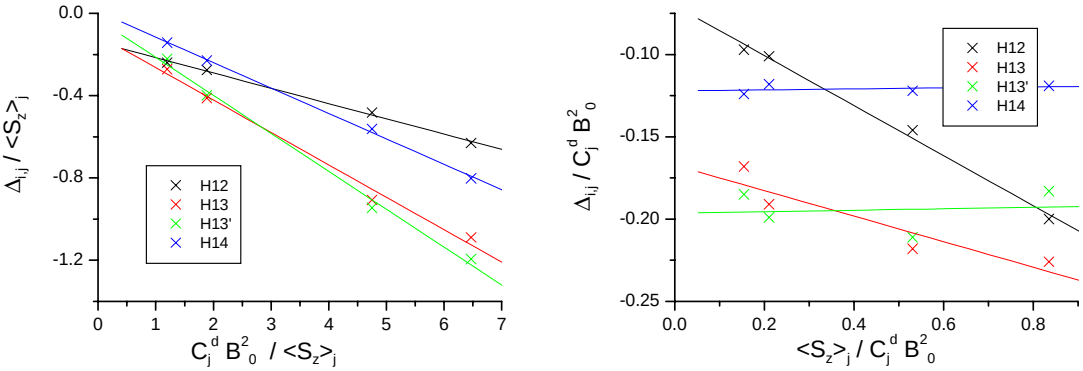

Figure 285 Modified one proton plots of LnLu(L^{AB3})$_3$ complexes

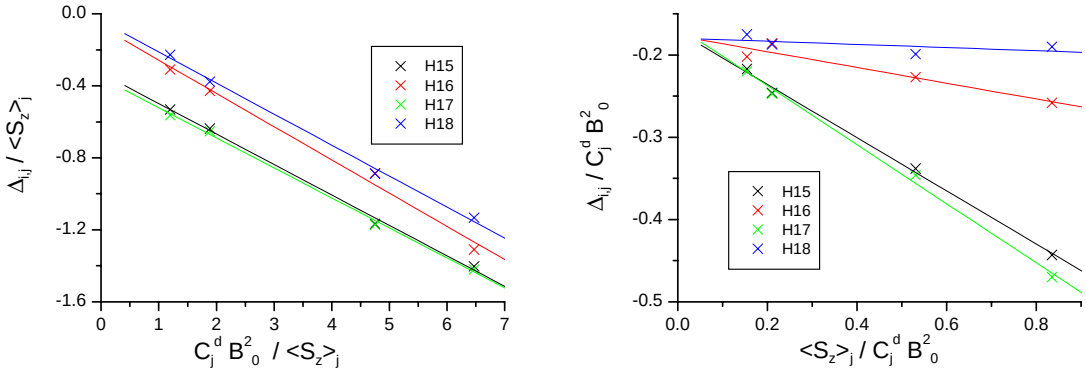

Figure 286 Modified one proton plots of LnLu(L^{AB3})$_3$ complexes

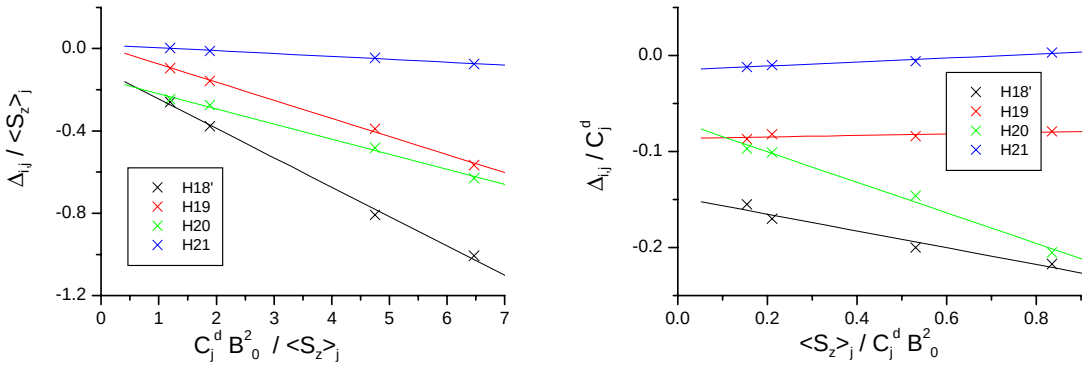

Figure 287 Modified one proton plots of LnLu(L^{AB3})$_3$ complexes

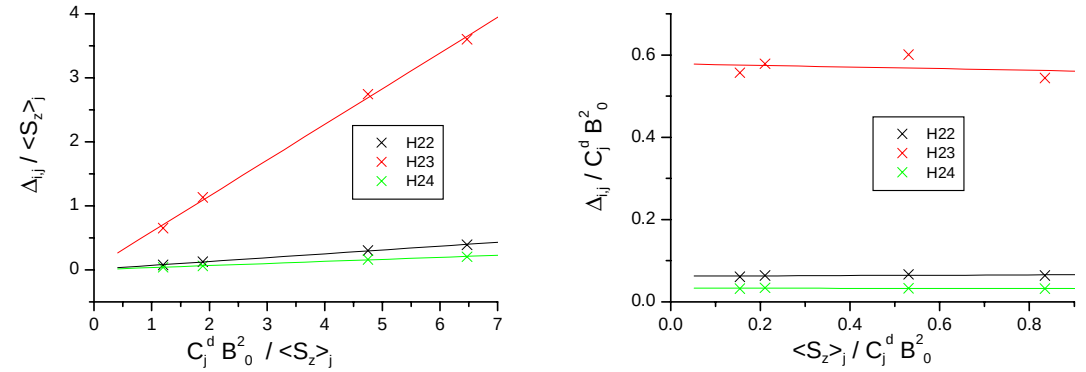

Figure 288 Modified one proton plots of LnLu(L^{AB3})$_3$ complexes

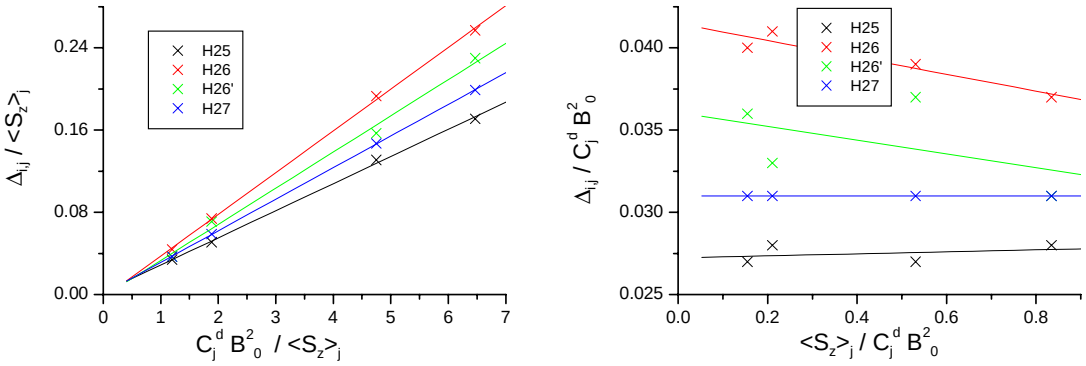

Figure 289 Modified one proton plots of LnLu(L^{AB3})$_3$ complexes

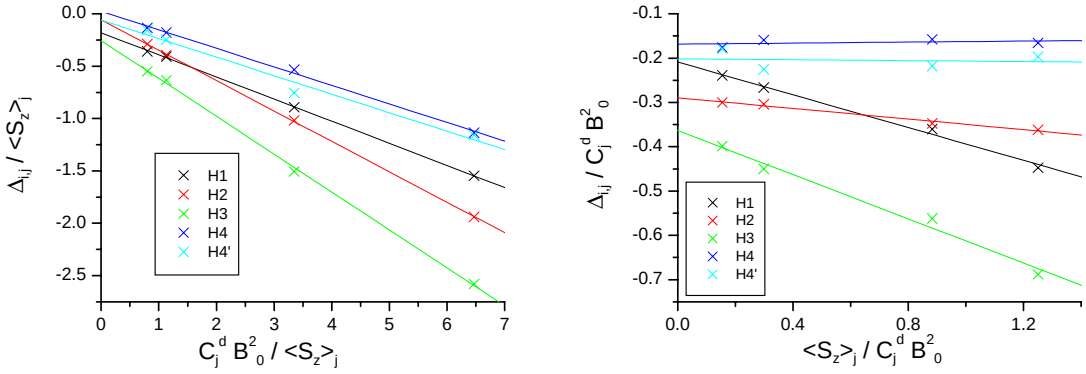

Figure 290 Modified one proton plots of LaLn(L^{AB4})$_3$ complexes

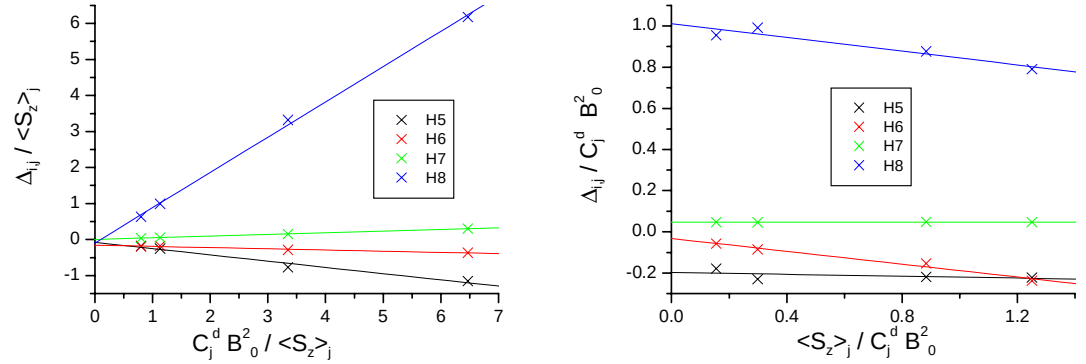

Figure 291 Modified one proton plots of LaLn(L^{AB4})$_3$ complexes

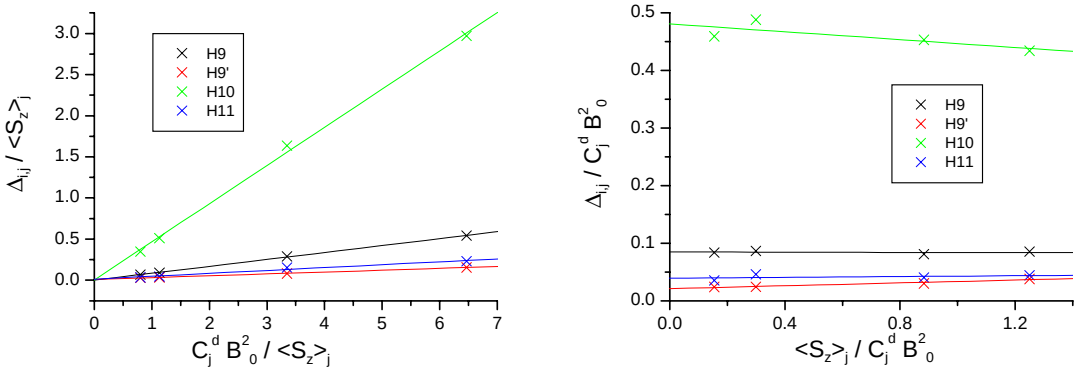

Figure 292 Modified one proton plots of LaLn(L^{AB4})$_3$ complexes

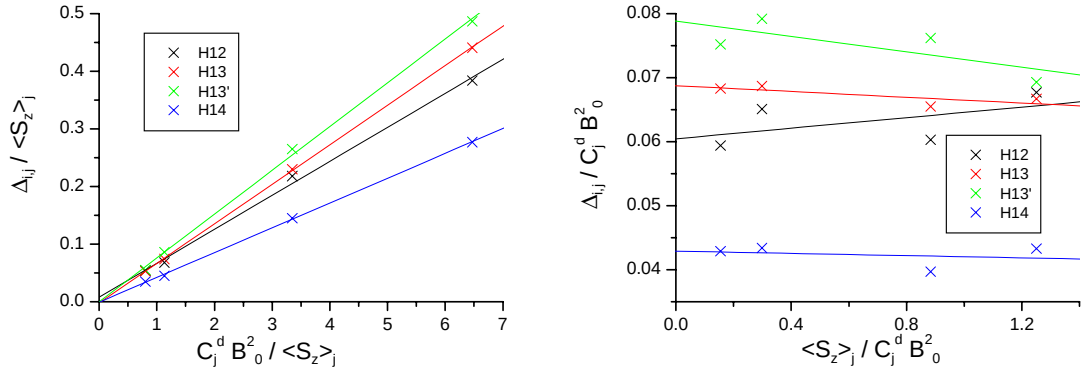

Figure 293 Modified one proton plots of LaLn(L^{AB4})$_3$ complexes

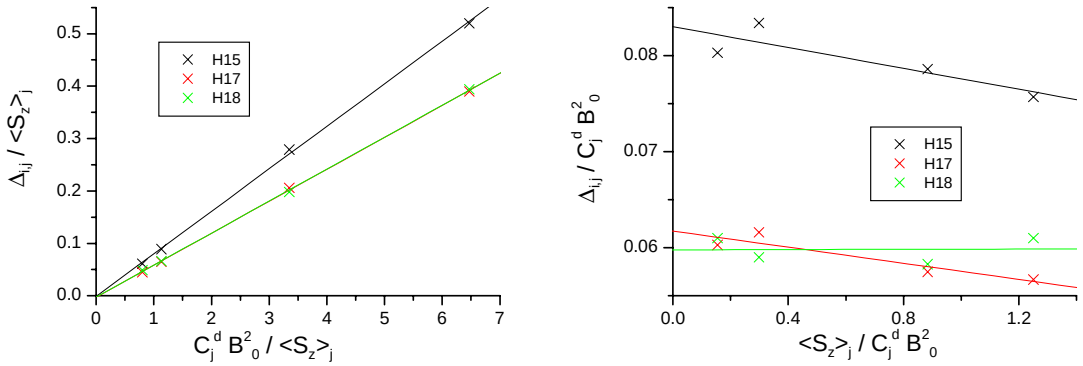

Figure 294 Modified one proton plots of LaLn(L^{AB4})$_3$ complexes

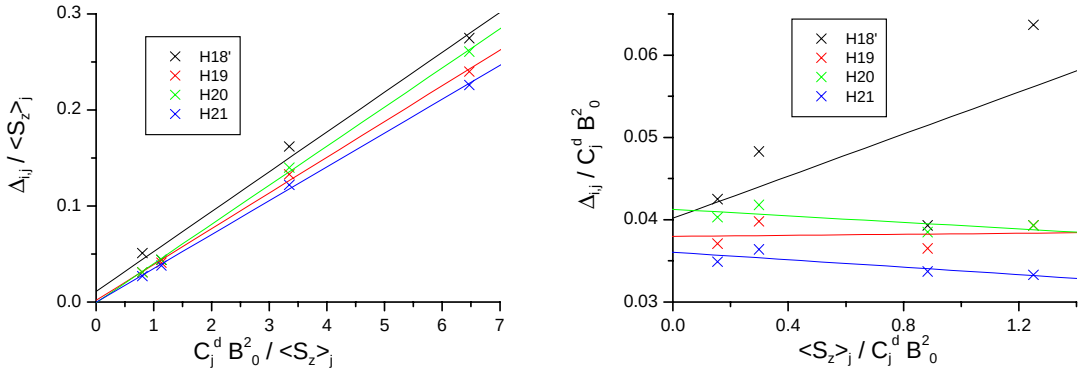

Figure 295 Modified one proton plots of LaLn(L^{AB4})$_3$ complexes

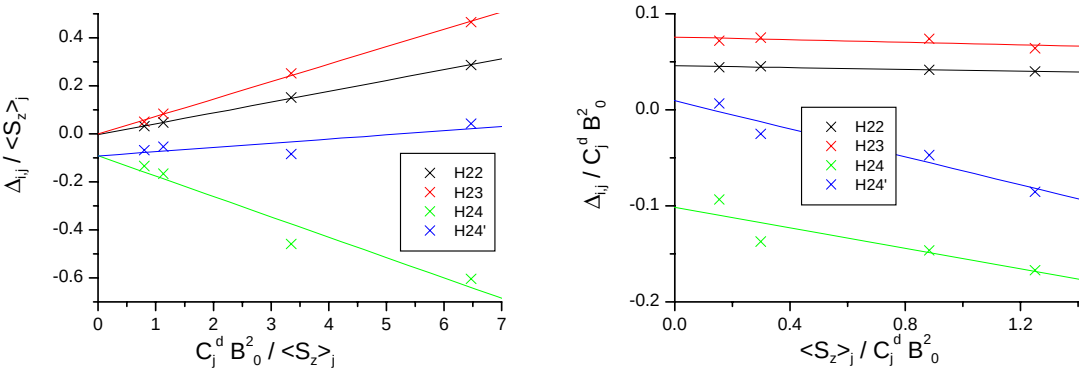

Figure 296 Modified one proton plots of LaLn(L^{AB4})$_3$ complexes

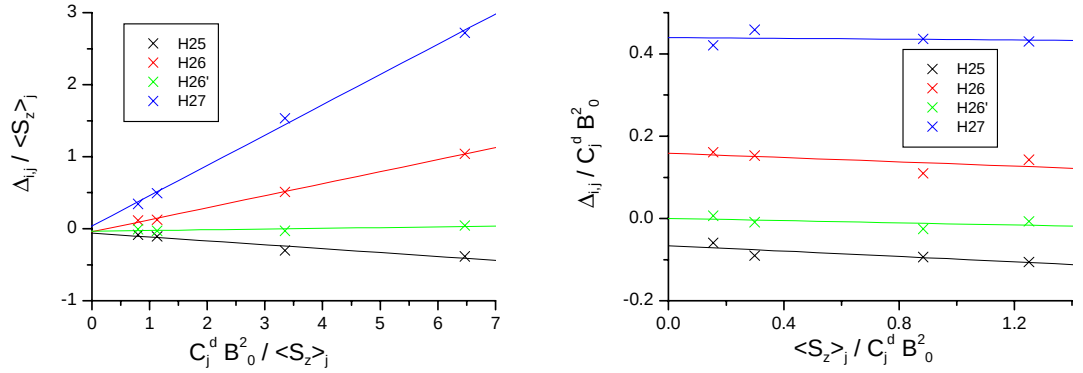

Figure 297 Modified one proton plots of LaLn(L^{AB4})$_3$ complexes

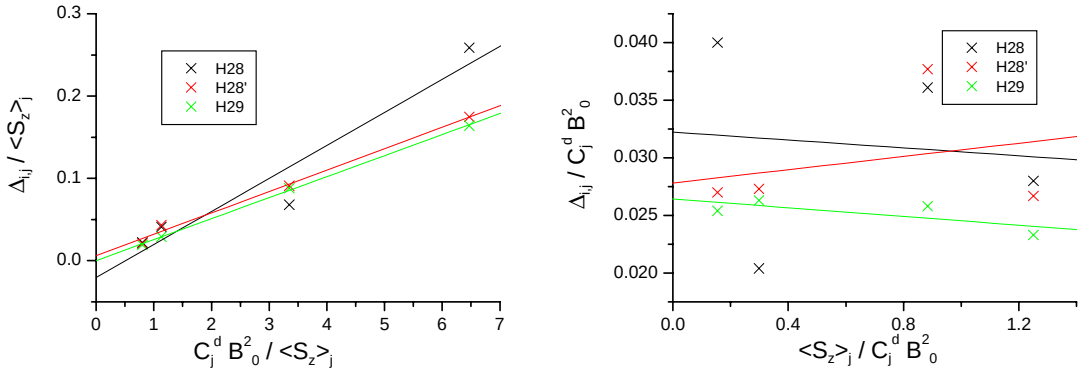

Figure 298 Modified one proton plots of LaLn(L^{AB4})$_3$ complexes

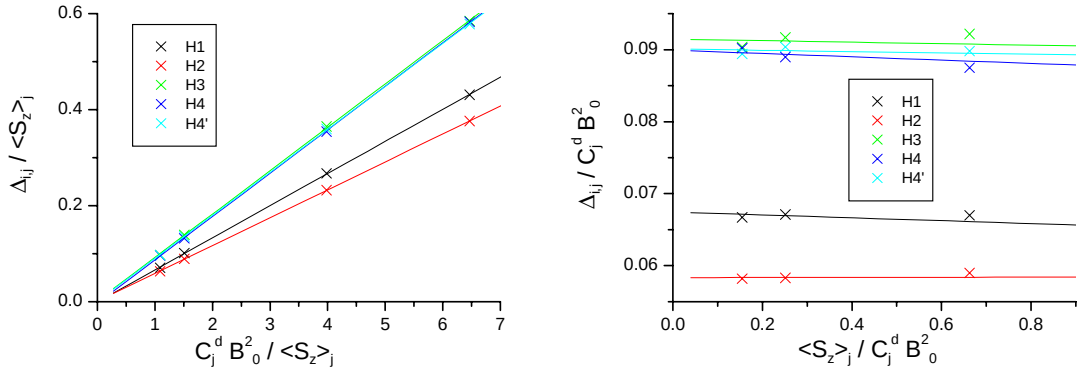

Figure 299 Modified one proton plots of LnLu(L^{AB4})$_3$ complexes

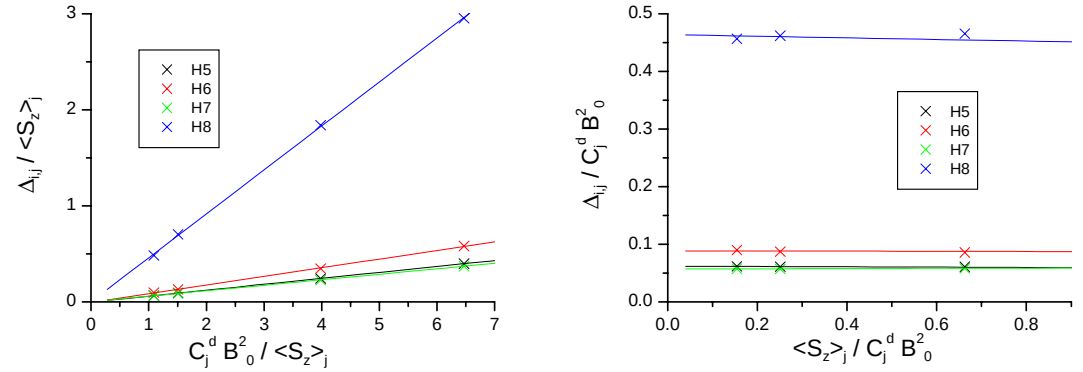

Figure 300 Modified one proton plots of LnLu(L^{AB4})$_3$ complexes

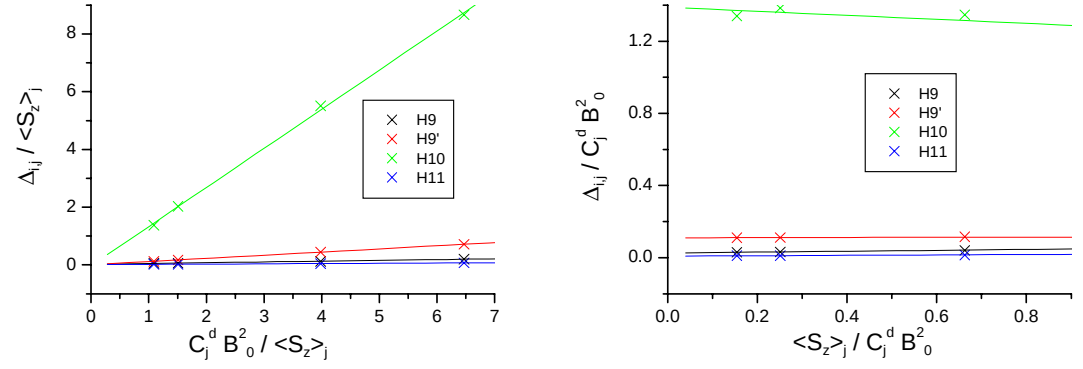

Figure 301 Modified one proton plots of LnLu(L^{AB4})$_3$ complexes

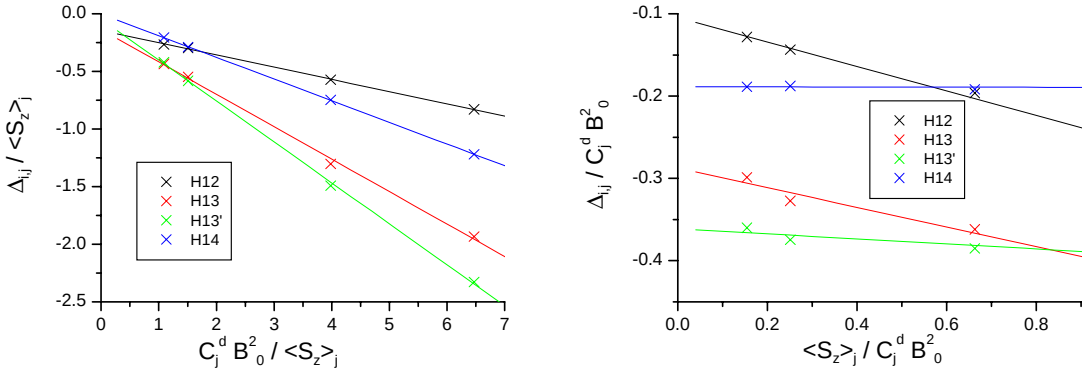

Figure 302 Modified one proton plots of LnLu(L^{AB4})$_3$ complexes

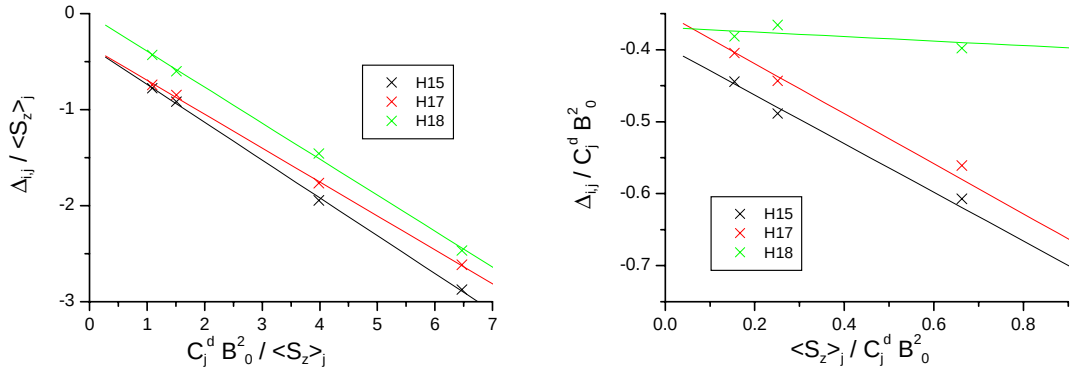

Figure 303 Modified one proton plots of LnLu(L^{AB4})$_3$ complexes

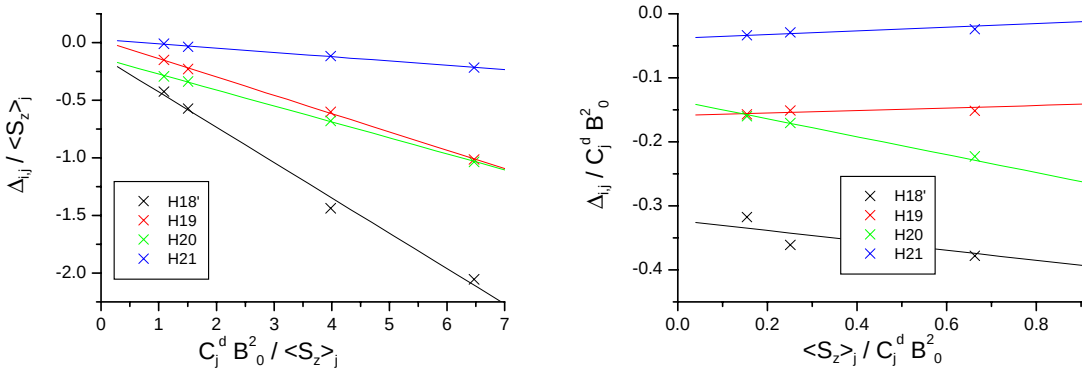

Figure 304 Modified one proton plots of LnLu(L^{AB4})$_3$ complexes

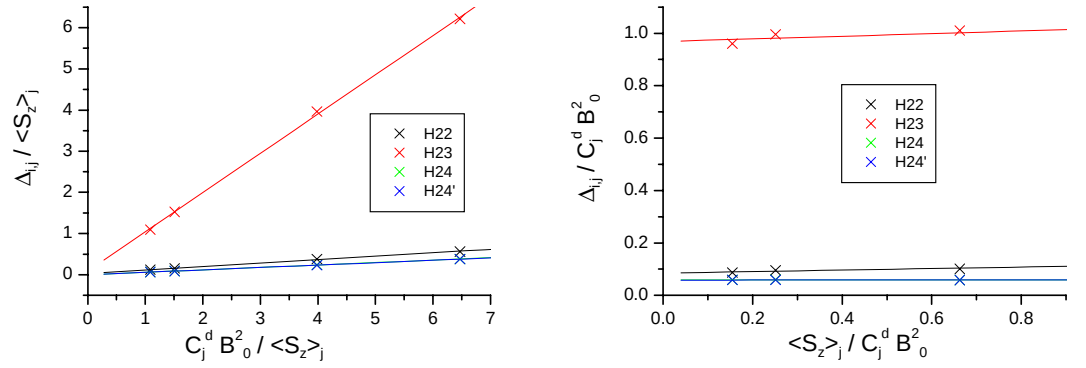

Figure 305 Modified one proton plots of LnLu(L^{AB4})$_3$ complexes

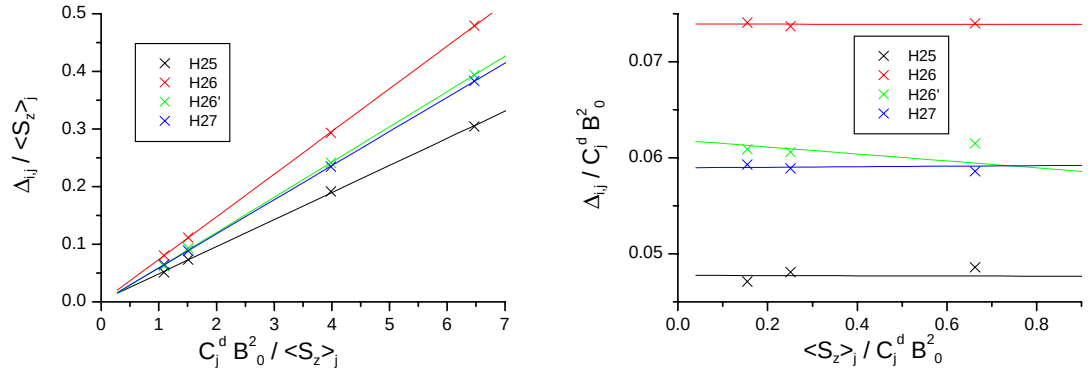

Figure 306 Modified one proton plots of LnLu(L^{AB4})$_3$ complexes

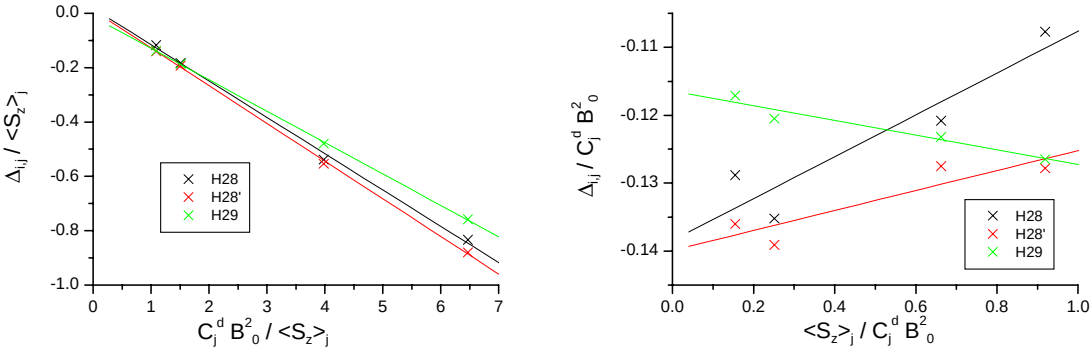

Figure 307 Modified one proton plots of LnLu(L^{AB4})$_3$ complexes

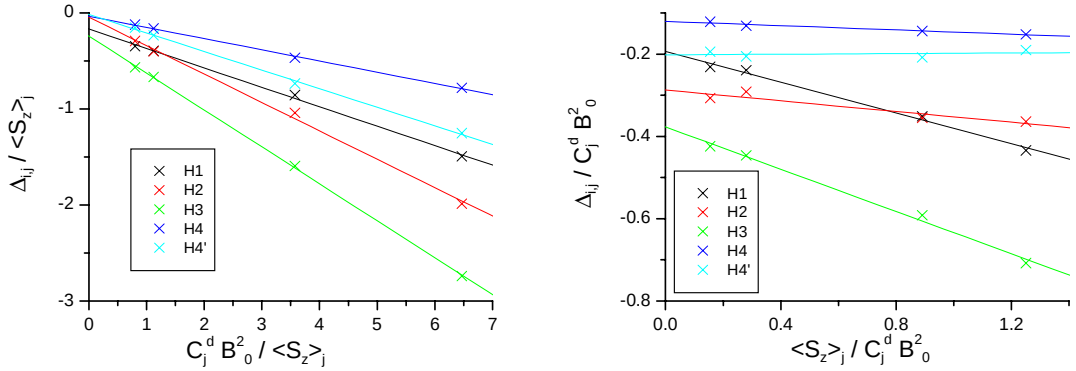

Figure 308 Modified one proton plots of LaLn(L^{AB5})$_3$ complexes

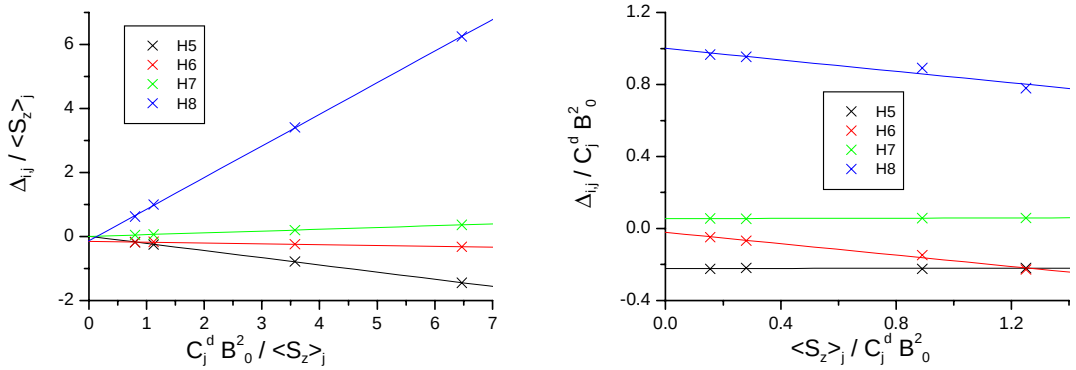

Figure 309 Modified one proton plots of LaLn(L^{AB5})$_3$ complexes

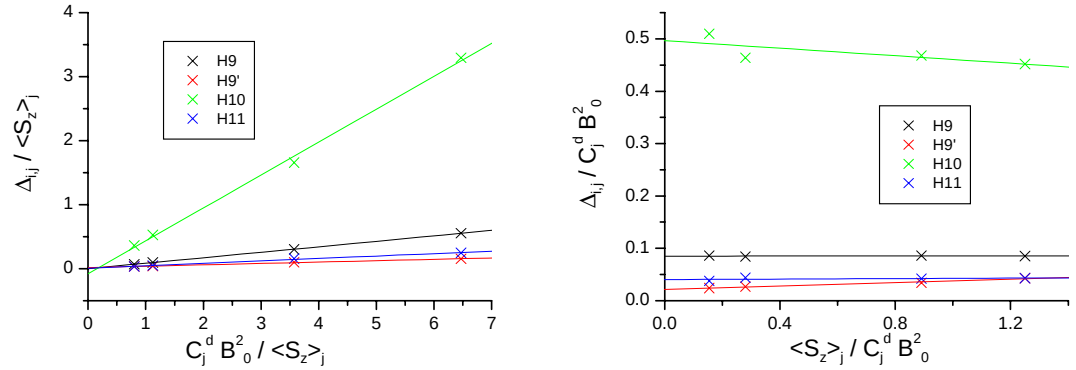

Figure 310 Modified one proton plots of LaLn(L^{AB5})$_3$ complexes

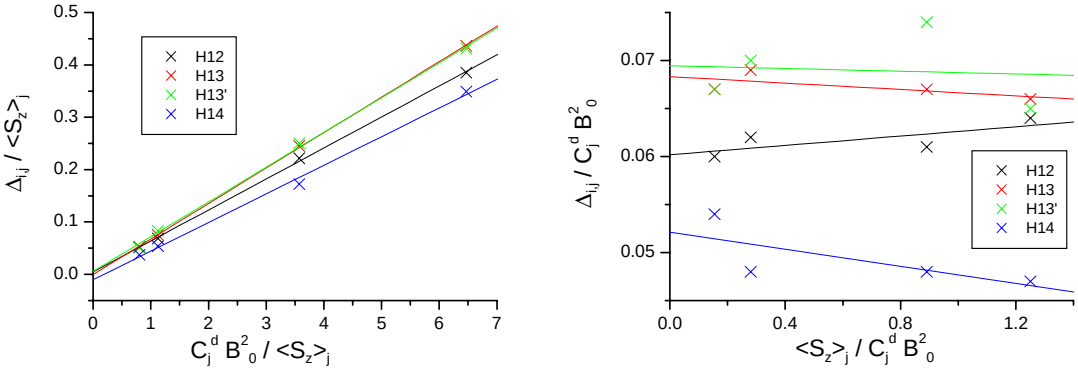

Figure 311 Modified one proton plots of LaLn(L^{AB5})$_3$ complexes

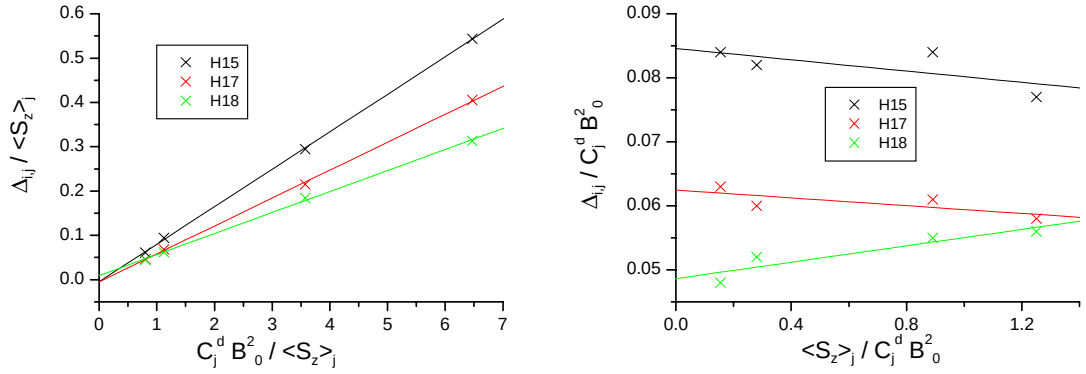

Figure 312 Modified one proton plots of LaLn(L^{AB5})$_3$ complexes

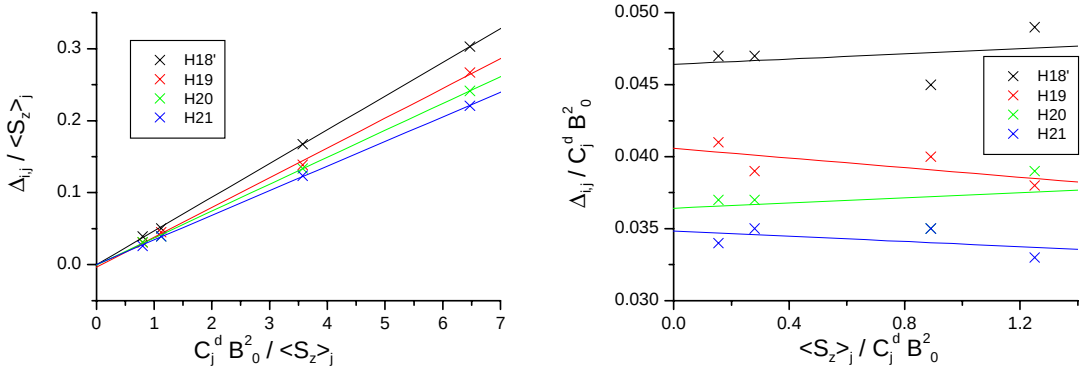

Figure 313 Modified one proton plots of LaLn(L^{AB5})$_3$ complexes

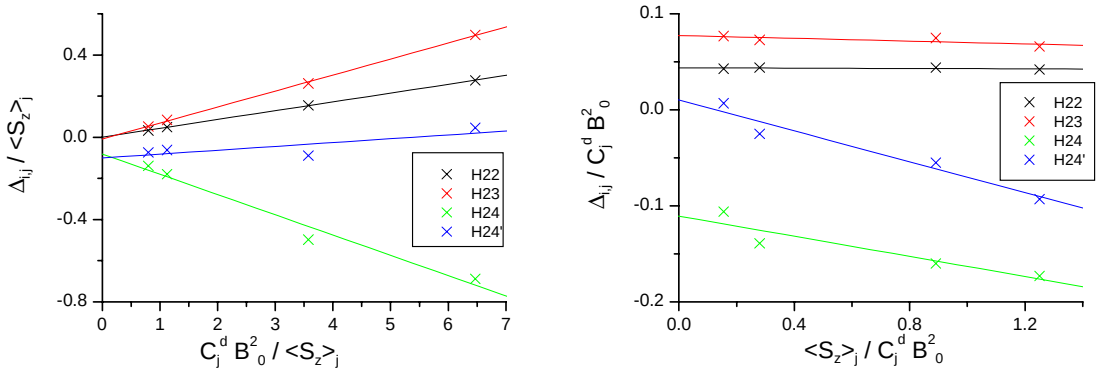

Figure 314 Modified one proton plots of LaLn(L^{AB5})$_3$ complexes

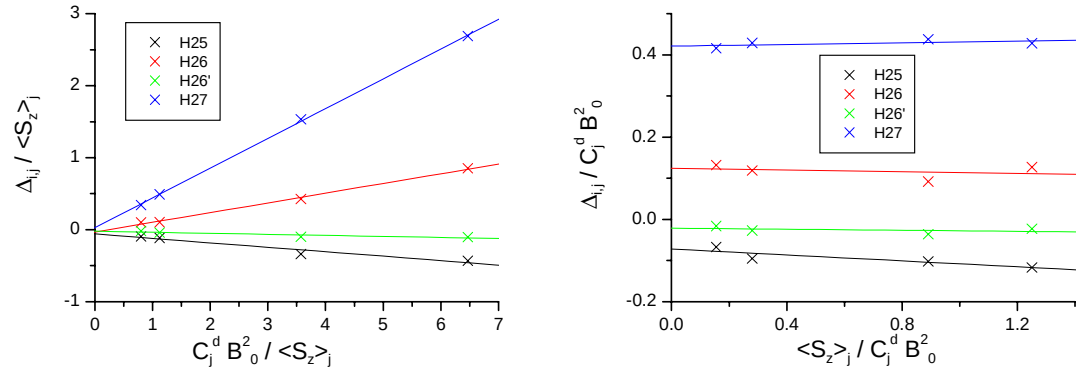

Figure 315 Modified one proton plots of LaLn(L^{AB5})$_3$ complexes

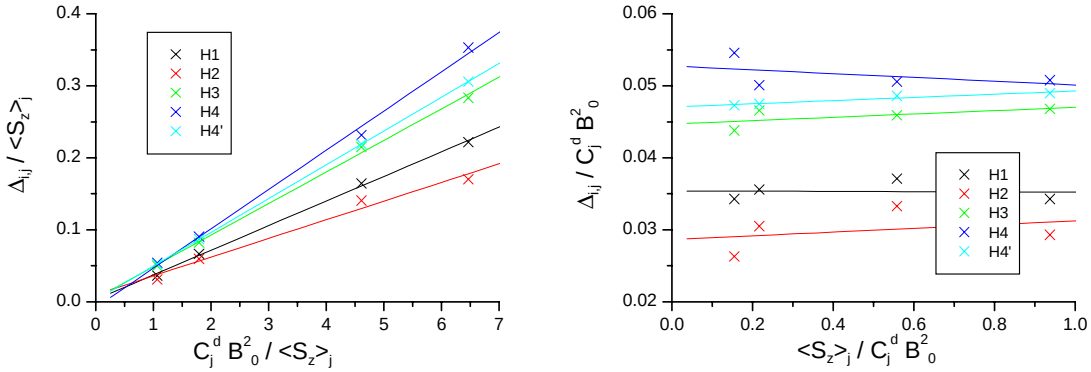

Figure 316 Modified one proton plots of LnLu(L^{AB5})$_3$ complexes

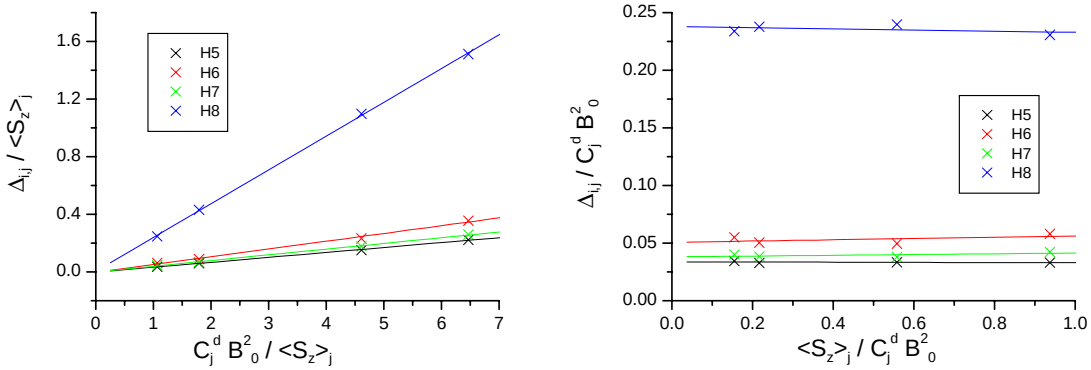

Figure 317 Modified one proton plots of LnLu(L^{AB5})$_3$ complexes

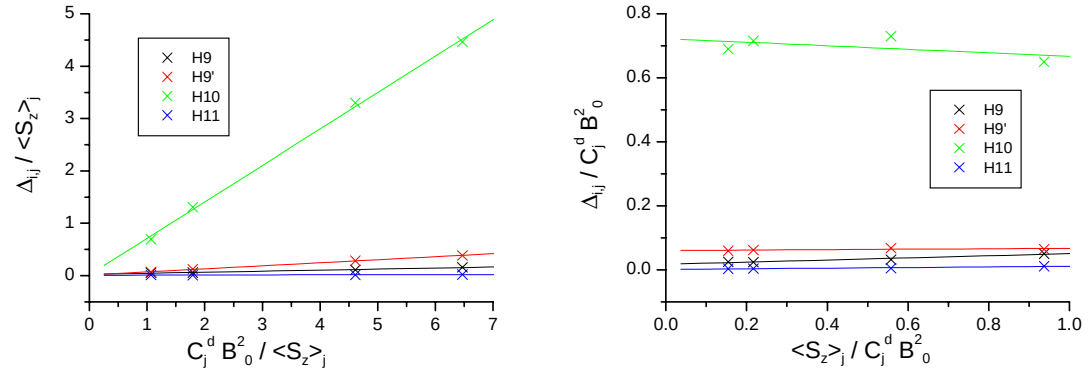

Figure 318 Modified one proton plots of LnLu(L^{AB5})$_3$ complexes

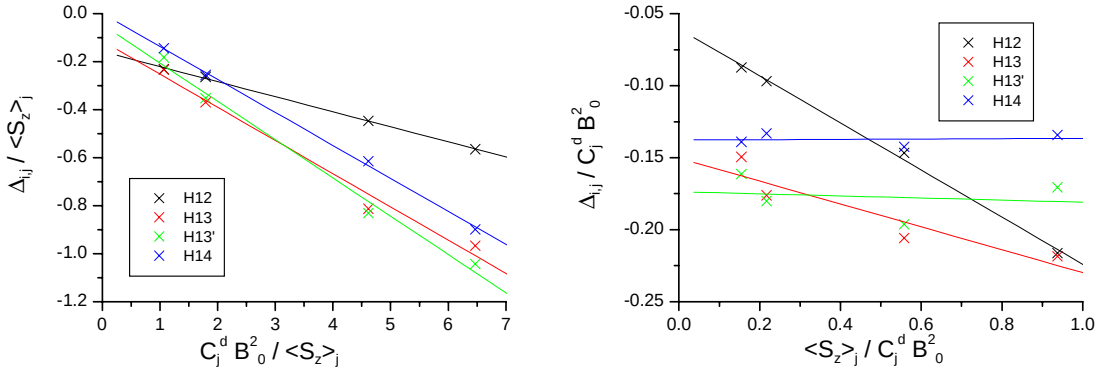

Figure 319 Modified one proton plots of LnLu(L^{AB5})$_3$ complexes

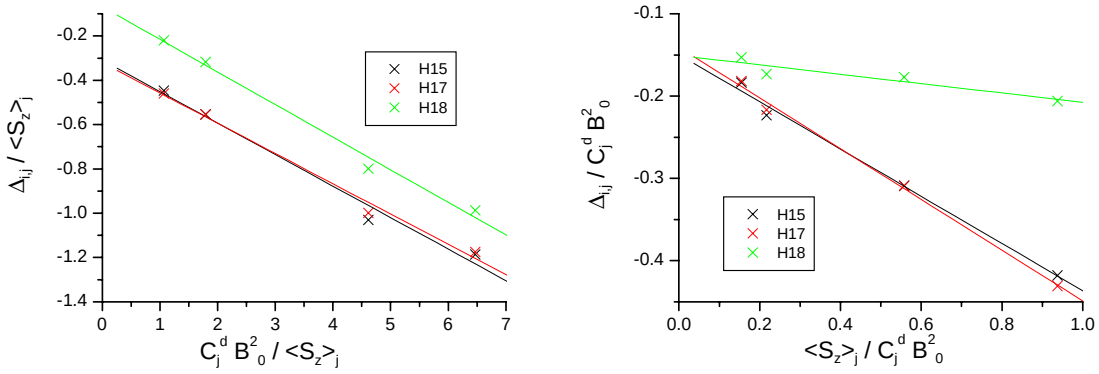

Figure 320 Modified one proton plots of LnLu(L^{AB5})$_3$ complexes

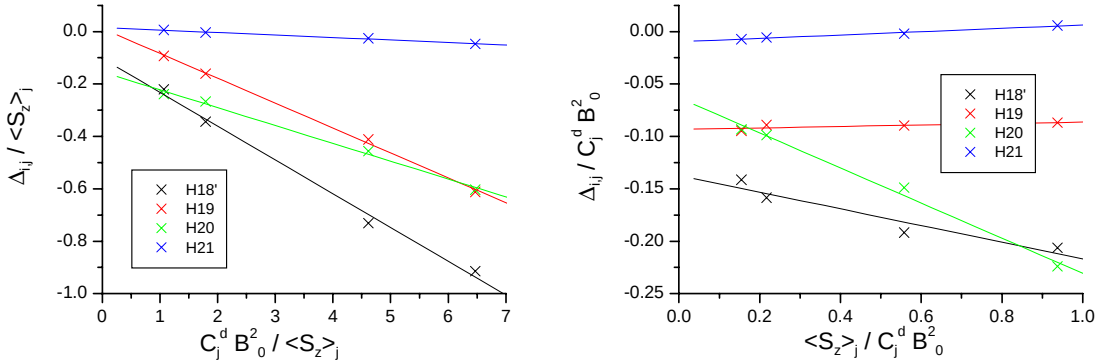

Figure 321 Modified one proton plots of LnLu(L^{AB5})$_3$ complexes

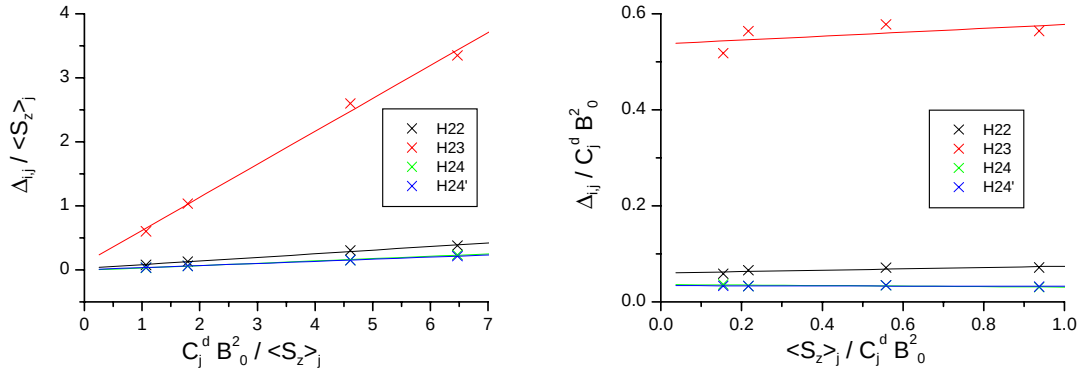

Figure 322 Modified one proton plots of LnLu(L^{AB5})$_3$ complexes

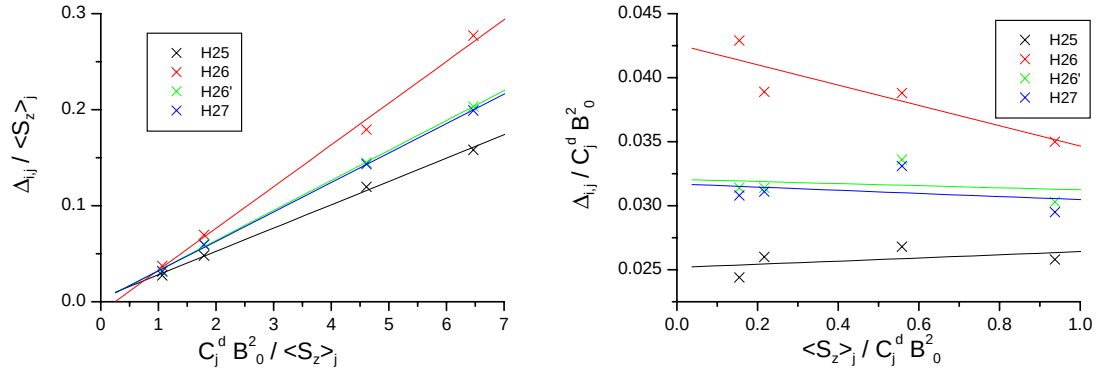

Figure 323 Modified one proton plots of LnLu(L^{AB5})$_3$ complexes

Curriculum vitae

Personal data

Address Rue Du Maupas 15
1004 Lausanne
E-mail t_b_jensen@yahoo.com
Date of birth 20th October 1971
Nationality Danish
Marital status Married to Micaela Vaerini Jensen (Swiss)

Education

02.2002 - 05.2006 Ph.D. in chemistry at the Laboratoire de chimie supramoleculaire des lanthanides, École Polytechnique Fédérale de Lausanne
Supervisor: Prof. Jean-Claude G. Bünzli
09.1990 - 07.1999 Cand.scient. (M.Sc.) in Chemistry at the Department of Chemistry, University of Copenhagen, Denmark
Supervisor: Prof. Jørgen Glerup
08.1987 - 06.1990 Allerød Gymnasium, Denmark
08.1978 - 06.1987 Lillerød Skole, Denmark

Work

02.2002 - 05.2006 Assistant at the École Polytechnique Fédérale de Lausanne. Teaching general chemistry (laboratory and excercices). Language: French.
08.1999 - 01.2001 Hilfsassistent and Ph.D. student at the Department of Chemistry and Biochemistry, University of Bern. Teaching general chemistry (in German) and EPR spectroscopy (in English).
1993 - 1998 Part time teaching assistant (inorganic and analytical chemistry) at the Department of Chemistry, University of Copenhagen, Denmark. Language: Danish.
1982 - 1990 Paper boy.

Languages

Danish Mother tongue
English Perfect knowledge
German Very good knowledge
French Very good knowledge
Italian Good knowledge
02.2001 - 06.2001 Intensive German course at the Migros Klubschule, Bern
11.2001 - 01.2002 Intensive French course at the École Club Migros, Lausanne

Publications

Sanzenbacher, R.; Böttcher, A.; Elias, H.; Hüber, M.; Haase, W.; Glerup, J.; Jensen, T. B.; Neuburger, M.; Zehnder, M.; Springborg, J.; Olsen, C. E.: Synthesis, Crystal Structure, and Magnetic Properties of a Ferromagnetically Coupled Difluoro-Bridged Dinuclear Chromium(III) Complex with a Substituted Tetrahydrosalen Derivative as Ligand *Inorg. Chem.* **1996**, *35*, 7493-7499.

André, N.; Jensen, T. B.; Scopelliti, R.; Imbert, D.; Elhabiri, M.; Hopfgartner, G.; Piguet, C.; Bünzli, J.-C. G.: Supramolecular Recognition of Heteropairs of Lanthanide Ions: A Step toward Self-Assembled Bifunctional Probes *Inorg. Chem.* **2004**, *43*, 515 - 529.

Posters

Solution Structure of Heterodimetallic Triple Helicates Studied by Analysis of Lanthanide Induced Shift and Relaxation *Fifth International Conference on f-Elements* (Geneva, Switzerland, August 24-29 2003)

HHH/HHT Equilibria in Lanthanide Containing Helicates *Swiss Chemical Society Fall Meeting* (EPFL, Lausanne, Switzerland, October 9 2003)

Homo- and Heterobimetallic Lanthanide Helicates *5th Symposium of the Polish Supramolecular Chemistry Network* (Piotrowo, Poland, October 23-26 2003)

Heterobimetallic Lanthanide Containing Helicates *Swiss Chemical Society Fall Meeting* (University of Zürich, Switzerland, October 7 2004)

Solution Structure of Bimetallic Lanthanide Complexes with Asymmetric Ligands *NRP 47 Spring School on Supramolecular Chemistry* (Murten, Switzerland, April 11-15 2005)

Solution Structure of Bimetallic Triple Helicates of Heterobitopic Ligands Studied by Analysis of the Lanthanide Induced Shift *24th Rare Earth Research Conference* (Keystone, Colorado, USA, June 26-30, 2005)

Lanthanide Induced Shift Analysis of Asymmetric Bimetallic Triple Helicates in Solution *Swiss Chemical Society Fall Meeting* (EPFL, Lausanne, Switzerland, October 13 2005)

References

[1] Piguet, C.; Bünzli, J.-C. G. *Chem. Soc. Rev.* **1999**, *28*, 347.

[2] Bünzli, J.-C. G.; Piguet, C. *Chem. Rev.* **2002**, *102*, 1897.

[3] Bünzli, J.-C. G.; Piguet, C. *Chem. Soc. Rev.* **2005**, *34*, 1048.

[4] Bünzli, J.-C. G. *Acc. Chem. Res.* **2006**, *39*, 53.

[5] Piguet, C.; Williams, A. F.; Bernardinelli, G.; Bünzli, J.-C. G. *Inorg. Chem.* **1993**, *32*, 4139.

[6] Petoud, S.; Bünzli, J.-C. G.; Renaud, F.; Piguet, C.; Schenk, K. J.; Hopfgartner, G. *Inorg. Chem.* **1997**, *36*, 5750.

[7] Piguet, C.; Bünzli, J.-C. G.; Bernardinelli, G.; Bochet, C. G.; Froidevaux. P. *J. Chem. Soc. Dalton Trans.* **1995**, 83.

[8] André, N. *Des complexes monométalliques 4f aux hélicates hétérodimétalliques 4f-4f' par reconnaissance spécifique ligand-cation lanthanide. Synthèse, structure, stabilité et propriétés photophysiques*. Ph.D. Thesis, EPFL, Lausanne **2002**.

[9] Ouali, N.; Bocquet, B.; Rigault, S.; Morgantini, P.-Y.; Weber, J.; Piguet, C. *Inorg. Chem.* **2002**, *41*, 1436.

[10] Patroniak, V.; Baxter, P. N. W.; Lehn, J.-M.; Hnatejko, Z.; Kubicki, M. *Eur. J. Inorg. Chem.* **2004**, 2379.

[11] Frey, S. T.; Chang, A.; Carvalho, J. F.; Varadarajan, A.; Schultze, L. M.; Pounds, K. L.; Horrocks, W. DeW., Jr. *Inorg. Chem.* **1994**, *33*, 2882.

[12] Powell, D. H.; Dhubhghaill, O. M. N.; Pubanz, D.; Helm, L.; Lebedev, Y. S.; Schlaepfer, W.; Merbach, A. E. *J. Am. Chem. Soc.* **1996**, *118*, 9333.

[13] Albrecht, M. *Chem. Rev.* **2001**, *101*, 3457.

[14] Piguet, C.; Bernardinelli, G.; Hopfgartner, G. *Chem. Rev.* **1997**, *97*, 2005.

[15] Piguet, C. *J. Incl. Phen. Macrocyc. Chem.* **1999**, *34*, 361.

[16] Watson, J. D.; Crick, F. C. H. *Nature*, **1953**, *171*, 737.

[17] Lehn, J.-M.; Rigault, A.; Siegel, J.; Harrowfield, J. Chevrier, B.; Moras, D. *Proc. Natl. Acad. Sci. USA* **1987**, *84*, 2565.

[18] Albrecht, M.; Blau, O.; Fröhlich, R. *Proc. Natl. Acad. Sci. USA* **2002**, *99*, 4867.

[19] Albrecht, M.; Schmid, S.; deGroot, M.; Weis, P.; Fröhlich, R. *Chem. Commun.* **2003**, 2526.

[20] Albrecht, M.; Janser, I.; Kamptmann, S.; Weis, P.; Wibbeling, B.; Fröhlich, R. *Dalton. Trans.* **2004**, 37.

[21] Albrecht, M.; Janser, I.; Lützen, A.; Hapke, M.; Fröhlich, R.; Weis, P. *Chem. Eur. J.* **2005**, *11*, 5742.

[22] Mamula, O.; Lama, M.; Telfer, S. G.; Nakamura, A.; Kuroda, R.; Stoeckli-Evans, H.; Scopelliti, R. *Angew. Chem. Int. Ed.* **2005**, *44*, 2527.

[23] Albrecht, M. *Angew. Chem. Int. Ed*. **2005**, *44*, 6448.

[24] Goodgame, D. M. L.; Hill, S. P. W.; Williams, D. J. *Chem. Commun.* **1993**, 1019.

[25] Bassett, A. P.; Magennis, S. W.; Glover, P. B.; Lewis, D. J.; Spencer, N.; Parsons, S.; Williams, R. M.; De Cola, L.; Pikramenou, Z. *J. Am. Chem. Soc.* **2004**, *126*, 9413.

[26] Lessmann, J. J.; Horrocks, W. DeW., Jr. *Inorg. Chem.* **2000**, *39*, 3114.

[27] Piguet, C.; Bünzli, J.-C. G.; Bernardinelli, G.; Hopfgartner, G.; Williams, A. F. *J. Am. Chem. Soc.* **1993**, *115*, 8197.

[28] Bernardinelli, G.; Piguet, C.; Williams; A. F. *Angew. Chem. Int. Ed. Engl.* **1992**, *31*, 1622.

[29] Hamacek, J.; Blanck, S.; Elhabiri, M.; Leize, E.; Van Dorsselaer, A.; Piguet, C.; Albrecht-Gary, A.-M. *J. Am. Chem. Soc.* **2003**, *125*, 1541.

[30] Martin, N.; Bünzli, J.-C. G.; McKee, V.; Piguet, C.; Hopfgartner, G. *Inorg. Chem.* **1998**, *37*, 577.

[31] Iglesias, C. P.; Elhabiri, M.; Hollenstein, M.; Bünzli, J.-C. G.; Piguet, C. *J. Chem. Soc., Dalton Trans.* **2000,** 2031.

[32] Elhabiri, M.; Scopelliti, R.; Bünzli, J.-C. G.; Piguet, C. *Chem. Commun.* **1998**, 2347.

[33] Elhabiri, M.; Scopelleti, R.; Bünzli, J.-C. G.; Piguet, C. *J. Am. Chem. Soc.* **1999**, *121*, 10747.

[34] Gonçalves e Silva, F. R.; Malta, O. L.; Reinhard, C.; Güdel, H.-U.; Piguet, C.; Moser, J. E.; Bünzli, J.-C. G. *J. Phys. Chem. A* **2002**, *106*, 1670.

[35] Elhabiri, M.; Hamacek, J.; Bünzli, J.-C. G.; Albrecht-Gary, A.-M. *Eur. J. Inorg. Chem.* **2004**, 51.

[36] Elhabiri, M.; Hamacek, J.; Humbert, N.; Bünzli, J.-B.; Albrecht-Gary, A.-M. *New J. Chem.* **2004**, *28*, 1096.

[37] Costes, J.-P.; Dahan, F.; Dupuis, A.; Lagrave, S.; Laurent, J.-P. *Inorg. Chem.* **1998**, *37*, 153.

[38] Costes, J.-P.; Nicodème, F. *Chem. Eur. J.* **2002**, *8*, 3442.

[39] Costes, J.-P.; Dahan, F.; Nicodème, F. *Inorg. Chem.* **2003**, *42*, 6556.

[40] Tóth, E.; Helm, L.; Merbach, A. E.; Hedinger, R.; Hegetschweiler, K.; Jánossy, A.

Inorg. Chem. **1998**, *37*, 4104.

[41] Hedinger, R.; Ghisletta, M.; Hegetschweiler, K.; Tóth, E.; Merbach, A. E.; Sessoli, R.; Getteschi, D.; Gramlich, V. *Inorg. Chem.* **1998**, *37*, 6698.

[42] Chapon, D.; Husson, C.; Delangle, P.; Lebrun, C.; Vottéro, P. J. A. *J. Alloys Compd.* **2001**, *323-324*, 128.

[43] Chapon, D.; Morel, J.-P.; Delangle, P.; Gateau, C.; Pécaut, J. *Dalton Trans.* **2003**, 2745.

[44] Chapon, D.; Delangle, P.; Lebrun, C. *J. Chem. Soc., Dalton Trans.* **2002**, 68.

[45] Ouali, N.; Rivera, J.-P.; Chapon, D.; Delangle, P.; Piguet, C. *Inorg. Chem.* **2004**, *43*, 1517.

[46] Shannon, R. D. *Acta Crystallogr.* **1976**, *A32*, 751.

[47] Le Borgne, T.; Altmann, P.; André, N.; Bünzli, J.-C. G.; Bernardinelli, G.; Morgantini, P.-Y.; Weber, J.; Piguet, C. *Dalton Trans.* **2004**, 723.

[48] André, N.; Scopelliti, R.; Hopfgartner, G.; Piguet, C.; Bünzli, J.-C. G. *Chem. Commun.* **2002**, 214.

[49] Bocquet, B.; Bernardinelli, G.; Ouali, N.; Floquet, S.; Renaud, F.; Hopfgartner, G.; Piguet, C. *Chem. Commun.* **2002**, 931.

[50] Floquet, S.; Ouali, N.; Bocquet, B.; Bernardinelli, G.; Imbert, D.; Bünzli, J.-C. G.; Hopfgartner, G.; Piguet, C. *Chem. Eur. J.* **2003**, *9*, 1860.

[51] Ouali, N.; Rivera, J.-P.; Morgantini, P.Y.; Weber, J.; Piguet, C. *J. Chem. Soc., Dalton Trans.* **2003**, 1251.

[52] Floquet, S.; Borkovec, M.; Bernardinelli, G.; Pinto, A.; Leuthold, L.-A.; Hopfgartner, G.; Imbert, D.; Bünzli, J.-C. G.; Piguet, C. *Chem. Eur. J.* **2004**, *10*, 1091.

[53] Zeckert, K.; Hamacek, J.; Rivera, J.-P.; Floquet, S.; Pinto, A.; Borkovec, M.; Piguet, C. *J. Am. Chem. Soc.* **2004**, *126*, 11589.

[54] Hamacek, J.; Borkovec, M.; Piguet, C. *Chem. Eur. J.* **2005**, *11*, 5217.

[55] Hamacek, J.; Borkovec, M.; Piguet, C. *Chem. Eur. J.* **2005**, *11*, 5227.

[56] Zeckert, K.; Hamacek, J.; Senegas, J.-M.; Della-Favera, N.; Floquet, S.; Bernardinelli, G.; Piguet, C. *Angew. Chem. Int. Ed.* **2005**, *44*, 7954.

[57] Piguet, C.; Borkovec, M.; Hamacek. J.; Zeckert, K. *Coord. Chem. Rev.* **2005**, *249*, 705.

[58] Borkovec, M.; Hamacek, J.; Piguet, C. *Dalton Trans.* **2004**, 4096.

[59] Hamacek, J.; Borkovec, M.; Piguet, C. *Dalton Trans.* **2006**, 1473.

[60] Piguet, C.; Hopfgartner, G.; Williams, A. F.; Bünzli, J.-C. G. *Chem. Commun.* **1995**, 491.

[61] Piguet, C.; Rivara-Minten, E.; Hopfgartner, G.; Bünzli, J.-C. G. *Helv. Chim. Acta* **1995**, *78*, 1541.

[62] Piguet, C.; Bernardinelli, G.; Bünzli, J.-C. G.; Petoud, S.; Hopfgartner, G. *Chem. Commun.* **1995**, 2575.

[63] Piguet, C.; Bünzli, J.-C. G.; Bernardinelli, G.; Hopfgartner, G.; Petoud, S.; Schaad, O. *J. Am. Chem. Soc.* **1996**, *118*, 6681.

[64] Piguet, C.; Rivara-Minten, E.; Bernardinelli, G.; Bünzli, J.-C. G.; Hopfgartner, G. *J. Chem. Soc., Dalton Trans.* **1997**, 421.

[65] Rigault, S.; Piguet, C.; Bernardinelli, G.; Hopfgartner, G. *Angew. Chem. Int. Ed.* **1998**, *37*, 169.

[66] Piguet, C.; Edder, C.; Rigault, S.; Bernardinelli, G.; Bünzli, J.-C. G.; Hopfgartner, G. *J. Chem. Soc., Dalton Trans.* **2000**, 3999.

[67] Rigault, S.; Piguet, C.; Bünzli, J.-C. G. *J. Chem. Soc., Dalton Trans.* **2000**, 2045.

[68] Rigault, S.; Piguet, C.; Bernardinelli, G.; Hopfgartner, G. *J. Chem. Soc., Dalton Trans.* **2000**, 4587.

[69] Cantuel, M.; Bernardinelli, G.; Imbert, D.; Bünzli, J.-C. G.; Hopfgartner, G.; Piguet, C. *J. Chem. Soc., Dalton Trans.* **2002**, 1929.

[70] Imbert, D.; Cantuel, M.; Bünzli, J.-C. G.; Bernardinelli, G.; Piguet, C. *J. Am. Chem. Soc.* **2003**, *125*, 15698.

[71] Cantuel, M.; Bernardinelli, G.; Muller, G.; Riehl, J. P.; Piguet, C. *Inorg. Chem.* **2004**, *43*, 1840.

[72] Telfer, S. G.; Tajima, N.; Kuroda, R.; Cantuel, M.; Piguet, C. *Inorg. Chem.* **2004**, *43*, 5302.

[73] Torelli, S.; Imbert, D.; Cantuel, M.; Bernardinelli, G.; Delahaye, S.; Hauser, A.; Bünzli, J.-C. G.; Piguet, C. *Chem. Eur. J.* **2005**, *11*, 3228.

[74] Lamm, B. *Acta Chem. Scand.* **1965,** 2316.

[75] Piguet, C.; Bernardinelli, G.; Bocquet, B.; Quattropani, A.; Williams, A. F. *J. Am. Chem. Soc.* **1992**, *114*, 7440.

[76] Johansen, J. E.; Christie, B. D.; Rapoport, H. *J. Org. Chem.* **1981**, *46*, 4914.

[77] Robinson, M. *J. Am. Chem. Soc.* **1958**, *80*, 5481.

[78] Vögtle, F.; Ohm, C. *Chem. Ber.* **1984**, *117*, 948.

[79] Achremovicz, L. ; Mlochowski, J. ; Mora, C. ; Skarzewski, J. *J. für prakt. Chemie*, **1982**, *324*, 735.

[80] André, N.; Jensen, T. B.; Scopelliti, R.; Imbert, D.; Elhabiri, M.; Hopfgartner, G.; Piguet, C.; Bünzli, J.-C. G. *Inorg. Chem.* **2004**, *43*, 515.

[81] Tripier, R.; Hollenstein, M.; Elhabiri, M.; Chauvin, A.-S.; Zucchi, G.; Piguet, C.; Bünzli, J-.G. G. *Helv. Chim. Acta* **2002**, *85*, 1915.

[82] Pauling, L. *The Nature of the Chemical Bond*, Cornell University Press, Ithaca, New York, 1960. Page 260.

[83] Piguet, C.; Geraldes, G. F. G. C. in *Handbook on the Physics and Chemistry of Rare Earths*, Gschneidner, K. A. Jr.; Bünzli, J.-C. G.; Pecharsky, V., Eds., Elsevier B. V., Amsterdam, The Netherlands, 2003. Vol. 33, Chapter 215.

[84] Golding, R. M.; Halton, M. R. *Aust. J. Chem.* **1972**, *25*, 2577.

[85] Pinkerton, A. A.; Rossier, M.; Spiliadis, S. *J. Magn. Res.* **1985**, *64*, 420.

[86] Bleaney, B. *J. Magn. Res.* **1972**, *8*, 91.

[87] Bleaney, B.; Dobson, C. M.; Levine, B. A.; Martin, R. B.; Williams, R. J. P.; Xavier, A. V. *Chem. Comm*. **1972**, 791.

[88] Reilley, C. N.; Good, B. W.; Desreux, J. F. *Anal. Chem.* **1975**, *47*, 2110.

[89] Reilley, C. N.; Good, B. W.; Allendoerfer, R. D. *Anal. Chem.* **1976**, *48*, 1446.

[90] Abragam, A.; Bleaney, B. *Electron Paramagnetic Resonance of Transition Ions*, Clarendon Press, Oxford, 1970. Tables 5.7, 5.8 and 5.11.

[91] Ouali, N.; Bocquet, B.; Rigault, S.; Morgantini, P.-Y.; Weber, J.; Piguet, C. *Inorg. Chem.* **2002**, *41*, 1436.

[92] Reuben, J. *J. Magn. Res.* **1982**, *50*, 233.

[93] Platas, C.; Avecilla, F.; de Blas, A.; Geraldes, C. F. G. C.; Rodríguez-Blas, T.; Adams, H.; Mahía, J. *Inorg. Chem.* **1999**, *38*, 3190.

[94] Görller-Walrand, C.; Binnemans, K. in *Handbook on the Physics and Chemistry of Rare Earths*, Gschneidner, K. A. Jr.; Eyring, L., Eds., Elsevier B. V., Amsterdam, The Netherlands, 1996. Vol. 23, Chapter 155.

[95] Vold, R. L.; Waugh, J. S.; Klein, M. P.; Phelps, D. E. *J. Chem. Phys.* **1968**, *48*, 3831.

[96] Peters, J. A.; Huskens, J.; Raber, D. J. *Prog. NMR Spec.* **1996**, *28*, 283.

[97] Rodríguez-Cortiñas, R.; Avecilla, F.; Platas-Iglesias, C.; Imbert, D.; Bünzli, J.-C. G.; de Blas, A.; Rodríguez-Blas, T. *Inorg. Chem.* **2002**, *41*, 5336.

[98] Desreux, J. F. in *Lanthanide Probes in Life, Chemical and Earth Sciences. Theory and*

Practice Bünzli, J.-C. G.; Choppin, G. R., Eds.; Elsevier Science Publ. B. V., Amsterdam, The Netherlands, 1989; Chapter 2.

[99] Wosley, W. C. *J. Chem. Educ.* **1973**, *50*, A335.

[100] Raymond, K. N. *Chem. Eng. News* **1983,** *Dec 12***,** 2.